ERDC/CHL TR-05-2

Coastal and Hydraulics Laboratory

US Army Corps of Engineers®
Engineer Research and Development Center

Geomorphic Analysis of Mattituck Inlet and Goldsmith Inlet, Long Island, New York

Michael J. Morgan, Nicholas C. Kraus, and Jodi M. McDonald

July 2005

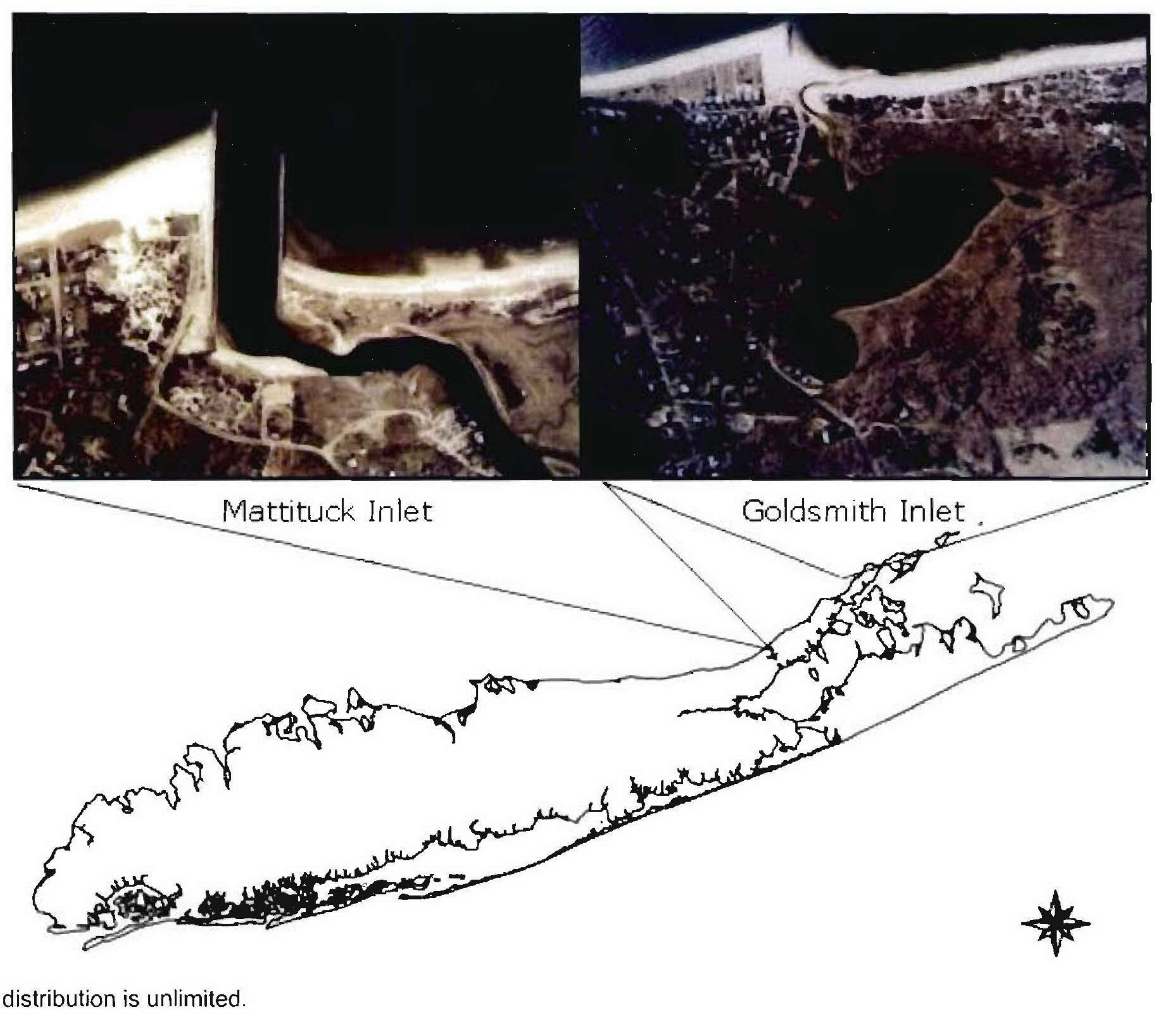

Coastal Inlets Research Program

ERDC/CHL TR-05-2
July 2005

Geomorphic Analysis of Mattituck Inlet and Goldsmith Inlet, Long Island, New York

Michael J. Morgan

Department of Geography
Hunter College, City University of New York
695 Park Avenue
New York, NY 10021

Nicholas C. Kraus

Coastal and Hydraulics Laboratory
U.S. Army Engineer Research and Development Center
3909 Halls Ferry Road
Vicksburg, MS 39180-6199

Jodi M. McDonald

U.S. Army Engineer District, New York
26 Federal Plaza
New York, NY 10278-0090

Final report

Prepared for U.S. Army Corps of Engineers
Washington, DC 20314-1000

ABSTRACT: This study of Mattituck Inlet and Goldsmith Inlet, Long Island, NY, covers the historic and geomorphic background, literature, field measurements, numerical modeling of tidal circulation, and analysis of inlet morphologic properties. The inlets are located 8.2 km apart on the eastern end of the north shore of Long Island, NY, facing Long Island Sound Mattituck Inlet has a federally maintained channel and dual jetties, and it connects the sound to Mattituck Creek. Mattituck Inlet is the only major harbor on the north fork of Long Island is a commercial and recreational boating center. The navigation channel is maintained to a depth of 7 ft mean low water with a 2-ft allowable overdraft. Goldsmith Inlet connects the sound to Goldsmith Pond. The inlet has a nonfunctional jetty on its west side and is non-navigable, with typical depths ranging from 0.5 to 3 ft.

Tidal inlets on the north shore of Long Island have received little study compared to those on the south shore that open to the Atlantic Ocean. It appears that most inlets on the north shore have been more stable and in existence longer than the inlets on the south shore. Inlets on the north shore, therefore, hold value for further understanding of basic inlet processes, in particular, of channel cross section and locational stability. Another motivation for the study of inlets along the north shore of Long Island is the large range in grain size of the sediments on this coast.

Given their significant differences, it is remarkable that Mattituck Inlet and Goldsmith Inlet have remained open for more than two centuries and likely much longer. The stability of inlets on the north shore derives in part from a relatively steep inner shore face, presence of geologic controls such as glacial erratics or hard points on shore, origins of ponds as low-lying areas created after glaciation, and relatively weak longshore sediment transport that is about an order of magnitude less than that on the south shore of Long Island. However, other factors enter in controlling stability, in particular, commercial mining of sediment, such as at Mattituck Inlet.

Contents

Preface ... xxii

Conversion Factors Non-SI to SI Units of Measurement ... xxiv

1—Introduction ... 1

Background ... 1
Study Site ... 3
Previous Studies ... 6
Motivaton ... 9
Study Objective ... 10

2—Study Area and Physical Setting ... 12

Regional Setting - Long Island Sound ... 12
Geomorphic environment ... 12
Oceanographic environment ... 15
Longshore sediment transport ... 18
Mattituck Inlet - History and Site Description ... 20
Physical description ... 22
Physical setting ... 27
Goldsmith Inlet - History and Site Description ... 32
Physical description ... 35
Physical setting ... 39
Present condition ... 40

3—Field Data Collection and Analysis ... 46

Overview of Measurements and Vertical Datums ... 46
Mattituck Inlet ... 49
Bathymetry ... 49
Water level ... 65
Current ... 68
Sediment ... 69
Goldsmith Inlet ... 74
Bathymetry ... 74
Water level ... 88
Current ... 91
Sediment ... 92

4—Morphology Change, and Channel Shoaling and Migration 101

Mattituck Inlet 101
Offshore morphology change 101
Navigation channel and flood shoal morphology change 117
East bank spit migration 162
Bank encroachment analysis 164
Goldsmith Inlet 168
Offshore morphology change 168
Channel migration 174
Channel and flood shoal morphology change 187
Summary of morphology change at Goldsmith Inlet 200

5—Circulation Analysis 204

Mattituck Inlet 204
Model validation 206
Pre-dredging condition (2002) 213
Alterntive 1: Post-dredging morphology 222
Alterntive 2: Natural morphology with offshore shoal 228
Goldsmith Inlet 243
Model validation 243
Discussion of tidal asymmetry 249
Discussion of current velocity 255

6—Inlet Morphology and Stability 265

General Inlet Properties 265
Inlet classification and sedimentation patterns 265
Inlet stability 268
Hydraulic efficiency 269
Ebb shoal volume 270
Flood shoal volume 270
Mattituck Inlet 271
Mattituck Inlet channel cross-sectional area stability 272
Mattituck Inlet offshore shoal 275
Mattituck Inlet flood shoal 276
Goldsmith Inlet 278
Goldsmith Inlet channel cross-sectional area stability 279
Goldsmith Inlet ebb shoal 282
Goldsmith Inlet flood shoal 282
Discussion of Channel Cross-Sectional Area Relations 284

7—Comparative Analysis and Conclusions 286

Summary of Inlet Characteristics 287
Comparative Analysis 288
Forcing 288
General features of geomorphology 289

Anthropogenic influences....290
Hydrodynamic and tidal shoals....291
Channel cross-sectional area stability....291
Mattituck Inlet, Conclusions....292
Goldsmith Inlet, Conclusions....294
Recommendations for Future Studies....295

References....297

List of Figures

Figure 1-1. Long Island, NY, inlets and harbors....4
Figure 1-2. Long Island, NY, with study area inset....5
Figure 1-3. Study area with Mattituck Inlet and Goldsmith Inlet insets....5
Figure 1-4. Mattituck Inlet and Mattituck Creek, 16 April 2003....6
Figure 1-5. Goldsmith Inlet and Goldsmith Pond, 16 April 2003....7
Figure 1-6. Shoreline from Duck Pond Point to Horton Point....8
Figure 1-7. Goldsmith Inlet with view northeast into Long Island Sound, showing substantial gravel and cobble, 22 March 2003....10
Figure 2-1. Long Island Sound region bathymetry....13
Figure 2-2. Harbor Hill and Ronkonkoma Moraine locations....14
Figure 2-3. Study area headlands....15
Figure 2-4. Mattituck Inlet as depicted in NOS T-sheet 55 (1838)....21
Figure 2-5. Mattituck Inlet and northern end of Mattituck Creek, 11 May 1955....21
Figure 2-6. The Mattituck Mill at Mattituck Creek....22
Figure 2-7. Dredging and mining activities in and near Mattituck Inlet....23
Figure 2-8. Mattituck Inlet and jetties, view looking south, 28 March 2003....26
Figure 2-9. Mattituck Inlet and jetties, view looking north, 28 March 2003....26
Figure 2-10. Mattituck Inlet channel, after turn eastward inside jetties....27
Figure 2-11. Bluffs east of Mattituck Inlet, 21 November 2003....28
Figure 2-12. Bailie's Beach primary dune, 21 November 2003....29
Figure 2-13. Dunes east of Mattituck Inlet, looking west, 8 October 2002....29

Figure 2-14. Dunes at base of Mattituck Inlet east jetty, looking south, 21 November 2003 30

Figure 2-15. Dunes at base of Mattituck Inlet east jetty, looking north, 8 October 2003 30

Figure 2-16. Vegetated dune protected by revetment at Bailie's Beach, view looking east, 9 July 2004 31

Figure 2-17. Sparsely vegetated and unprotected dune at Bailie's Beach, view looking west, 9 July 2004 31

Figure 2-18. Mattituck Inlet perimeter, view looking south, 21 November 2003 32

Figure 2-19. Goldsmith Inlet as depicted in NOS T-sheet 55 (1838) 33

Figure 2-20. Peconic Mill at Goldsmith Inlet 34

Figure 2-21. Headstone of James H. and Sarah C. Goldsmith, Old Burial Ground, Southold, New York 35

Figure 2-22. Goldsmith Inlet and Goldsmith Pond, 11 May 1955, 9 years before jetty construction 36

Figure 2-23. Typical gravel and some cobble armoring at Goldsmith Inlet, 28 March 2003 37

Figure 2-24. Proposed marinas, 1960 37

Figure 2-25. Goldsmith Inlet, west perimeter, view looking south, circa winter 2001 39

Figure 2-26. Bluffs west of Goldsmith Inlet, 28 March 2003 40

Figure 2-27. Goldsmith Inlet entrance with view of east beach, 28 March 2003 40

Figure 2-28. Sediment impoundment west of Goldsmith Inlet jetty, circa winter 2001 42

Figure 2-29. Goldsmith Inlet orientation, 8 October 2002 43

Figure 2-30. Goldsmith Inlet orientation, 28 March 2003 43

Figure 2-31. Goldsmith Inlet orientation and ice, 16 February 2004 44

Figure 2-32. Goldsmith Inlet orientation after emergency dredging, 6 April 2004 44

Figure 3-1a. Datum elevation differences, Port Jefferson 47

Figure 3-1b. Datum elevation differences, Bridgeport 48

Figure 3-2. Mattituck Inlet bathymetry survey coverage, 6-8 October 2002 50

Figure 3-3. Mattituck Inlet elevation contours, 6-8 October 2002 51

Figure 3-4. Mattituck Inlet offshore west survey transects, 6-8 October 2002 52

Figure 3-5a. Beach profiles W1-W5, west of Mattituck Inlet, 6-8 October 2002 52

Figure 3-5b. Beach profiles W6-W10, west of Mattituck Inlet, 6-8 October 2002 53

Figure 3-6. Shoreline west of Mattituck Inlet, 21 November 2003 53

Figure 3-7a. Longshore bars west of Mattituck Inlet, 16 April 2003 54

Figure 3-7b. Offshore east of Mattituck Inlet, 16 April 2003 54

Figure 3-8. Mattituck Inlet offshore east survey transects, 6-8 October 2002 55

Figure 3-9a. Beach profiles E1-E5, east of Mattituck Inlet, 6-8 October 2002 56

Figure 3-9b. Beach profiles E6-E10, east of Mattituck Inlet, 6-8 October 2002 56

Figure 3-10. Beach east of Mattituck Inlet, 16 April 2003, showing irregular shoreline 57

Figure 3-11 Cuspate shoreline features east of Mattituck Inlet, 21 November 2003 57

Figure 3-12. Mound of *Crepidula fornicata* shells, east of Mattituck Inlet, 21 November 2003 58

Figure 3-13. Mattituck Inlet offshore shoal and channel contour elevation, 6-8 October 2002 59

Figure 3-14. Features offshore of Mattituck Inlet, 6-8 October 2002 59

Figure 3-15. Mattituck Inlet flood shoal, 6-8 October 2002 60

Figure 3-16. Mattituck Inlet flood shoal on eastern bank, view looking west, March 2003 60

Figure 3-17. Mattituck Inlet flood shoal on eastern bank, view looking east, 21 November 2003 61

Figure 3-18. Mattituck Inlet Federal navigation channel elevation, 6-8 October 2002 62

Figure 3-19. Mattituck Inlet channel transects 1-10, 6-8 October 2002 62

Figure 3-20a. Mattituck Inlet channel cross sections 1-4, 6-8 October 2002 63

Figure 3-20b. Mattituck Inlet channel cross sections 5-7, 6-8 October 2002 63

Figure 3-20c. Mattituck Inlet channel cross sections 8-10, 6-8 October 2002 64

Figure 3-21. Mattituck Inlet shore-attached flood shoals on northern and southern banks of channel, view looking east, 21 November 2003 64

Figure 3-22. Mattituck Inlet tide gauge and current meter locations, 19 September – 8 October 2002 65

Figure 3-23a. Mattituck Inlet water level, 19 September – 8 October 2002 66

Figure 3-23b. Mattituck Inlet water level, 4-8 October 2002 67

Figure 3-24. Mattituck Inlet along-channel current velocity, 7-8 October 2002 68

Figure 3-25. Mattituck Inlet sediment sample locations, 6-7 May 2003 70

Figure 3-26a. Mattituck Inlet cumulative grain size distribution MH1-MH4, 6-7 May 2003 71

Figure 3-26b. Mattituck Inlet cumulative grain size distribution MH5, MH6, MH8, and MH10, 6-7 May 2003 71

Figure 3-27. Mattituck Inlet, New York District (1969) sediment sampling profile locations 72

Figure 3-28a Goldsmith Inlet bathymetry survey coverage, 6-8 October 2002 75

Figure 3-28b. Goldsmith Inlet elevation contours, 6-8 October 2002 75

Figure 3-29. Goldsmith Inlet offshore survey transects, 6-8 October 2002 76

Figure 3-30a. Beach profiles W1-W3, west of Goldsmith Inlet, 6-8 October 2002 77

Figure 3-30b. Beach profiles W4-W7, west of Goldsmith Inlet, 6-8 October 2002 77

Figure 3-31a. Beach profiles E1-E5, east of Goldsmith Inlet, 6-8 October 2002 78

Figure 3-31b. Beach profiles E6-E10, east of Goldsmith Inlet, 6-8 October 2002 78

Figure 3-32. Aerial view of shoreline west of Goldsmith Inlet, 16 April 2003 79

Figure 3-33. Ground view of shoreline west of Goldsmith Inlet, 28 March 2003 79

Figure 3-34. Aerial view of shoreline east of Goldsmith Inlet, 16 April 2003 80

Figure 3-35. Ground view of inlet entrance and shoreline east of Goldsmith Inlet, 28 March 2003 80

Figure 3-36. Goldsmith Pond flood shoal formations, 16 April 2003 81

Figure 3-37. Goldsmith Inlet flood shoal, west lobe, view looking south, 28 March 2003 81

Figure 3-38. Goldsmith Inlet flood shoal, east lobe, view looking south, 9 July 2004 82

Figure 3-39. Goldsmith Inlet flood shoal, east and west lobe, view looking south, 9 July 2004 82

Figure 3-40a. Goldsmith Inlet contours at low tide, 8 October 2002 83

Figure 3-40b. Goldsmith Inlet contours at mean tide, 8 October 2002 83

Figure 3-40c. Goldsmith Inlet contours at high tide, 8 October 2002 84

Figure 3-41. Goldsmith Inlet, channel with shoal, 28 March 2003 85

Figure 3-42. Goldsmith Inlet attached shoal, 28 March 2003 85

Figure 3-43. Goldsmith Inlet channel transects, 8 October 2002 86

Figure 3-44a. Goldsmith Inlet channel cross sections 1-4, 8 October 2002 86

Figure 3-44b. Goldsmith Inlet channel cross sections 5-8, 8 October 2002 87

Figure 3-44c. Goldsmith Inlet channel cross sections 9-12, 8 October 2002 87

Figure 3-45. Goldsmith Inlet channel center-line elevation, 8 October 2002 88

Figure 3-46. Goldsmith Inlet tide gauge locations, 19 September - 8 October 2002 89

Figure 3-47a. Goldsmith Inlet water level, 19 September – 8 October 2002 89

Figure 3-47b. Goldsmith Inlet water level, 5-7 October 2002 90

Figure 3-48. Goldsmith Inlet midchannel current velocity, 8 October 2002 92

Figure 3-49a. Goldsmith Inlet sediment sample locations, 8 October 2002 93

Figure 3-49b. Goldsmith Inlet sediment sample locations, 31 July 2003 93

Figure 3-50a. Goldsmith Inlet cumulative grain size S1-S4 and S15, 8 October 2002 and 31 July 2003 94

Figure 3-50b. Goldsmith Inlet cumulative grain size S5-S8 and S16, 8 October 2002 and 31 July 2003 94

Figure 3-50c. Goldsmith Inlet cumulative grain size S9-S12 and S17, 8 October 2002 and 31 July 2003 95

Figure 3-50d. Goldsmith Inlet cumulative grain size S13, S14, S18, S19, 8 October 2002 and 31 July 2003 95

Figure 3-50e. Goldsmith Inlet cumulative grain size S20-S23, 8 October 2002 and 31 July 2003 96

Figure 3-50f. Goldsmith Inlet cumulative grain size S24-S27, 8 October 2002 and 31 July 2003 96

Figure 3-50g. Goldsmith Inlet cumulative grain size S28-S31, 8 October 2002 and 31 July 2003 97

Figure 3-51. Goldsmith Inlet median grain-size distribution of surface samples, 8 October 2002 and 31 July 2003 98

Figure 3-52. Goldsmith Inlet, New York District (1969) profile locations 100

Figure 4-1a. Beach profile W1, west of Mattituck Inlet, March 1998 and 6-8 October 2002 102

Figure 4-1b Beach profile W2, west of Mattituck Inlet, March 1998 and 6-8 October 2002 102

Figure 4-1c. Beach profile W3, west of Mattituck Inlet, March 1998 and 6-8 October 2002 103

Figure 4-1d. Beach profile W4, west of Mattituck Inlet, March 1998 and 6-8 October 2002 103

Figure 4-1e. Beach profile W5, west of Mattituck Inlet, March 1998 and 6-8 October 2002 104

Figure 4-1f. Beach profile W6, west of Mattituck Inlet, March 1998 and 6-8 October 2002 104

Figure 4-1g. Beach profile W7, west of Mattituck Inlet, March 1998 and 6-8 October 2002 105

Figure 4-1h Beach profile W8, west of Mattituck Inlet, March 1998 and 6-8 October 2002 105

Figure 4-2a. Offshore shoal cross-shore profile E4, March 1998 and 6-8 October 2002 106

Figure 4-2b. Offshore shoal cross-shore profile E5, March 1998 and 6-8 October 2002 106

Figure 4-2c. Offshore shoal cross-shore profile E6, March 1998 and 6-8 October 200 107

Figure 4-2d. Offshore shoal cross-shore profile E7, March 1998 and 6-8 October 2002 107

Figure 4-2e. Offshore shoal cross-shore profile E8, March 1998 and 6-8 October 2002 108

Figure 4-2f. Offshore shoal cross-shore profile E9, March 1998 and 6-8 October 2002 108

Figure 4-3. Mattituck Inlet and offshore elevation contours, 8 December 1927 110

Figure 4-4. Mattituck Inlet, circa 1930 and offshore elevation contours, 1969 110

Figure 4-5a. Mattituck Inlet offshore elevation change, 1927-1969 111

Figure 4-5b. Mattituck Inlet offshore elevation change, 1969-2002 111

Figure 4-5c. Mattituck Inlet offshore elevation change, 1927-2002 112

Figure 4-6. Volume change polygons, east of Mattituck Inlet, with elevation change 1927-2002 113

Figure 4-7. Offshore shoal elevation change, 1969-2002 and Mattituck Inlet 16 April 2003 114

Figure 4-8. Mattituck Inlet offshore shoal center lines, 8 December 1927 and 6-8 October 2002 116

Figure 4-9. Offshore feature center lines, 8 December 1927 and 6-8 October 2002 117

Figure 4-10. Mattituck Inlet orientation, 1891 119
Figure 4-11. Mattituck Inlet orientation, 1900 119
Figure 4-12. Mattituck Inlet, 1891-1900, hypothesized reorientation 120
Figure 4-13. Mattituck Inlet orientation, 1901 121
Figure 4-14. Mattituck Inlet orientation, 1905-1907 121
Figure 4-15. Mattituck Inlet orientation, 1913/14 122
Figure 4-16. Mattituck Inlet with shoaling along inside of west jetty, circa 1930s 123
Figure 4-17. Mattituck Inlet east jetty landward breach, 1941 123
Figure 4-18a. Mattituck Inlet channel elevation, 1935 127
Figure 4-18b. Mattituck Inlet flood shoal area, 1935 127
Figure 4-19a. Mattituck Inlet channel elevation, 4 May 1936 128
Figure 4-19b. Mattituck Inlet flood shoal area, 4 May 1936 129
Figure 4-19c. Channel elevation change, 1935 to 4 May 1936 129
Figure 4-20. Federal navigation channel study area 130
Figure 4-21a. Mattituck Inlet channel elevation, 3 July 1937 131
Figure 4-21b. Mattituck Inlet flood shoal area, 3 July 1937 132
Figure 4-21c. Channel elevation change, 4 May 1936 to 3 July 1937 132
Figure 4-22a. Mattituck Inlet channel elevation, 1938 133
Figure 4-22b. Mattituck Inlet flood shoal area, 1938 134
Figure 4-22c. Channel elevation change, 4 May 1936 to 1938 134
Figure 4-23a. West lobe morphology change, 1936–1938 135
Figure 4-23b. East lobe morphology change, 1936–1938 135
Figure 4-24. Mattituck Inlet west jetty seaward extension, 1938 136
Figure 4-25 Shoreline recession and east jetty landward breach 1927 to 1941 137
Figure 4-26a. Mattituck Inlet east bank spit morphology, 1891-1927, with jetty configuration of 1914 included for reference 138
Figure 4-26b. Mattituck Inlet east bank spit morphology, 1935-1955, with jetty configuration of 1914 and 1946 included for reference 139
Figure 4-27. Mattituck Inlet Federal navigation channel configuration, prior to and after October – November 1950 140
Figure 4-28. Federal navigation channel and Federal anchorage dredging areas, September – October 1965 141
Figure 4-29a. Mattituck Inlet, circa 1930 142
Figure 4-29b. Mattituck Inlet, 1938 142

Figure 4-29c. Mattituck Inlet, 1941 143
Figure 4-29d. Mattituck Inlet, 11 May 1955 143
Figure 4-29e. Mattituck Inlet, 1 April 1964 144
Figure 4-29f. Mattituck Inlet, 25 April 1969 144
Figure 4-29g. Mattituck Inlet, 6 April 1976 145
Figure 4-29h. Mattituck Inlet, 23 March 1980 145
Figure 4-29i. Mattituck Inlet, 5 April 1993 146
Figure 4-29j. Mattituck Inlet, 26-30 April 2001 146
Figure 4-29k. Mattituck Inlet, 16 April 2003 147
Figure 4-29l. Mattituck Inlet, 15 April 2004 147
Figure 4-30. Mining related companies and locations at Mattituck Inlet 149
Figure 4-31a. Channel elevation, June 1961 (pre-dredging) 151
Figure 4-31b. Channel elevation, September 1961 (post-dredging) 152
Figure 4-31c. Channel elevation change, June 1961 - September 1961 152
Figure 4-32a. Channel elevation, January 1980 (pre-dredging) 153
Figure 4-32b. Channel elevation, May 1980 (post-dredging) 153
Figure 4-32c. Channel elevation change, January 1980 - May 1980 154
Figure 4-33a. Channel elevation, September 1990 (pre-dredging) 154
Figure 4-33b. Channel elevation, October 1990 (post-dredging) 155
Figure 4-33c. Channel elevation change, September 1990 - October 1990 155
Figure 4-34a. Channel elevation change, May 1980 to August 1983 158
Figure 4-34b. Channel elevation change, May 1980 to June 1985 158
Figure 4-34c. Channel elevation change, May 1980 to September 1987 159
Figure 4-34d. Channel elevation change, May 1980 to June 1988 159
Figure 4-34e. Channel elevation change, May 1980 to October 1989 160
Figure 4-35. Channel elevation change, October 1990 to January 2002 161
Figure 4-36. Mattituck Inlet shoreline, pre- and post-dredging, 16 April 2003 and 15 April 2004 162
Figure 4-37a. East bank spit migration, 1941-1976 163
Figure 4-37b. East flood shoal migration, 1976-2003 163
Figure 4-38. Mattituck Inlet channel cross sections 164
Figure 4-39a. Mattituck Inlet channel cross-section A 165
Figure 4-39b. Mattituck Inlet channel cross-section B 166
Figure 4-39c. Mattituck Inlet channel cross-section C 167

Figure 4-40a. Boat approaching turn at base of jetties, Mattituck Inlet, 9 July 2004, view looking northwest 167

Figure 4-40b. Boat wake obliquely incident on area of flood shoal at base of east jetty, Mattituck Inlet, 9 July 2004 168

Figure 4-41a. Beach profile W1, west of Goldsmith Inlet, March 1998 and 6-8 October 2002 169

Figure 4-41b Beach profile W2, west of Goldsmith Inlet, March 1998 and 6-8 October 2002 169

Figure 4-41c. Beach profile W4, west of Goldsmith Inlet, March 1998 and 6-8 October 2002 170

Figure 4-41d. Beach profile E1, east of Goldsmith Inlet, March 1998 and 6-8 October 2002 170

Figure 4-41e. Beach profile E2, east of Goldsmith Inlet, March 1998 and 6-8 October 2002 171

Figure 4-41f. Beach profile E3, east of Goldsmith Inlet, March 1998 and 6-8 October 2002 171

Figure 4-41g. Beach profile E4, east of Goldsmith Inlet, March 1998 and 6-8 October 2002 172

Figure 4-41h. Beach profile E5, east of Goldsmith Inlet, March 1998 and 6-8 October 2002 172

Figure 4-41i. Beach profile E6, east of Goldsmith Inlet, March 1998 and 6-8 October 2002 173

Figure 4-41j. Beach profile E7, east of Goldsmith Inlet, March 1998 and 6-8 October 2002 173

Figure 4-41k. Beach profile E8, east of Goldsmith Inlet, March 1998 and 6-8 October 2002 174

Figure 4-42a. Goldsmith Inlet channel entrance, 1938 175

Figure 4-42b. Goldsmith Inlet channel entrance, 11 May 1955 175

Figure 4-42c. Goldsmith Inlet channel entrance, 1 April 1964 176

Figure 4-42d. Goldsmith Inlet channel entrance, 5 October 1966 176

Figure 4-42e. Goldsmith Inlet channel entrance, 28 April 1969 177

Figure 4-42f. Goldsmith Inlet channel entrance, 6 April 1976 177

Figure 4-42g. Goldsmith Inlet channel entrance, 24 May 1980 178

Figure 4-42h. Goldsmith Inlet channel entrance, 5 April 1993 178

Figure 4-42i. Goldsmith Inlet channel entrance, 21 April 1996 179

Figure 4-42j. Goldsmith Inlet channel entrance, 26-30 April 2001 179

Figure 4-42k. Goldsmith Inlet channel entrance, 16 April 2003 180

Figure 4-42l. Goldsmith Inlet, 15 April 2004 180

Figure 4-43a. Goldsmith Inlet channel entrance, 1938 and 11 May 1955 181

Figure 4-43b. Goldsmith Inlet channel entrance, 11 May 1955, 1 April 1964, and 5 October 1966 182

Figure 4-43c. Goldsmith Inlet channel entrance, 28 April 1969, 28 April 1976, and 24 May 1980 182

Figure 4-43d. Goldsmith Inlet channel entrance , 21 April 1996 and 5 April 1996 184

Figure 4-43e. Goldsmith Inlet channel entrance, 16 April 2002, 16 April 2003, and 15 April 2004 184

Figure 4-44a. Goldsmith Inlet channel entrance orientation, 1993-2003 185

Figure 4-44b. Goldsmith Inlet channel entrance orientation, 2002-2004 186

Figure 4-45. Shoaling east of Goldsmith Inlet jetty, 1993-2004 187

Figure 4-46a. Goldsmith Inlet natural flood shoal, 1938 188

Figure 4-46b. Goldsmith Inlet natural flood shoal, 11 May 1955 188

Figure 4-46c. Goldsmith Inlet -channel with partially intact in-channel flood shoal, 1 April 1964 189

Figure 4-46d. Goldsmith Inlet channel, 5 October 1966 190

Figure 4-46e. Goldsmith Inlet channel, 28 April 1969 190

Figure 4-46f. Goldsmith Inlet channel, 6 April 1976 191

Figure 4-46g. Goldsmith Inlet channel, 24 May 1980 191

Figure 4-46h. Goldsmith Inlet channel, 5 April 1993 192

Figure 4-46i. Goldsmith Inlet channel, 21 April 1996 192

Figure 4-46j. Goldsmith Inlet channel, 16 April 2003 193

Figure 4-46k. Goldsmith Inlet channel, 15 April 2004 193

Figure 4-47a. Goldsmith Inlet channel center, 11 May 1955 and 1 April 1964 195

Figure 4-47b Goldsmith Inlet channel center, 5 October 1966 and 28 April 1969 195

Figure 4-47c. Goldsmith Inlet channel center, 6 April 1976 and 24 May 1980 196

Figure 4-47d. Goldsmith Inlet channel center, 5 April 1993 and 21 April 1996 196

Figure 4-47e. Goldsmith Inlet channel center, 16 April 2003 and 15 April 2004 197

Figure 4-48a. Goldsmith Inlet flood shoal, 11 May 1955 and 1 April 1964 198

Figure 4-48b. Goldsmith Inlet flood shoal, 5 October 1966 and 6 April 1976 198

Figure 4-48c. Goldsmith Inlet flood shoal, 5 April 1993 and 21 April 1996 199

Figure 4-48d. Goldsmith Inlet flood shoal, 16 April 2003 and 21 April 2004 199

Figure 4-49. Goldsmith Inlet, east bank wetlands, during current measurement, 8 October 2002 200

Figure 4-50. Goldsmith Inlet, east bank wetlands, with protective sand bank, 8 October 2002 201

Figure 4-51. Goldsmith Inlet, east bank wetland, 20 February 2004 201

Figure 5-1. Regional ADCIRC grid - New York Bight and Long Island Sound 205

Figure 5-2. Mattituck Inlet and Mattituck Creek, ADCIRC model bathymetry 205

Figure 5-3. Close view of Mattituck Inlet, ADCIRC model bathymetry 206

Figure 5-4. NOS stations and 19 September - 8 October 2002 survey tide gauge locations 207

Figure 5-5a. Water level at Eaton's Neck, Huntington Harbor; NOS measurements and ADCIRC calculations, 19 September - 8 October 2002 208

Figure 5-5b. Water level at Eaton's Neck, Huntington Harbor; NOS measurements and ADCIRC calculations, 5-8 October 2002 208

Figure 5-5c. Water level at New Haven Harbor, New Haven; NOS measurements and ADCIRC calculations, 19 September - 8 October 2002 209

Figure 5-5d. Water level at New Haven Harbor, New Haven; NOS measurements and ADCIRC calculations, 5-8 October 2002 209

Figure 5-5e. Water level at Kings Point; NOS measurements and ADCIRC calculations, 19 September - 8 October 2002 210

Figure 5-5f. Water level at Kings Point; NOS measurements and ADCIRC calculations, 5-8 October 2002 210

Figure 5-6a. Water level at Mattituck Inlet, near west jetty; measurements and ADCIRC calculations, 19 September - 8 October 2002 211

Figure 5-6b. Water level at Mattituck Inlet, near west jetty; measurements and ADCIRC calculations, 5-8 October 2002 211

Figure 5-6c. Water level at Mattituck Creek; measurements and ADCIRC calculations, 19 September - 8 October 2002 212

Figure 5-6d. Water level at Mattituck Creek; measurements and ADCIRC calculations, 5-7 October 2002 212

Figure 5-7. Current velocity at Mattituck Creek; measurements and ADCIRC calculations, 7-8 October 2002 213

Figure 5-8a. Near-maximum flood-tide velocity, Mattituck Inlet offshore area, 1200 GMT, 7 October 2002 214

Figure 5-8b. Near-maximum ebb-tide velocity, Mattituck Inlet offshore area, 1830 GMT, 7 October 2002 214

Figure 5-8c. Near-maximum flood-tide velocity, Mattituck Inlet ebb shoal area, 1200 GMT, 7 October 2002 215

Figure 5-8d. Near-maximum flood-tide velocity and depth, Mattituck Inlet offshore shoal area, 1200 GMT, 7 October 2002 215

Figure 5-8e. Near-maximum ebb-tide velocity, Mattituck Inlet offshore shoal area, 1830 GMT, 7 October 2002 216

Figure 5-8f. Near-maximum ebb-tide velocity and depth, Mattituck Inlet ebb shoal area, 1830 GMT, 7 October 2002 216

Figure 5-8g. Flood-current eddies and depth, directly west of Mattituck Inlet, 1200 GMT, 7 October 2002 217

Figure 5-8h. Ebb-current eddies and depth, directly east of Mattituck Inlet, 1830 GMT, 7 October 2002 217

Figure 5-9a. Near-maximum flood-tide velocity, Mattituck Inlet, 1200 GMT, 7 October 2002 218

Figure 5-9b. Near-maximum flood-tide velocity and depth, Mattituck Inlet, 1200 GMT, 7 October 2002 219

Figure 5-9c. Near-maximum ebb-tide velocity, Mattituck Inlet, 1830 GMT, 7 October 2002 219

Figure 5-9d. Near-maximum ebb-tide velocity and depth, Mattituck Inlet, 1830 GMT, 7 October 2002 220

Figure 5-10a. Near-maximum flood-tide velocity, Mattituck Inlet flood shoal area, 1200 GMT, 7 October 2002 220

Figure 5-10b. Near-maximum flood-tide velocity and depth, Mattituck Inlet flood shoal area, 1200 GMT, 7 October 2002 221

Figure 5-10c. Near-maximum ebb tide velocity, Mattituck Inlet flood shoal area, 1830 GMT, 7 October 2002 221

Figure 5-10d. Near-maximum ebb-tide velocity and depth, Mattituck Inlet flood shoal area, 1830 GMT, 7 October 2002 222

Figure 5-11a. Near-maximum flood-tide velocity, Mattituck Inlet, pre-dredging grid 223

Figure 5-11b. Near-maximum flood-tide velocity, Mattituck Inlet, post-dredging grid 223

Figure 5-11c. Near-maximum ebb-tide velocity, Mattituck Inlet, pre-dredging grid 224

Figure 5-11d. Near-maximum ebb tide velocity, Mattituck Inlet, post-dredging grid 224

Figure 5-11e. Near-maximum flood-tide velocity and depth, Mattituck Inlet pre-dredging grid 225

Figure 5-11f. Near-maximum flood-tide velocity and depth, Mattituck Inlet post-dredging grid 225

Figure 5-12. Comparative current velocity plot locations 226

Figure 5-13a. Current velocity directly north of Mattituck Inlet east bank flood shoal, pre-dredging and synthetic post-dredging condition (Location A) 226

Figure 5-13b. Current velocity directly north of Mattituck Inlet east bank flood shoal, pre-dredging and synthetic post-dredging condition (Location B) 227

Figure 5-13c. Current velocity directly north of Mattituck Inlet east bank flood shoal, pre-dredging and synthetic post-dredging condition (Location C) 227

Figure 5-14a. Mattituck Inlet natural state, near-maximum offshore spring flood-tide velocity, 1200 on 7 October 2002 229

Figure 5-14b. Mattituck Inlet natural state, near-maximum offshore spring flood-tide velocity, 1200 on 7 October 2002 229

Figure 5-14c. Mattituck Inlet natural state, offshore and inlet spring flood-tide velocity, 1230 on 7 October 2002 230

Figure 5-14d. Mattituck Inlet natural state, offshore spring flood-tide and near-maximum inlet spring flood-tide velocity, 1430 on 7 October 2002 230

Figure 5-14e. Mattituck Inlet natural state, offshore spring ebb-tide and inlet spring flood-tide velocity, 1530 on 7 October 2002 231

Figure 5-14f. Mattituck Inlet natural state, near maximum offshore spring ebb-tide and inlet spring ebb-tide velocity, 1830 on 7 October 2002 231

Figure 5-14g. Mattituck Inlet natural state, offshore spring ebb-tide and inlet near maximum spring ebb-tide velocity, 2100 on 7 October 2002 232

Figure 5-14h. Mattituck Inlet natural state, offshore spring flood-tide and inlet spring ebb-tide velocity, 2200 on 7 October 2002 232

Figure 5-14i. Mattituck Inlet natural state, near maximum offshore spring flood tide and inlet spring ebb-tide velocity, 0030 on 8 October 2002 233

Figure 5-15. Mattituck Inlet assumed (synthetic) natural state and offshore water level and current velocity comparison locations 233

Figure 5-16a. Mattituck Inlet natural state and offshore water level comparison (Locations A and B) 234

Figure 5-16b. Mattituck Inlet natural state and offshore water level comparison (Locations A and C) 234

Figure 5-16c. Mattituck Inlet natural state and offshore water level comparison (Locations A and D) 235

Figure 5-17a. Mattituck Inlet natural state and offshore current velocity comparison (Locations A and B) 235

Figure 5-17b. Mattituck Inlet natural state and offshore current velocity comparison (Locations A and C) 236

Figure 5-17c. Mattituck Inlet natural state and offshore current velocity comparison (Locations A and D) 236

Figure 5-18a. Near-maximum offshore flood-tide velocity, Mattituck Inlet offshore shoal area, 1200 GMT on 7 October 2002 237

Figure 5-18b. Near-maximum offshore flood-tide velocity and depth, Mattituck Inlet offshore shoal area, 1200 GMT on 7 October 238

Figure 5-18c. Near-maximum inlet flood-tide velocity, Mattituck Inlet offshore shoal area, 1430 GMT on 7 October 2002 238

Figure 5-18d. Near-maximum inlet flood-tide velocity and depth, Mattituck Inlet offshore shoal area, 1430 GMT on 7 October 239

Figure 5-18e. Near-maximum offshore ebb-tide velocity, Mattituck Inlet offshore shoal area, 1830 GMT on 7 October 2002 239

Figure 5-18f. Near-maximum offshore ebb-tide velocity and depth, Mattituck Inlet offshore shoal area, 1830 GMT on 7 October 240

Figure 5-18g. Near-maximum inlet ebb-tide velocity, Mattituck Inlet offshore shoal area, 2030 GMT on 7 October 2002 241

Figure 5-18h. Near-maximum inlet ebb-tide velocity and depth, Mattituck Inlet offshore shoal area, 2030 GMT on 7 October 2002 241

Figure 5-19. Current velocity comparison plot locations 242

Figure 5-20a. Current velocity at Mattituck Inlet entrance (Locations A and B) 242

Figure 5-20b. Current velocity between Mattituck Inlet entrance and offshore shoal (Locations C through E) 243

Figure 5-21. DYNLET grid of Goldsmith Inlet, with nodes and extents of nodal cross sections 244

Figure 5-22a. Water-level measurements offshore of Goldsmith Inlet and Node 2 calculations, 20 September - 8 October 2002 246

Figure 5-22b. Water-level measurements offshore of Goldsmith Inlet and Node 2 calculations, 5-8 October 2002 246

Figure 5-22c. Water-level measurements at Goldsmith Pond and DYNLET Node 30 calculations, 20 September - 8 October 2002 247

Figure 5-22d. Water-level measurement offshore of Goldsmith Pond and DYNLET Node 30 calculations, 5-8 October 2002 247

Figure 5-23a. Current velocity measurement and calculated velocities at Nodes 13 and 14, 7-8 October 2002 248

Figure 5-23b. Current velocity measurement and Nodes 13 and 14 calculations, 8 October 2002 248

Figure 5-24a. Water-level measurements offshore of Goldsmith Inlet and DYNLET Nodes 5 and 8 calculations, 5-8 October 2002 250

Figure 5-24b. Water-level measurements offshore of Goldsmith Inlet and DYNLET Nodes 8 and 9 calculations, 5-8 October 2002 251

Figure 5-24c. Water-level measurements offshore of Goldsmith Inlet and DYNLET Nodes 9 and 10 calculations, 5-8 October 2002 251

Figure 5-24d. Water-level measurements offshore of Goldsmith Inlet and DYNLET Nodes 10 and 15 calculations, 5-8 October 2002 252

Figure 5-24e. Water-level measurements offshore of Goldsmith Inlet and DYNLET Nodes 15 and 20 calculations, 5-8 October 2002 252

Figure 5-24f. Water-level measurements offshore of Goldsmith Inlet and DYNLET Nodes 20 and 30 calculations, 5-8 October 2002 253

Figure 5-25a. Discharge at Goldsmith Inlet, DYNLET Nodes 5 and 8 calculations, 5-8 October 2002 253

Figure 5-25b. Discharge at Goldsmith Inlet, DYNLET Nodes 9 and 10 calculations, 5-8 October 2002 254

Figure 5-25c. Discharge at Goldsmith Inlet, DYNLET Nodes 15 and 20 calculations, 5-8 October 2002 254

Figure 5-26a. Current velocity calculations offshore of Goldsmith Pond and DYNLET Nodes 6 and 7 calculations, 5-8 October 2002 255

Figure 5-26b. Current velocity calculations offshore of Goldsmith Inlet and DYNLET Nodes 7 and 8 calculations, 5-8 October 2002 256

Figure 5-26c. Current velocity calculations offshore of Goldsmith Pond and DYNLET Nodes 8 and 9 calculations, 5-8 October 2002 256

Figure 5-26d. Current velocity calculations offshore of Goldsmith Pond and DYNLET Nodes 9 and 10 calculations, 5-8 October 2002 257

Figure 5-26e. Current velocity calculations offshore of Goldsmith Pond and DYNLET Nodes 10 and 11 calculations, 5-8 October 2002 257

Figure 5-26f. Current velocity calculations offshore of Goldsmith Pond and DYNLET Nodes 11 and 13 calculations, 5-8 October 2002 258

Figure 5-26g. Current velocity calculations offshore of Goldsmith Pond and DYNLET Nodes 13 and 16 calculations, 5-8 October 2002 258

Figure 5-26h. Current velocity calculations offshore of Goldsmith Pond and DYNLET Nodes 16 and 17 calculations, 5-8 October 2002 259

Figure 5-26i. Current velocity calculations offshore of Goldsmith Pond and DYNLET Nodes 17 and 21 calculations, 5-8 October 2002 259

Figure 5-26j. Current velocity calculations offshore of Goldsmith Pond and DYNLET Nodes 21 and 22 calculations, 5-8 October 2002 260

Figure 5-26k. Current velocity calculations offshore of Goldsmith Pond and DYNLET Nodes 22 and 30 calculations, 5-8 October 2002 260

Figure 5-27. Maximum calculated flood- and ebb-spring-tide current velocities and channel elevation at Goldsmith Inlet, 7 October 2002 261

Figure 5-28a. Goldsmith Inlet spring flood-tide maximum current velocity, total calculation domain 262

Figure 5-28b. Goldsmith Inlet spring ebb-tide maximum current velocity, total calculation domain 262

Figure 5-28c. Goldsmith Inlet spring flood-tide maximum current velocity, inlet channel 263

Figure 5-28d. Goldsmith Inlet spring ebb-tide maximum current velocity, inlet channel 263

Figure 5-28e. Goldsmith Inlet spring flood-tide and ebb-tide maximum current velocity difference 264

Figure 6-1. Classification of tidal inlet morphology 266

Figure 6-2. Tidal prism-channel area relation, Mattituck Inlet and Atlantic coast dual jettied inlets 273

Figure 6-3. Mattituck Inlet offshore water-level measurements and calculations by CEA model 273

Figure 6-4. Mattituck Creek water-level measurements and calculations by CEA model 274

Figure 6-5. Escoffier curve calculated for Mattituck Inlet, CEA model 275

Figure 6-6. Shoaling at Mattituck Inlet and Mattituck Creek, 6-8 October 2002 277

Figure 6-7. Goldsmith Pond water-level measurements and calculations by CEA model 280

Figure 6-8. Escoffier curve calculated for Goldsmith Inlet, CEA model 281

Figure 6-9. Tidal prism-channel area relations, Goldsmith Inlet, Chesapeake Bay small inlets, and Puget Sound inlets 281

Figure 6-10 Shoaling at Goldsmith Inlet and Goldsmith Pond, 8 October 2002 283

Figure 6-11. Comparison of channel cross section and tidal prism relations 285

List of Tables

Table 2-1. Selected Tide Ranges for Long Island Sound 16

Table 2-2. Average Wind Direction for Long Island Sound 16

Table 2-3. Calculated Significant Wave Height and Period 17

Table 2-4. Mean and Maximum Measured Current Velocities for Long Island Sound 18

Table 2-5. Mattituck Inlet Dredging History 24

Table 2-6. Mattituck Inlet Maintenance History....24

Table 2-7. Summary of Federal Commercial Sand Mining Permits....25

Table 2-8. Mattituck Park District Permit Mining Volume Estimates 1960-1975....25

Table 2-9. Goldsmith Inlet Dredging History....41

Table 3-1. Phi Units and Millimeter Equivalents....69

Table 3-2. Grain-Size Analysis, Mattituck Inlet Offshore Area, Profiles 56 and 57....73

Table 3-3. Grain-Size Analysis, Goldsmith Inlet Offshore Area, Profiles 59 and 60....99

Table 4-1. Estimated Offshore Volume Change, Mattituck Inlet, 1927-2002...114

Table 4-2. Mattituck Inlet Flood Shoal Area 1935-1938....124

Table 4-3. Estimated Mattituck Inlet Flood Shoal Volumes and Areas, 1935-1938....125

Table 4-4. Calculated Versus Measured Dredging Volumes, Mattituck Inlet Channel....156

Table 4-5. Estimated Sediment Accumulation Rates, Mattituck Inlet Federal Navigation Channel....157

Table 4-6. Summary of Morphology Change at Goldsmith Inlet, 1955 to Present....202

Table 5-1. Goldsmith Inlet DYNLET Node Depths....249

Table 6-1. Inlet Bypassing and Channel Cross-Sectional Stability Classification of Inlets....267

Table 6-2. Tidal Prism and Minimum Channel Cross-Sectional Area Relationships....268

Table 6-3. Mattituck Inlet *r* Ratio and Associated Physical Quantities....272

Table 6-4. Channel Equilibrium Area Model Quantities for Mattituck Inlet....274

Table 6-5. Goldsmith Inlet *r* Ratio and Associated Physical Quantities....279

Table 6-6. Channel Equilibrium Area Information for Goldsmith Inlet....279

Table 6-7. Goldsmith Inlet Flood Shoal and Physical Quantities....284

Table 7-1. Mattituck Inlet and Goldsmith Inlet – Morphologic Characteristics....287

Table 7-2. Mattituck Inlet and Goldsmith Inlet, Nearshore Slopes and Sediment Grain Size....287

Table 7-3. Mattituck Inlet and Goldsmith Inlet – Hydrodynamic Characteristics....288

Table 7-4. Mattituck Inlet and Goldsmith Inlet, Summary of Key Engineering Activities....288

Preface

This study of the morphology and dynamics of Mattituck Inlet and Goldsmith Inlet, NY, was conducted at the U.S. Army Engineer Research and Development Center (ERDC), Coastal and Hydraulics Laboratory (CHL), Vicksburg, MS, and the Department of Geography, Hunter College, City University of New York (CUNY). Work was performed as an activity of the Coastal Morphology Modeling and Channel Evolution Work Unit of the Coastal Inlets Research Program (CIRP) administered at CHL under the Navigation Systems Program for Headquarters, U.S. Army Corps of Engineers (HQUSACE). Mr. Barry W. Holliday is HQUSACE lead technical monitor for CIRP. Dr. Sandra K. Knight is Technical Director for the Navigation Systems Program, and Dr. Nicholas C. Kraus, Senior Scientists Group (SSG), CHL, is CIRP Program Manager and Principal Investigator of the Coastal Morphology Modeling and Channel Evolution Work Unit.

CIRP conducts applied research to improve USACE capability to manage federally maintained inlets on all coasts of the United States, covering the Atlantic Ocean, Gulf of Mexico, Pacific Ocean, and Great Lakes, as well as other areas of responsibility of USACE. CIRP objectives are to improve understanding and develop predictive technology for (a) design, maintenance, and operation of inlet navigation projects, in particular, to reduce the cost of maintenance dredging, and (b) preservation of the beaches adjacent to inlets in a systems approach that treats the inlet and beaches as a sediment-sharing system. To achieve these objectives, CIRP is organized in work units that conduct research and development in hydrodynamic, sediment transport, and morphology change modeling; navigation channel performance; sediment bypassing and adjacent beaches; jetty performance; scour at jetties; laboratory and field investigations; and technology transfer.

This report was written by Mr. Michael J. Morgan, graduate student, Hunter College, CUNY, Dr. Kraus, and Ms. Jodi M. McDonald, U.S. Army Engineer District, New York. Ms. McDonald was formerly in the New York District Operations Division (OD), and is presently in the Plan Formulation Branch, Planning Division. The September and October 2002 data collection was performed under contract with Offshore and Coastal Technologies, Inc. (OCTI), Chadds Ford, PA. Mr. William G. Grosskopf, OCTI, led the data-collection effort and provided additional information in support of this study. Dr. Mark R. Byrnes, Applied Coastal Research and Science, Inc., supplied and provided information on various geospatial data sets and related metadata. Geographic Information System support was provided by Ms. Mary Claire Allison, Coastal Engineering Branch, CHL, and assistance in hydrodynamic modeling by Mr. Mitchell E. Brown, SSG. Dr. Brian K. Batten, Coastal Engineering Branch,

CHL, provided valuable information and discussion at the final stage of this study. Logistical support at Hunter College was provided by Dr. Jeffrey Osleeb, executive officer, Ph.D. Program in Earth and Environmental Sciences, CUNY. Mr. John F. Tavolaro, Acting Chief, OD, New York District, and Ms. Lynn M. Bocamazo, Engineering Division, New York District, provided bathymetric survey data and engineering and coastal processes information for Mattituck Inlet. Mr. James Richter, Town Engineer, Town of Southold, NY, provided information on dredging and coastal processes at Goldsmith Inlet. Messrs. Barry Pendergrass, New York State Department of State, Division of Coastal Resources, and Richard Tuers, New York State Department of Environmental Conservation, furnished copies of reports and aerial photographs. Dr. DeWitt Davis, Suffolk County Department of Planning organized a review meeting for the working draft of this report that resulted in many valuable suggestions and corrections by local and state government officials. The meeting was attended by: Dr. Davis, Mr. Thomas Isles, Ms. Lauretta Fischer, and Mr. Ronald Verbarg of the Suffolk County Department of Planning; Mr. William Shannon and Mr. Thomas Rogers of the Suffolk County Department of Public Works; Dr. Henry Bokuniewicz of the Marine Sciences Research Center at the State University of New York, Stony Brook; Mr. Jay Tanski of New York Sea Grant; Messrs. George Hamarth and Richard Tuers of the New York State Department of Environmental Protection; and Mr. Barry Pendergrass of the New York State Department of State.

Work at CHL was performed under the general administrative supervision of Mr. Thomas W. Richardson, Director, and Dr. William D. Martin, Deputy Director, respectively, CHL. Final report formatting was completed by Ms. J. Holley Messing, Coastal Engineering Branch, CHL.

At the time of publication of this report, Dr. James R. Houston was Director of ERDC, and COL James R. Rowan, EN, was Commander and Executive Director.

Conversion Factors: Non-SI to SI Units of Measurement

Non-SI units of measurement appearing in this report can be converted to SI units as follows:

Multiply	By	To Obtain
cubic yards	0.7645549	cubic meters
feet	0.3048	meters
miles (U.S. statute)	1.609347	kilometers
square feet	0.09290304	square meters
square yards	0.8361274	square meters
yards	0.9144	meters

1 Introduction

Coastal inlets are narrow waterways that connect a bay, lagoon, or similar water body with a larger water body that generates motion between them, such as forced by the tide in the oceans and by seiching in the Great Lakes. Inlets serve commercial, military, and recreational functions. They are also central to the health of marine and coastal terrestrial organisms by allowing water exchange and by being a conduit for movement of organisms and nutrients between the sea and estuaries or bays. Consequently, inlets have been the subject of considerable research in coastal engineering and science.

In the present study, motivation for improved understanding of inlet processes lies in reducing the cost of maintaining navigable channels and more reliably predicting the functioning of proposed inlet modifications. Related concerns are the influence of an inlet or planned inlet modification on the adjacent beaches and the associated ecosystem. The overall aim of an inlet maintenance program is to establish and sustain a dynamic state of equilibrium for the inlet morphology with minimal adjustment required of the adjacent beaches and minimal change to the ebb- and flood-tidal shoals.

Background

The physical environment of a tidal inlet is determined by the forcing of the periodically reversing tidal current, and by waves, wave-induced currents, wind-induced currents, and storms. The interaction includes the type of sediment (grain size) and sediment transport, and the morphologic response of the inlet to the hydrodynamic forcing, which then feed back to the hydrodynamics. Two types of inlet stability are commonly recognized, one referring to locational stability and orientation of the inlet channel or gorge, and the other to stability of the inlet channel cross-sectional area. The stability of an inlet depends on the balance between two physical processes, the wave-induced longshore current that transports sediment toward the inlet, creating a tendency towards closure and migration, and the tidal flow within the inlet that tends to scour the bottom and banks of the channel, removing sediment from the inlet throat (Johnson 1919; Bruun and Gerritsen 1959).

Most field and theoretical studies of inlet stability have concerned large tidal inlets with sand-sized sediment, as commonly found on all coasts of the United States. Such inlets are prevalent and have great economic and environmental functions. However, coastal inlets are also found on rocky coasts, and small inlets that tend to close are of environmental concern (Goodwin 1996). Although inlet channel cross-sectional area has been investigated (e.g., Le Conte 1905; O'Brien 1931, 1969; Jarrett 1976; Byrne et al. 1980; Moody 1988; Hume and Merdendorf (1990); Kraus 1998; Hughes 2002), the role of sediment size in the stability of inlets has received almost no investigation (Simpson

1976). The present study attempts to contribute to understanding of small inlets and the role of grain size by examining two relatively small inlets on a mixed sediment coast that includes gravel.

Inlets along the south shore of Long Island, NY, have received substantial study owing to their easy access and proximity to the New York metropolitan area. On the south shore, there are presently six federally maintained permanent inlets (from west to east: Rockaway Inlet, East Rockaway Inlet, Jones Inlet, Fire Island Inlet, Moriches Inlet, and Shinnecock Inlet), and they serve long and broad bays surrounded by towns and commercial entities. Of the large literature on Long Island south shore inlets, representative examples are:

a. Geomorphology, sedimentology, and sediment budgets: Taney (1961), Kumar and Sanders (1974), Leatherman and Allen (1985), Leatherman (1989), Kana (1995), Morang et al. (1999), Schwaab et al. (1999).

b. Coastal and inlet processes: Panuzio (1968), Tanski et al. (1990), Militello et al. (2000).

c. Site-specific inlet studies: Gofseyeff (1952), Czerniak (1977), Schmeltz et al. (1982), Militello and Kraus (2001), Kraus et al. (2003).

Inlets along the south shore of Long Island have been dynamic, both in location and channel cross section, as documented in many of the these references.

In contrast to south shore inlets of Long Island, inlets on the north shore have received little study. Many of these inlets are small and serve small and isolated water bodies. Significantly, north shore inlets appear to be more stable in location than the south shore inlets.[1] Why are these inlets more stable and, apparently, longer lived, as compared to the south shore inlets?

Although glacial processes dominate the surficial sediments and geologic structure of Long Island, the sediment along the south shore consists predominantly of fine to medium sand, with a median grain size of 0.3 mm being typical. In contrast to the sandy beaches backed by dunes found along the south shore of Long Island, high bluffs and a wide range in grain size, with gravel and cobble common, characterize its north shore. The tide range along the north shore is about double that of the south shore. Longshore sediment transport is an order of magnitude less on the north shore as compared to the south shore, and the waves along the north shore are steeper. The inner shelf on the north shore is steeper than along the south shore.

---

[1] The World Wide Web site http://www.ilovelbny.com/LongBeachMaps.html displays several historic maps of East Rockaway Inlet, Jones Inlet, and several ephemeral inlets on the western end of the south shore of Long Island. These maps clearly indicate inlet opening, closing, and significant migration of the westernmost inlets from the first map, dated 1797. Sometimes the easternmost inlets are absent (closed). The names of the inlets may be different, and inlets with other names and that no longer exist can also be seen.

It appears that much can be learned about inlet stability through study of the inlets of the north shore of Long Island because of the substantial difference in coastal environment as compared to the south shore and to most inlets on sandy coasts in general.

Study Site

The inlets investigated in this study, Mattituck Inlet and Goldsmith Inlet, are located 5.2 miles apart on the eastern end of the north shore of Long Island, NY. Inlets of varying size are found along the south and north shores, as well as in the bays of Long Island. Inlets on the north shore of Long Island have received little study, with the exception of Stony Brook Harbor (Cooke 1985; Park 1985; Zarillo and Park 1987). The inlets of Long Island's north shore vary greatly in size and configuration, from large ones, such as Port Jefferson Harbor and Oyster Bay, to small inlets such as Mattituck Inlet and Goldsmith Inlet (Figure 1-1). Port Jefferson Harbor and the entrance to Oyster Bay are of comparable scale to the more extensively studied inlets of the south shore, but their bay systems are much smaller.

Mattituck Inlet and Goldsmith Inlet are connected to Long Island Sound. Long Island Sound is a semienclosed tide-dominated water body that communicates with the Atlantic Ocean at both its eastern and western ends, via Block Island Sound and the East River (and ultimately, New York Harbor) respectively. The relatively large mean tide (5.2 ft)[1] and spring tide range (6.0 ft) along the Eastern Long Island Sound is one controlling factor for the stability of both inlets (Figures 1-2 and 1-3).

Mattituck Inlet is a federally maintained channel and connects Long Island Sound to Mattituck Creek (Figure 1-4). Mattituck Inlet is the only major harbor on the north fork of Long Island and is a commercial and recreational boating center. Two jetties stabilize this inlet, and the navigation channel is maintained to a depth of 7 ft mean low water (mlw) with a 2-ft allowable overdraft. Overdraft refers to the contractually allowable depth of dredging greater than the authorized depth to account for equipment limitations and survey accuracy. The inlet was sometimes dredged from the mid 1920s to mid 1970s for local commercial mineral operations (sand and gravel mining). The tidal prism, the volume of water entering or exiting an inlet during a flood or ebb tide, is a primary control on inlet stability and channel cross-sectional area. The present study calculates a tidal prism of 4.32×10^7 cu ft at Mattituck Inlet based on measured bay area and half the spring tide range.

---

[1] Engineering activities such as surveying and dredging, as well as historic documentation of tide ranges associated with this study are reported in their original units, U.S. Customary (non-SI) units. As an aid to those ongoing activities and to maintain continuity with previous publications employing non-SI units, those units are preserved in the present context. Oceanographic quantities are expressed in SI units. A table for converting non-SI to SI units is given on page xxiv.

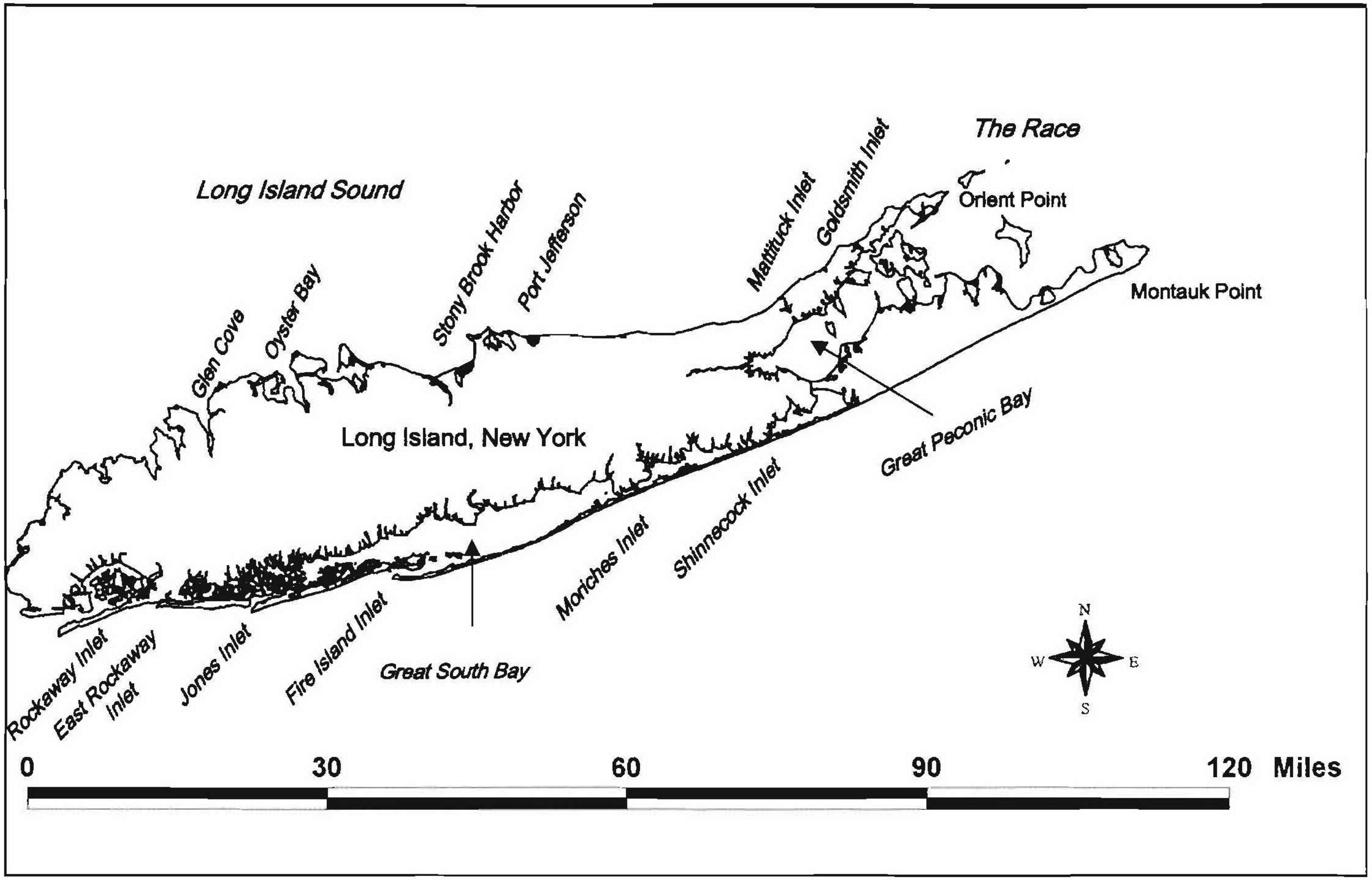

Figure 1-1. Long Island, NY, and selected inlets and harbors

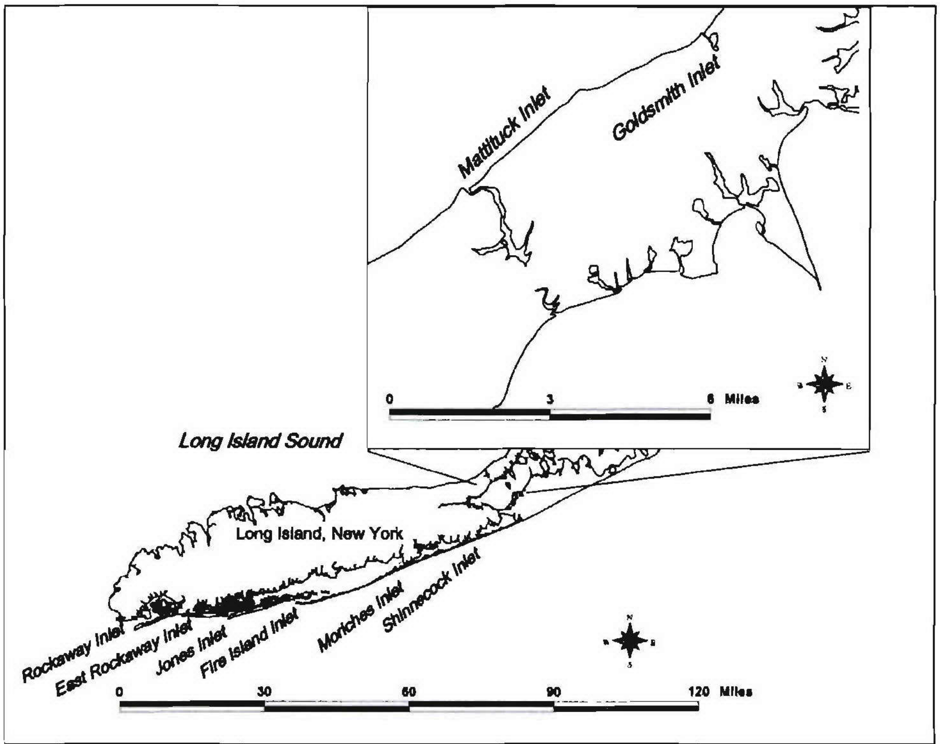

Figure 1-2. Long Island, NY, with study area inset

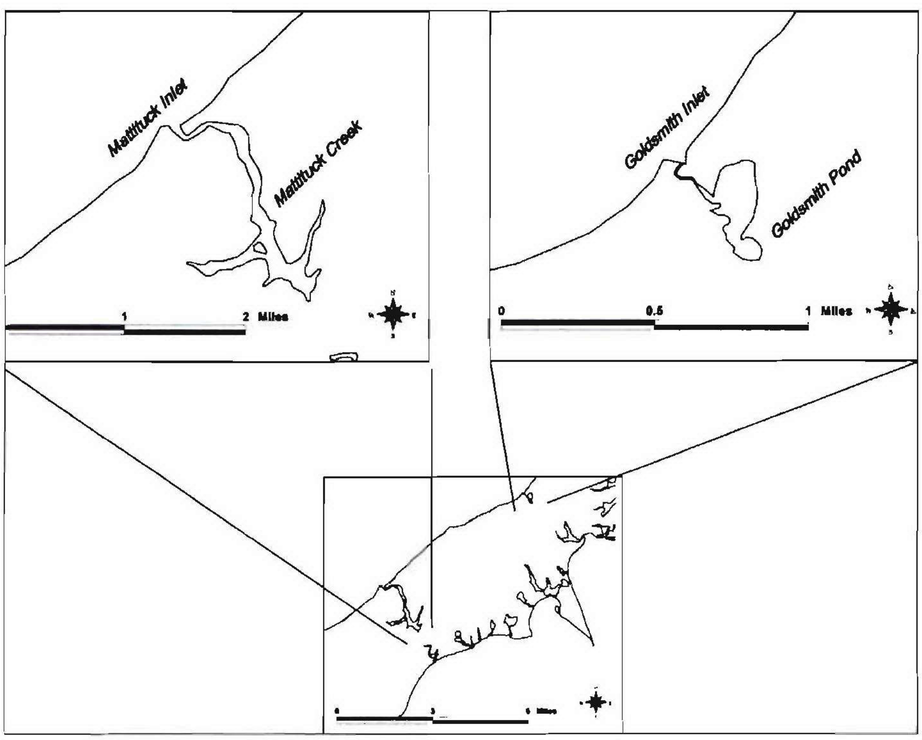

Figure 1-3. Study area with Mattituck Inlet and Goldsmith Inlet insets

Figure 1-4. Mattituck Inlet and Mattituck Creek, 16 April 2003

Goldsmith Inlet (Figure 1-5) is much smaller than Mattituck Inlet and is maintained as needed by the Town of Southold (and, in the past, by Suffolk County). It has been occasionally dredged as a source of sand and gravel for upland activities and to provide sediment for renourishment of Kenneys Road Beach, located east and downdrift of the inlet. In recent times, Goldsmith Inlet has been dredged on an emergency basis, when the inlet has experienced closure, with the dredged material placed on the downdrift (eastern) adjacent beach. Goldsmith Inlet received an emergency dredging in the winter of 2001 and in March 2004.

Goldsmith Inlet connects Long Island Sound to Goldsmith Pond. The inlet has a nonfunctional jetty on its west side and is non-navigable, with typical depths ranging from 0.5 to 3 ft NAVD88. The present study calculated a tidal prism of 3.04×10^6 cu ft at Goldsmith Inlet, 14 times smaller than that of Mattituck Inlet based on pond area and measured spring tide range.

Previous Studies

A small number of coastal processes studies and shoreline change analysis reports are available for the eastern end of the north shore of Long Island. Few studies have been made of north shore inlets, with the exception of Stony Brook Harbor (Cooke 1985; Park 1985; Zarillo and Park 1987), which lies about 37.5 miles west of the Mattituck Inlet. The literature pertaining to this area is reviewed here.

Figure 1-5. Goldsmith Inlet and Goldsmith Pond, 16 April 2003

The U.S. Army Engineer District, New York, quantified beach recession and accretion and storm-related damage for the north shore of Long Island in Suffolk County in 1969. The New York District issued an update of this report in 1996. This report notes the high rate of bluff erosion for the areas directly adjacent to Mattituck Inlet and the area east of Goldsmith Inlet as a primary issue. The New York District (1969) report estimates a recession rate of approximately 1 ft/year for these areas and classified erosion as moderate. Erosion of the area directly east of Mattituck Inlet was identified as a concern. The report also identified beach erosion as the primary concern for the areas west of Goldsmith Inlet and classified erosion for the Kenneys Road Beach area as severe.

In 1987, The New York State Department of Environmental Conservation (NYSDEC) conducted a coastal erosion reconnaissance study of the shoreline from Duck Pond Point (approximately 16,000 ft west of Goldsmith Inlet) to Horton Point (approximately 16,000 ft east of Goldsmith Inlet) (Figure 1-6). The NYSDEC report reaches similar conclusions as the New York District (1969) report and notes the influence of Goldsmith jetty and a series of privately installed groins on the shoreline, where accretion on the west side and erosion on the east side is observed.

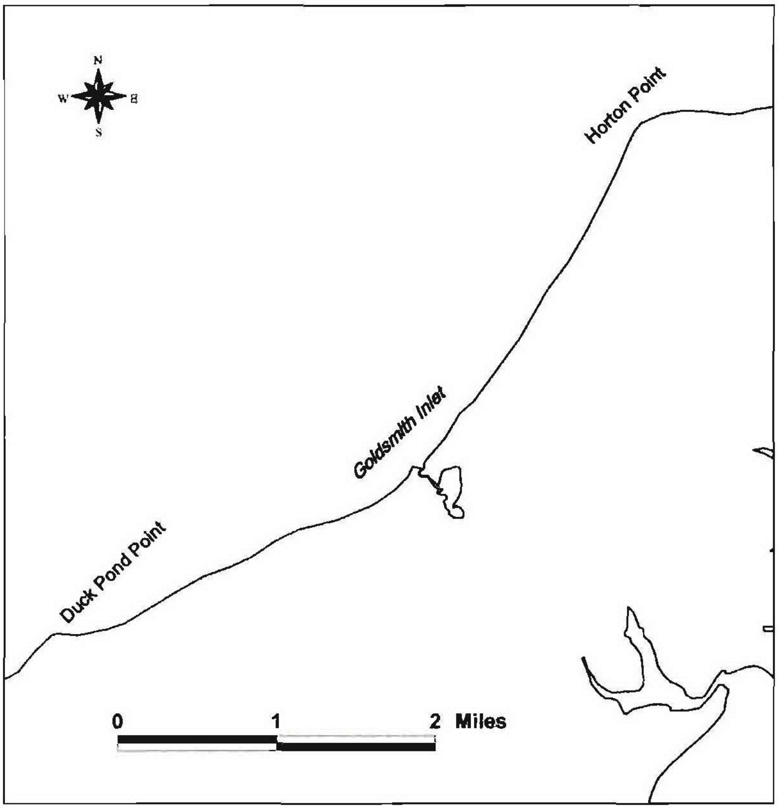

Figure 1-6. Shoreline from Duck Pond Point to Horton Point

Davies et al. (1971) and Davies (1972) studied erosion of the north shore of Long Island, and Offshore and Coastal Technologies, Inc. (OCTI 1998) surveyed the shoreline and beach profile from the Southold town line to Horton Point. Fields et al. (1999) conducted a historical shoreline change analysis for the same area. In these studies, the observed rates of erosion were attributed to the lack of sediment supply, storms, and the impoundment of sediment by jetties and other coastal structures. Omholt (1974) conducted a study of the effects of small groins on the shorelines of the north shore of Long Island. Schubel (1976) studied the consequence of commercial mining operations, conducted on the beach directly west of Mattituck Inlet. Alpine Ocean Seismic Survey, Inc. (1998) conducted a geophysical investigation of the offshore area from Duck Pon Point to Horton Point in 1998. Greenman-Pedersen Associates, P.C. (1981) studied the response of the adjacent east shoreline to the Goldsmith Inlet jetty through analysis of historic aerial photography. The report concluded that the Goldsmith Inlet jetty and a private groin located 3,400 ft east of the jetty were responsible for significant downdrift erosion from 1964 to 1978.

An Erosion Management Plan for the Town of Southold was prepared in 1995 (Allee King Rosen and Fleming, Inc. et al. 1995). In 1996, the Town of Southold conducted a workshop examining erosion between Duck Pond Point and Horton Point. One result of this workshop was a set of recommendations by Leatherman (1996)[1] that included

[1] Leatherman, S. P. (1996). "Workshop observations and recommendatons," in report of the workshop examining erosion of the coastal barrier landform between Duck Pond Point and Horton, Town of Southold,

shortening of the Goldsmith Inlet jetty to half its length and installation of groins at selected locations downdrift of the inlet. Although the stability of Goldsmith Inlet was not explicitly addressed, its possible closure and the resulting environmental and water quality problems were considered in the recommendations.

Contemporaneously with the present study, in support of the New York District, Batten and Kraus (2005) performed a Section 111 analysis for the downdrift (east) shore at Mattituck Inlet. Section 111 of the River and Harbor Act of 1968 authorizes studies for the prevention or mitigation of shore damages attributable to Federal navigation works. Batten and Kraus (2005) analyzed shoreline change both updrift and downdrift of Mattituck Inlet in a regional context, including development of a sediment budget for the coastal area adjacent to the inlet.

Motivation

Inlet properties of bay size, tide range, wave height, sediment size, and location on a wave-sheltered or unsheltered coast have been found to influence the stability relation between inlet tidal prism and cross-sectional area. These and other processes, such as potential geologic controls and wave steepness, can be investigated at Mattituck Inlet and Goldsmith Inlet. The apparent longevity and locational stability of Mattituck Inlet and Goldsmith Inlet, as compared to much larger inlets on the south shore of Long Island warrants attention. Why should such relatively small inlets be so stable?

Small inlets offer a convenient opportunity to investigate inlet morphodynamics because of their limited size and greater accessibility. Byrne et al. (1980) found that the relationship between changes in inlet cross-sectional area and flow regime differed for small inlets. Through the analysis of width-to-depth ratios found at both small and large inlets, they concluded that small inlets must be more hydraulically efficient than large inlets to maintain stability. Goldsmith Inlet is similar in size to those studied by Byrne et al. (1980), whereas Mattituck Inlet is larger, but yet small as compared to the 108 inlets analyzed by Jarrett (1976) in developing predictive relationships for inlet channel cross-sectional area.

The close proximity of these inlets, one a federally maintained inlet (Mattituck Inlet), and the other a seminatural inlet (Goldsmith Inlet), provides an opportunity to examine the dynamics and stability of small inlets in an engineered condition and an almost natural condition, respectively. Although they share the same wave climate and the same tidal forcing, the differences in tidal prism and number of jetties benefit a comparative study of inlet stability. Mattituck Inlet is dredged for navigation, is stabilized by two jetties, and has a channel composed predominantly of sand and gravel-sized sediment. Goldsmith Inlet is dredged infrequently, is shallow and non-navigable, has one jetty that is fully impounded, and is substantially armored by gravel (Figure 1-7).

NY, Appendix II-A1, unpublished report.

Study Objective

The stability in location and in cross-sectional channel area of coastal inlets is of central interest for the operation and maintenance of navigation channels, as well as for understanding the interaction of inlets and beaches. The control of coarse sediment (gravel) on inlet morphology and hydrodynamics is also of scientific and engineering interest. In an effort to improve understanding of tidal inlet stability, this study was undertaken at two Long Island, NY, north shore inlets, Mattituck Inlet and Goldsmith Inlet.

The study covers review of the literature, compilation and analysis of historic New York District survey records, site visits, short-term measurements of water level and current, bathymetric surveys, sediment sampling, bathymetry change and aerial photography analysis, mathematical analysis, and numerical modeling. In support of this study, a bathymetric survey of both inlets was made in October 2002, together with limited measurements of the water level and current. The acquired process data, together with previous measurements, modeling, and morphologic analysis, allow examination of the stability of the subject inlets.

Figure 1-7. Goldsmith Inlet with view northeast into Long Island Sound, showing substantial gravel and cobble, 22 March 2003

The objective of this study is to improve understanding of the factors that contribute to the stability of channel cross-sectional area and location and orientation for small inlets that may in part be controlled by the presence of coarse sediment. The morphology and morphology change at Mattituck Inlet and Goldsmith Inlet are explored through comparisons of channel cross sections and beach profiles and by generating topographic difference maps for Mattituck Inlet. Morphologic analysis identifies areas of erosion and deposition, while yielding information on sediment bypassing and ebb and flood shoal formation. Waves and currents combine to form the longshore current, the predominant mechanism of coastal sediment transport. Numerical modeling of the tidal

hydrodynamics for each inlet serves to identify the mechanisms that contribute to the observed morphologic formations.

2 Study Area and Physical Setting

This chapter describes the study area, the physical setting of Mattituck Inlet and Goldsmith Inlet, and the regional setting of the north shore of Long Island, the Long Island Sound. The configuration of Long Island Sound exerts significant control on the tide, waves, and current that act upon the two inlets. Aspects of the geomorphology of the north shore of Long Island are also reviewed as they pertain to the sediment source for these inlets. Discussion of the history and setting of each inlet follows to understand the regional, economic, and environmental significance of the inlets.

Regional Setting – Long Island Sound

Mattituck Inlet and Goldsmith Inlet connect to the Long Island Sound, a semienclosed water body open to the Atlantic Ocean at both ends (Figure 2-1). Long Island Sound is approximately 110 miles long and 20 miles wide at its center. It narrows to about 10 miles at its eastern extreme, where it meets the Atlantic Ocean through Block Island Sound, and to less than 1 mile at its western extreme where it meets the East River, New York Harbor, and ultimately the Atlantic Ocean. Long Island Sound has a surface area of 1,268 square miles (Koppelman et al. 1976) and is oriented along a southwest-northeast axis, as is the depression that runs along its center. The depth of Long Island Sound along this depression is 110-130 ft, and the mean depth of the sound is 60 ft. The maximum depth of near 300 ft is found in an area known as The Race, a constricted channel that connects Long Island Sound to Block Island Sound.

Geomorphic environment

Long Island Sound lies on the northern edge of the Atlantic Coastal Plain and is one of several basins that occupy the New England part of the Atlantic Coastal Plains province. Long Island Sound can be characterized as five separate basins separated by shoals of varying relief. Mattituck Inlet and Goldsmith Inlet connect to the sound in an area bounded by the New Haven shoal and Six Mile Reef (Williams 1981). The southern boundary of Long Island Sound, the north shore of Long Island is classified as a glacial deposition coast (Shepard 1963) and is composed primarily of glacial till deposits. These deposits originated from a group of terminal moraines created by the continental glaciers that advanced upon the area during the Wisconsin stage of the Pleistocene Epoch, 70,000 to 10,000 years ago.

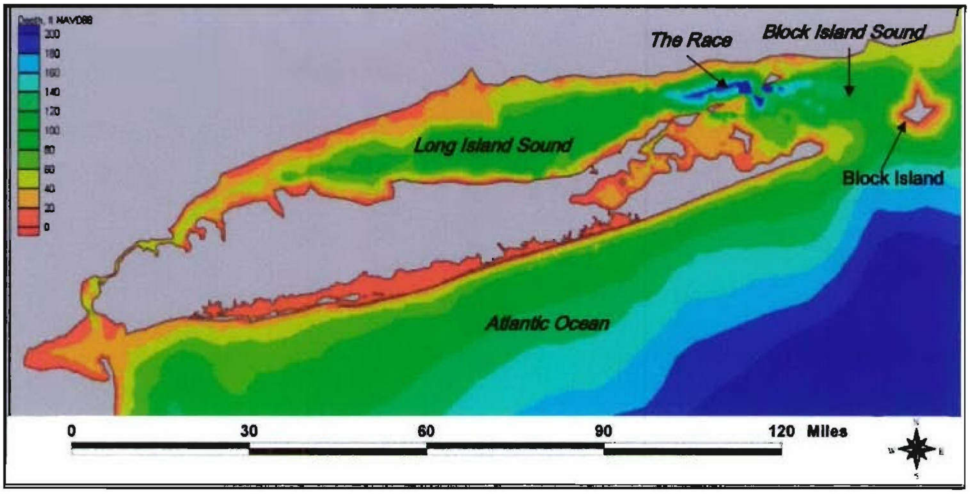

Figure 2-1. Long Island Sound region bathymetry

The south shore and north shore of Long Island differ significantly. The south shore is an outwash plain characterized by sand-sized sediments and a gentle slope. The gentle slope found on the south shore is a controlling factor in the observed large bay sizes and the presence of barrier islands. In contrast, the proximity of the north shore to the Harbor Hill moraine is a controlling factor in the coarser sediment, steeper slope, and absence of barrier islands found here. The Harbor Hill moraine begins in the west end of Long Island and extends in a northeasterly direction to form the northern fork of Long Island with its terminus at Orient Point. A second terminal moraine, the Ronkonkoma Moraine, begins in the western portion of Long Island and extends to the southeast (Figure 2-2).

The western extent of the north shore of Long Island is characterized by a series of narrow bays that extends south to the Harbor Hill Moraine. These bays are believed to have been formed by protruding lobes of ice attached to the Wisconsin stage glacier that advanced upon the region. The ice lobes carved the valleys that form the bays and thrust the material southward, forming the steep bluffs found there. A secondary factor may have been the action of "spring sapping," where underground springs loosen the sand found in these valleys, allowing for rapid erosion (Fuller 1914).

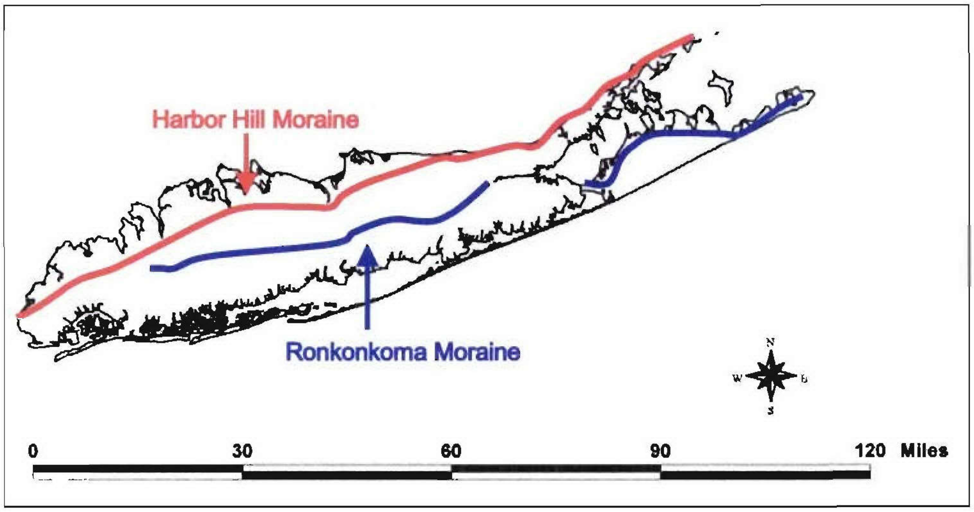

Figure 2-2. Harbor Hill and Ronkonkoma Moraine locations (approximate)

The eastern portion, where Mattituck Inlet and Goldsmith Inlet are located, largely comprises steep bluffs separated by headland areas. The remnant headlands (Herod, Roanoke, Jacobs, Duck Pond, and Horton Points) are composed of clay and till, and are more resistant to erosion than adjacent areas (New York District 1969). The bluffs are characterized by loosely consolidated material, as a mixture of moraine material and glacial outwash, and they are often directly exposed to waves, thus acting as a sediment source for longshore transport. McClimans (1970)[1] studied bluff erosion along the Suffolk County portion of the north shore of Long Island and estimated annual recession rates of 0.5 m/year (1.64 ft/year) at Horton Point, and 0.6 m/year (1.97 ft/year) 0.7 miles west of Orient Point. Bokuniewicz and Tanski (1983) studied erosion of 50 miles of coastal bluffs along the eastern end of the north shore of Long Island and concluded that bluff erosion rates were large enough to satisfy the longshore sediment transport potential along the eastern portion of the north shore of Long Island. Batten and Kraus (2005) discuss loss of finer sediments from the beach to the offshore because of the predominant steep wind waves in the Long Island Sound.

Mattituck Inlet is bounded by two headlands, Jacobs Point to the west and Duck Pond Point to the east. Goldsmith Inlet is bounded by Duck Pond Point to the west and by Horton Point to the east (Figure 2-3). Geological evidence suggests that Goldsmith Pond was once an embayment that was filled by sediment supplied from these headlands. As sediment deposition narrows the entrance of an embayment, the tidal current increases in velocity and scouring efficiency. An inlet achieves equilibrium if the deposition caused by longshore sediment transport is balanced by the erosion caused by tidal current scour (Johnson 1919). Goldsmith Inlet appears to be an inlet in such a near-equilibrium state.

[1] McClimans, R. J. (1970). "Suffolk County bluff and shore recession," U.S. Department of Agriculture, Soil Conservation Service, Riverhead, NY, unpublished manuscript.

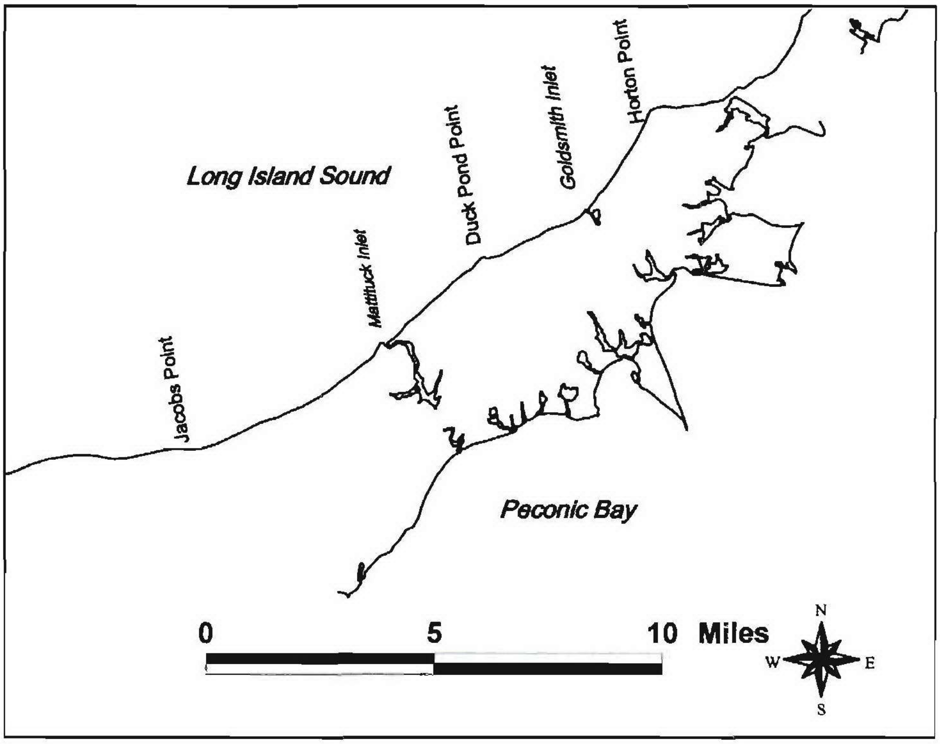

Figure 2-3. Study area headlands

Oceanographic environment

Water movement within Long Island Sound is controlled by the tide and is influenced by wind waves, wave-induced current, wind-induced current, and storms. The geometry and length of Long Island Sound create a wide variation of tidal range and tidal current speed.

Tide and storm surge. The tide within Long Island Sound is predominantly semidiurnal. The length and depth of the water body is such that it is approximately a quarter-wave resonator for the semidiurnal tide, resulting in mean tide amplitudes that increase by a factor of three from Block Island Sound to the western end of the sound. Table 2-1 summarizes mean and spring tide ranges for various locations throughout Long Island Sound. Tide duration in Long Island Sound is asymmetric, owing to frictional decay, with ebb tide lasting 15 min longer than flood tide at its eastern end and 30 min longer at its western end (Signell et al. 2000).

Storm surge is the difference between the observed water level and that predicted at a given time and location in the absence of a storm, and it is a major agent of coastal erosion and of inlet and shoreline morphology change. The hurricane of 21 September 1938 produced the water level of record (13.3 ft above mean sea level (msl)) within Long Island Sound, and the hurricane of 31 August 1954 produced the water level of record (9.45 ft above msl) for the Suffolk County portion of the north shore of Long Island. Hurricanes and tropical cyclones are relatively rare in the Long Island region, however, and are usually oriented to cause water buildup along southern facing coasts, such as the south shore of Long Island and the southern coast of Connecticut.

Table 2-1
Selected Tide Ranges for Long Island Sound[1]

Location	Mean Tidal Range (ft)	Spring Tidal Range (ft)
Plum Island (Block Island Sound)	2.6	3.1
Mattituck Inlet (Eastern third)	5.2	6.2
Port Jefferson (Central third)	6.6	7.6
Hempstead Harbor (Western third)	7.3	8.6

[1] Information obtained from National Oceanic and Atmospheric Administration (NOAA) National Ocean Service (NOS), Web site: http://tidesandcurrents.noaa.gov/tides03/tab2ec2a.html.

Extratropical cyclones, colloquially referred to as "northeasters," are common to this region and are often oriented to produce water buildup along the north shore of Long Island (Davies et al. 1971; Davies 1972). New York District (1969) states that 65 moderate to severe northeasters struck the New York coastal area in the 100 years previous to 1965. Northeasters of lesser intensity occur with much greater frequency and can also alter inlet morphology. Northeasters are slow moving and can remain in a region for a number of days, and they can also arrive in succession with short intervals, days to weeks, in-between.

A severe storm can alter coastal morphology equivalent to months or years of normal or typical-condition hydrodynamic forcing. The consequences of storm surge and wave setup on the north shore of Long Island are not explicitly analyzed in this study.

Waves. Wave direction corresponds with wind direction for the limited-fetch water body of Long Island Sound, and peak wave height corresponds with wind speed. Table 2-2 summarizes the average wind direction taken from wind data at LaGuardia Airport, located on the western end of the north shore of Long Island. These data can be considered to be qualitatively representative of wind conditions for the study area.

Table 2-2
Average Wind Direction for Long Island Sound (Town of Southold 2003)

Direction	Percent Occurrence
Northeast	20
Southeast	17
Northwest	30
Southwest	33

Because Long Island Sound is a semienclosed basin, fetch and wind duration are limited. Wind over Long Island Sound typically originates from the south during the summer and from the north during the winter. Wind speed and storm duration tend to be greater during the winter months. Typical summer and winter winds originate from the

western quadrant, producing longshore current and sediment transport directed toward the east for the central and eastern portions of Long Island. For the study sites, fetch length for waves originating from the west is considerably larger than the fetch length from the east. Fetch length for the study area is approximately 50 miles from the northwest and 20 miles from the northeast (New York District 1969). Larger fetch length will yield comparatively larger wave heights from the west under similar conditions, further augmenting the dominant direction of sediment transport.

A wave analysis performed by New York District (1999)[1] calculated significant wave heights and wave periods for various long-term return periods for waves approaching Mattituck Inlet (Table 2-3). The calculated wave heights listed are for extreme weather events. Calculated wave directions were from 260 to 280 deg at 10-deg intervals. Wave height and period for the 10- through 200-year storms have a limited spread because of the restricted fetch of Long Island Sound.

Table 2-3
Calculated Significant Wave Height and Period (New York District 1999[1])

Return Period (year)	Significant Wave Height (ft)	Period (sec)
10	12.3	6.9
25	13.7	7.3
50	15	7.6
100	16.4	7.9
200	17.4	8.2

Tidal currents. During flood tide, water enters Long Island Sound from the Atlantic Ocean. Current strength is greatest during this time and greatest at The Race, with a consistent westward decrease in velocity. Circulation within Long Island Sound is counterclockwise, with flood current entering to the north and preceding west, and ebb current running from west to east along the north shore of Long Island (U.S. Environmental Protection Agency (USEPA) and USACE (2001)). The tidal current has been observed to decrease consistently with water depth throughout the sound. Current speed for Long Island Sound is asymmetric. Western and Central Long Island Sound are flood-dominant, where flood-tide speeds are about 1-3 cm/sec greater than ebb speeds. In eastern Long Island Sound, ebb tide speeds were found to be about 1-5 cm/sec greater than flood speeds. Table 2-4 summarizes mean and maximum currents from the study by the USEPA and USACE (2001). Mean current velocities were calculated by averaging the mean velocities of a number of current meters that were deployed throughout the region.

[1] U.S. Army Engineer District, New York. (1999). "Mattituck Inlet, New York," unpublished memorandum.

Table 2-4
Mean and Maximum Measured Tidal Current Velocities for Long Island Sound (USEPA and USACE 2001)

Location	Mean Velocity (cm/sec)	Maximum Velocity (cm/sec)
Block Island Sound	37.4	156.9
Eastern third	38.8	136.2
Central third	28.1	91.5
Western third	23.6	110.7

Longshore sediment transport

The ebb tidal current runs from west to east along the Long Island north shore (USEPA and USACE 2001). Wind-generated surface waves and wave-induced current combine to produce a longshore current and associated longshore sediment transport. In Long Island Sound, the predominant wind direction is from the northwest. Wind from this direction dominates in the winter, when wind speed tends to be greatest and duration tends to be longest. As a result of their longer fetch from the west as compared to the east, waves approaching Mattituck Inlet and Goldsmith Inlet from the west will, on average, tend to be larger and have longer duration than waves originating from the east. Based on considerations of waves and currents, predominant direction of longshore sediment transport for this study region is, therefore, from west to east. Storms can also produce offshore transport of sediment from the headlands and cliffs during times of high tide combined with storm surge. Bokuniewicz and Tanski (1983) conducted visual observations of wave height, period, and angle of attack for the eastern portion of the north shore of Long Island for the period 7-31 May 1981. They concluded that the transport of sediment was consistently towards the east with the exception of the area directly on the west side of Mattituck Inlet, where a local reversal in transport, to the west, was observed.

Only a few estimates of the annual east-directed longshore sediment transport rate are available for the vicinity of the study sites. Omholt (1974) calculated a longshore transport potential of 96,000 cu yd/year and noted that the longshore current is not carrying its full capacity of sediment. Leatherman et al. (1997) arrived at an east-directed transport rate of 25,000 cu yd/year. This estimate was inferred through the analysis of volume change of the accretion fillet west of the Goldsmith jetty as seen in historic aerial photographs. Fields et al. (1999) estimated an east-directed net annual transport rate of 8,000 cu yd/year at Goldsmith Inlet by the same method. They note that this estimate does not include sediment that may have moved through or around the jetty, and should be considered a minimum net longshore transport rate to the east. This figure is, therefore, an estimate of the annual accumulation rate of the fillet west of the Goldsmith Inlet jetty. Fields et al. (1999) described the maximum potential error for their estimate as +/- 35 percent (for a maximum fillet accumulation rate of 10,800 cu/yd year).

Bokuniewicz and Tanski (1983) discuss two estimates from other references that were based on wave hindcasts. Of these, TetraTech (1979) calculated an annual net longshore transport rate directed to the east of 9×10^7 kg/year. Here, this estimate is converted to volume by the equation:

$$V = \frac{M}{\rho_s(1-a)} \tag{6-7}$$

where

V = sediment volume

M = sediment mass

ρ_s = specific density of the sediment

a = sediment porosity

For this calculation, the porosity was taken to be 0.4 and the specific density 2,650 kg/cu m, corresponding to quartz sand. The resultant value of 57,000 cu m/year converts to 73,000 cu yd/year and must be considered doubtful because it is inconsistent with estimates of Leatherman et al. (1997) and Fields et al. (1999), as well as with channel maintenance volumes, which are much less at Mattituck Inlet. Such a large net rate implies an even larger gross transport that is not considered feasible for the north shore of Long Island and the waves in the Long Island Sound.

To estimate the gross longshore sediment transport rate at Goldsmith Inlet, the present study considers the rate of accumulation at the fillet west of the Goldsmith Inlet jetty, the annual rate of sediment accumulation in Goldsmith Inlet , the rate of sediment transported offshore, and the rate of west-directed longshore sediment transport. The annual rate of accumulation at the fillet is taken to be 8,000 cu yd/year, as inferred from the analysis by Fields et al. (1999). The annual sediment accumulation rate in Goldsmith Inlet is at least 5,000 cu yd/year, based on dredging records (1977 to 1990) and the fact that sediment is observed to accumulate beyond the point of typical dredging. The rate of transport offshore is not known, but may be significant given the pronounced depression located directly offshore of Goldsmith Inlet. The rate of west-directed transport is not known. Given the previous information and unknowns, the authors conclude that a gross longshore sediment transport rate of 25,000 cu yd/year at Goldsmith Inlet is a reasonable upper limit estimate.

The coast from Duck Pond Point to Horton Point (Figure 2-3) can be considered as a littoral cell, with the bluffs serving as the sediment source. A littoral cell is a semienclosed reach of the coast that is relatively isolated sedimentologically from adjacent coastal reaches and that may contain its own sources and sinks of sediment. The shoreline from Duck Pond Point to Goldsmith Inlet increases in orientation toward the east. This change in orientation increases the angle between the crests of the predominant waves and the shoreline, thereby increasing potential longshore sediment transport directed to the east. In contrast, the section of shore that includes Mattituck Inlet is oriented more parallel to the crests of the predominant waves and would, therefore, be expected to have a smaller east-directed longshore sediment transport rate for some wave conditions.

As described in Chapter 4, the present study estimates an average-annual sediment accumulation rate of 8,000 cu yd/year for Mattituck Inlet prior to jetty modifications in 1938 and 1946. Based on this range of rates, a gross sediment transport rate of 25,000 cu yd/year as found for Goldsmith Inlet is judged to be an overestimate for Mattituck Inlet. Recently, Batten and Kraus (2005) analyzed shoreline change, beach profile surveys, and dredging records at Mattituck Inlet, and developed a local sediment budget within the context of a regional budget. The local sediment budget was balanced

with an easterly longshore sediment transport rate of 16,000 cu yd/year and a westerly rate of 5,000 cu yd/year, yielding a net rate of 11,000 cu yd/year to the east and a gross rate of 21,000 cu yd/year.

Mattituck Inlet – History and Site Description

Much of the information presented in this section was taken from the Town of Southold (2003) Local Waterfront Revitalization Plan.

Mattituck Inlet is located in the Village of Mattituck, in the Town of Southold, Suffolk County, NY. Mattituck Inlet in its natural condition, is depicted in an 1838 NOS topographic sheet T-55 (Figure 2-4). In its natural condition, Mattituck Inlet is shown to be directed towards the east. The inlet is of regional economic significance as the only major harbor east of Port Jefferson Harbor, a distance of 35 miles. The inlet is identified as one of 10 maritime centers on Long Island Sound by the New York Department of State (NYDOS). Mattituck Inlet and Creek have historically been of economic importance as well, as seen from the infrastructure in 1955 (Figure 2-5). The creek was the site of a tide-gristmill, constructed in 1821, which operated until 1902 (Figure 2-6). The structure is now the Old Mill Inn Restaurant.

Mattituck Creek serves four marinas and is a commercial and recreational boating center. The oysters of Mattituck Creek were historically considered to be of the finest quality and taste (Craven 1906). In 1988, the NYSDEC listed Mattituck Creek as a high-priority water body problem and the water quality problem as "severe," an action that precluded shell fishing in the area. These problems were listed by the NYSDEC as having "high resolution potential," and the creek has been the subject of an effort to improve water quality. At present, the NYSDEC permits conditional shellfish harvesting in the northern section of Mattituck Creek, whereas the southern portion remains closed. The water at the mouth of Mattituck Inlet is listed as high quality.

The area around Mattituck Inlet has seen gradual improvement. In 2002, New York State purchased 9.5 acres of surrounding land to further restore the waterfront and promote public access.

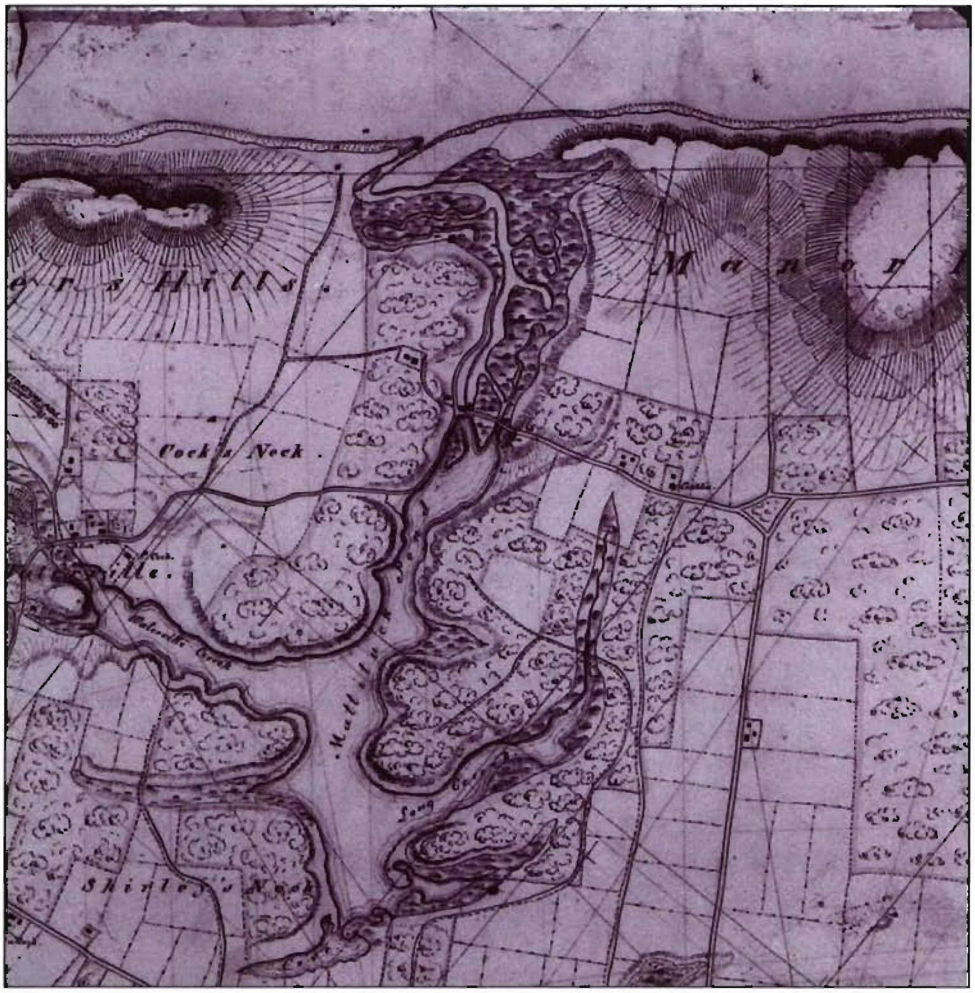

Figure 2-4. Mattituck Inlet as depicted in NOS T-sheet 55 (1838)

Figure 2-5. Mattituck Inlet and northern end of Mattituck Creek, 11 May 1955

Figure 2-6. Mattituck Mill at Mattituck Creek (by permission Southold Historical Society, Southold, NY, undated)

Physical description

Mattituck Inlet is a federally maintained inlet with a channel dredged to 7 ft mlw, with 2-ft overdraft. The New York District dredges Mattituck Inlet every 10-15 years. Mattituck Creek is 2.5 miles long and two creeks emerge from it. One, Howard's Creek, extends to the west and is navigable for its entire length. The other, Long Creek, extends east and is navigable for about 100 ft beyond its entrance. Mattituck Inlet and Creek have a surface area of approximately 7,200,000 sq ft, as determined by analysis of an aerial photograph dated 16 April 2003.

Prior to inlet stabilization, the Mattituck Inlet entrance was narrow, winding, and shallow (non-navigable). In the Rivers and Harbor Act of 1896, the U.S. Congress authorized the construction of two jetties to stabilize the inlet and provide reliable navigation. Work on the jetties commenced in 1901, and construction of the east jetty was completed in 1906.

Mattituck Inlet has been subject to considerable anthropogenic modification. The first dredging for channel improvement took place in 1907, and the Federal channel was completed in 1914 (Ralston 1928). The new work volumes dredged from Mattituck Inlet and Mattituck Creek are not known. Analysis of New York District condition surveys indicate that the entire creek had been dredged as of a survey dated August 1913 to April 1914. Mattituck Inlet and Creek were formerly the site of commercial sand and gravel handling facilities and asphalt tanks. Commercial mining of sand and gravel is known to have been conducted intermittently within the inlet from 1925 to 1948, under Federal permit, and mining activities took place on the beach directly west of the west jetty under Mattituck Park District permit. The beach directly east of Mattituck Inlet has been nourished by sediment dredged from the inlet. Figure 2-7 displays the approximate locations of engineering and mining activities in and around Mattituck Inlet.

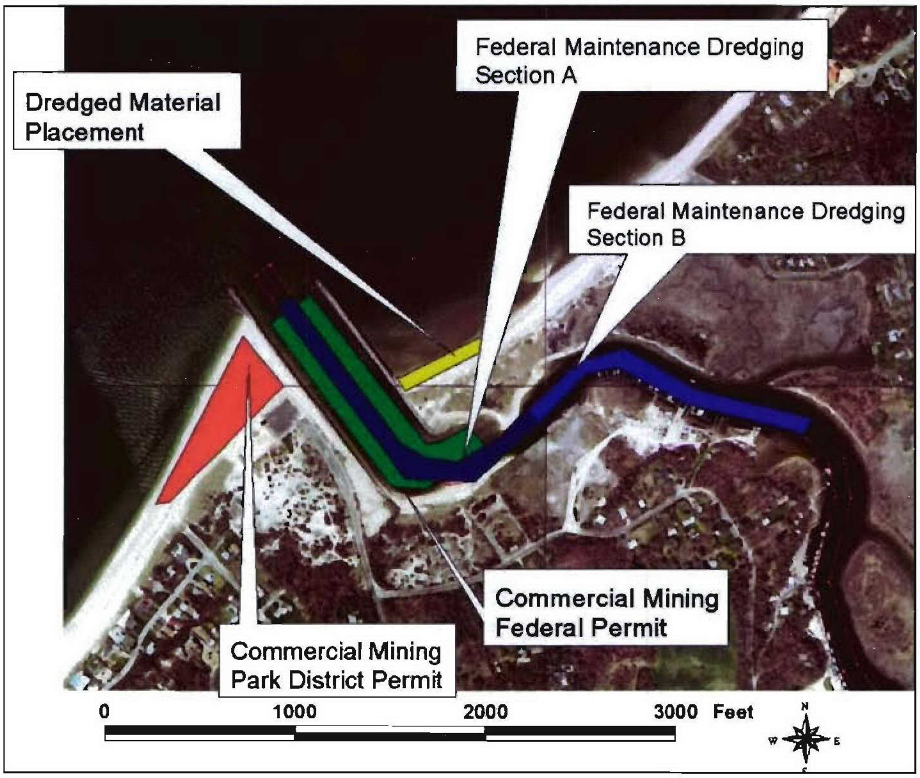

Figure 2-7. Dredging and mining activities in and near Mattituck Inlet

A chronology of maintenance dredging is given in Table 2-5, and a chronology of jetty construction, repairs, and modifications is given in Table 2-6. Table 2-7 provides a summary of the mining permits issued by the New York District. The Mattituck Park District permitted mining operations on the beach directly west of the west jetty. These mining operations are documented from 1960 to 1975, and, according to local sources, continued "on and off" for more than 50 years, as of 1976 (Schubel 1976). Mining operations came to an end in 1977, a result of a lawsuit brought against the Mattituck Park District by nearby property owners.[1]

Schubel (1976) calculated the volumes removed from the beach adjacent to the west jetty, from 1960 to 1975, based on the rates charged by the Mattituck Park District to the mining contractors. An overall average rate of $0.50 cu yd was assumed. These calculations, which partially document the volumes removed through mining, are presented in Table 2-8. Maintenance dredging at Mattituck Inlet is analyzed in Chapter 4. The implications of the mining practices on sediment transport within and adjacent to Mattituck Inlet are discussed in Chapters 4 and 7.

---

[1] Personal Communication, 30 August 2004, Mr. Frank Murphy, Mattituck Park District Supervisor (retired).

Table 2-5
Mattituck Inlet Dredging History[1]

Date Dredged	Dredged Depth (ft, mlw)	Volume Removed (cu yd)	Disposal Site (If Known)
1907	Unknown	Unknown	
1914	7	Unknown	
June – November 1921	7	13,468	
August – September 1923	7	49,500	
September – October 1927	7	49,186	
November 1935 – May 1936	7	50,785	
July – August 1938	7	18,312	
September – November 1946	7	53,893	Beach east of east jetty
October – November 1950	7	22,913[2]	Beach east of east jetty
August – September 1955	7	31,552	Beach east of east jetty
August – October 1961	7	43,550	
September – October 1965	7	6,285[3] 40,980[4]	
May 1980	7	24,137	Beach east of east jetty
October 1990	7	13, 241	Beach east of east jetty
17-24 March 2004	7	13,785	Beach east of east jetty

[1] Source: New York District undated compilation; (Ralston 1928).
[2] Channel reorientation.
[3] Dredged from channel entrance.
[4] Dredged from Federal anchorage and southern portion of the channel within Mattituck Creek.

Table 2-6
Mattituck Inlet Jetty Maintenance History[1]

Date	Action Taken	Quantity (tons)
1901	Commencement of Federal navigation project	
1906	East jetty completed	
1910	Sand tightening of landward 680 ft of east jetty, sand tightening of landward 485 ft of west jetty	
1914	First full dredging of the Federal navigation channel	
October 1937-August 1938	Repair of outer 100 ft of west jetty 280 ft seaward extension of west jetty	10,000
August – September 1946	Repair of 110 ft of east jetty 100 ft shoreward extension of east jetty	1,300
May – July 1975	Repairs to east jetty	13,500
1996	Repairs to west jetty Elevation of seaward 100 ft of west jetty by 1 ft	~16,000

[1] Sources: New York District undated compilation; Ralston (1928); Smith (1988)

Table 2-7[1]
Summary of Federal Commercial Sand Mining Permits

Applicant	Location	Depth, ft (mlw)	Date Granted	Date Expired	Work Completed
J.H. Rambo	Channel Entrance	10	4/9/1925	12/31/1928	N
Northport Sand and Gravel	S.W. flood shoal	10	9/1/1925	12/31/1928	N
J.H. Rambo	Channel Entrance	10	1/29/1929	12/31/1932	Partial
C.H. Benjamin	Channel Entrance	12	2/10/1928	12/31/1934*	Partial
F.M. Lewis	Channel Entrance	12	6/16/1928	12/31/1931	Y
Seely & Walsh	W. Channel Entrance	20	9/8/1931	12/31/1934	N
Bickel & Wichert Dredging	Channel Entrance	20	8/19/1932	12/31/1933	Partial
Bickel & Wichert Dredging	Channel Entrance	20	6/30/1934**	unknown	unknown
Seaboard Sand and Gravel	unknown	unknown	unknown	unknown	unknown
J. Cancro	Channel Entrance	20	6/30/1933	12/31/1936	Partial
J. Cancro	Channel Entrance	20	2/25/1937**	12/31/1943	None

[1]Source: Batten and Kraus (2005)
*extension granted
**extension of previous permit

Table 2-8[1]
Mattituck Park District Permit Sand Mining Volume Estimates 1960-1975

Year	Volume Mined (cu yd)
1960	23,214
1961	17,694
1962	14,734
1963	36,098
1964	20,032
1965	26,534
1966	25,808
1967	24,914
1968	15,914
1969	6,482
1970	7,208
1971	8,532
1972	9,502
1973	3,356
1974	364
1975	3.965

[1] Source: Schubel (1976)

Specifications of the original navigation project called for construction of two jetties to the 9-ft mlw contour depth. The distance between the jetties is 400 ft (Figure 2-8 and Figure 2-9). The jetties, at their original length, did not effectively protect the navigation channel. The west jetty therefore received a seaward extension in 1938, and it is now 1,320 ft long. An undated compilation of maintenance history at Mattituck Inlet from the New York District indicates that the east jetty was to receive a shoreward extension of 100 ft in 1946. Analysis of aerial photographs prior to and after this extension indicates that this extension was approximately 280 ft, an adjustment probably made during construction to close the breach. The east jetty is now 1,020 ft long. The east jetty was last repaired in 1975. In 1996, the west jetty was tightened, and the seaward 100-ft section was elevated 1 ft to reduce sediment intrusion to the inlet (New York District 2003). A condition survey was completed in May 2003, and dredging took place over 17-24 March 2004, removing 13,785 cu yd of sediment. Sediment dredged in 1946, and thereafter, with the possible exception of the dredging of 1965, was placed on the beach directly east of Mattituck Inlet. The area of placement for other dredging operations at Mattituck Inlet is not known.

Figure 2-8. Mattituck Inlet and jetties, view looking south, 28 March 2003

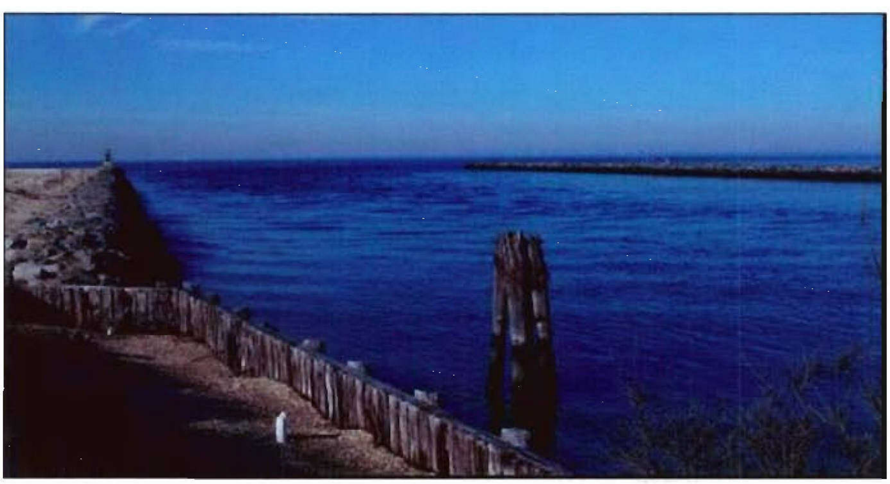

Figure 2-9. Mattituck Inlet and jetties, view looking north, 28 March 2003

The Federal navigation channel is 100 ft wide at the inlet and 80 ft wide in the interior. Mattituck Creek makes two sharp turns just south of the inlet. The channel narrows at the turns, where the greatest sediment shoaling takes place (Figure 2-10). Mattituck Inlet is characterized by sand-sized sediment, shell, and gravel. A recent grain size sampling of the navigation channel found the main shoaling areas to be composed mostly of sand and gravel (New York District 2003).

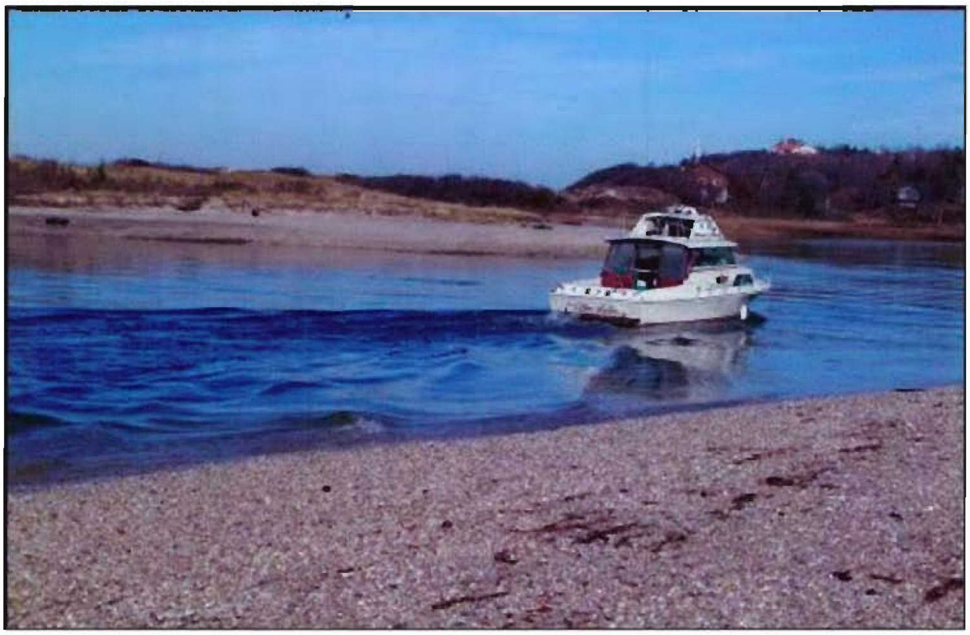

Figure 2-10. Mattituck Inlet channel, after turn eastward inside jetties. Large deposits of gravel and sand line both sides of channel, 21 November 2003

The Federal navigation channel runs from the inlet entrance to the Village of Mattituck. The New York District also completed a one-time dredging at the head of Mattituck Creek in 1965 to create a 460 × 570 ft Federal anchorage. Suffolk County has twice dredged this area. In 1955, Mattituck Creek was dredged, resulting in the removal of 1.5×10^6 cu yd of sediment (Allee, King Rosen and Fleming, Inc. et al. 1995). In 1967, Long Creek, a tributary of Mattituck Creek, was dredged, removing 13,000 cu yd.

Physical setting

Steep bluffs bound the beaches surrounding Mattituck Inlet. The bluffs are composed of loosely consolidated moraine material and glacial outwash. The bluffs reach maximum elevation (160 ft) to the west (Mattituck Hills), where elevations are consistently greater than 150 ft. The elevation of the bluffs east of Mattituck Inlet (Oregon Hills) average 100 ft. Narrow beaches front large sections of the bluffs on either side. These bluffs serve as a primary sediment source for littoral transport, and portions of this supply have been removed from the littoral system by recent construction of large retaining walls (Figure 2-11). The offshore on both sides of Mattituck Inlet contains

large submerged or partially submerged glacial erratics (boulders) that are a hazard to navigation.

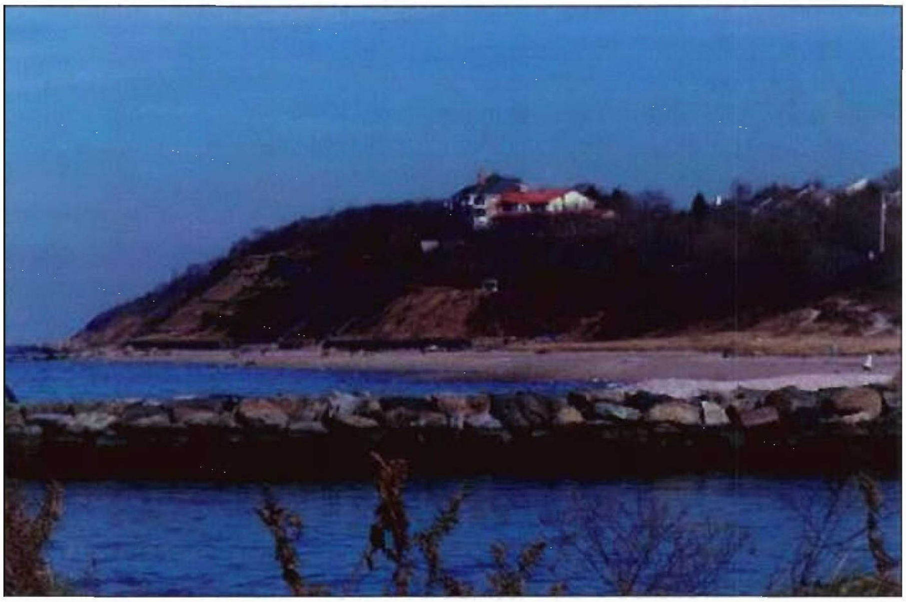

Figure 2-11. Bluffs east of Mattituck Inlet, 21 November 2003

Beach width west of Mattituck Inlet (Breakwater Beach) ranges between 50-100 ft and can be attributed to impoundment by the west jetty. The beach west of the jetties is composed mainly of sand. The beach east of the jetty, Bailie's Beach, is narrower and is composed of a mixture of sand and gravel. In the past, there was concern that a breach could occur adjacent to the east jetty. A breach at this location would expose the Oregon Hills Tidal Wetlands (located just south of the dunes that back Bailie's Beach) to waves and would reduce effectiveness of the Federal channel. A study by New York District (1999)[1] concluded that a breach was improbable, because the beach is backed by a row of primary and secondary dunes (Figures 2-12 to 2-15). Inspection of the area performed on several occasions during 3 years as part of the present study confirmed the presence of high dunes and a wide barrier spit (large volume of sediment that will resist storm erosion). The large sediment volume of the back beach adjacent to the east jetty indicates a local reversal in longshore transport against the regional west-to-east trend. The dunes east of Mattituck Inlet appear to be subject to erosion as a result of anthropogenic use (e.g., Boy Scouts climbing on them.) Figures 2-16 and 2-17 display a vegetated dune protected by a revetment adjacent to an accessible and unprotected dune with sparse vegetation.

---

[1] U.S. Army Engineer District, New York. (1999). op cit. p. 16.

Figure 2-12. Bailie's Beach primary dune, 21 November 2003. Boy Scouts of America facility is located south of dunes

Figure 2-13. Dunes east of Mattituck Inlet, looking west, 8 October 2002

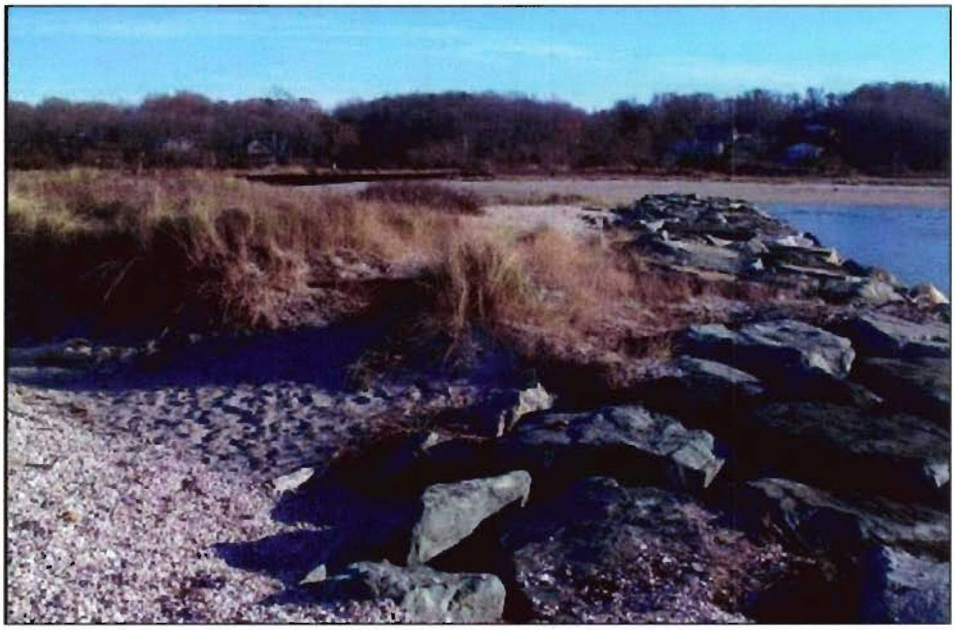

Figure 2-14. Dunes at base of Mattituck Inlet east jetty, looking south, 21 November 2003

Figure 2-15. Dunes at base of Mattituck Inlet east jetty, looking north, 8 October 2002

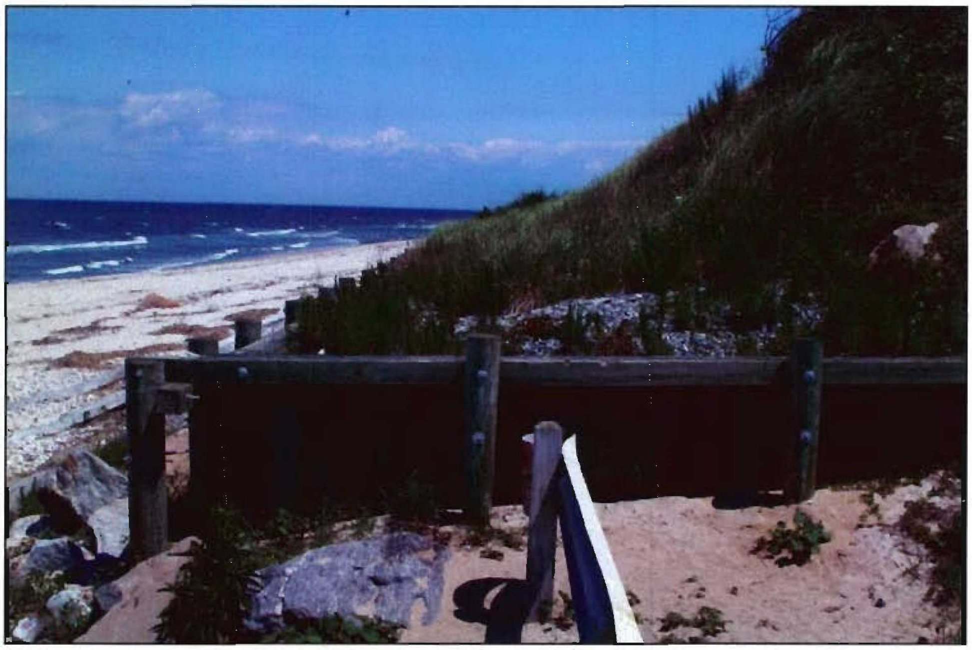

Figure 2-16. Vegetated dune protected by revetment at Bailie's Beach, view looking east, 9 July 2004

Figure 2-17. Sparsely vegetated and unprotected dune at Bailie's Beach, view looking west, 9 July 2004, at same location as photograph shown in Figure 2-16

Mattituck Inlet, Mattituck Creek, and the land surrounding it have been designated as the Mattituck Inlet Significant Coastal Fish and Wildlife Habitat by the NYDOS. The perimeter of Mattituck Inlet is fringed with tidal marshes with both intertidal and high marsh vegetation (Figure 2-18). These wetlands have high primary productivity and support a variety of wildlife. There are also areas of deposited dredged material along the shore. The most extensive wetland system is the state-owned Oregon Marsh Tidal Wetlands, located behind the secondary dunes of Bailie's Beach. This system supports juvenile marine finfish, clams, mussels, and osprey.

Figure 2-18. Mattituck Inlet perimeter, view looking south, 21 November 2003

Goldsmith Inlet – History and Site Description

Much of the information presented in this section was taken from the Town of Southold (2003) Local Waterfront Revitalization Plan and from Comes (1954).

Goldsmith Inlet is located in the Hamlet of Peconic in the Town of Southold, Suffolk County, NY. Goldsmith Inlet in 1838, as depicted in 1838 NOS topographic sheet T-55, is shown in Figure 2-19. Similar to Mattituck Inlet in a natural condition (Figure 2-4), the entrance of Goldsmith Inlet is directed towards the east and has a winding sigmoidal planform. Although it remains an area of historic, scenic, and environmental significance, for much of its history it was a site of economic significance also, owing to a gristmill that was located there. The inlet's first gristmill was constructed in 1760. This tidal mill failed to work satisfactorily, was remade into a horse-driven mill, and then fell into disuse as the local money crop changed from wheat and corn to flax around the time of the American Revolution.

In 1841, at a cost of $2,100, a group of 80 farmers bought shares to finance the construction of a new tide-gristmill (Figure 2-20). The Peconic Mill was completed in 1843 and was successful for much of the remainder of the century. The mill stood on the west bank of Goldsmith Inlet. Owing to the large, semidiurnal tide range (5.2 ft), the

inlet experienced large tidal runs twice a day. Two wooden gates attached to a footbridge crossing the inlet impounded the high-tide waters that filled Goldsmith Pond.

For much of its existence, the mill was owned by Mr. Gilbert Terry. Mr. Terry added a windmill wheel to the top tower sometime in the 1870s, allowing the mill to continue to produce when the creek was frozen (and possibly during times of temporary inlet closure). The mill ceased operating when the local money crop changed to potatoes and cauliflower in the 1890s. Newspaper accounts note, "the channel was allowed to fill up with sand, seaweed, and mussel shoals" (Comes 1954). A large storm on 26-27 November 1889 caused the windmill wheel to fall, and the mill deteriorated. The structure was torn down in 1906.

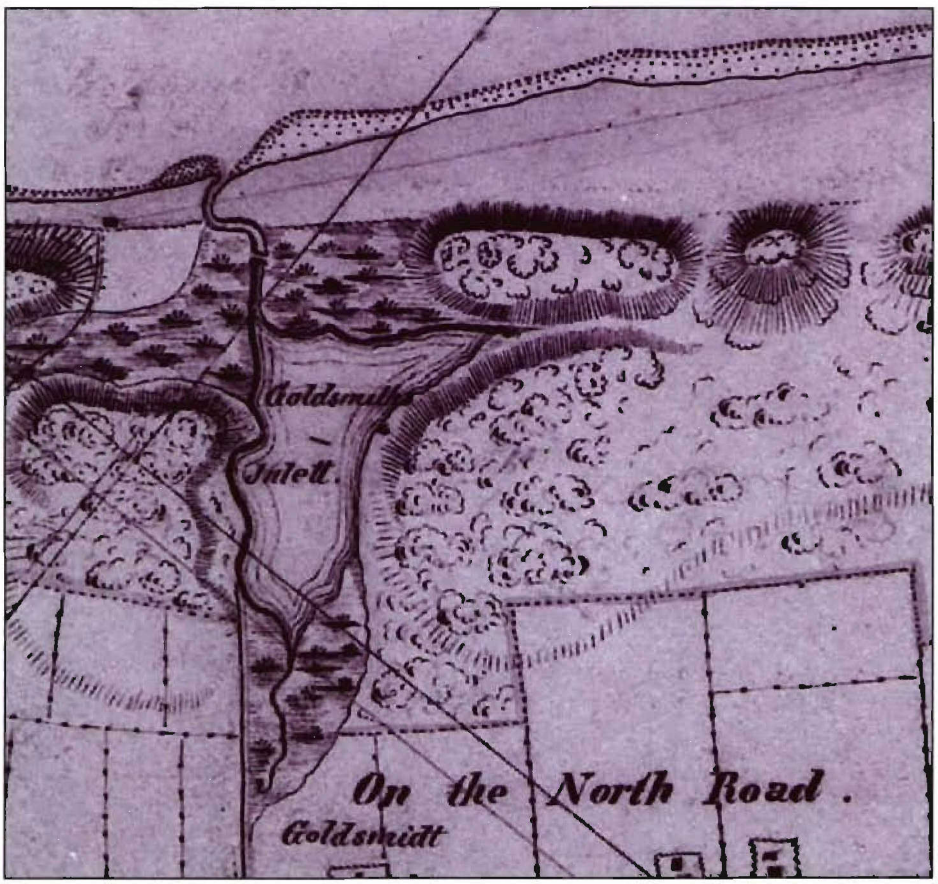

Figure 2-19. Goldsmith Inlet as depicted in NOS T-sheet 55 (1838)

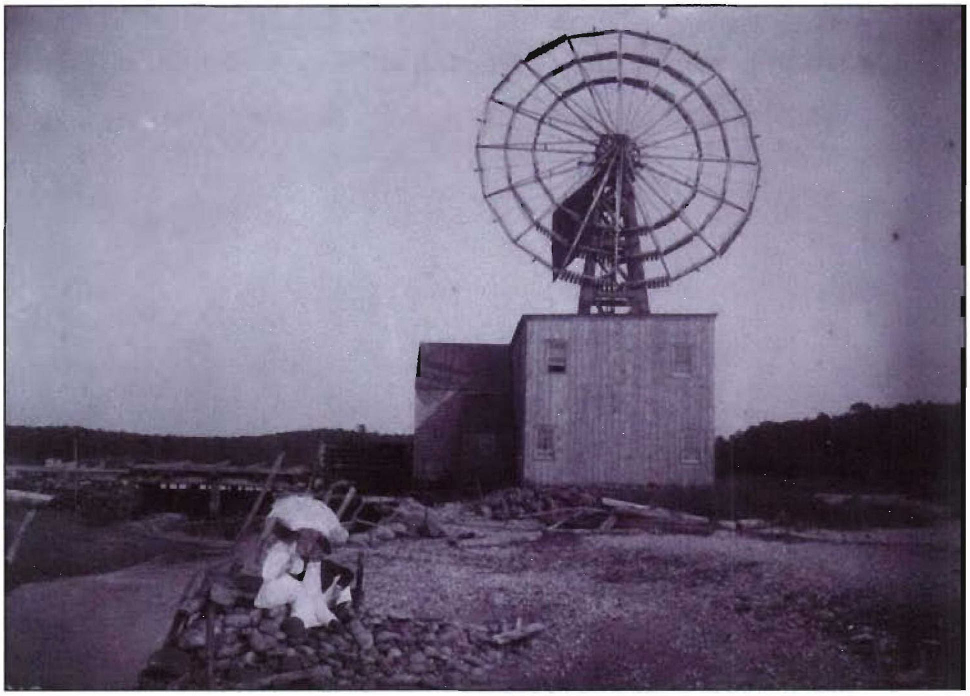

Figure 2-20. Peconic Mill at Goldsmith Inlet (by permission Southold Historical Society, Southold, NY, undated)

Although it is not known when the inlet was first called Goldsmith Inlet, the presence of a Goldsmith family in the town of Southold can be traced to at least 1668. Southold was founded in 1640 and is the oldest English town in New York State. The old burying ground in Cutchogue, also founded in 1640 and believed to be the oldest European burial ground in New York State, contains many tombstones with the surname Goldsmith on them from the 1800s (Figure 2-21).

Figure 2-21. Headstone of James H. and Sarah C. Goldsmith, Old Burial Ground, Cutchogue, NY

Physical description

Goldsmith inlet is now a locally maintained inlet that connects Goldsmith Pond to Long Island Sound (Figure 2-22). The inlet is non-navigable, and numerous site visits by the authors indicate it reaches depths of about 0.5-4 ft msl, depending on location and stage of tide. The inlet width ranges from about 10 to 100 ft, has a mean width of about 50 ft, and is approximately 1,200 ft long. Goldsmith Pond has a mean depth of 2.5 ft msl (based on survey) and a surface area of approximately 950,000 sq ft as determined from analysis of an aerial photograph dated 16 April 2003. Goldsmith Inlet is composed of medium to coarse-grained sand armored with gravel (Figure 2-23).

In 1960, the Suffolk County Department of Public Works proposed the development of marinas in locations throughout the county, including Goldsmith Inlet (Figure 2-24). The primary motivation for the construction of the jetty at Goldsmith Inlet is unclear.

The summary report on the workshop examining erosion of the baymouth barrier bar between Duck Pond Point and Horton Point (Town of Southold 1996)[1] concludes "it is uncertain if the project was meant to address shoreline erosion or prepare the inlet for construction of a marina and harbor of refuge at Goldsmith Pond." An introductory geographic sketch within this same report, however, states "the jetty was intended to protect the inlet and mitigate erosion immediately to the west." The transcripts of this workshop proceedings document discussion on this matter (Town of Southold 1996).

Figure 2-22. Goldsmith Inlet and Goldsmith Pond, 11 May 1955, 9 years before jetty construction

[1] Town of Southold, NY, and New York State Department of State Division of Coastal Resources and Waterfront Revitalization. (1996). "Report of the workshop examining erosion of the coastal barrier landform between Duck Pond Point, Town of Southold, NY," unpulished report.

Figure 2-23. Typical gravel and some cobble armoring at Goldsmith Inlet, 28 March 2003 (view looking west)

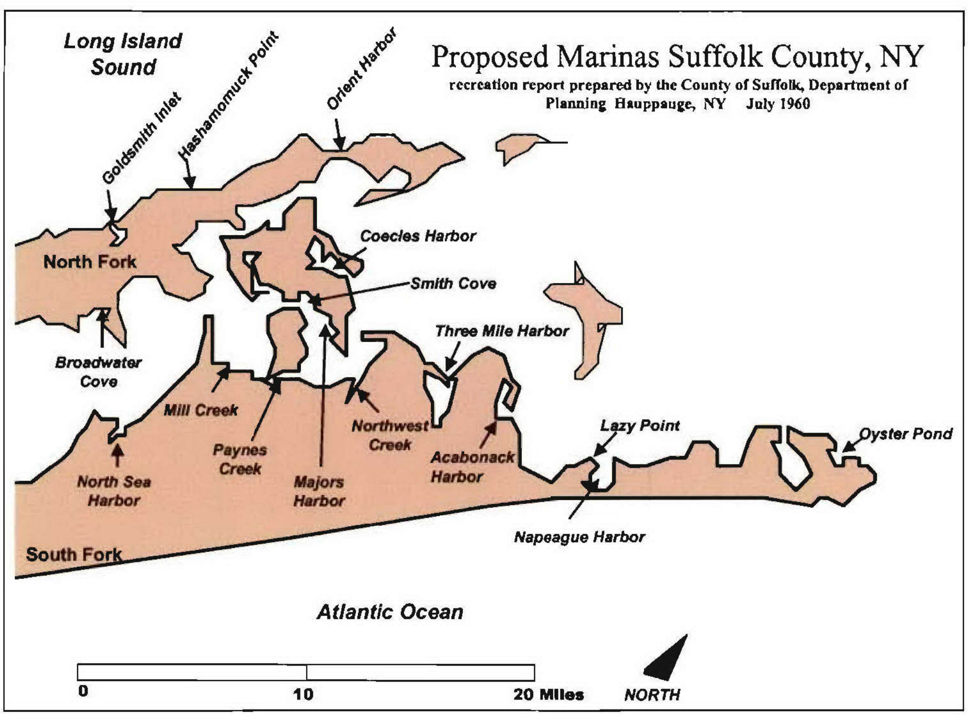

Figure 2-24. Proposed marinas, 1960 (redrawn after map of proposed marinas, Suffolk County, NY, Department of Planning, July 1960)

On 13 August 1962, proceedings by the Suffolk County Board of Supervisors approved funding for "... the construction of a stone jetty for beach protection on Long Island Sound at Goldsmith Inlet." A request by the New York State Department of Public Works (NYSDPW 1963) to construct a jetty at Goldsmith Inlet was approved by the New York District on 12 September 1963. An attached drawing plan of the proposed jetty by the NYSDPW lists the project as "Beach Protection Project 192." On the same day, a press release by the NYSDPW announced the receipt of a low-contract bid "for beach protection work at Goldsmith Inlet." A memorandum from the NYSDEC, dated 15 May 1979, states "The purpose of the jetty was to maintain the opening at Goldsmith Inlet and to allow for future development of the Town's recreational facilities." Available literature on the construction of the jetty at Goldsmith Inlet and its subsequent impact on the adjacent shoreline cite beach protection and the construction of a marina at Goldsmith Inlet as the motivation for jetty construction (Leatherman 1996;[1] Greenman-Pederson Associates 1981).

Construction of a marina at Goldsmith Inlet was still being considered in 1967. The transcript of the workshop proceedings indicates that this remained true as of 1973. Documentation for this date was not, however, provided. A letter dated 30 January 1967 from the Town of Southold Office of the Supervisor to the NYSDPW requests assistance in procuring state funding to further this aim: "It is the intention of the County Board of Supervisors to open Goldsmith's Inlet as a harbor of refuge off Long Island Sound and it is necessary at this time to construct a jetty on the east side of the inlet, as well as providing for beach stabilization on the east side." It is not known whether this request was made as part of a continuing plan to develop Goldsmith Inlet into a marina, dating back to the construction of the west jetty, or as a new initiative. The east jetty was never built, and the project was never completed.

Construction of the jetty was completed in 1964. The cost of construction was divided equally between New York State and Suffolk County (Town of Southold 1996). Leatherman (1996) cites a jetty length of 400 ft and Dean (1996),[2] in his recommendations to the Town of Southold, puts the length of the jetty at 460 ft. Original documents (New York District 1963) and subsequent literature (NYSDEP 1987)[3] indicate that the length of the jetty is 310 ft. From analysis of aerial photographs from 1964 to 2003, the present authors conclude that the jetty length is greater than 310 ft, although a definitive length could not be determined without excavation.

Goldsmith Inlet and Goldsmith Pond have no direct water-dependent uses. The water quality is considered to be environmentally acceptable at present, but the pond has been closed for shell fishing since 1996 owing to high bacteria counts. The high coliform bacteria counts are thought to originate from a stream that discharges into the inlet and from Autumn Pond, a 1.5-acre pond located to the west that is connected via a drainage pipe. Non-point sources such as road runoff, septic tanks, and waterfowl waste reduce

---

[1] Leatherman. (1996). op cit p. 9.

[2] Dean, R. G. (1996). "Beach erosion control and recommendations," in Report of the Workshop Examining Erosion of the Coastal Barrier Landform Between Duck Point and Horton Point, Town of Southold, NY, Appendix II-B1, unpublished report.

[3] New York State Department of Environmental Conservation (NYSDEC). (1987). "Coastal erosion reconnaissance study," in Report of the workshop examining erosion of the coastal barrier landform between Duck Pond Point and Horton Point, Town of Southold, NY, unpublished report.

the pond's water quality. For these reasons, Goldsmith Inlet has consistently appeared on the NYSDEC Priority Water Problem List and the Priority Waterbodies List. Closure of Goldsmith Inlet would be expected to further reduce water quality in the pond.

Physical setting

Goldsmith Inlet is owned by Suffolk County and is located within the county's 34-acre Goldsmith Inlet Park. The jetty at Goldsmith Inlet is owned by the Town of Southold. The park serves the community for nature walks and fishing. The site supports a variety of wildlife species, including deer, heron, osprey, and piping plovers. The piping plover is an endangered species whose breeding grounds are protected by the NYSDEC. A 1998 environmental inventory marked the area as a piping plover nesting site. This is a factor entering scheduled inlet maintenance, because the NYSDEC will only allow dredging from October through March. This same inventory also found that the western side of Goldsmith Inlet contains diverse vegetative habitats including Pitch Pine and Oak Forest, Maritime Shrubland, Maritime Grassland, Shrub Swamp, Emergent Marsh, and Estuary and Salt Marsh.

Behind the beach, a narrow fringe of habitat that is classified as an estuary and salt marsh containing intertidal marsh and high marsh rings the western and southwestern edge of Goldsmith Inlet and Pond (Figure 2-25). Goldsmith Inlet Park, together with the Peconic Dunes County Park located directly east of it, contain a system of primary and secondary dunes not found elsewhere along the North Fork coast. Goldsmith Inlet Park has been designated as a "critical environmental area" by the Suffolk County Department of Health and is protected.

Figure 2-25. Goldsmith Inlet, west perimeter, view looking south, circa winter 2001

The bluff-backed beaches and land surrounding the inlet represent the advanced stages of a bay barrier, where the pond was once a bay and the barrier beach was formed from the erosion of coastal glacial deposits. Approaching the inlet from the west, the bluffs (Figure 2-26) average 40 to 60 ft in elevation and are exposed to waves during extreme high water. The bluffs decrease in height of 20 to 40 ft with proximity to the

inlet and turn landward, merging with dunes and beaches. Dunes are found east of Goldsmith Inlet that lead into the Peconic Dunes County Park (Figure 2-27). Kenneys Road Beach is located further to the east. Sediment removed by periodic dredging of Goldsmith Inlet is a source of nourishment for this beach, as well as for the beaches directly east of the inlet.

Figure 2-26. Bluffs west of Goldsmith Inlet, 28 March 2003

Figure 2-27. Goldsmith Inlet entrance with view of east beach, 28 March 2003

Present condition

Suffolk County ceased annual dredging of Goldsmith Inlet in the 1990s. Since then, the Town of Southold has conducted dredging operations on an as-needed basis. Emergency dredging took place in winter 2001 and in April 2004. In the past, the

primary motivation for dredging was not necessarily to prevent inlet closure. The town undertook annual dredging because the sediment found in Goldsmith Inlet, which is coarser than that found in the beaches, was considered a good source of material for the eastern beaches. Dredging activities at Goldsmith Inlet are summarized in Table 2-9. The Town of Southold has dredged Goldsmith Inlet annually since 1991, with the exceptions of 2002 and 2003.

Table 2-9
Goldsmith Inlet Dredging History (Augmented from Fields et al. 1999)

Date Dredged	Volume (cu yd)	Placement Location
1977	4,000	Goldsmith Inlet beach, directly east of inlet
July 1980	3,720	Goldsmith Inlet beach, directly east of inlet
June 1982	6,000	Stockpiled west of inlet, removed off site
July 1985	2,640	Goldsmith Inlet beach, directly east of inlet
June 1987	4,800	Stockpiled and trucked to Kenneys Road Beach
June 1989	4,320	Stockpiled and trucked to Kenneys Road Beach
June 1990	NA	Stockpiled and trucked to Kenneys Road Beach
March 2004	Approx. 5,000	Goldsmith Inlet beach, directly east of inlet
Records not available after 1990. It is estimated that approximately 5,000 cu yd of sediment was dredged annually and trucked to Kenneys Road Beach.		

Since 1964, the jetty has gradually deteriorated. Lack of maintenance has caused the jetty to become porous and lower. Jetty degradation and impoundment of sediment on the west side of the jetty (Figure 2-28) have apparently led to greater sediment intrusion into the inlet.[1] Records are not available for the volumes dredged in the 1990s. It can be assumed that the increased sediment intrusion has resulted in continually increasing dredging volumes since the mid-1990s. The increased sedimentation and lack of recent dredging have resulted in an inlet that is continually approaching closure.

The unusually cold weather of the winters of 2002 and 2003 may have contributed to delay closure by the buildup of ice along the shore that reduced wave action and sediment transport towards the jetty and inlet. Orientation of the inlet entrance to the east may reduce the effectiveness of the flushing action of the ebb tide by lengthening the channel, but may be beneficial overall for maintaining inlet stability, discussed in Chapter 6.

[1] Personal communication, 24 March 2003, Mr. James McMahon, Community Development Director, Town of Southold.

Figure 2-28. Sediment impoundment west of Goldsmith Inlet jetty (view looking north), circa winter 2001

After the bathymetric survey of 6-8 October 2002 (discussed in Chapter 3), the mouth of Goldsmith Inlet migrated to the east. In the winter months of 2003 and 2004, a west-oriented spit accreted at the inlet mouth, redirecting the mouth slightly toward the west. The presence of ice directly east of the inlet may have been partially responsible for buildup of this west-oriented spit as well as the redirecting of the inlet mouth to the west.

The Town of Southold requested that Suffolk County dredge the inlet. A permit for dredging, and the creation of a 4-ft-deep, 40-ft-wide straight channel, was requested in the winter of 2003/2004[1]. Restrictions brought by piping plover breeding concerns precluded any action after April 2004. The New York District denied the permit application because of environmental concerns. A permit was issued to conduct smaller scale emergency dredging, however, and during 22-26 March 2004, approximately 5,000 cu yd of sediment was removed from the mouth of Goldsmith Inlet to prevent inlet closure. The material was placed on the adjacent downdrift beach.

Figure 2-29 shows the orientation of the Goldsmith Inlet entrance on 8 October 2002, Figures 2-30 and 2-31 show the orientation on 28 March 2003 and 16 February 2004, respectively. The orientation of the Goldsmith Inlet entrance on 6 April 2004, soon after the emergency dredging of March 2004, is shown in Figure 2-32.

---

[1] Personal communication, 27 January 2004, Mr. James A Richter, Office of the Engineer, Town of Southold.

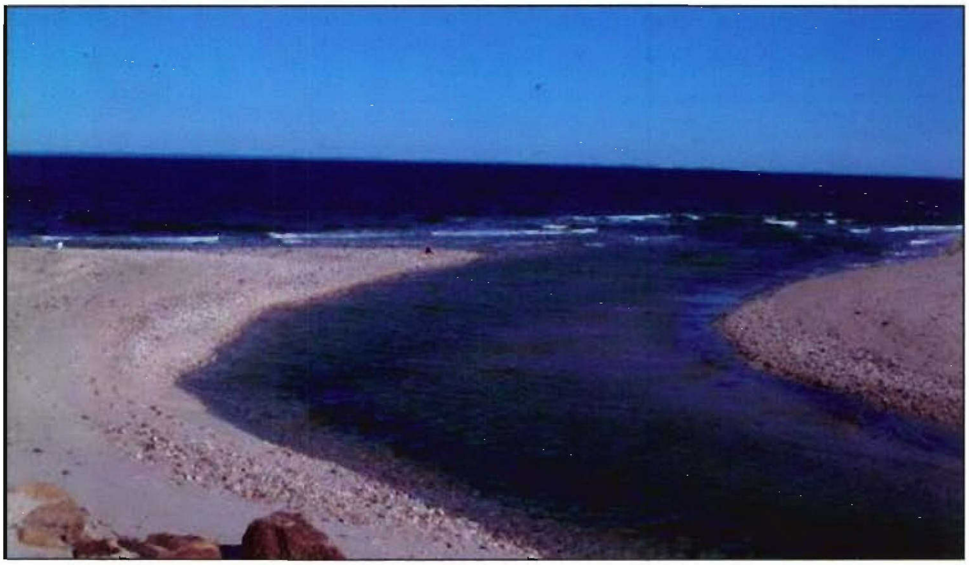

Figure 2-29. Goldsmith Inlet orientation, 8 October 2002 (view looking northeast)

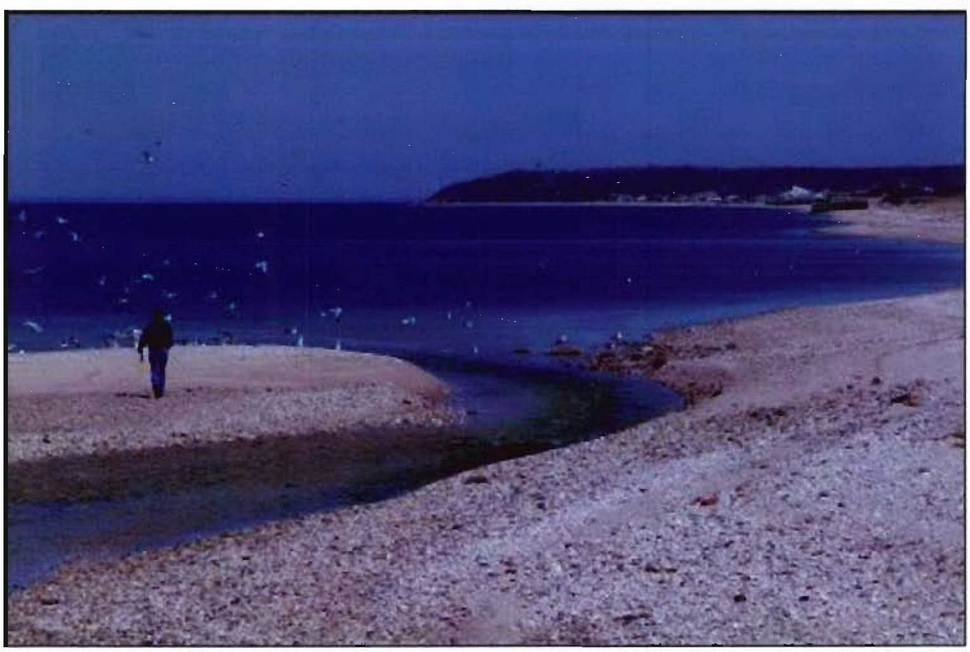

Figure 2-30. Goldsmith Inlet orientation, 28 March 2003 (view looking east)

Figure 2-31. Goldsmith Inlet orientation and ice, 16 February 2004 (view looking east)

Figure 2-32. Goldsmith Inlet orientation, after emergency dredging, 6 April 2004 (view looking northeast)

The Town of Southold has discussed the futures of Goldsmith Inlet and the Goldsmith Inlet jetty. Beyond the creation of a new deeper channel, an option being considered is shortening of the jetty, which may mitigate erosion east of the jetty yet still preserve a portion of the beach fillet west of it.

The presence of Autumn Pond must also be considered in assessing the environmental consequences of actions at Goldsmith Inlet. Autumn Pond connects to Goldsmith Pond through a drainage pipe. If the inlet were to experience closure, the relative elevation of the ponds is expected to change, potentially resulting in a reversal of drainage. Elevated water level in the pond could be a concern for the homeowners in the vicinity of Autumn Pond,[1] as well as alter the environment along the perimeter.

---

[1] Personal communication, 24 March 2003, Mr. James McMahon, Community Development Director, Town of Southold.

3 Field Data Collection and Analysis

As part of this study, a bathymetric survey was performed, and measurements were made of the water level and current at Mattituck Inlet and Goldsmith Inlet from mid-September to mid-October 2003. Measurement procedures and results are presented in this chapter. Previous sediment analysis studies at Mattituck Inlet and Goldsmith Inlet are also discussed.

Overview of Measurements and Vertical Datums

Shoreline position east and west of these inlets have been surveyed previously (OCTI 1998; Fields et al. 1999), and the New York District surveys the Federal navigation channel at Mattituck Inlet regularly. Prior to the present study, synoptic bathymetry data were lacking for the channels and offshore at Mattituck Inlet and Goldsmith Inlet. At Goldsmith Inlet, prior to the present work, no bathymetric survey of Goldsmith Pond was available, and at Mattituck Inlet offshore surveys covering the offshore shoal were available from 1927 and 1967 (the 1927 survey was recovered from archives as part of this study). Comprehensive surveys allow analysis of morphology change at the inlet channels and their shoals.

The bathymetric surveys were conducted during 6-8 October 2002. Survey data presented here are referenced to the horizontal datum New York State Plane Grid, Long Island Lambert, North American Datum 1983 (NAD83), in feet. Elevations are referenced to the North American Vertical Datum 1988 (NAVD88) in feet. Horizontal and vertical controls for the land-based survey were obtained from a March 1998 shoreline survey performed by OCTI (1998). For the period of record of the water-level gauges deployed in this study, the tidal datum mean sea level was found to be within survey error of NAVD88 offshore of Mattituck Inlet, at the tip of the west jetty, and 0.25 ft higher than the NAVD88 datum in Mattituck Creek. At Goldsmith Pond, msl datum for the period of record was found to be 0.91 ft higher than NAVD88. Datum trees that illustrate the relations between the various datums referenced in this study are provided in Figures 3-1a and 3-1b.

Water level and current measurements were scheduled for spring tide. The data collection occurred in autumn, when water level in Long Island Sound tends to be slightly higher than the annual or long-term average (Lyles et al. 1988). Because of the wide range in sediment grain size at Goldsmith Inlet (from sand

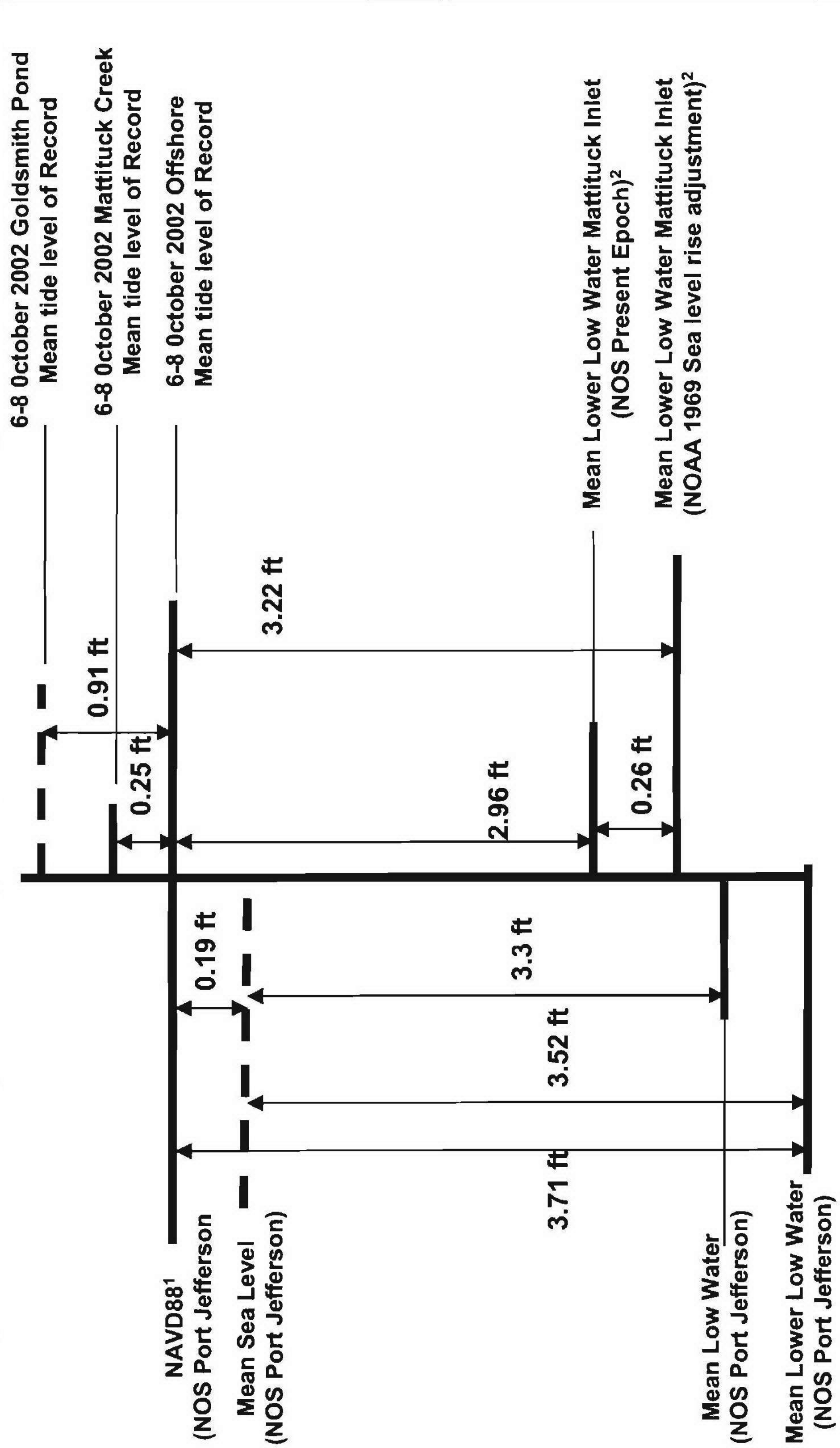

[1] At Port Jefferson, New York, NOS tide gauge (Station ID 8514560), located approximately 48 km west of Mattituck Inlet, 1983-2001 tidal epoch tidal datums mtl and msl are given as 1.076 and 1.073 m, respectively, and NAVD88 datum is at 1.132 m with respect to mllw
[2] At Port Jefferson, New York, NOS tide gauge (Station ID 8514560), mean sea level rise is given as 2.44 mm/year.

Figure 3-1a. Datum elevation differences, Port Jefferson (not to scale)

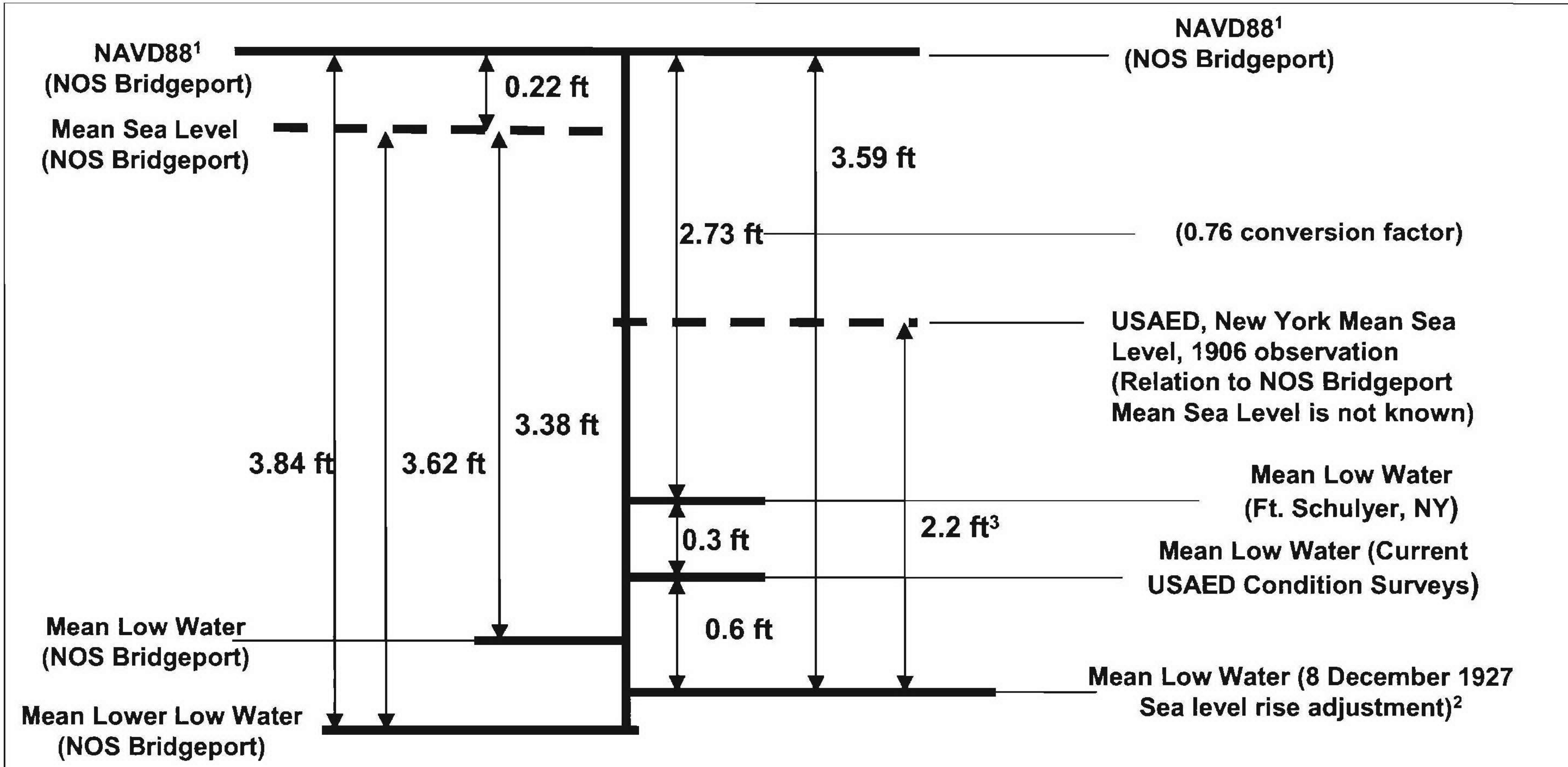

[1] At Bridgeport, Connecticut, NOS tide gauge (Station ID 8514560), located approximately 48 km west of Mattituck Inlet, 1983-2001 tidal epoch tidal datums mtl and msl are given as 1.101 and 1.104 m, respectively, and NAVD88 datum is at 1.171 m with respect to mllw

[2] At Bridgeport, New York, NOS tide gauge (Station ID 8514560), mean sea level rise is given as 2.58 mm/year.

[3] New York District Condition Surveys

Figure 3-1b. Datum elevation differences, Bridgeport (not to scale)

to cobble), sediment samples were collected there and analyzed to explore possible relations among grain size, water movement, and inlet channel cross-sectional stability.

Mattituck Inlet

The 6-8 October 2002 survey of Mattituck Inlet, Mattituck Creek, and the offshore area adjacent to Mattituck Inlet, was made with an Innerspace 448 high-precision echo sounder and a Global Positioning System (GPS). Horizontal positional accuracy is approximately +/-1 m. The Innerspace 448 is a survey-grade depth sounder that employs a transducer with an 8-deg sounding beam and operates at a frequency of 208 kHz. The beaches adjacent to the inlet and the area from the shoreline seaward to wading depth were surveyed with land-based equipment (total station and surveying rod).

At Mattituck Inlet, two Seabird26 Paroscientific Digiquartz Pressure Sensor-based tide gauges were deployed for the period 19 September - 8 October 2002. Two SonTek side-looking (SL) acoustic Doppler current meters were deployed for the period 7-8 October 2002. Current Meter 1 was placed adjacent to Tide Gauge 2. Grain-size properties of sediment samples collected 6-7 May 2003 and analyzed by the New York District are also discussed.

Bathymetry

The extent of the survey for the Mattituck Inlet study area is shown in Figure 3-2, and interpolated elevation contours for the Mattituck Inlet study area are plotted in Figure 3-3. The survey data were brought into ArcView 3.3 for display and data cleaning. Areas of shoaling within the inlet, the Federal navigation channel, the channel that runs through Mattituck Creek, and the Federal anchorage at the end of the creek are observed. A shoal of unknown origin is located east of the inlet. It is doubtful that this feature is an ebb shoal. This morphologic feature, longshore bars west of the inlet, the Federal navigation channel, and the areas of shoaling within the inlet are discussed in the following sections.

Offshore and east offshore shoal morphology. Figure 3-4 shows the locations of the offshore survey transects of 6-8 October 2002 west of Mattituck Inlet. Beach profiles derived from the survey are shown in Figures 3-5a and 3-5b. From the berm crest to a depth of approximately 10 ft, the beach slope is 1:15. Three longshore sandbars and a relatively uniform shoreline are observed. The relatively uniform shoreline west of the inlet is shown in Figure 3-6. Figure 3-7a indicates these longshore bars west of the inlet and Figure 3-7b indicates the lack of longshore bars east of the inlet. The most landward or inner longshore bar is located approximately 250 ft offshore, trends toward the shoreline 2,500 ft west of the inlet, and extends for approximately 7,500 ft west. The second longshore bar, referred to in this report as the main longshore bar, is located approximately 750 ft offshore. The main longshore bar begins approximately 2,000 ft west of Mattituck Inlet, where it trends in towards the shoreline, and continues for at least 28,000 ft. The most seaward bar runs from the tip of the west jetty to 4,300 ft west of the jetty, where it attaches to the main longshore bar. Adjacent to the east jetty, a bypassing bar is observed, that connects to the most seaward longshore bar east of the inlet. Seaward of these bars, the slope is gentler, at approximately 1:125, from 1,400 to 2,500 ft offshore.

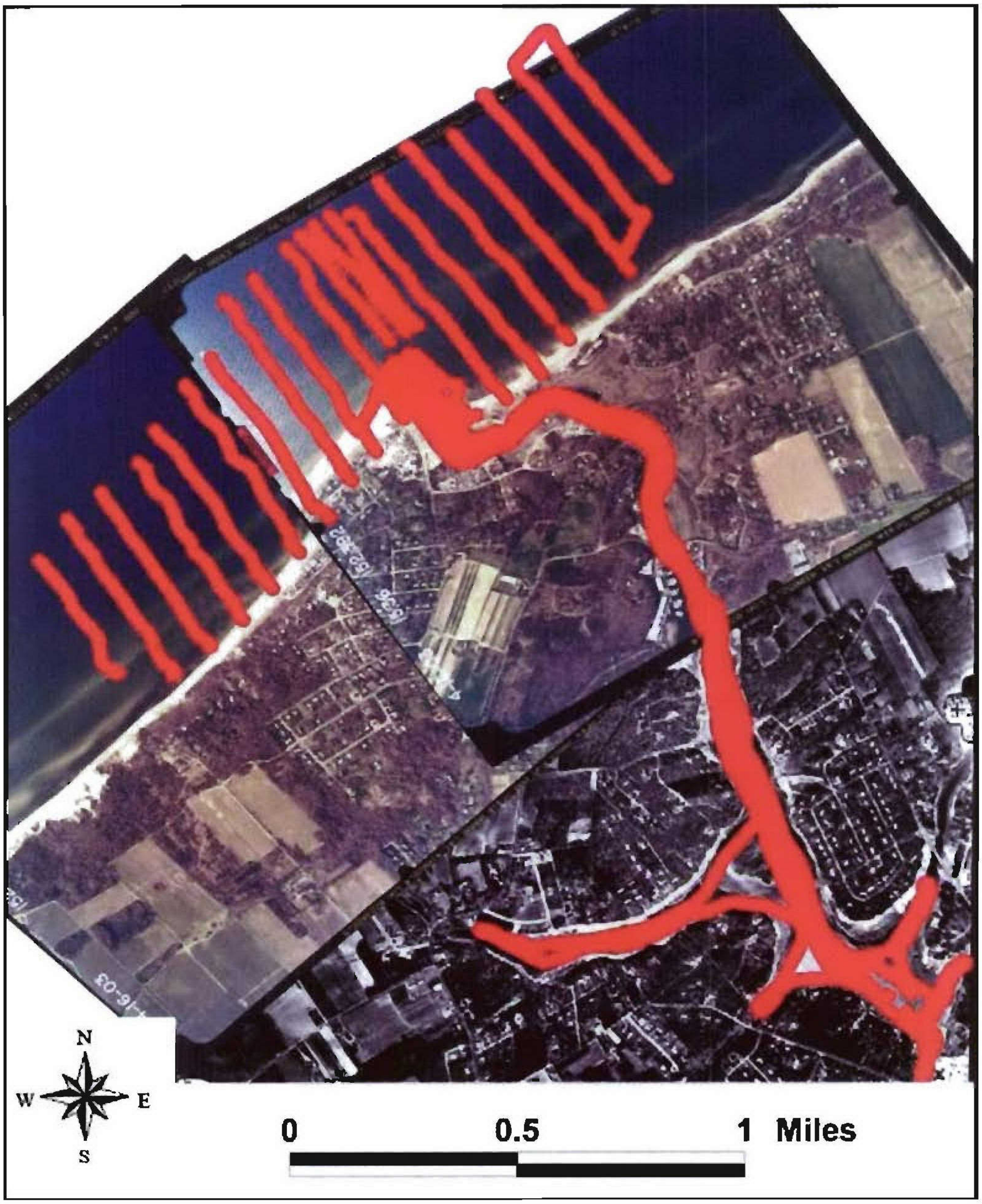

Figure 3-2. Mattituck Inlet bathymetry survey coverage, 6-8 October 2002

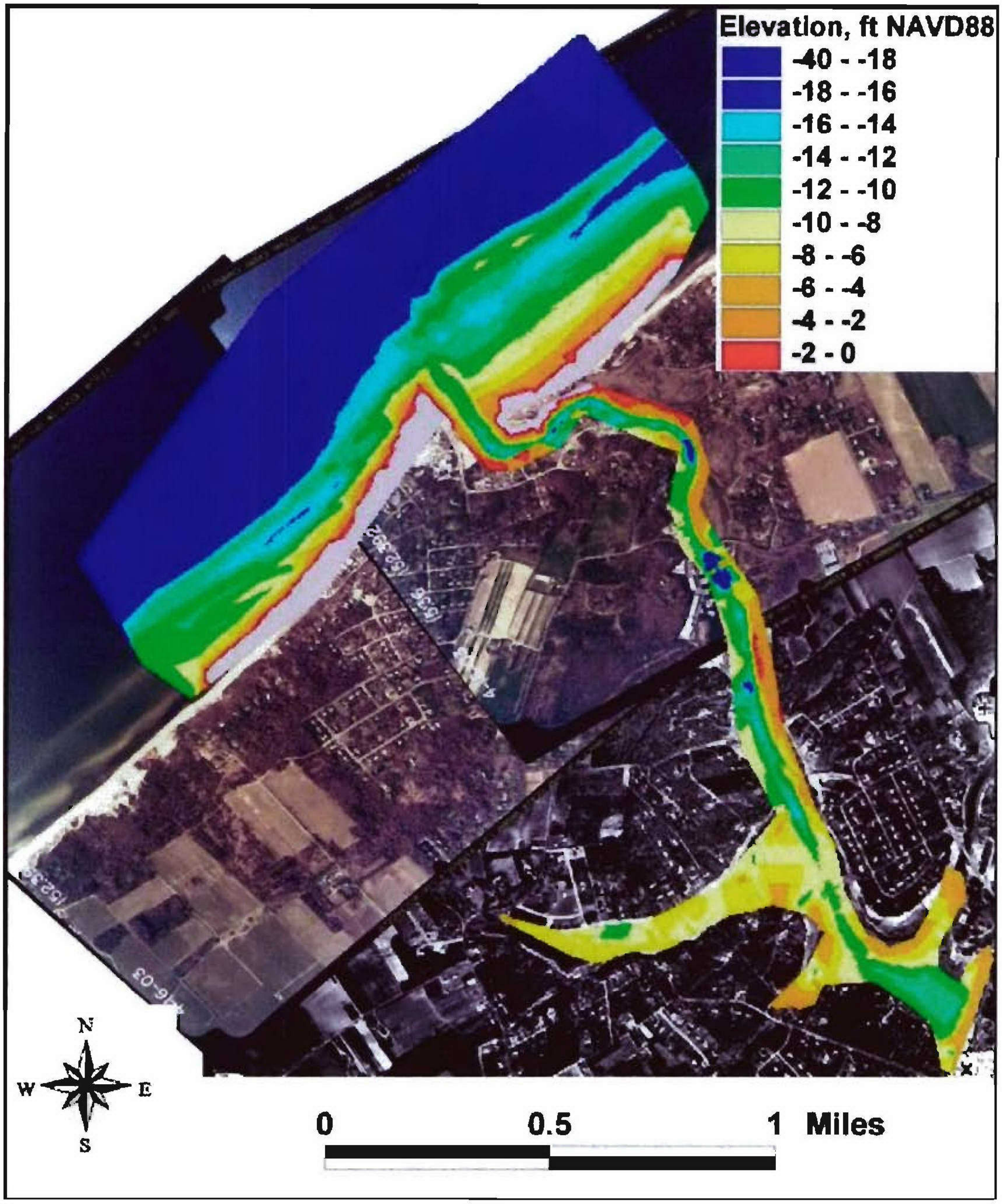

Figure 3-3. Mattituck Inlet elevation contours, 6-8 October 2002

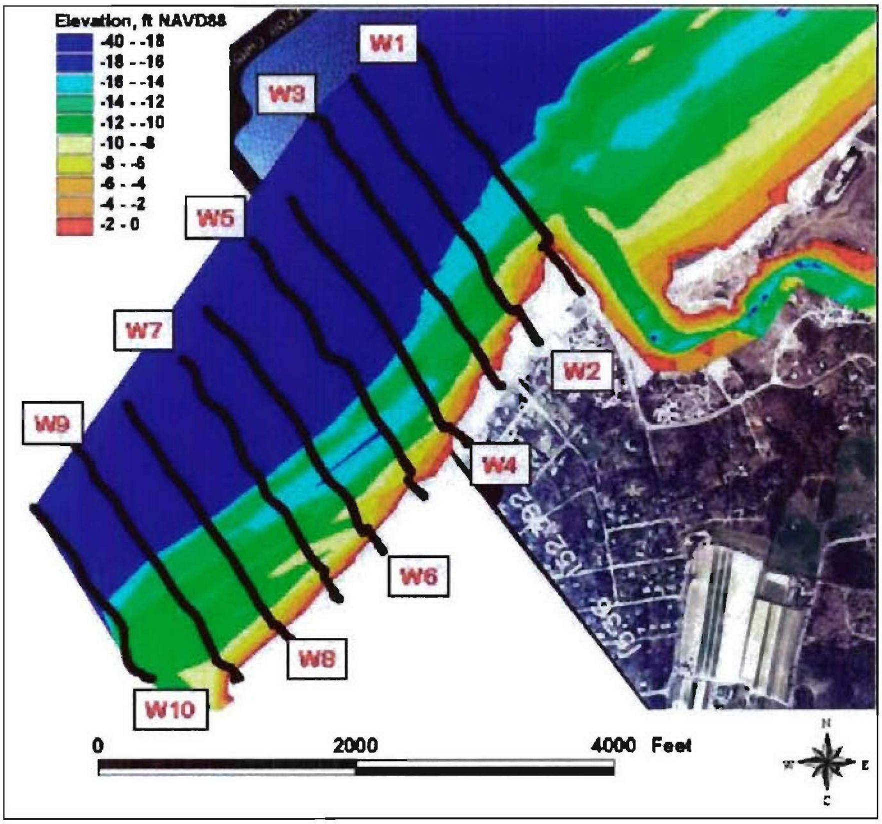

Figure 3-4. Mattituck Inlet offshore west survey transects, 6-8 October 2002

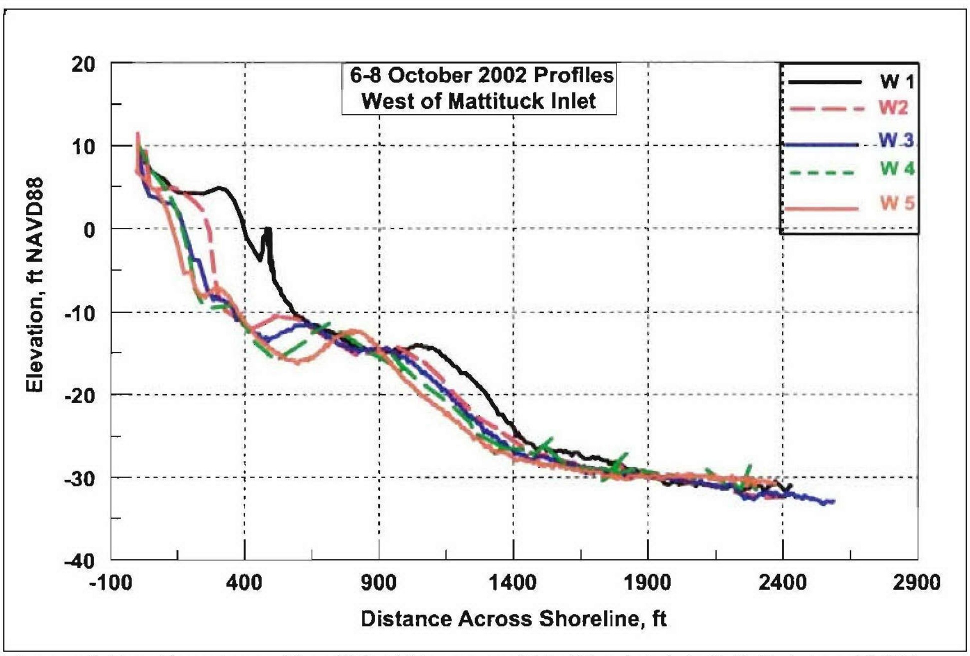

Figure 3-5a. Beach profiles W1-W5, west of Mattituck Inlet, 6-8 October 2002

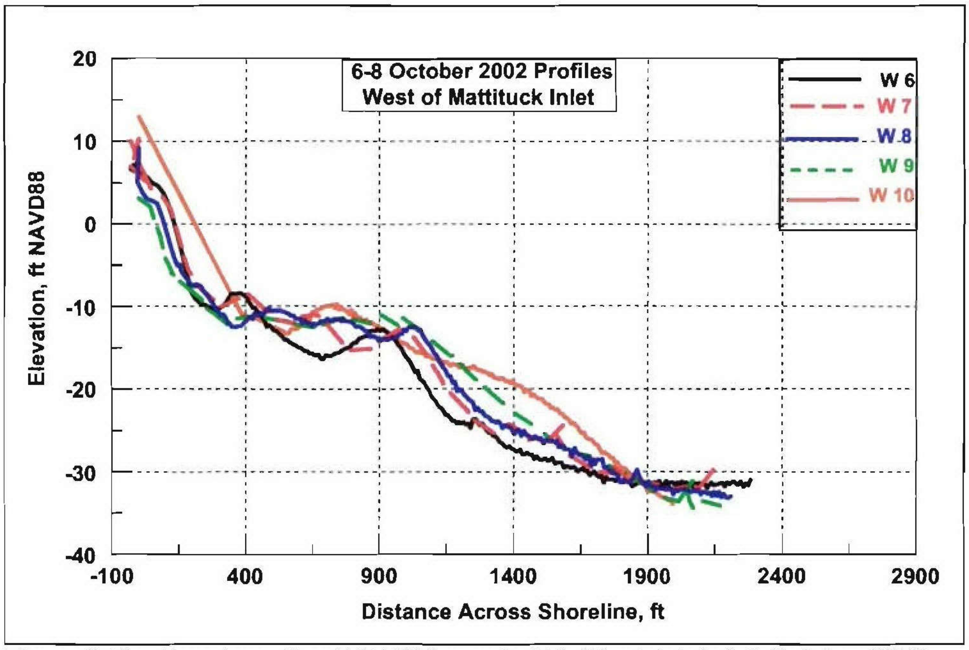

Figure 3-5b. Beach profiles W6-W10, west of Mattituck Inlet, 6-8 October 2002

Figure 3-6. Shoreline west of Mattituck Inlet, 21 November 2003

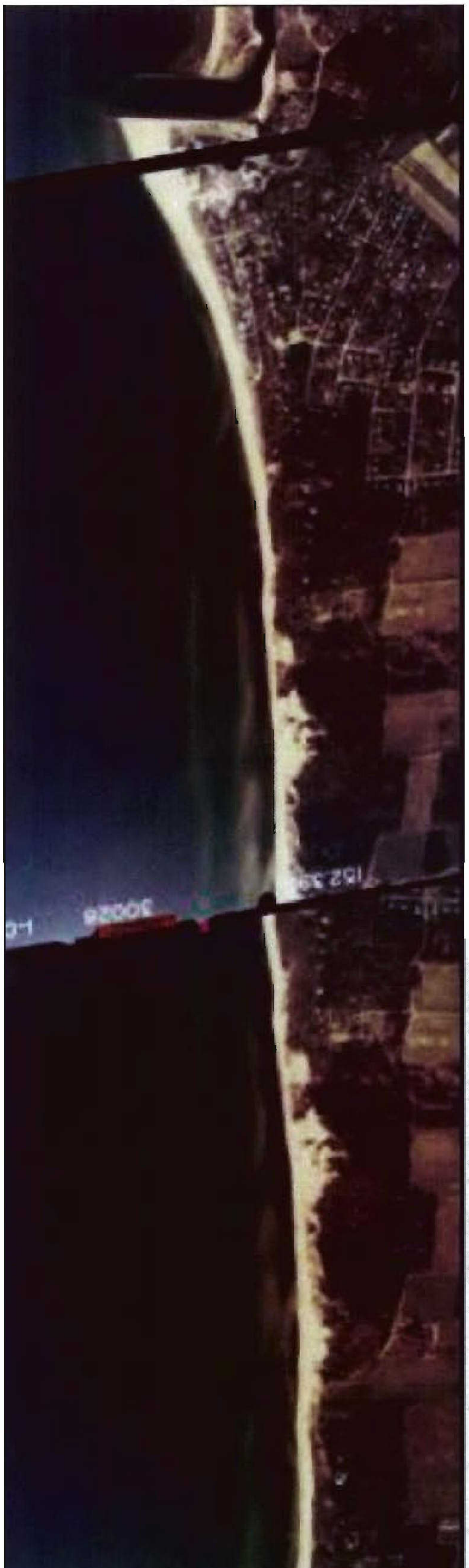

Figure 3-7a. Longshore bars west of Mattituck Inlet, 16 April 2003

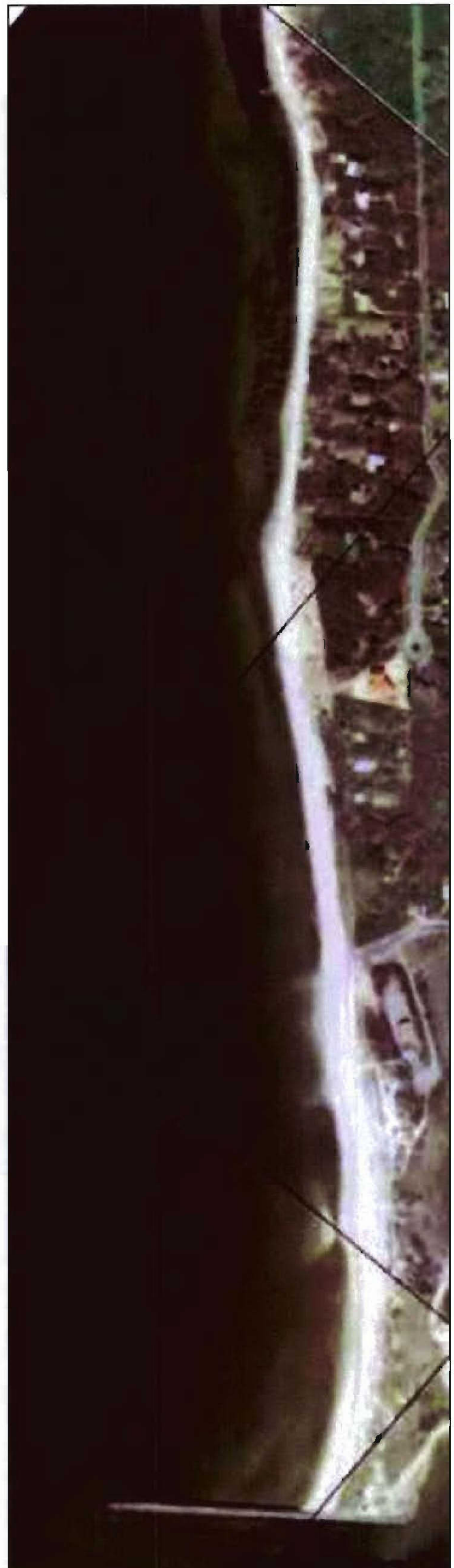

Figure 3-7b. Offshore east of Mattituck Inlet, 16 April 2003

Locations of the survey transects of 6-8 October 2002 for the offshore area east of Mattituck Inlet are shown in Figure 3-8, and beach profiles derived from this survey are shown in Figures 3-9a and 3-9b. In contrast to the almost uniform or smooth shoreline west of the inlet, the shoreline east of the inlet is characterized by a series of cuspate formations composed of a sand and gravel mix (Figures 3-7b, 3-10 and 3-11). The beaches directly east of Mattituck Inlet also contain an abundance of shells from the bivalve *Crepidula fornicata*, a native species known as a slipper limpet or common boat shell (Figure 3-12) that attaches to shells and stones on substrata around the lower range of the tidal zone.

The slope from the berm crest to approximately 10 ft mlw is 1:25 for the area directly east of the inlet to approximately 500 ft. The slope becomes gentler after this point, at 1:50.

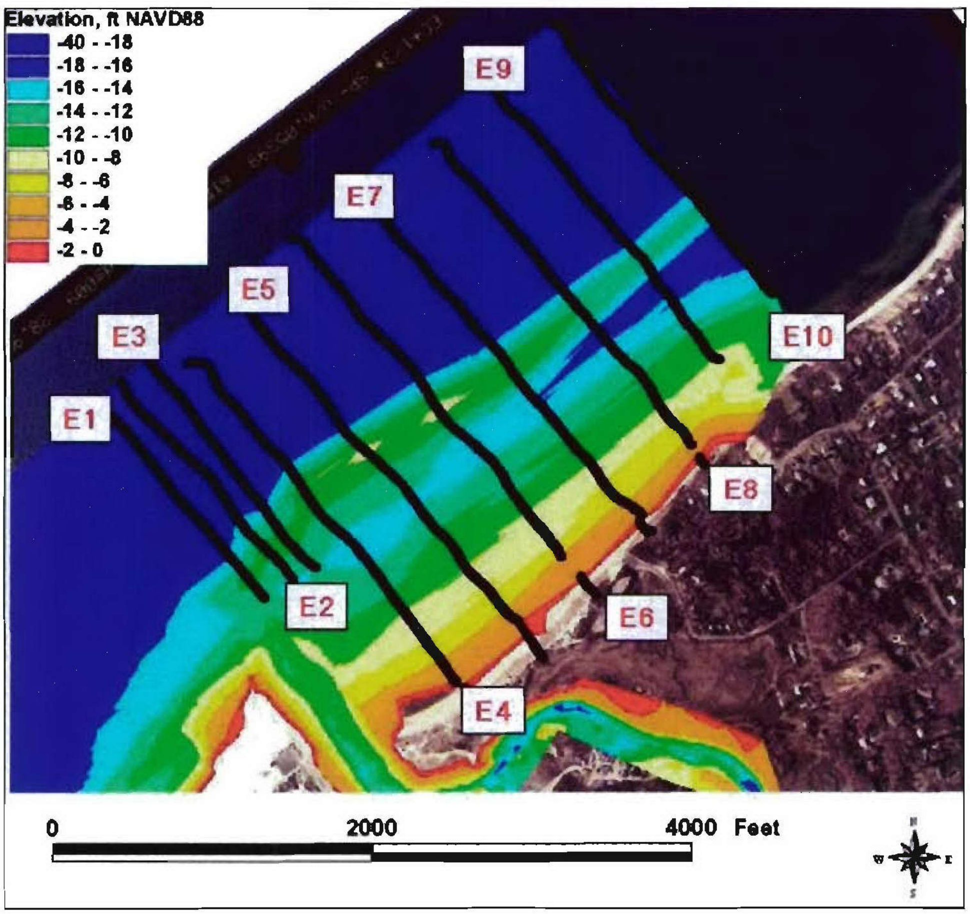

Figure 3-8. Mattituck Inlet offshore east survey transects, 6-8 October 2002

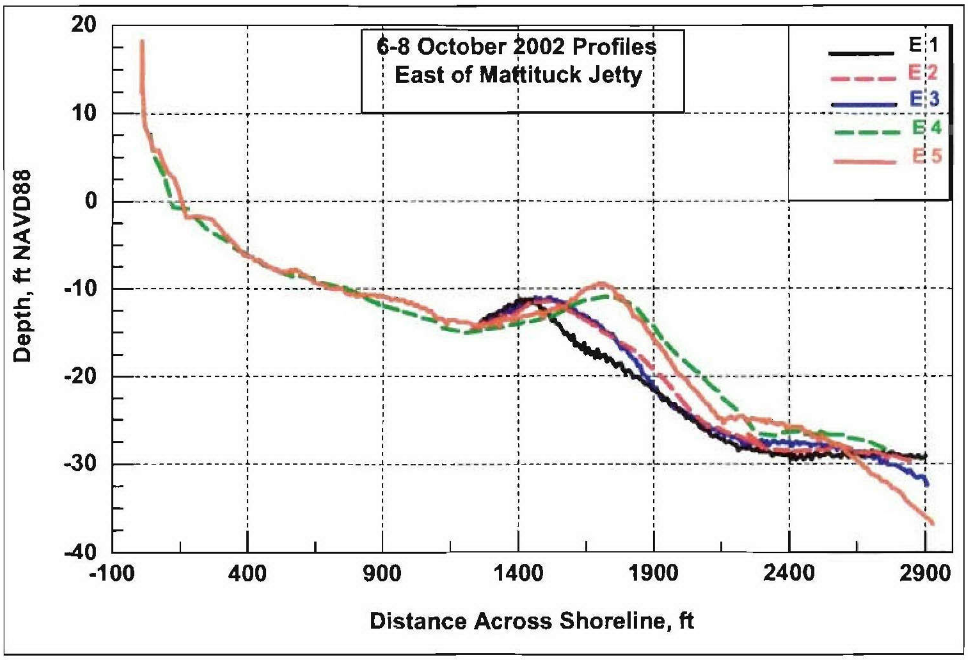

Figure 3-9a. Beach profiles E1-E5, east of Mattituck Inlet, 6-8 October 2002

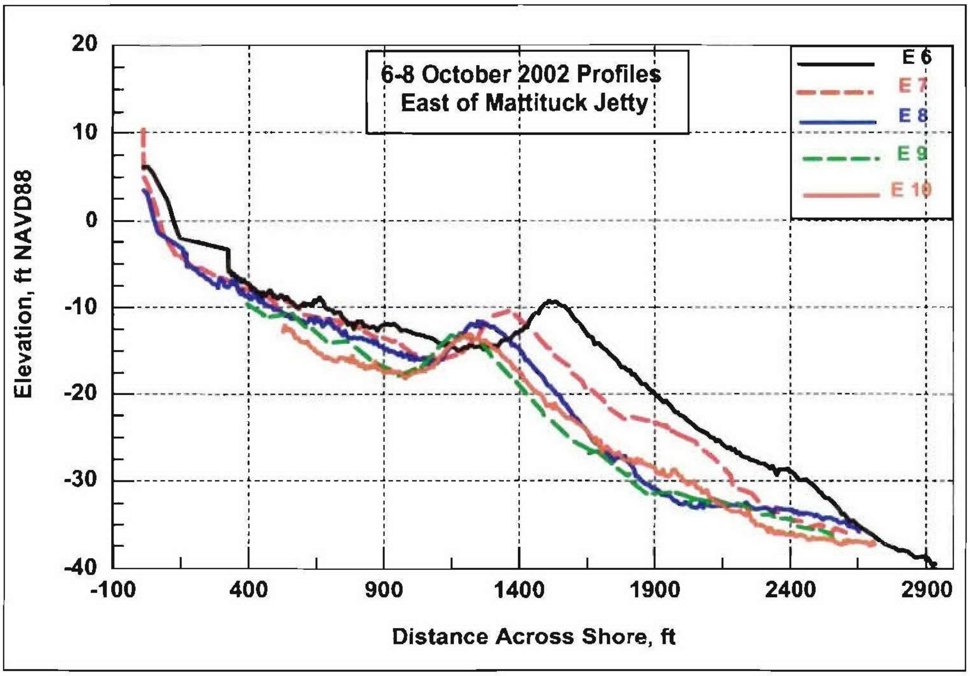

Figure 3-9b. Beach profiles E6-E10, east of Mattituck Inlet, 6-8 October 2002

Figure 3-10. Beach east of Mattituck Inlet, 16 April 2003, showing irregular shoreline

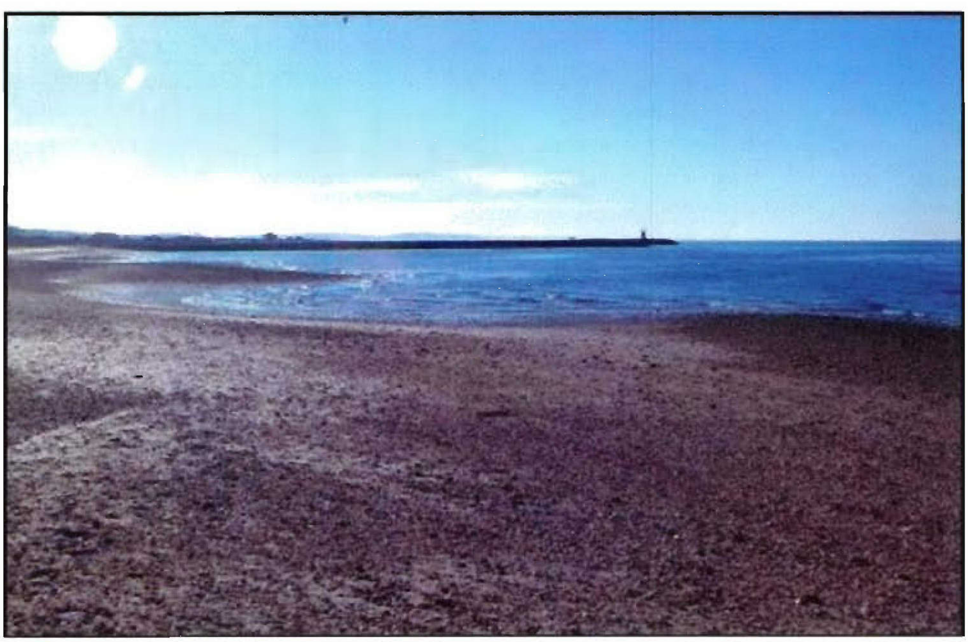

Figure 3-11. Cuspate shoreline features east of Mattituck Inlet, 21 November 2003

Figure 3-12. Mound of slipper limpet shells, east of Mattituck Inlet, 21 November 2003

The area offshore east of the inlet lacks longshore sandbars and possesses a shoal, displayed in Figure 3-13, oriented parallel to the shoreline. Its center line is located approximately 1,600 ft offshore, and the shoal is approximately 2,100 ft long and 400 ft wide at its center. The minimum water depth above the crest is 9.3 ft NAVD88. The volume of the shoal is approximately 460,000 cu yd, measured from a reference datum of –21.5 ft NAVD88 (Chapter 4). The feature has an unusual rectangular shape that contrasts with the more characteristic semi-circular or horseshoe shape of ebb shoals found at many Atlantic Ocean inlets, including the south shore of Long Island. For this and other reasons discussed in Chapter 6, the feature is not considered to be an ebb shoal.

Figure 3-14 displays elevation contours for the main longshore bar, the seaward longshore bar adjacent to the west jetty tip, the bypassing bar adjacent to the east jetty, and the offshore shoal. Collectively, these features comprise the sediment bypassing complex for the area offshore of Mattituck Inlet.

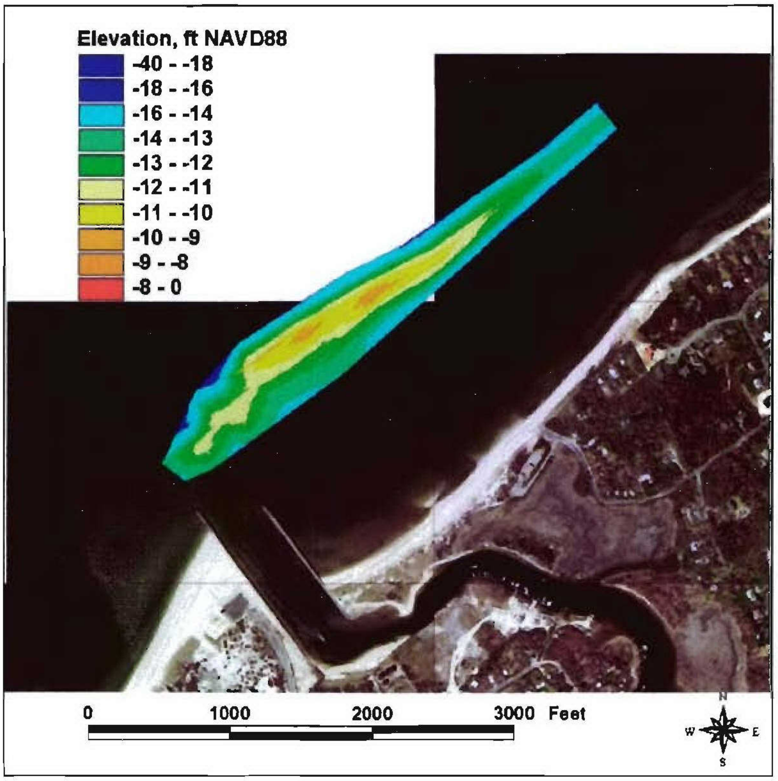

Figure 3-13. Mattituck Inlet offshore shoal and channel contour elevation, 6-8 October 2002

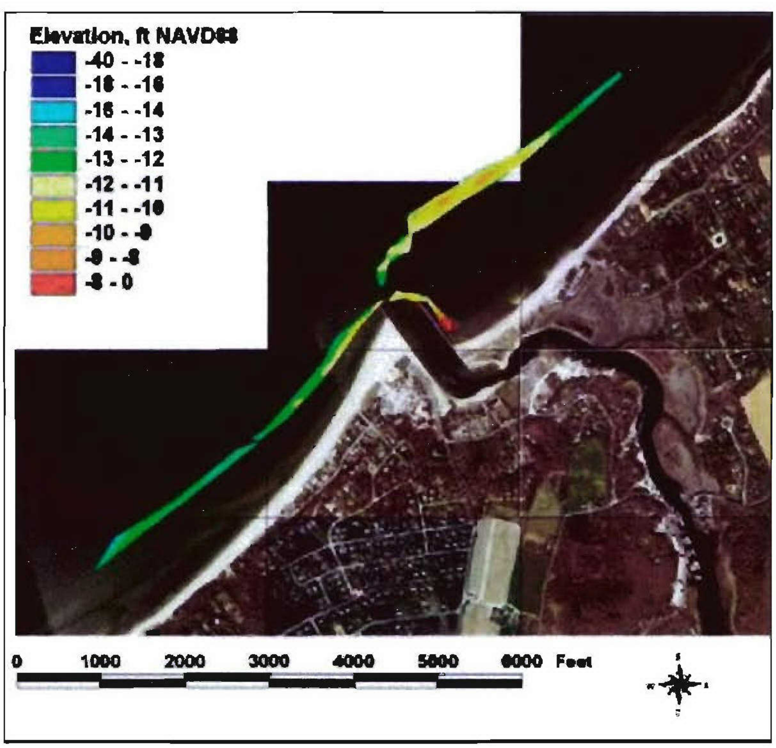

Figure 3-14. Features offshore of Mattituck Inlet, 6-8 October 2002

Flood shoal morphology. Mattituck Creek takes a sharp turn to the northeast just beyond the landward end of the east jetty. A major portion of the flood shoal is located on the north bank, directly behind this turn. Shoaling also occurs on the south bank and at the inlet mouth, along the west jetty (Figures 3-15 to 3-17).

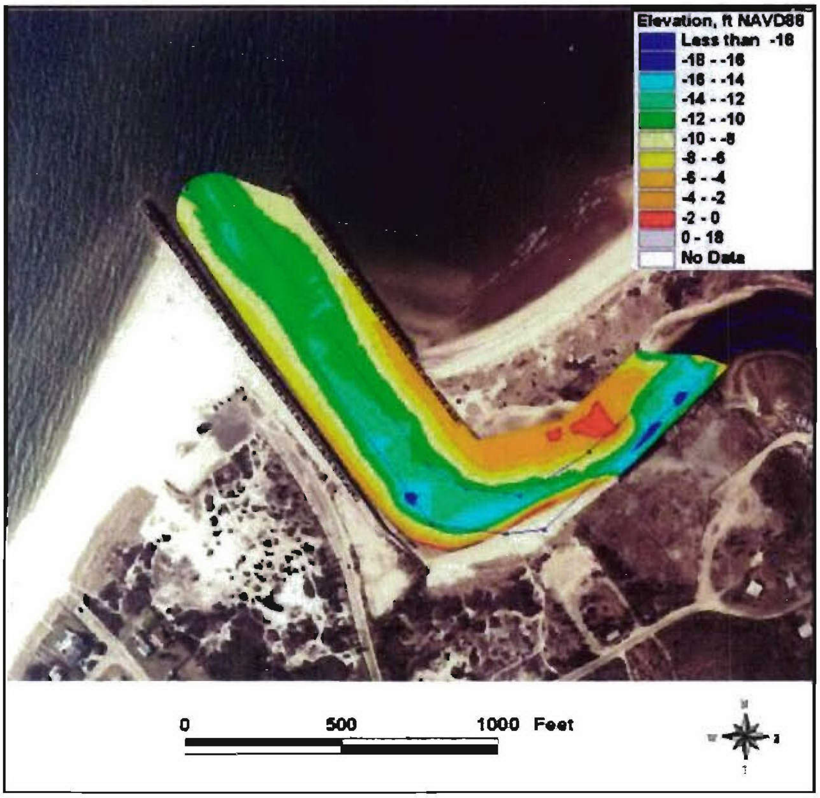

Figure 3-15. Mattituck Inlet flood shoal, 6-8 October 2002

Figure 3-16. Mattituck Inlet flood shoal, eastern bank, view looking west, March 2003

Figure 3-17. Mattituck Inlet flood shoal, eastern bank, view looking east, 21 November 2003

Navigation channel morphology. The Mattituck Inlet Federal navigation channel is maintained to a depth of 7 ft mlw with 2 ft allowable overdraft. The most recent dredgings took place in October 1990 and in March 2004. Figure 3-18 illustrates channel elevations for the 6-8 October 2002 bathymetric survey. The navigation channel has an approximate average depth of 12 ft NAVD88 (approximately 9 ft mlw), but depth reaches 16 ft at the turn east from the entrance.

Locations of channel transects are shown in Figure 3-19. Figures 3-20a through 3-20c display cross sections of the channel, the area of the flood shoal, and the progressive narrowing of the channel. Figure 3-21 shows the approximate location where this narrowing occurs. The Federal navigation channel is widest between the jetties. Channel infilling occurs on the west side near the channel entrance (Transect 2) and on the east side thereafter. At the channel turn, the bank is steep on the southwest side (Transects 5 through 7), indicating scouring by the ebb current and by waves. Beyond the turn, the channel narrows and is constricted by the growth of the gravelly beach on the southwest side (Transects 7 and 8) and by the shore-attached flood shoal on the northern bank (Transects 9 and 10).

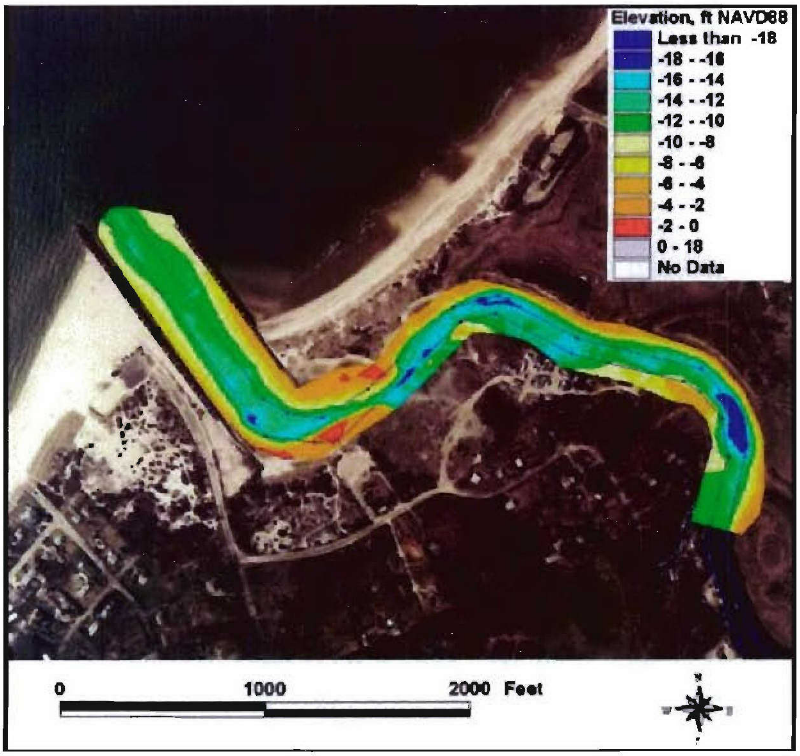

Figure 3-18. Mattituck Inlet Federal navigation channel elevation, 6-8 October 2002

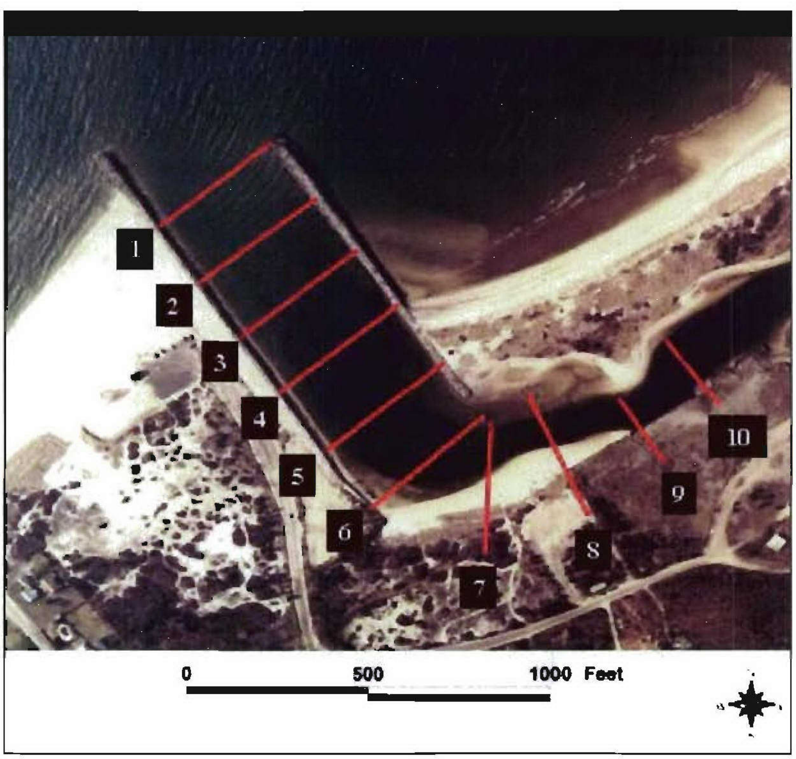

Figure 3-19. Mattituck Inlet channel transects, 6-8 October 2002

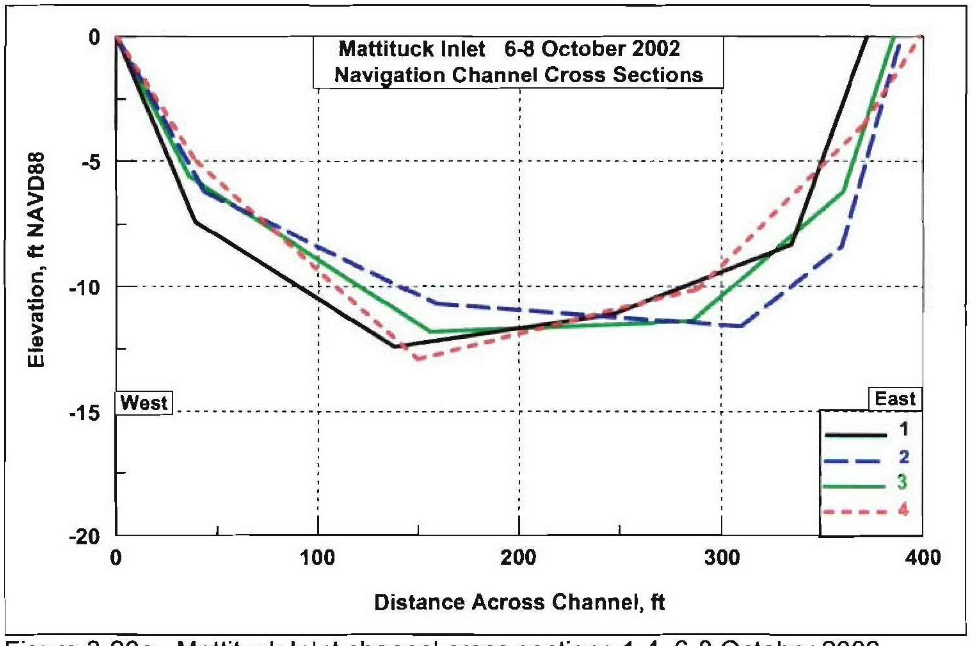

Figure 3-20a. Mattituck Inlet channel cross sections 1-4, 6-8 October 2002

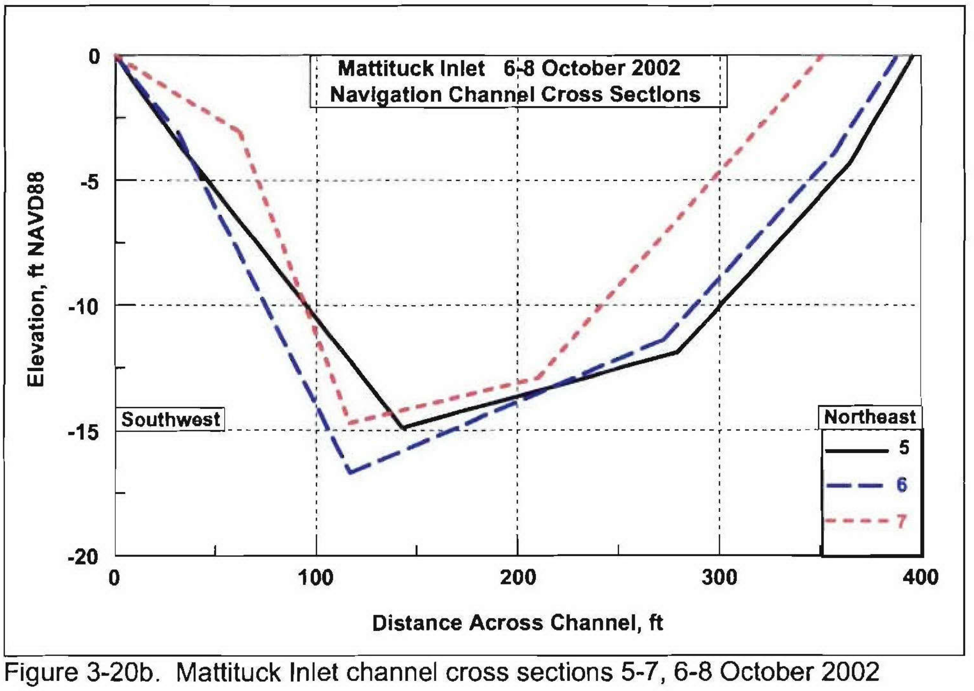

Figure 3-20b. Mattituck Inlet channel cross sections 5-7, 6-8 October 2002

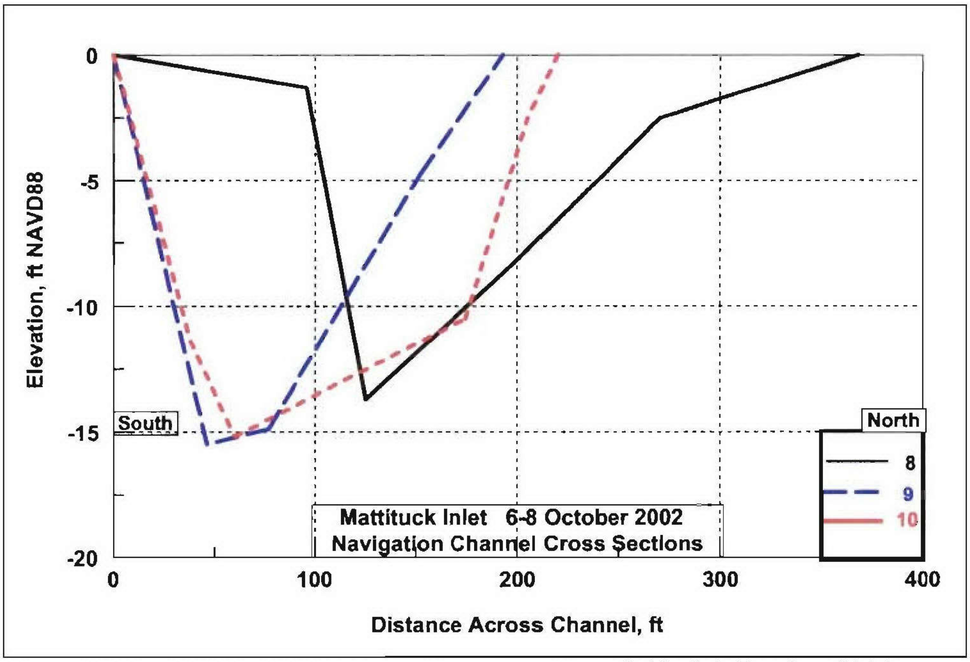

Figure 3-20c. Mattituck Inlet channel cross sections 8-10, 6-8 October 2002

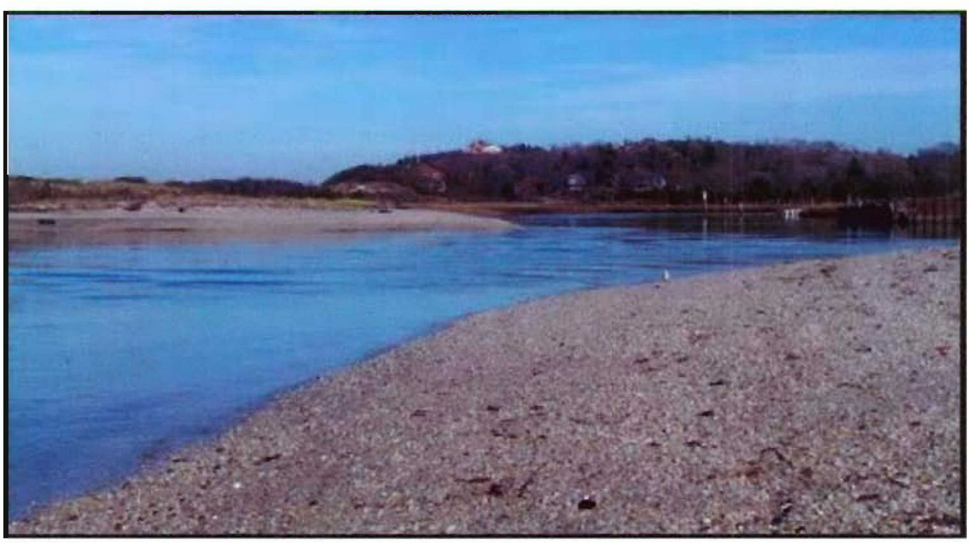

Figure 3-21. Mattituck Inlet shore-attached flood shoals on northern and southern banks of channel, view looking east, 21 November 2003

Water level

Water level was measured at the two locations shown in Figure 3-22. Tide Gauge 1 was secured to the end of the Mattituck Inlet west jetty. Tide Gauge 2 was secured to a piling near the town bulkhead and the Old Mill Inn Restaurant (GPS location lat. 41°00.552′N, long. 72°32.942′W). The data were referenced to msl datum of record (time duration of the October data collection) and converted to the NAVD88 datum. No conversion was done for the areas offshore, because NAVD88 is 0.059 m (0.2 ft) above msl in this area of the Long Island Sound[1], and the sea surface was not sufficiently calm to make meaningful the geodetic datum conversion to 0.05-ft accuracy.

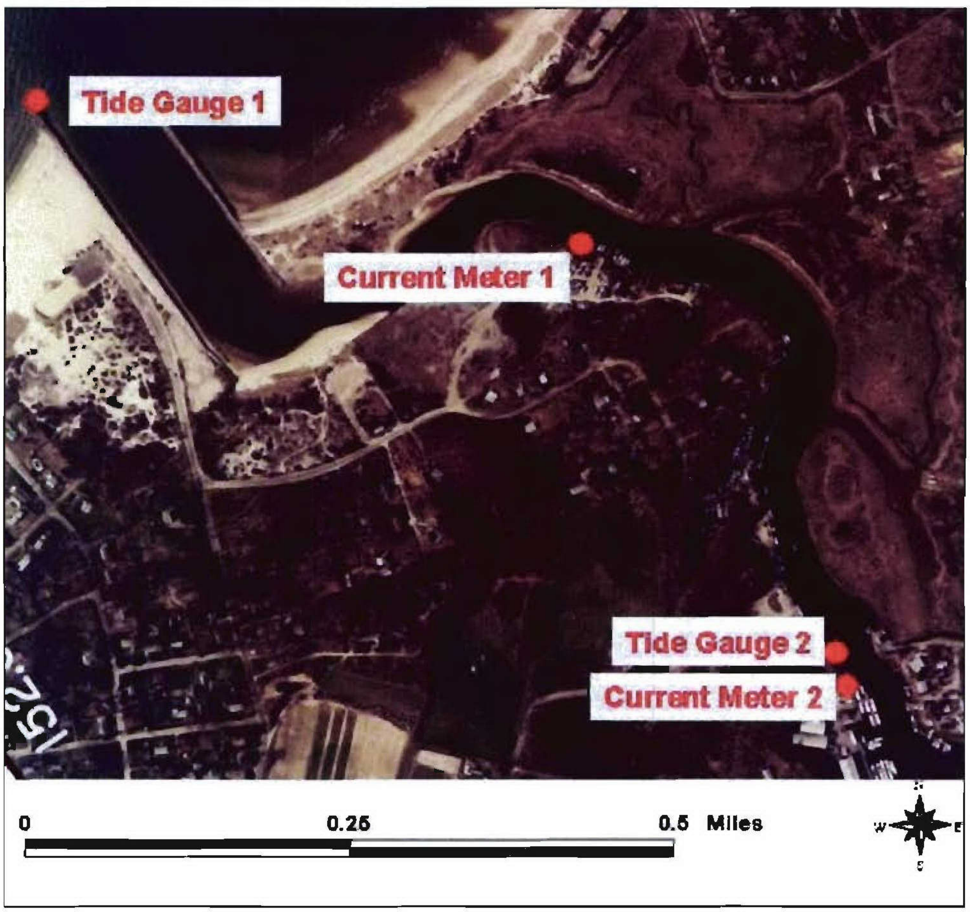

Figure 3-22. Mattituck Inlet tide gauge and current meter locations, 19 September-8 October 2002

Water-level data collected during the survey are plotted in Figure 3-23a with respect to Greenwich Mean Time (GMT). At the time of the data collection, GMT led local time

[1] At the Port Jefferson, NY, NOS tide gauge (Station ID 8514560), located approximately 48 km west of the study site, the 1983-2001 tidal epoch tidal datums mean tide level (mtl) and msl are given as 1.076 and 1.073 m, respectively, and NAVD88 datum is at 1.132 m with respect to mllw.

(Daylight Savings Time) by 4 hr. Figure 3-23b shows water levels for 5-7 October 2002, during spring tide. The distance between Tide Gauge 1 and Tide Gauge 2 is approximately 5,200 ft. Measured tidal ranges varied from 3.8 to 7.2 ft (at both locations). The mean tide range offshore for the deployment was calculated to be 5.21 ft, and the mean tide range in Mattituck Creek was calculated to be 5.26 ft. A 1-day spring tidal range of approximately 6 ft was observed at both locations. Offshore at Mattituck Inlet, the duration of the average ebb tide (defined as peak to trough) of record was 6 hr, 5 min, and the duration of the average flood tide (trough to peak) was 6 hr, 19 min. In Mattituck Creek, the duration of the average ebb tide of record was 6 hr, 13 min and the duration of the average flood tide was 6 hr 10 min. Signell et al. (2000) found that the duration of the ebb tide in the eastern portion of Long Island Sound is 15 min longer than the duration of the flood tide in that water body. The reversal to slightly longer flood tide than ebb in the inlet is attributed to generation of overtides and other nonlinearities as the tidal wave propagates into shallow water.

The measured mean tide range and spring tide range are consistent with those provided by NOS for this area.[1] The 20-day record indicates a slight increase in tide range in the inlet as compared to the offshore, attributed to tidal wave shoaling in shallow water and slight resonance in the enclosed channel system.

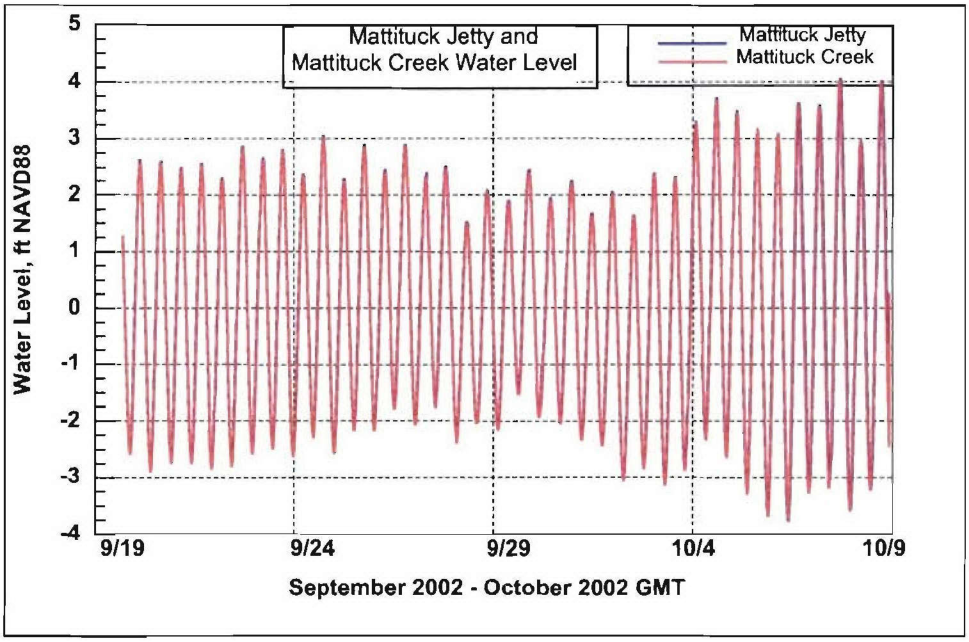

Figure 3-23a. Mattituck Inlet water level, 19 September – 8 October 2002

[1] At the Mattituck Inlet, NY, NOS subordinate station, NOS lists 5.4 ft as mean tide range and 6.2 ft as spring tide range for Mattituck Inlet.

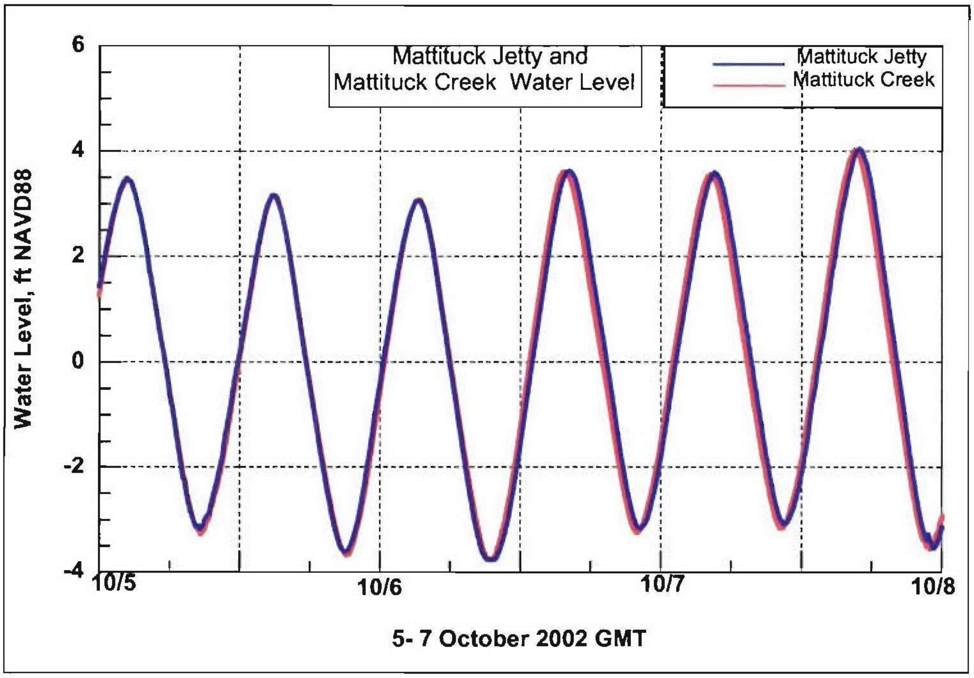

Figure 3-23b. Mattituck Inlet water level, 4-8 October 2002

The phase lag, τ, between the two water-level gauge locations was calculated by determining the time difference between the respective peaks and troughs of each tidal cycle. The modal phase lag for the measurement duration was 6 min, with the median value of 5.1 min. As expected, the peaks and troughs at Tide Gauge 1 typically led those of Tide Gauge 2. Because there was a time interval indicating a phase reversal, only those cycles when the offshore led the back bay were selected to calculate the median phase lag. From approximately 1400 GMT on 6 October 2002 to 1500 GMT on 7 October 2002, a phase reversal was recorded, when the peaks and troughs inside Mattituck Creek led those offshore by 12 to 18 min. A change in phase was not observed at Goldsmith Inlet for this time period. The reason for the reversal is not known.

The median phase lag allows an estimation of the equivalent cross-channel depth of Mattituck Creek between the two tide gauges. The celerity C of a long wave is $C = \sqrt{gh_*}$, where g = acceleration of gravity (32.2 ft/sec^2), and h_* = equivalent average along-channel and cross-channel depth between the two gauges. With the length λ = 5,200 ft between water-level gauges, the equivalent depth is $h_* = \lambda^2 / g\tau^2$ = 9 ft, for τ = 5.1 min (median lag). This value is consistent with the average water depth in the dredged channel at msl.

Current

Current Meter 1 was secured to a piling at Peterson's Marina (GPS coordinates lat. 41°00.842'N, long. 72°33.172'W), adjacent to Tide Gauge 2, at approximately 3-ft water depth. The instrument was deployed on 7 October 2002 at 2236 GMT and retrieved on 8 October 2002 at 2130 GMT. Current Meter 2 was mounted on a floating barge secured to shore near the town bulkhead (GPS coordinates lat. 41°00.552'N, long. 72°32.942'W) in approximately 2-ft water depth. Current Meter 2 was deployed on 7 October 2002 at 2306 GMT and retrieved on 8 October 2002 at 2352 GMT.

A maximum velocity of 0.43 m/sec was recorded at Current Meter 1, and instantaneous velocities exceeding 0.50 m/sec were recorded at Current Meter 2 (Figure 3-24). The second half of the data record from Current Meter 2, which failed after about 11 hr, was considered questionable and is not presented. Flood current is directed positive and ebb current is directed negative. The maxima on 8 October 2002 correspond to the near maximum water elevation at spring tide (Figure 3-23b). This instrument was secured to a floating barge, and the high-frequency fluctuations are attributable to movement of the barge with surface waves and wind. The velocity phases and magnitudes at both locations are consistent. Relative velocities at these point measurements are not readily compared because of the different water depths and proximities of the gauges to the channel or jetty. The measurements show plateaus in the maxima and minima, indicative of nonlinearities in water motion due to tidal wave shoaling and bottom friction.

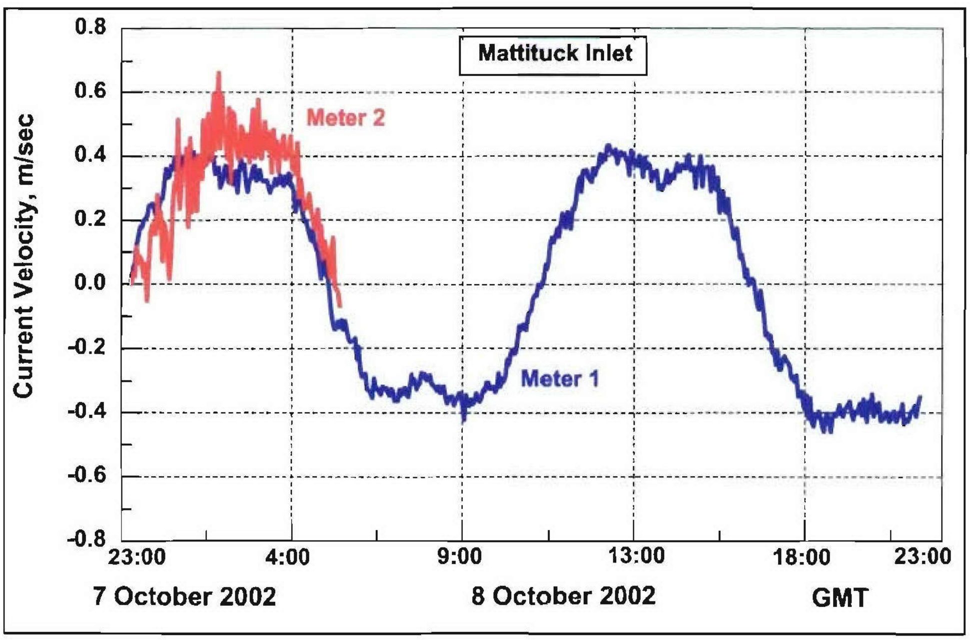

Figure 3-24. Mattituck Inlet along-channel current velocity, 7-8 October 2002

Sediment

The New York District collected 16 sediment samples at Mattituck Inlet and Mattituck Creek on 6 and 7 May 2003. The sampling locations are shown in Figure 3-25. Of the samples, two (MH7 and MH9) were not analyzed and are not shown. The location of sample MH14 was uncertain and is not shown. Inspection of samples MH11 through MH16 (taken from the southern portion of Mattituck Creek) indicated that they contained more than 90 percent silt and clay, so they were not further processed. The upper and lower portions of samples MH5 and MH8 were analyzed separately because substrate layering was apparent.

Only the results of the upper portion are presented here for the data interpretation to be consistent with surface samples taken at Goldsmith Inlet. The New York District (2003) analysis presented the data grouped in United States Department of Agriculture (USDA) particle size classes. These results are presented here in phi units. Selected ϕ unit conversions to millimeters are given in Table 3-1. Figures 3-26a and 3-26b show the cumulative grain size for all the samples that were analyzed.

Sediment from the Federal navigation channel near the mouth of the inlet consists of a mixture of coarse, medium, and fine sand (0 to 3 ϕ). Sediment from the west side of the Federal navigation near the landward edge of the west jetty (an area of shoaling) consisted of gravel and coarse sand (> 0 ϕ). It is inferred that this is an area where the flood current initially deposits much of the sediment brought into the inlet. The gravel and coarse sand remains as a lag deposit under the action of waves striking shore after entering the inlet, and finer (sand-sized) sediments are transported further into the inlet.

Table 3-1
Phi (ϕ) Units and Millimeter (mm) Equivalents

Phi (ϕ) Units	Millimeters
-6	64
-5	32
-4	16
-3	8
-2	4
-1	2
0	1
1	0.5
2	0.25
3	0.125
4	0.0625

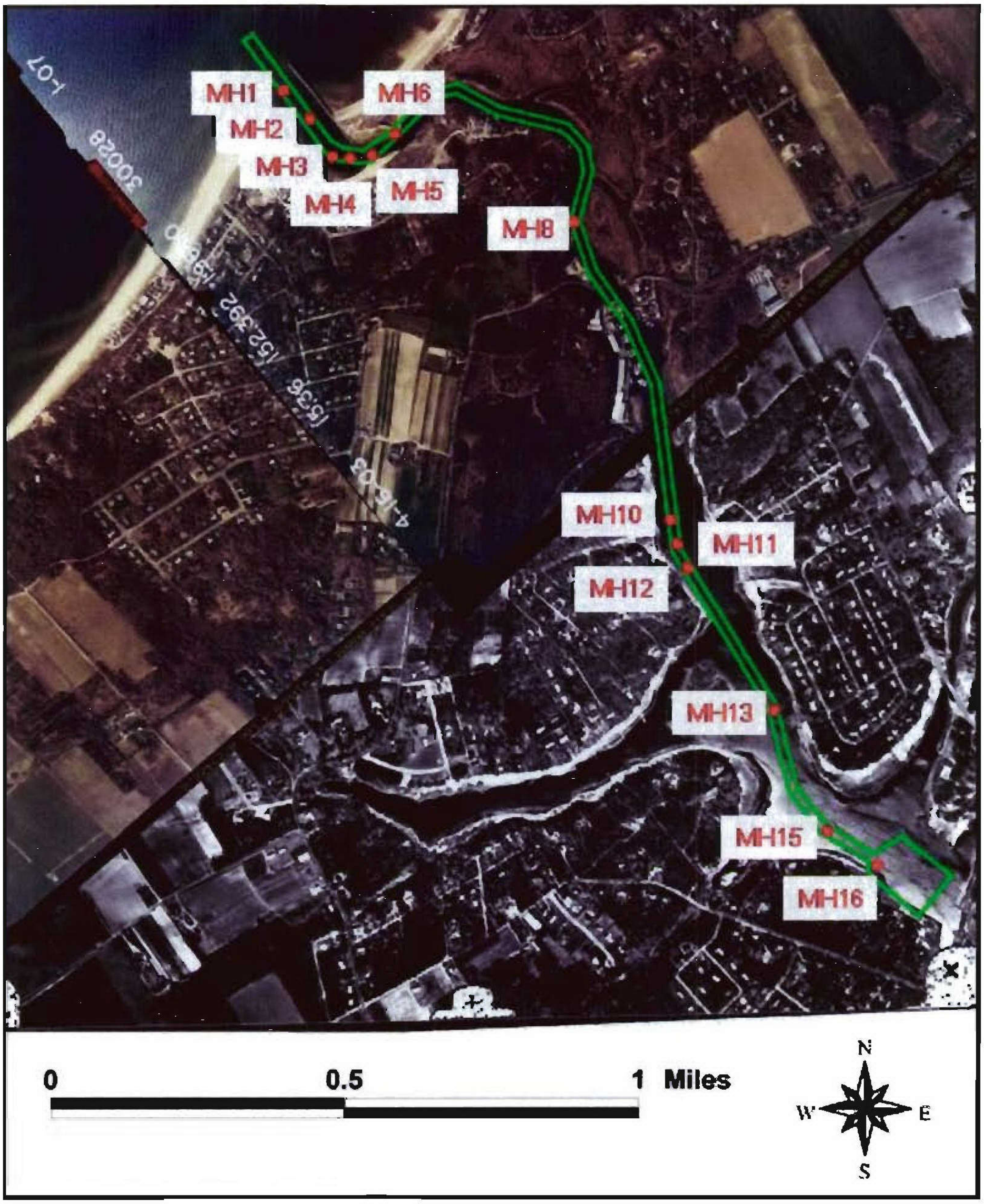

Figure 3-25. Mattituck Inlet sediment sample locations, 6-7 May 2003

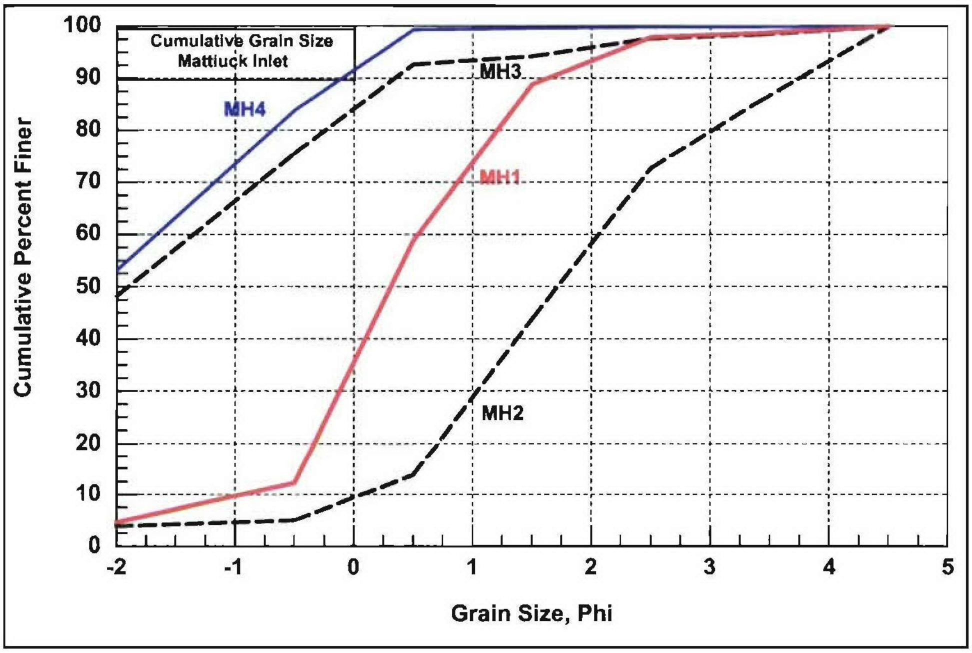

Figure 3-26a. Mattituck Inlet cumulative grain size distribution MH1-MH4, 6-7 May 2003, (data from New York District (2003))

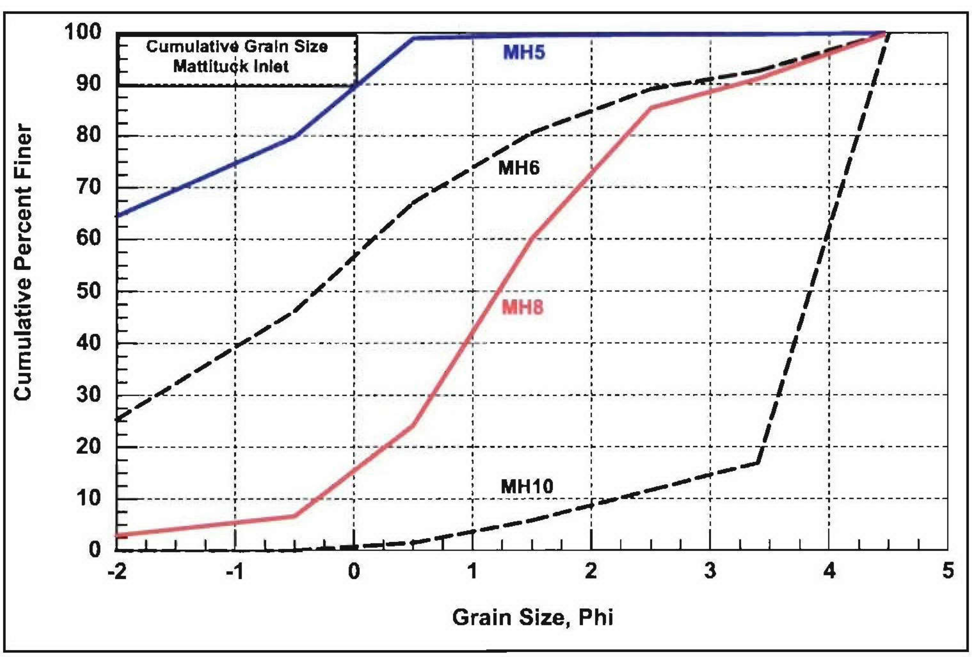

Figure 3-26b. Mattituck Inlet cumulative grain size distribution, MH5, MH6, MH8, and MH10, 6-7 May 2003, (data from New York District (2003))

Sediment from the main area of shoaling, near the base of the east jetty, was composed primarily of very coarse to coarse sand (-1 to 1 ϕ). Sediment mobilized by waves that reflect from the west bank, where the inlet turns, may be moved by the flood current and redeposited here, whereas finer sediments can be transported further into the inlet. Sediment from approximately 1.5 km up the channel consisted primarily of medium to fine grained sand (1 to 3 ϕ), and samples taken beyond this location are primarily composed of silt and clay (< 4 ϕ). In summary, it appears that the mixture of sediment brought into the entrance by the tidal current tends to sort, with the coarser materials remaining at the bend, where the ebb-tidal current weakens, and the finer material transported further east into the channel.

Offshore sediment samples were collected and analyzed by the New York District (1969). Figure 3-27 shows the approximate profile locations for the New York District study against the interpolated bathymetry data of the 6-8 October 2002 survey. The profile locations were approximated from a hard copy map of the 1969 survey. Table 3-2 lists the median grain sizes found at Profiles 56 and 57 of this study. Profile 56 is located 500 ft west of the inlet, and Profile 57 is 2,000 ft east of the inlet and, therefore, intersects the offshore shoal. The report gives the median grain size together with location depth, and no reference datum is provided. It is assumed that the datum depth of sampling was the New York District mlw.

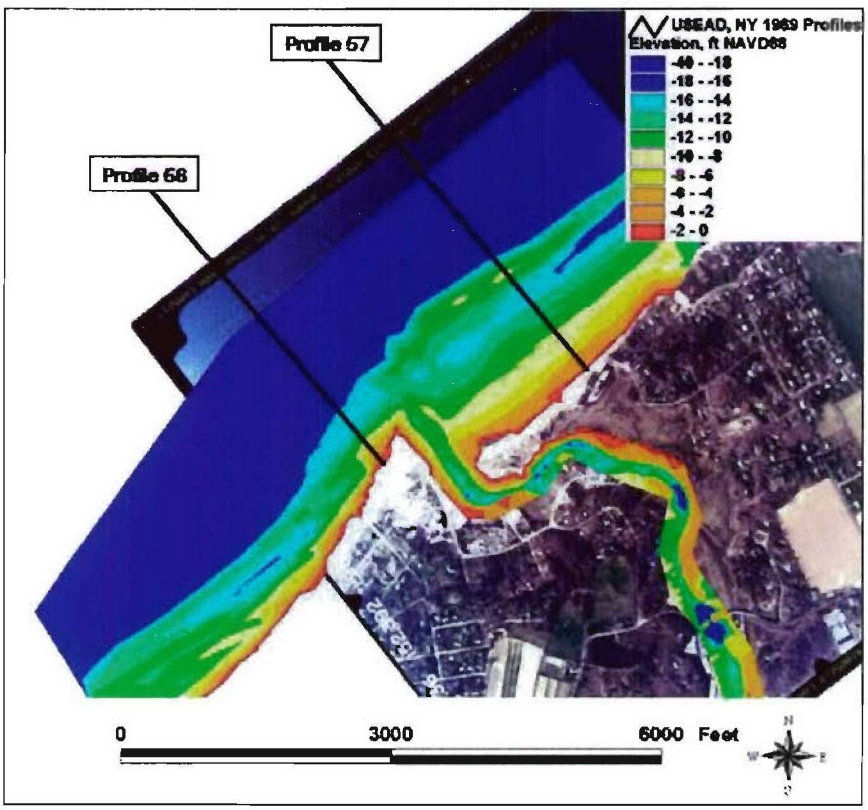

Figure 3-27. Mattituck Inlet, New York District (1969) sediment sampling profile locations

Table 3-2
Grain-Size Analysis, Mattituck Inlet Offshore Area, Profiles 56 and 57 (New York District 1969)

Location Depth (ft) (mlw assumed)	Grain Size		Classification of Material (percent)			
	Range of sizes (mm)	Median grain size (mm)	Fine Sand	Medium Sand	Coarse Sand	Gravel
Profile 56, 500 ft west of Mattituck Inlet						
Backshore	0.25 - 19.0	1.09	5	72	9	14
High water	0.25 - 25.4	7.45	3	25	11	61
Midtide	0.50 - 25.4	3.15	0	42	14	44
Low water	0.40 - 19.0	5.95	0	10	26	64
6	0.10 – 4.76	0.57	27	71	2	0
12	0.10 - 1.00	0.40	65	35	0	0
18	0.08 – 2.36	0.25	86	14	0	0
24	0.07 - 2.36	0.26	88	12	0	0
30	0.07 - 2.36	0.37	65	34	1	0
Profile 57, 2,000 ft East of Mattituck Inlet						
Backshore	0.10 – 25..4	0.56	34	39	6	21
High water	0.15 – 4.76	0.55	15	83	2	0
Midtide	0.29 – 4.76	0.49	24	75	1	0
Low water	0.27 – 38.1	4.75	7	35	8	50
6	0.13 – 2.36	0.38	60	40	0	0
12	0.10 – 38.1	0.55	21	47	1	31
18	0.10 – 2.36	0.23	90	10	0	0
24	0.09 – 4.76	0.21	90	9	1	0
30	0.08 – 4.76	0.38	59	40	1	0

The center line of the offshore shoal at Mattituck Inlet is located 1,600 ft offshore at a depth of 10 ft NAVD88. The New York District sample at the depth of 12 ft mlw (approximately 14.5 ft NAVD88) on Profile 57 is, therefore, located on or near the ebb shoal. This sample location has a median grain size of 0.55 mm and, significantly, is composed of 47 percent medium-grain sand and 31 percent gravel. The large amount of coarse material represents a departure from characteristics of other samples in this study, where fine to medium grain sand predominate. The coarseness of material on the offshore shoal as compared to adjacent areas indicates the shoal is a lag deposit under the tidal current and storm waves breaking on it.

Goldsmith Inlet

The 6-8 October 2002 bathymetric survey of the offshore adjacent to Goldsmith Inlet was conducted with an Innerspace 448 high-precision echo sounder and a Global Positioning System (GPS). Positional accuracy is estimated at +/-1 m. Goldsmith Inlet and Pond, the beaches adjacent to the inlet, and the area from the shoreline to wading depth were surveyed with land-based equipment (total survey station and surveying rod). The survey of Goldsmith Inlet and Goldsmith Pond was conducted on 8 October 2002.

A Seabird26 Paroscientific Digiquartz Pressure Sensor-based tide gauge (Tide Gauge 3) was deployed from 19 September to 8 October 2002. Flood current velocity was measured in the inlet from 1323 to 1643 GMT, 8 October 2002 by means of a hand-held current meter mounted on a pole that was sunk into the bed (see Figure 4-49). Values were read visually and recorded by hand. Fourteen sediment grab samples were collected from Goldsmith Inlet on 8 October 2002, supplemented by 17 samples collected on 31 July 2003. In addition, sediment samples collected and analyzed by the New York District (2003) for the offshore area at Goldsmith Inlet are discussed here.

Bathymetry

The extent of the survey for the Goldsmith Inlet study area is presented in Figure 3-28a, and interpolated elevation contours for the Goldsmith Inlet study area are plotted in Figure 3-28b. An interesting finding of the survey is that Goldsmith Inlet lacks an ebb shoal. An implication from this observation is that bypassing from west to east occurs around the jetty, along the spit, and then back to the shore on the east side along a bypassing bar. In contrast, Goldsmith Inlet possess a well-developed flood shoal consisting of three lobes. The lobes are located on the east bank, center channel, and west bank, where Goldsmith Inlet enters Goldsmith Pond.

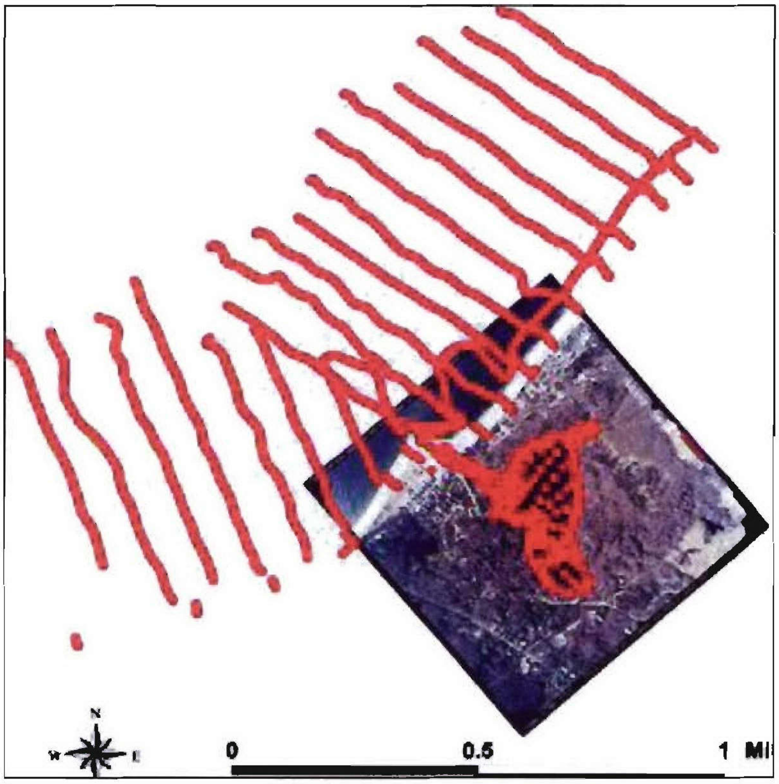

Figure 3-28a. Goldsmith Inlet bathymetry survey coverage, 6-8 October 2002

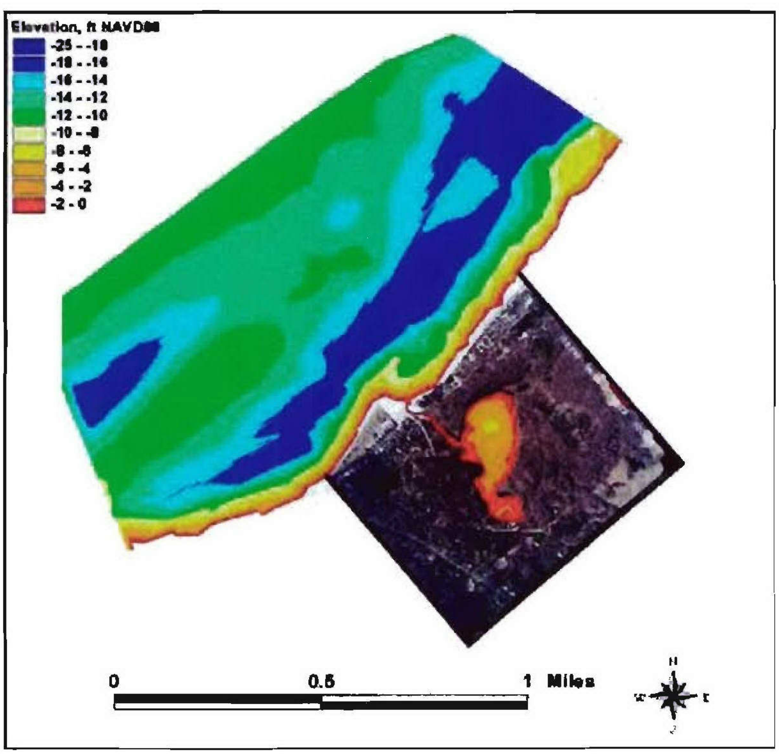

Figure 3-28b. Goldsmith Inlet elevation contours, 6-8 October 2002

Offshore morphology. The location of the offshore transects of the 6-8 October 2002 survey are shown in Figure 3-29. Figures 3-30a and 3-30b display beach profiles west of the inlet, and Figures 3-31a and 3-31b display beach profiles west of the inlet. The area offshore on both sides of Goldsmith Inlet has a steep gradient, with a slope of approximately 1:10 from the beach to a depth of approximately 18 ft NAVD88 (to approximately 700 ft offshore). A depression that is oriented parallel to the shoreline is located from 750 to 2,000 ft offshore, where the depth reaches 22 ft NAVD88.

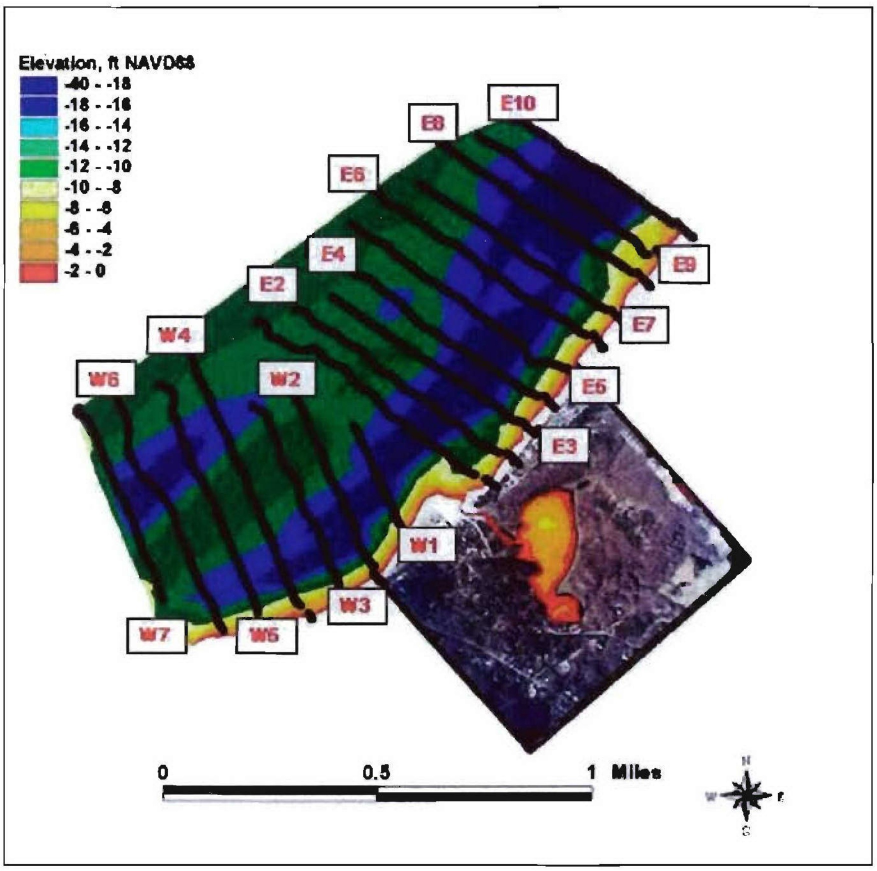

Figure 3-29. Goldsmith Inlet offshore survey transects, 6-8 October 2002

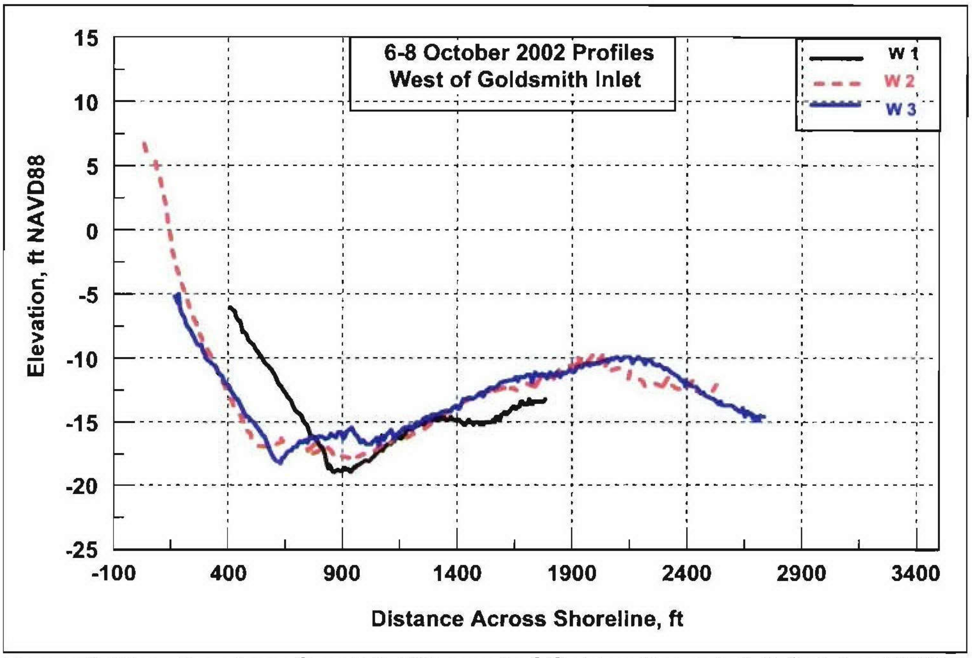

Figure 3-30a. Beach profiles W1-W3, west of Goldsmith Inlet, 6-8 October 2002

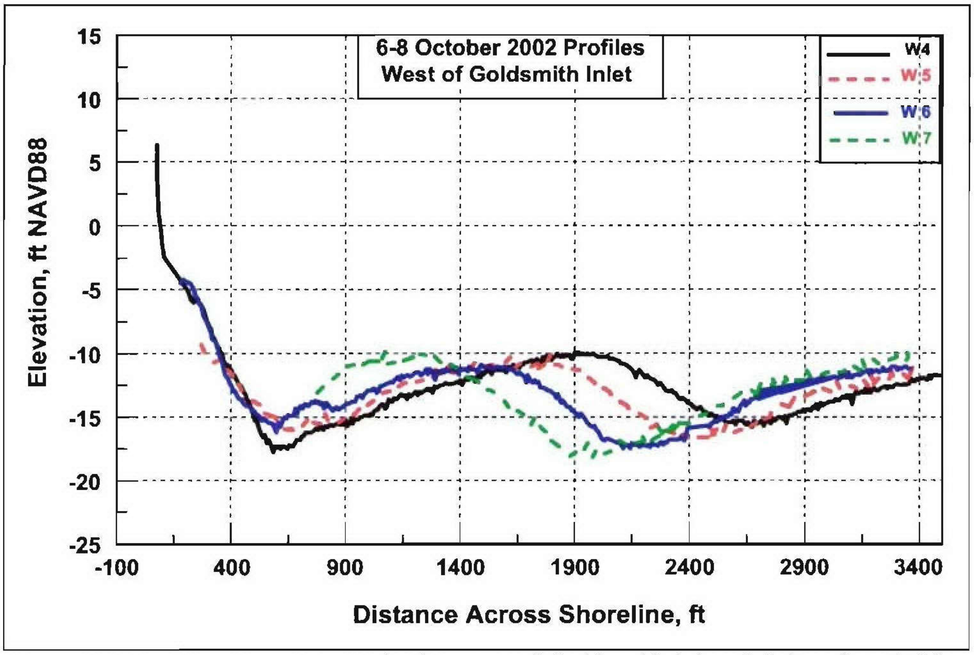

Figure 3-30b. Beach profiles W4-W7, west of Goldsmith Inlet, 6-8 October 2002

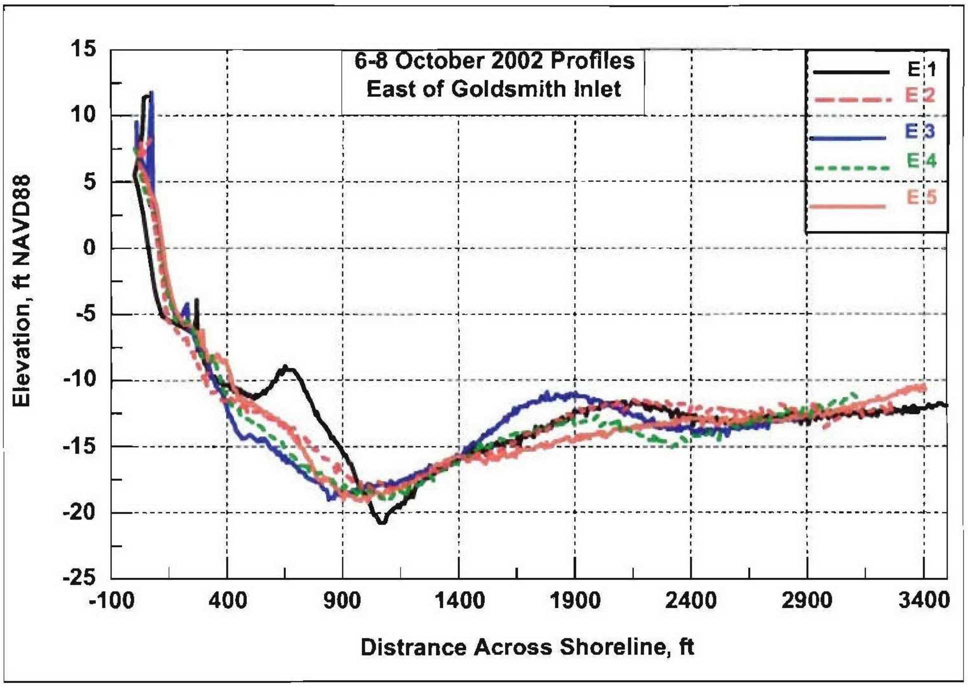

Figure 3-31a. Beach profiles E1-E5, east of Goldsmith Inlet, 6-8 October 2002

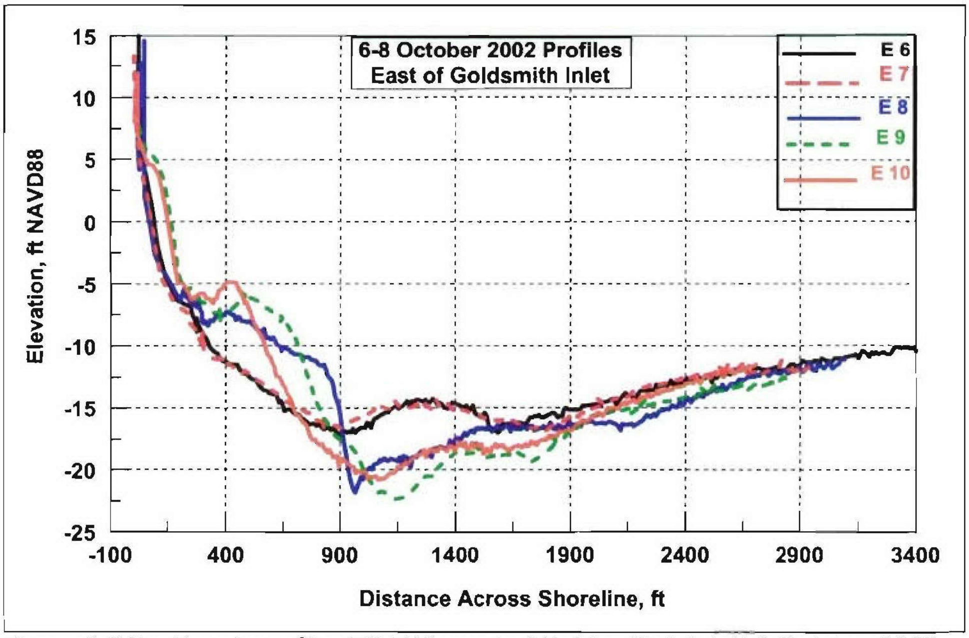

Figure 3-31b. Beach profiles E6-E10, east of Goldsmith Inlet, 6-8 October 2002

To the west of the inlet, an elevated formation (shoal) is located 1,000 to 2,000 ft offshore. Because of this distance, the presence of this formation is not considered to be a consequence of the presence of either the modern or the historic inlet. The shoreline west of Goldsmith Inlet is characterized by a relatively uniform shoreline (Figure 3-32 and Figure 3-33), and a large number of glacial erratics. The shoreline east of Goldsmith Inlet is less uniform (Figure 3-34 and Figure 3-35). The offshore is covered with glacial erratics as well. In contrast to Mattituck Inlet, there are no longshore bars near Goldsmith Inlet, which may be attributed to the pronounced depression discussed in the preceding paragraph.

Figure 3-32. Aerial view of shoreline west of Goldsmith Inlet, 16 April 2003

Figure 3-33. Ground view of shoreline west of Goldsmith Inlet, 28 March 2003

Figure 3-34. Aerial view of shoreline east of Goldsmith Inlet, 16 April 2003

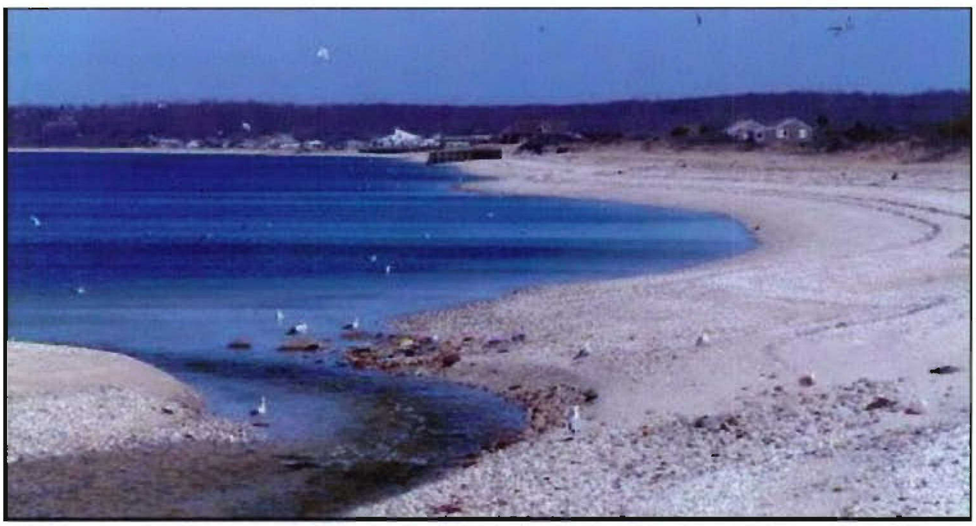

Figure 3-35. Ground view of inlet entrance and shoreline east of Goldsmith Inlet, 28 March 2003

Flood shoal morphology. The flood shoal at Goldsmith Inlet consists of three lobes that are located on the east bank, on the west bank, and in the channel where the inlet enters Goldsmith Pond (Figure 3-36). Because of the mild elevation relief at Goldsmith Pond, the east and west lobes of the flood shoal are exposed during low water (Figures 3-37 through 3-39). Figures 3-40a through 3-40c depict the contours of Goldsmith Pond at low tide, mean tide, and high tide for 8 October 2002. The current velocity and water level for both study areas were measured during 6-8 October 2002, in coordination with the bathymetric survey. The current and water-level measurements are discussed in the following sections.

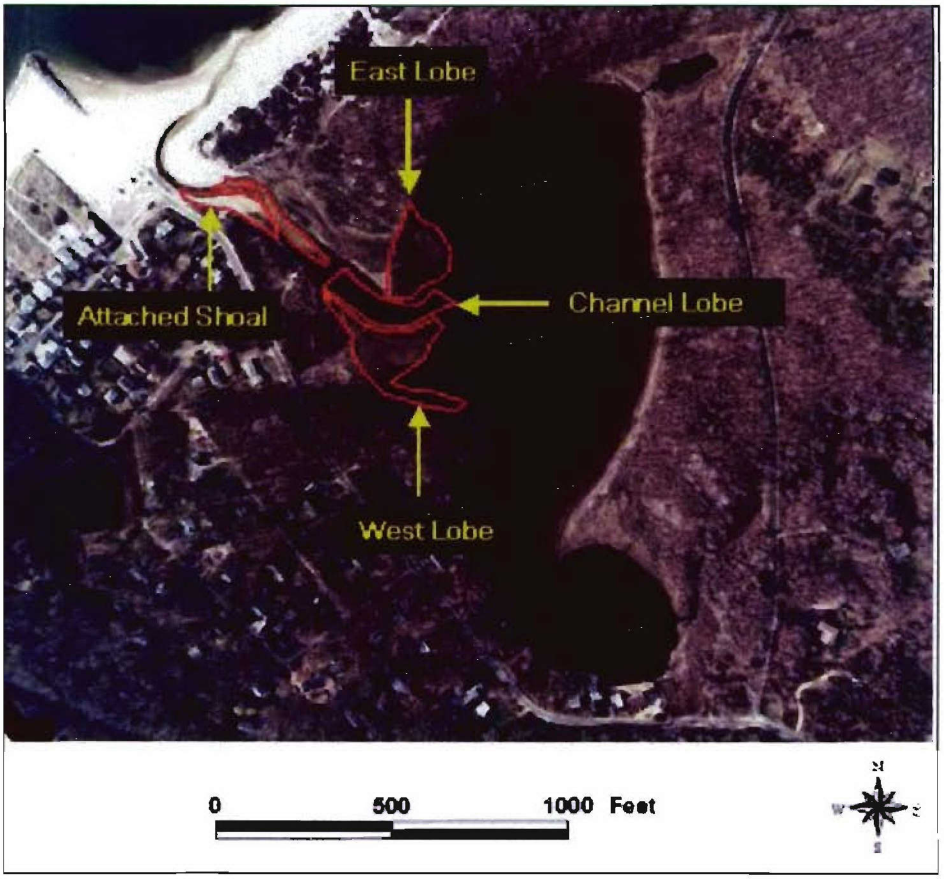

Figure 3-36. Goldsmith Pond flood shoal formations, 16 April 2003

Figure 3-37. Goldsmith Inlet flood shoal, west lobe, view looking south, 28 March 2003

Figure 3-38. Goldsmith Inlet flood shoal, east lobe, view looking south, 9 July 2004

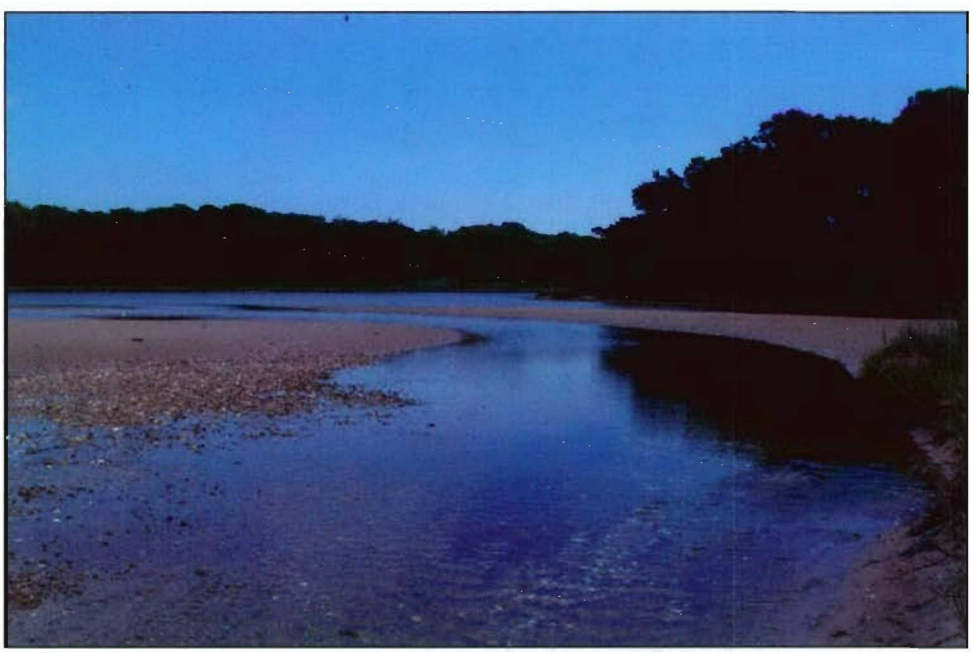

Figure 3-39. Goldsmith Inlet flood shoal, east and west lobe, view looking south, 9 July 2004

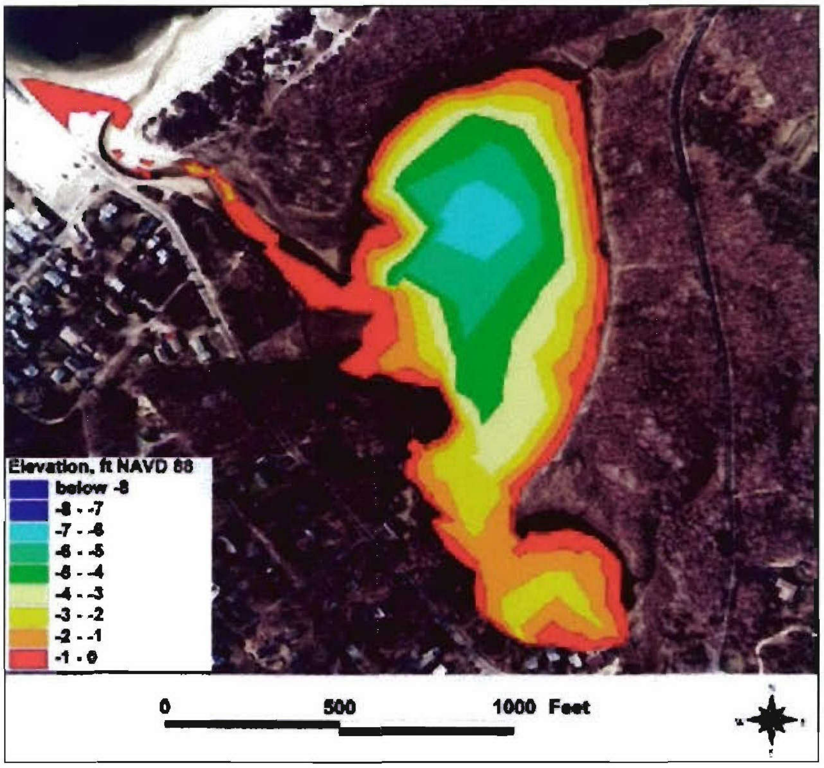

Figure 3-40a. Goldsmith Inlet contours at low tide, 8 October 2002

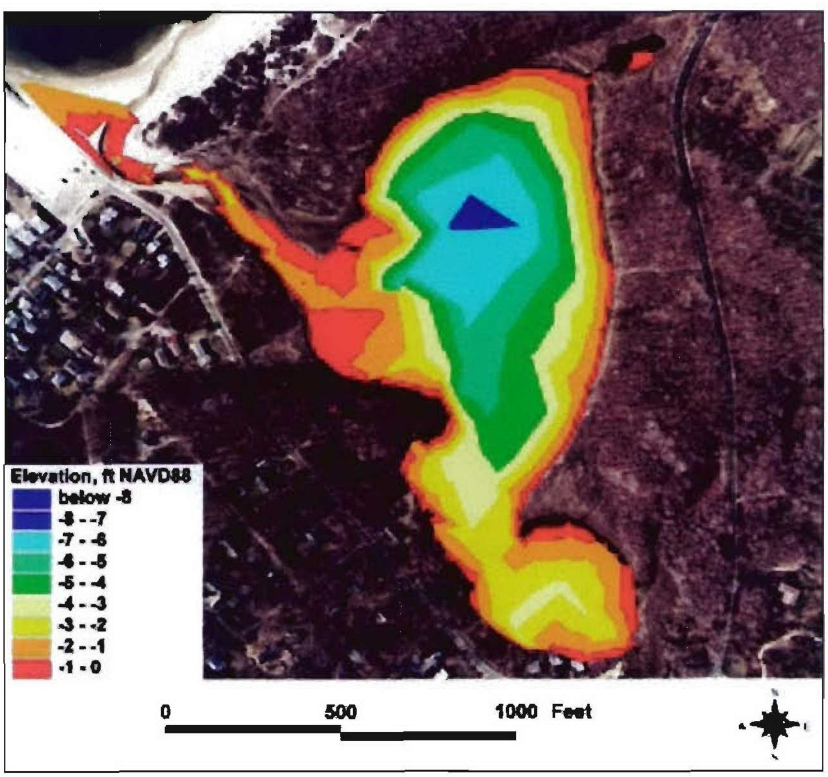

Figure 3-40b. Goldsmith Inlet contours at mean tide, 8 October 2002

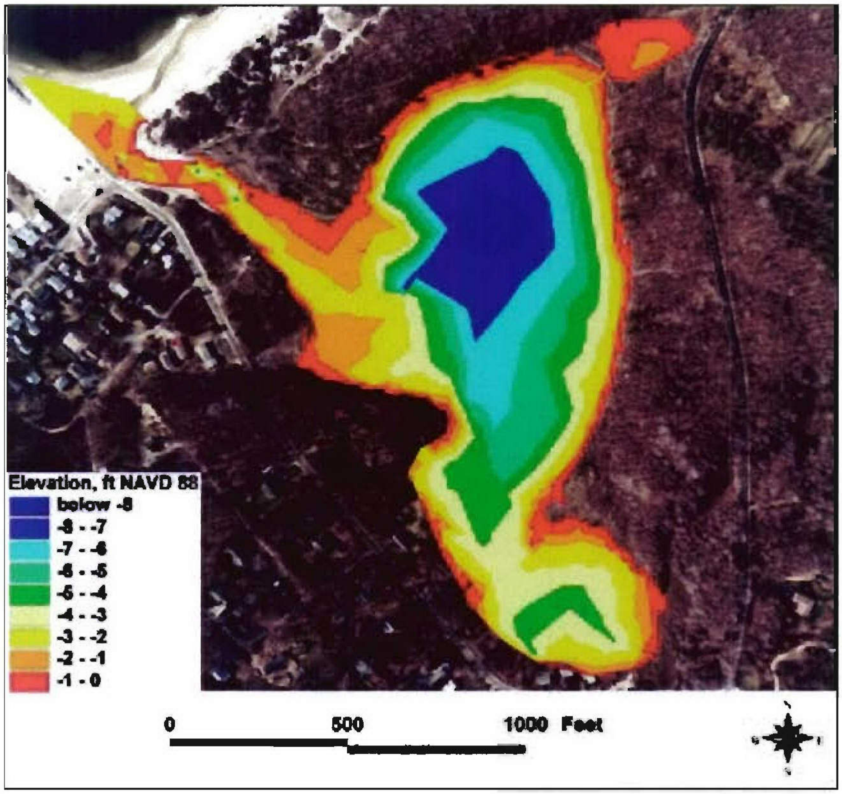

Figure 3-40c. Goldsmith Inlet contours at high tide, 8 October 2002

Channel morphology. The entrance channel at Goldsmith Inlet is narrow and shallow. Depths range between 1 and 4 ft NAVD88, and a large in-channel bar formation in the center of the channel becomes exposed during low tide (Figure 3-41). The channel has been observed to contain running water at all times during numerous field visits. At the time of the 6-8 October 2002 survey, the channel was 12 ft wide at the entrance to the Long Island Sound and expanded to 100 ft at the entrance to Goldsmith Pond.

An attached shoal is located approximately 800 ft into the inlet on the west bank. Sediment entering the inlet attaches to the inlet bank, occupying a portion of the inlet channel (Figure 3-42). Sediment entering the inlet during flood tide is inferred to have formed this feature. This attachment on the west bank may redirect the ebb and flood tidal current and decrease the flushing capacity of the inlet. Sediment also approaches the inlet entrance from the spit that forms adjacent to the jetty. The entrance channel tends to align to the east, a characteristic that has become more pronounced with growth of the attachment shoal and the buildup of sediment along the jetty.

Transects were extracted from the 8 October 2002 survey. Because Goldsmith Inlet is shallow, the survey was made based on changes in relief. Two-dimensional (2-D) transects were created from a three-dimensional (3-D) bathymetry grid to analyze of the morphology of Goldsmith Inlet. The transect lines are displayed in Figure 3-43, and channel cross sections are shown in Figures 3-44a through 3-44c. Figure 3-44a displays the shallow water at the inlet mouth. A longitudinal linear shoal that is dry during low tide can be seen in Transects 2 and 3. The relatively large attached shoal that has formed

on the west bank is illustrated in Figure 3-44b (Transects 5 and 6) and the east lobe of the flood shoal formation is depicted in Figure 3-44c (Transects 11 and 12).

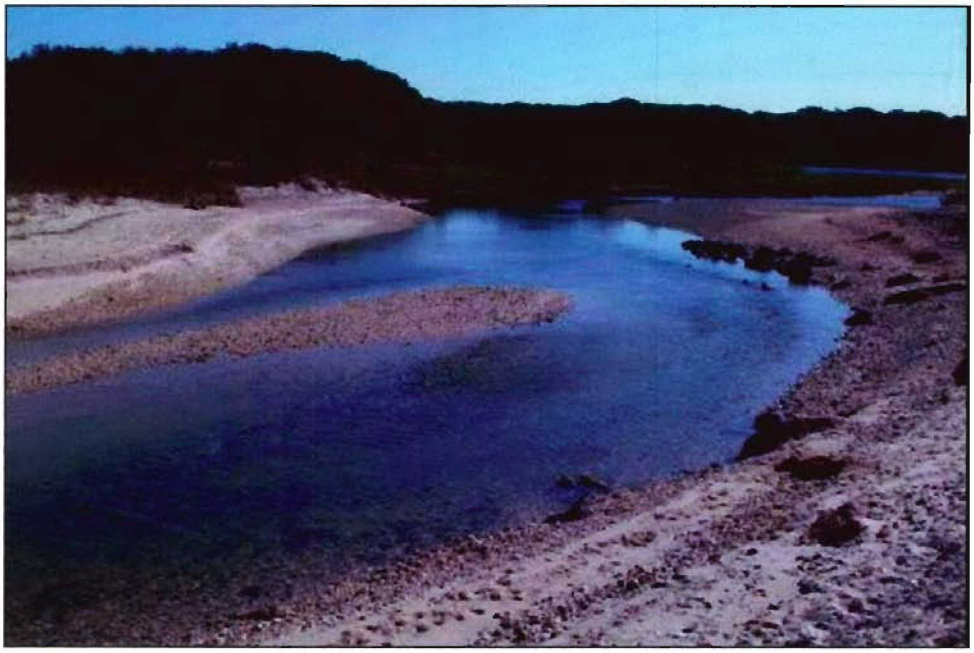

Figure 3-41. Goldsmith Inlet, channel with shoal, 28 March 2003

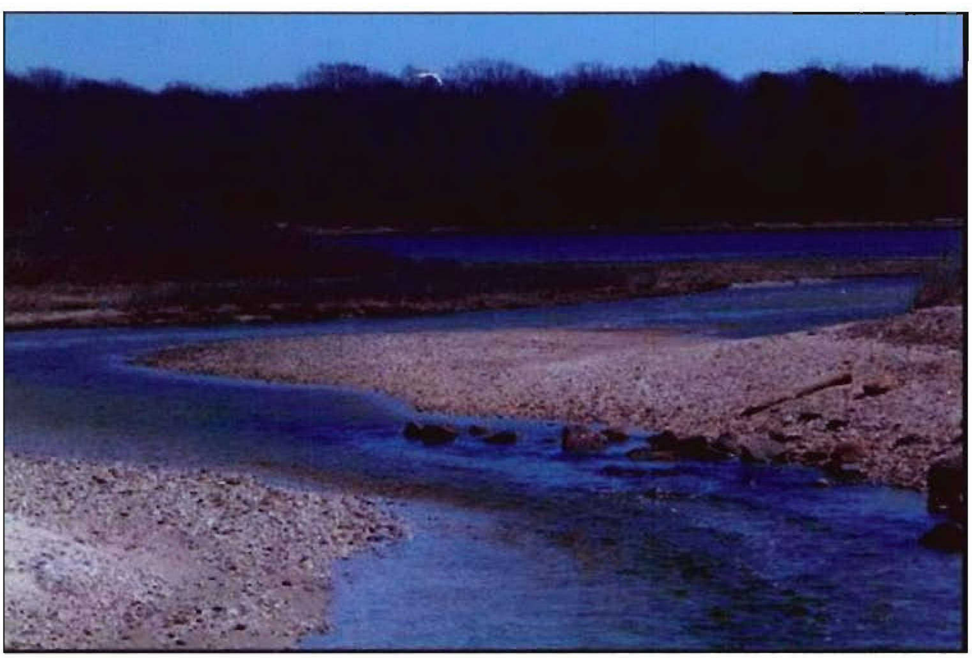

Figure 3-42. Goldsmith Inlet attached shoal, 28 March 2003

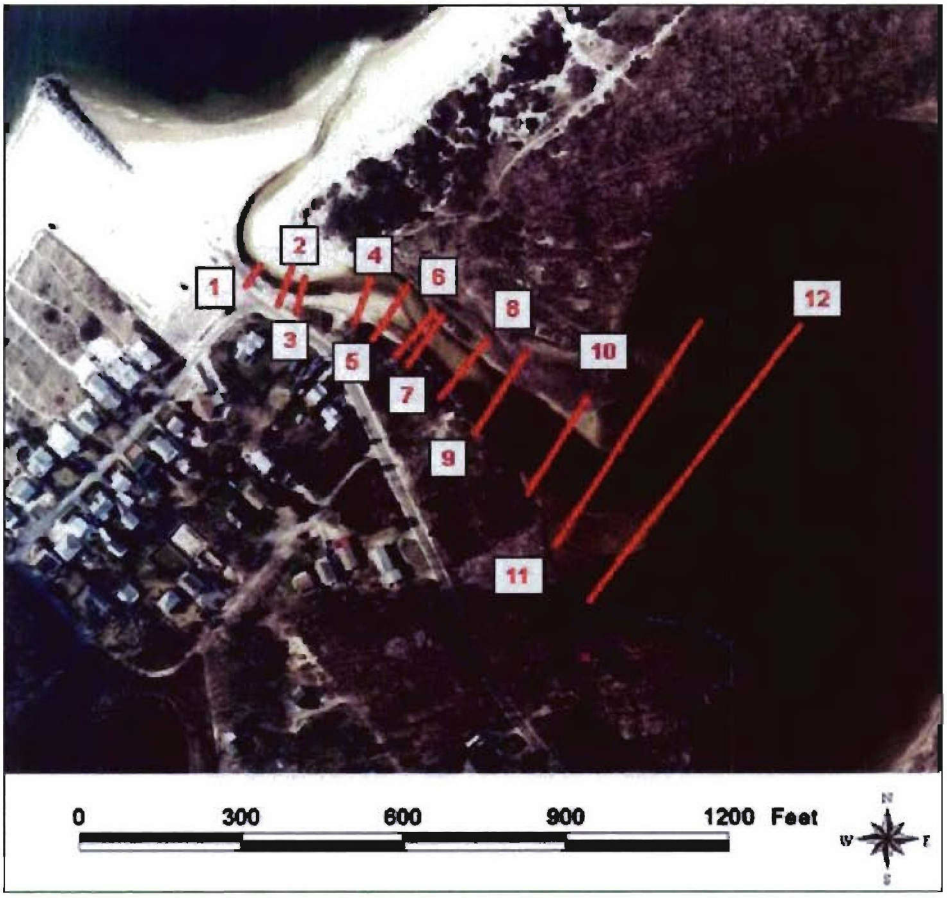

Figure 3-43. Goldsmith Inlet channel transects, 8 October 2002

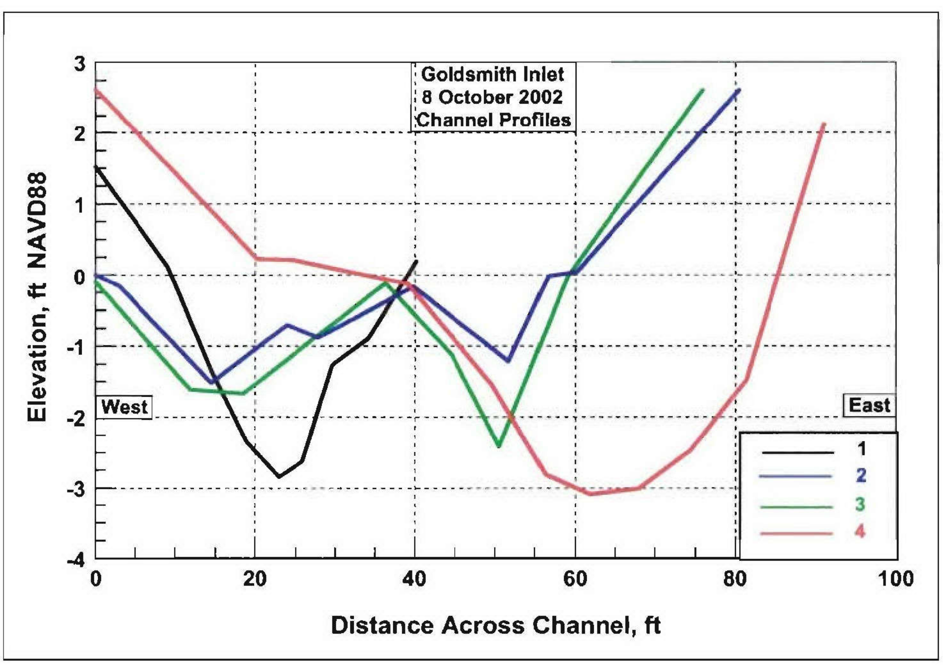

Figure 3-44a. Goldsmith Inlet channel cross sections 1-4, 8 October 2002

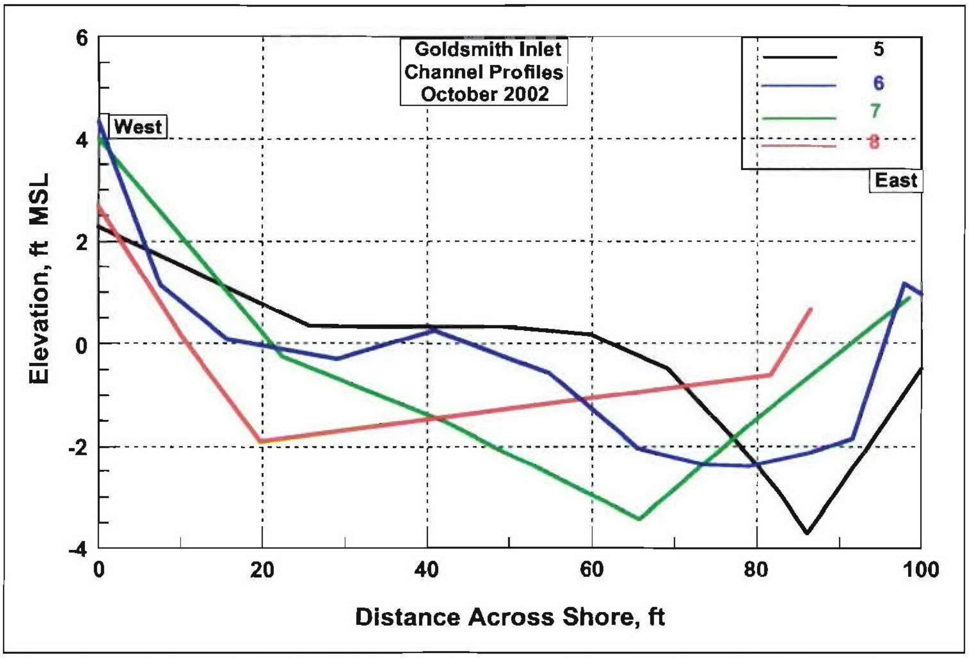

Figure 3-44b. Goldsmith Inlet channel cross sections 5-8, 8 October 2002

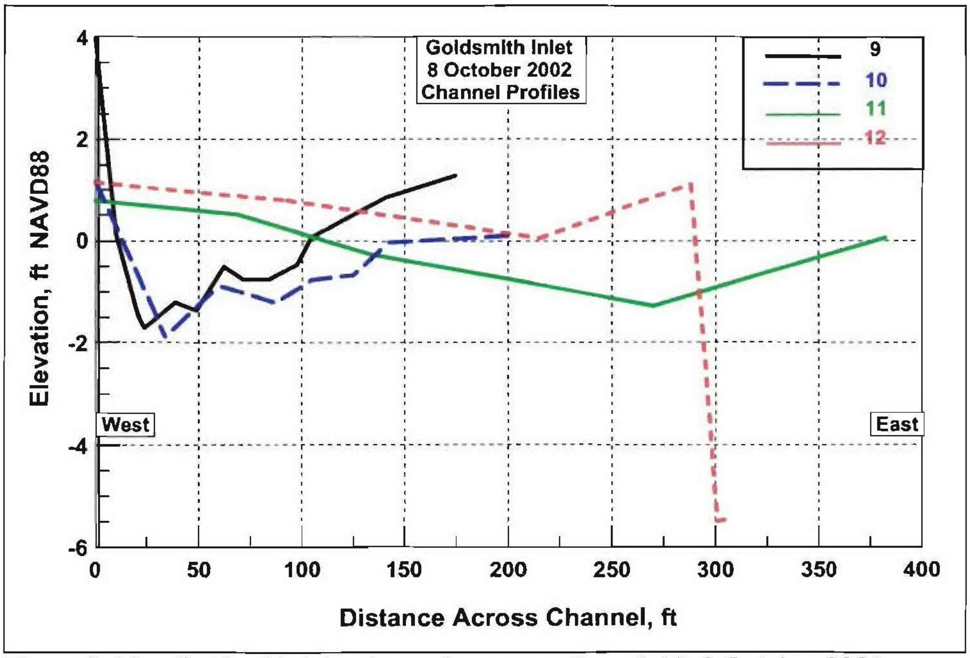

Figure 3-44c. Goldsmith Inlet channel cross sections 9-12, 8 October 2002

Elevation changes along the channel center line at Goldsmith Inlet are summarized in Figure 3-45. The entrance, located at the shoreline, presents a sill to tidal flow, as does the interior of the channel toward the pond. The response of the tidal flow to the sill at Goldsmith Inlet is discussed in the following paragraphs.

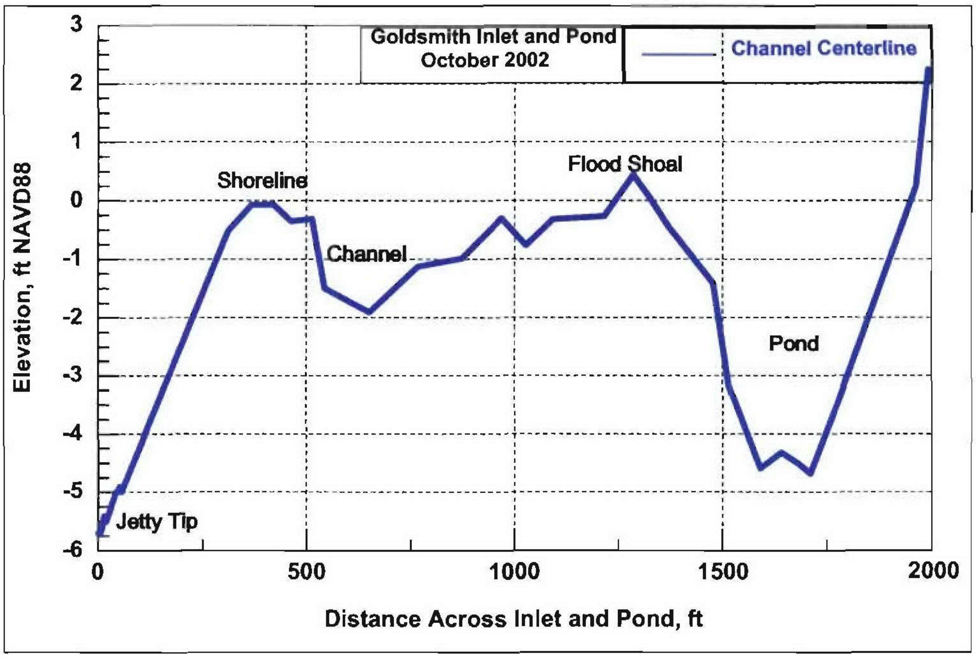

Figure 3-45. Goldsmith Inlet channel center line elevation, 8 October 2002

Water level

The locations of the tide gauge and the current meter are indicated in Figure 3-46. Tide Gauge 3 was placed near the southern bank of Goldsmith Pond and secured to the pond bottom by rebar, because there were no structures available to serve as a mounting platform. Water level at Goldsmith Pond is plotted in Figure 3-47a, together with that in Long Island Sound measured at the Mattituck Inlet jetty (Tide Gauge 1). In Goldsmith Pond, the average water level of the record was 0.91 ft above NAVD88. This means that the pond does not completely empty to mean sea level, because the water flow is retarded by the sill in the area of the flood shoal, as indicated in Figure 3-47a and, to a lesser extent, by the sill near the Long Island Sound shoreline.

The measured tidal range within Goldsmith Pond varied from 1.2 to 3.5 ft NAVD88. The mean tidal range for the deployment was calculated to be 2.15 ft, with a spring tidal range of approximately 2.9 ft for the period of record. With the measured tidal range offshore of Mattituck Inlet as an accurate representation of the tidal range offshore of Goldsmith Inlet, the reduction in tide at Goldsmith Pond is about 3 ft or half the tidal range in Long Island Sound.

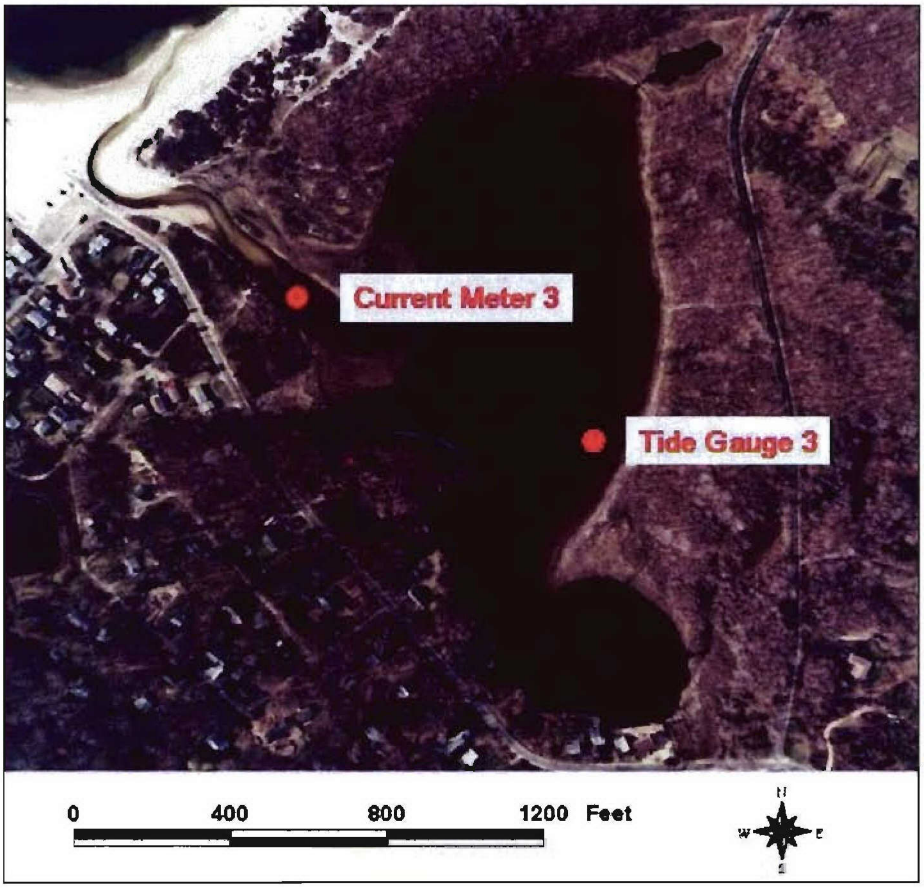

Figure 3-46. Goldsmith Inlet tide gauge location, 19 September – 8 October 2002

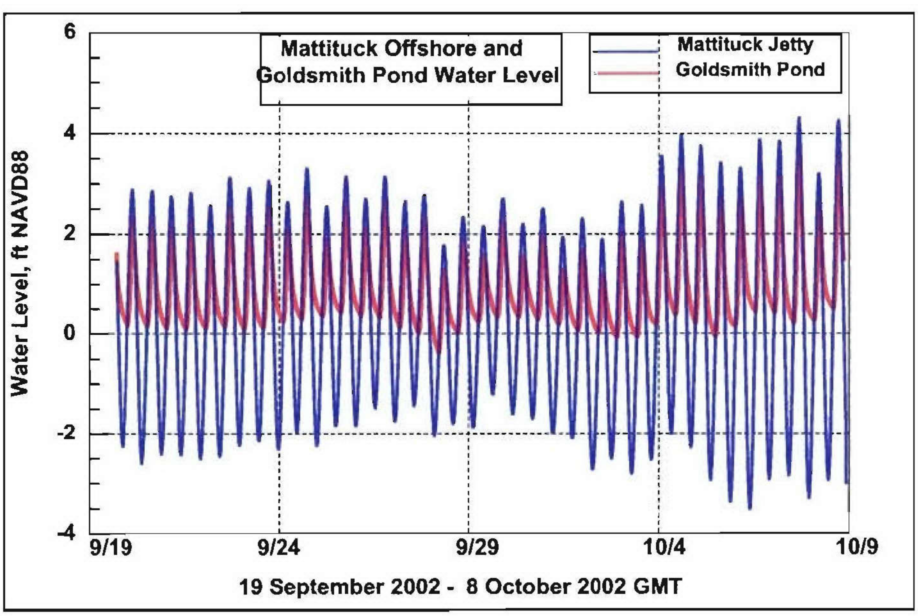

Figure 3-47a. Goldsmith Inlet water level, 19 September – 8 October 2002

Figure 3-47b plots water levels for 5–7 October 2002, a period of spring tide, and illustrates the phase lag observed at Goldsmith Inlet. Because the tidal wave travels from east to west in Long Island Sound, the phase of the tide at Goldsmith Inlet, located 5.2 miles east of Mattituck Inlet will slightly lead that outside of Mattituck Inlet. Therefore, the calculated phase lags for Goldsmith Inlet are slightly less than the values given.

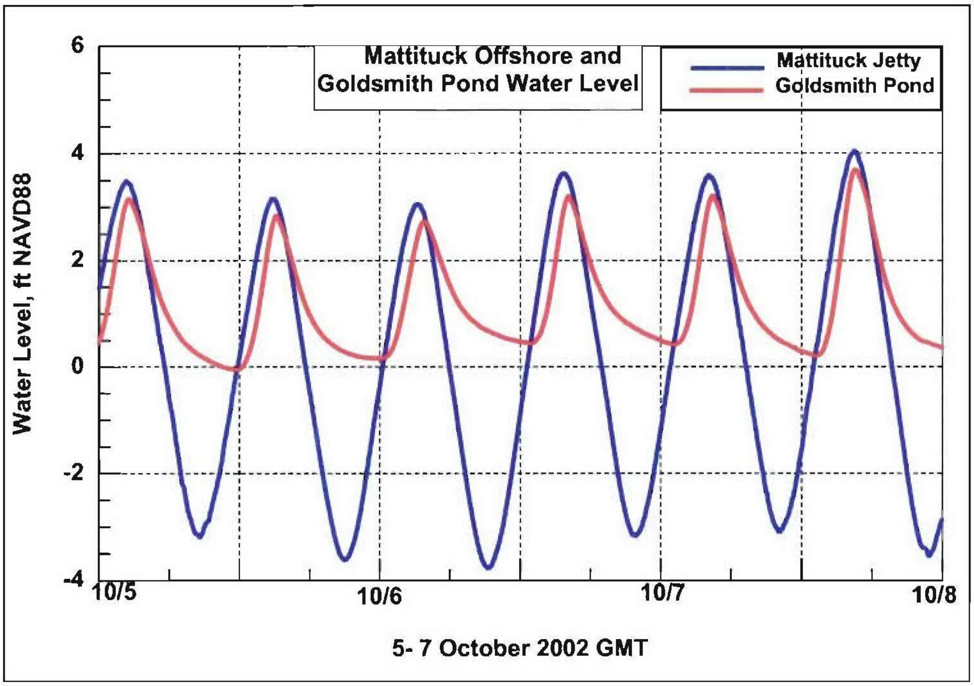

Figure 3-47b. Goldsmith Inlet water level, 5–7 October 2002

The times series of water level in Goldsmith Pond, as shown in Figure 3-47a and more clearly in Figure 3-47b, exhibits three remarkable properties:

a. Low tide usually does not reach 0 NAVD88, which is approximately msl at the site.

b. The tide range in the pond is less than half that in the Long Island Sound.

c. Water level rises much more rapidly than it falls, and the duration of ebb is much longer than flood.

Properties (*a*) and (*b*) are related. In Goldsmith Pond, the duration of the average ebb tide (peak to trough) of record was 8 hr, 56 min, and the duration of the average flood tide (trough to peak) was 3 hr, 28 min.

The bottom of the mouth of Goldsmith Inlet is located approximately at the elevation of the NAVD88 datum, near the visually observed mean shoreline position. The relation between NAVD88 and msl at the mouth of Goldsmith Inlet is not known with confidence. In any case, flow into the inlet and pond can only occur if the water level in Long Island Sound is above the NAVD88 or msl datums, according to modeling results described in Chapter 5. When high tide is reached in the sound, high tide in the pond occurs about 29 min later (median lag) and is 0.25 ft lower. In contrast, the median phase

lag for the low waters is 195 min. (3.24 hr). Therefore, flow into the inlet and pond can only occur when the water level in the sound is above msl.

The long-term average water level in Goldsmith Pond is expected to be constant. The time duration of the high water is much shorter than the duration of the low water about the mean water level. Because the same amount of water must enter on flood as leaves at ebb to maintain the average water level in the pond, but in a shorter time, the average of the inlet channel cross-sectional current velocity on flood must be much greater than on ebb. Such an inlet is called "flood dominant," referring to the greater magnitude, but shorter duration of the flood tide.

Tidal asymmetry of coastal inlets has been well studied (e.g., Boon 1975; Boon and Byrne 1981; Aubrey and Speer 1985; Speer and Aubrey 1985; Speer et al. 1991, as summarized by Walton (2002). For example, shoaling in channels truncates the lowest portion of the tide, resulting in a longer falling tide and a weaker ebb current as compared to the flood current. Such a truncation is a hypsometric effect, the control of water-surface elevation by the bathymetry or depth. In the case of Goldsmith Inlet, the elevation of the entire inlet entrance is located near msl datum in the Long Island Sound. At the lower water levels of ebb tide, the sills at the flood shoal and shoreline become effective in retarding flow. In addition, water entering the fringing marsh of Goldsmith Pond on flood tide has greater velocity than when it exits on ebb. The effective friction of the marsh, creating storage capacity, releases water slowly on ebb as compared to its entrance at flood tide.

Current

The hand-held current meter (Current Meter 3) was located approximately at middepth position (Figure 4-49). Along-channel current velocity at this location is plotted in Figure 3-48. The flood current velocity reached 1.30 m/sec, when the current meter had to be removed because of concerns over the rising water level and strong current on the pole holding the meter. Corresponding to discussion of water level, there must be a strong asymmetry in current velocity at Goldsmith Inlet, with flood current being significantly stronger than ebb current. Sediment transport is proportional to a power of water velocity, typically the third power. Therefore, a flood-dominant inlet will tend to have net sediment transport directed into the bay, or into Goldsmith Pond in the present situation.

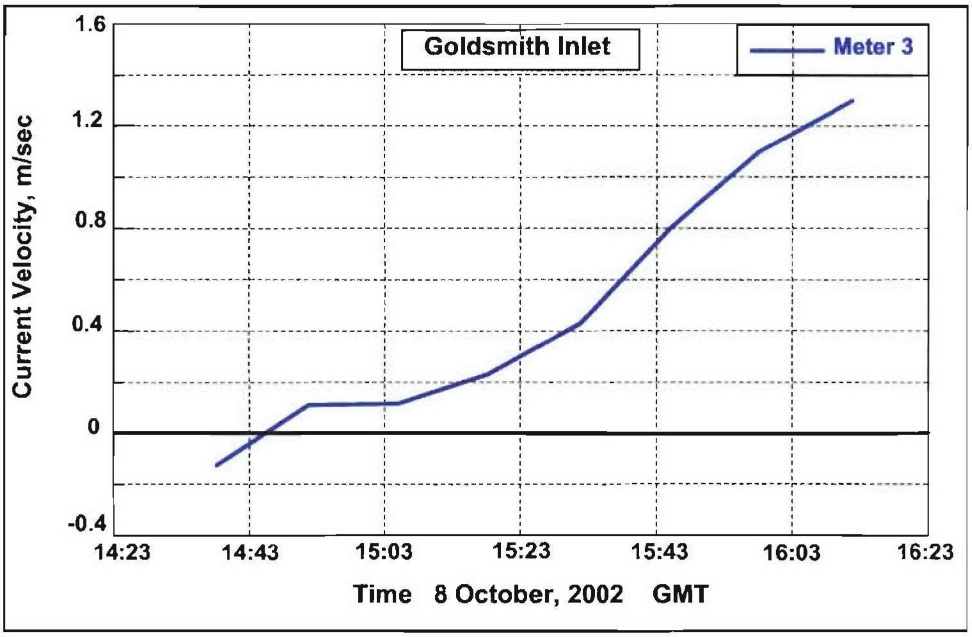

Figure 3-48. Goldsmith Inlet midchannel current velocity, 8 October 2002

Sediment

Sample collection sites for 8 October 2002 are shown in Figure 3-49a, and Figure 3-49b shows the sites of the 31 July 2003 sampling. The photograph serving as background in these two figures was taken 16 April 2003. For the 8 October 2002 sampling, the inlet mouth was located somewhat to the west as compared to April 2003. The samples were sieved to determine the grain-size distribution and median grain size of the surficial sediments at each location. Figures 3-50a through 3-50g show the grain size cumulative frequency for each sample site.

The surficial sediment at the inlet entrance (Samples 1-10; 15-17) is predominantly composed of gravel (-6 to -2 ϕ). A transitional area is located around the shoal attached to the west bank of the channel (Samples 11-13; 18, and 19), where smaller gravel (-4 to -2 ϕ) dominates sand and larger gravel. The area of the inlet south of the transition region, which includes the flood shoal, and the bottom of Goldsmith Pond, where samples were taken, is composed primarily of fine gravel and very coarse to coarse sand (-1 to 1 ϕ).

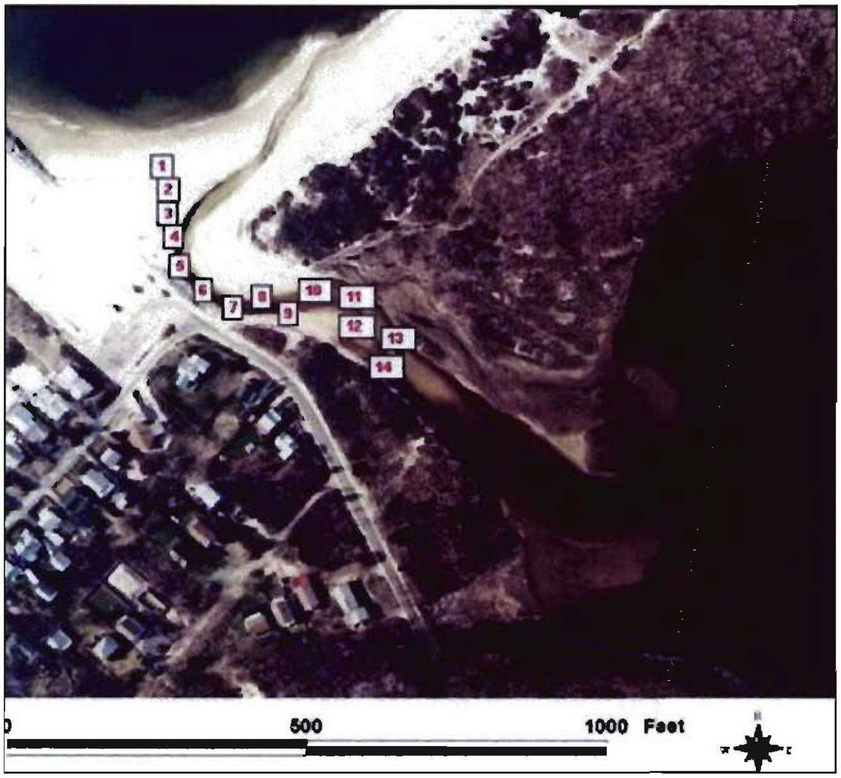

Figure 3-49a. Goldsmith Inlet sediment sample locations, 8 October 2002

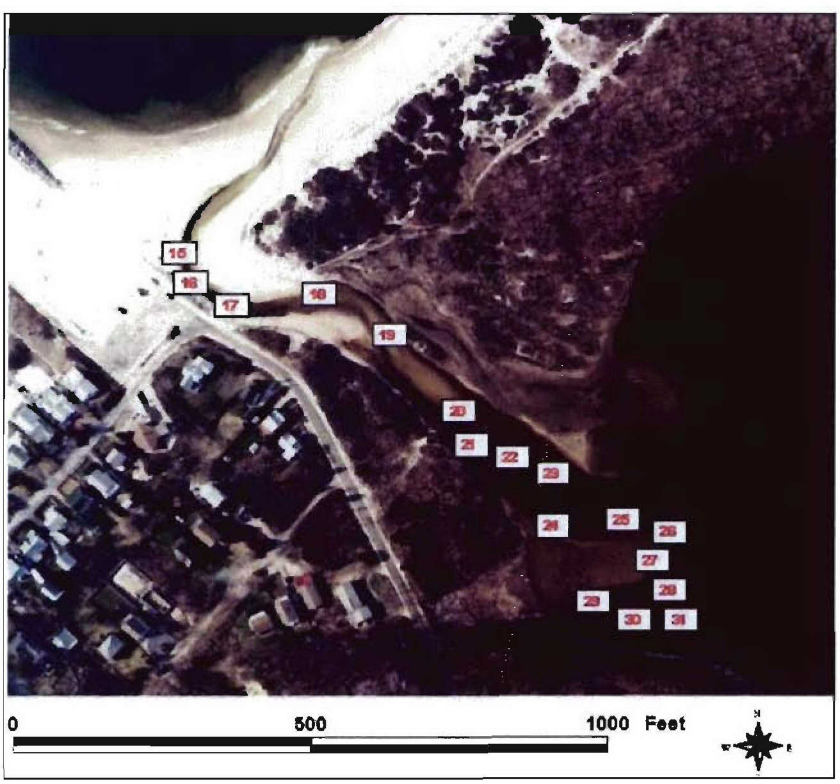

Figure 3-49b. Goldsmith Inlet sediment sample locations, 31 July 2003

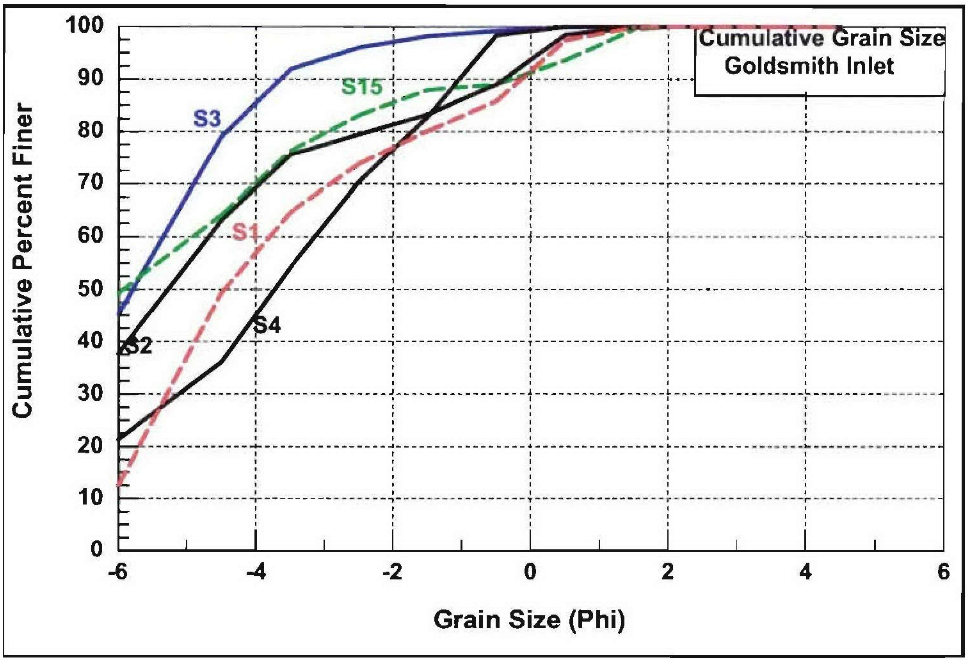

Figure 3-50a. Goldsmith Inlet cumulative grain size S1-S4 and S15, 8 October 2002 and 31 July 2003

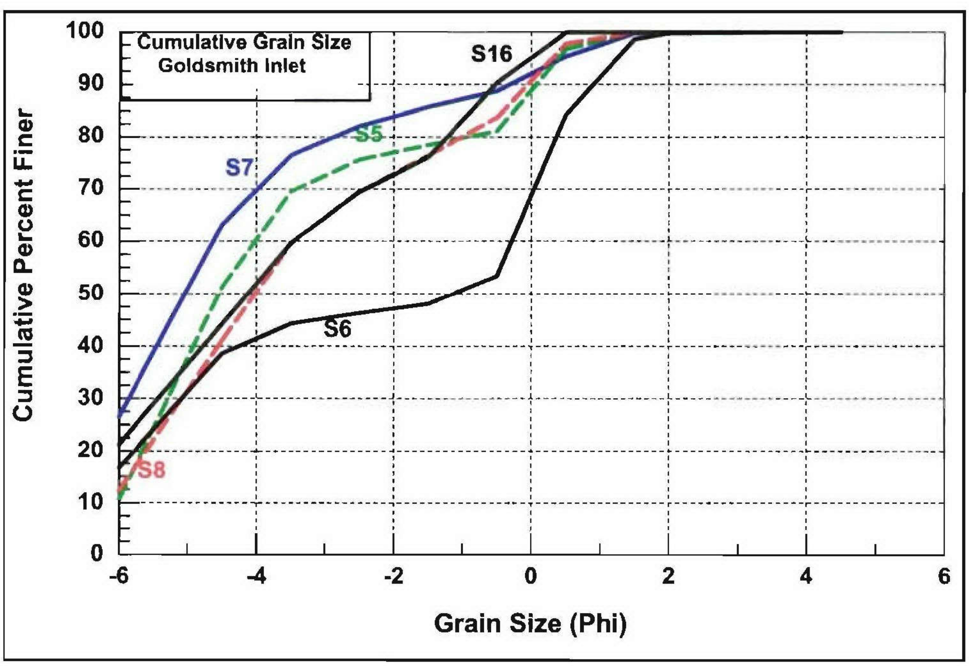

Figure 3-50b. Goldsmith Inlet cumulative grain size S5-S8 and S16, 8 October 2002 and 31 July 2003

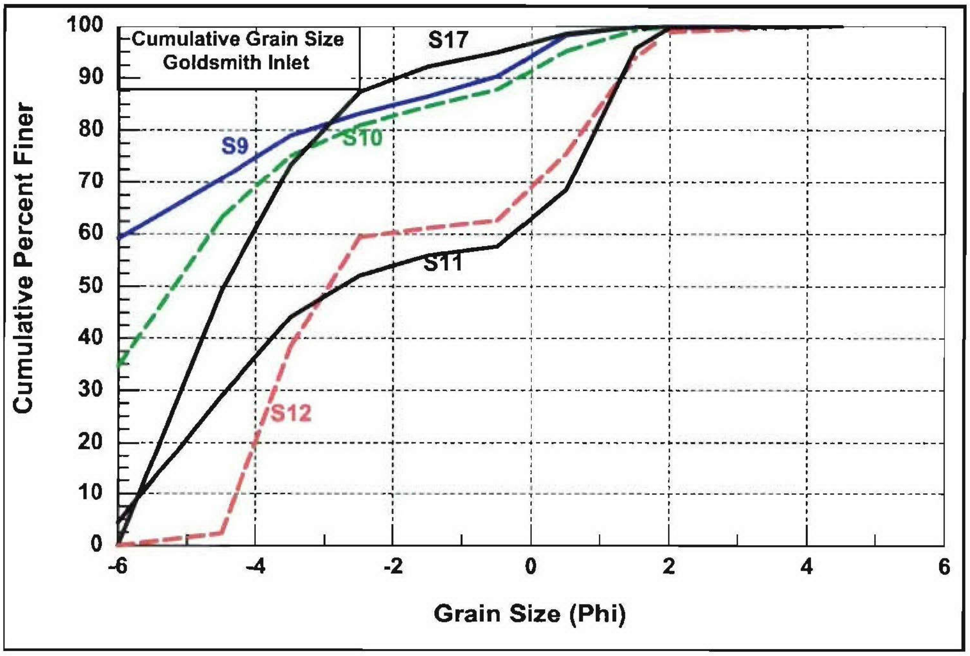

Figure 3-50c. Goldsmith Inlet cumulative grain size S9-S12 and S17, 8 October 2002 and 31 July 2003

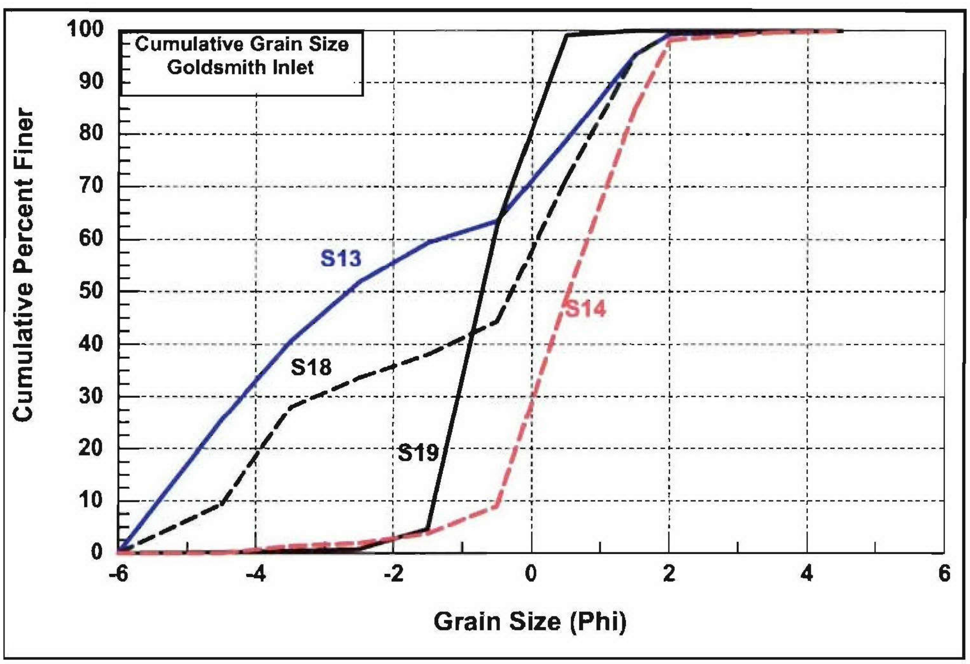

Figure 3-50d. Goldsmith Inlet cumulative grain size S13, S14, S18, and S19, 8 October 2002 and 31 July 2003

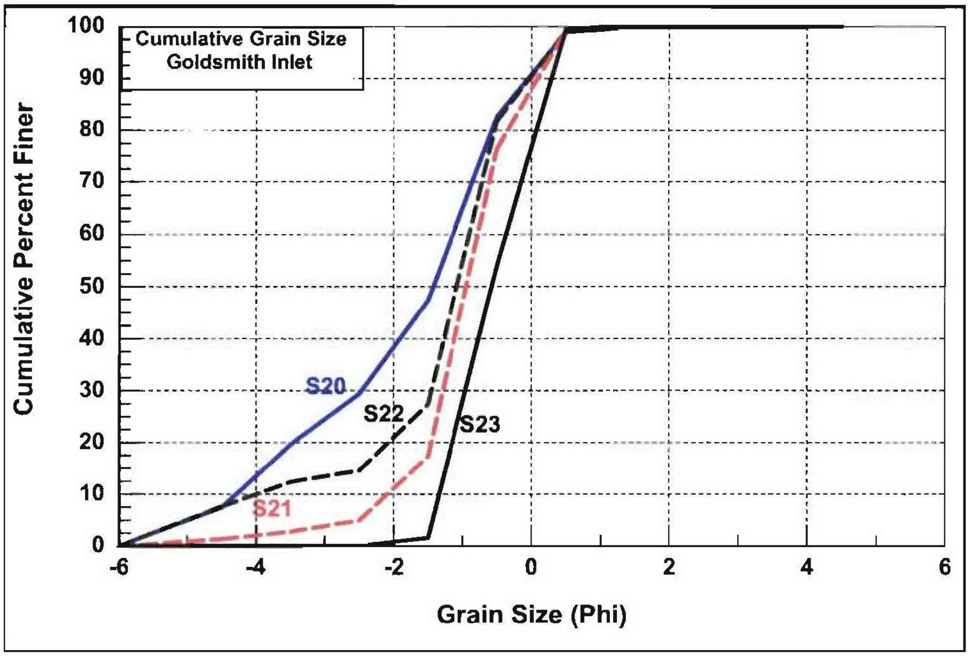

Figure 3-50e. Goldsmith Inlet cumulative grain size S20-S23, 8 October 2002 and 31 July 2003

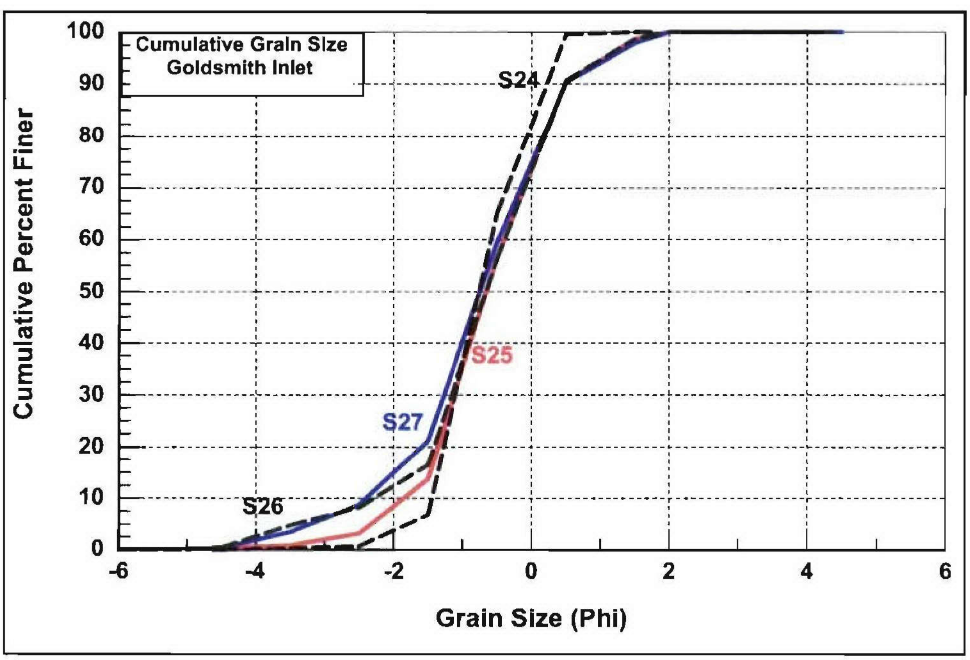

Figure 3-50f. Goldsmith Inlet cumulative grain size S24-S27, 8 October 2002 and 31 July 2003

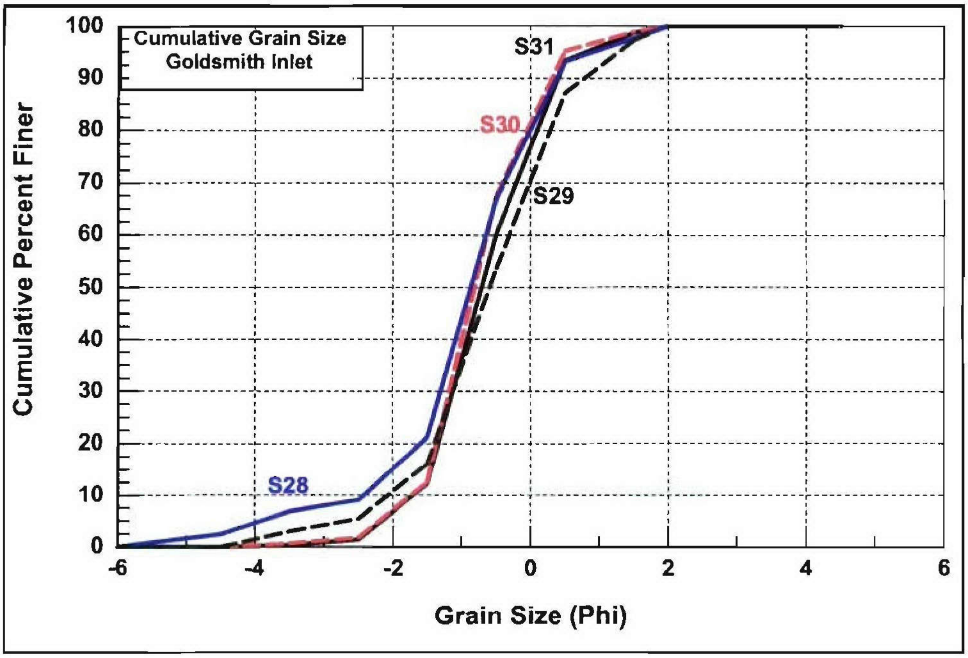

Figure 3-50g. Goldsmith Inlet cumulative grain size S28-S31, 8 October 2002 and 31 July 2003

Figure 3-51 displays a plan view distribution of sediment grain size at Goldsmith Inlet. Because exact sampling locations were not recorded, as by GPS, the grain-size map is approximate. The plan view clearly shows the fining of sediment with distance into the inlet and pond from the entrance. Current velocity magnitude plays a major role in determining the distribution of grain size within an inlet, resulting in a graded deposit and sorting within the channel. The greater velocity magnitude at the inlet mouth will entrain and transport increasingly larger grain sizes. As the current velocity magnitude decreases, the larger grain size fractions will be deposited, whereas finer sediments will be transported further into the inlet.

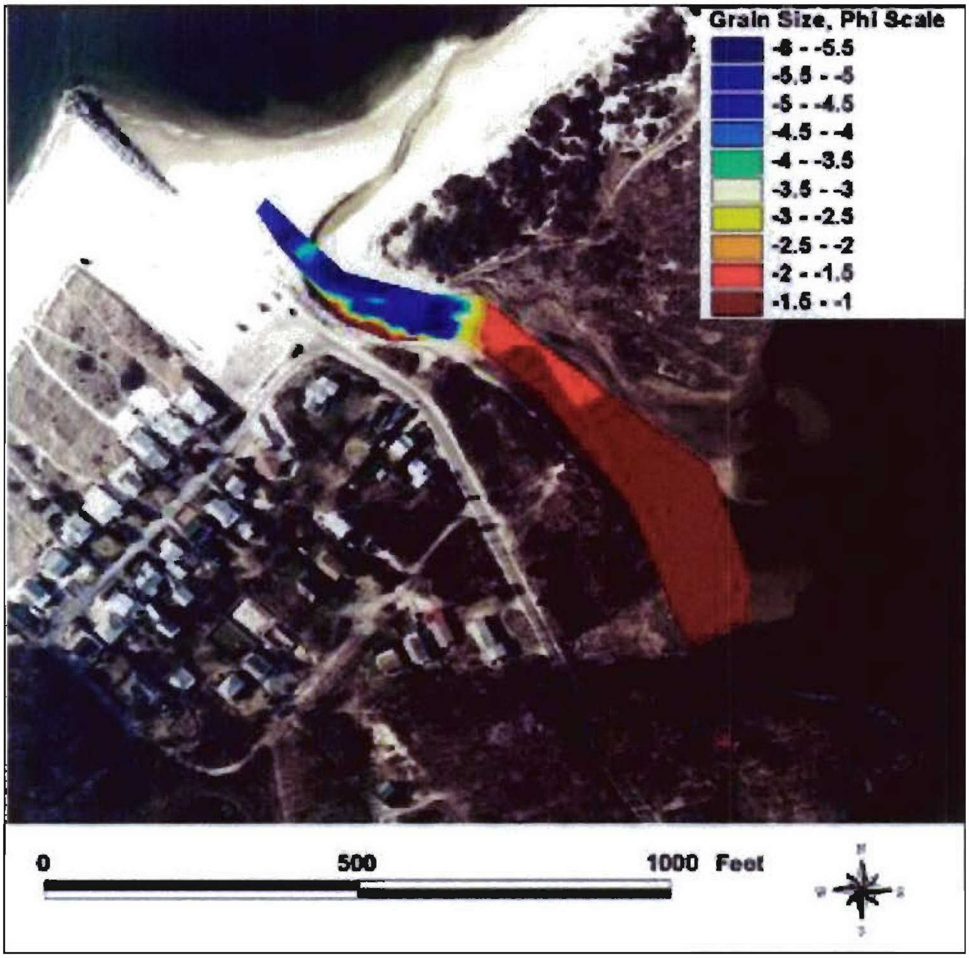

Figure 3-51. Goldsmith Inlet median grain-size distribution of surface samples, 8 October 2002 and 31 July 2003

Table 3-3 lists the median grain sizes found at Profiles 59 and 60 from the New York District (1969) study. Profile 59 is located approximately 200 ft west of Goldsmith Inlet and Profile 60 is approximately 500 ft east of Goldsmith Inlet. The profile locations are shown in Figure 3-52. The 1969 study indicates that sediment grain size west of Mattituck and Goldsmith Inlet is consistently larger than the grain sizes found east of the inlet.

Table 3-3
Grain-Size Analysis, Goldsmith Inlet Offshore Area, Profiles 59 and 60 (New York District 1969)

Location Depth (ft)	Grain Size		Classification of Material (percent)			
	Range of sizes (mm)	Median grain size (mm)	Fine Sand	Medium Sand	Coarse Sand	Gravel
Profile 59, 200 ft west of Goldsmith Inlet						
Backshore	0.10 - 25.4	1.50	4	57	14	25
High water	0.15 – 38.1	1.28	7	52	7	34
Midtide	0.15 – 38.1	3.00	7	41	6	46
Low water	0.10 – 38.1	6.00	3	24	14	59
6	0.07 – 25.4	9.50	0	6	10	84
12	0.07 – 2.36	0.45	42	53	2	0
18	0.08 – 25.4	0.23	70	21	2	7
24	0.04 – 9.52	0.23	66	24	6	2
30	0.07 - 2.36	0.22	95	4	1	0
Profile 60, 500 ft east of Goldsmith Inlet						
Backshore	0.15 – 2.36	0.52	20	80	0	0
High water	0.15 – 25.4	0.43	49	16	0	35
Midtide	0.17 – 2.36	0.49	25	75	0	0
Low water	0.05 – 19.0	0.69	27	45	5	22
6	0.15 – 2.36	0.40	62	38	0	0
12	0.07 – 4.76	0.43	50	48	2	0
18	0.16 – 4.76	0.48	40	58	2	0
24	0.10 – 4.76	0.43	45	54	1	0
30	0.09 – 2.36	0.44	47	53	0	0

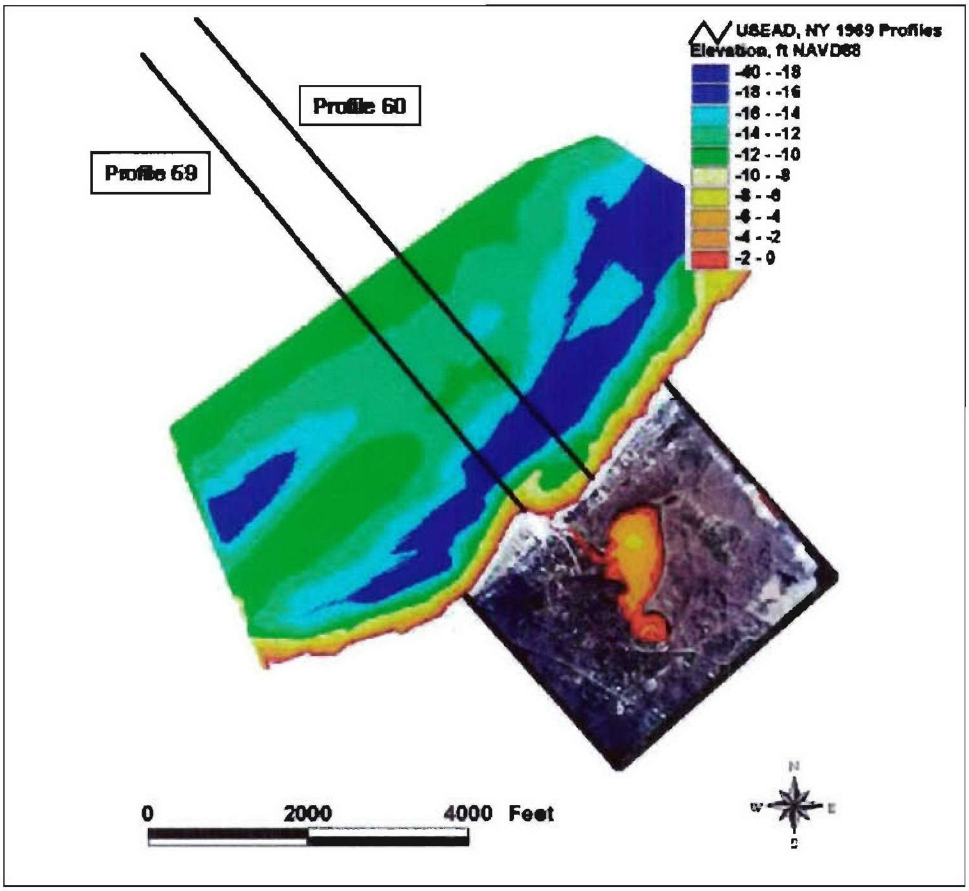

Figure 3-52. Goldsmith Inlet, New York District (1969) profile locations

4 Morphology Change, and Channel Shoaling and Migration

This chapter describes and quantifies morphology change at Mattituck Inlet from 1891 to present and at Goldsmith Inlet from 1964 to present. For Mattituck Inlet, change in the offshore and flood shoals, and in the inlet response to the original navigation project and to subsequent modifications, is analyzed. For Goldsmith Inlet, change in the channel, inlet orientation, and flood shoal is analyzed.

Mattituck Inlet

To analyze morphology change for the offshore area at Mattituck Inlet, beach profiles from the 6-8 October 2002 survey are compared to those from a March 1998 survey (OCTI 1998), spanning a 4-1/2 year interval. The long-term morphology change of the offshore shoal associated with Mattituck Inlet is analyzed by comparing a 1927 survey to the survey of 6-8 October 2002. For the Mattituck Inlet navigation channel and flood shoal, morphology change and response to jetty modifications is analyzed based upon historic aerial photographs and data provided by the New York District.

Historic sounding data received from the New York District had been archived on aperture cards, a form of media that requires a high-resolution reader. The Hudson Blueprint Company was engaged to read the aperture cards. Paper maps were produced and scanned in a large-format scanner, and the resulting images were then calibrated, digitized, and converted into ArcView® shape files by means of Didger® software.

Offshore morphology change

Beach profiles. Figures 4-1a to 4-1h plot the 1998 (OCTI 1998) and 2002 beach profile survey data for the offshore area west of Mattituck Inlet. Profile transects were referenced to established monuments (OCTI 1998). Two longshore bars can be identified on most of the profile lines, and cross-shore, primarily seaward movement of the bars occurred between 1998 and 2002 (Figures 4-1e to 4-1h). More data sets are required over several years and with greater frequency to determine the cause of movement as due to seasonal changes

in waves, as a response to seasonal water level, or another cause. The profile surveys indicate a shoreline near equilibrium with small amounts of advance at some locations to the west of Mattituck Inlet.

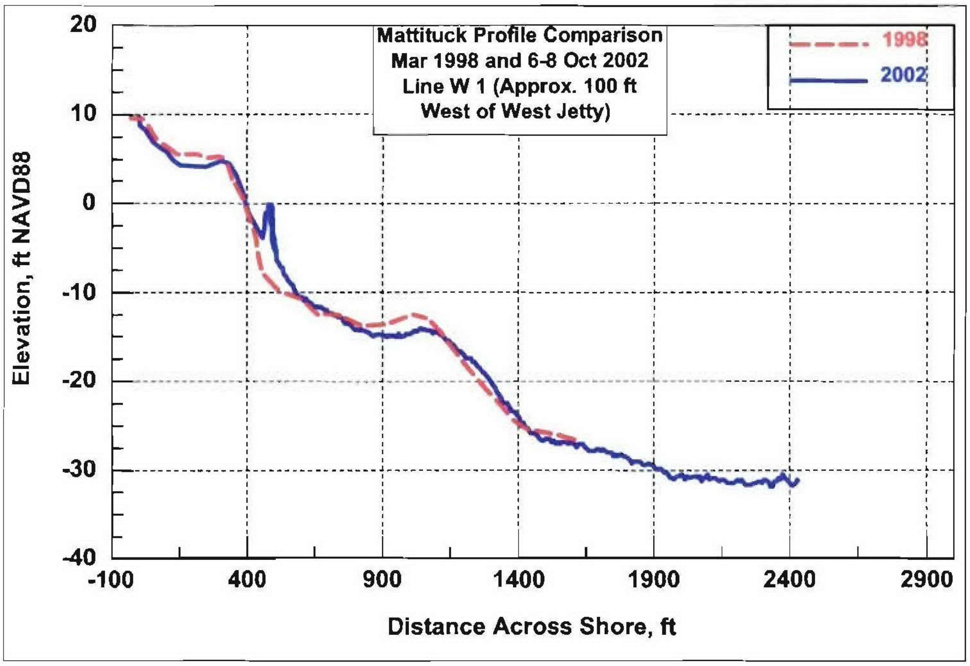

Figure 4-1a. Beach profile W1, west of Mattituck Inlet, March 1998 and 6-8 October 2002

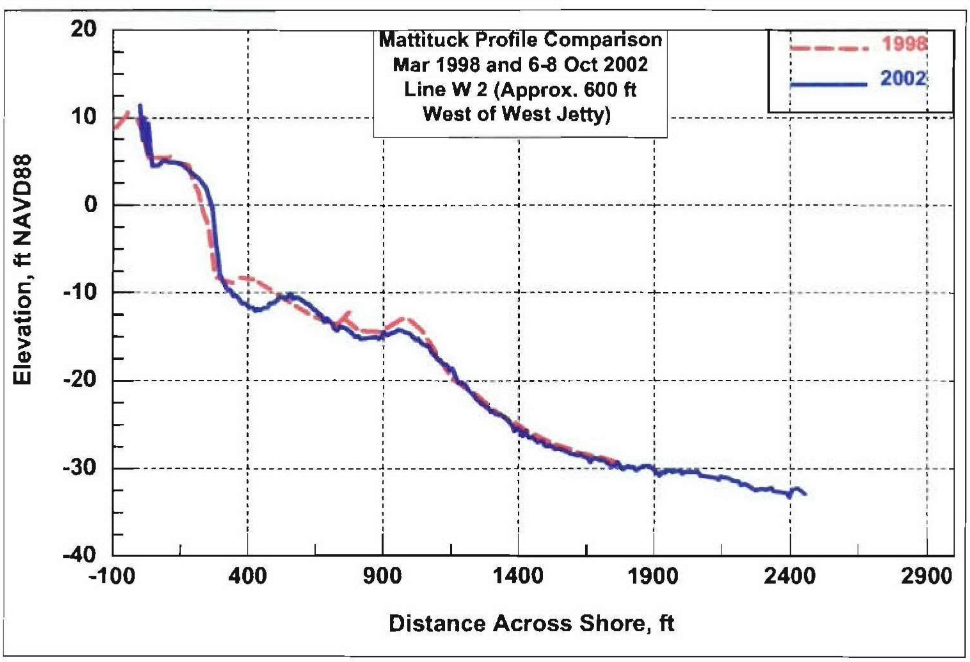

Figure 4-1b. Beach profile W2, west of Mattituck Inlet, March 1998 and 6-8 October 2002

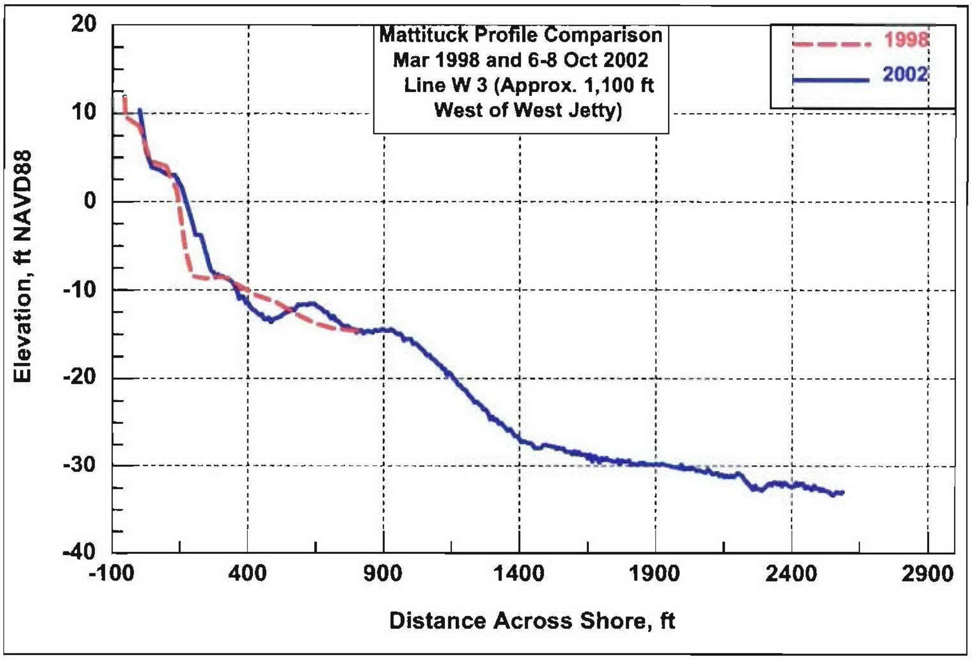

Figure 4-1c. Beach profile W3, west of Mattituck Inlet, March 1998 and 6-8 October 2002

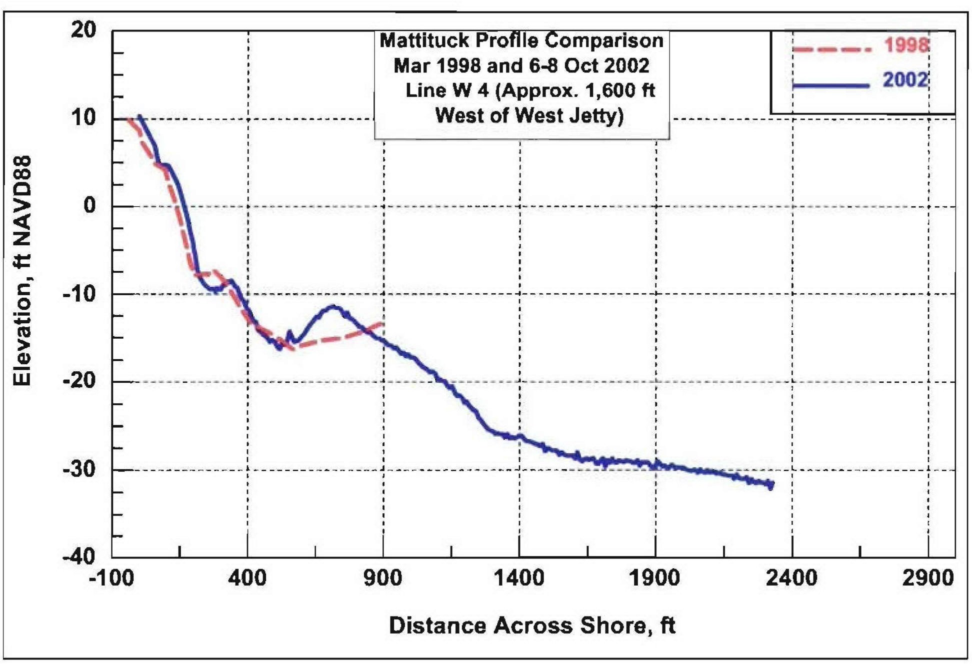

Figure 4-1d. Beach profile W4, west of Mattituck Inlet, March 1998 and 6-8 October 2002

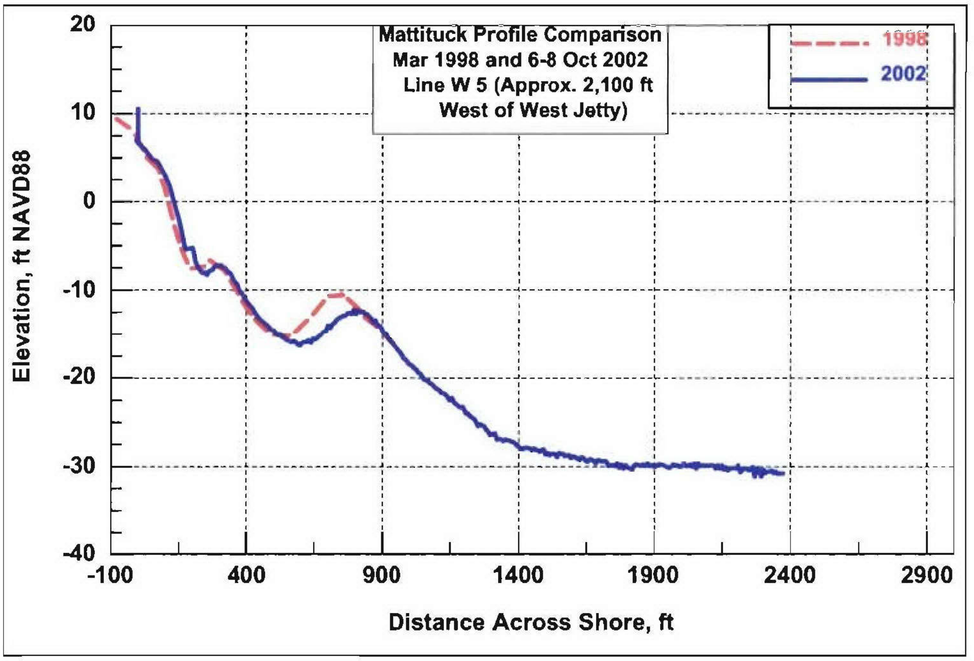

Figure 4-1e. Beach profile W5, west of Mattituck Inlet, March 1998 and 6-8 October 2002

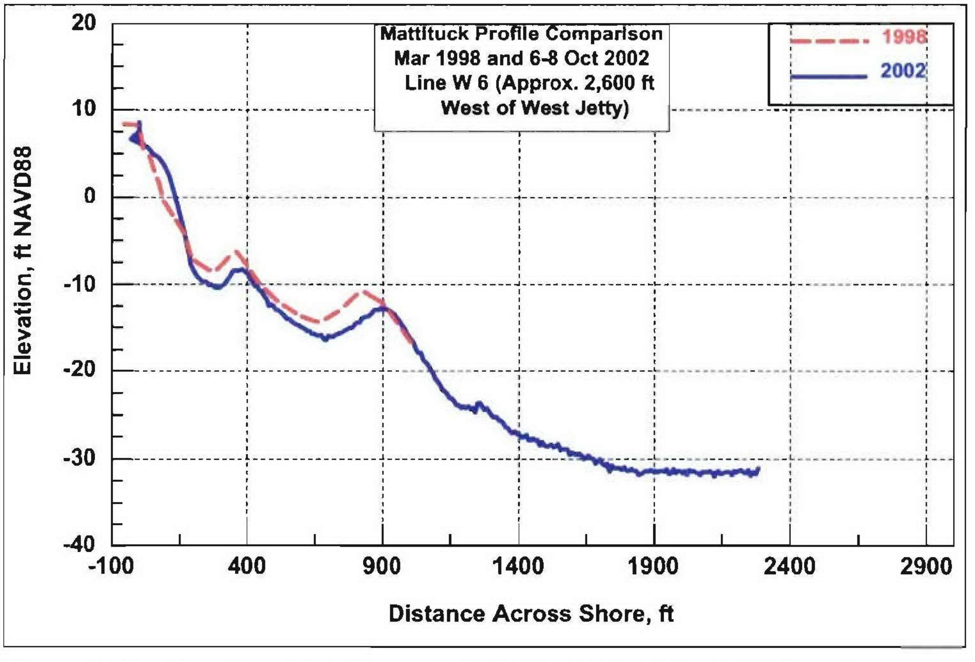

Figure 4-1f. Beach profile W6, west of Mattituck Inlet, March 1998 and 6-8 October 2002

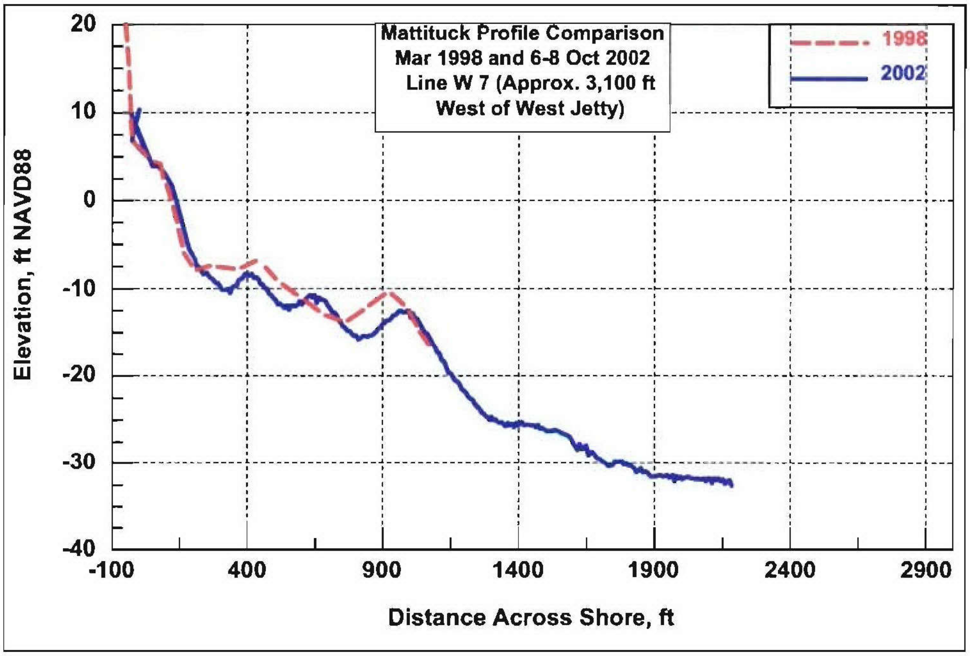

Figure 4-1g. Beach profile W7, west of Mattituck Inlet, March 1998 and 6-8 October 2002

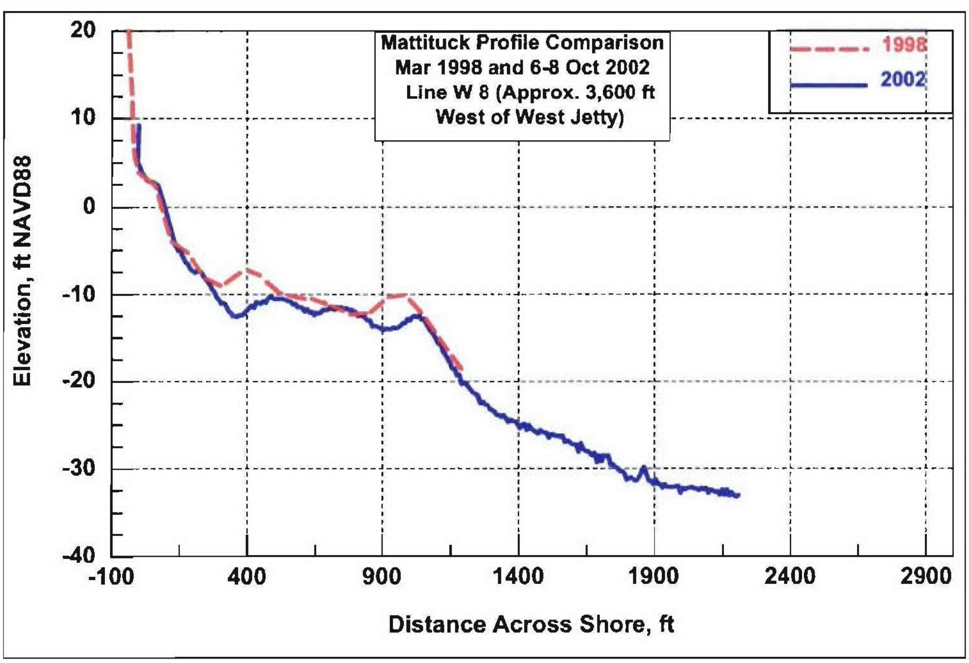

Figure 4-1h. Beach profile W8, west of Mattituck Inlet, March 1998 and 6-8 October 2002

Figures 4-2a to 4-2f plot 1998 (OCTI 1998) and 2002 beach profile survey for the offshore area east of Mattituck Inlet and cover the shoal located approximately 1,660 ft offshore. The profiles indicate stability of this feature for the 4-1/2-year interval and a stable shoreline with small amounts of recession at some locations to the east of Mattituck Inlet.

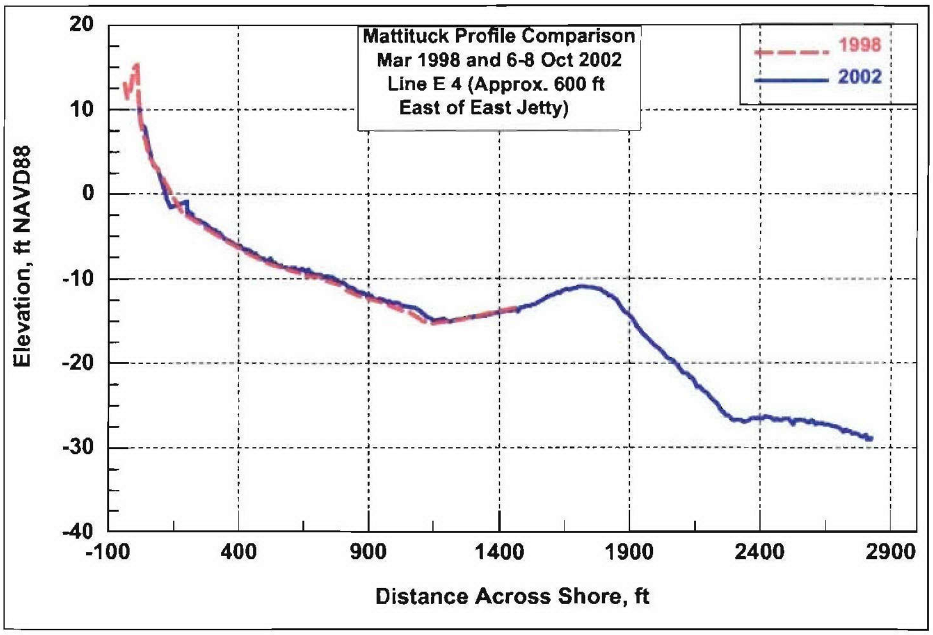

Figure 4-2a. Offshore shoal cross-shore profile E4, March 1998 and 6-8 October 2002

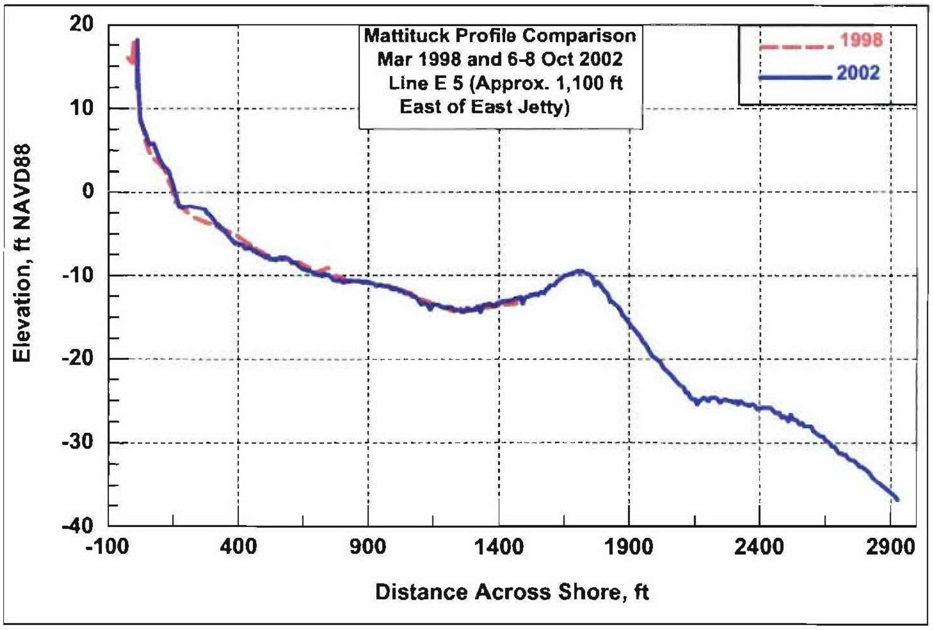

Figure 4-2b. Offshore shoal cross-shore profile E5, March 1998 and 6-8 October 2002

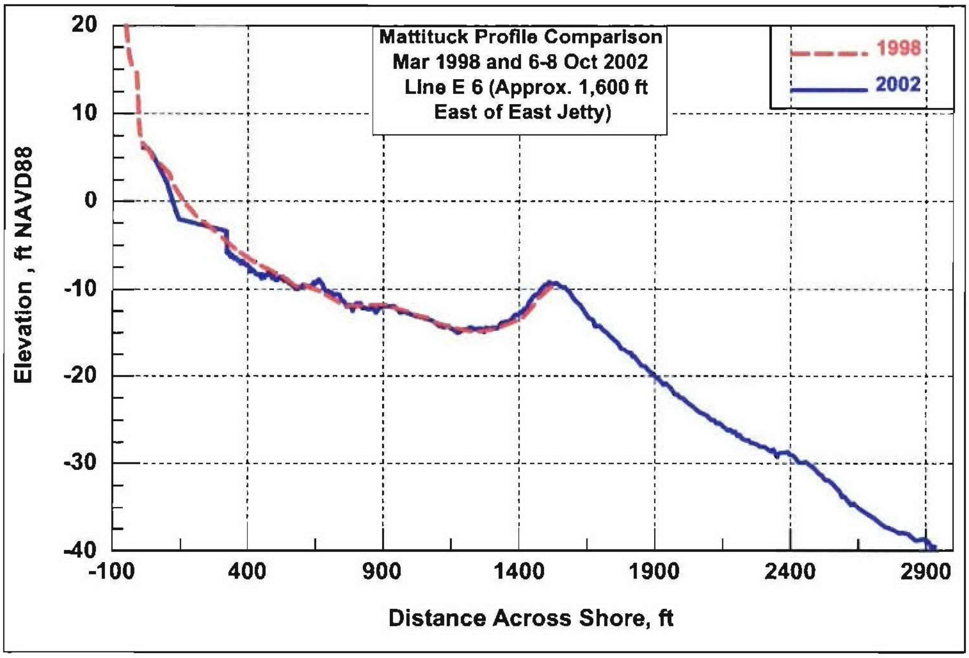

Figure 4-2c. Offshore shoal cross-shore profile E6, March 1998 and 6-8 October 200

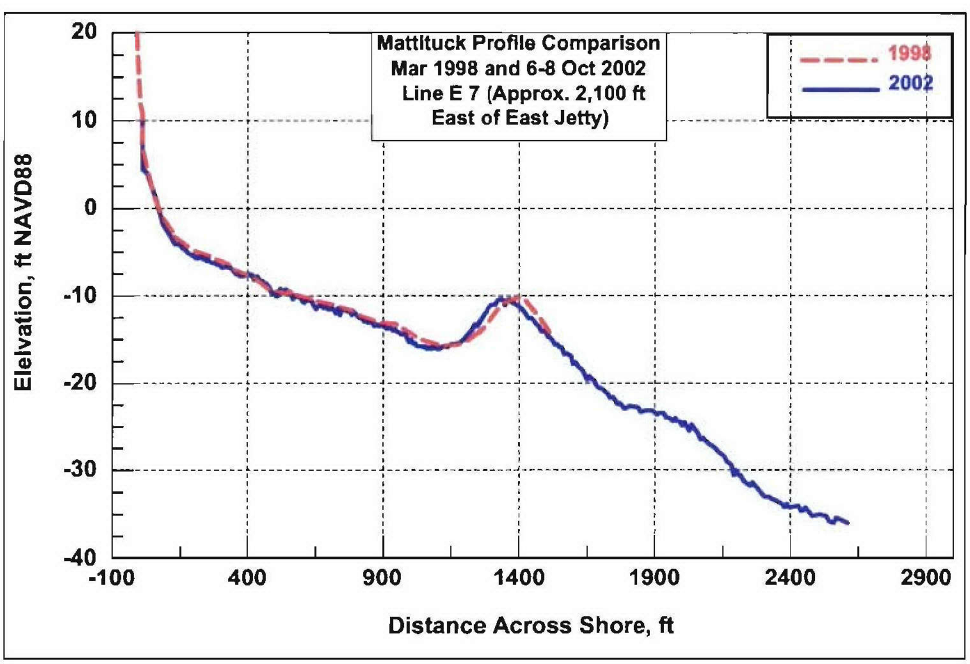

Figure 4-2d. Offshore shoal cross-shore profile E7, March 1998 and 6-8 October 2002

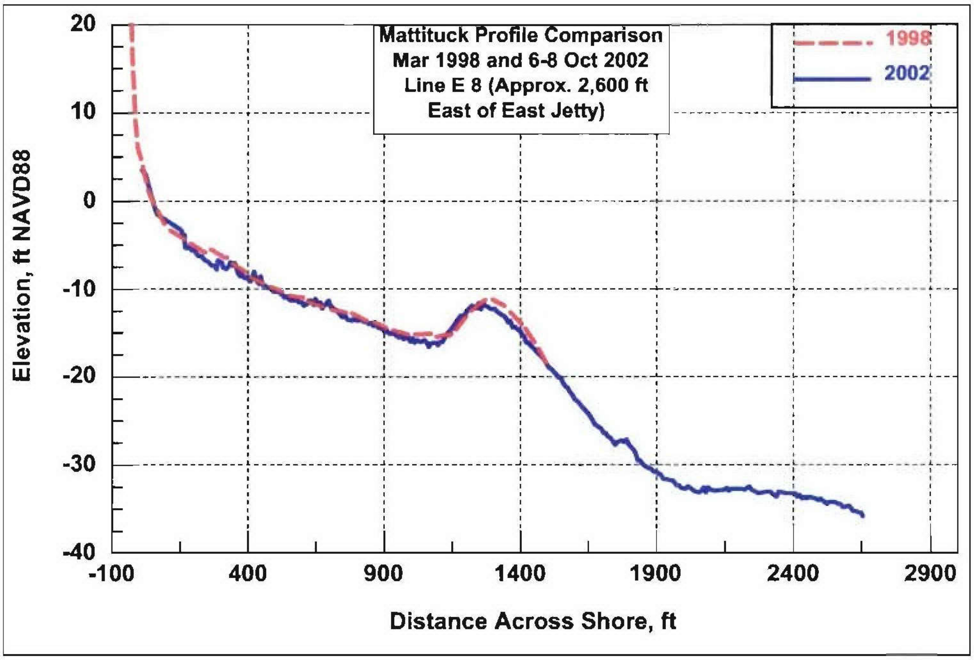

Figure 4-2e. Offshore shoal cross-shore profile E8, March 1998 and 6-8 October 2002

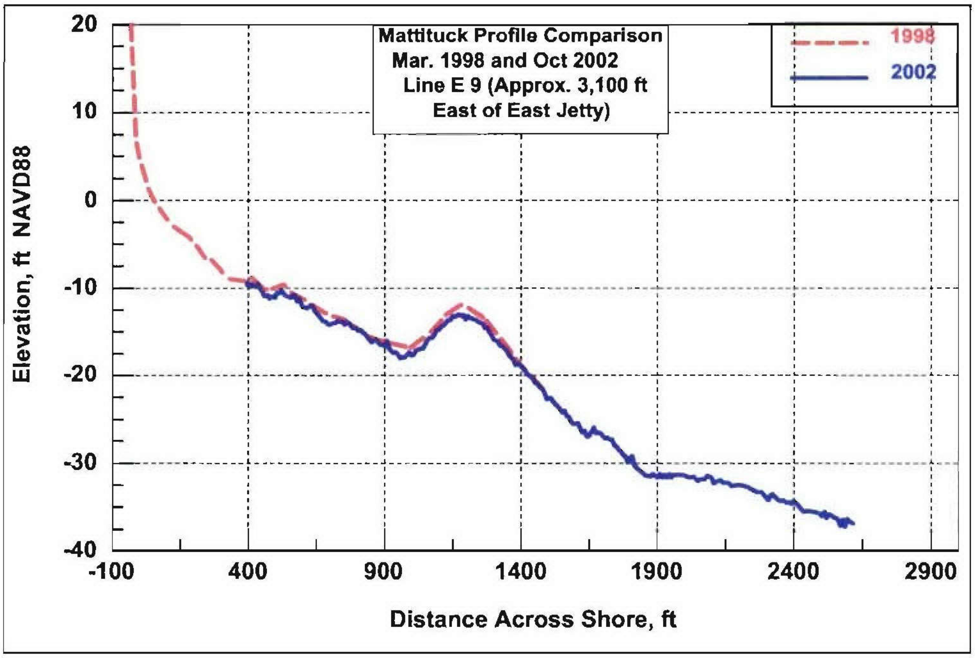

Figure 4-2f. Offshore shoal cross-shore profile E9, March 1998 and 6-8 October 2002

Change of offshore shoal morphology. To assess long-term change offshore of Mattituck Inlet, a comparative analysis of the 6-8 October 2002 survey, a 1969 survey by the National Oceanic and Atmospheric Administration (NOAA) (survey #H09087), and an 8 December 1927 New York District survey was conducted. Because the 8 December 1927 covered the smallest area, the spatial extent of this survey defined the area of examination of elevation change for the periods considered. Elevation change was obtained through surface differencing, calculated between triangulated irregular network (TIN) grids generated in ArcView 3.3.

The 8 December 1927 condition survey was conducted approximately 2 months after the dredging of September – October 1927. The New York District condition survey of 8 December 1927 was referenced to a mlw datum that lies 2.2 ft below a New York District msl datum as determined in April-May 1906. To adjust the 8 December 1927 survey to the NAVD88 datum, 3.63 ft was subtracted from the elevation values of this condition survey. The difference between the datums was derived after Batten and Kraus (2005), and can be accounted for in the following manner. The mlw datum of reference for the 1927 survey was determined at the NOS tide station at Ft. Schuyler, NY. At Mattituck Inlet, mlw is 0.3 ft below mlw at Ft Schuyler, NY. According to the NOS, the conversion factor between Mattituck Inlet and the NOS Bridgeport, CT, reference station is 0.76, and the difference between mlw and NAVD88 at Bridgeport, CT, is 3.59 ft. The difference between the present day mlw and NAVD88 at Mattituck Inlet is therefore 2.73 ft. Sea level has risen approximately 0.6 ft at Port Jefferson for the 75-year period considered. The difference between mlw at Mattituck Inlet and Ft. Schuyler (0.3 ft), sea level rise (0.6 ft), and the calculated elevation of mlw datum in the present tidal epoch (2.73 ft), yield the adjustment of 3.63 ft applied here. The datum relations are illustrated in Figure 3-1a and 3-1b.

The 1969 NOAA survey was referenced to mean lower low water (mllw). The NOS published conversion factor for the 1983-2001 epoch at Mattituck Inlet defines NAVD88 at 2.96 ft above mllw. According to the NOS tide station at Port Jefferson, sea level has risen approximately 0.26 ft between 1969 and 2002. To adjust the mllw datum of this survey to NAVD88, 3.22 ft was subtracted from the elevation values of this survey. The datum relations discussed here are illustrated in Figure 3-1a.

The condition survey of 8 October 1927 is referenced to a local coordinate system. The background aerial photograph shown in Figures 4-3 through 4-5c is circa 1930. Horizontal conversion to the New York State Plane Grid, Long Island Lambert, NAD83, was accomplished by georeferencing the data to this aerial photograph of Mattituck Inlet, and the subsequent digitization of the adjusted survey points. The root mean square (rms) error in the georeferencing was 60 ft. The circa 1930 aerial photograph is large scale (1:24,000), and covers more than 10 miles of shoreline. The rms error is considered reasonable because Mattituck Inlet is near the center of the aerial photograph, where the estimated error is less. Overall, mapped high-water line (hwl) lines and jetty and channel location matched well, and visual inspection of the alignment of the jetties between the aerial photograph and the 8 December 1927 bathymetry survey indicated error between 10 to 30 ft.

Figures 4-3 and 4-4 displays the elevation contours from the 8 December 1927 survey and the 1969 NOAA survey. Elevation change for the periods 1927-1969, 1969-2002, and 1927-2002 are shown in Figures 4-5a through 4-5c. The observed morphology changes are discussed in the following paragraphs.

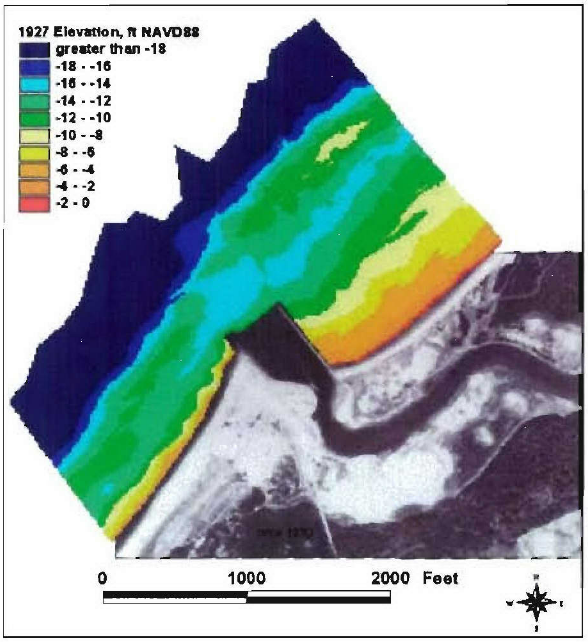

Figure 4-3. Mattituck Inlet, circa 1930 and offshore elevation contours, 8 December 1927

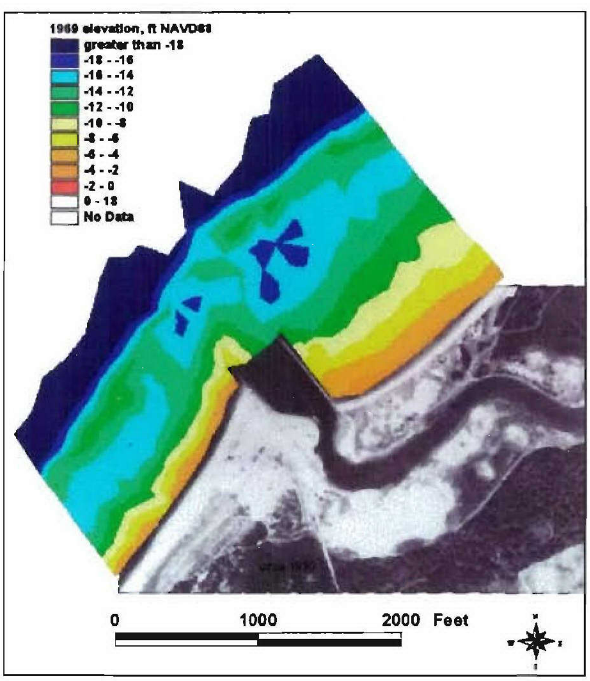

Figure 4-4. Mattituck Inlet, circa 1930 and offshore elevation contours, 1969

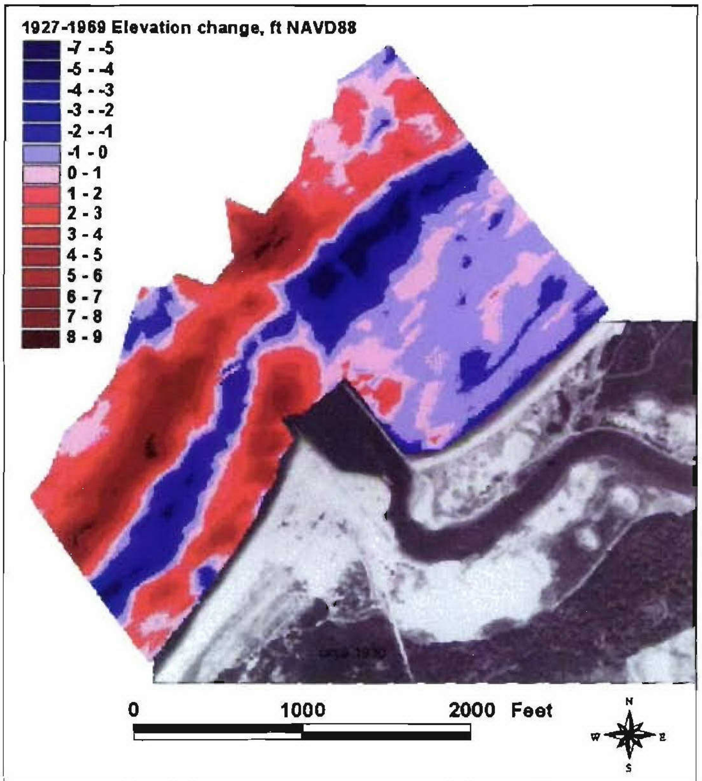

Figure 4-5a. Mattituck Inlet offshore elevation change, 1927-1969

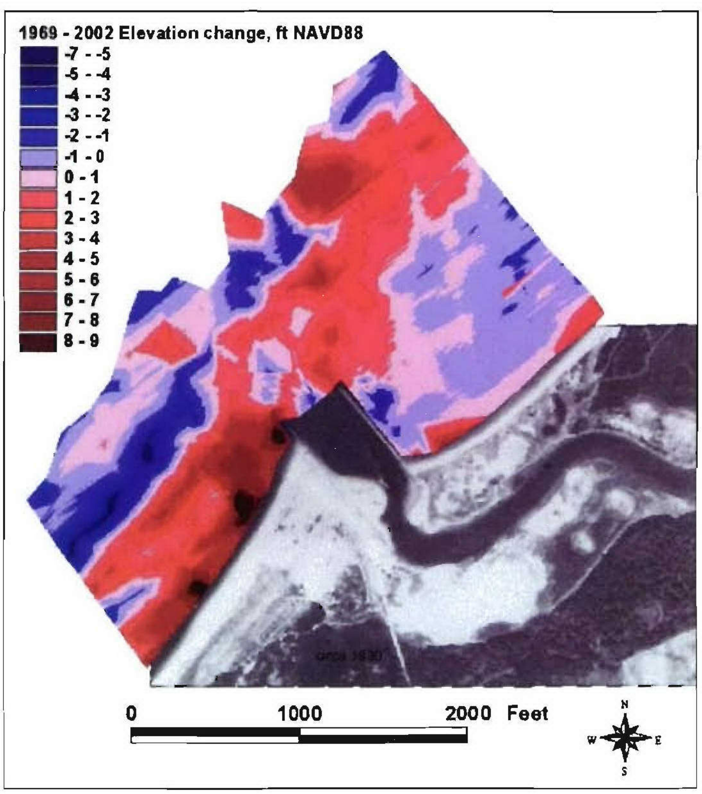

Figure 4-5b. Mattituck Inlet offshore elevation change, 1969-2002

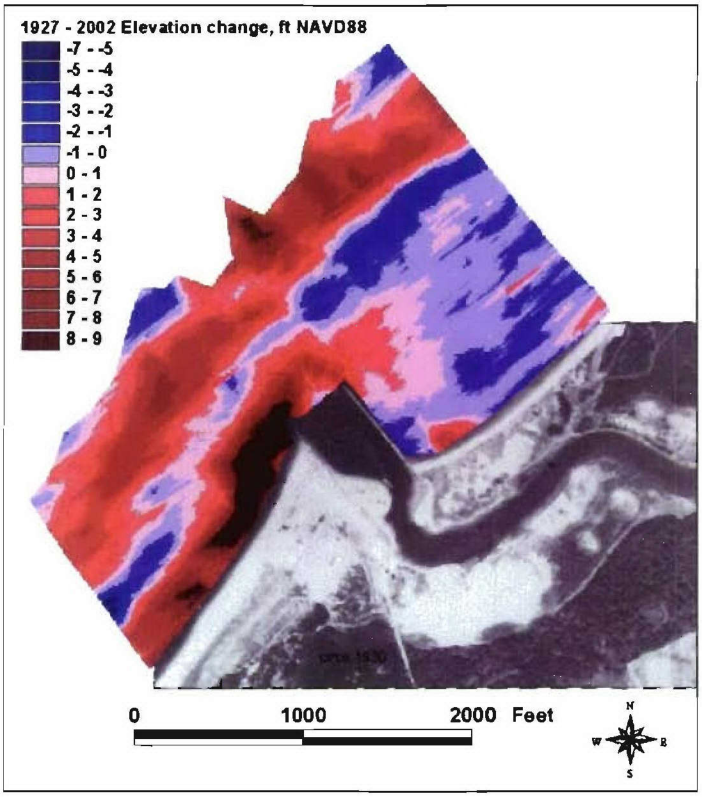

Figure 4-5c. Mattituck Inlet offshore elevation change, 1927-2002

From 1927 to 1969, the offshore shoal migrated seaward, and this is indicated in Figure 4-5a as a landward area of erosion and a seaward area of deposition east of the inlet. West of the inlet, the main longshore bar migrated seaward as well. The seaward movement of the longshore bar during this period may be interpreted as a response to shoreline advance, because the shoreline west of the inlet advanced as a result of sediment impoundment by the west jetty.

The surface difference of the 1969 and 2002 surveys (Figure 4-5b) shows that the shoal reached locational equilibrium by 1969, and the main longshore bar west of the inlet had migrated shoreward. This migration may be attributable to the steepening of the beach slope over this 33-year period (Batten and Kraus 2005). This period is also characterized by deposition in front of the offshore shoal and formation of a new longshore bar adjacent to the east jetty, which apparently acts to bypass sediment to the downdrift beach.

To further investigate and quantify morphology change of the offshore shoal and patterns of deposition and erosion near Mattituck Inlet, each grid was sub-sampled, and TINS were generated from which volume change for the three periods (1927-1969, 1969-2002, and 1927-2002) was calculated. Figure 4-6 illustrates the areas covered in these calculations. The 8 December 1927 survey did not fully cover the shoal east of the inlet. Volume change calculations for the western portion of this feature were conducted, as well as a volume change calculation for the spatial extent of the feature in the 6-8 October 2002 survey for the period 1969-2002 (Figure 4-7). Polygons A and B cover the seaward and landward portions of the offshore shoal area, respectively, and polygon C covers

the area where a longshore bypassing bar has developed. Elevation changes for the total offshore shoal were calculated from a reference datum of -21.5 ft NAVD88, taken to be the ambient depth found at the base of the shoal. Table 4-1 summarizes the results of this analysis.

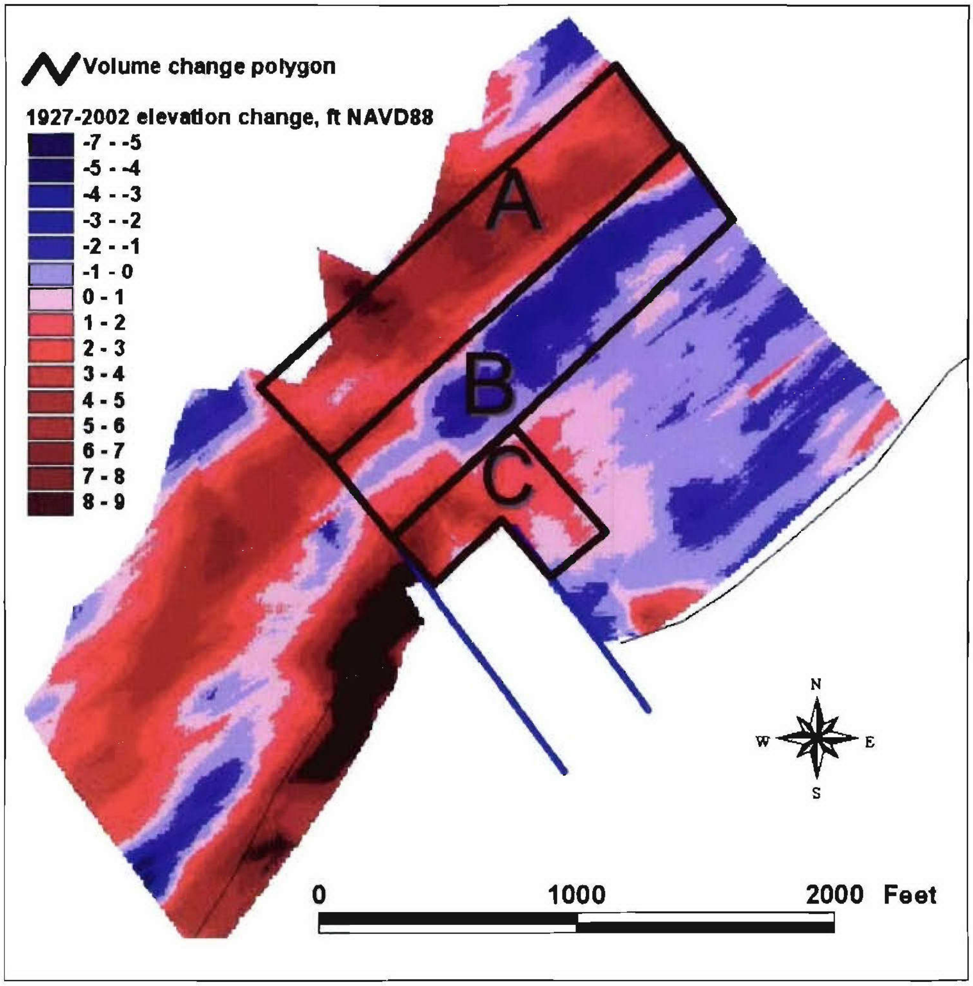

Figure 4-6. Volume change polygons, east of Mattituck Inlet, with elevation change 1927-2002

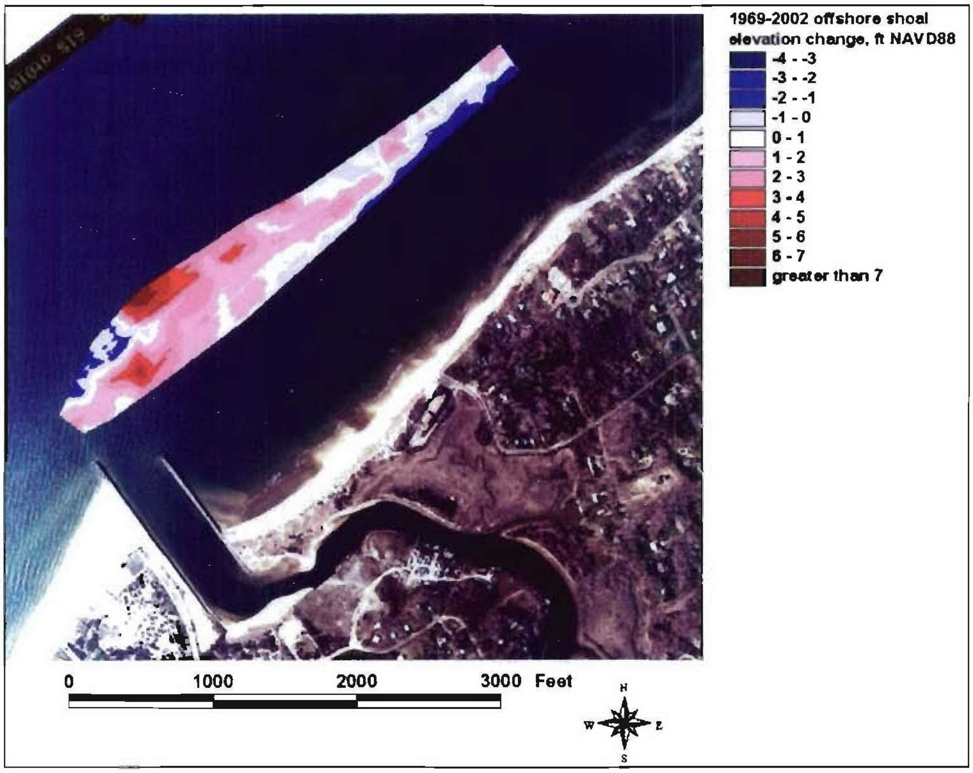

Figure 4-7. Offshore shoal elevation change, 1969-2002 and Mattituck Inlet 16 April 2003

Table 4-1
Estimated Offshore Volume Change, Mattituck Inlet, 1927-2002

Volume Change (cu yd)			
Area	**1927-1969**	**1969-2002**	**1927-2002**
Total study area	**155,000**	**188,000**	**343,000**
Seaward shoaling area (polygon A)	**78,000**	**35,000**	**113,000**
Landward shoaling area (polygon B)	**negative 45,000**	**44,500**	**negative 500**
Total shoaling area (polygon A/B)	**33,000**	**78,500**	**111,500**
East bypass bar area (polygon C)	**13,500**	**12,000**	**25,500**
Total offshore shoal area from –21.5 ft NAVD88		**13,500**	

Deposition Rate (cu yd/ year)			
Area	**1927-1969**	**1969-2002**	**1927-2002**
Total study area	**3,700**	**5,700**	**4,700**
Seaward shoaling area (polygon A)	**2,000**	**1,000**	**1,500**
Landward shoaling area (polygon B)	**negative 1,000**	**1,000**	**0**
Total shoaling area (polygon A/B)	**1,000**	**2,000**	**1,500**
East bypass bar area (polygon C)	**300**	**400**	**350**
Total offshore shoal area from –21.5 ft NAVD88		**500**	

Estimation of volume change of the offshore shoal for the spatial extents shown in Figure 4-6 provides insight into the morphology change and patterns of erosion and deposition for the 75-year period considered. The total study area gained 343,000 cu yd, yielding a rate of deposition of approximately 4,500 cu yd/year. A considerable portion of this deposition is contributed by impoundment directly west of the west jetty, as shown in Figure 4-5c. As a result of seaward migration of the shoal, the seaward area of the shoal (polygon A) was an area of deposition from 1927 to 2002, and the landward portion (polygon B) was an area of erosion. Deposition took place in both areas between 1969 and 2002. Polygons A and B are of equal area. Considered collectively, polygon A+B experienced a net growth of 33,000 cu yd from 1927 to 1969, and a net growth of 10,000 cu yd for the period 1969-2002.

The rate of deposition for the seaward area was approximately 2,000 cu yd/year between 1927 and 2002. One thousand cu yd/year of this deposition can be attributed to migration of the offshore shoal, because the landward area is shown to be eroding at a rate of 1,000 cu yd/year. Deposition of new material, therefore, accounts for 1,000 cu yd/year, and can be considered the actual growth rate of this feature for the period considered. The east bypassing bar is accreting at a rate of 300 to 400 cu yd/year. The areas of growth are along the seaward edge of this feature and at the western tip, nearest to the jetty entrance.

Volume change for the total spatial extent of the offshore shoal surveyed on 6-8 October 2002 survey was calculated for the period 1969-2002. The lowest elevation of either TIN, -21.5 ft NAVD88, was selected as the reference datum. The calculated volume growth is 13,500 cu yd, and the calculated rate of volume change is 500 cu yd/year. The volume of the spatial extent of the offshore shoal shown in Figure 4-7 was calculated to be 460,000 cu yd.

The relative movement of the features offshore of Mattituck Inlet has the potential to alter the sediment transport pathways. Figure 4-8 shows the center lines of the offshore shoal in 1927 and 2002. Figure 4-9 shows the relative location of this feature as well as the relative location of the center lines of the main longshore bar east of Mattituck Inlet. By 2002, the center line of the main longshore bar had migrated landward (referenced to its contemporary shoreline), the shoal has migrated seaward, and the two features no longer directly connected. The separation of the features resulted in the formation of a secondary longshore bar adjacent to the east jetty, which may bypass finer sediment to the downdrift beach.

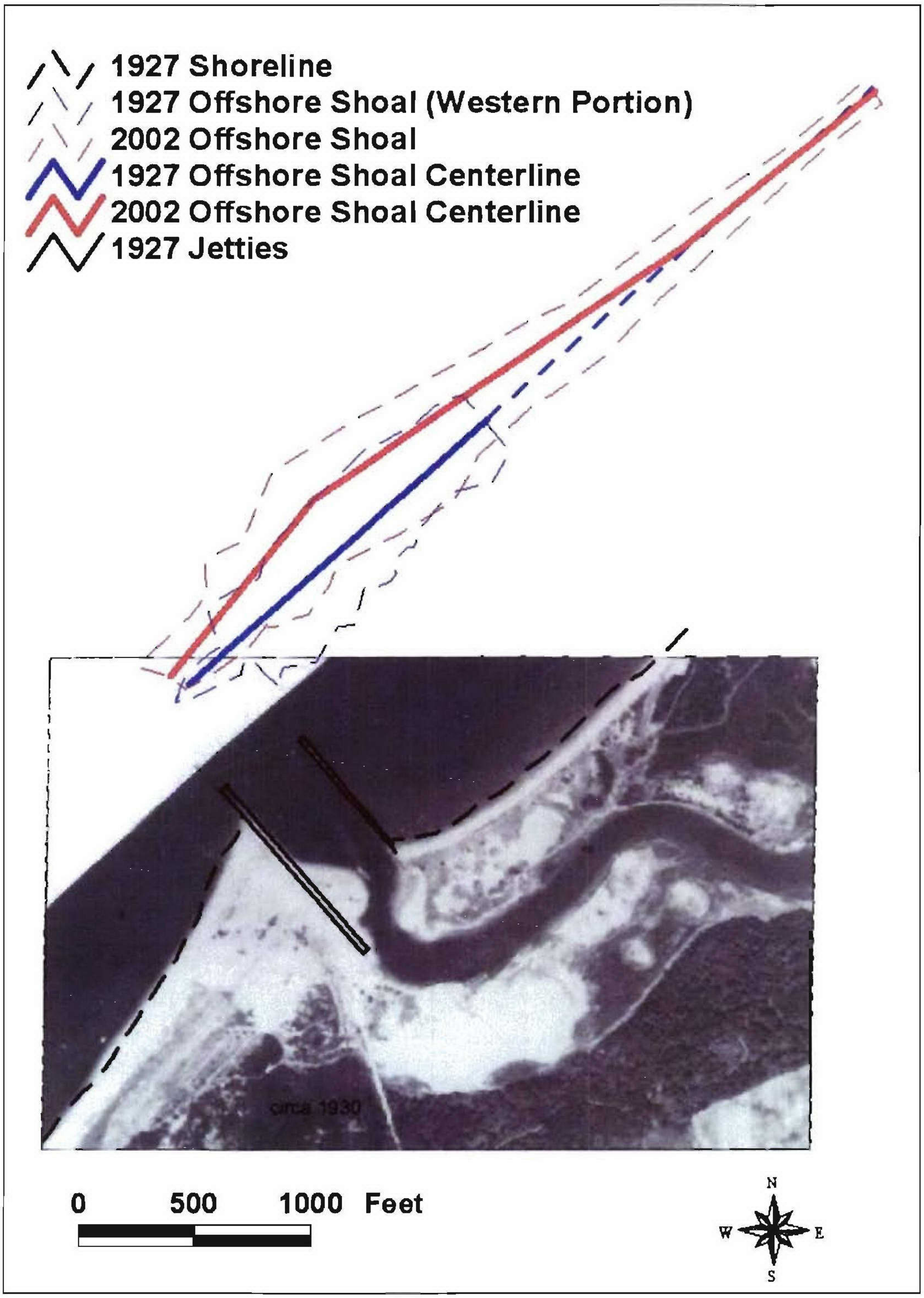

Figure 4-8. Mattituck Inlet offshore shoal center lines, 8 December 1927 and 6-8 October 2002

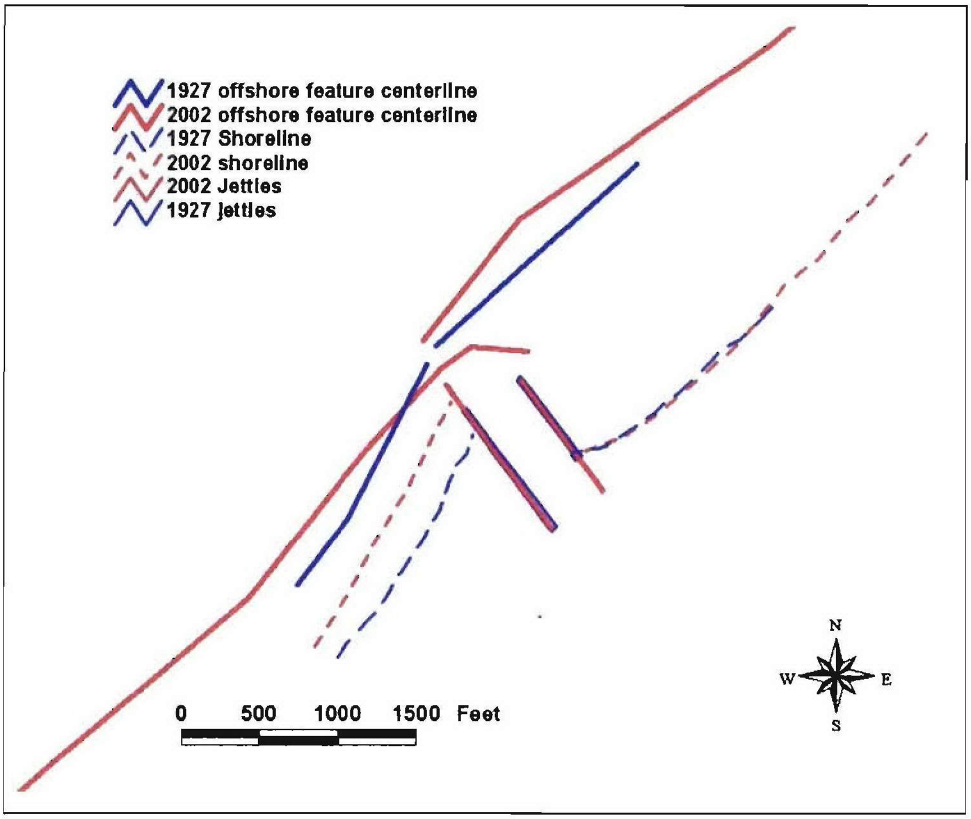

Figure 4-9. Offshore feature center lines, 8 December 1927 and 6-8 October 2002

In summary, the offshore shoal located east of Mattituck Inlet migrated seaward from 1969 to 2002. This movement, and the landward migration of the main longshore bar located to the west of the inlet, indicate a change in the sediment pathways. The increased rate of deposition at the landward area of shoaling (from −1,000 to +1,000 cu yd/year in polygon B), the decreased rate of deposition at the seaward area (from 2,000 to 1,000 cu yd/year in polygon A) and the formation of a bypassing bar directly east of the inlet support this conclusion.

Navigation channel and flood shoal morphology change

This section begins with a review of the natural morphology of Mattituck Inlet and the modifications introduced by construction of the jetties and by channel dredging. The evolution, morphology, and migration of the flood shoal at Mattituck Inlet in response to modifications of the jetties and dredging is analyzed. For the period 1980 to 2002, volume and elevation changes associated with dredging activities are calculated. Based upon GIS-generated grids, the volume changes for three dredging events are estimated. The results are compared to dredging volumes reported by the New York District. To understand shoaling patterns within Mattituck Inlet, temporal changes of selected channel cross sections are analyzed.

The channel condition surveys discussed in this section are referenced to the mlw datum employed by the surveyors. As discussed in the previous section, the New York District mlw datum for this time period is believed to be 3.63 ft below NAVD88.

The dredging history of Mattituck Inlet (Table 2-5) can be consulted to estimate the rate of sediment accumulation in the navigation channel. Dredging is usually performed on an as-need basis (every 10 to 15 years), and sometimes advance dredging is undertaken. These physical and economic constraints confound interpretation of dredging records and obscure efforts to make a one-to-one comparison between volume of sediment shoaled and volume of sediment dredged (Kraus and Rosati 1998). Dredging at Mattituck Inlet has also been conducted over varying spatial extents. If records are available over a sufficiently long interval, however, as is the case for Mattituck Inlet, uncertainties are reduced.

Natural morphology and initial modifications (1891-1914). The Rivers and Harbors Act of 19 September 1890 authorized a preliminary examination and survey of Mattituck Inlet that resulted in a favorable recommendation for inlet modification. The inlet was considered to have modest economic potential and was seen as a good harbor of refuge. Mattituck Creek in its natural state was winding and approximately 2-4 ft deep. Figure 4-10 shows the Mattituck Inlet hwl shoreline of 1891, referenced against the original configuration of the Federal navigation channel jetty, the present configuration of the Federal navigation channel, and the original jetty lengths of 1914. Kraus and Rosati (1997) discuss definitions of the shoreline, including the hwl.

The orientation of Mattituck Inlet in its natural state resembled that of Goldsmith Inlet prior to the recent dredging of 22-26 March 2004 (Figure 4-106), where a narrow spit directed to the east, the dominant direction of sediment transport, developed. Another example of similar morphology on the north shore of Long Island is found at Stony Brook Harbor, where a large, well-developed east-directed spit exists (Cooke 1985; Park 1985; Zarillo and Park 1987).

Figure 4-11 shows the hwl shorelines of Mattituck Inlet for the year 1900. The morphology of Mattituck Inlet has changed significantly, and a west-directed spit is observed. This west-directed spit is believed to have evolved into what is now the eastern lobe of the flood shoal. The reversal in the inlet entrance orientation observed here is consistent with temporary closure and subsequent reopening of the inlet.

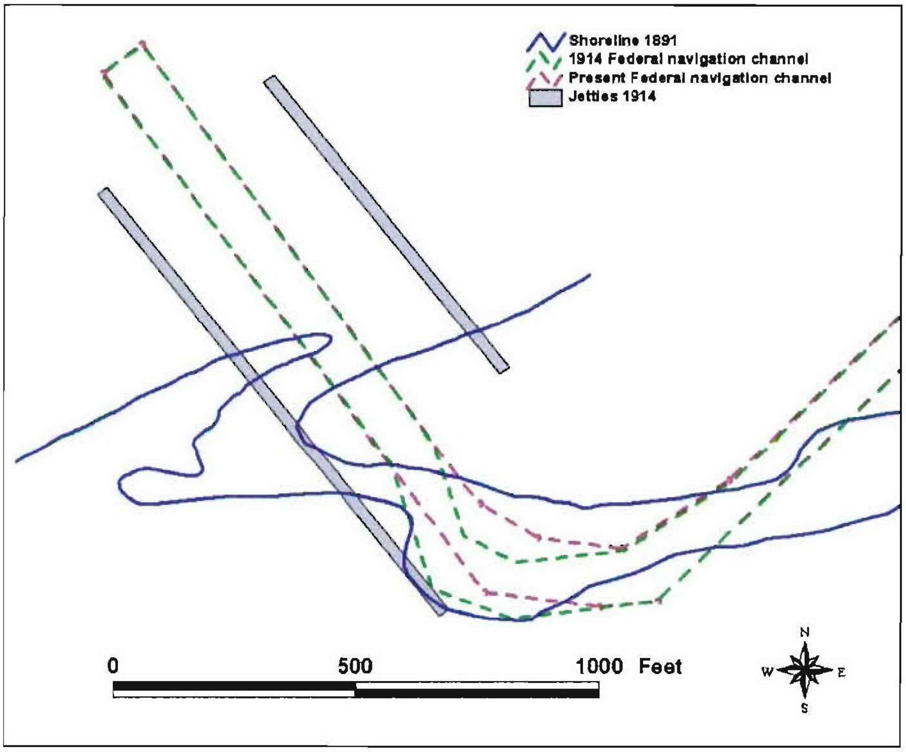

Figure 4-10. Mattituck Inlet orientation, 1891

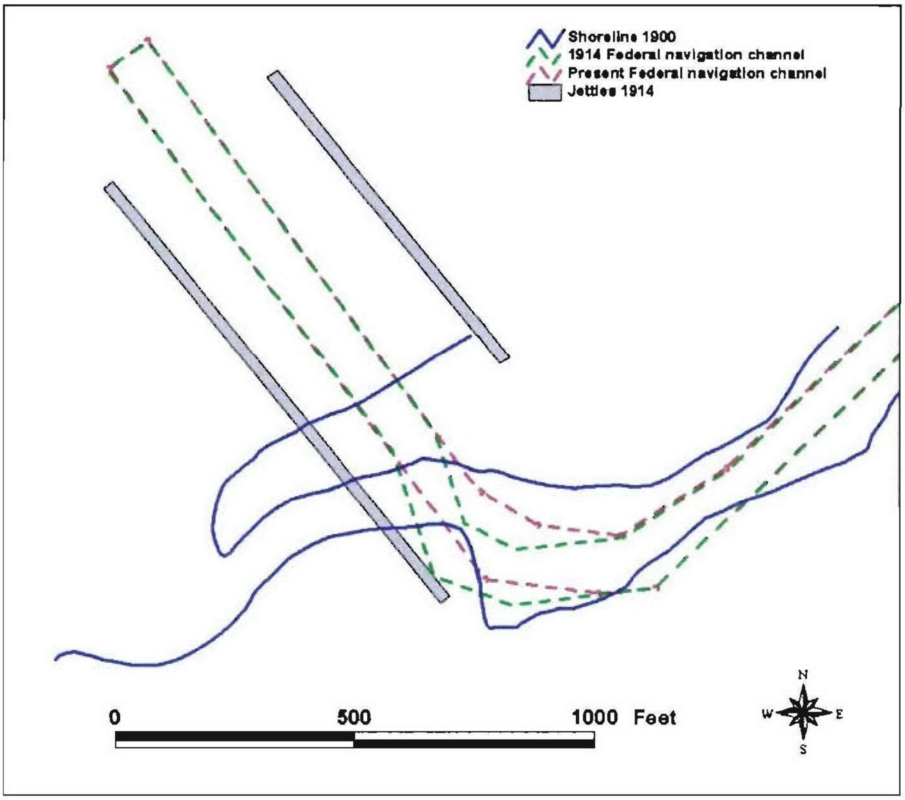

Figure 4-11. Mattituck Inlet orientation, 1900

New York District (1969) documents that between the 1830s and 1880s, the entrance to Mattituck Inlet migrated 600 ft to the west, and the spit length was about 1,000 ft. It is probable that this reported configuration is the result of lengthening of the spit to the east, making the inlet hydraulically inefficient, leading to a breach to the west, closer to the inland source channel, and the present day entrance. Observed after the breach, the channel would have appeared to migrate west. Figure 4-12 illustrates a hypothesized sequence (a to d) of spit growth, closure, and reopening that would yield the observed change in orientation. The sequence resembles one of a number of proposed models described by FitzGerald et al. (2000).

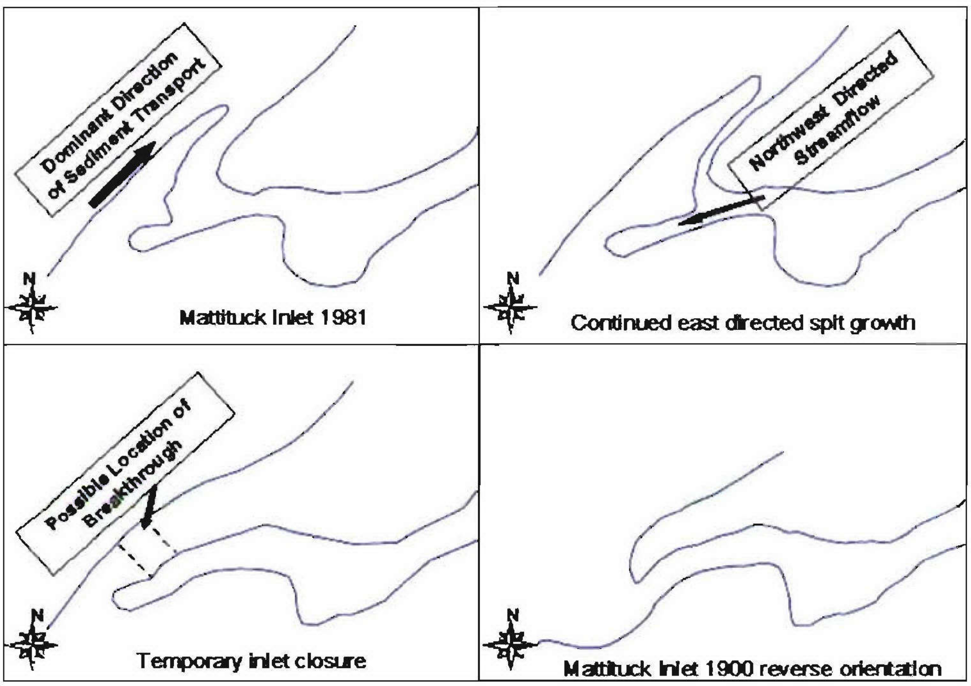

Figure 4-12. Mattituck Inlet, 1891-1900, hypothesized reorientation

The creation of the Federal navigation channel and construction of the jetties was approved in the Rivers and Harbor Act of 3 June 1896, and work commenced in 1901. Figure 4-13 shows the morphology of Mattituck Inlet at this time. It is assumed that the inlet opening shown here was the result of an initial partial dredging and that the natural opening to the west was filled in.

The morphology of Mattituck Inlet for 1905 and 1907 is illustrated in Figure 4-14. Construction of the east jetty was completed in 1906, and a partial dredging for improvement took place in 1907 (U.S. Engineers Office, First District 1928). It is not known whether the morphology of 1907 shown in Figure 4-14 was that prior to or after the partial dredging of 1907. It is believed that the morphology illustrated was prior to the initial dredging of 1907, because shoaling is observed along the inside of the west jetty and near the base of the east jetty.

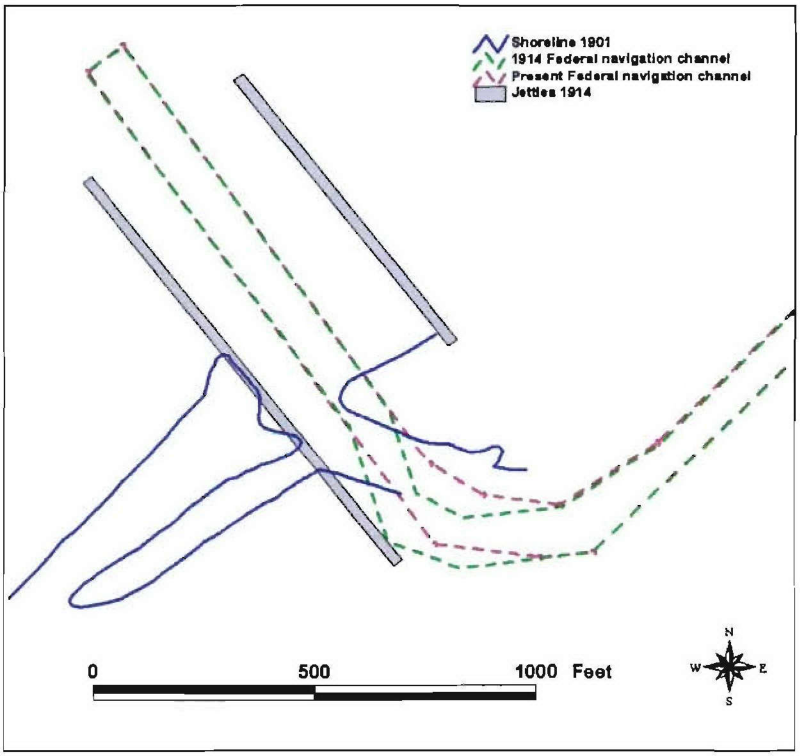

Figure 4-13. Mattituck Inlet orientation, 1901

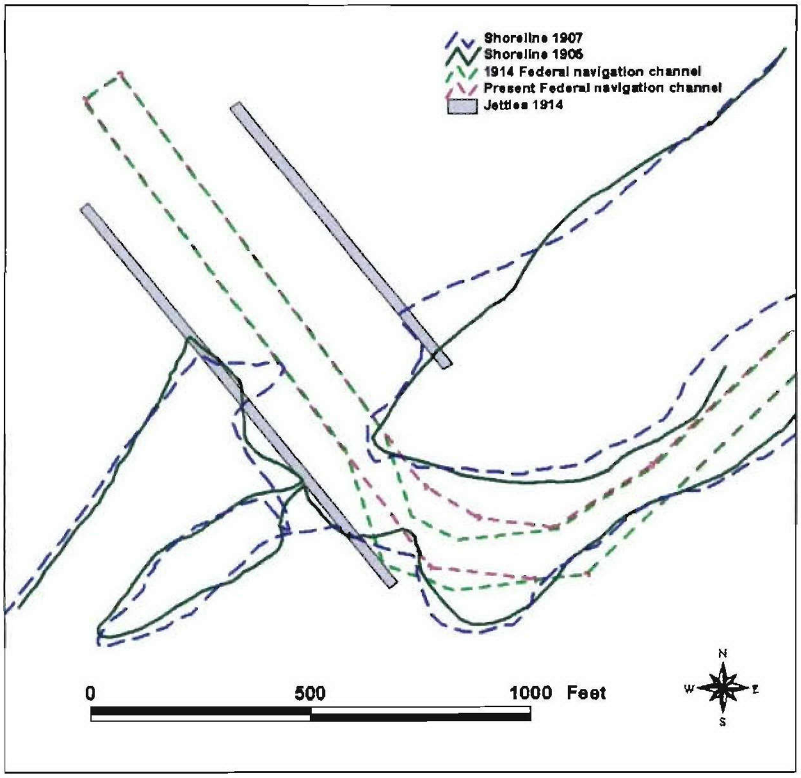

Figure 4-14. Mattituck Inlet orientation, 1905-1907

In 1914, the Federal navigation channel was completed by dredging. Analysis of New York District condition surveys indicate that Mattituck Creek had been dredged as of a survey dated August 1913 to April 1914. The morphology of Mattituck Inlet for the period 1913-1914, as listed on the New York District shoreline survey map, is illustrated in Figure 4-15. Shoals along the inside of the west jetty had been cleared, shoaling near the base of the east jetty no longer encroaches upon the Federal navigation channel, and the inlet was widened along the west bank, directly behind the turn to the east. The morphology shown here is, therefore, believed to be for a period after the full dredging of 1914.

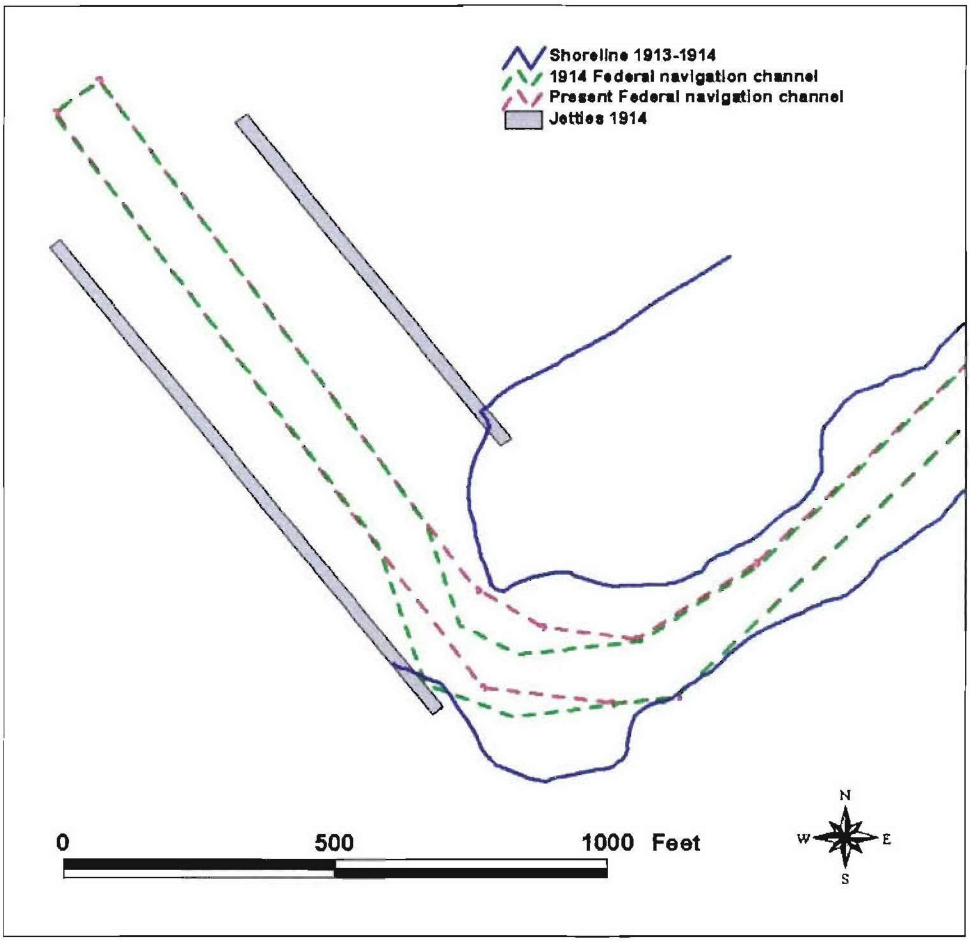

Figure 4-15. Mattituck Inlet orientation, 1913/14

Inlet response. This section describes and quantifies sediment shoaling along the inlet adjacent to the west jetty, sedimentation patterns and shoaling at the base of the east jetty, the volume and rates of channel infilling, and the area, volume, and growth of each lobe of the flood shoal for the period 1935 to 1938. Mattituck Inlet, and the extent of shoaling along the inside of the west jetty, is shown in Figure 4-16, circa the 1930s (exact year and date unknown). An apparent landward breach at the base of the east jetty occurred on or around 1935 (Figure 4-17).

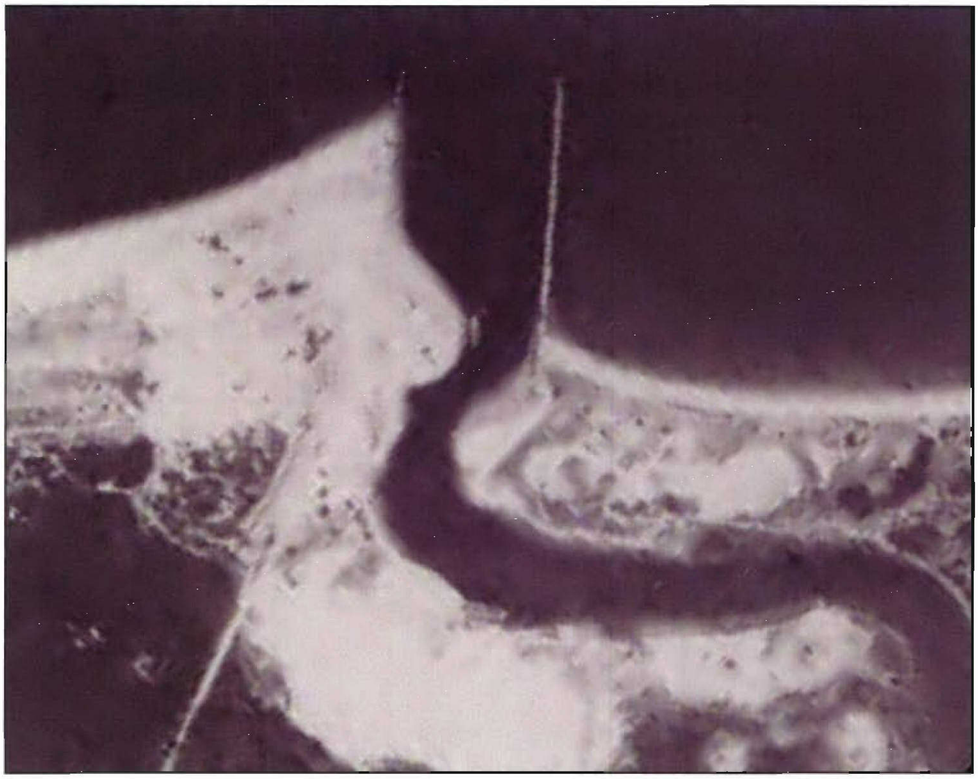

Figure 4-16. Mattituck Inlet with shoaling along inside of west jetty, circa 1930s (exact year and date unknown)

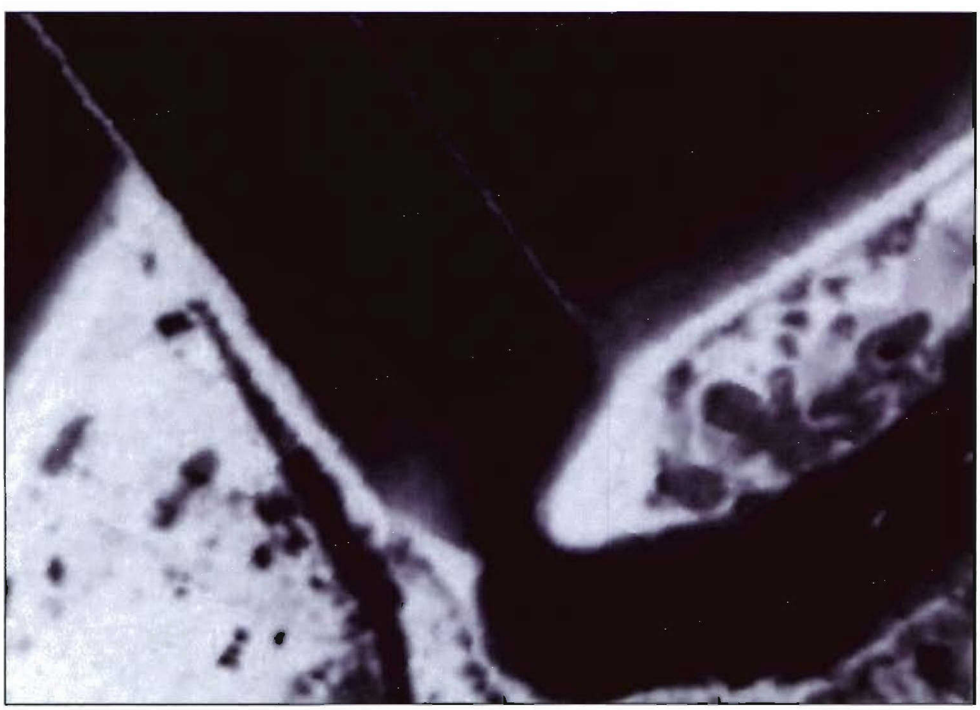

Figure 4-17. Mattituck Inlet east jetty landward breach, 1941

To quantify areal changes of the flood shoal at Mattituck Inlet from 1935 to 1938, each lobe was divided into two sections, the portion that lies below mlw datum, and the portion that is above mlw. The attached spit, located at the base of the east jetty and not considered to be a portion of the flood shoal proper, is also analyzed. Table 4-2 lists the corresponding areas for each portion of the flood shoal in square feet.

Table 4-2
Mattituck Inlet Flood Shoal Area 1935-1938

	Area (sq ft)			
Year	**1935**	**1936**	**1937**	**1938**
West lobe below mlw	77,000	55,800	66,000	30,100
West lobe above mlw	48,800	63,200	75,600	81,000
West lobe total	125,800	119,000	141,600	121,100
East lobe below mlw	107,200	33,400	61,900	66,800
East lobe above mlw	50,500	21,500	25,200	45,100
East lobe total	157,700	54,900	87,100	111,900
Flood shoal total	283,500	174,400	228,700	233,000

Volumes dredged from Mattituck Inlet during November 1935 to May 1936, the annual volume of shoaling within Mattituck Inlet, and the volume of channel infilling for the period 1936 through 1938, were calculated by differencing bathymetry surfaces digitized from the original survey sheets. Difference surfaces generated by map calculations of raster grids for each survey are analyzed to understand the observed volume change. To quantify volume changes, TIN's were generated for each condition survey, and the volume for each TIN was calculated. Volume changes were calculated for the entire study area and a selected portion of the Federal navigation channel (to estimate the average rate of channel infilling). The volumes calculated represent those of sediment in the study area found above a datum located beneath the lowest elevation contained in the grids considered.

Each lobe of the flood shoal was divided into two sections, the portion outside the navigation channel and the portion inside the navigation channel. The volume above a selected datum was then calculated for each TIN. For the portions outside the navigation channel, a reference datum at a depth of 3 ft mlw was specified, corresponding to be the average ambient depth outside the channel. For the portion within the navigation channel, a reference datum at a depth of 9 ft mlw was specified, corresponding to the average depth after dredging. The volume and area of each portion of the flood shoal are listed in Table 4-3. This method does not necessarily consider shoaling along the sloping walls of the Federal navigation channel, which may introduce error.

Table 4-3
Estimated Mattituck Inlet Flood Shoal Volumes and Areas, 1935-1938

Feature	1935	1936	1937	1938
Volume (cu yd)				
West lobe outside channel	11,600	19,400	23,400	16,100
West lobe inside channel	7,100	0	3,100	6,400
West lobe total	18,700	19,400	26,500	22,500
East lobe outside channel	9,800	5,800	5,700	9,300
East lobe inside channel	17,600	0	3,400	4,200
East Lobe total	27,400	5,800	9,100	13,500
Flood shoal total	46,100	25,200	35,600	36,000
Area (sq ft)				
West lobe outside channel	102,800	109,200	113,600	86,200
West lobe inside channel	25,600	0	14,000	17,200
West lobe total	128,400	109,200	127,600	103,400
East lobe outside channel	90,000	56,300	53,600	80,900
East lobe inside channel	58,100	0	24,100	28,200
East lobe total	148,100	56,300	77,700	109,100
Flood shoal total	276,500	165,500	205,300	212,500

The original navigation project authorized the jetties to the 9-ft mlw depth contour (Ralston 1928). The authorized jetty lengths, 1,030 ft for the west jetty and 775 ft for the east jetty, did not adequately protect the inlet from shoaling. Sediment intrusion from the west to east, associated with the predominant direction of longshore transport, augmented by storms from the northwest quadrant, resulted in rapid shoaling within the channel along the west jetty. In addition, the shoreline directly east of Mattituck Inlet receded rapidly, causing a landward breach at the base of the east jetty sometime in the mid-1930s. Evidence of this landward breach can be seen in Figure 4-17 (circa 1941).

The initial new work dredging of the Federal navigation channel at Mattituck Inlet was completed in 1914. From June to November 1921, the first maintenance dredging occurred, removing 13,498 cu yd of sediment. Given the fact that the next dredging occurred only 2 years later, this dredging is considered to be an emergency dredging to restore the Federal navigation channel to project dimensions. Visual inspection of a New York District condition survey dated 30 April 1920 confirms that the channel had greatly shoaled and was nearly non-navigable.

Figure 4-18a shows the approximate hwl position in 1927, indicating considerable accretion on the west side of Mattituck Inlet. Dredging from August to September 1923 removed 49,168 cu yd of sediment. Of this dredging and the dredging of September-October 1927, Ralston (1928) states that the removed sediment was "principally from the entrance channel between the jetties." Newly dredged channels will often be subject to sediment slumping, in which sediment falls into a channel as the inlet trends towards equilibrium morphology. Given the large volumes dredged in the period 1921 - 1927, it is hypothesized that sediment slumping is responsible for a portion of the sediment dredged, and that the volumes dredged during this early period cannot be totally attributable to longshore sediment transport rates for this area.

Condition surveys indicates that the Federal navigation channel had narrowed to less than 50 ft at the base of the east jetty by May 1925, and that controlling depths of the channel had decreased to 5 ft mlw by May 1925, to 3 ft by June 1926, and to 2.5 ft by August 1927 (Ralston 1928). Preliminary examination (submitted 29 April 1927) and subsequent survey (submitted 22 June 1928), concluded that "shoaling is caused mainly by heavy material (sand and gravel) being driven into the inlet by the action of storms from the northwest quadrant, to which the inlet is directly exposed" (Ralston 1928). The report notes that sand fences had been erected with no appreciable effect, which precludes wind-blown sand as a significant sediment source (or that the sand fencing was ineffective). These surveys produced a recommendation that the west jetty be extended seaward 350 ft, or to the 12-to-15 ft mlw depth contour. The survey also recommends a possible further seaward extension of 150 ft for the west jetty and a seaward extension of 300 ft for the east jetty "if required and conditions indicate" (Ralston 1928). The Rivers and Harbor Act of 30 August 1935 authorized a 250-ft seaward extension of the west jetty.

The dredging from September to October 1927 restored Mattituck Inlet to the specified project depth. Figure 4-18a shows channel elevations, and Figure 4-18b shows the areal extent of the flood shoal, for 23 September 1935, 8 years after this dredging. The east and west lobes of the flood shoal have joined, and the controlling depth is 2 ft mlw. At this time, the Federal navigation channel was presumably navigable only during times of high water. Infilling along the insides of both jetties created significant tracts of dry shoals. The condition survey of 23 September 1935 did not fully record the shoreline position. The landward breach at the base of the east jetty can be discerned. Evidence of this breach becomes clearer in successive surveys. The shoreline fragments for this period that were recorded are indicated in black, referenced against the hwl shoreline of 8 December 1927. A portion of this area, within the channel at the base of the east jetty, appears to be below mlw, further indicating that the breach had begun to form at this point.

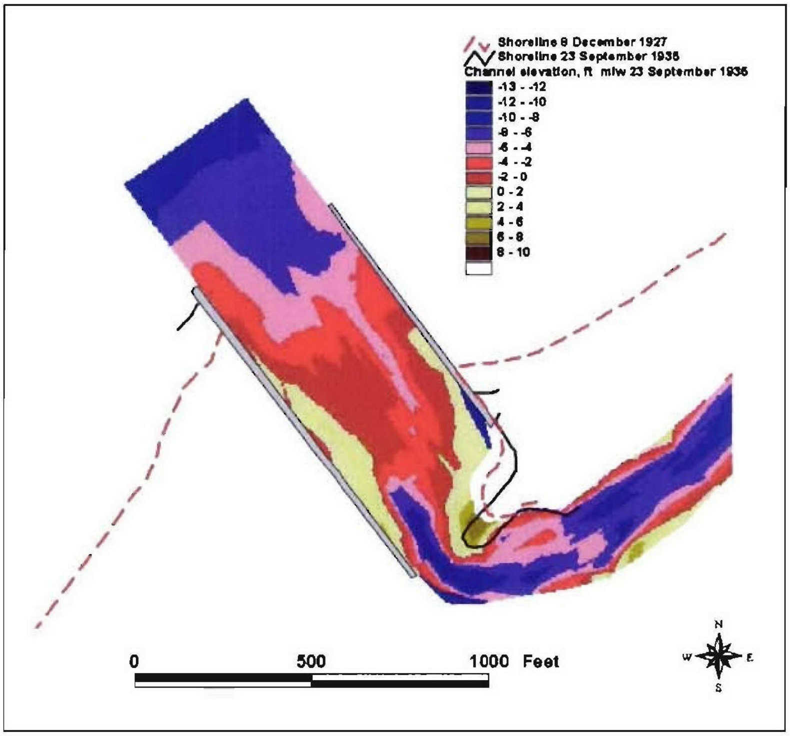

Figure 4-18a. Mattituck Inlet channel elevation, 1935

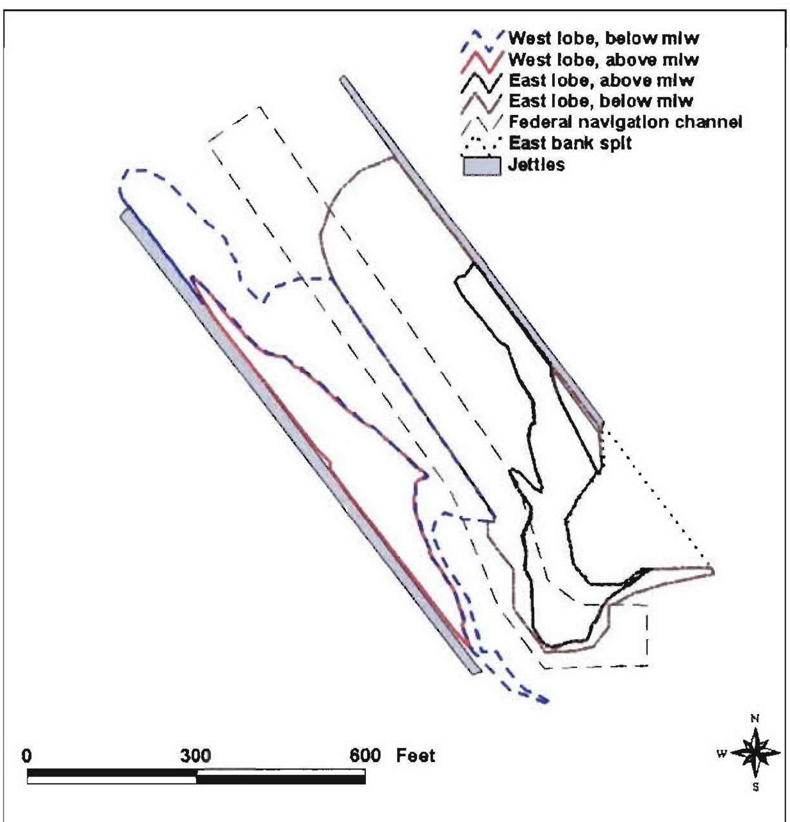

Figure 4-18b. Mattituck Inlet flood shoal area, 1935

Channel elevations and hwl location for 4 May 1936, immediately after the dredging of November 1935 to May 1936, are shown in Figure 4-19a. The areal extent of the flood shoal is illustrated in Figure 4-19b. The shoreline of 4 May 1936 is illustrated in Figure 4-19a, referenced against the shoreline of 8 December 1927, and the landward breach near the base of the east jetty is clearly apparent. It is inferred that sediment was transported to the east bank by landward bypassing during times of high tide and storms. It is appropriate to consider this feature a spit onto which the east lobe of the flood shoal attaches itself. Because this spit is dredged only if it encroaches upon the Federal navigation channel, a portion was not removed. This portion remains in the system and has evolved into what is considered as the modern-day flood shoal.

The dredging of November 1935 to May 1936 restored the Federal navigation channel to project depth. Figure 4-19c plots the net change in elevation as a result of the maintenance dredging of November 1935 to May 1936. In some areas, the elevation change is extreme. Near the base of the jetties, the channel has a tendency to migrate to the west, and dredging served to reposition the navigation channel back to project specifications. Dredging reduced elevation by 16 ft in the area where the flood shoal was removed. An increase of 12 ft occurred where landward bypassing deposited sediment along the inside of the base of the east jetty. An increase of 8 ft occurred near the west bank of the channel, presumably a result of repositioning the channel.

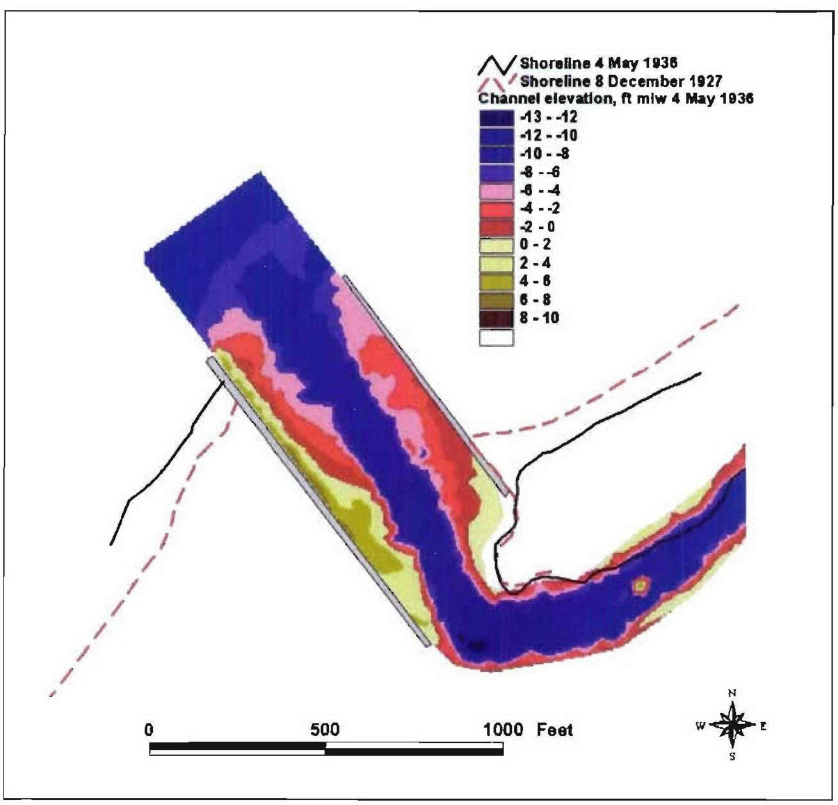

Figure 4-19a. Mattituck Inlet channel elevation, 4 May 1936

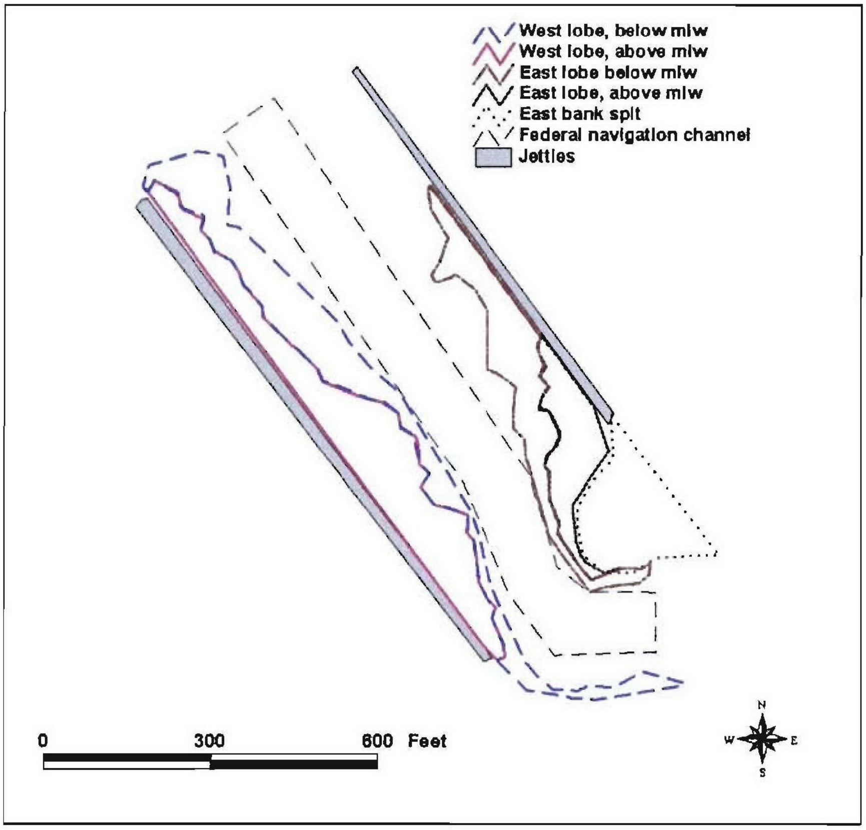

Figure 4-19b. Mattituck Inlet flood shoal area, 4 May 1936

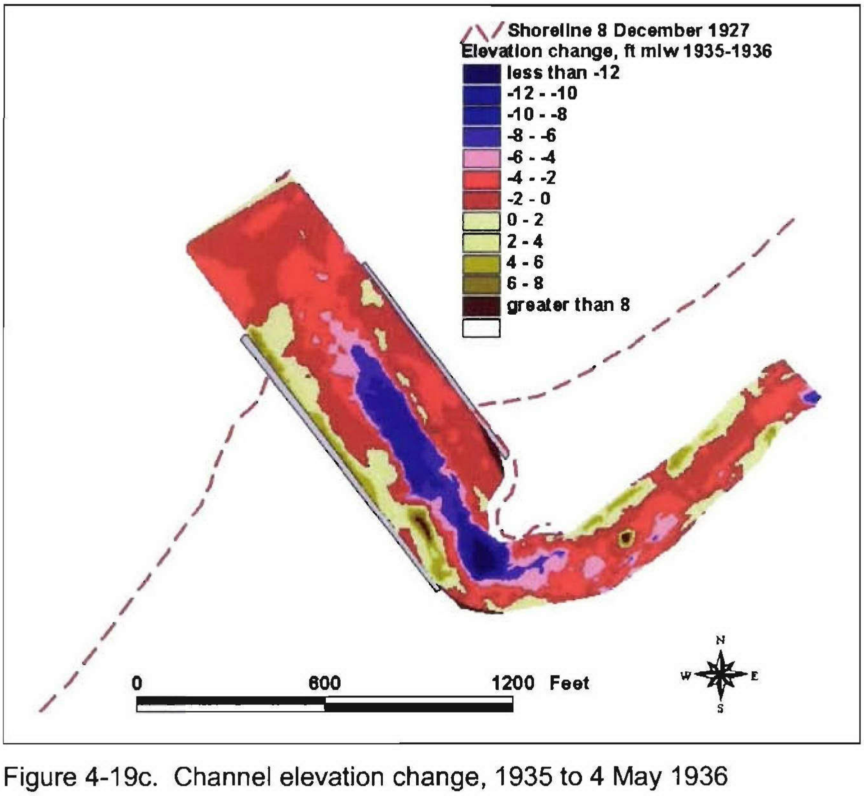

Figure 4-19c. Channel elevation change, 1935 to 4 May 1936

Dredging records indicate that 50,785 cu yd of sediment was removed during the period November 1935 to May 1936. The volume change for the total study area below mlw is here calculated to be 44,000 cu yd. The volume change for a selected portion of the Federal navigation channel below mlw, as indicated in Figure 4-20, was calculated to be 25,500 cu yd. The average pre-dredging depth for the Federal navigation channel was calculated to be 3.2 ft mlw, and the average depth after dredging was calculated to be 9 ft, a figure which conforms to the specified project depth of 7 ft mlw with 2 ft allowable overdraft. The volume change for what was defined to be the flood shoal proper, as outlined in Figure 4-19a and 4-19b, was calculated to be 20,100 cu yd. The lobes of the flood shoal within the Federal navigation channel were removed, as were a considerable portion of the east lobe outside the channel and a small portion of the west lobe outside the channel.

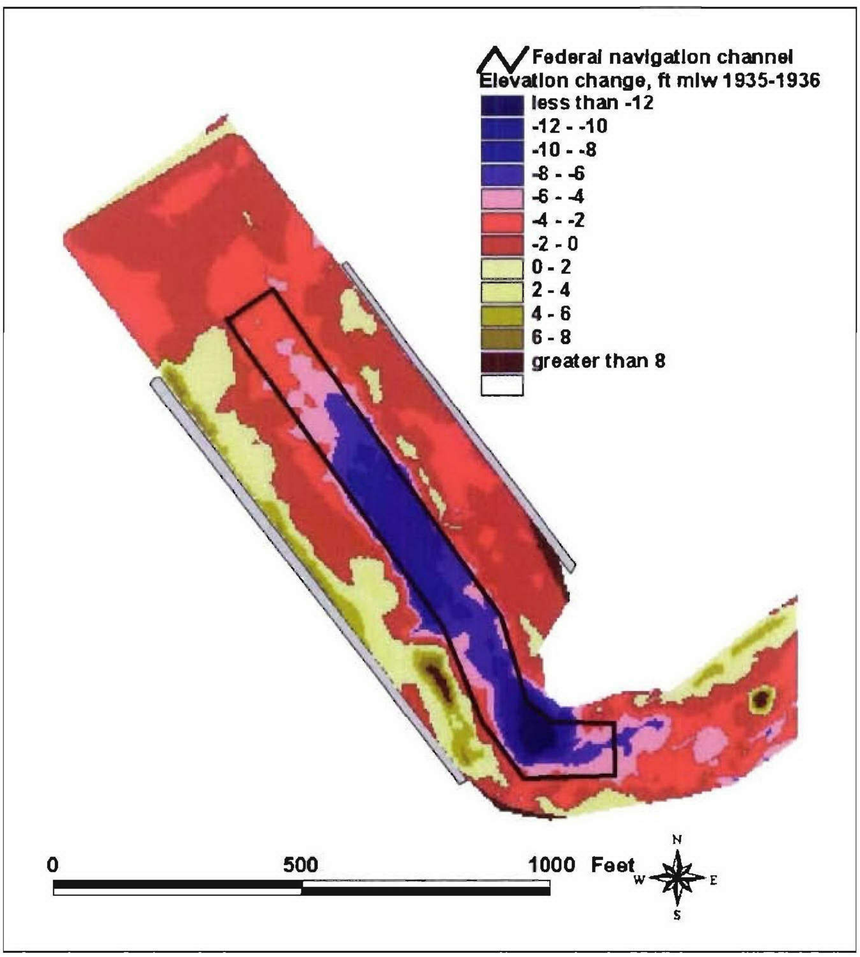

Figure 4-20. Federal navigation channel study area

Channel elevations for 3 July 1937 are shown in Figure 4-21a. The areal extent of the flood shoal at this time is shown in Figure 4-21b, and channel elevation change between 4 May 1936 and 3 July 1937 is plotted in Figure 4-21c. For this 14-month period, the net volume change for the study area was calculated to be 12,000 cu yd, yielding an annual sediment accumulation rate of 10,500 cu yd/year. The portion of the Federal navigation channel considered was calculated to have 5,200 cu yd of infilling, for an average channel infilling rate of 4,500 cu yd/year for the period. The area of the Federal navigation channel considered is 194,000 sq ft. The average depth of the channel for 3 July 1937 was calculated to be 7.8 ft. The flood shoal was calculated to have grown from 25,200 to 35,600 cu yd.

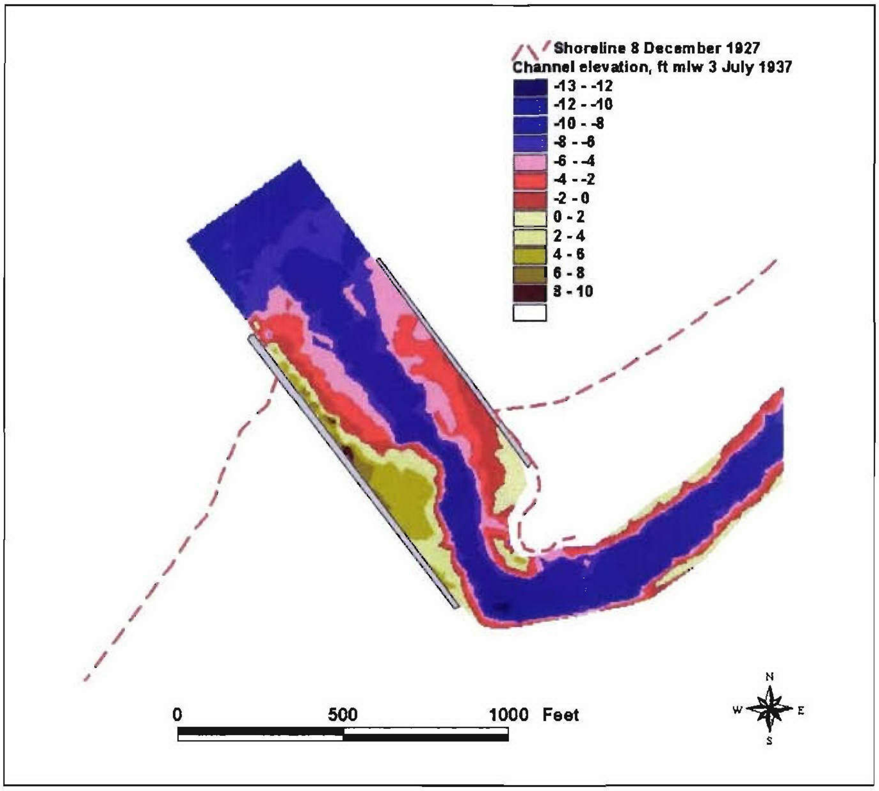

Figure 4-21a. Mattituck Inlet channel elevation, 3 July 1937

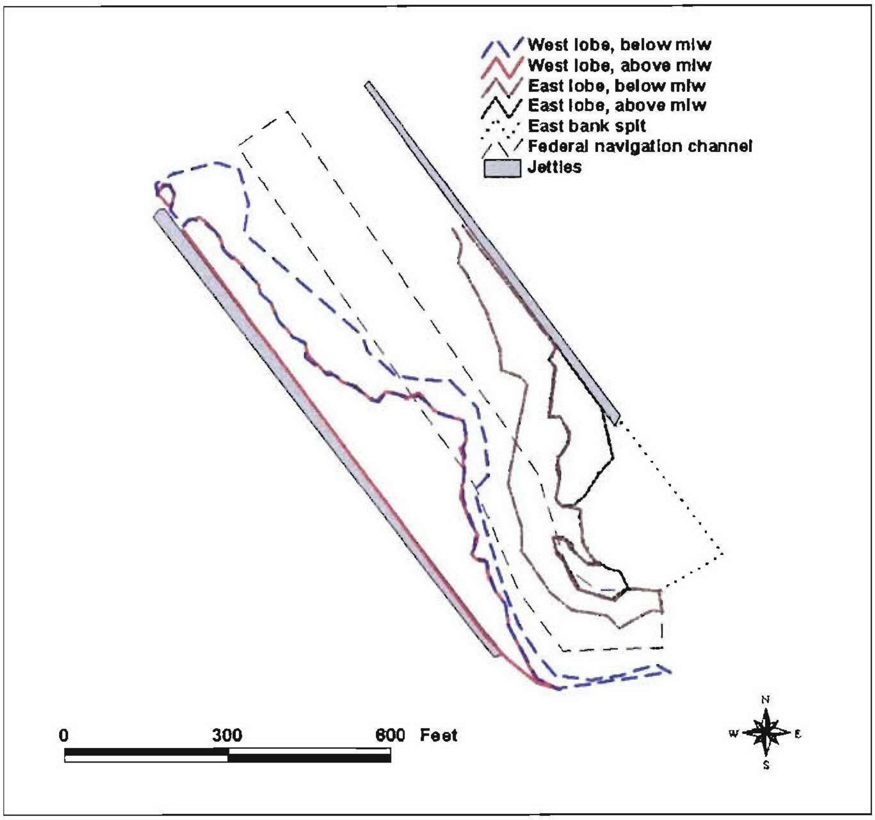

Figure 4-21b. Mattituck Inlet flood shoal area, 3 July 1937

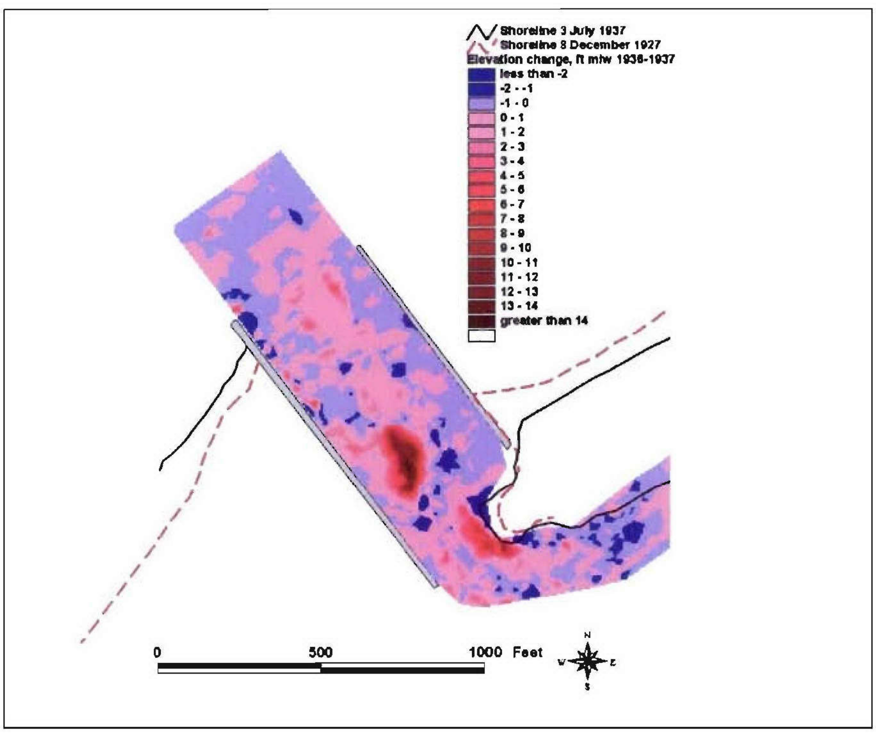

Figure 4-21c. Channel elevation change, 4 May 1936 to 3 July 1937

Figure 4-22a shows channel elevations for July 1938 (exact date not available), and the areal extent of the flood shoal is illustrated in Figure 4-22b. Channel elevation changes between 4 May 1936 and July 1938 are plotted in Figure 4-22c. For the 26-month period, the net volume change for the study area was calculated to be 13,882 cu yd, yielding an annual sediment accumulation rate of 6,500 cu yd/year. The portion of the Federal navigation channel considered was calculated to have 6,600 cu yd of infilling for the 26-month period, for an average channel infilling rate of 3,000 cu yd/year for the period.

The average depth of the Federal navigation channel for July 1938 was calculated to be 7.5 ft. The flood shoal was calculated to have grown by only 400 cu yd during this period. This small volume change can be attributed to the fact that the condition survey of 1938 did not fully record elevations along the west side of the inlet. The area of elevations not recorded can be discerned by comparing the survey extent shown in Figure 4-40 to that of prior condition surveys. The extent of this area is approximately 26,000 sq ft. Because the area not surveyed is dry shoal, the depth was taken to be at least 7.5 ft, based on the morphology of 3 July 1937 and the ambient depth at this location, resulting in a volume of shoaling that is estimated to be at least 7,000 cu yd. This figure, in addition to the 400 cu yd calculated, yields an estimated growth of the total flood shoal of 7,400 cu yd.

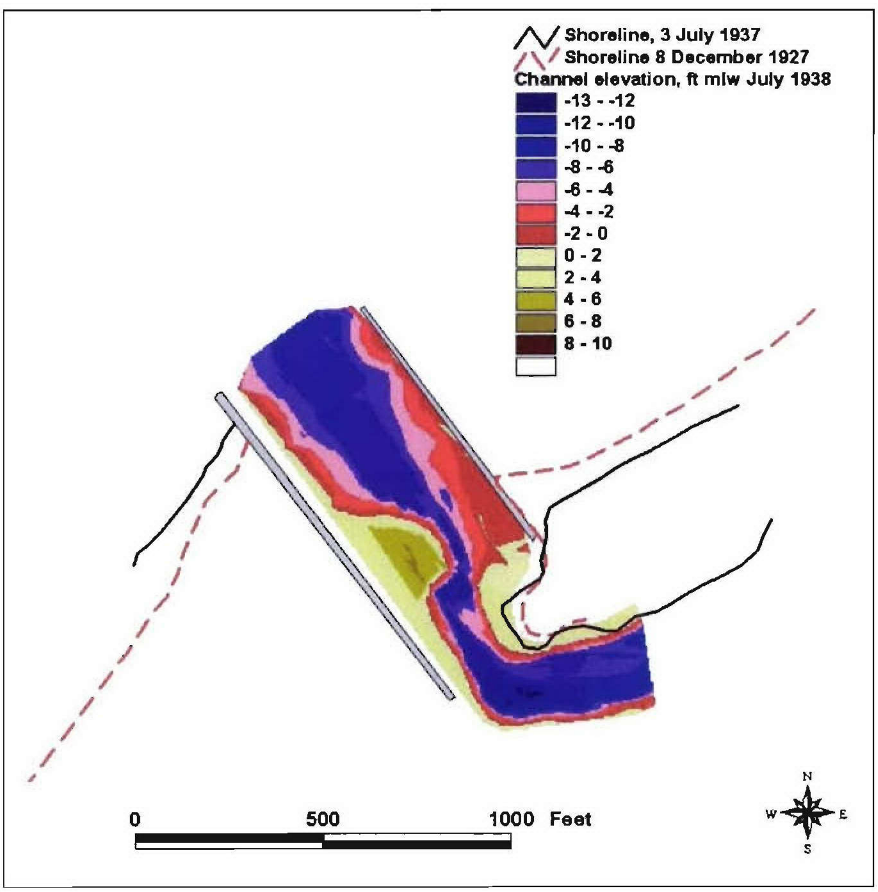

Figure 4-22a. Mattituck Inlet channel elevation, 1938

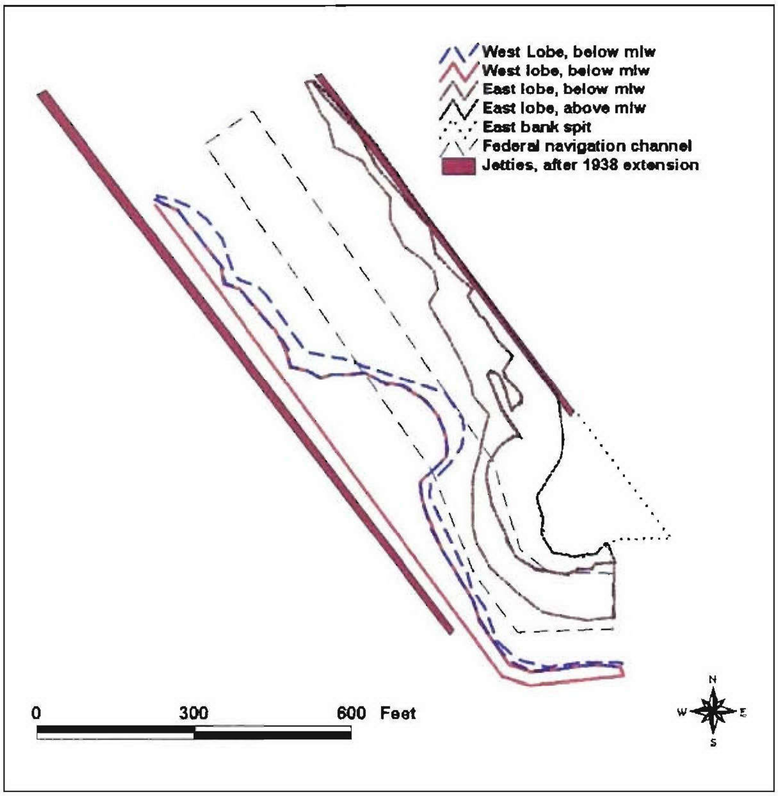

Figure 4-22b. Mattituck Inlet flood shoal area, 1938

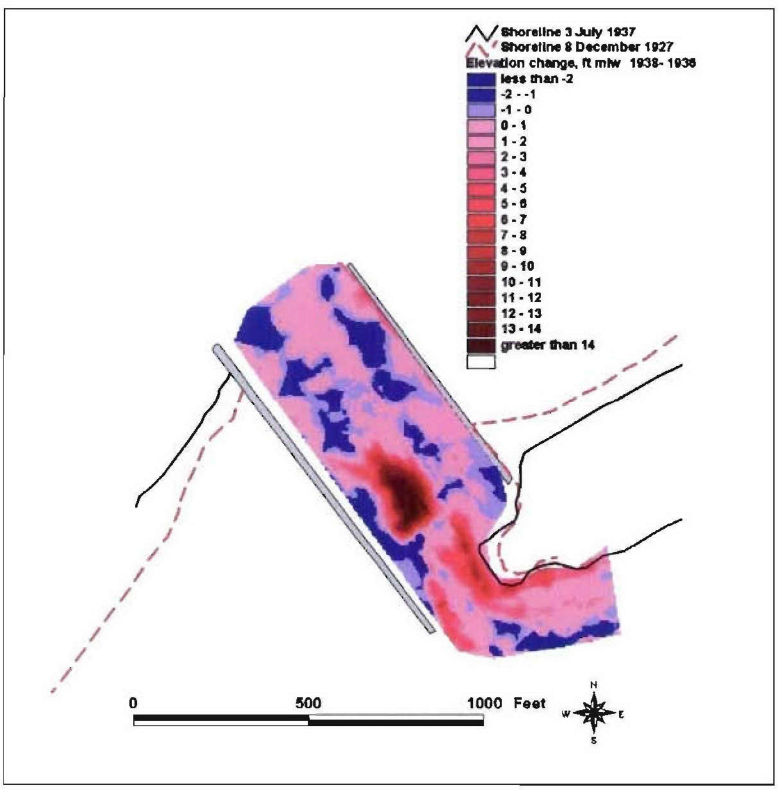

Figure 4-22c. Channel elevation change, 4 May 1936 to 1938

Changes in planform morphology for the west and east lobes of the flood shoal for the period 1936-1938 are illustrated in Figures 4-23a and 4-23b. The observed morphology change for both lobes may indicate the transport of sediment from the west lobe to the east lobe, further into the channel.

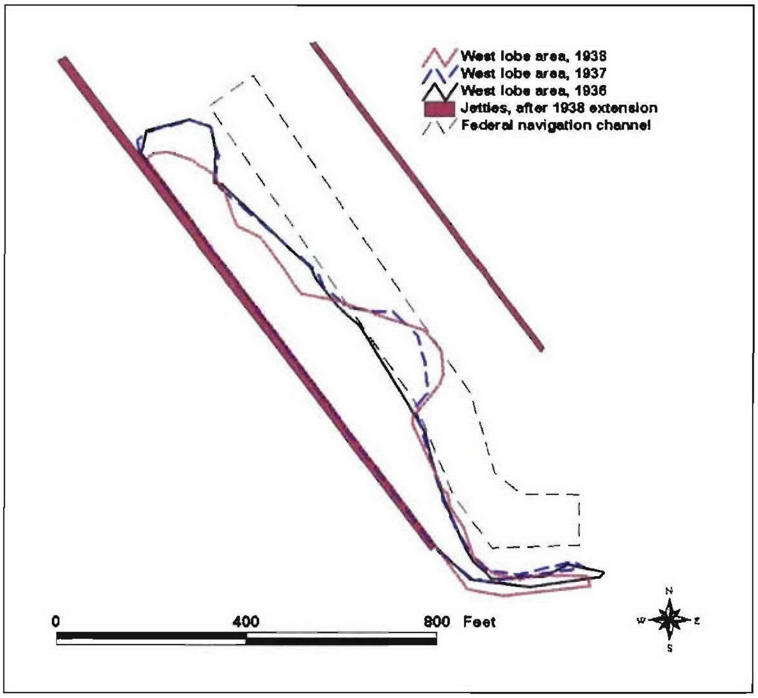

Figure 4-23a. West lobe morphology change, 1936–1938

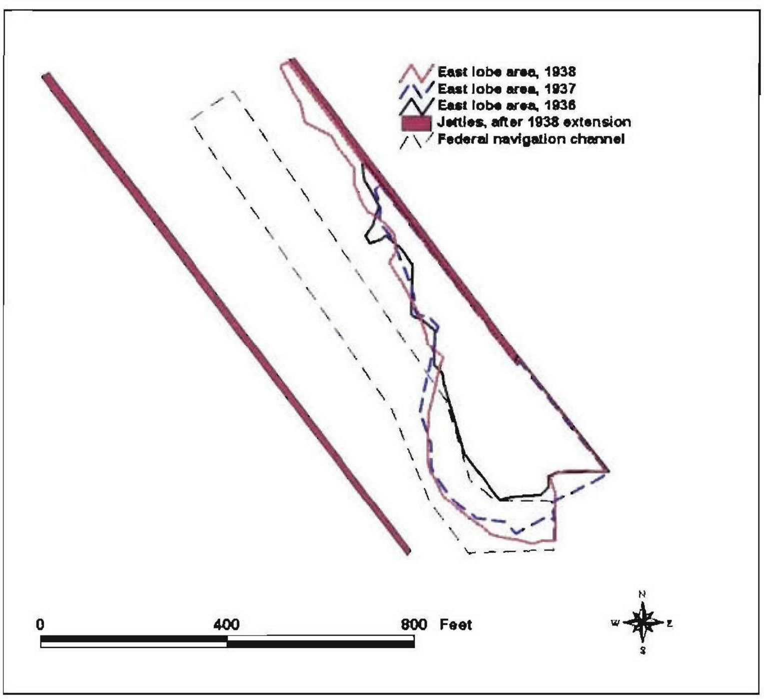

Figure 4-23b. East lobe morphology change, 1936–1938

Landward breaching, spit formation, and jetty modification. In response to rapid sediment accumulation, the west jetty at Mattituck Inlet was repaired and extended seaward 250 ft from October 1937 to September 1938 (Figure 4-24 and Table 2-6). Prior to this, on or before 1935, a breach next to the east jetty occurred as the shoreline receded. Figure 4-25 shows the shoreward breach and the approximate hwl recession from 1927 to 1941. Contour elevations are drawn to reveal shoaling of sediment within the inlet from 1935 to 1938. The condition survey of 1938 did not contain a shoreline (panel e), so it cannot be shown. The 1941 shoreline (panel f) was derived from an 1941 aerial photograph and should be regarded as an estimate. This series of figures documents the widening breach. The contour elevations illustrate the rapid buildup of sediment, where the inlet, directly inside of the east jetty has negative elevations in 1935 and positive elevations in 1936.

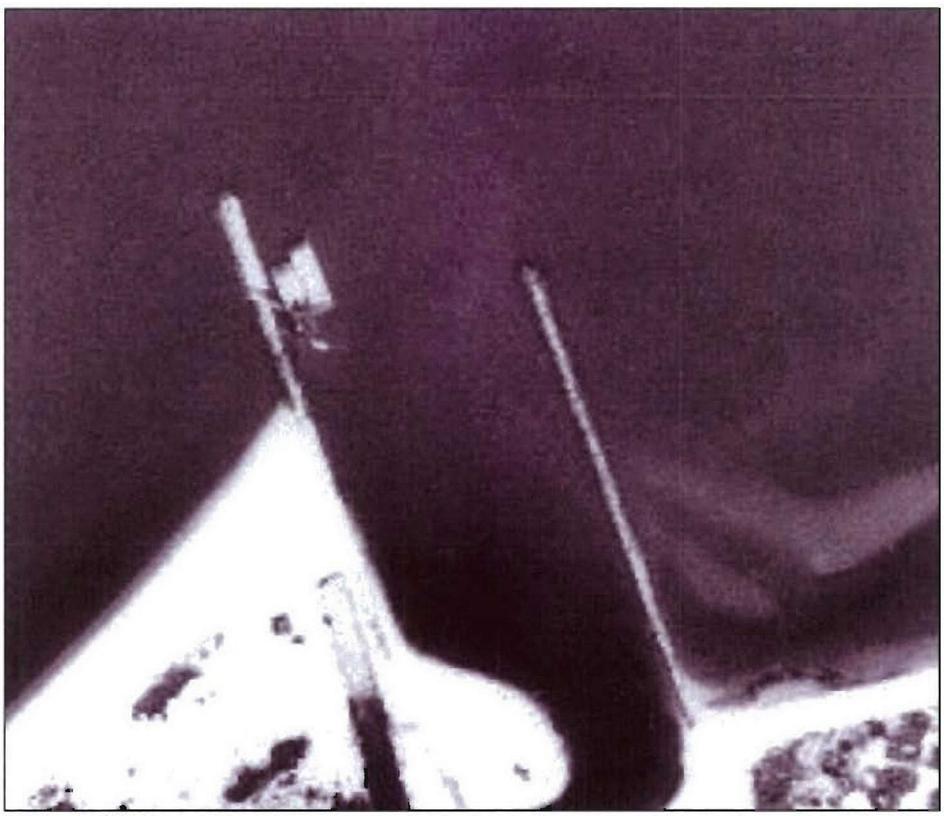

Figure 4-24. Mattituck Inlet west jetty seaward extension, 1938

The dredging of July to August 1938 removed 18,312 cu yd of sediment. Prior to this, the November 1935 to May 1936 dredging removed a large volume of sediment (50,785 cu yd) that restored the Federal navigation channel to project depth. As of 1938, the large volume of exposed shoal along the inside of the west jetty was still present (Figure 4-25). This exposed shoal is not apparent in the aerial photograph of 1941 (Figure 4-17) so it is reasonable to believe that the dredging of July–August 1938 removed a large portion of the west lobe of the flood shoal.

The seaward extension of the west jetty reduced sediment intrusion into the inlet from the west. Dredging of 53,893 cu yd and the repair and 280-ft landward extension of the east jetty took place between August-November 1946. Post-dredging surveys indicate that the west shoal was dredged in its entirety by this time. The dredging of September – November 1946 extended beyond the area of normal dredging (section A in Figure 2-7), and included a portion of Mattituck Creek (approximately half of section B in Figure 2-7). However, only the portion of the east lobe of the flood shoal that encroached in the Federal navigation channel was dredged. The exposed portion of this lobe, a westward-directed spit, is not considered to be a part of the flood shoal because it was formed from landward bypassing. This spit has remained nearly stable from 1950 until present and can be traced to the inlet morphology exhibited in 1891 (Figure 4-10), prior to placement of the jetties.

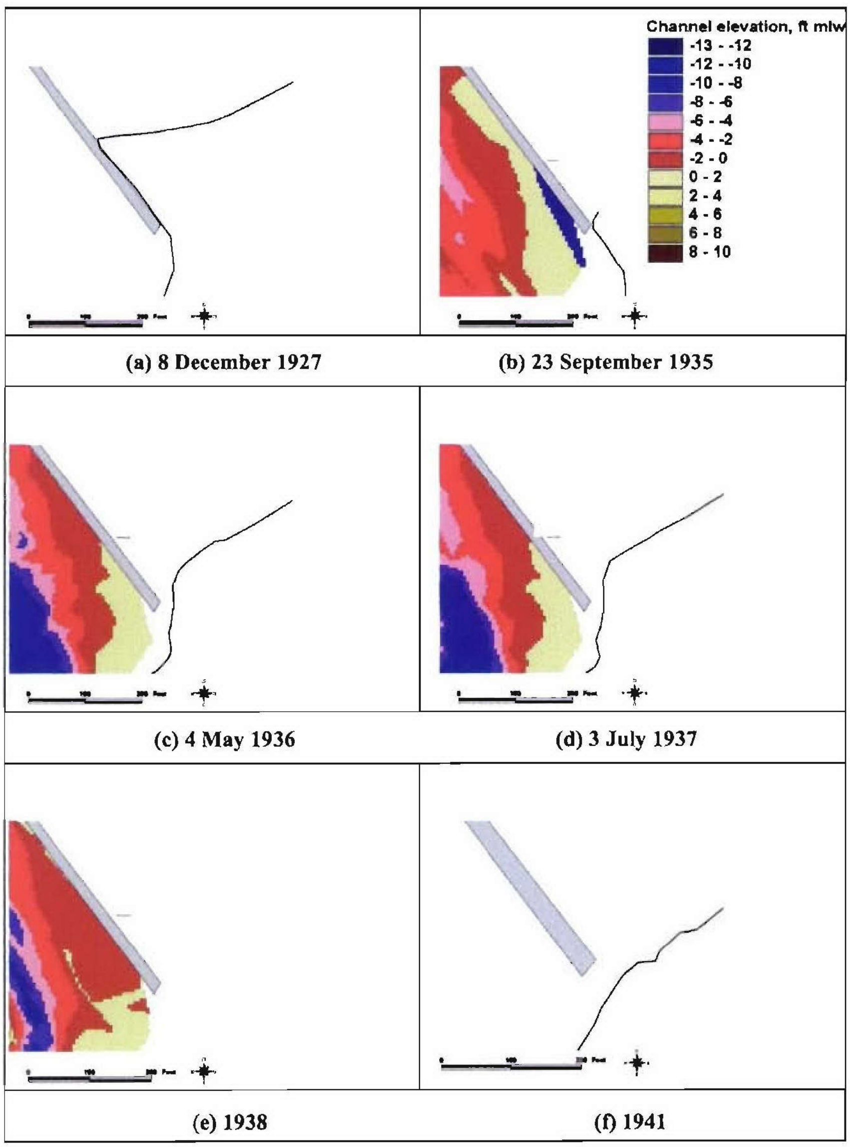

Figure 4-25. Shoreline recession and east jetty landward breach 1927 to 1941

Figures 4-26a and 4-26b illustrate the morphology of this spit in 1891, when Mattituck Inlet was in a natural state, to 1955. The spit experienced rapid growth due to the landward breach in the 1930s. After the landward extension of the east jetty in 1946, this spit began to migrate south and east under wave attack and to transport by the flood current. Panel d of Figure 4-26b shows the spit in 1955, when it had begun migrating. The migration of this spit and its evolution into the present-day flood shoal are analyzed next.

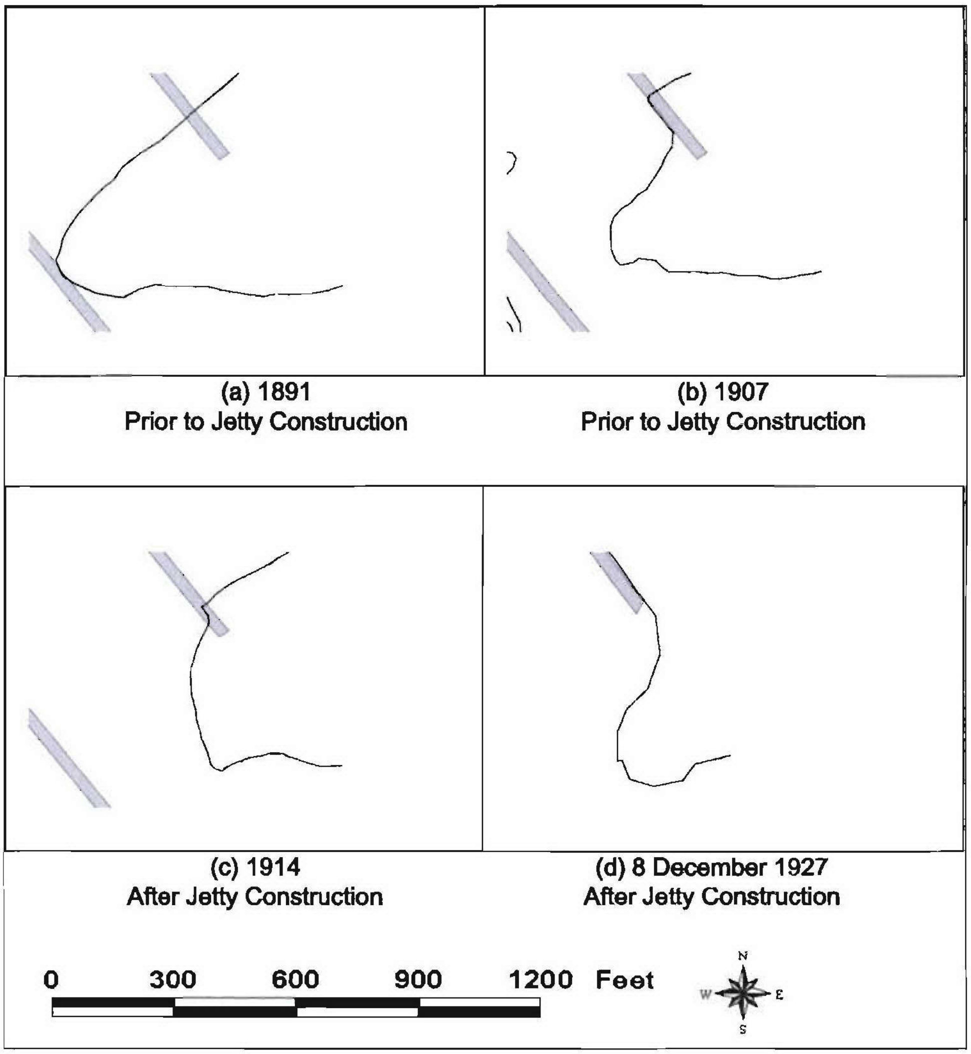

Figure 4-26a. Mattituck Inlet east bank spit morphology, 1891-1927, with jetty configuration of 1914 included for reference

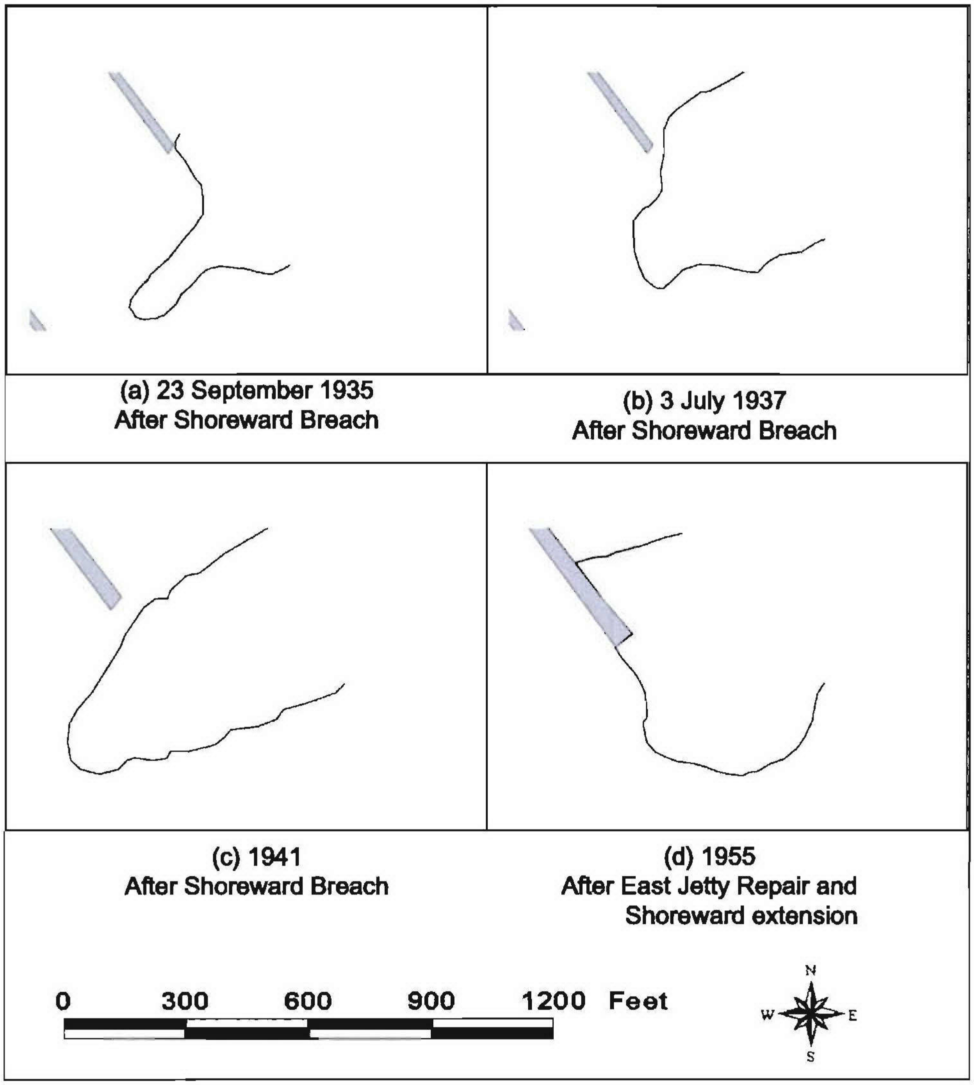

Figure 4-26b. Mattituck Inlet east bank spit morphology, 1935-1955, with jetty configuration of 1914 and 1946 included for reference

Condition survey maps indicate that the present configuration of the Federal navigation channel was introduced, and maintenance dredging took place, during the period October-November 1950 (Tables 2-5 and 2-6). The post- dredging survey of September-November 1946 and the pre-dredging survey of 4-6 October 1950 indicate that much of the east bank spit was left intact. Removal of the portion of the flood shoal that was located within the location of the new navigation channel apparently involved the dredging of an estimated 10,000-12,000 cu yd of sediment. This value accounts for approximately 40 to 50 percent of the 22,913 cu yd of sediment dredged in October–September 1950. Figure 4-27 illustrates the configuration of the Federal navigation channel prior to and after 1950.

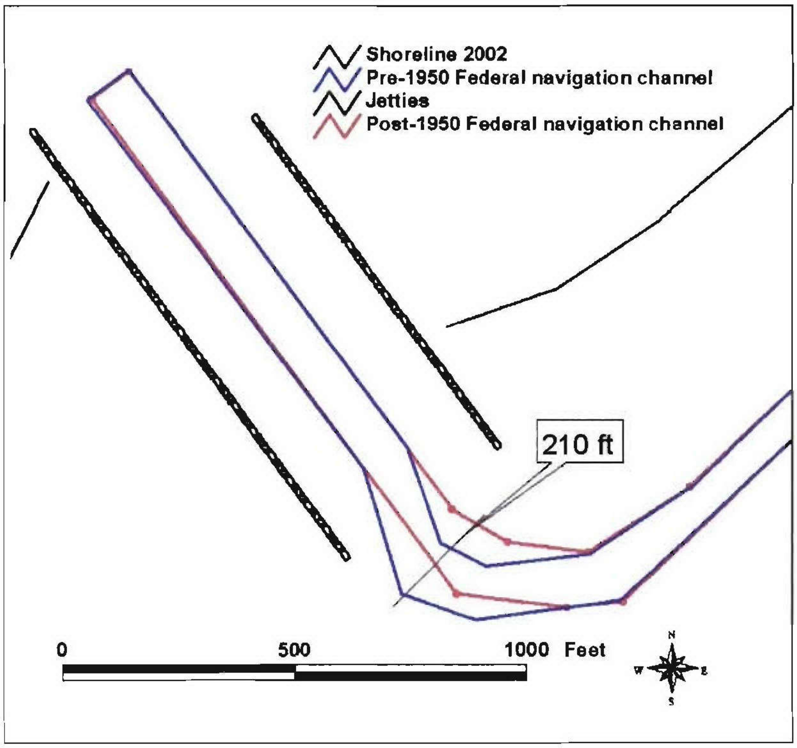

Figure 4-27. Mattituck Inlet Federal navigation channel configuration, prior to and after October – November 1950

Repositioning of the Federal navigation channel increased the maximum channel cross-section width to approximately 210 ft. The repairs of October 1937 - August 1938 and August-September 1946, together with the clearing of the west flood shoal and the introduction of the present navigation channel position in October-November 1950, brought the configuration of Mattituck Inlet close to its present configuration.

The dredging of August–September 1955 removed 31,552 cu yd of sediment. Dredging took place only in section A (Figure 2-7), from the channel entrance to the location of the east flood shoal. The dredging of August-October 1961 removed 43,550 cu yd of sediment. The extent of this dredging included section A and all of section B (Figure 2-7). Elevation change in section A for this dredging is discussed in the next section of this chapter.

During September–October 1965, a one-time dredging was performed to create a Federal anchorage at the head of Mattituck Creek, in addition to the dredging of the entrance of the Federal navigation channel. Areas dredged at this time are indicated in Figure 4-28. A total 47,265 cu yd of sediment was dredged. As indicated in Figure 4-28, only portions of section A and of section B adjacent to the flood shoal were dredged, removing 6,285 cu yd of sediment. The remaining 40,980 cu yd of sediment was dredged from the Federal anchorage and southern section of Mattituck Creek.

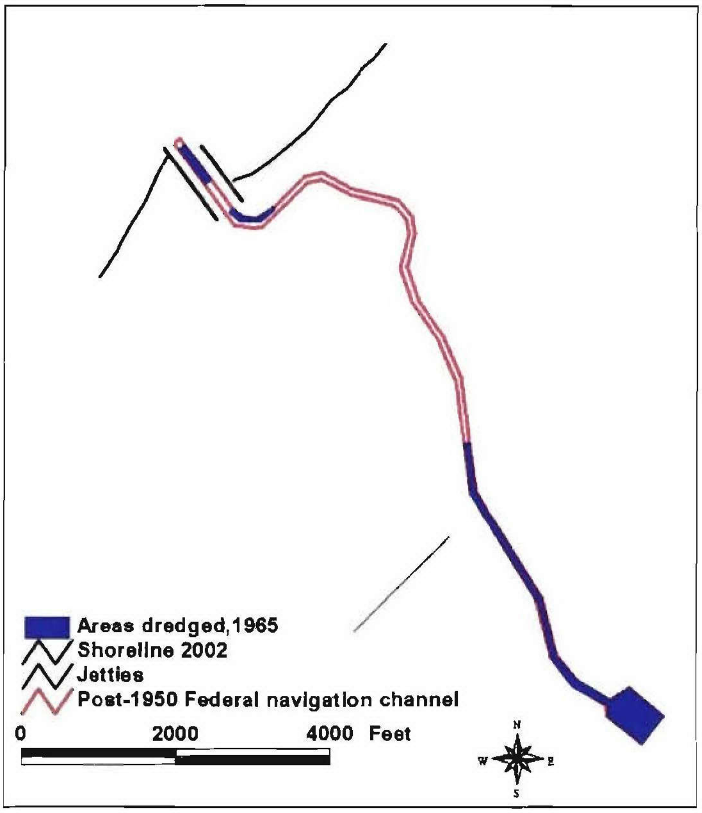

Figure 4-28. Federal navigation channel and Federal anchorage dredging areas, September – October 1965

Figures 4-29a through 4-29l show Mattituck Inlet at different times from 1930 to April 2004. Figure 4-29d shows Mattituck Inlet on 11 May 1955, immediately prior to a maintenance dredging. According to the conditions surveys of 1946 and 1950, sediment dredged during these periods was placed to nourish the beach east of Mattituck Inlet. The 1955 aerial photograph indicates that width of the beach directly adjacent to the east jetty had increased by approximately 50 ft (as compared to 1941).

The migration of the attached formation from 1941 to present can be seen in this series of figures. The formation appears to have begun migrating after 1950, apparently in response to the prior jetty modifications. The post-dredging survey of 7-8 November 1950 shows the now-truncated formation to be oriented perpendicular to the east jetty and generally oriented along an east-west axis, as it was in 1941. The orientation of this formation in 1976 and thereafter is approximately along a north-south axis. Subsequent aerial photographs show that this formation continued to migrate further into the inlet. Waves and the flood current are presumed to have caused this formation to migrate, and because much of this formation presently lies below mlw, it can now be considered to be a flood shoal.

The morphology of Mattituck Inlet on 16 April 2003, 11 months prior to the recent dredging of 17-24 March 2004, is shown in Figure 4-29k. Figure 4-29l shows the morphology of Mattituck Inlet on 15 April 2004, immediately after this dredging.

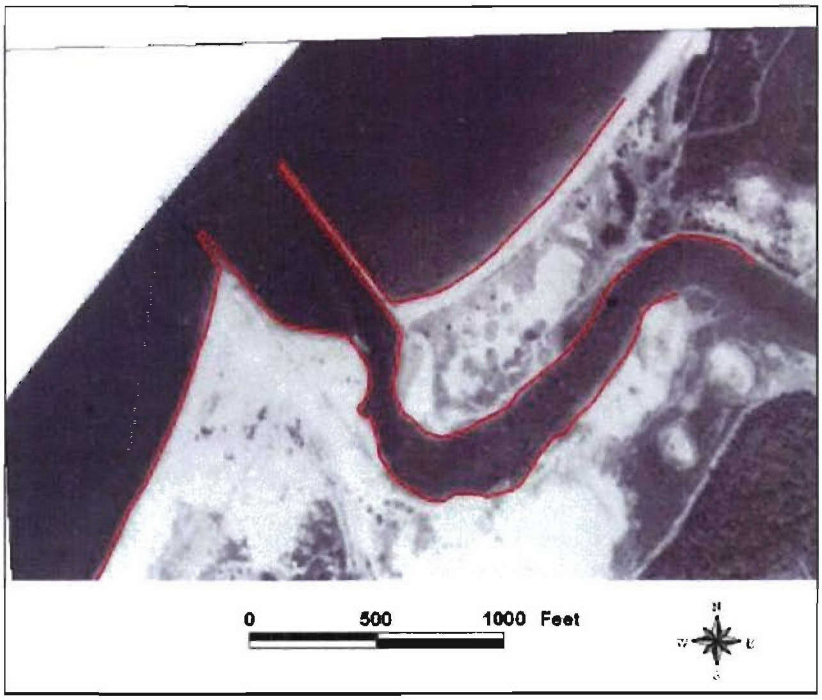

Figure 4-29a. Mattituck Inlet, circa 1930

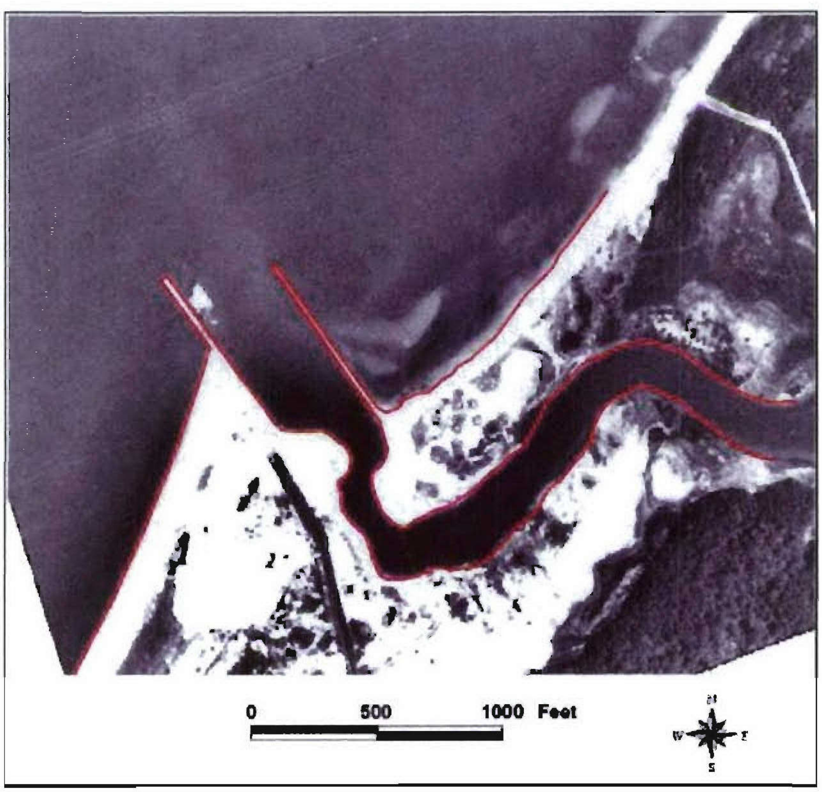

Figure 4-29b. Mattituck Inlet, 1938 (exact month and day unknown)

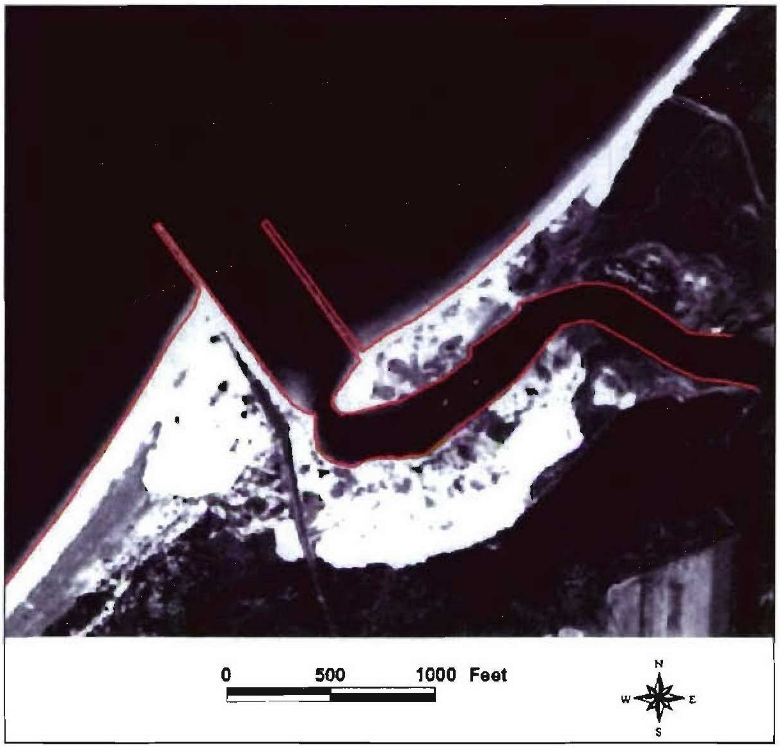

Figure 4-29c. Mattituck Inlet, 1941(exact month and day unknown)

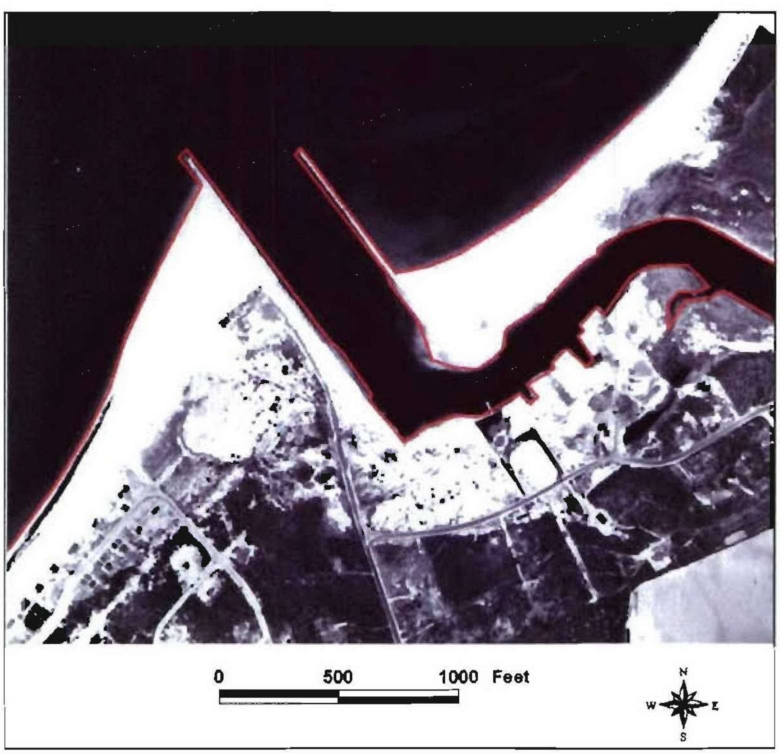

Figure 4-29d. Mattituck Inlet, 11 May 1955

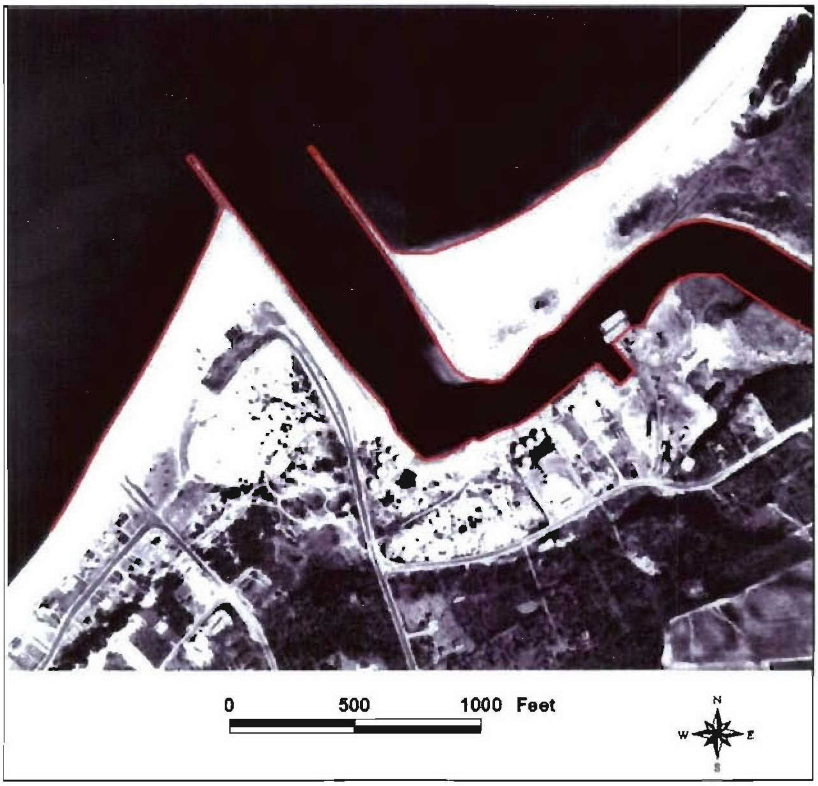

Figure 4-29e. Mattituck Inlet, 1 April 1964

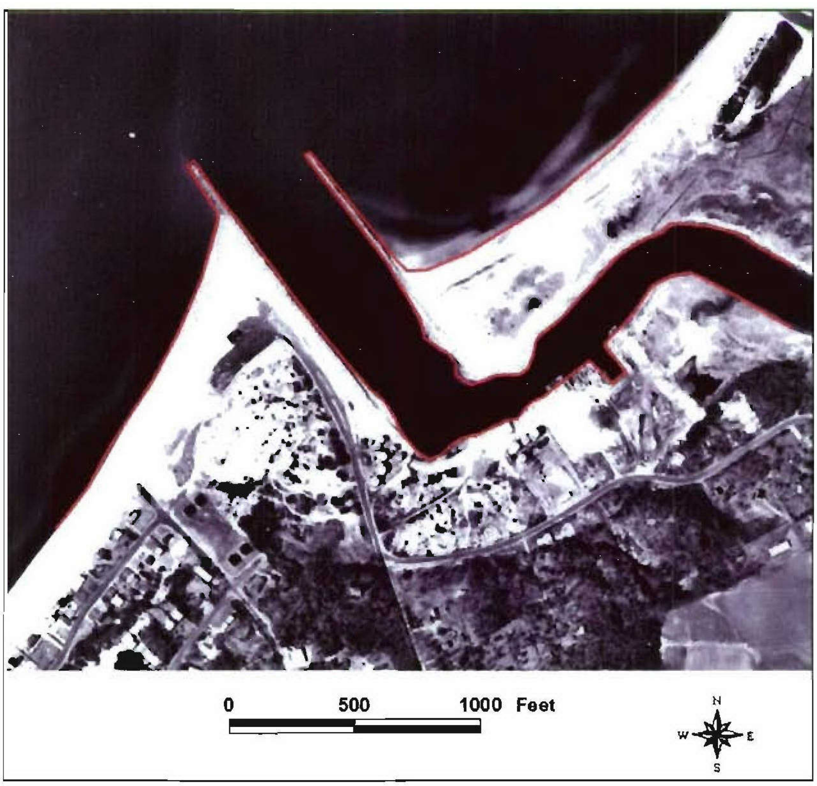

Figure 4-29f. Mattituck Inlet, 25 April 1969

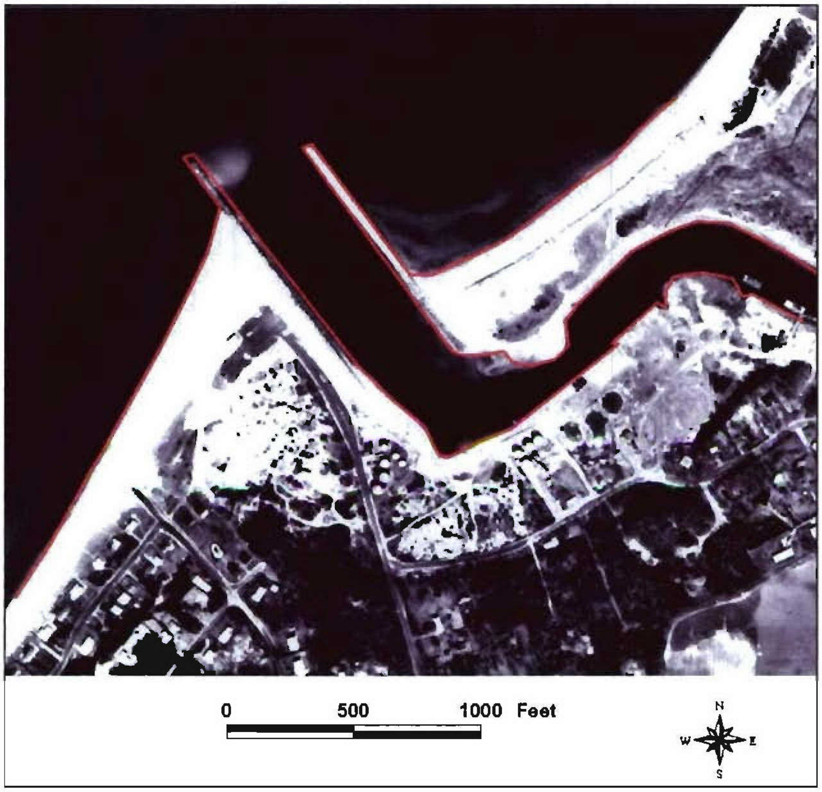

Figure 4-29g. Mattituck Inlet, 6 April 1976

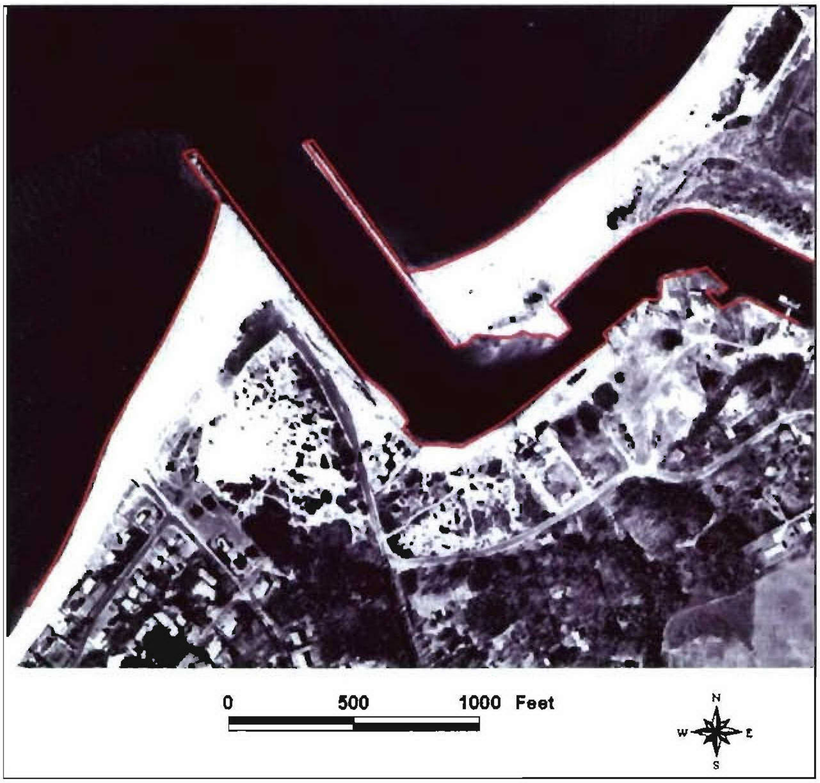

Figure 4-29h. Mattituck Inlet, 23 March 1980

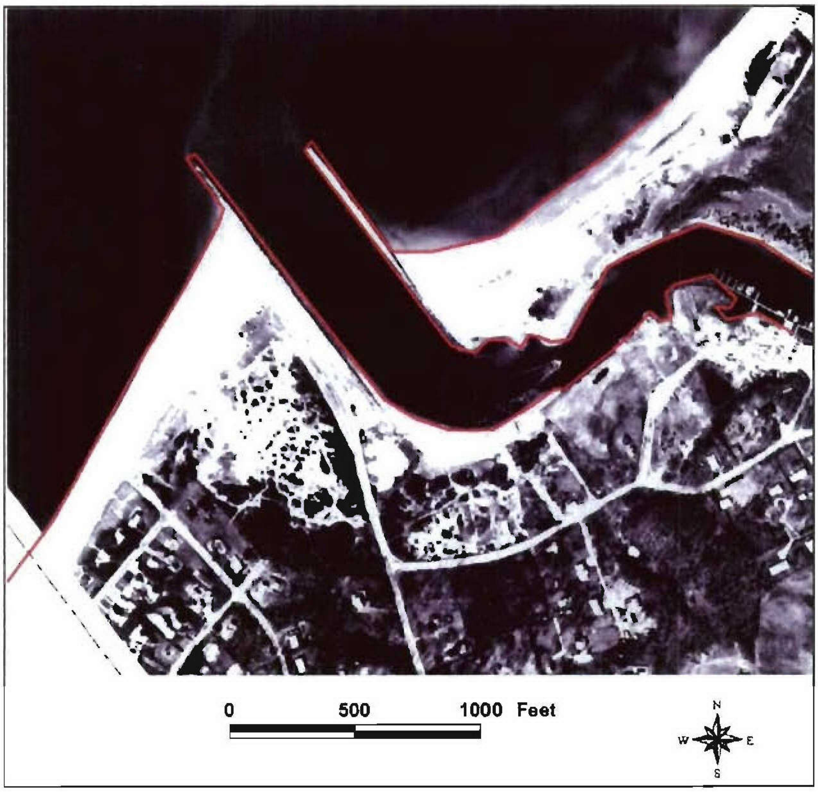

Figure 4-29i. Mattituck Inlet, 5 April 1993

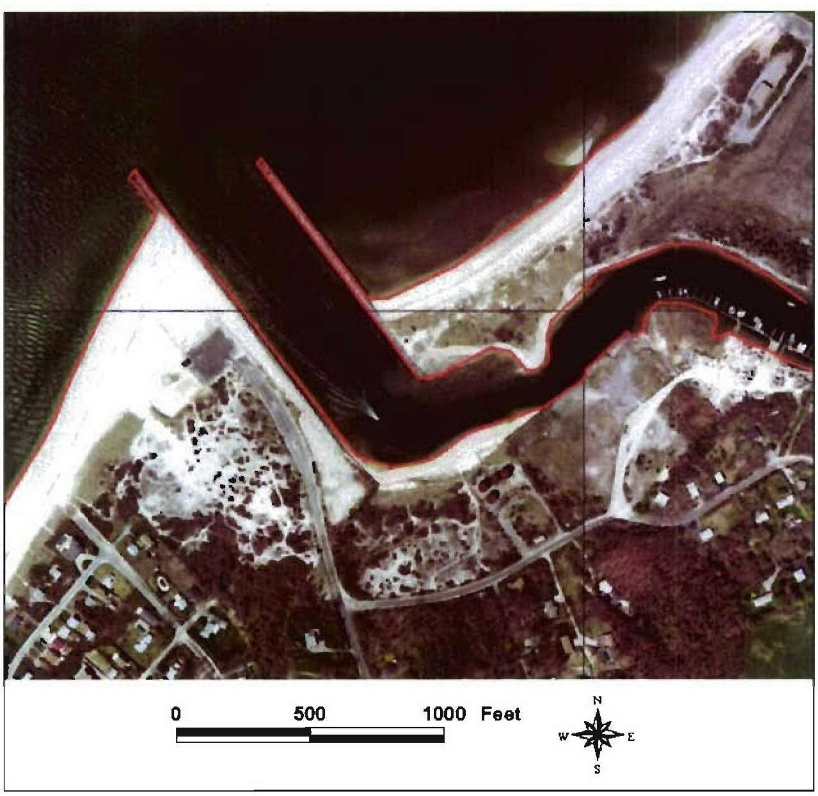

Figure 4-29j. Mattituck Inlet, 26-30 April 2001

Figure 4-29k. Mattituck Inlet, 16 April 2003

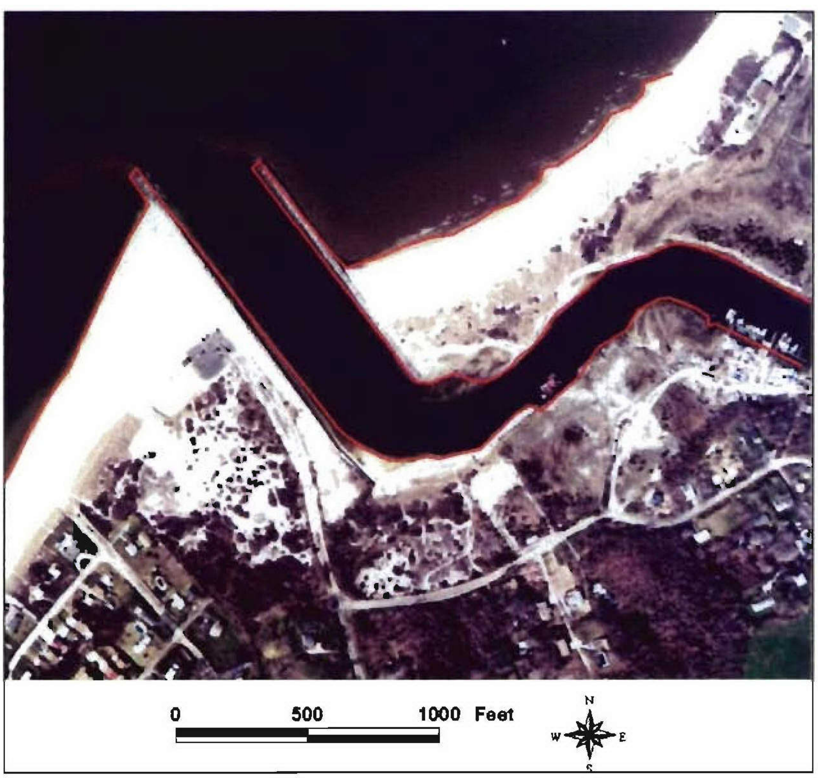

Figure 4-29l. Mattituck Inlet, 15 April 2004

Commercial mining activities. Mattituck Inlet has been the site of considerable commercial mining. Mining of the Federal navigation channel, under Federal permit, and mining of the beach directly west of the west jetty under local permit, removed a large volume of sediment from this system from 1920 to 1977. These activities, and their possible implications on sediment transport at Mattituck Inlet are discussed here.

In the course of the present study, the archive of New York District dredging permits was accessed to investigate permitted commercial dredging for gravel and sand within the limits of the Federal navigation project (Table 2-7). The New York District could only issue permits for dredging within the Federal navigation project, because adjacent submerged land falls under jurisdiction of the State of New York, a point repeatedly raised in local agency review of the permit requests. Permit applications and associated documentation of New York District actions were found for the interval 1925 to 1948 and primarily concerned shoaling areas adjacent to the west jetty. During this interval, the Federal navigation channel was configured such that it abutted the west bank of Mattituck Inlet at the base of the west jetty (see Figure 4-27).

Federal permits allowed dredging to depths ranging from 7 to 20 ft mlw. Most of the permit applicants did not complete planned work, as indicated by requests for extensions or renewals, or by comments from New York District inspectors. Therefore, it is uncertain how much dredging occurred for commercial use, although it is expected to have been intermittent, but substantial at times.

The functional duration of commercial mining activities is not known, and the Federal permits provide no information on the volumes dredged. However, because of the asphalt-handling infrastructure that was present near the inlet, there is evidence of a robust mining industry at Mattituck Inlet for a long span of time. Ralston (1928) states that the sand and gravel industry at Mattituck Inlet could dredge "50 cu yd, daily, of sand and gravel from between the jetties at the entrance to the harbor, under permit from the War Department, and its transportation to the south end of the harbor for manufacture into concrete tile." Three permits were issued prior to the Ralston (1928) report. Two of these (J.H. Rambo, and Northport Sand and Gravel) apparently indicate offsite disposal of the dredged material, and the third (C. H. Benjamin) indicates disposal on the Wickert estate, located adjacent to the area of mining. It is, therefore, apparent that the activities referred to by Ralston (1928), which note "transportation to the south end of the harbor," are different than those referred to in the Federal dredging permits.

The existence of a robust mining industry at Mattituck Inlet is further evidenced in New York District condition surveys, which document physical plants of sand and gravel companies. The condition survey map dated 20 May 1965 notes the existence of an abandoned "Sand Plant" on the west bank of Mattituck Creek. The condition survey map dated 20 May 1965 notes the physical plants of Asphalts, Inc. and the Gotham Sand and Gravel Company, both near the area of mining. The condition survey map dated 27 July 1971 notes the physical plant of the New Sand and Gravel Company near this same location. The locations of the physical plants are shown in Figure 4-30.

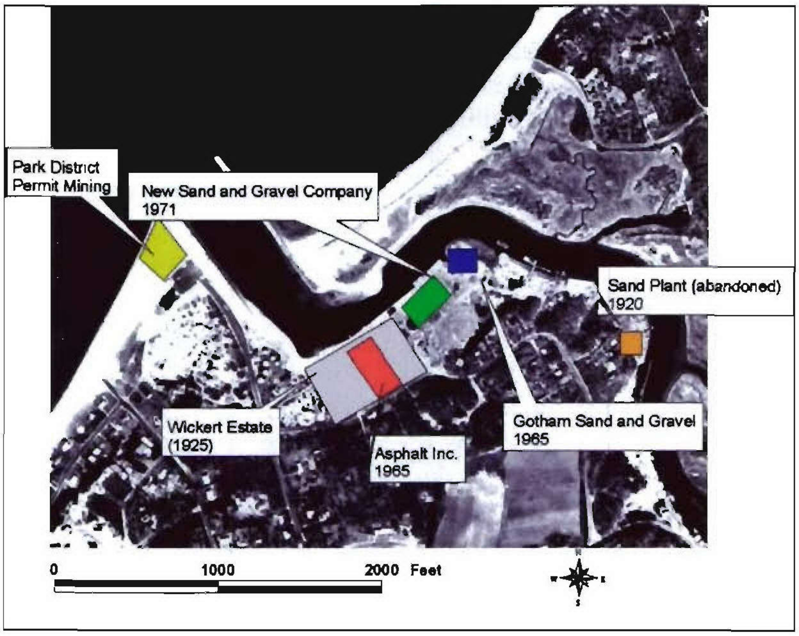

Figure 4-30. Mining related companies and locations at Mattituck Inlet

The only estimated volume information is that given by Ralston (1928) in reference to "50 cu yd, daily." This figure translates to 10,000 cu yd annually (for 200 working days). Known Federal dredging permits cover a time period of approximately 30 years. Given the evidence of commercial activity associated with sediment mining, the possibility of substantial undocumented mining at Mattituck Inlet is strong, as is the evidence that mining practices continued beyond the 1940s. The authors of the present study therefore estimate that from 250,000 to 500,000 cu yd of sediment was removed from Mattituck Inlet from 1920 to 1970.

The extent of sediment mining on the beach directly west of the west jetty is unclear as well. Schubel (1976) documents mining of sand and gravel from the beach directly west of the west jetty for the period 1960-1975, under permit of the Mattituck Park District (Table 2-8). The area of permitted removal was bounded by the hwl, a line "parallel to and 25 yards from the west jetty" and a second parallel line located near a refreshment stand (Schubel 1976). According to local sources, these activities have continued "on and off" for a period of over 50 years, up to 1976.[1] Analysis of aerial photographs from 11 May 1955 (Figure 4-29d) and 1 April 1964 (Figure 4-29e) support the presence of mining activities at this location prior to 1960. The noted area would normally experience a net gain of sediment through jetty impoundment, and the aerial photographs indicate shoreline recession.

[1] Personal Communication, 30 August 2004, Mr. Frank Murphy, Mattituck Park District Supervisor (retired).

The authors of the present study estimate that these mining activities removed 260,000 to 380,000 cu yd from the system. The consequence of this mining on sediment accumulation within Mattituck Inlet can be seen in the dredging records (Table 2-5), where a substantial decrease in dredged volume within the channel is observed after 1965. Cessation of these mining activities can also, in turn, be expected to eventually increase sediment accumulation rates within Mattituck Inlet. Impoundment west of the west jetty is observed to have increased in recent years, and the shoreline there has advanced (see Figures 4-29h through 4-29l; Batten and Kraus 2005). Sediment accumulation rates can be expected to increase significantly when the west jetty has reached impoundment capacity.

Elevation change and dredging volume. In its present condition, Mattituck Inlet is a hydraulically efficient channel that experiences small rates of sediment accumulation. Gradual shoaling within the Federal navigation channel eventually leads to constriction, and this shoaling is the main requirement for periodic dredging, jetty repair, and jetty extension. The good performance of the Mattituck Inlet navigation project in its present condition is largely the result of proper maintenance and jetties of adequate length. Sand and gravel mining that occurred directly west of the inlet which served to keep the volume of sediment located there below the impoundment capacity of the west jetty, is also a significant factor. Dredging records (Table 2-5) indicate that the Federal navigation channel at Mattituck Inlet accumulated sediment at a rate of 1,000-2,000 cu yd/year from 1965 to 1990. The repair of the west jetty in 1975 may partially explain the decrease in accumulation rate. (The west jetty was last repaired in 1996.) Improvements in dredging technology may also account for the smaller volumes that have been dredged in recent years, where the channel is more accurately dredged to the project depth of 7 ft mlw with 2-ft overdraft.

The volume dredged in August to October 1961 was 43,550 cu yd. This volume resulted in average channel depths of about 10 to 11 ft mlw, 1 to 2 ft greater than the authorized depth of 7 ft mlw with 2 ft advance dredging. The volume change for the September to October 1965 dredging was not calculated because a full pre-dredging condition survey was not available. The channel depth observed after dredging in May 1980 and October 1990 for this same location is 9 ft mlw, equal to the authorized project depth of 7 ft mlw with 2-ft advance dredging.

Maintenance dredging of Mattituck Inlet was performed in May 1980 and October 1990 (Table 2-5). The most recent maintenance dredging of the channel took place on 17-24 March 2004. Dredging volume changes for years 1961, 1980, and 1990 are analyzed here. The dredging of 1965 included section B as shown in Figure 2-7 as well as section A. The dredgings of 1980 and 1990 covered only section A, the area of typical dredging. Figure 4-31a plots channel elevations for June 1961, prior to dredging, and Figure 4-31b shows channel elevations for September 1961, immediately after dredging. Figure 4-31c plots the net change in elevation as a result of the maintenance dredging of September 1961. Figures 4-32a through 3-32c show channel elevation and elevation change for the maintenance dredging of 1980. Figures 3-33a through 3-33c show channel elevation and elevation change for the maintenance dredging of 1990.

The shoaling patterns observed in these figures are largely the same as those that followed the 1946 landward extension of the east jetty, though the rate of

sediment accumulation diminished greatly after 1965. Shoaling now occurs mainly along the east bank, directly behind the shoreward end of the east jetty. Shoaling is also observed along the west bank, directly opposite the main flood shoal and alongside the seaward tip of the west jetty. Based on the amount of sediment dredged from these locations (Figures 4-31c, 4-32c and 4-33c), sediment accumulates at these locations along the sloped walls of the channel, causing the channel to become increasingly constricted. Shoaling also occurs at the mouth of the inlet, where sediment accumulates at the bottom of the channel (channel infilling). Dredging serves to deepen the channel, as well as widen it in areas where bank encroachment constricts the channel.

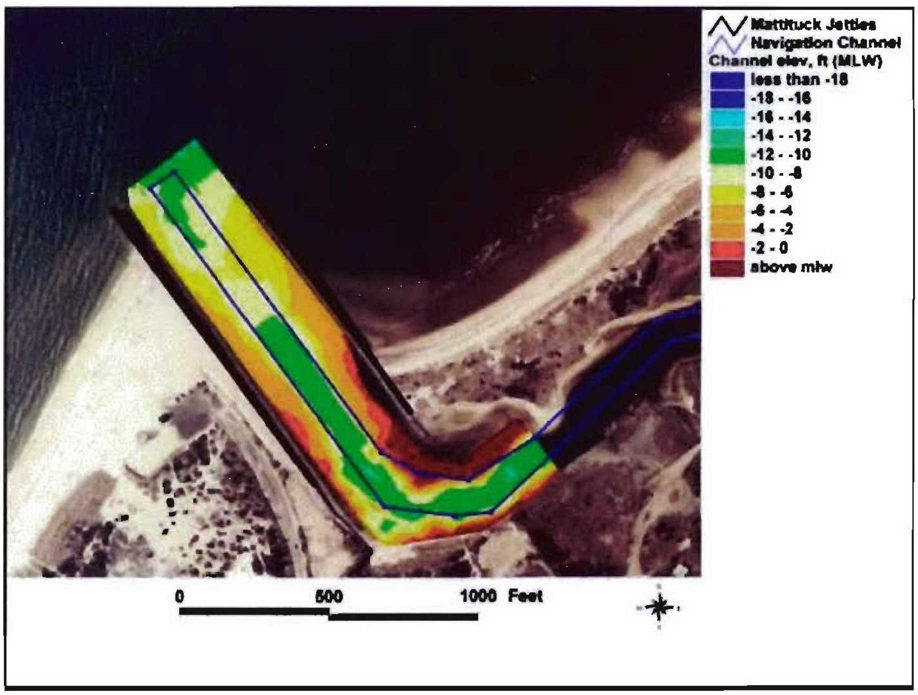

Figure 4-31a. Channel elevation, June 1961 (pre-dredging)

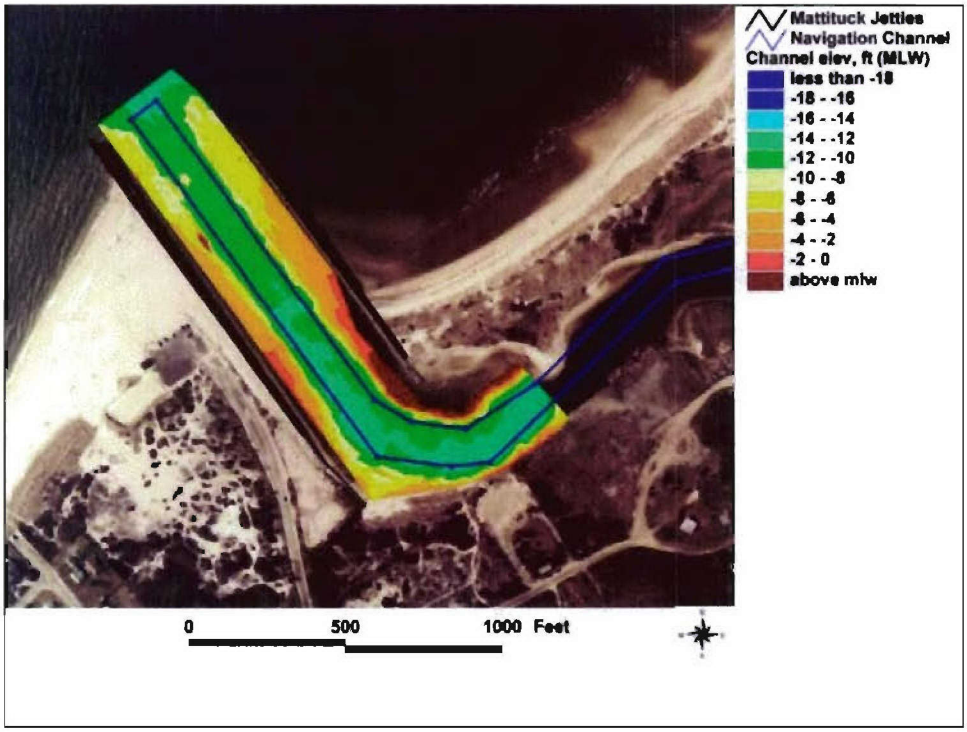

Figure 4-31b. Channel elevation, September 1961 (post-dredging)

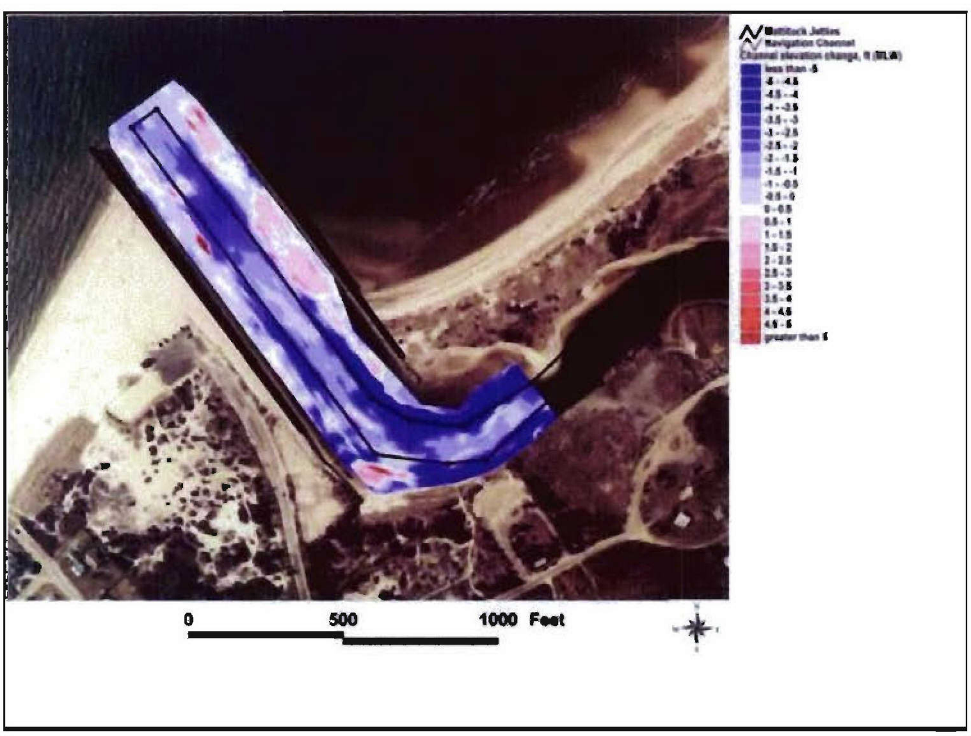

Figure 4-31c. Channel elevation change , June 1961 - September 1961

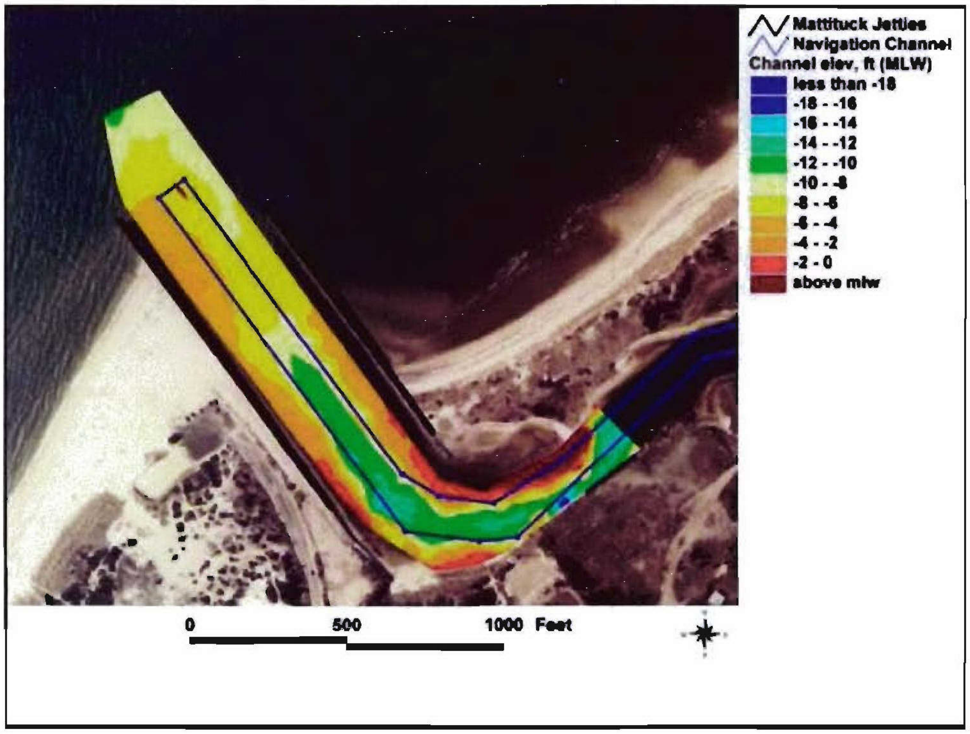

Figure 4-32a. Channel elevation, January 1980 (pre-dredging)

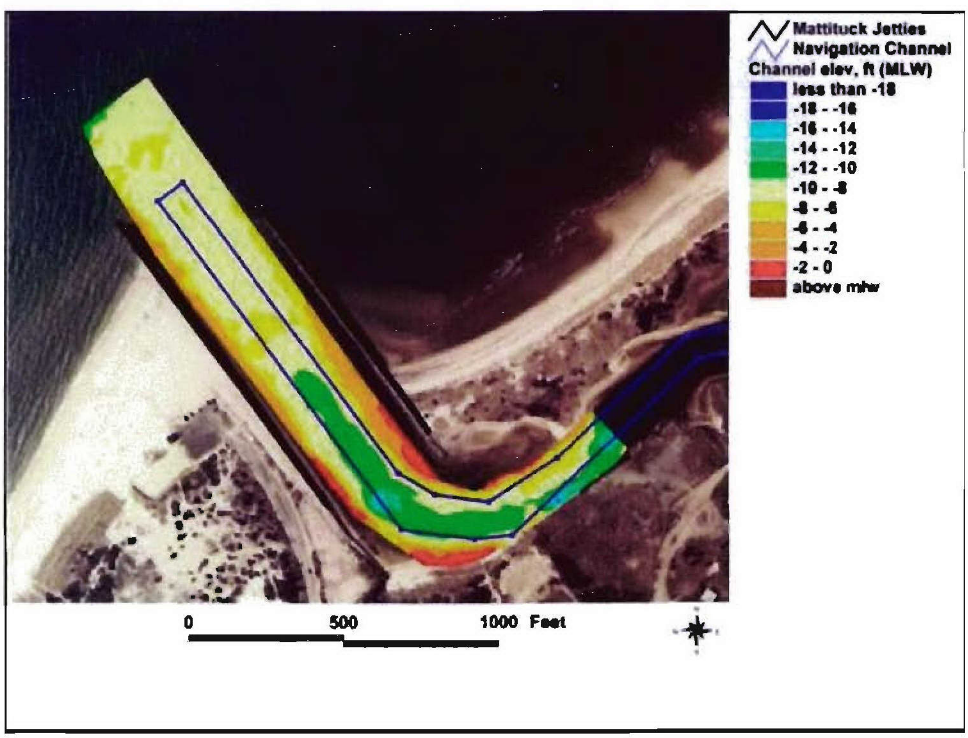

Figure 4-32b. Channel elevation, May 1980 (post-dredging)

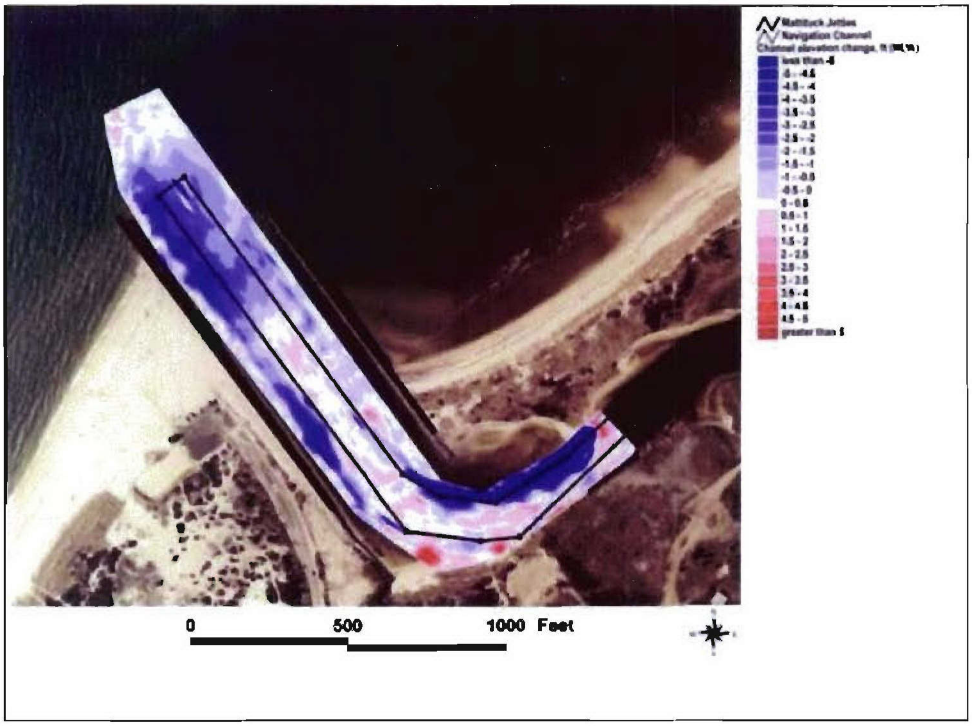

Figure 4-32c. Channel elevation change, January 1980 - May 1980

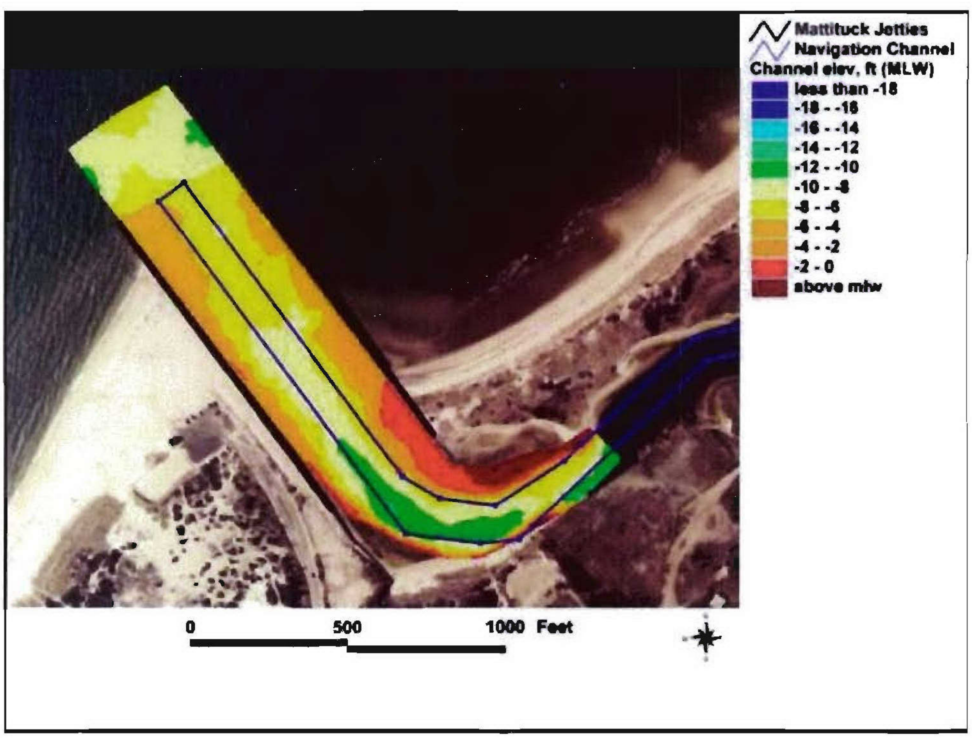

Figure 4-33a. Channel elevation, September 1990 (pre-dredging)

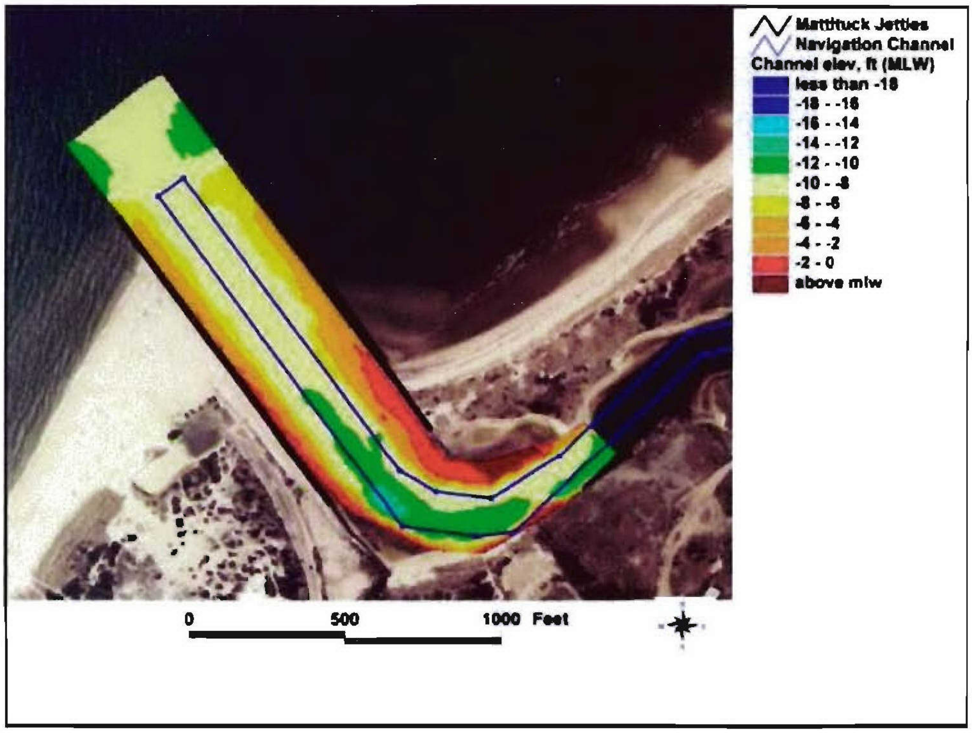

Figure 4-33b. Channel elevation, October 1990 (post-dredging)

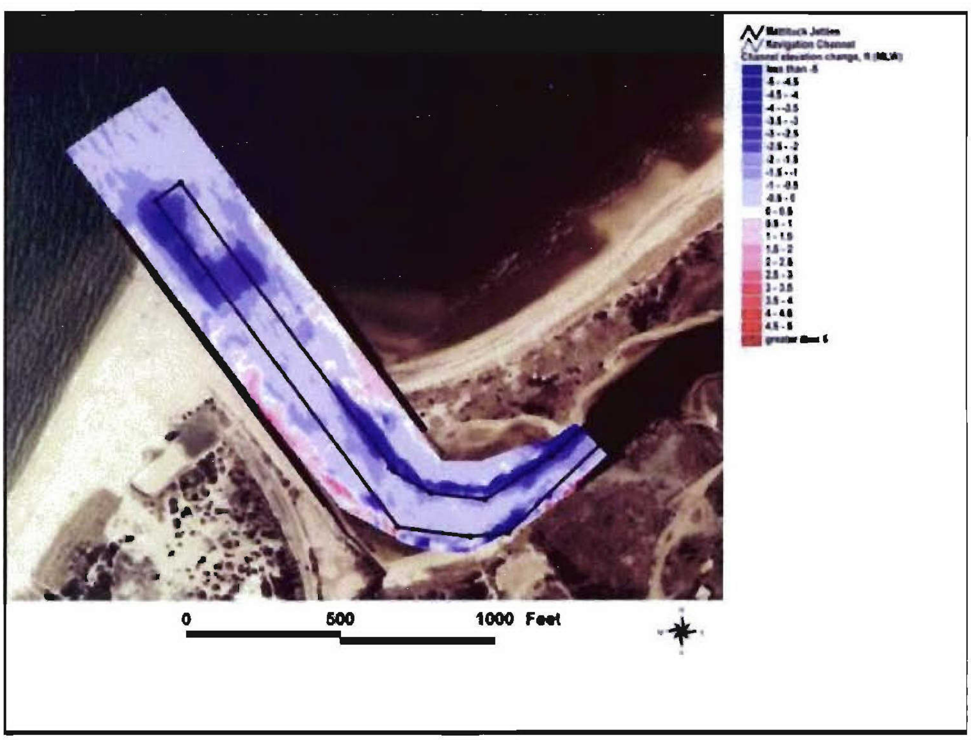

Figure 4-33c. Channel elevation change, September 1990 - October 1990

Volumes dredged from the navigation channel were calculated by differencing bathymetry surfaces. A TIN was generated for each condition survey, and the volume for each TIN was then calculated. The volumes calculated represent the volumes of sediment in the study area found above a datum located beneath the lowest elevation found. Because ArcView GIS introduces surface area variation in generating grids, the surface areas compared were normalized to represent equal surface areas. The volume of the post-dredging grid was divided by its planimetric surface area, yielding an average height above the reference datum. This height was then multiplied by the planimetric surface area of the pre-dredging grid. The total volume of a post-dredging TIN was then subtracted from its corresponding pre-dredging TIN.

Results of these calculations are listed in Table 4-4 and compared to the reported volumes dredged. The data indicate an accumulation rate of 1,000 to 2,000 cu yd/year for the period following the jetty repairs of 1975 for the area considered. Good agreement is found between calculated and reported volume for January 1980 to May 1980. Agreement between June 1961 and September 1961 is reasonable as well. The dredging of September 1961 included a section of the channel not normally dredged. The volumes dredged from this extra portion are not, however, expected to be large. Given this fact, the calculated volume, which is less than the reported volume, is considered to be reasonably accurate. The calculated volume for the September 1980 to October 1990 is only 50 percent of the reported volume. The cause of this discrepancy is unknown.

Table 4-4
Calculated Versus Measured Dredging Volumes, Mattituck Inlet Channel

Pre-Dredging Date	Post-Dredging Date	Calculated Volume (cu yd)	Reported Volume (cu yd)
June 1961	September 1961	40, 473	43,550
January 1980	May 1980	26,459	24,137
September 1990	October 1990	26,595	13,241

Table 4-5 provides estimated sediment accumulation rates at Mattituck Inlet for selected periods. Certain periods are not included, in instances when the extent or purpose of the dredging is beyond normal maintenance (as with the October–November 1950, which served to reposition the Federal navigation channel).

Table 4-5
Estimated Sediment Accumulation Rates, Mattituck Inlet Federal Navigation Channel

Perlod	Rate (cu/yd year)
1914 – August 1923*	7,000
September 1923 – September 1927	12,000
October 1927 – November 1935	6,500
May 1936 – July 1938	8,500
August 1938 – September 1946	6,500
November 1950 – August 1955	7,000
September 1955 – August 1961	7,000
October 1961 – September 1965	1,500
October 1965 – May 1980	1,500
May 1980 – October 1990	1,300
October 1990 – March 2004	1,000

* Includes dredging of June - November 1921

The average sediment accumulation rate from 1914 to 1946, the period prior to the modification of both jetties, is 8,100 cu yd/year and the range is 6,500 to 12,000 cu yd/year. The previous repairs and extensions appear to have greatly mitigated shoaling along the west jetty, and a reduction in the sediment accumulation rate is expected after the major rehabilitation of 1946. The continued high rate indicated from 1946 to 1961 is interpreted as a transitional period containing adjustments of the morphology of Mattituck Inlet to a new hydrodynamic equilibrium condition. The decrease in rates for the period 1961 to the present is considerable. The efficiency of the current Federal navigation project and the mining of sediment directly west of the jetty are identified as the major factors in the observed decrease.

Seventeen condition survey maps from the years 1969 to 2003 were digitized, and quantitative analysis of sediment deposition within the Mattituck Inlet navigation channel was attempted through surface differencing. It was found that the annual volume difference between successive condition surveys was too small to detect because the volume error was three to six times the annual volume change (1,000 to 2,000 cu yd). The surface areas analyzed measure approximately 60,000 sq yd. A survey error of 0.33 ft, or 0.1 yd, yields a volume error of +/- 6,000 cu yd. The volumes obtained based on the post-dredging condition surveys are considered reliable because of the large change relative to the pre-dredging surveys.

The difference maps generated do, however, provide qualitative information on the location and persistence of shoaling within the channel. Sediment accumulation within the channel appears to be constant and evenly distributed, with the exception of the inlet entrance, where considerable shoaling is observed along the west jetty. Near the shoreward end, areas of scour and shoaling are apparent. Figures 4-43a through 4-34e illustrate elevation changes from May 1980 (immediately after a dredging) through October 1990.

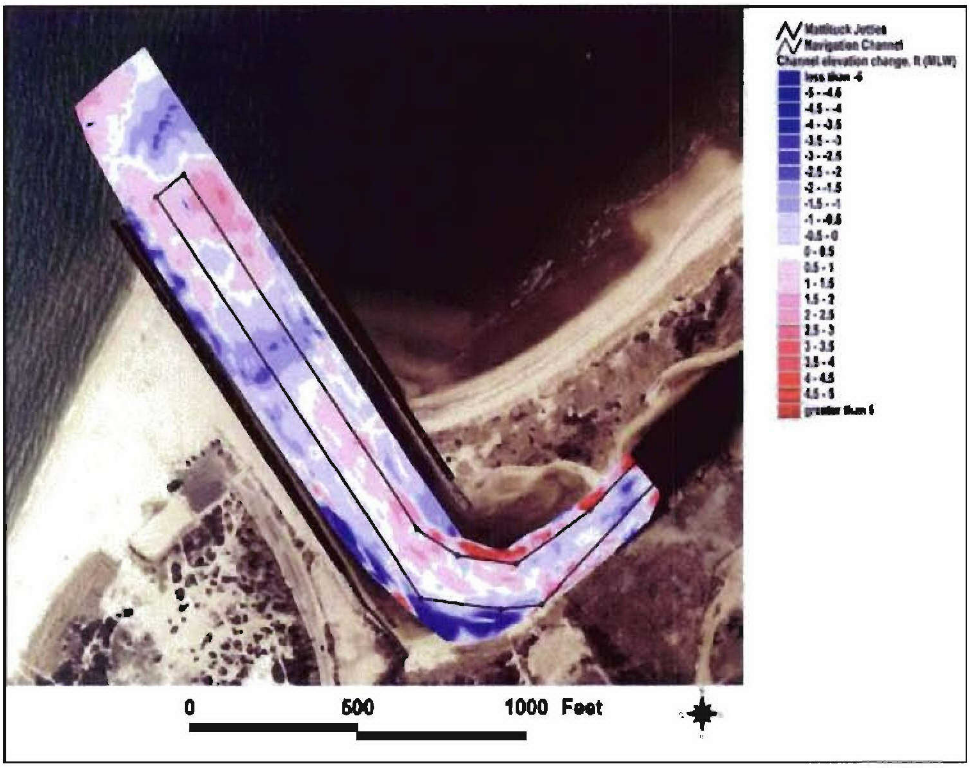

Figure 4-34a. Channel elevation change, May 1980 to August 1983

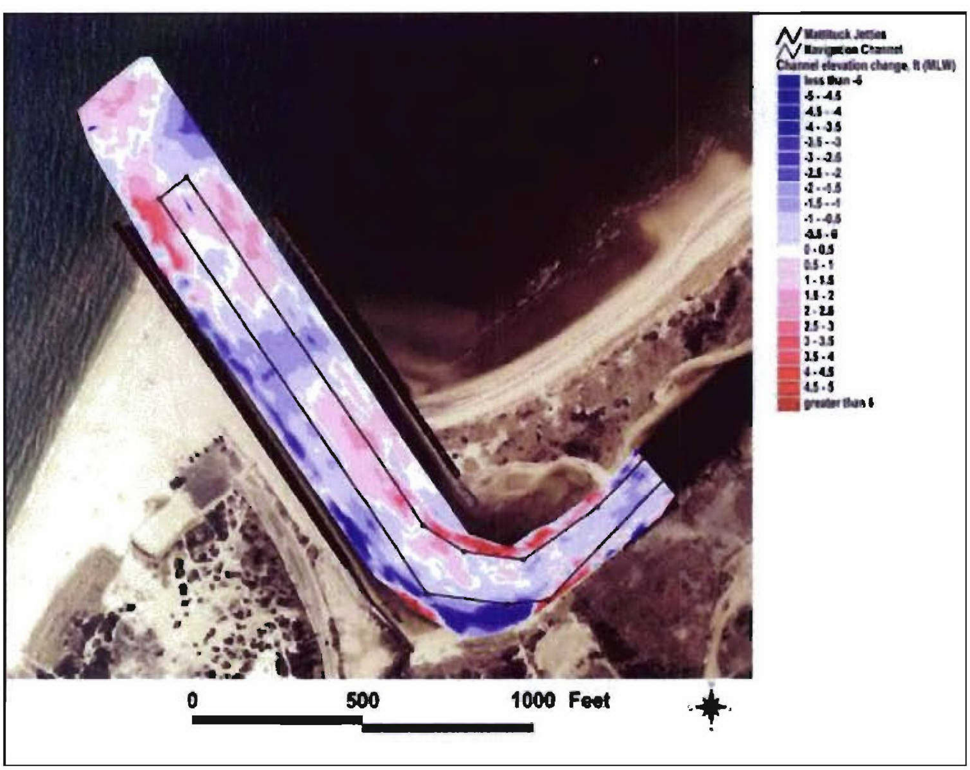

Figure 4-34b. Channel elevation change, May 1980 to June 1985

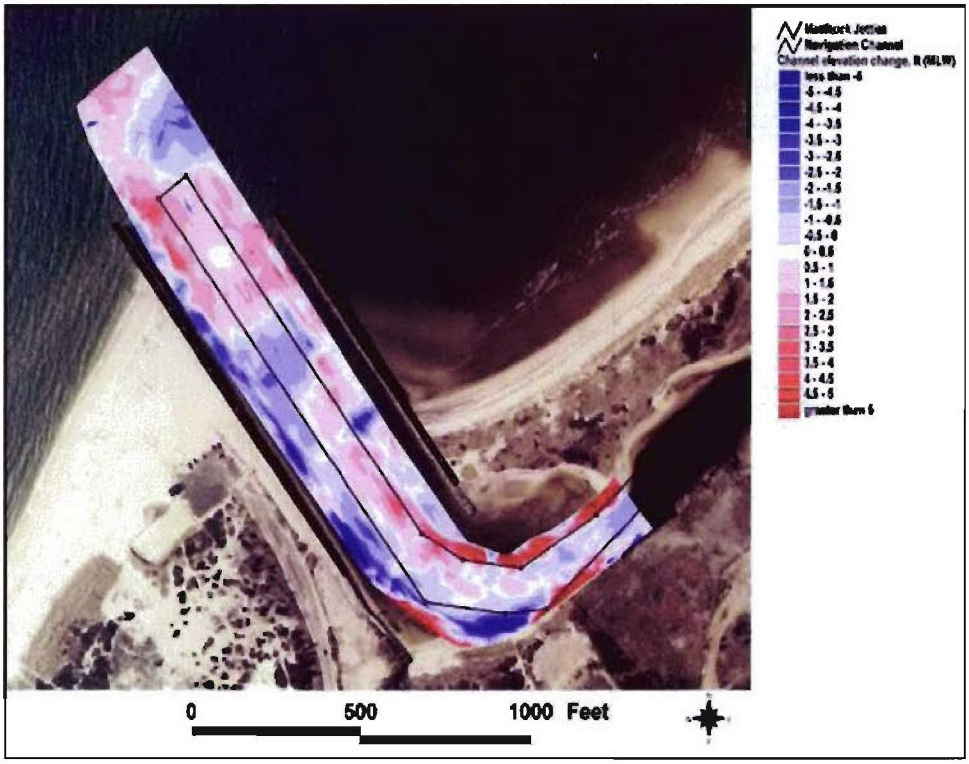

Figure 4-34c. Channel elevation change, May 1980 to September 1987

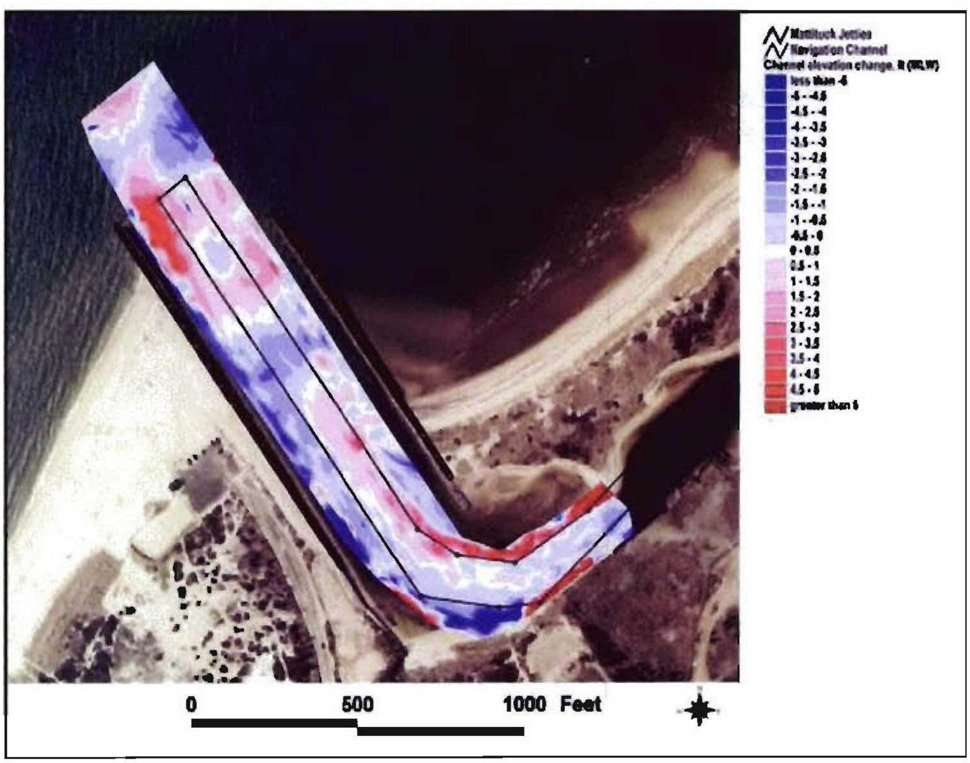

Figure 4-34d. Channel elevation change, May 1980 to June 1988

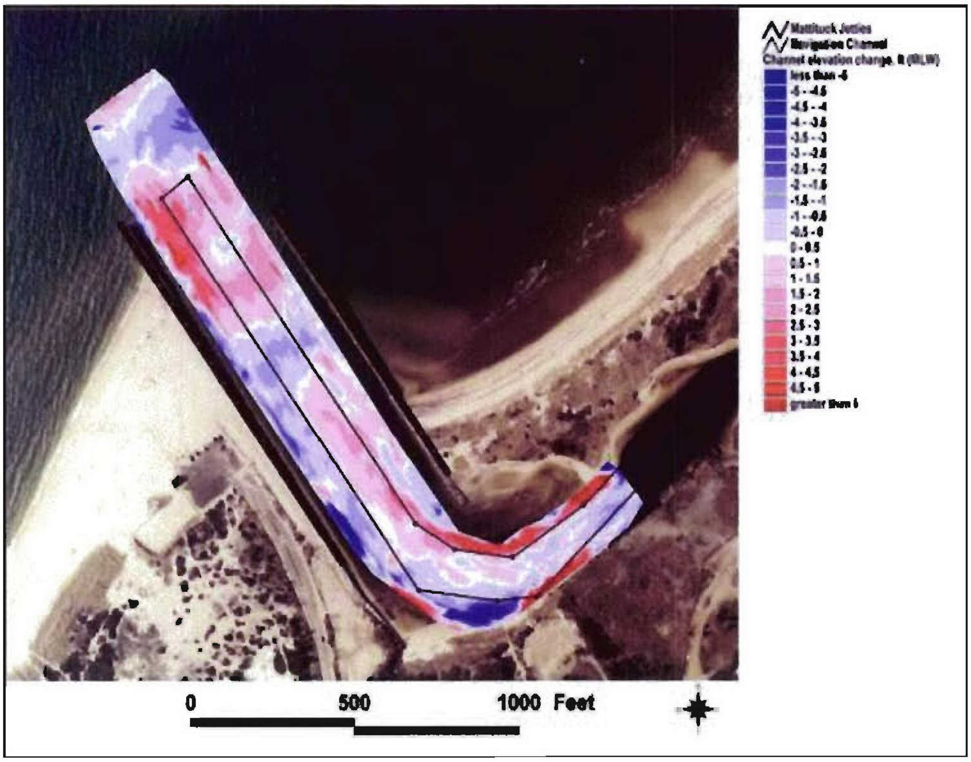

Figure 4-34e. Channel elevation change, May 1980 to October 1989

The total volume of sediment that accumulated within the channel for the period from October 1990 to January 2002 was calculated to be 24,600 cu yd. This figure is considered reasonable in indicating an annual deposition rate within the inlet of 2,000 cu yd/year. The grids analyzed in this calculation do not cover the full flood shoal (Figure 4-35), so the actual amount accumulated may be larger. The survey of January 2002 did not fully capture the flood shoal, presumably because it was inaccessible. Scour along the east jetty can also be seen.

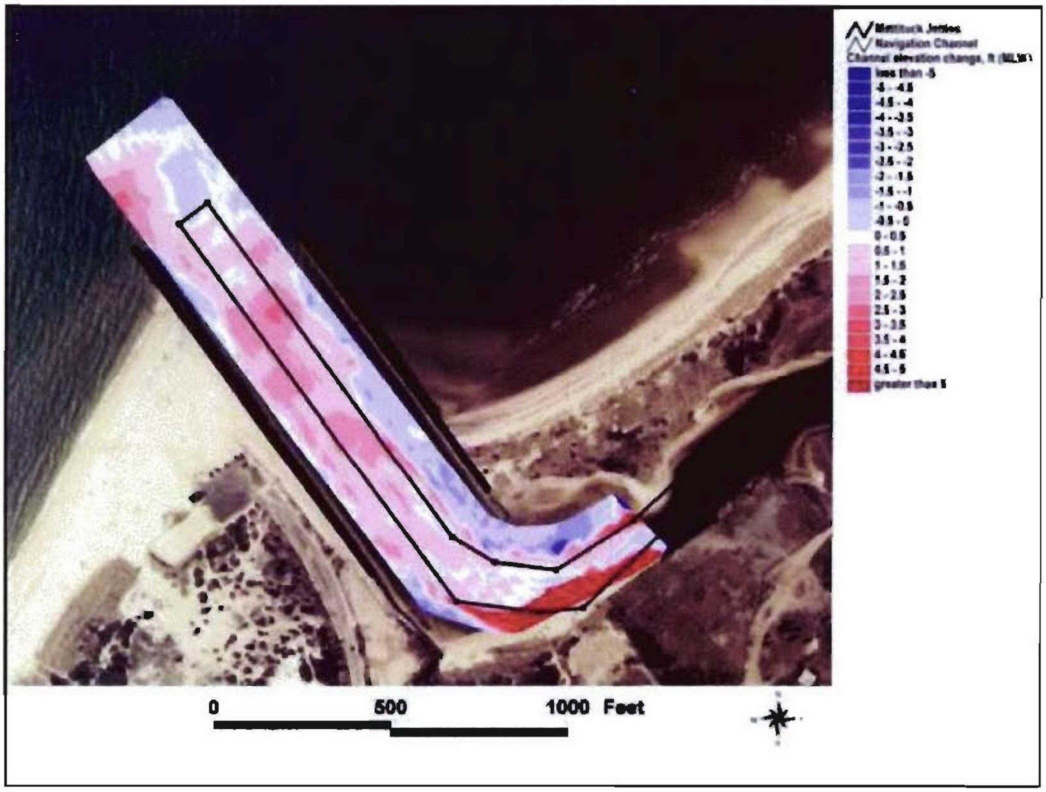

Figure 4-35. Channel elevation change, October 1990 to January 2002

A post-dredging condition survey following the recent dredging of 17-24 March 2004 was not available at the time of this writing. Figure 4-36 compares the shoreline of Mattituck Inlet of 16 April 2003 (11 months prior to the most recent dredging) to the shoreline of 15 April 2004 (immediately after dredging). The volume of 13,786 cu yd was removed from Mattituck Inlet and the sediment was placed on the beach directly east of the inlet. The observed morphology change clearly illustrates the placement of this sediment and dredging of the main area of shoaling on the east bank, as well as the dredging of the area of secondary shoaling in the west bank.

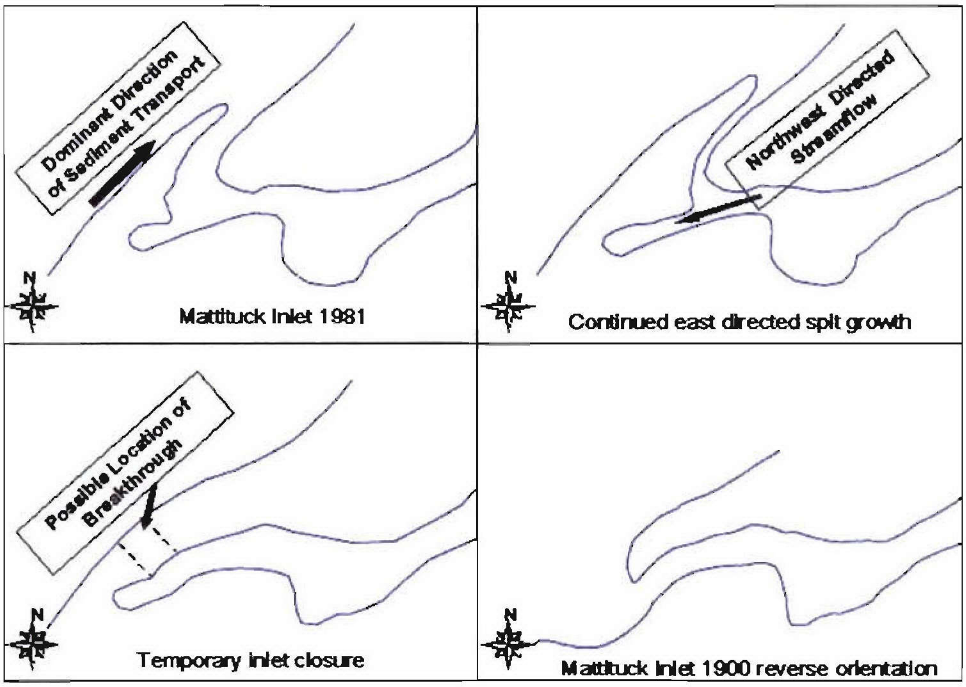

Figure 4-36. Mattituck Inlet shoreline, pre- and post-dredging, 16 April 2003 and 15 April 2004

East bank spit migration

Migration of the east bank spit from 1941 to present is summarized in Figures 4-37a and 4-37b. The orientation of the axis of this formation rotated from east-west to north-south between 1941 and 1969. This reorientation took the formation from the end of the east jetty to the mouth of Mattituck Creek. Estimates of the center lines for the formation for each photograph are approximated in Figure 4-37a to illustrate the rotation and reorientation. The spit began to migrate after 1969. It migrated 260 ft from 1969 to 1976, and 80 ft from 1976 to 1980, with corresponding rates of 37 and 20 ft/year, respectively. After 1980, the formation appears to have reached locational equilibrium, which may indicate the limit of transporting capacity of the flood current. However, this feature could continue to grow into the channel if sediment is supplied to it.

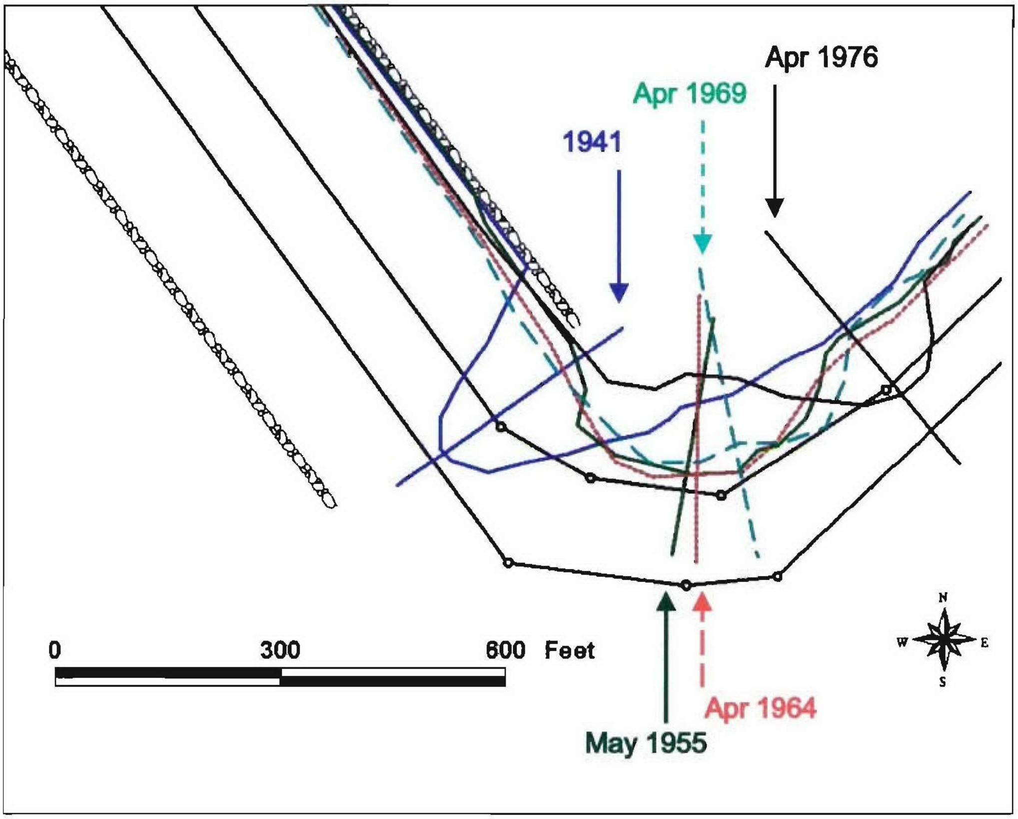

Figure 4-37a. East bank spit migration, 1941-1976

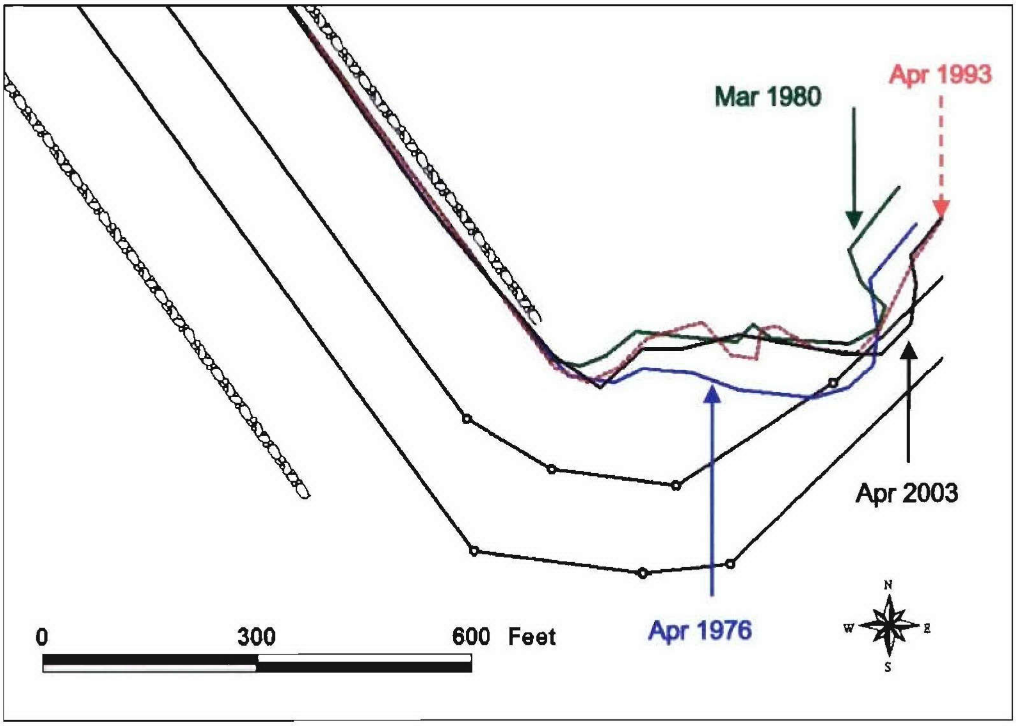

Figure 4-37b. East flood shoal migration, 1976-2003

Bank encroachment analysis

To further quantify the shoaling patterns within Mattituck Inlet, temporal changes in channel width were analyzed. Three cross sections were extracted from the 1980 to 2002 conditions surveys. The locations of these cross sections are shown in Figure 4-38. The temporal changes in cross-sections A and B are analyzed for the period 1980 to 1990, because the data from this period provide the best spatial and temporal coverage. Cross-section C was analyzed for the period 1990 to 2002 to illustrate recent and current morphology changes in this area.

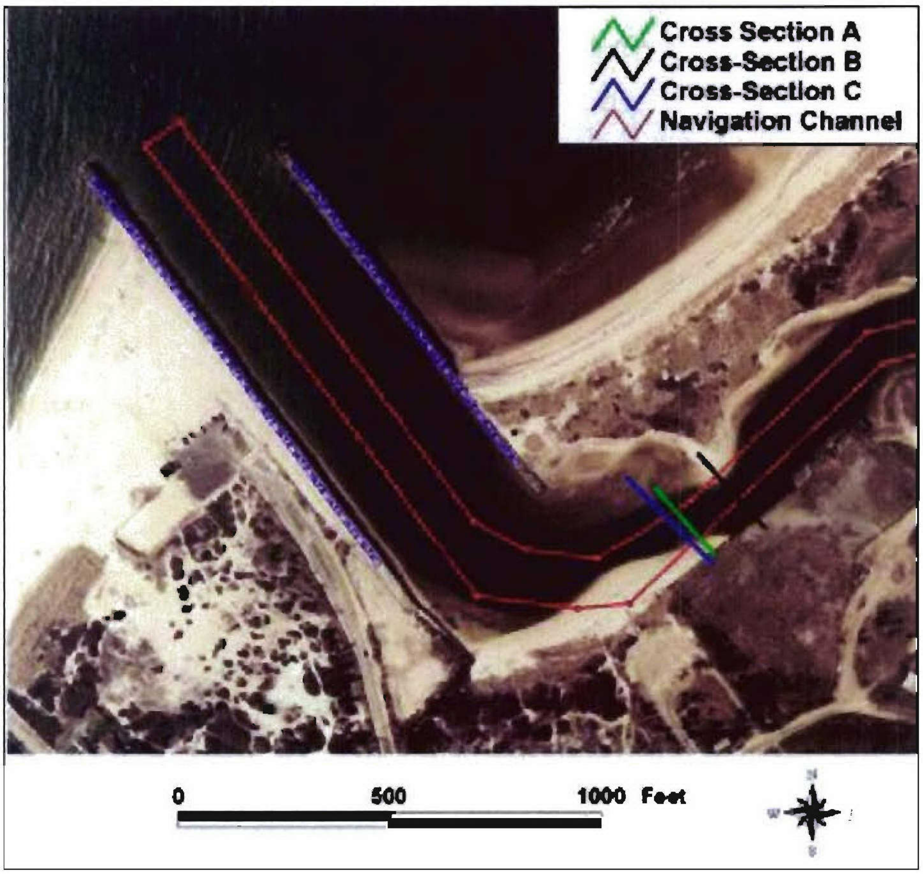

Figure 4-38. Mattituck Inlet channel cross sections

Figure 4-39a shows changes in cross-section A from May 1980 to March 1990, and Figure 4-39b shows changes in cross-section B for the same period. Because these cross sections are not surveyed at identical locations, there is spatial variation between annual surveys. Some of the morphology changes indicated are within survey error. Trends of channel infilling and bank encroachment can be seen over the periods considered. Cross-section A was surveyed for 6 years, and cross-section B was surveyed for only 4 years because there were no surveys near this location in June 1985 and September 1987. Cross-section A is located approximately 150 ft north of the east flood shoal, and

cross-section B is directly adjacent to, and partially cuts through the east flood shoal.

Cross-section A shows areas of scour on the west side of Mattituck Inlet, with channel depths averaging 15 ft. A high degree of variability is indicated. The variability may be the result of differences in survey position, although it is possible that these changes reflect episodes of scour at specific times. Bank encroachment can be seen on the east wall of the navigation channel. Referenced to a depth of 5 ft mlw, sediment accumulation has added approximately 25 ft to the eastern wall of the navigation channel over the 10-year period. This estimate seems reasonable and is supported by the trend over time seen in this figure. Referenced from the center of this cross section, the figure indicates that channel infilling added 1.5 ft of sediment to the channel bottom. Although this value is within survey error, it is consistent with previous assessments of sediment accumulation.

Cross-section B is directly adjacent to the east flood shoal and shows similar trends of scour along the west bank and infilling within the channel, although depths along the areas of scour are not as great. Bank encroachment along the east wall of the navigation channel is more pronounced. Referenced at a depth of 5 ft mlw, sediment deposition added approximately 50 ft to the eastern wall of the Federal navigation channel over the 10-year period.

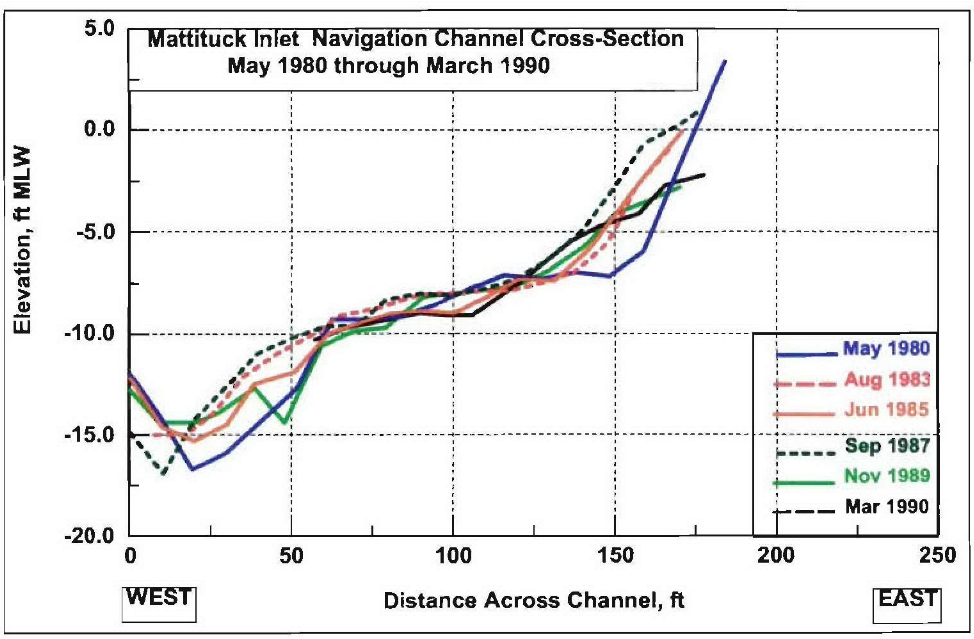

Figure 4-39a. Mattituck Inlet channel cross-section A

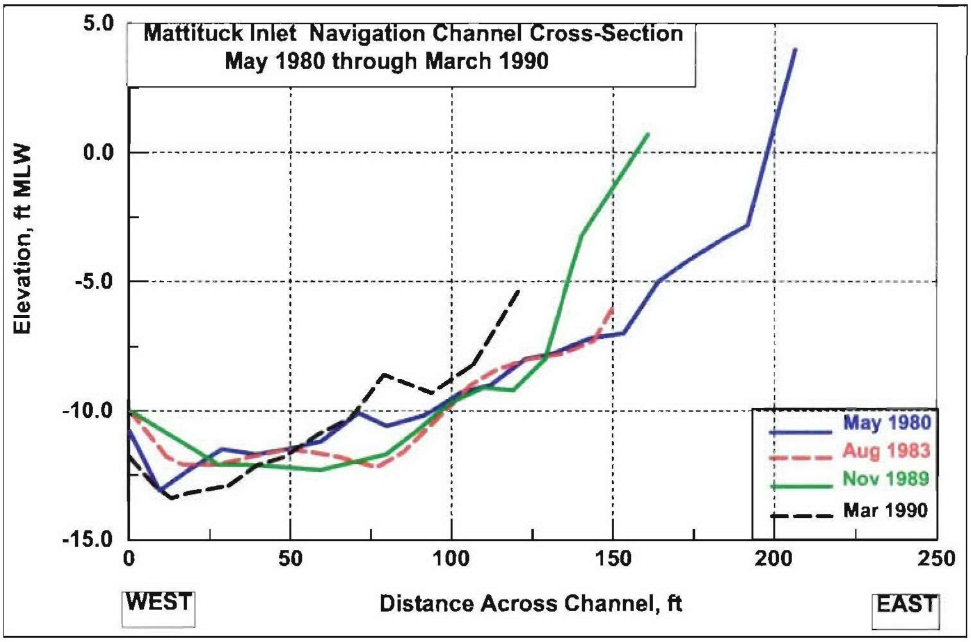

Figure 4-39b. Mattituck Inlet channel cross-section B

Cross-section C (Figure 4-39c) provides information on the present morphology of Mattituck Inlet and is close in location to cross-section A. For comparison to previous figures, the cross section from May 1990 has been included. The cross section of May 1990 is from a pre-dredging survey, and the cross section of October 1990 is from a post-dredging survey. Cross-section C tracks changes in channel width from May 1990 to 2 June 2002. Referenced to a depth of 5 ft mlw, the east bank appears to have grown only 6-7 ft in thickness from October 1990 to 20 June 2001. The 2002 survey at this location shows no indication of growth. Because the other cross sections indicate a trend of bank encroachment, this cross section was not included in the calculation. The 2 June 2002 cross section does, however, indicate encroachment below this reference that generally agrees with the bank encroachment indicated in the other cross sections.

A large of amount of shoaling can be seen along the west bank on cross-section C, and this portion of the shoal was not dredged in October 1990. This portion of the flood shoal was presumably allowed to grow because it was not located within the navigation channel. The eastern edge of the navigation channel starts at approximately 40 ft into the cross sections shown. The shoaling indicated did not begin to encroach upon the navigation channel until the mid-1990s. These cross sections indicate that the east wall of the channel encroached approximately 10 ft between March 1999 and 2002.

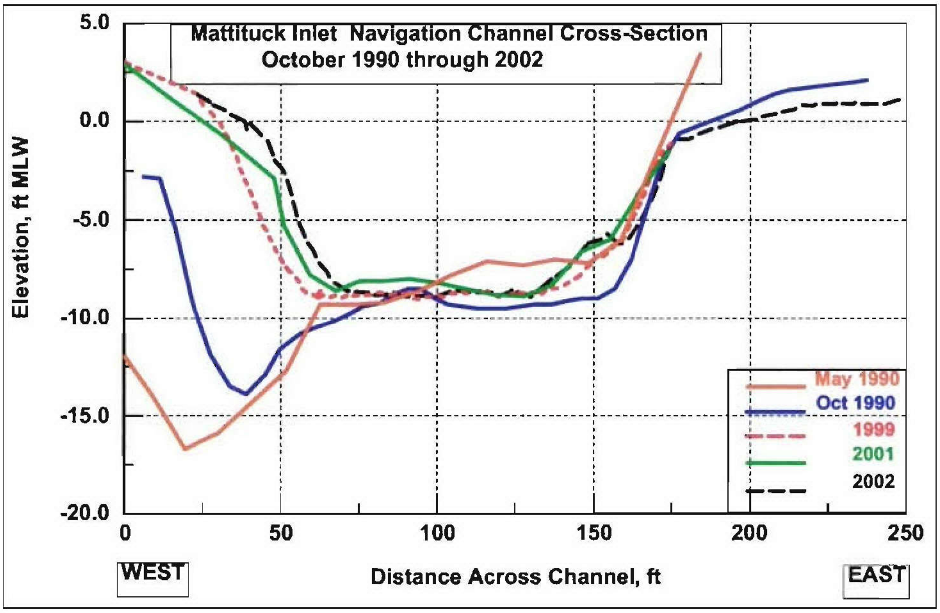

Figure 4-39c. Mattituck Inlet channel cross-section C

Observations during site visits indicate that boat wake action may be a significant mechanism for the redistribution of sediment within the inlet in the areas of shoaling. Figures 4-40a and 4-40b show a boat of medium size entering Mattituck Inlet and the resulting wake arriving obliquely on the area of shoaling located at the base of the east jetty. The obliquely incident waves can transport sediment alongshore.

Figure 4-40a. Boat approaching turn at base of jetties, Mattituck Inlet, 9 July 2004, view looking northwest

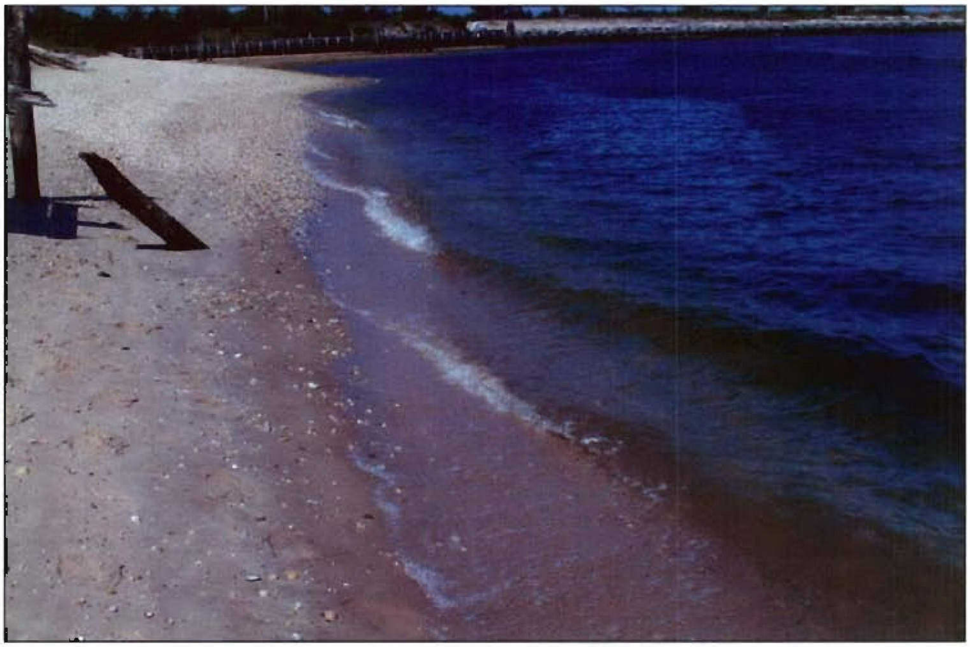

Figure 4-40b. Boat wake obliquely incident on area of flood shoal at base of east jetty, Mattituck Inlet, 9 July 2004

Goldsmith Inlet

To analyze morphology change for the offshore at Goldsmith Inlet, beach profiles from the 6-8 October 2002 survey are compared to those from a March 1998 survey (OCTI 1998), spanning a 4-1/2 year interval. Analysis of the migration of the inlet entrance and the inlet channel, growth of the fillet at the jetty, growth of an attached west bank fillet, and the flood shoal is conducted by reference to aerial photography.

Offshore morphology change

Figures 4-41a to 4-41k plot comparisons of 1998 (OCTI 1998) and 2002 beach profiles for the areas offshore of Goldsmith Inlet. In some instances, profile transects were referenced to previously established monuments (OCTI 1998). East of Goldsmith Inlet, the profiles often did not overlap. The profile surveys indicate a shoreline near equilibrium from 1998 to 2002.

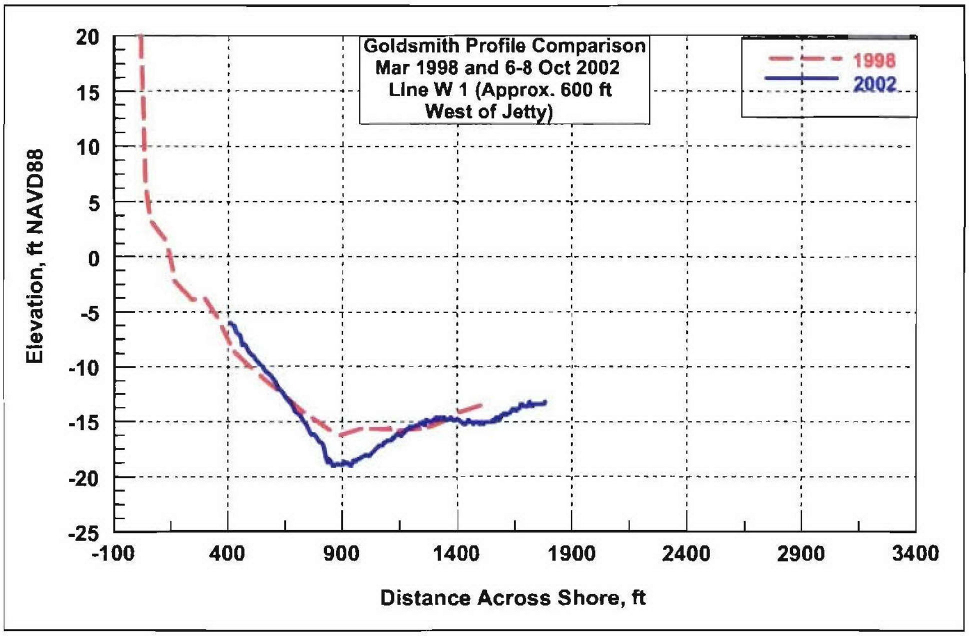

Figure 4-41a. Beach profile W1, west of Goldsmith Inlet, March 1998 and 6-8 October 2002

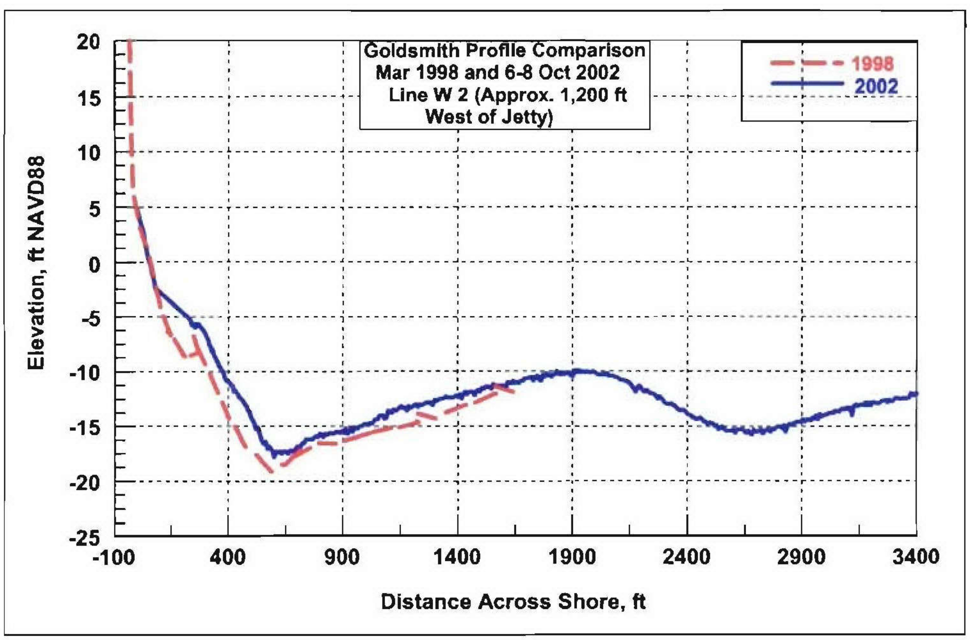

Figure 4-41b. Beach profile W2, west of Goldsmith Inlet, March 1998 and 6-8 October 2002

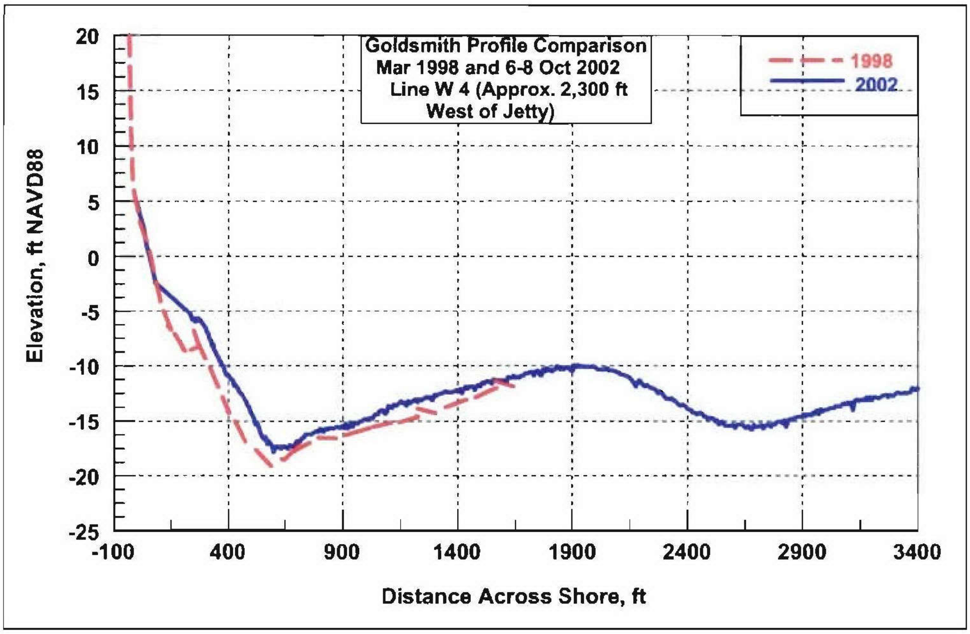

Figure 4-41c. Beach profile W4, west of Goldsmith Inlet, March 1998 and 6-8 October 2002

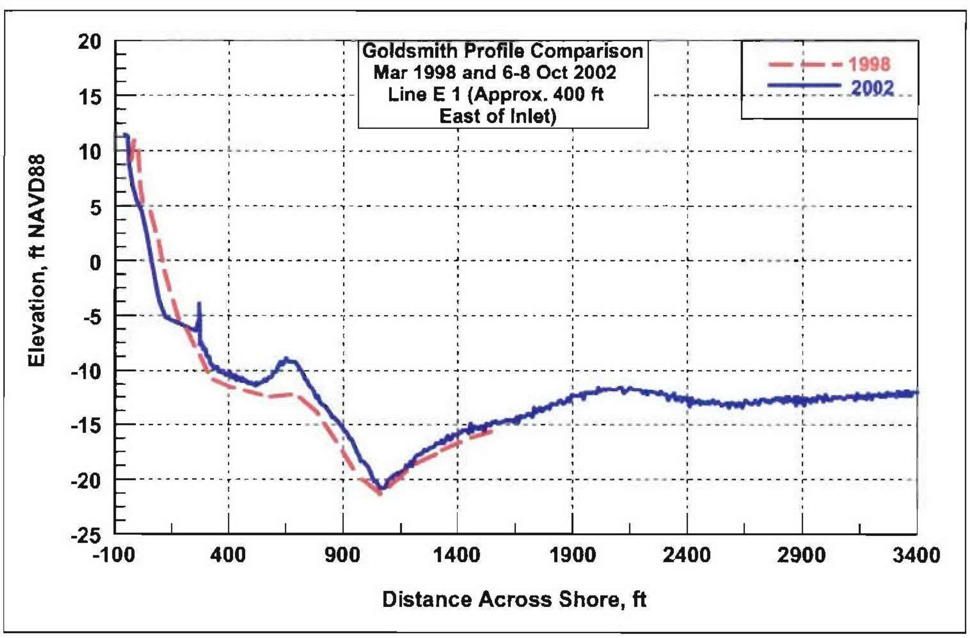

Figure 4-41d. Beach profile E1, east of Goldsmith Inlet, March 1998 and 6-8 October 2002

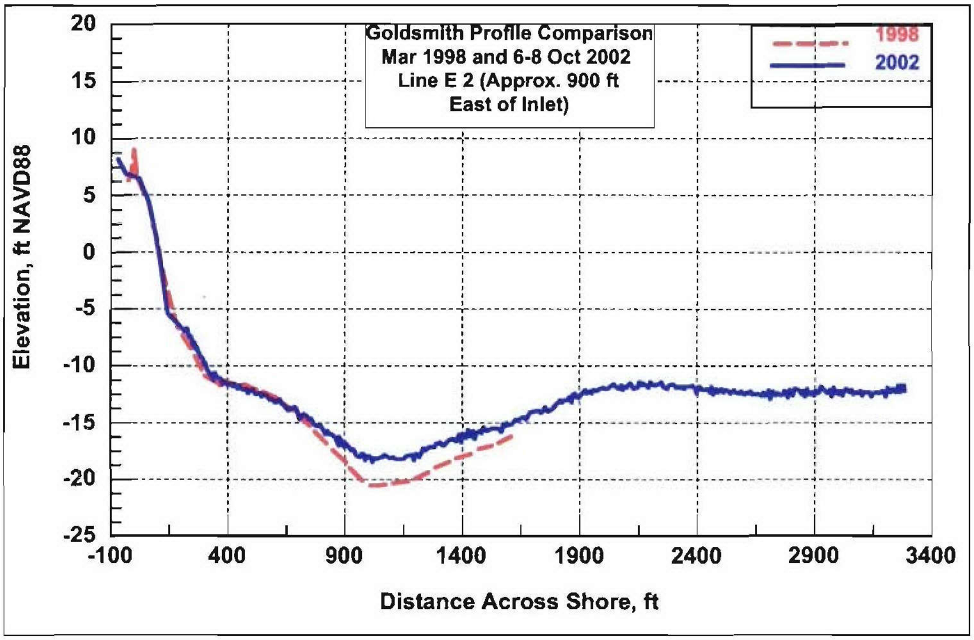

Figure 4-41e. Beach profile E2, east of Goldsmith Inlet, March 1998 and 6-8 October 2002

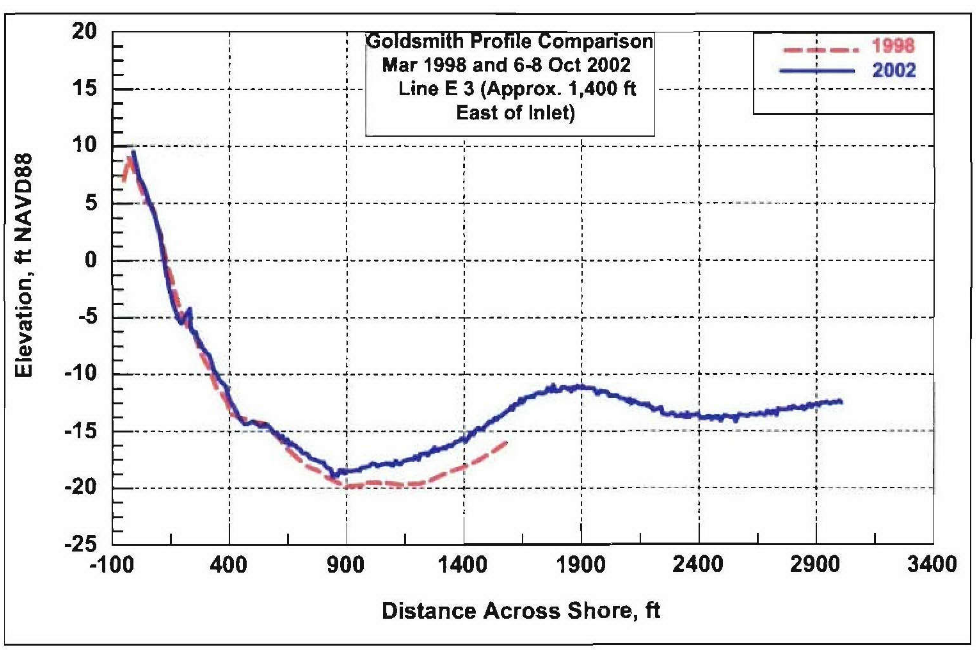

Figure 4-41f. Beach profile E3, east of Goldsmith Inlet, March 1998 and 6-8 October 2002

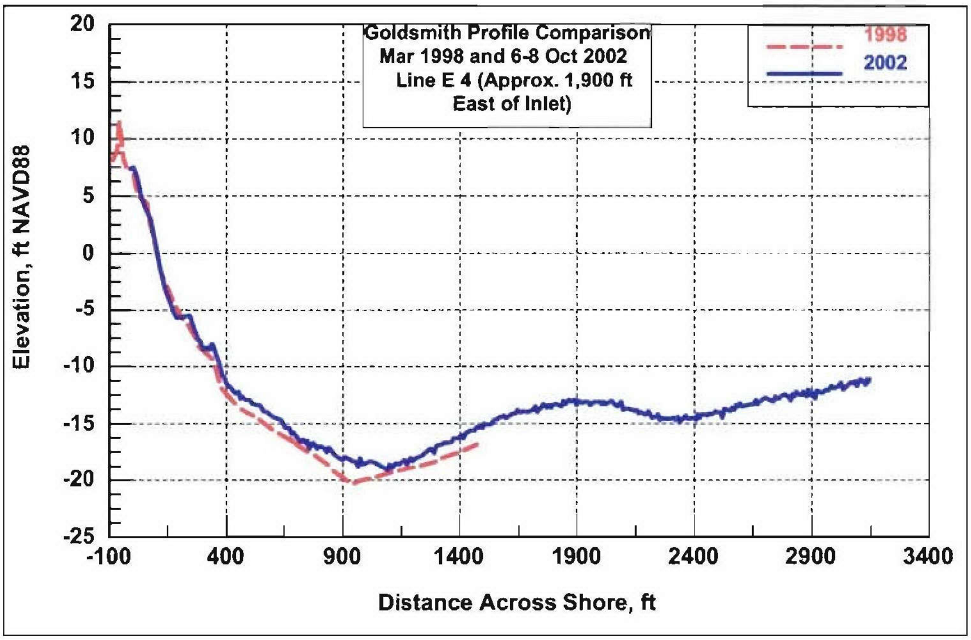

Figure 4-41g. Beach profile E4, east of Goldsmith Inlet, March 1998 and 6-8 October 2002

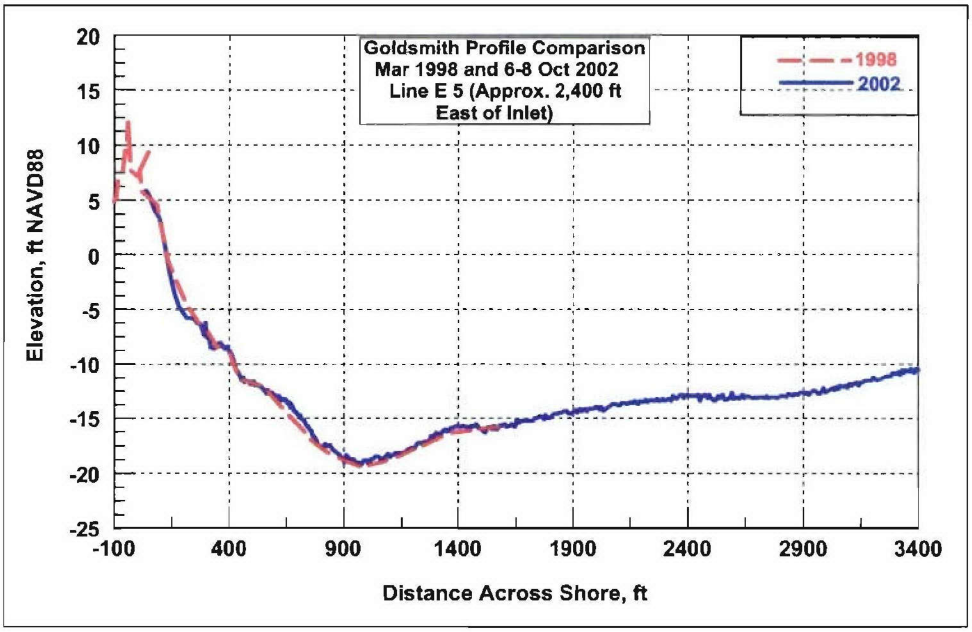

Figure 4-41h. Beach profile E5, east of Goldsmith Inlet, March 1998 and 6-8 October 2002

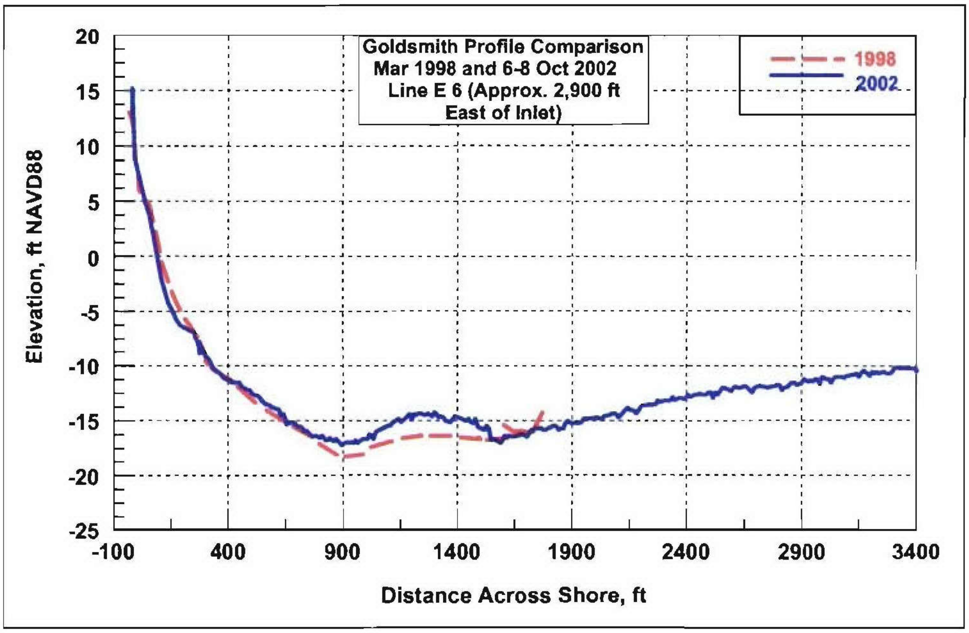

Figure 4-41i. Beach profile E6, east of Goldsmith Inlet, March 1998 and 6-8 October 2002

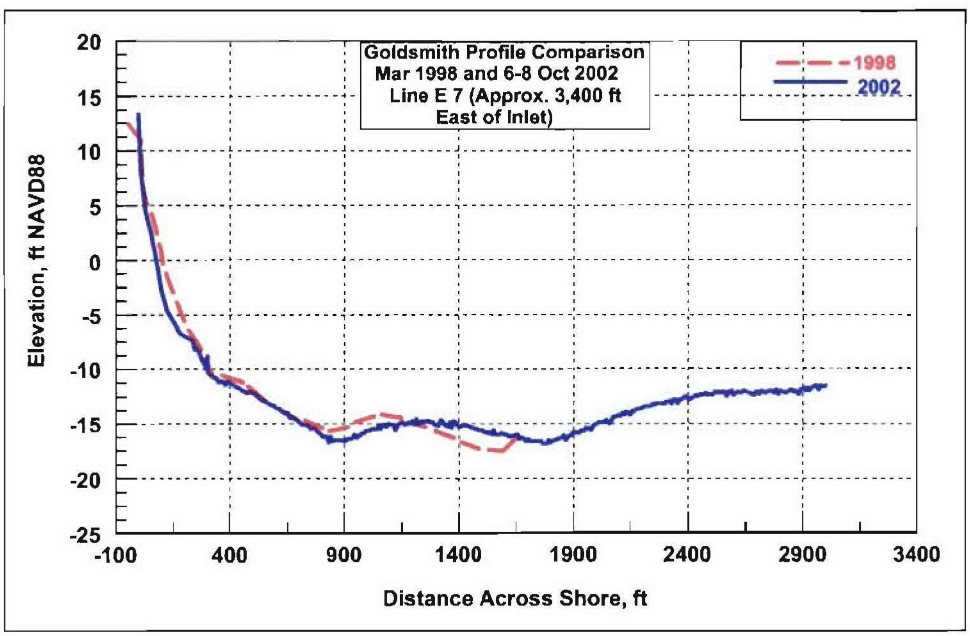

Figure 4-41j. Beach profile E7, east of Goldsmith Inlet, March 1998 and 6-8 October 2002

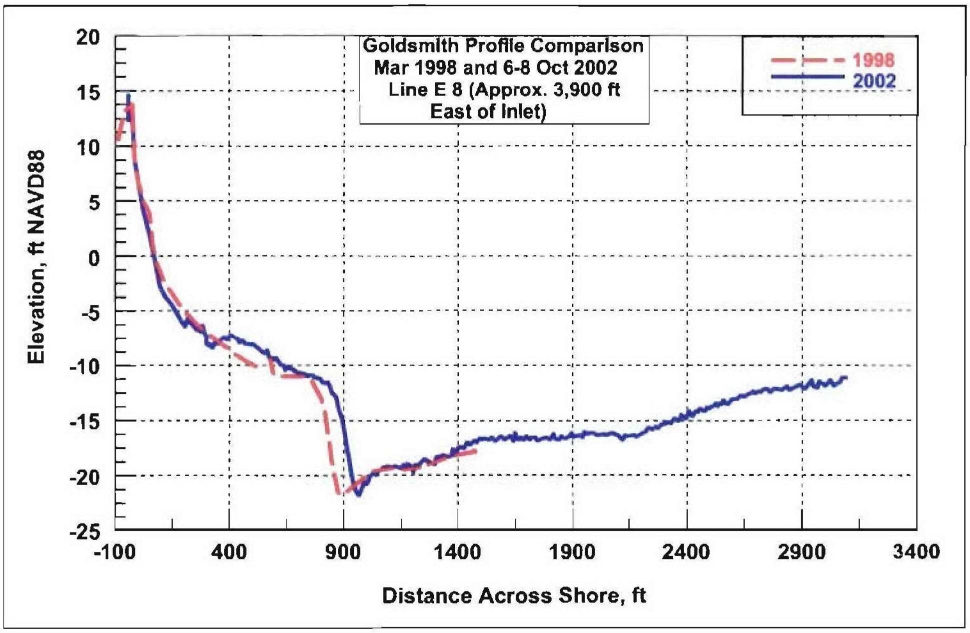

Figure 4-41k. Beach profile E8, east of Goldsmith Inlet, March 1998 and 6-8 October 2002

Channel migration

Because Goldsmith Inlet is free to migrate to the east and away from the jetty, the location of its entrance channel is dynamic. The orientation of the channel, sediment impoundment west of the jetty, and formation of a fillet east of the jetty are analyzed for times available from aerial photographs. The reorientation indicates that Goldsmith Inlet is presently an ephemeral inlet, in contrast to the preceding century when it was apparently more stable and open (Chapter 2).

Goldsmith Inlet in 1938 and 1955, prior to the 1964 construction of the jetty, is shown in Figures 4-42a and 4-42b. A small promontory or cusp directly to the west of the inlet mouth is observed in Figure 4-42b. The promontory may be associated with blockage by a geological hard point from the glacial moraine. Alternatively, this feature may be a small relict groin. A hard point would promote and preserve the stability of Goldsmith Inlet and Goldsmith Pond. The Goldsmith Inlet channel in its natural state had a width of approximately 10 ft for the first 450 ft, and widened to an average of approximately 120 ft for the remainder of the channel issuing into Goldsmith Pond. Sediment grain size analysis shows the median grain size for the first 500 ft to range from -4 to -6 ϕ (16-64 mm). The median grain size of the channel beyond this point ranges from -1 to -3 ϕ (2-8 mm).

Figures 4-42c though 4-42l document the location and width of the inlet entrance of Goldsmith Inlet from 1964 to the present. The relation among sediment impoundment (1964-1976), the formation of an accretion spit directly east of the jetty (1976-present), and the eastward migration of the channel entrance are discussed in the following paragraphs (1976-present).

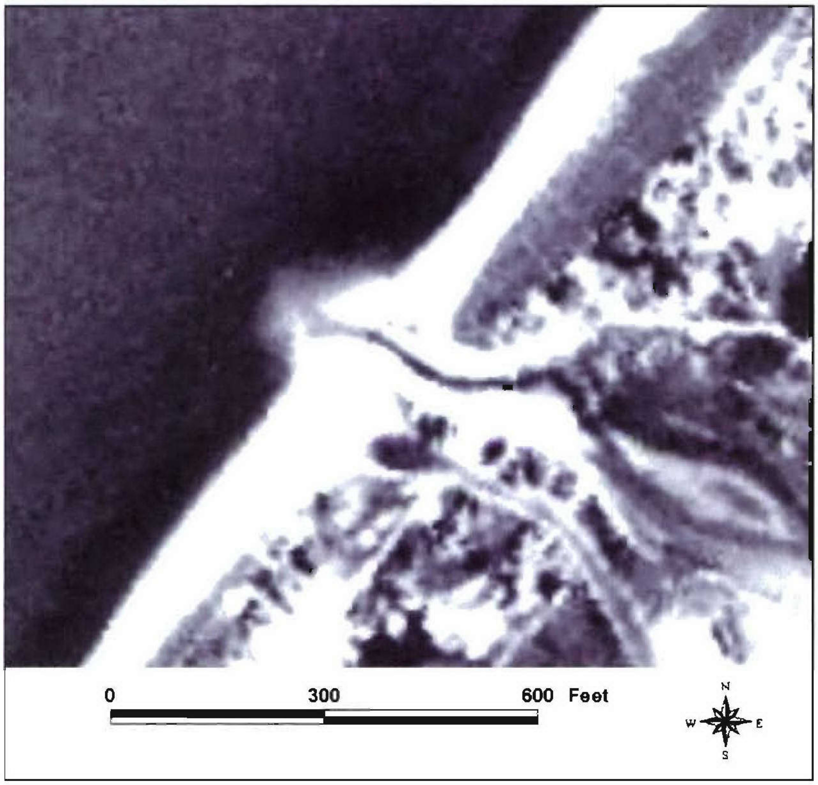

Figure 4-42a. Goldsmith Inlet channel entrance, 1938 (exact month and day unknown)

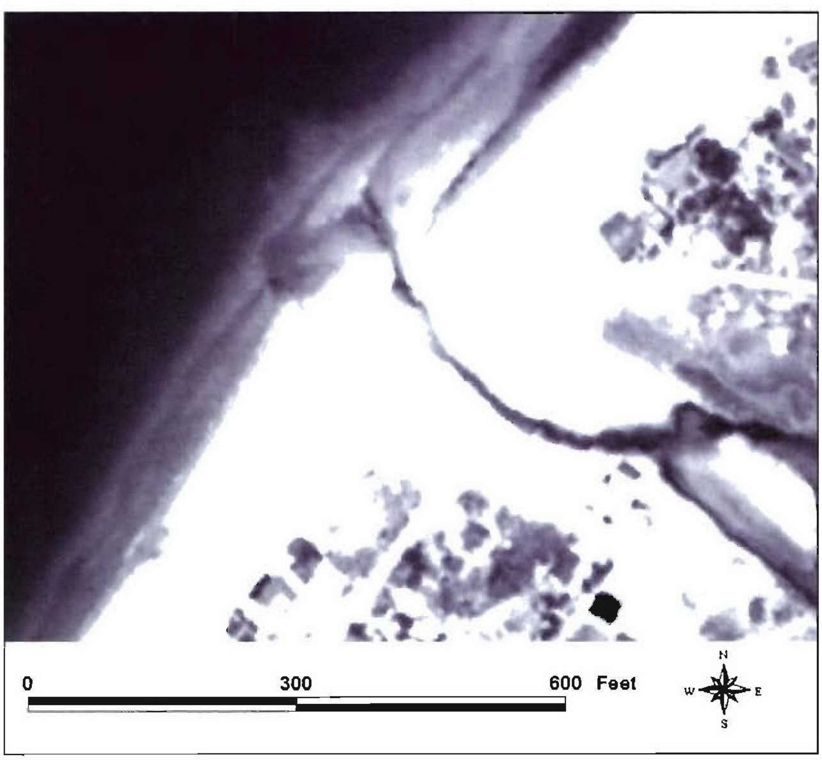

Figure 4-42b. Goldsmith Inlet channel entrance, 11 May 1955

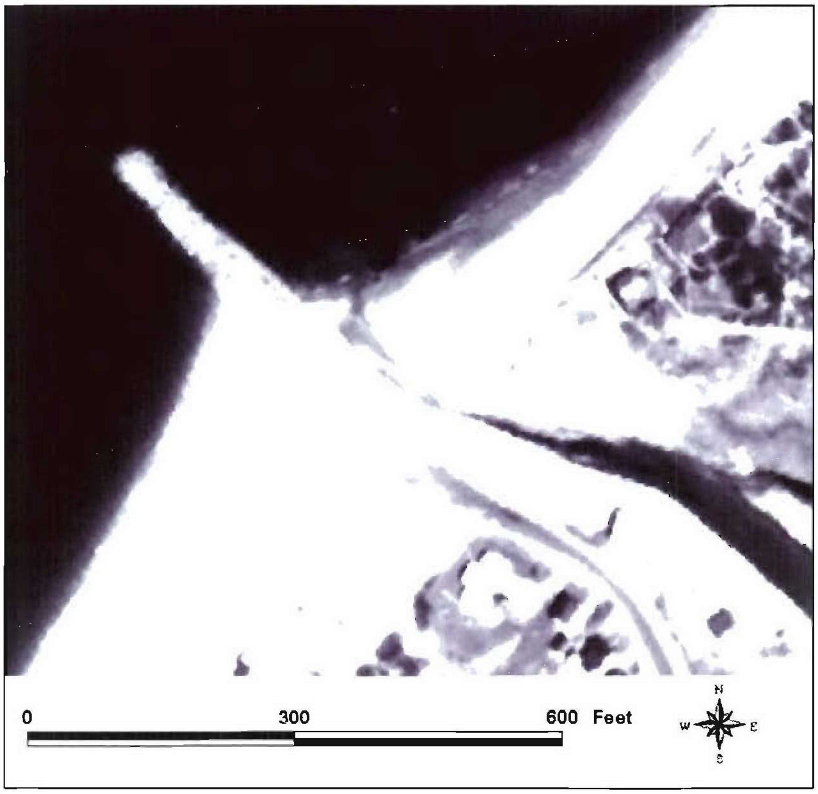

Figure 4-42c. Goldsmith Inlet channel entrance, 1 April 1964

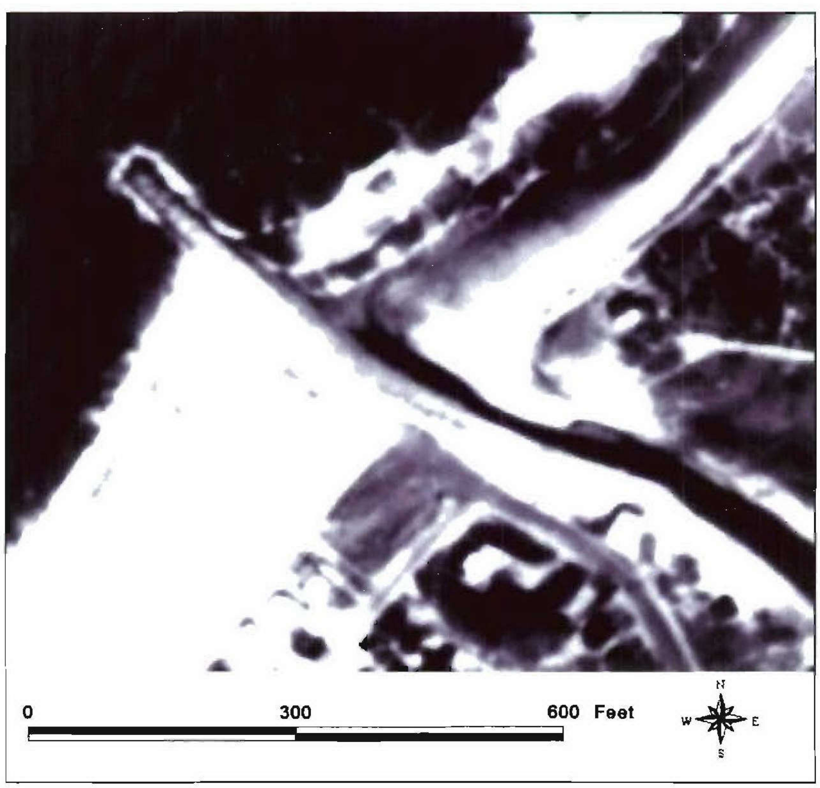

Figure 4-42d. Goldsmith Inlet channel entrance, 5 October 1966

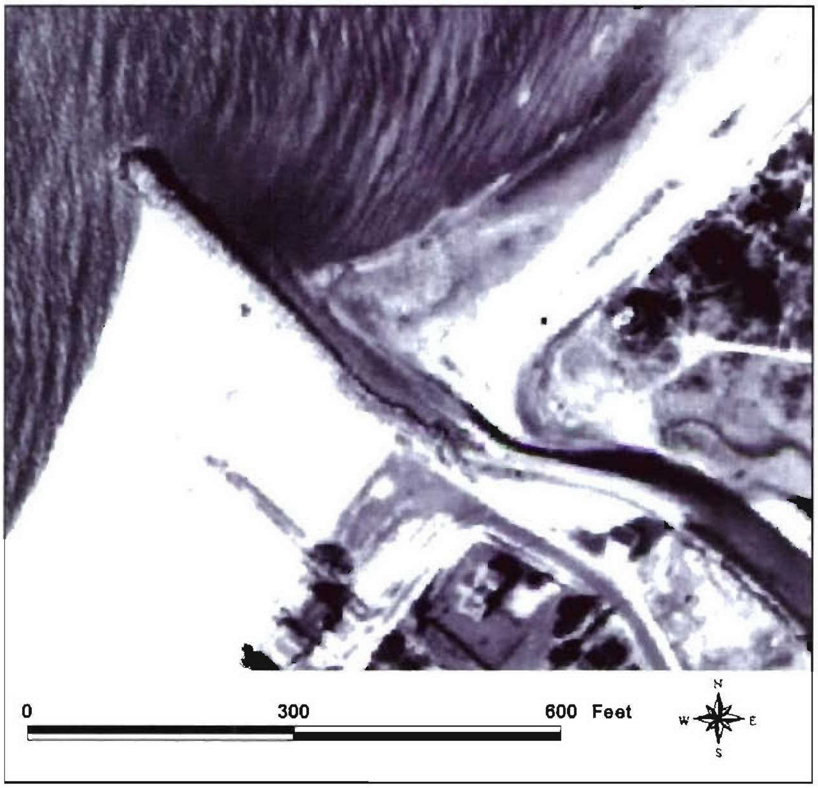

Figure 4-42e. Goldsmith Inlet channel entrance, 28 April 1969

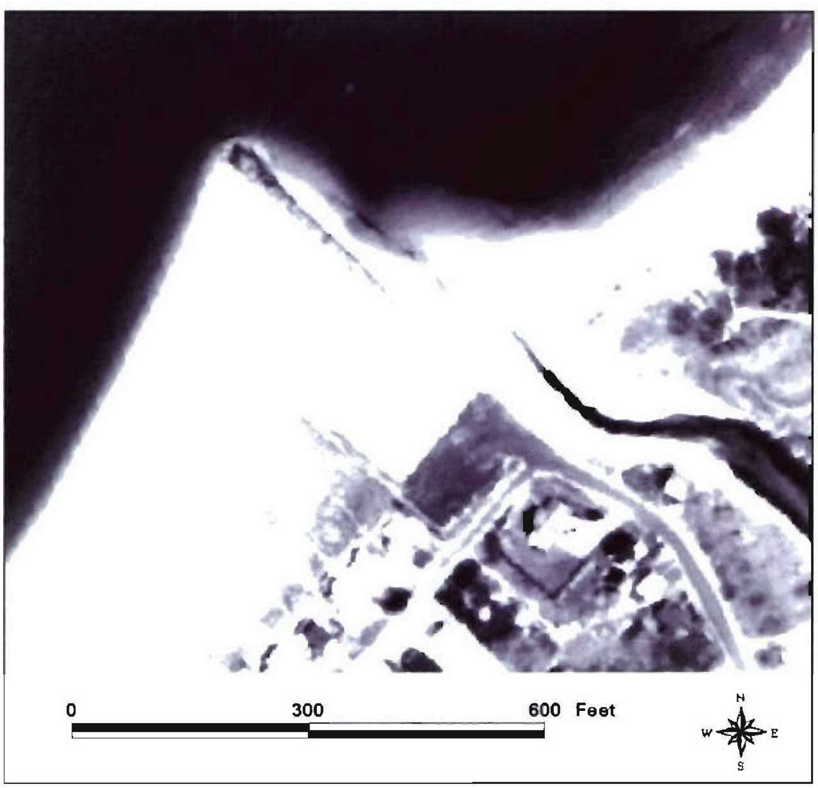

Figure 4-42f. Goldsmith Inlet channel entrance, 6 April 1976

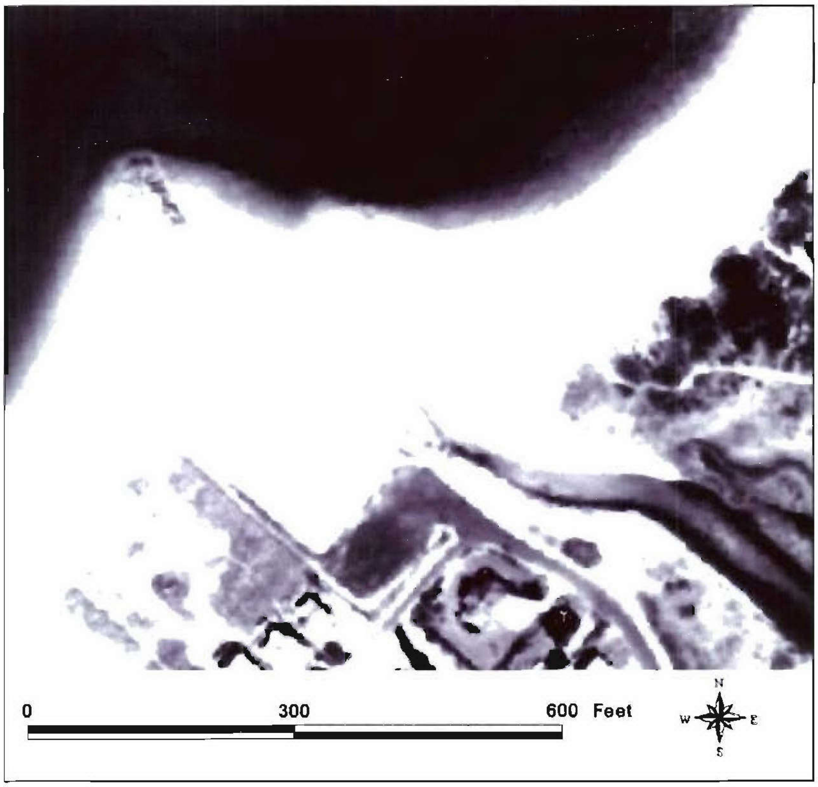

Figure 4-42g. Goldsmith Inlet channel entrance, 24 May 1980

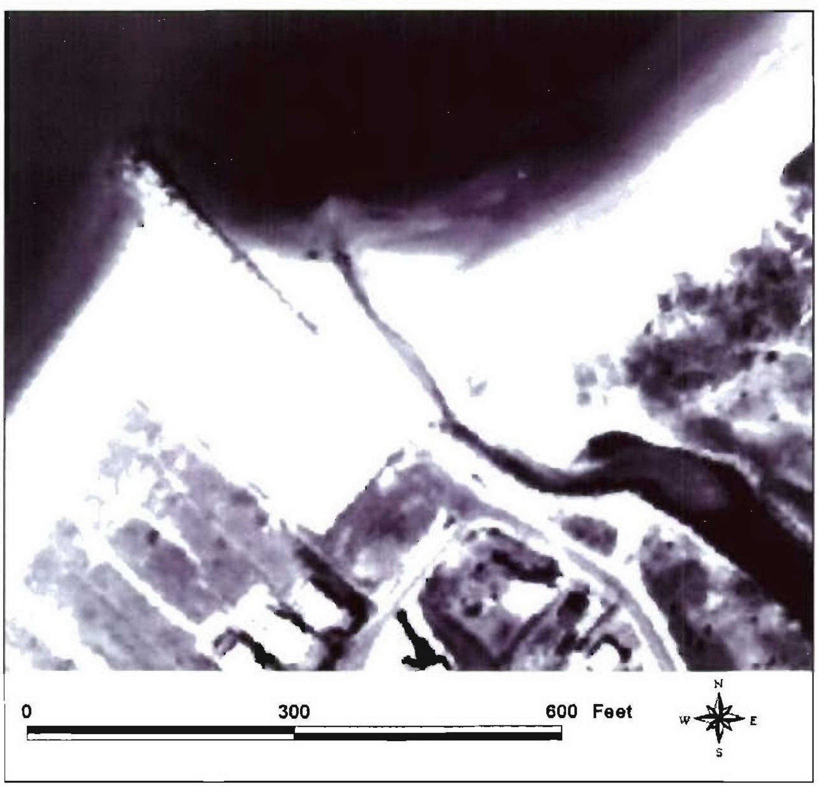

Figure 4-42h. Goldsmith Inlet channel entrance, 5 April 1993

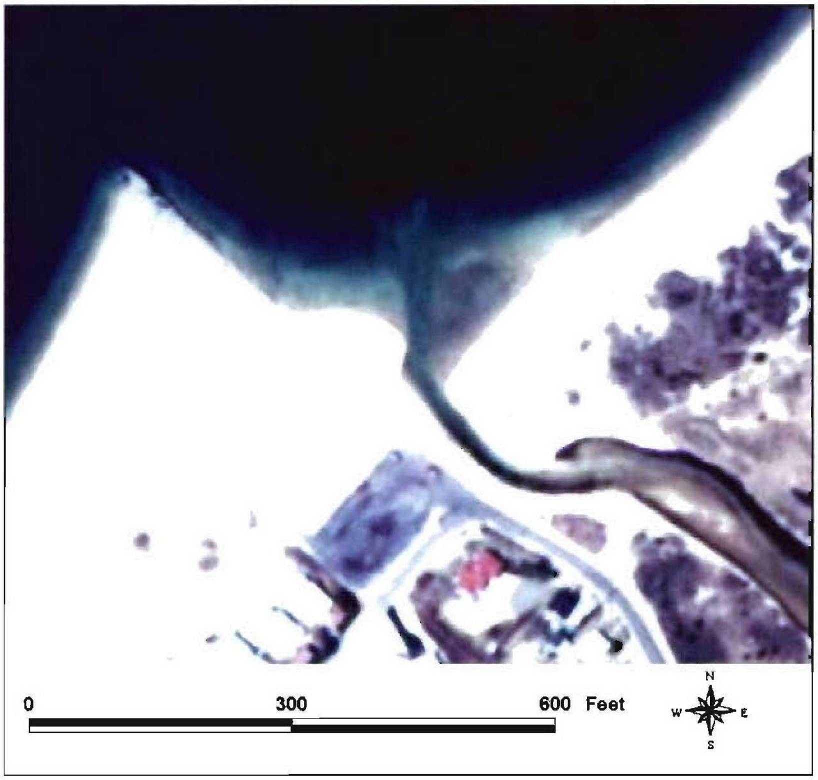

Figure 4-42i. Goldsmith Inlet channel entrance, 21 April 1996

Figure 4-42j. Goldsmith Inlet channel entrance, 26-30 April 2001

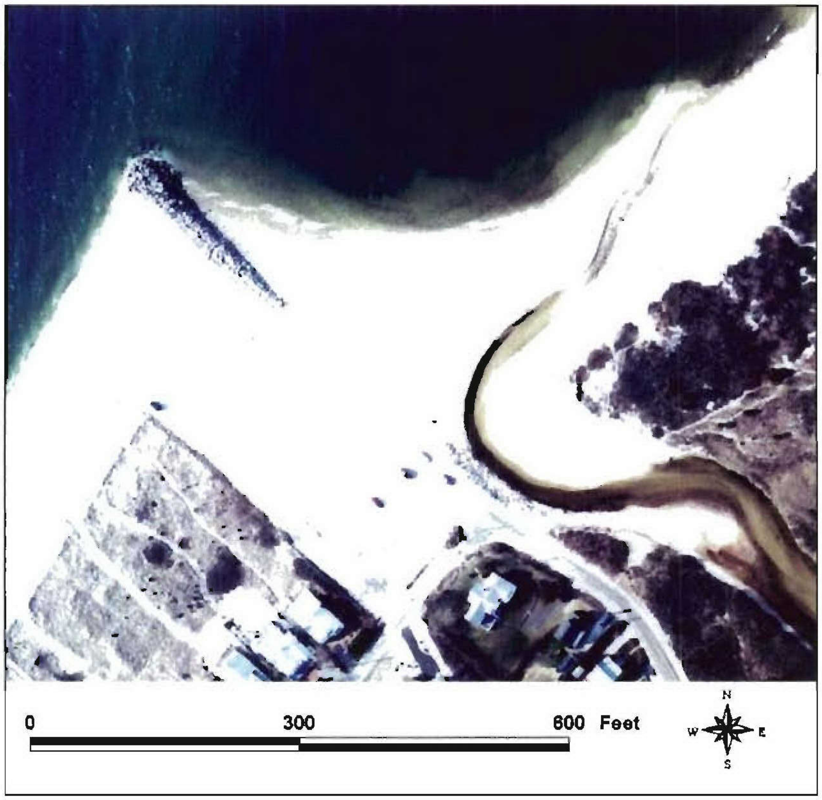

Figure 4-42k. Goldsmith Inlet channel entrance, 16 April 2003

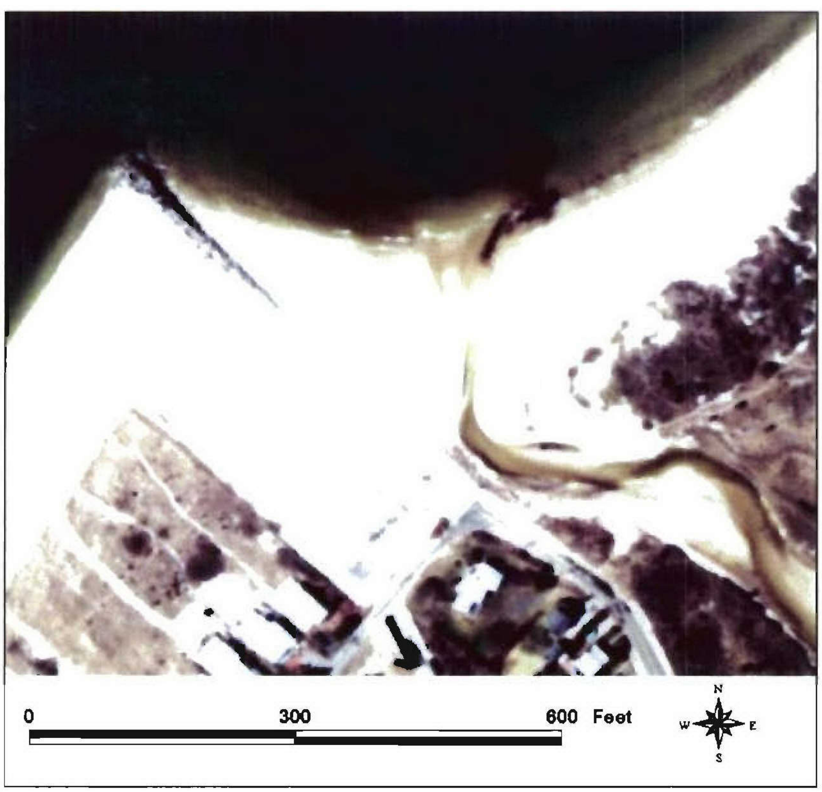

Figure 4-42l. Goldsmith Inlet, 15 April 2004

Channel orientation at Goldsmith Inlet in 1938 and 1955, prior to the construction of the jetty, is illustrated in Figure 4-43a. Channel orientation and shoreline extent directly east and west of Goldsmith Inlet from 1955 to 1966 are illustrated in Figure 4-43b, referenced to the location of the jetty. Morphology change at the entrance of Goldsmith Inlet for this period is characterized by the introduction of the jetty, the relocation of the inlet entrance, and resulting impoundment of sediment west of the jetty and shoreline recession east of the jetty.

Figure 4-43c illustrates channel orientation and shoreline extent directly east and west of Goldsmith Inlet from 1969 to 1980. The impoundment capacity of the jetty at Goldsmith Inlet is rapidly being approached in 1969, and the jetty reached near-field capacity by 1976. Formation of the present-day spit directly east of the jetty at Goldsmith Inlet had begun by 1976. The inlet experienced closure at least once in the photographic record (March 1980) and appeared to be approaching closure in April 1976.

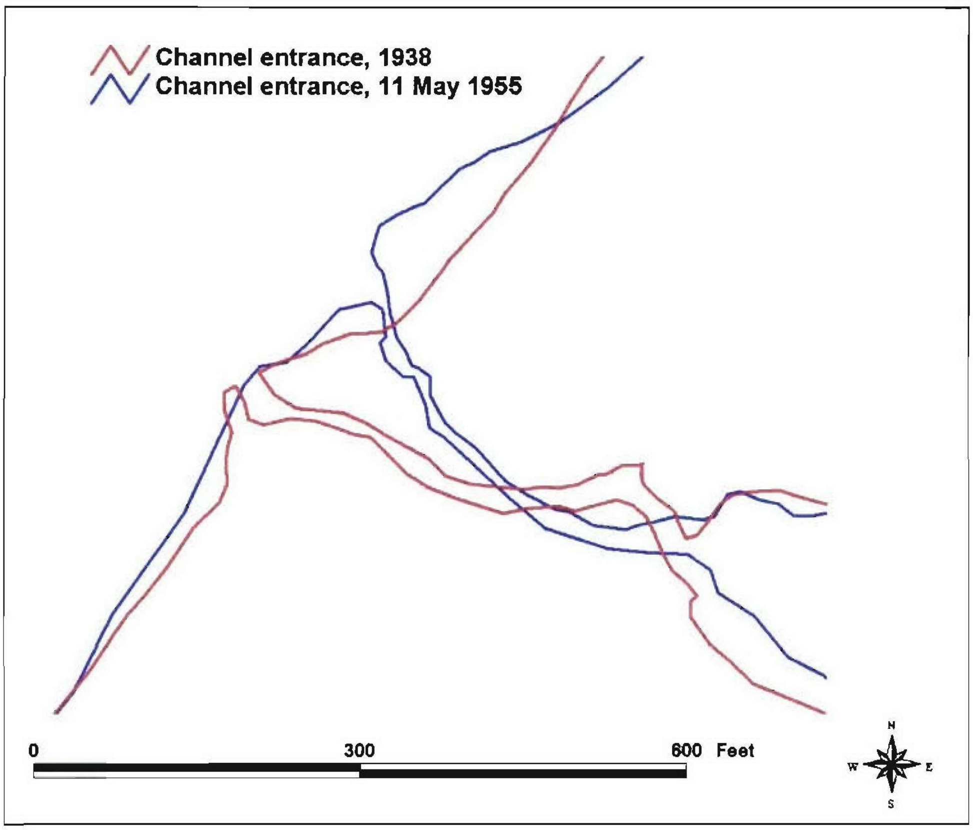

Figure 4-43a. Goldsmith Inlet channel entrance, 1938 and 11 May 1955

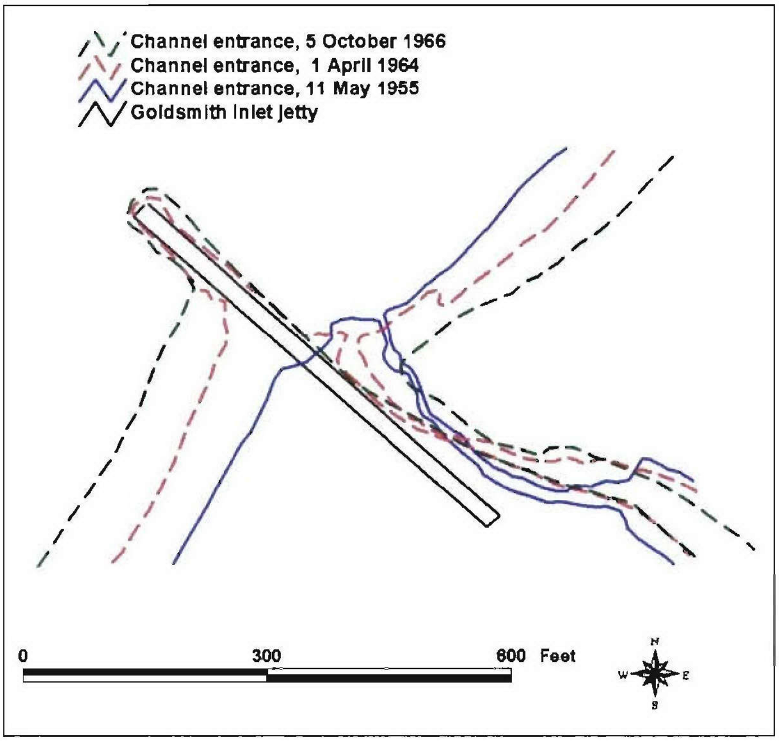

Figure 4-43b. Goldsmith Inlet channel entrance, 11 May 1955, 1 April 1964, and 5 October 1966

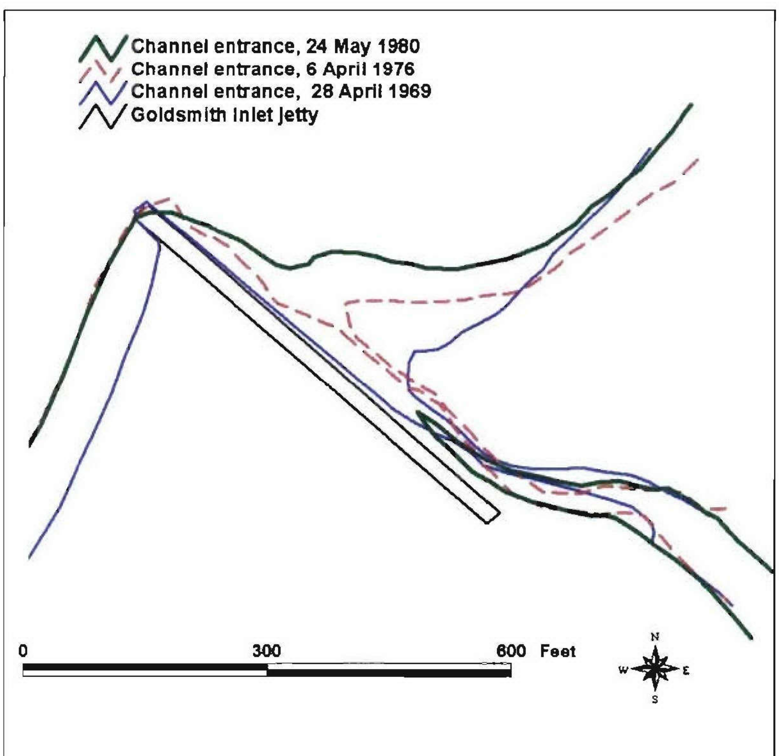

Figure 4-43c. Goldsmith Inlet channel entrance, 28 April 1969, 28 April 1976, and 24 May 1980

According to Greenman-Pedersen Associates, P.C. (1981), the Goldsmith Inlet jetty reached impoundment capacity in 1972 and had become an effective sediment bypasser. Their analysis, however, indicates that the greatest rates of erosion on the downdrift beach occurred between 1972-1978. The report concludes that there is no apparent reason for this acceleration. Analysis in the present study indicates that an effective sediment bypassing system was not established until the jetty-attached spit directly east of the jetty had reached a certain volume and areal extent. The impoundment fillet directly west of the jetty was the apparent primary sediment sink in this area prior to 1972. After this, the formation of the spit adjacent to the east side of the jetty became the primary sediment sink for the local sand-sharing system. This period may have also been characterized by greater rates of sediment intrusion within the inlet.

Goldsmith Inlet was dredged in 1977 and again in July 1980. Figure 4-42g shows Goldsmith Inlet was closed on 24 May 1980. This dredging reopened the inlet. The inlet also appears to have been approaching closure in 1976, and the dredging of 1977 is assumed to have prevented closure or reopened the inlet soon after closure. Aerial photographs for the period 1981–1993 were not found. Records indicate, however, that the Town of Southold regularly dredged the inlet during this time (Table 2-9). Based on comparison of areal extent of the spit directly east of the jetty in 1976 and 1993, it is assumed that these dredgings served to keep the inlet open and the location at the entrance of the inlet relatively stable.

The present, dynamic morphology of the Goldsmith Inlet channel is apparent in Figures 4-43d and 4-43e. No dredging records are available for Goldsmith Inlet after 1990. Fields et al. (1999) estimates that 5,000 cu yd of sediment had been dredged annually from Goldsmith Inlet. The Southold Town Engineer, however, has indicated that all dredging operations ceased sometime in the mid-1990s.[1] Ceasing of dredging is apparently reflected in the growth of the spit directly west of the jetty between 1993 and 1996 (Figure 4-43d).

Channel orientation for 2002-2004 is illustrated in Figure 4-43e. There appears to have been little migration of the channel entrance between 1996 and 2002, although locational stability may have owed to dredging for which accurate records are not available. The observed rapid migration and spit formation of recent times is discussed in the following paragraphs.

---

[1] Personal communication, 22 March 2003, Mr. James. A Richter, Office of the Engineer, Southold Town Hall, 53095 Main Road, Southold, NY.

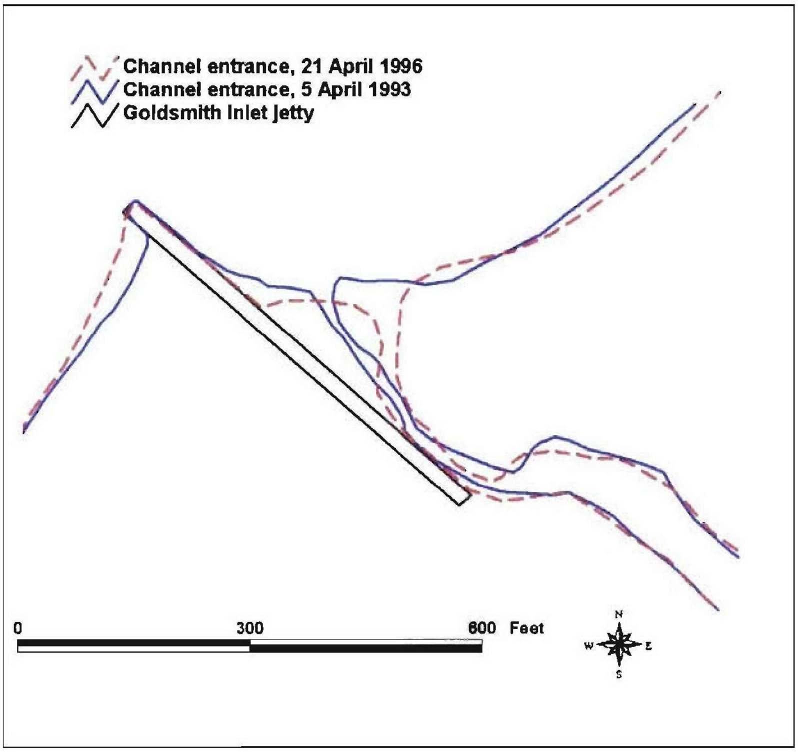

Figure 4-43d. Goldsmith Inlet channel entrance , 5 April 1993 and 21 April 1996

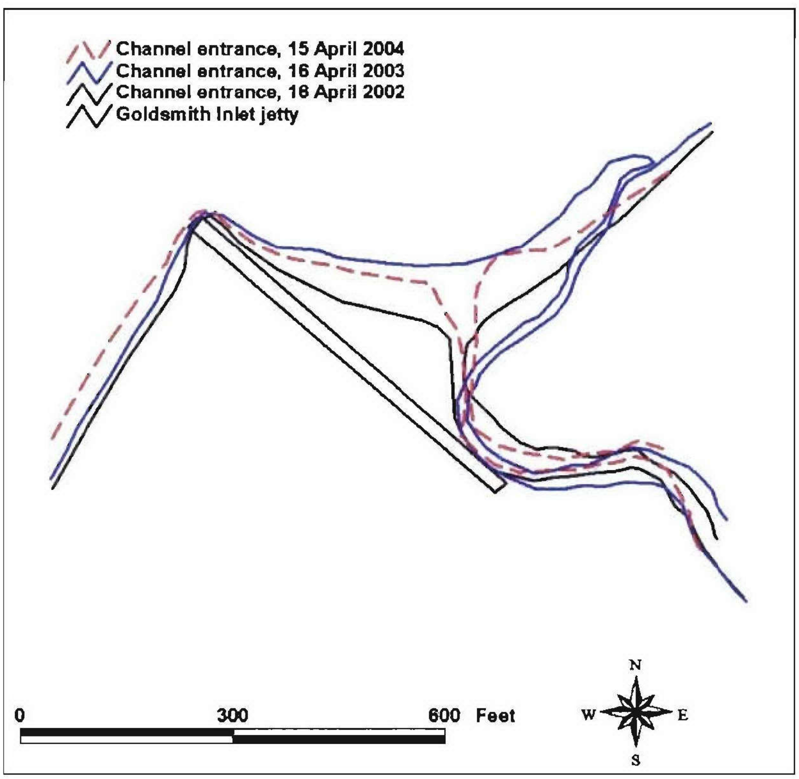

Figure 4-43e. Goldsmith Inlet channel entrance, 16 April 2002, 16 April 2003, and 15 April 2004

Figures 4-44a and 4-44b summarize orientations of the inlet entrance from 1993 to 2004. The aerial photograph of 16 April 2002 approximates the location and orientation of the channel at the time of the bathymetry survey of 6-8 October 2002. Change in location and morphology of the Goldsmith Inlet channel entrance between 6-8 October 2002 and 16 April 2003 is substantial. Sediment accumulation extended the beach 60-80 ft for the 500 ft directly east of the jetty, and the entrance channel mouth migrated 350 ft to the east. The effective greater length of the channel diminished the flushing capability of the inlet and contributed to closure. The acute angle of the inlet relative to the shoreline, in contrast, allows for more effective sediment bypassing. An emergency dredging at Goldsmith Inlet took place on 22-26 March 2004, and the inlet entrance and channel were repositioned.

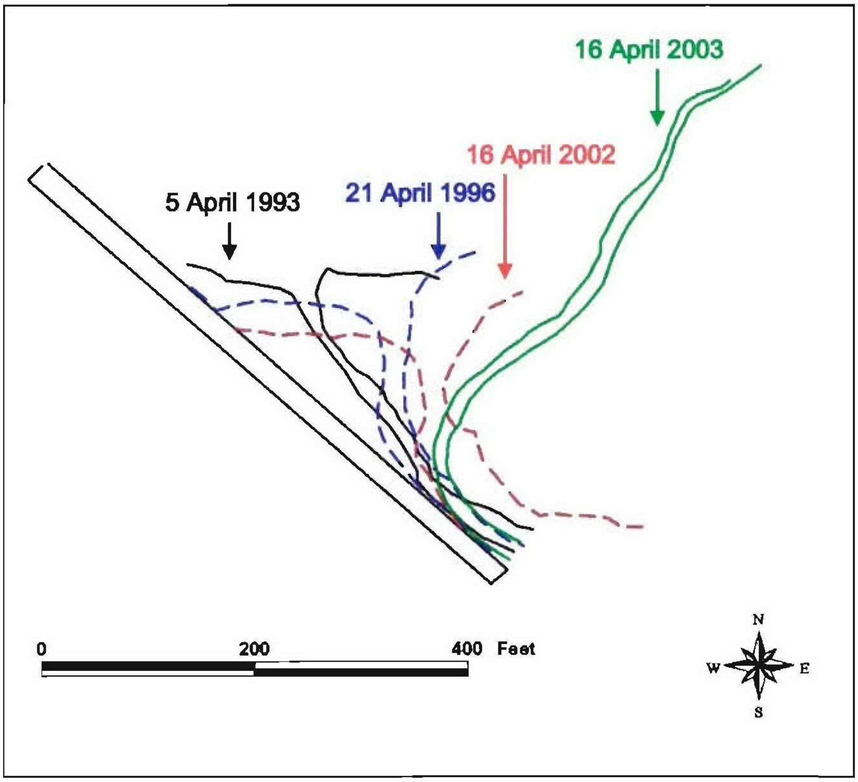

Figure 4-44a. Goldsmith Inlet channel entrance orientation, 1993-2003

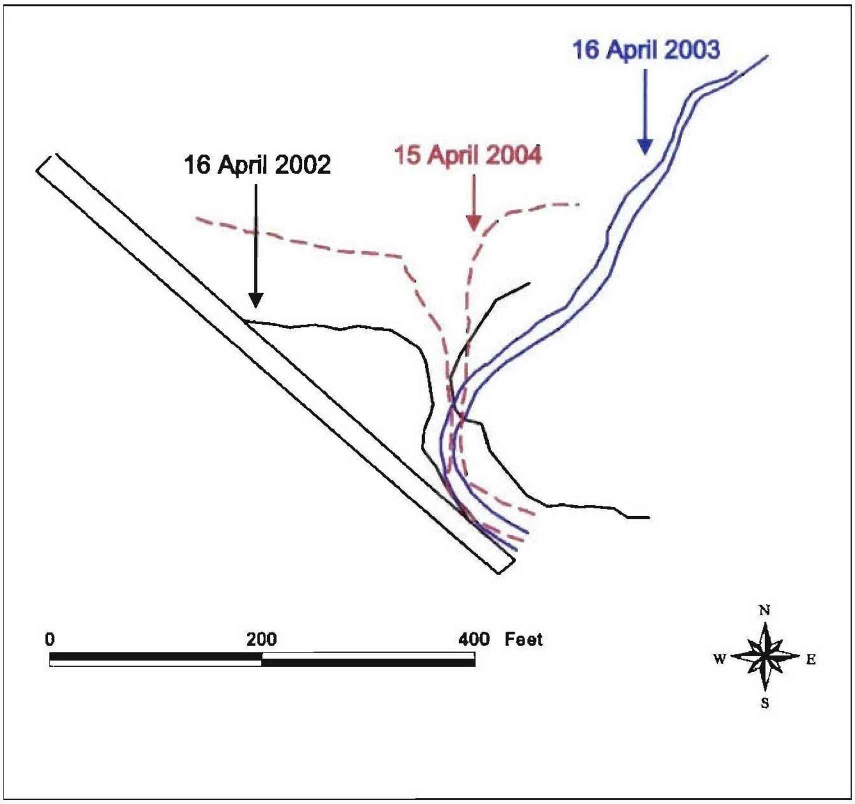

Figure 4-44b. Goldsmith Inlet channel entrance orientation, 2002-2004

Areal changes of the spit directly east of the jetty are illustrated in Figure 4-45. Bypassing along the east side of the jetty resulted in 12,000 sq ft of accreted sediment in 1996 and 17,000 sq ft in 2002. The elevation of the Goldsmith Inlet jetty is 7 ft NAVD88. Because this spit for the most part covered the landward portion of the jetty, the thickness of the shoal at both times is estimated to be 6 ft above the NAVD88 datum. Volume of the spit is estimated to be 2,700 cu yd in 1996 and 3,800 cu yd in 2002. The average rate of sediment accumulation along the east side the jetty from 1996 to 2002 is estimated to be 140 cu yd/year.

The area of the spit along the east side of the jetty increased from 17,000 sq ft on 16 April 2002 to 68,000 sq ft on 16 April 2003. The volume of sediment located between the jetty and entrance channel is estimated to be 9,000-12,000-cu yd, with 5,200 to 8,200 cu yd accumulating in a 6-month period. The areal extent of the spit after the emergency dredging of 22-26 March 2004 is estimated to be 35,000 sq ft.

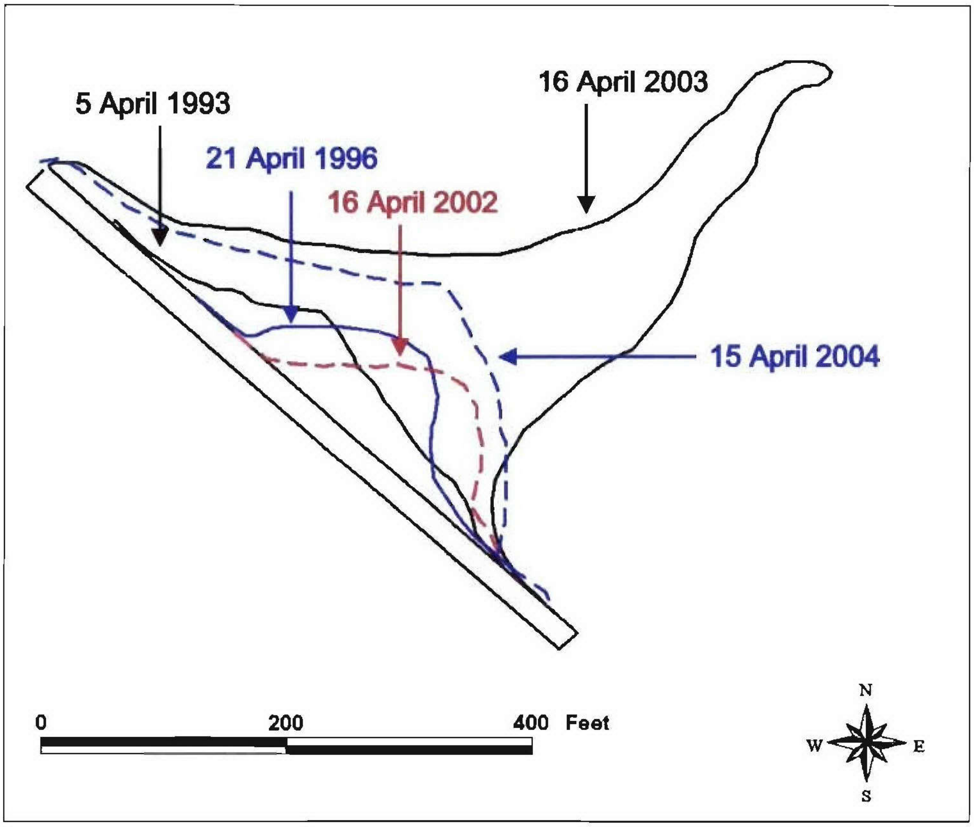

Figure 4-45. Shoaling east of Goldsmith Inlet jetty, 1993-2004

Channel and flood shoal morphology change

This section begins with a review of the natural morphology of the channel at Goldsmith Inlet and modifications identified or interpreted to have been introduced by channel dredging. Evolution and morphology change of the flood shoal at Goldsmith Inlet in response to these modifications is then analyzed.

The morphology of the channel at Goldsmith Inlet prior to jetty construction (1938 and 11 May 1955) is shown in Figures 4-46a and 4-46b. Figure 4-46c shows the morphology of the channel soon after the construction of the jetty (1 April 1964). The exact date of initial dredging of Goldsmith Inlet in association with jetty construction is not known. It is apparent from the aerial photographs that the new-work dredging had taken place by 1 April 1964.

In its natural condition (prior to jetty construction), Goldsmith Inlet had a well-developed partially dry flood shoal within an area that is now part of the present-day channel. The northern 450-ft section of the channel was narrow, and it widened considerably beyond this point, where the natural flood shoal begins. The original modified channel was dredged along the western bank of the inlet, while the eastern natural channel was left unmodified. As seen in Figures 4-46c, a considerable dry portion of the natural flood shoal was left intact as well. The volume of shoaling at the location of the present-day flood shoal was minimal. It is believed that material from the initial dredging was placed on the beach directly east of the inlet.

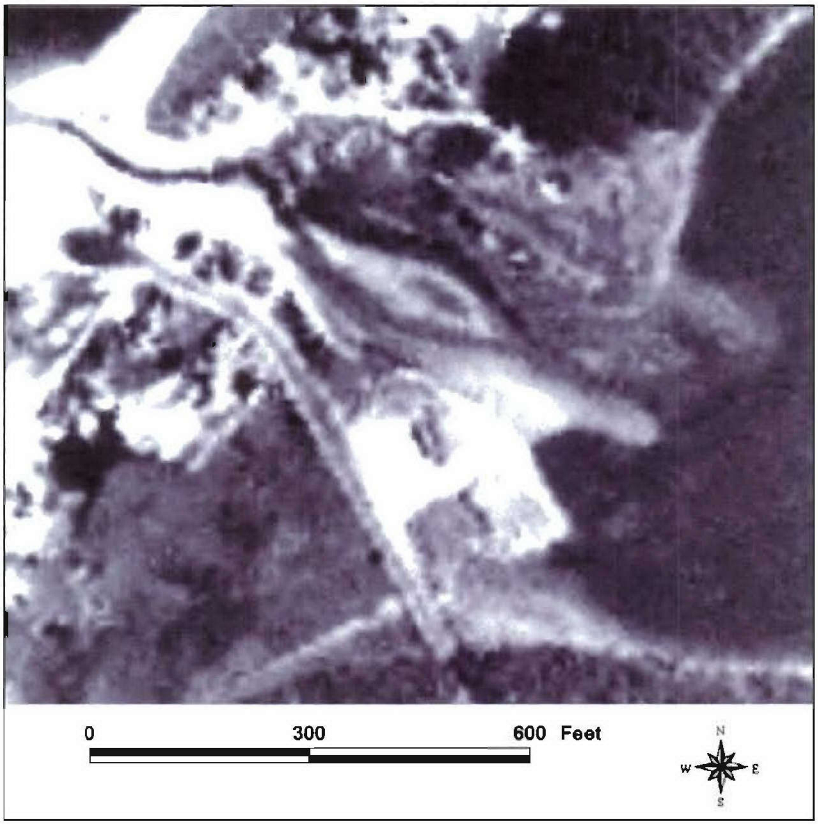

Figure 4-46a. Goldsmith Inlet natural flood shoal, 1938 (exact month and day unknown)

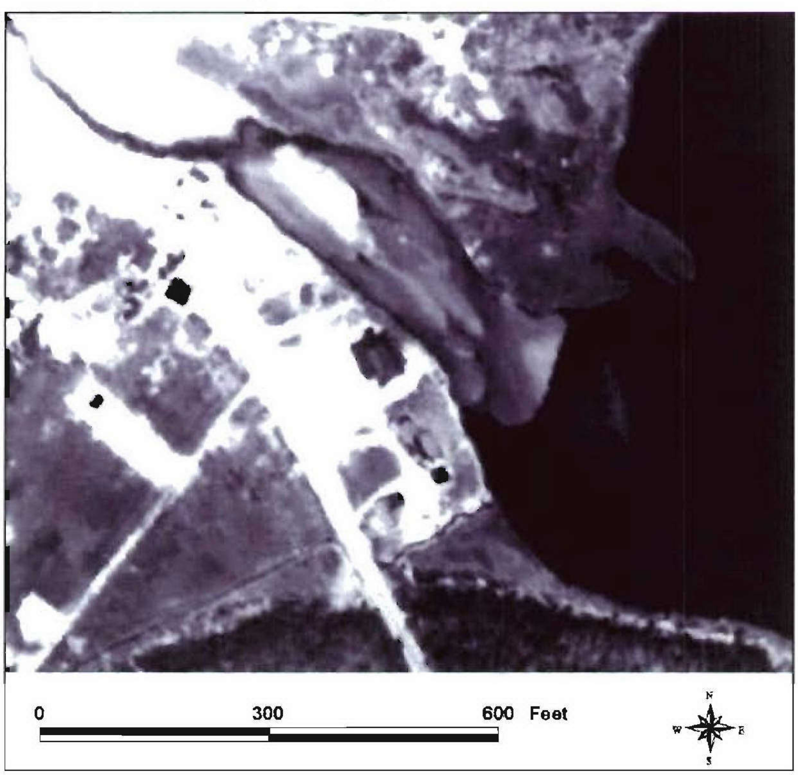

Figure 4-46b. Goldsmith Inlet natural flood shoal, 11 May 1955

Figure 4-46c. Goldsmith Inlet channel with partially intact in-channel flood shoal, 1 April 1964

The morphology of the in-channel flood shoal, apparent morphology changes along the east bank, and the evolution of the west bank attached shoal, from 1969 to the present are illustrated and analyzed in Figures 4-46d through 4-46k. Because the aerial photographs are not tide corrected, and the wet-dry line along the banks of Goldsmith Inlet is blurred, particularly in areas bounded by wetlands, these figures should be regarded as approximations. The figures do, however, present clear trends in morphology change for the features considered.

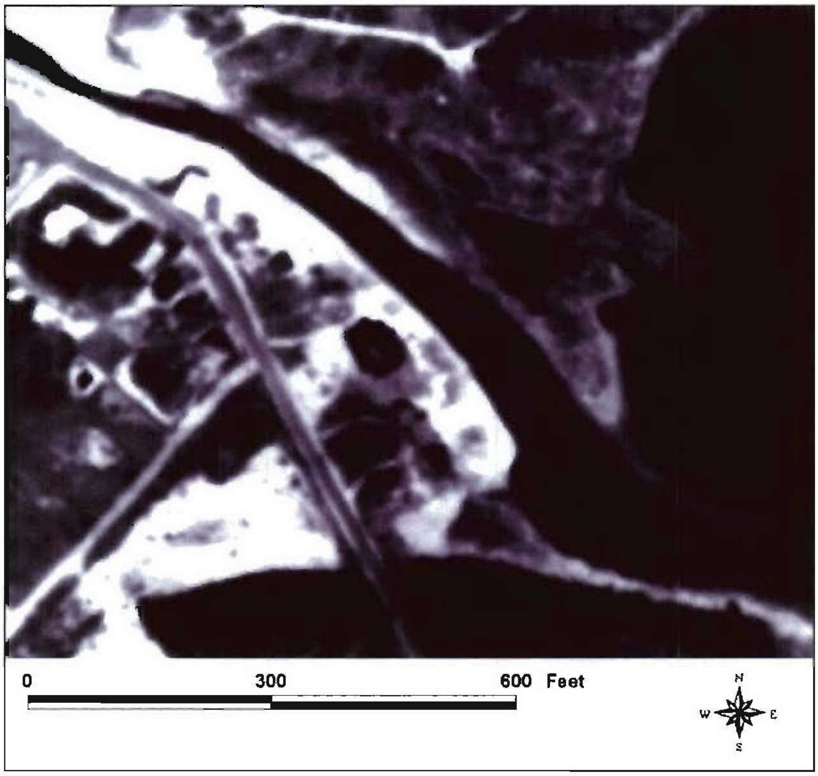

Figure 4-46d. Goldsmith Inlet channel with partially intact in-channel flood shoal, 5 October 1966

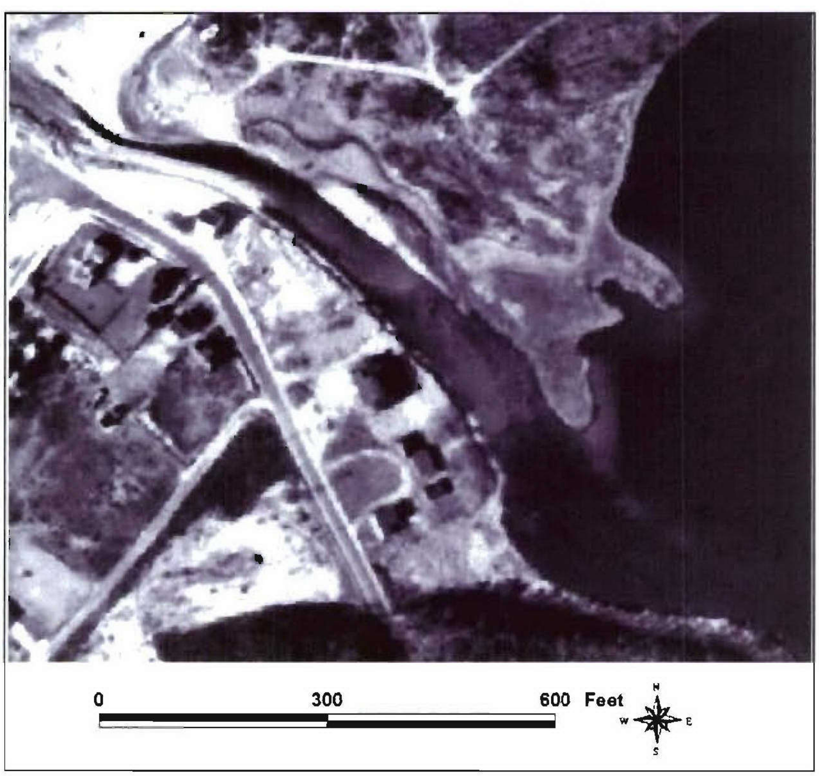

Figure 4-46e. Goldsmith Inlet channel, 28 April 1969

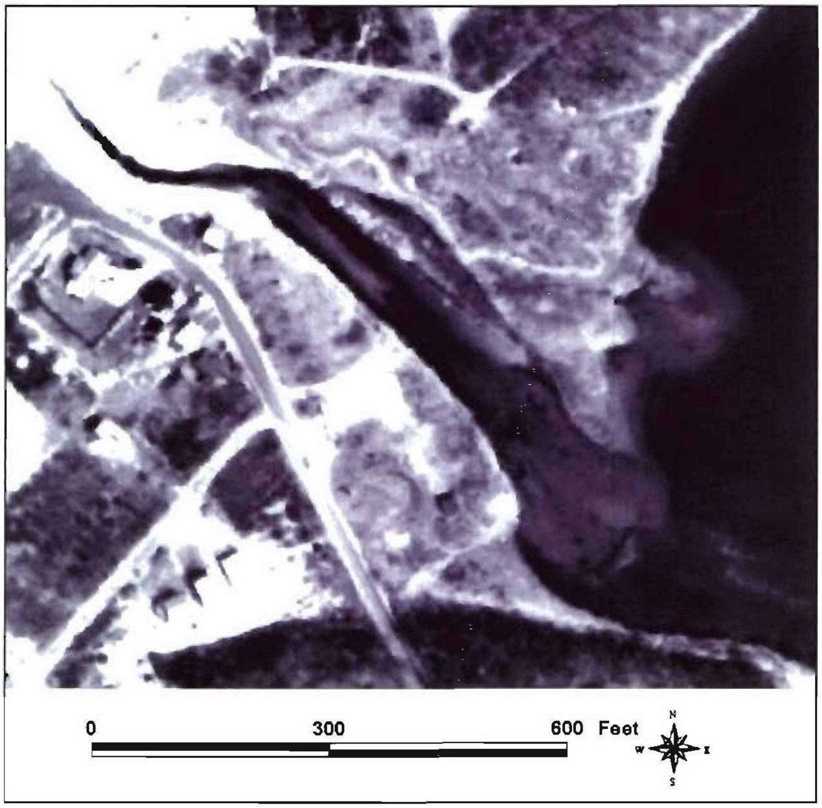

Figure 4-46f. Goldsmith Inlet channel, 6 April 1976

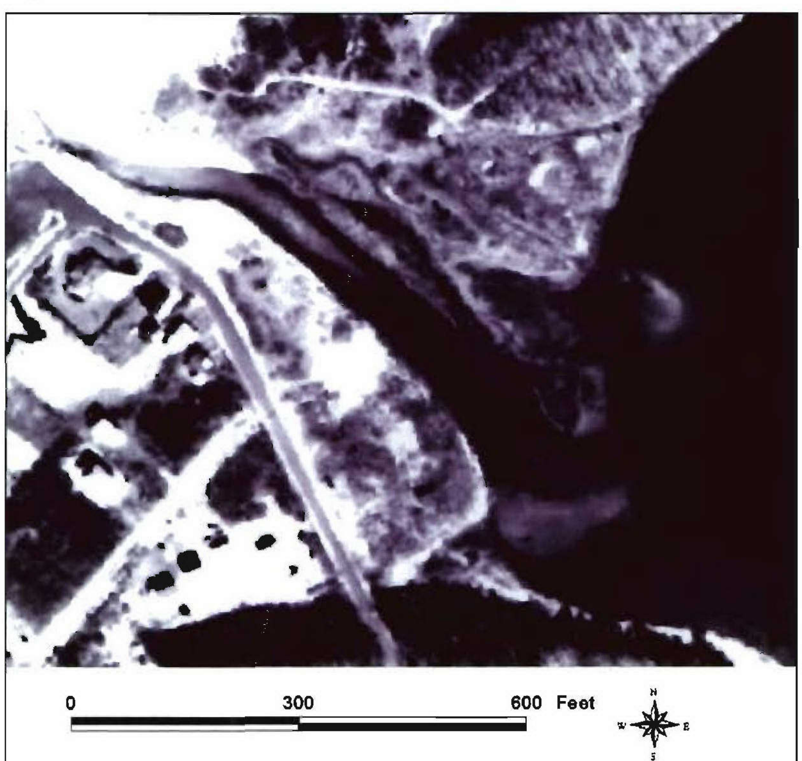

Figure 4-46g. Goldsmith Inlet channel, 24 May 1980

Figure 4-46h. Goldsmith Inlet channel, 5 April 1993

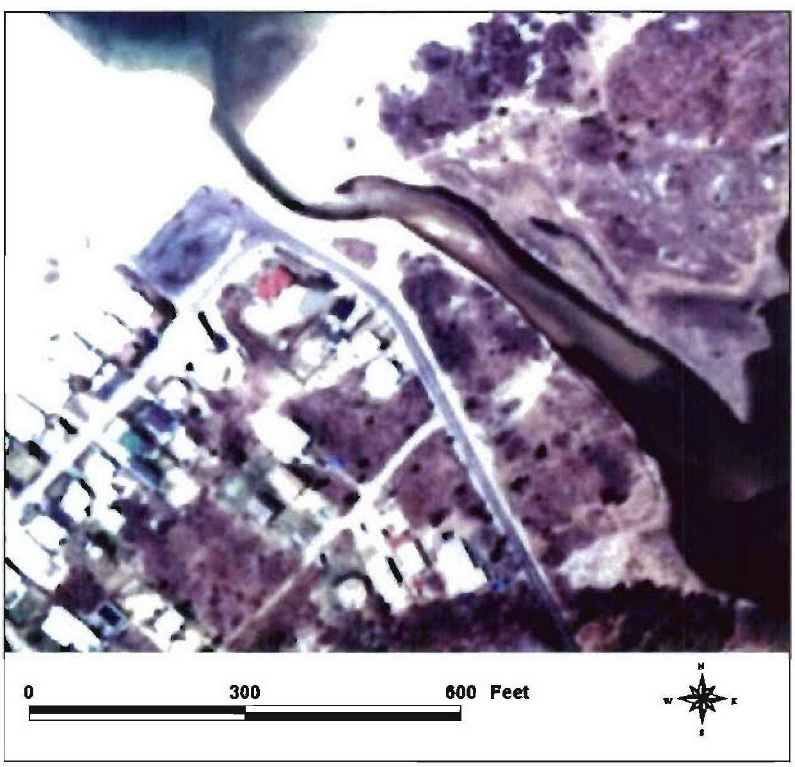

Figure 4-46i. Goldsmith Inlet channel, 21 April 1996

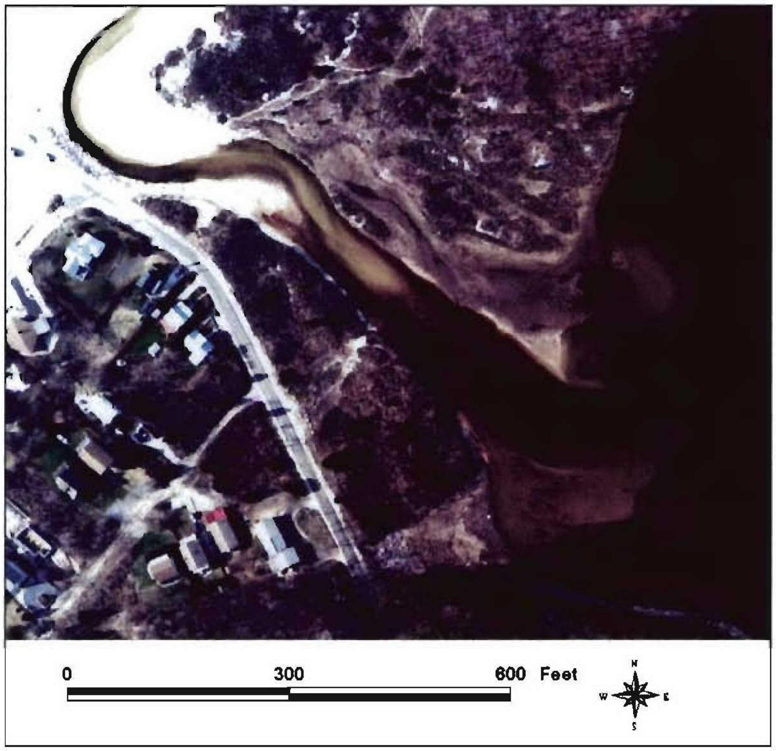

Figure 4-46j. Goldsmith Inlet channel, 16 April 2003

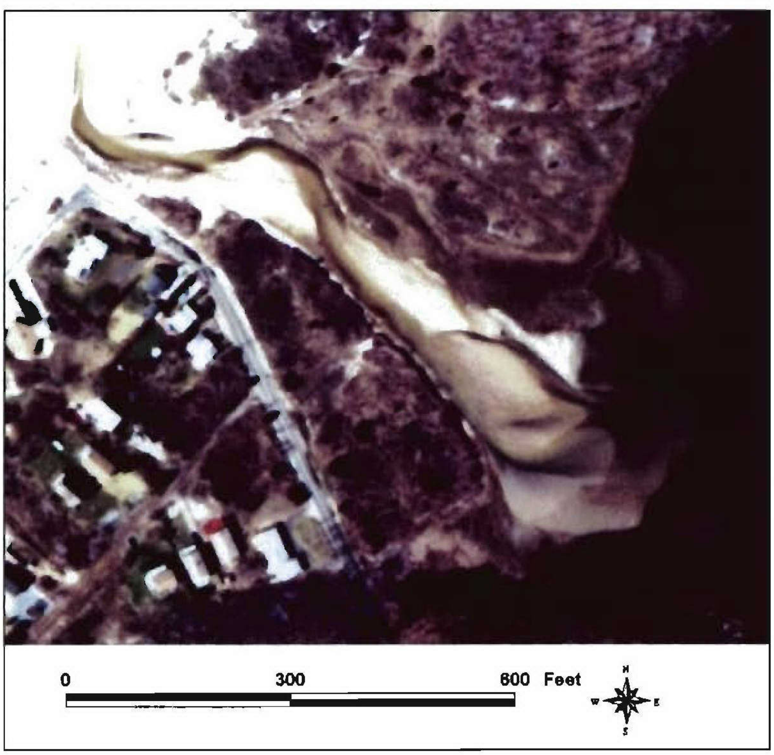

Figure 4-46k. Goldsmith Inlet channel, 15 April 2004

Figures 4-47a through 4-47e plot morphology change within the midchannel area, migration of the intact portion of the natural in-channel flood shoal, and eventual closure of the eastern, natural channel. The fact that a dry portion of the natural flood shoal was left intact may have greatly influenced evolution of the channel and the present-day flood shoal at Goldsmith Inlet. The continued existence of the dry portion of the natural flood shoal created two channels that begin 450 ft into the inlet (Figures 4-47a and 4-47b). The western, modified channel, as well as the initial 450 ft, would be considerably deeper than the eastern natural channel. During flood tide, gravel and coarse sediment would, therefore, tend to accumulate within the modified channel.

The sediment that constituted the portion of the natural flood shoal that was left intact appears to have been redistributed by tidal currents during the time period considered. Intrusion of new sediment resulted in the eventual closure of the eastern natural channel and the apparent creation of new wetland along the east bank (Figures 4-47c through 4-47e).

An attached shoal developed along the west bank and is illustrated in Figures 4-47c and 4-47e. The evolution of this attached shoal resulted in an increasingly sigmoidal channel morphology, which modifies the ebb and flood current (and resulting sediment deposition). Initial growth of this attached shoal could be discerned in 1976, and no growth was apparent in 1980 and 1993 (Figures 4-47c and 4-47d). The apparent absence of this attached shoal may be attributable to the aerial photographs for this period being taken at a time of higher water. It is also possible, however, that this attached shoal had been dredged. This attached shoal is observed to have grown rapidly in recent years, indicating increased sediment deposition within the channel (Figure 4-47e).

The location and areal morphology of the flood shoal for the time period considered is illustrated in Figures 4-48a through 4-48d, referenced against the present shoreline (15 April 2004). The photographs of 28 April 1969 and 24 May 1980 appear to have been taken at higher water, when only small portions of the submerged flood shoal were discernible, and are not shown. Because the extent of the flood shoal that is visible depends on several factors, particularly water level, values obtained are approximations. They do, however, indicate trends of movement and growth of the flood shoal at Goldsmith Inlet.

New work modifications introduced to Goldsmith Inlet resulted in the migration of the natural flood shoal along the east bank. The sediment that composed this feature apparently relocated to the eastern bank, where the inlet empties into Goldsmith Pond. This sediment apparently began the formation of the eastern lobe of the present-day flood shoal (Figures 4-48a and 4-48b).

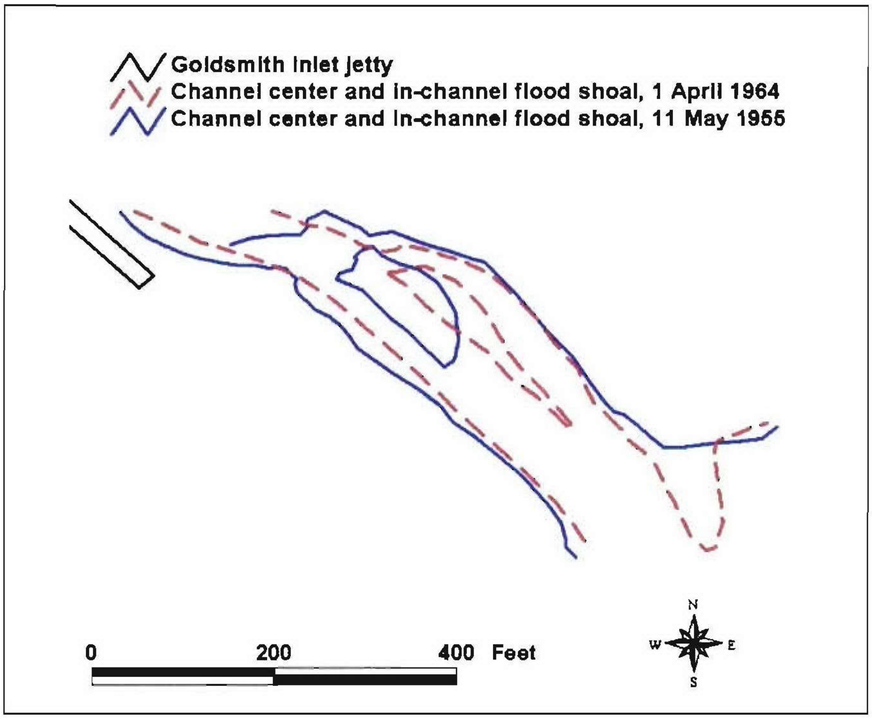

Figure 4-47a. Goldsmith Inlet channel center, 11 May 1955 and 1 April 1964

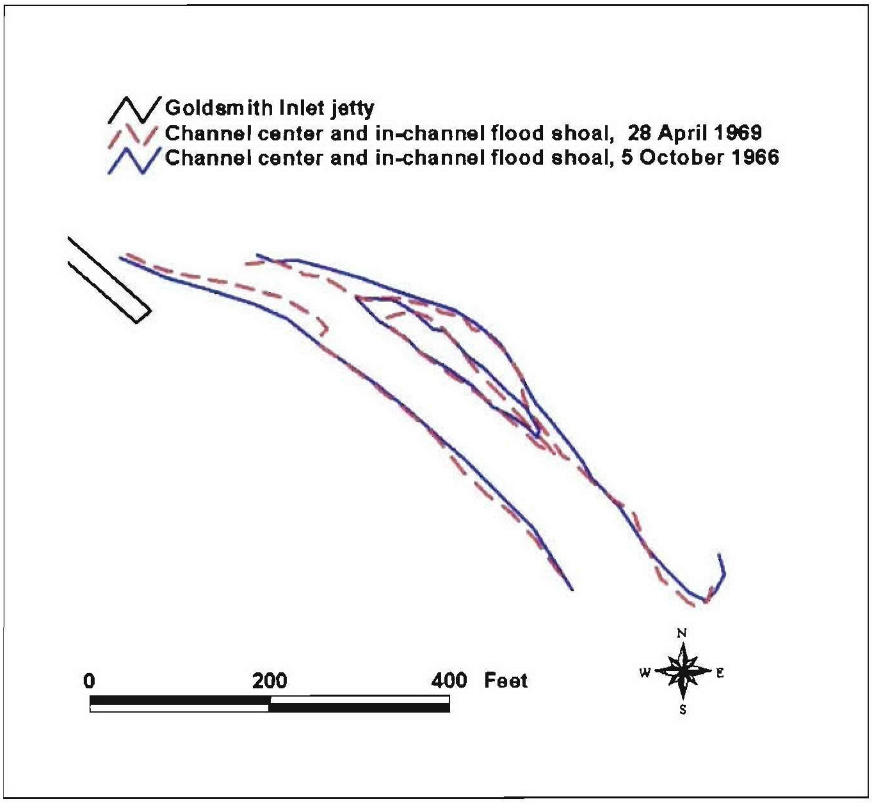

Figure 4-47b. Goldsmith Inlet channel center, 5 October 1966 and 28 April 1969

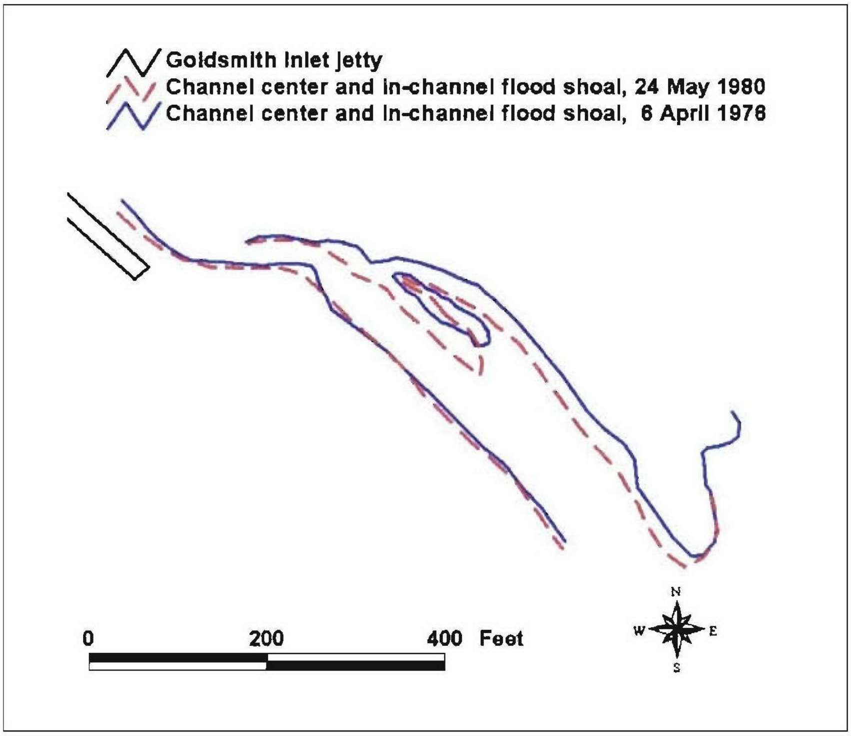

Figure 4-47c. Goldsmith Inlet channel center, 6 April 1976 and 24 May 1980

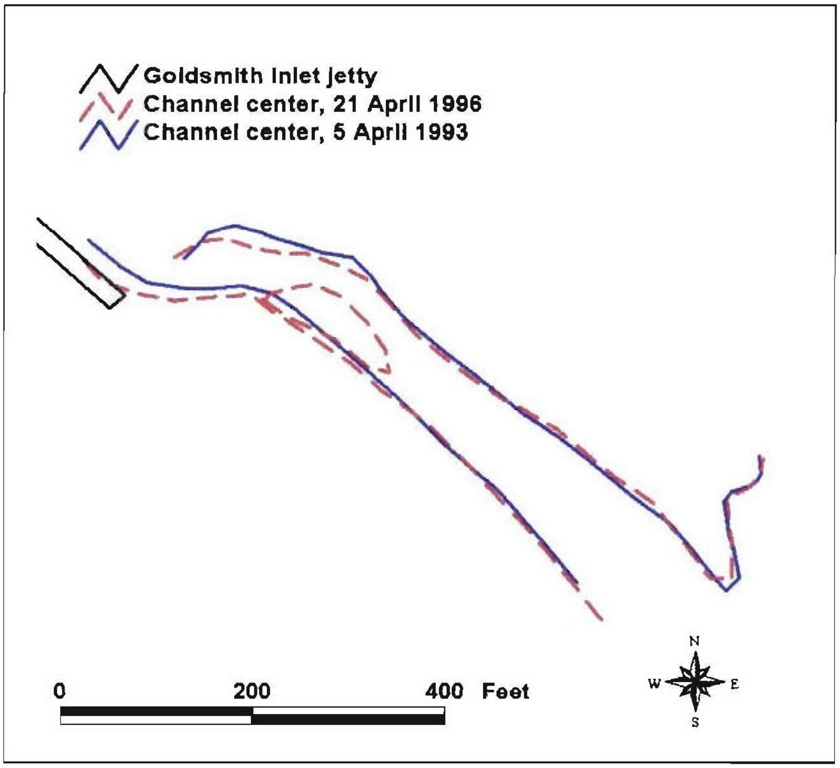

Figure 4-47d. Goldsmith Inlet channel center, 5 April 1993 and 21 April 1996

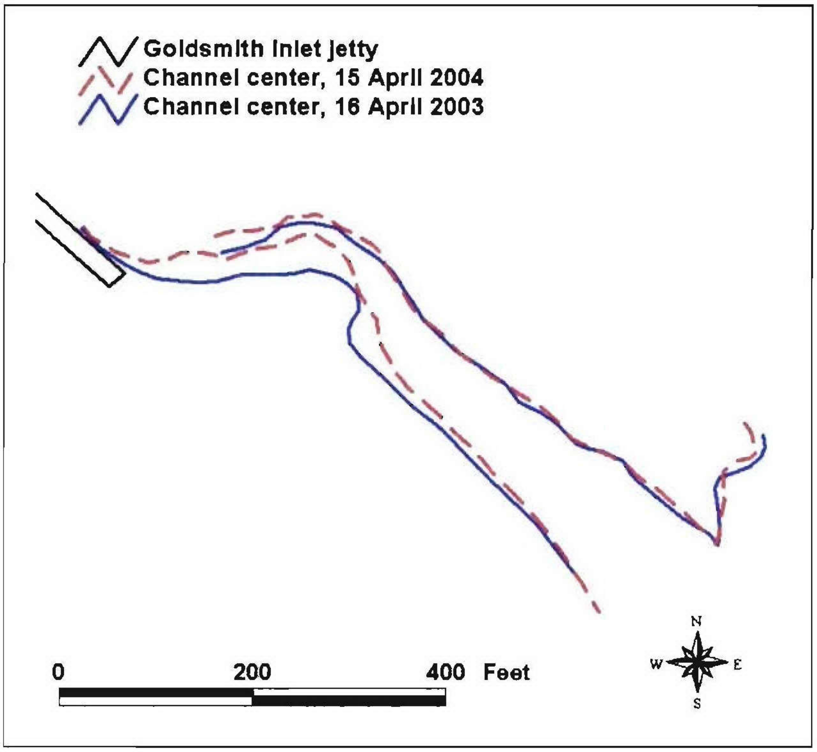

Figure 4-47e. Goldsmith Inlet channel center, 16 April 2003 and 15 April 2004

New shoaling along the west bank and the beginnings of the west lobe of the present-day flood shoal can be seen in Figure 4-48b, the apparent result of the deeper channel dredged along the west side of the inlet.

Figure 4-48c outlines the approximate extent of the flood shoal on 5 April 1993 and 21 April 1996. The flood shoal appeared to be reaching maturity at this point, where its morphology closely resembled its present manifestation. The eastern and western lobes appeared to be mature and well developed by 1993. Limiting depth at this location is a prominent control on the present hydrodynamics of Goldsmith Inlet. The period of flood shoal development appears to have been followed by a period of channel infilling, where a new lobe of the flood shoal developed, as seen in the morphology of 21 April 1996.

The areal extent of shoaling within the channel can be seen in Figure 4-48c for 21 April 1996 and in Figure 4-48d for 16 April 2003 and 15 April 2004. The well-developed flood shoal probably began blocking the transport of sediment into Goldsmith Pond, resulting in a new period that is characterized by deposition within the inlet channel. This observation is supported by the sediment grain sizes found at this location (Chapter 3). The southern portion of the inlet is characterized by course to medium sand that is distinct from the larger sediment found north of this location and the finer sediment that comprises the flood shoal proper. This period is also characterized by the formation of the attached west-bank shoal, further supporting the conclusion of flood shoal stability. The observed in-channel shoal resembles the natural flood shoal of 1955 in many respects.

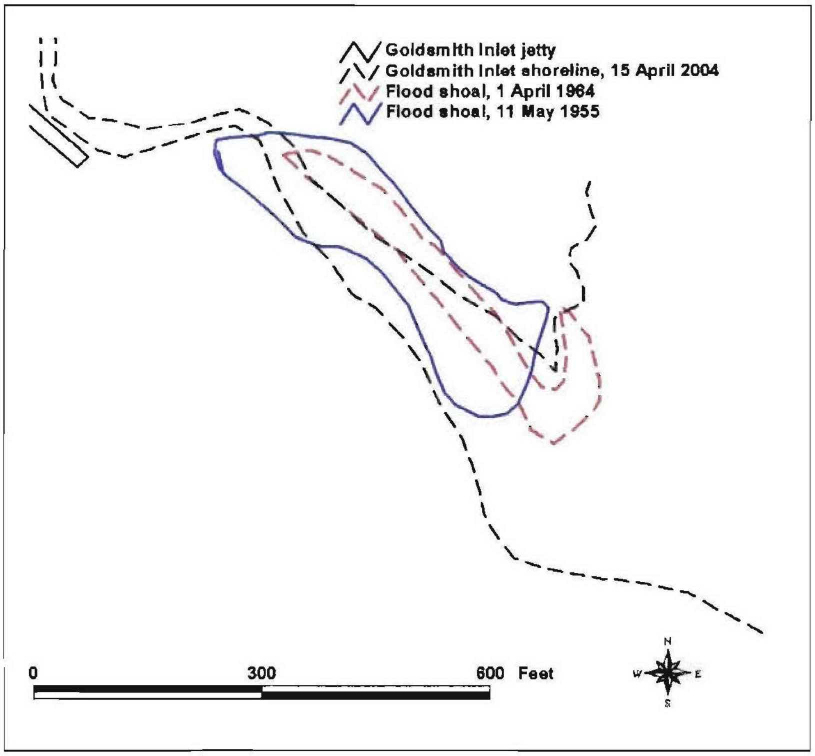

Figure 4-48a. Goldsmith Inlet flood shoal, 11 May 1955 and 1 April 1964

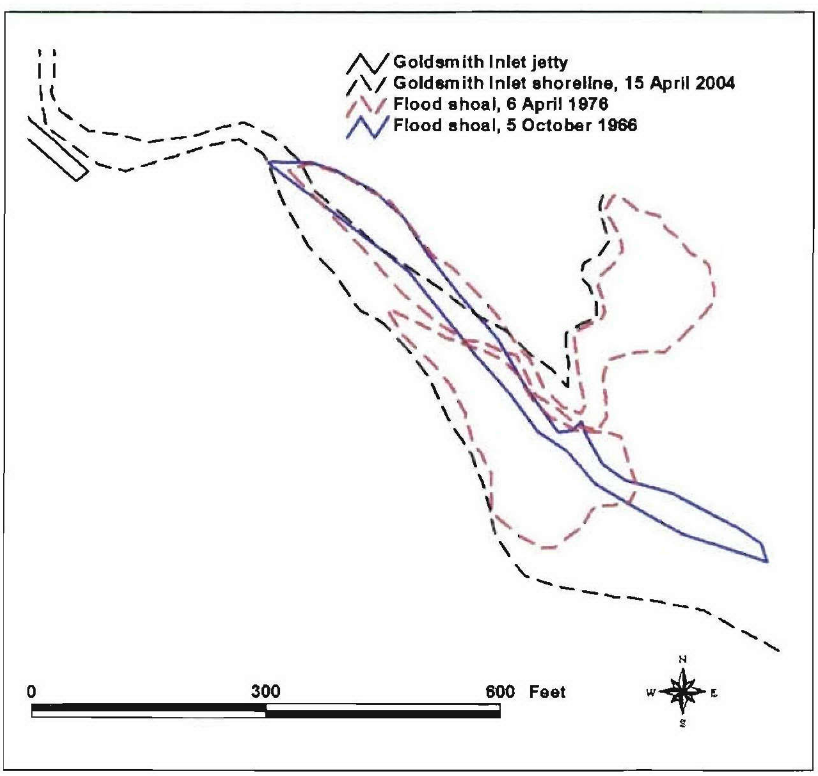

Figure 4-48b. Goldsmith Inlet flood shoal, 5 October 1966 and 6 April 1976

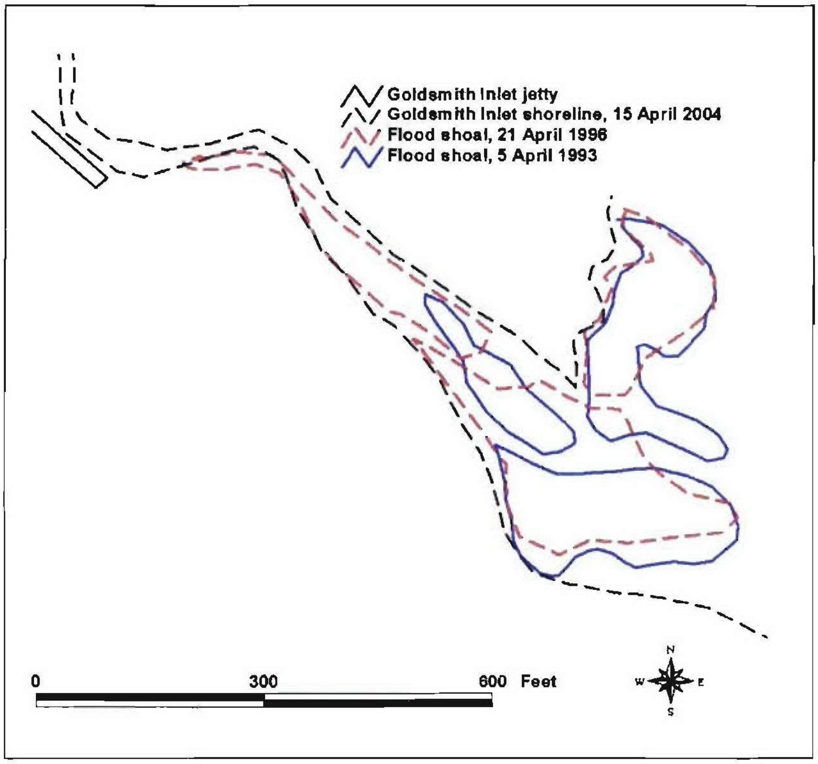

Figure 4-48c. Goldsmith Inlet flood shoal, 5 April 1993 and 21 April 1996

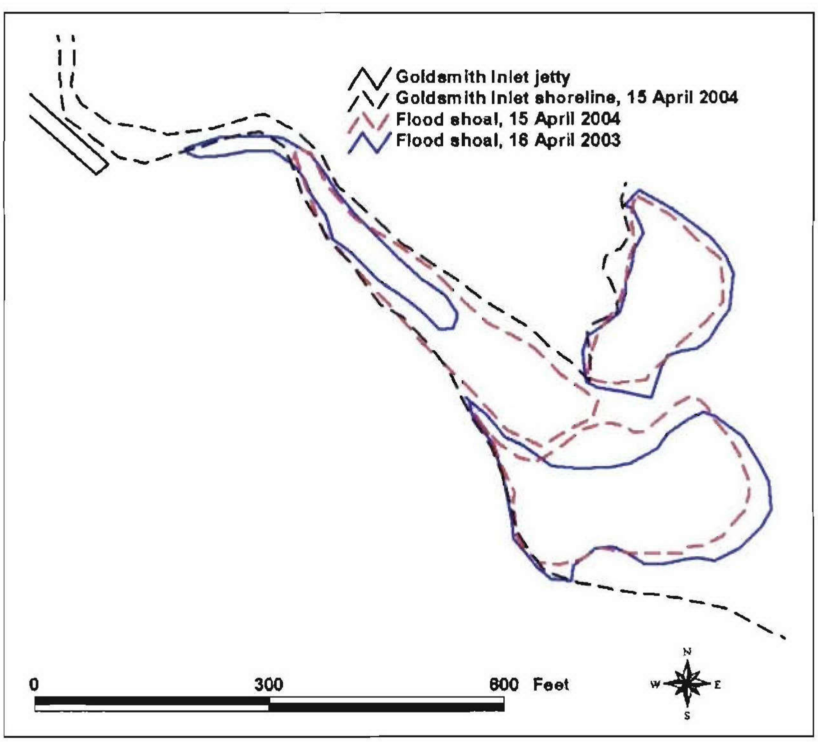

Figure 4-48d. Goldsmith Inlet flood shoal, 16 April 2003 and 21 April 2004

Figures 4-49 and 4-50 show the east bank of Goldsmith Inlet on 8 October 2002 during rising spring tide. Presently, the east bank of the inlet appears to be experiencing erosion. Erosion of the wetland perimeter is evident in Figure 4-49, and a protective bank of fine-grained sediment is seen in Figure 4-50. Figure 4-51 shows the east bank on 20 February 2004 at high tide. The wetlands are inundated, and the protective bank of sediment shows erosion and undercutting. The observed inundation may be related to increased elevation associated with channel infilling that began in the mid-1990s.

Summary of morphology change at Goldsmith Inlet

Modifications introduced to Goldsmith Inlet have produced a dynamic morphological response throughout the inlet. The response can be characterized by development of new features and distinct periods of sedimentation patterns. Table 4-6 summarizes the major aspects of interpreted morphology change from 1955 to the present and synopsizes discussion of change at the inlet entrance, within the channel, and at the location of the present-day flood shoal (inlet exit).

In summary, the west accretion fillet reached the seaward tip of the jetty prior to 6 April 1976 (Figure 4-42f), (by 1972, according to Greenman-Pederson (1981)), and it is assumed that sediment accretion rates along the east side of the jetty and within Goldsmith Inlet increased around this time. Construction of the jetty apparently stabilized the inlet for 17 years by blocking eastward-moving material, because the first dredging of record occurred in 1977. Subsequently, Goldsmith Inlet was dredged seven times until 1990, and several times in the early 1990s. Local sources have indicated that the inlet has not been dredged in recent years. The inlet apparently maintained a degree of stability from the mid-1990s to 2002.

Figure 4-49. Goldsmith Inlet, east bank wetlands, during current measurement, 8 October 2002

Figure 4-50. Goldsmith Inlet, east bank wetlands, with protective sand bank, 8 October 2002

Figure 4-51. Goldsmith Inlet, east bank wetland, 20 February 2004

The relatively large tidal range and large sediment grain size contribute to maintenance of inlet stability. Continual degradation of the jetty at Goldsmith Inlet, which allows sediment to enter the inlet, acts to reduce inlet stability.

Channel migration between 1996 and 2002 is not known. It is inferred that increasing rates of sediment bypassing around the jetty and close to shore, owing to full impoundment on the west side and spit growth on the east side, promote eastward migration of the inlet entrance. Migration of the channel creates an increasingly sigmoidal or "S"-shaped configuration, which decreases the flushing capacity of the inlet because of increasing length of channel and associated increase in friction.

Table 4-6
Summary of Morphology Change at Goldsmith Inlet, 1955 to Present

Date	Inlet entrance	Inlet channel	Inlet Exit
1955	--	Natural in-channel flood shoal	--
1963 - 1964	Construction of jetty		--
1964	New work dredging	New work dredging	New work dredging
1964 - 1972	Impoundment west of jetty and associated erosion east of jetty	Natural flood shoal migration	Initial formation of present east and west lobes
1972 - 1976	Initial formation of spit east of jetty Assumed acceleration of sediment intrusion	--	Mature and stable east lobe
1976 - 1980	Closure of Inlet (1980)	Closure of eastern natural channel	Continued flood shoal growth
1980 - 1990	Assumed stability through regular dredging Establishment of natural effective sediment bypassing	--	Mature and stable west lobe Period of channel infilling begins
1990 - 2002	Continued spit development Initial channel migration	Development of attached west bank shoal Channel infilling in mid - channel	Continued period of channel infilling
2002 - 2003	Rapid spit formation Rapid eastward channel migration	Inundation of Wetlands – presumably from raised elevation of channel infilling	Continued period of channel infilling
April 2004	Dredging and reorientation of inlet	--	–

Although a larger channel will increase friction presented to the flow within it, it can be inferred that alignment of the channel almost parallel to shore makes the inlet an efficient bypasser during ebb flow. At that stage of tide, an ebb current of any strength would reinforce wave action and the wave-induced longshore current directed to the east to transport material down the coast. Therefore, it may be feasible to maintain the inlet with less dredging by allowing the channel to remain oriented toward the east than it is to dredge and realign the channel straight out toward the sound. Likewise, the orientation toward the east makes it difficult for sediment streaming off of the spit on the east side of the jetty to turn almost 180 deg and enter the inlet entrance.

Finally, development and maturation of the existing flood shoal has served to block sediment transport into Goldsmith Pond, resulting in sediment deposition within the channel since 1993. The limiting depth that has resulted from the development of this feature has also served to accentuate asymmetries in flood and ebb current velocity (discussed in Chapter 5). At present, given the rapid eastward migration of the inlet entrance and the apparent increases in in-channel sedimentation rates, Goldsmith Inlet can be said to be an autonomic system, where changes within it promote a positive feedback cycle, thereby increasing the observed rates of change. Maintenance of the inlet mouth in an eastward orientation may only require minor dredging, thereby reinforcing the autonomous behavior. An eastward orientation would maximize sediment bypassing while allowing a minimal amount of sediment to enter the inlet channel.

5 Circulation Analysis

This chapter describes calculations of circulation and water level at Mattituck Inlet and Goldsmith Inlet performed to infer and interpret sediment-transport pathways associated with tidal flow. Field measurements (Chapter 4) made in October 2002 of bathymetry, water level, and current provided data for driving and validating the models.

For Mattituck Inlet, tidal hydrodynamics (water level and current) were simulated with the ADvanced CIRCulation (ADCIRC) model (Luettich et al. 1992), a two-dimensional (2-D) finite-element hydrodynamic model that calculates the depth-averaged horizontal circulation. For Goldsmith Inlet, tidal hydrodynamics were modeled with DYNLET (DYNamic Implicit Model of One-Dimensional Tidal Flow Through InLETs) (Amein and Kraus 1991), which is a one-dimensional (1-D) finite-difference model suited to narrow inlets and areas with minimal cross-channel and cross-bay circulation.

Mattituck Inlet

Water-surface elevation and current velocity for the Long Island Sound, Mattituck Inlet, and Mattituck Creek were calculated with ADCIRC. A regional ADCIRC grid of the New York Bight and the Long Island Sound (Figure 5-1) developed in the Coastal Inlets Research Program (Militello et al. 2000) was modified by increasing resolution at the study site and incorporating data from the October 2002 bathymetry survey at Mattituck Inlet. The model was then validated against regional and local measurements.

The finite-element ADCIRC grid allows fine resolution to be specified in areas of interest. The model domain for this study incorporated horizontal grid elements with lengths ranging from 2.8 km along the Atlantic Ocean southeastern model domain boundary to less than 10 m within Mattituck Creek. The model grid consisted of 15,113 nodes and 27,851 elements. The ADCIRC grid for the study area is shown in Figure 5-2, and the grid for Mattituck Inlet and Mattituck Creek is shown in Figure 5-3. The regional grid assures input of reliable forcing to accurately reproduce tidal phasing and amplitude.

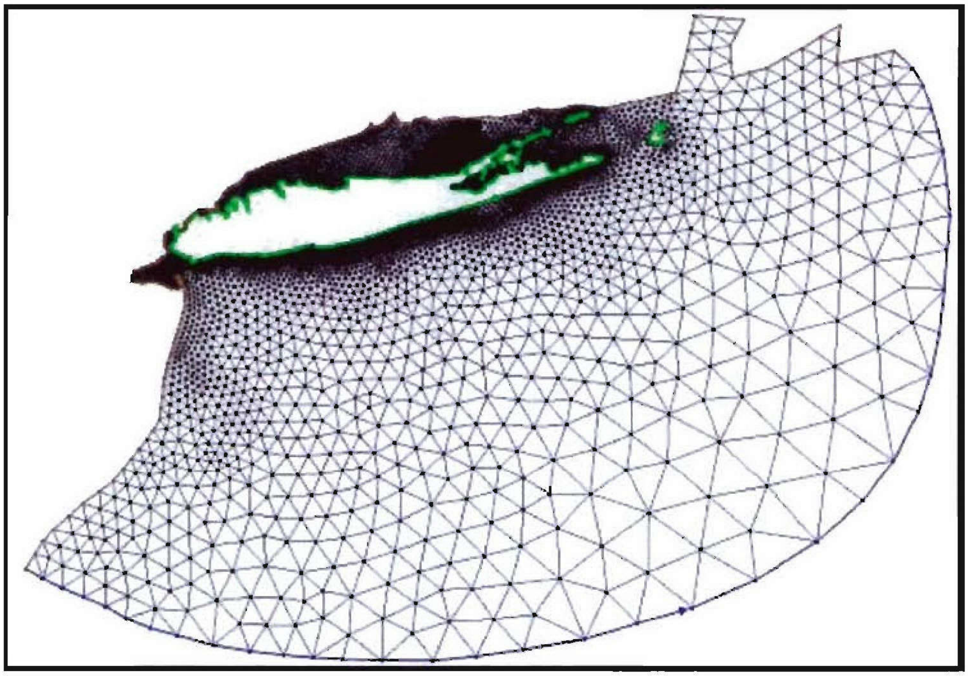

Figure 5-1. Regional ADCIRC grid – New York Bight and Long Island Sound (after Militello et al. 2000)

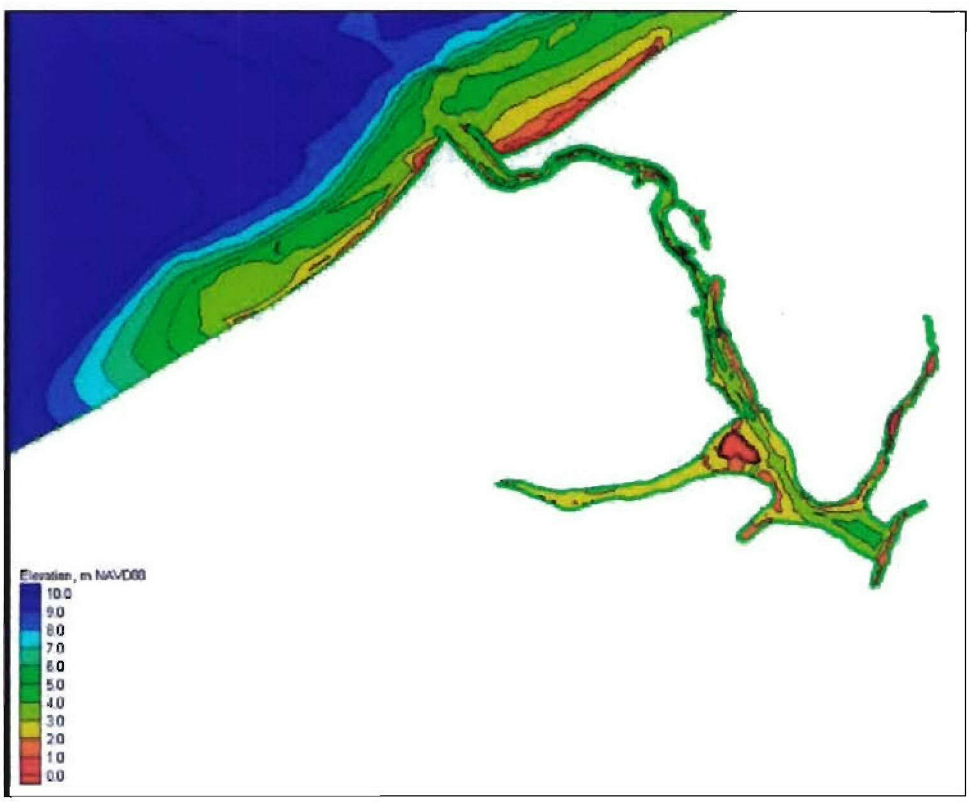

Figure 5-2. Mattituck Inlet and Mattituck Creek, ADCIRC model bathymetry

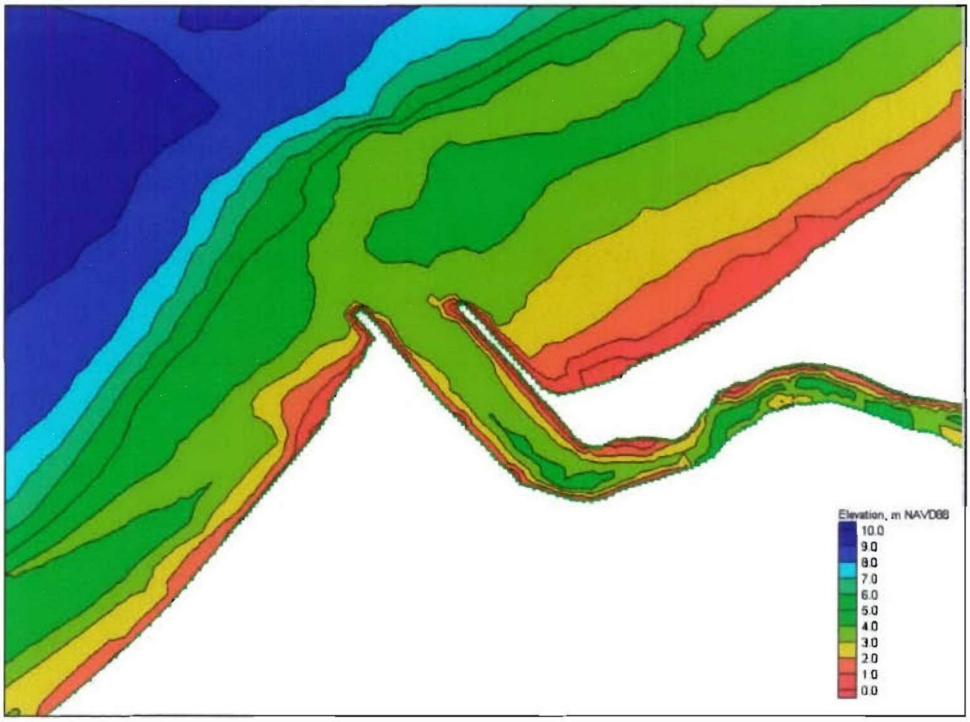

Figure 5-3. Close view of Mattituck Inlet, ADCIRC model bathymetry

To explore possible relations between the morphology and circulation (to infer sediment transport pathways) at Mattituck Inlet, three alternative morphologies were modeled. The initial ADCIRC grid incorporated the bathymetry survey of 6-8 October 2002 and represents a pre-dredging condition at Mattituck Inlet. The second grid (Alternative 1) had the same bathymetry except that the area at the flood shoal at the base of the east jetty was removed to represent a post-dredging condition. A third grid (Alternative 2) was developed to approximate the morphology of Mattituck Inlet circa 1891, before construction of the jetties and channel deepening by new-work dredging. Alternative 2 was created to examine the relation between tidal currents at Mattituck Inlet and the offshore shoal.

Model validation

ADCIRC was run with default value parameters. The bottom friction coefficient is the main parameter, and its default value is 0.0025. The model simulated water level and current velocity for the period 18 September 2002 to 18 October 2002, with a time-step of 0.25 sec. This relatively small time-step was necessary because of fine resolution required to represent the navigation channel and Mattituck Creek.

Regional validation. Predictions of the model were verified regionally by comparing calculations to published NOS water-level records of selected stations within Long Island Sound, with local water-elevation measurements at Mattituck Inlet and Mattituck Creek collected from 19 September to 8 October 2002, and with current velocity measurements within Mattituck Creek collected 7-8 October 2002. The three locations within Long Island Sound (Figure 5-4) are

Eaton's Neck in Huntington Harbor, Huntington, Long Island, NY (40°57.2'N, 73°24'W); New Haven Harbor, New Haven, CT (41°17.0'N, 72°54.5'W); and Kings Point, NY (40°48.6'N, 73°45.9'W).

Figures 5-5a, 5-5c, and 5-5e show comparisons for the period of field data collection (18 September – 8 October 2002), and Figures 5-5b, 5-5d and 5-5f show comparisons for 5-8 October 2002, a period of spring tide. The water-level plots for these locations validate the model output for the southern boundary of the Long Island Sound (the north shore of Long Island), the northern boundary of the Long Island Sound (the south shore of Connecticut), and the western portion of the Long Island Sound, respectively. These plots also illustrate the tidal signature of the Long Island Sound, where mean tide amplitudes increases from east to west (Chapter 2). Agreement with both tidal phase and amplitude is seen. Occasional deviation is observed between calculation and measurements, attributed primarily to neglect of wind forcing in the model for the present application. At Kings Point, under predictions of ADCIRC are believed to be related to the coarseness of the grid in the area of the NOS station. Increased resolution of the grid supplemented with recent and denser bathymetry measurements would improve agreement.

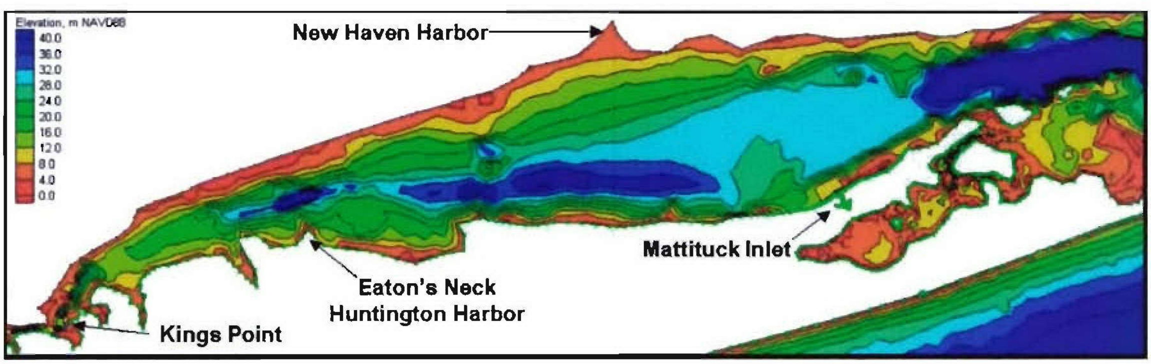

Figure 5-4. NOS stations and 19 September - 8 October 2002 survey tide gauge locations

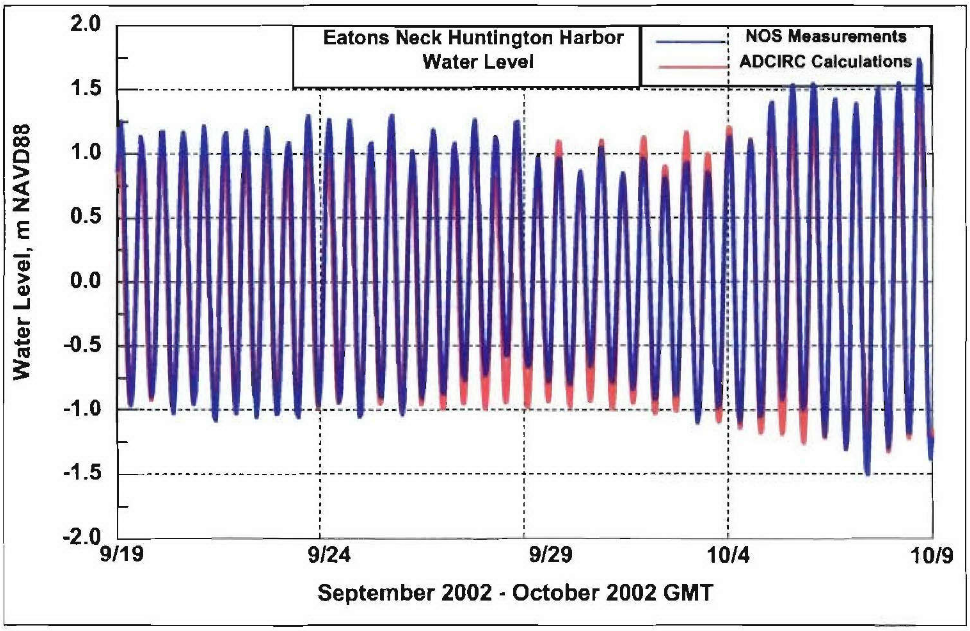

Figure 5-5a. Water level at Eaton's Neck, Huntington Harbor; NOS measurements and ADCIRC calculations, 19 September - 8 October 2002

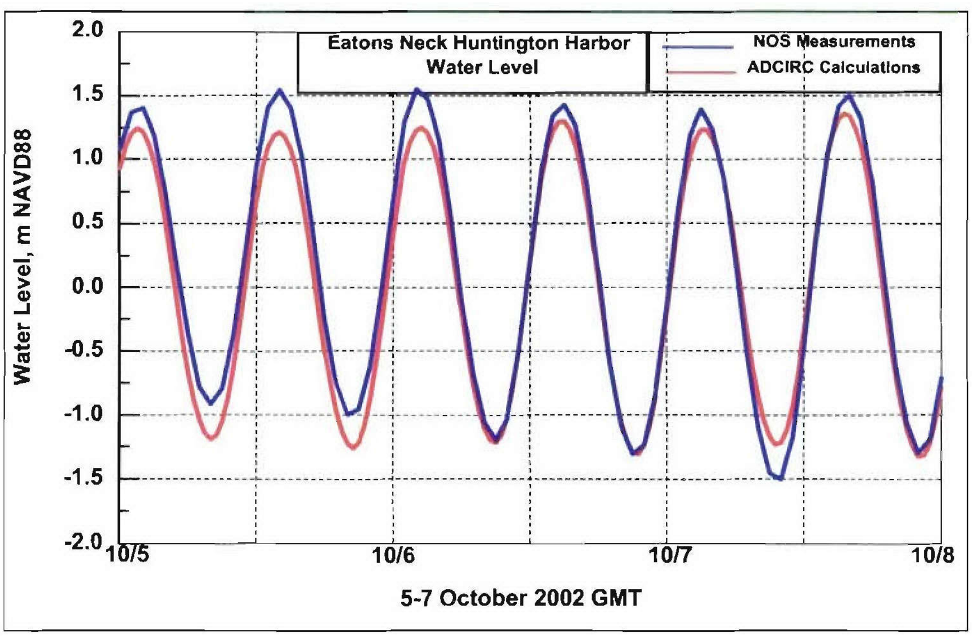

Figure 5-5b. Water level at Eaton's Neck, Huntington Harbor; NOS measurements and ADCIRC calculations, 5-8 October 2002

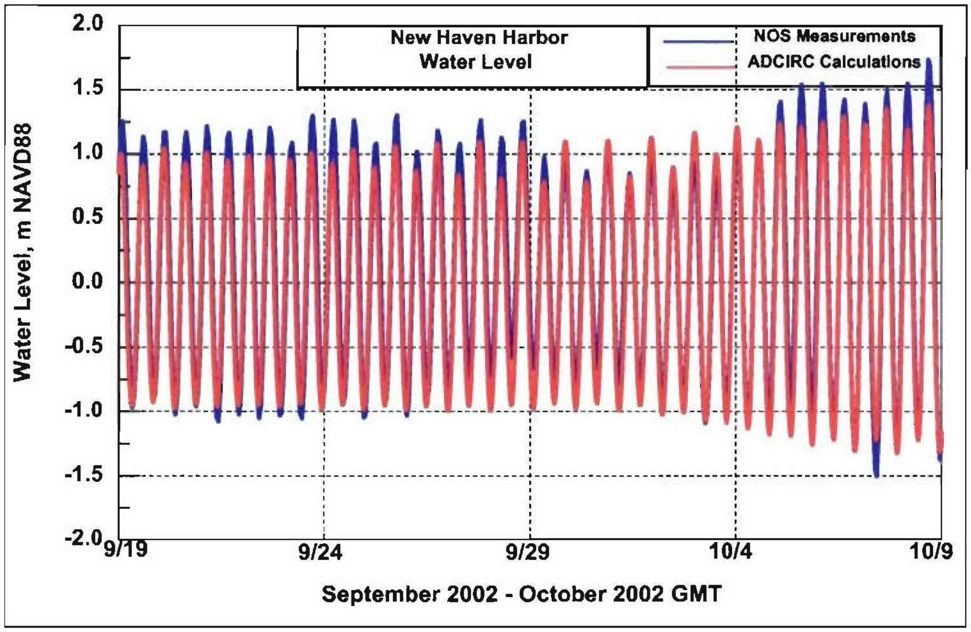

Figure 5-5c. Water level at New Haven Harbor, New Haven; NOS measurements and ADCIRC calculations, 19 September - 8 October 2002

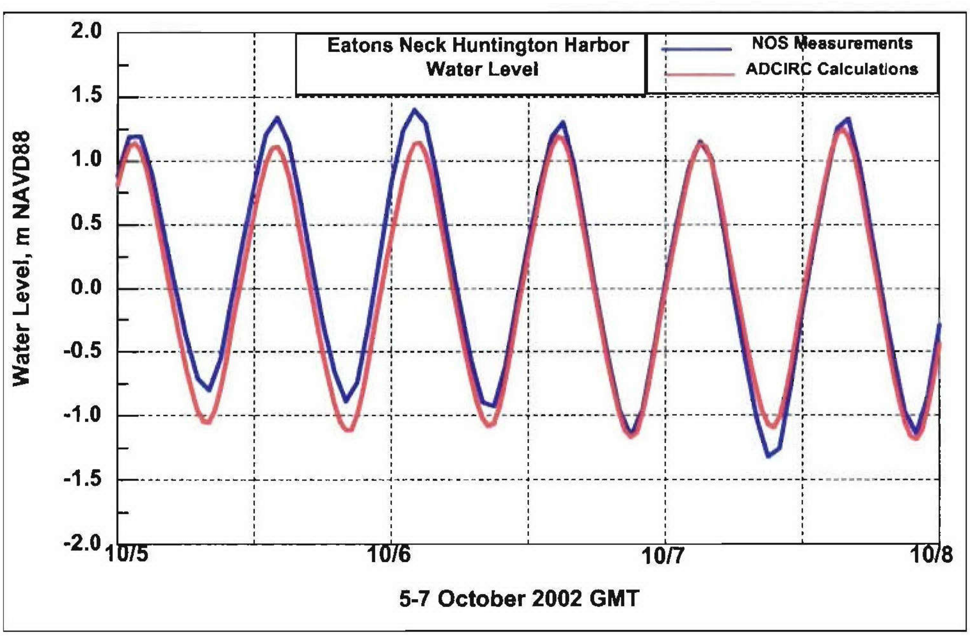

Figure 5-5d. Water level at New Haven Harbor, New Haven; NOS measurements and ADCIRC calculations, 5-8 October 2002

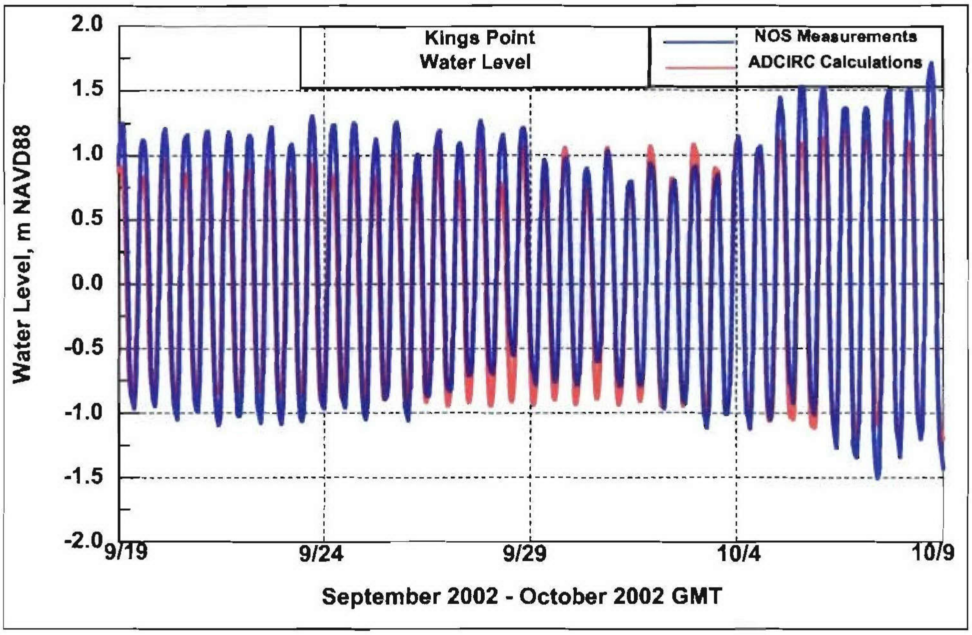

Figure 5-5e. Water level at Kings Point; NOS measurements and ADCIRC calculations, 19 September - 8 October 2002

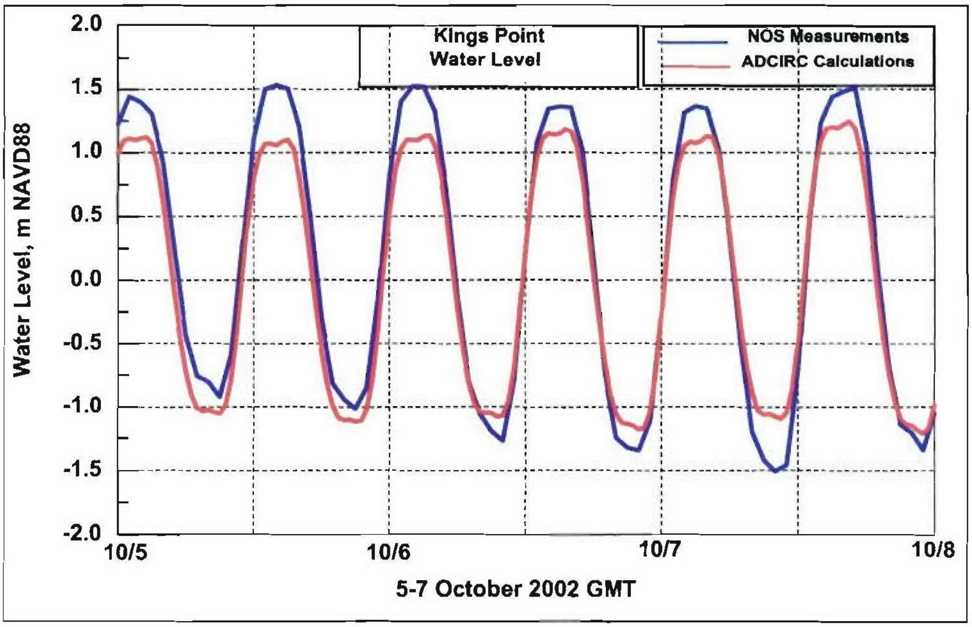

Figure 5-5f. Water level at Kings Point; NOS measurements and ADCIRC calculations, 5-8 October 2002

. ADCIRC calculations of water level were compared to measurements made at Mattituck Inlet and Mattituck Creek from 19 September to 8 October 2002 (Figures 5-6a through 5-6d). The locations of the tide gauges for this survey are given in Figure 3-23. Both amplitude and phase of the measurements are reproduced. The tidal signal maintains amplitude or increases in amplitude at the creek station because of the constricted flow there.

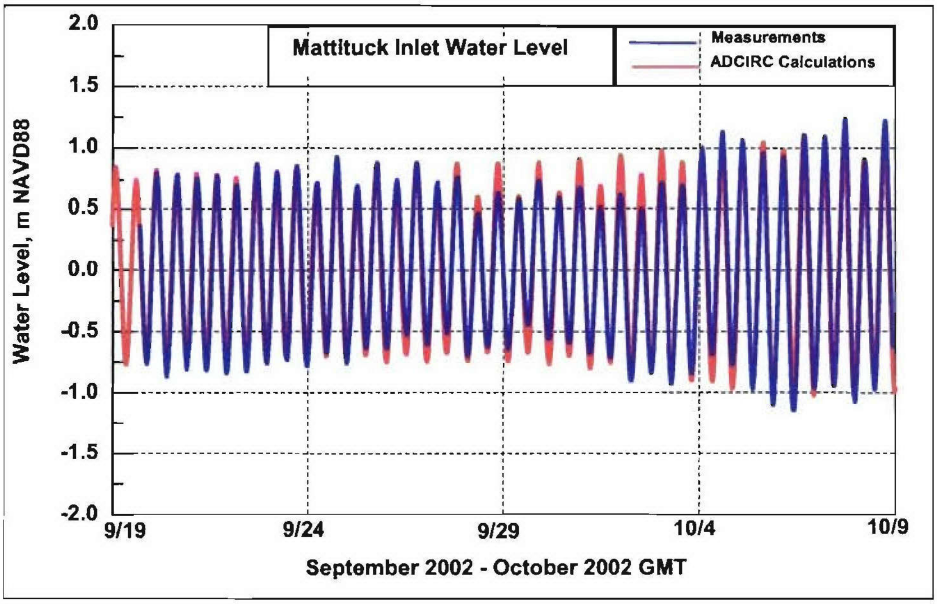

Figure 5-6a. Water level at Mattituck Inlet, near west jetty; measurements and ADCIRC calculations, 19 September - 8 October 2002

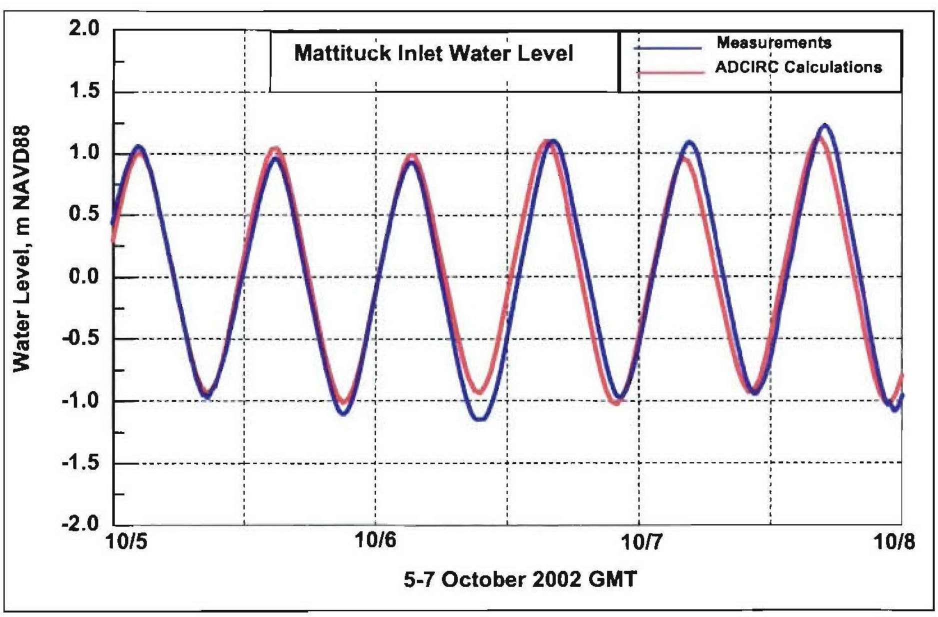

Figure 5-6b. Water level at Mattituck Inlet, near west jetty; measurements and ADCIRC calculations, 5-8 October 2002

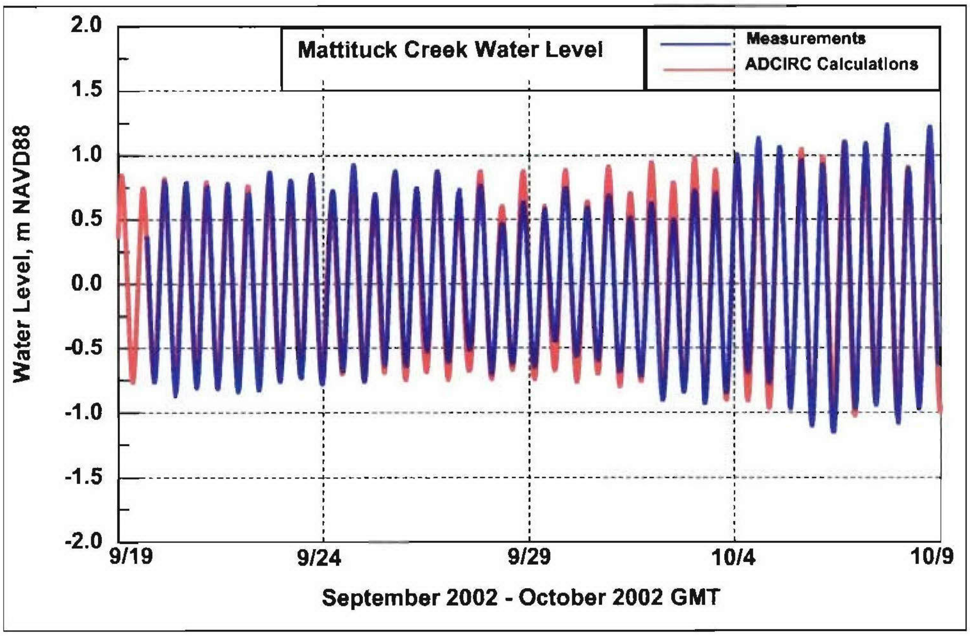

Figure 5-6c. Water level at Mattituck Creek; measurements and ADCIRC calculations, 19 September - 8 October 2002

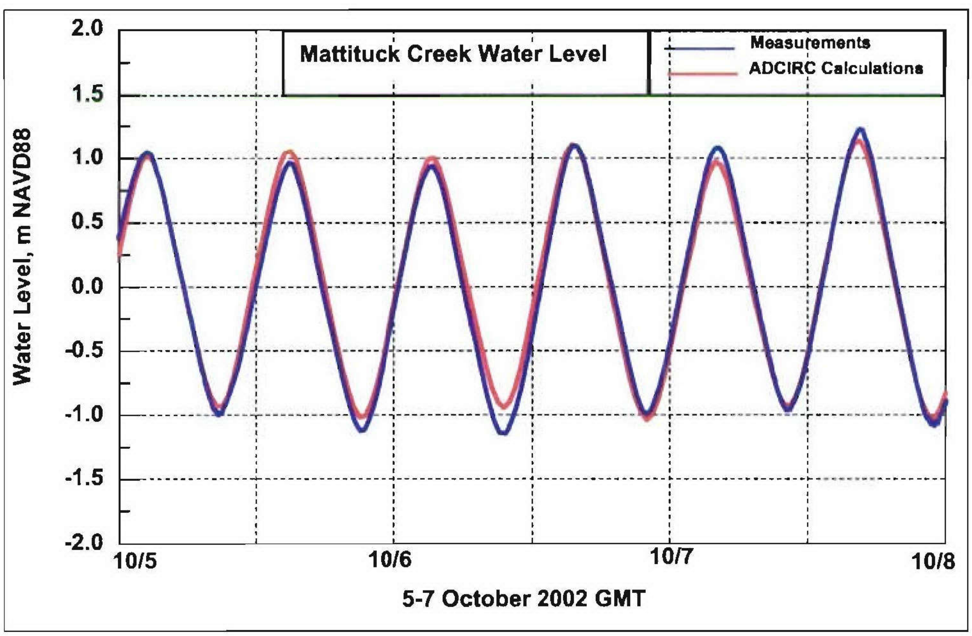

Figure 5-6d. Water level at Mattituck Creek; measurements and ADCIRC calculations, 5-7 October 2002

Figure 5-7 plots current velocity measurements collected 7-8 October 2002 (Current meter 1) and ADCIRC calculations. The model reproduces both the amplitude and phase of the current. The calculation exhibits a broad or double-peaked crest and trough in the current. The measurements contain these features, somewhat obscured by noise in the signal. The deviation from a sine curve is caused by nonlinearity in the tidal wave as it shoals into shallow water from Long Island Sound.

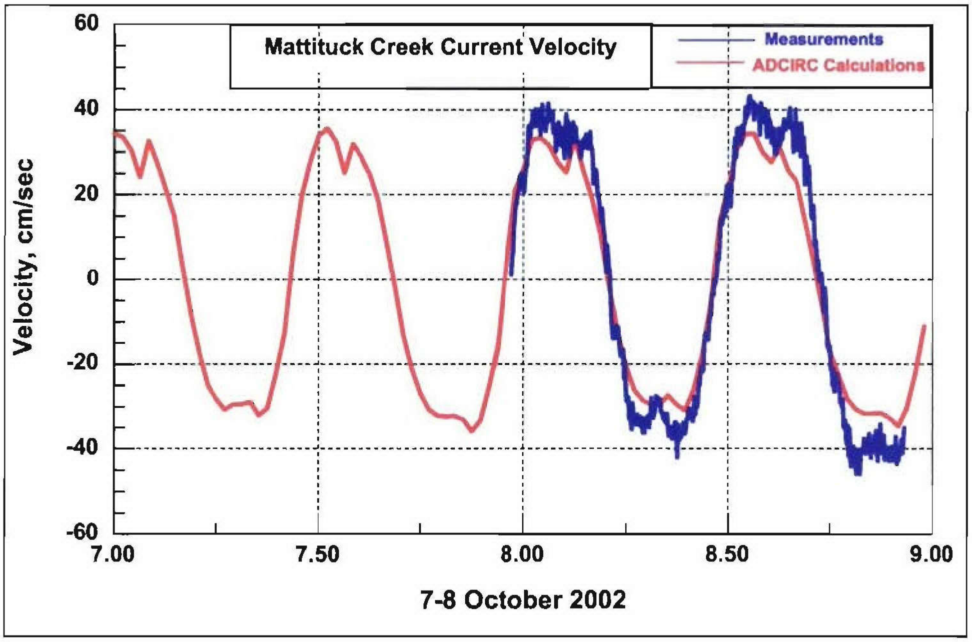

Figure 5-7. Current velocity at Mattituck Creek; measurements and ADCIRC calculations, 7-8 October 2002

Pre-dredging condition (2002)

Calculated current velocities, based on the bathymetric survey data of 6-8 October 2002, are presented here. Calculated velocities offshore of Mattituck Inlet range from 0 to 0.6 m/sec, and calculated velocities within Mattituck Inlet range from 0 to 0.5 m/sec. Near-maximum calculated flood and ebb current velocities for the offshore study area are shown in Figures 5-8a and 5-8b, respectively. These figures plot the calculated near-maximum flood and ebb tide velocities during a period of spring tide, at approximately 1200 and 1830 GMT on 7 October 2002, respectively. The velocities are termed near-maximum in that the time of maximum was sought for the area around the inlet, which may not be the maximum in the channel or in the nearshore.

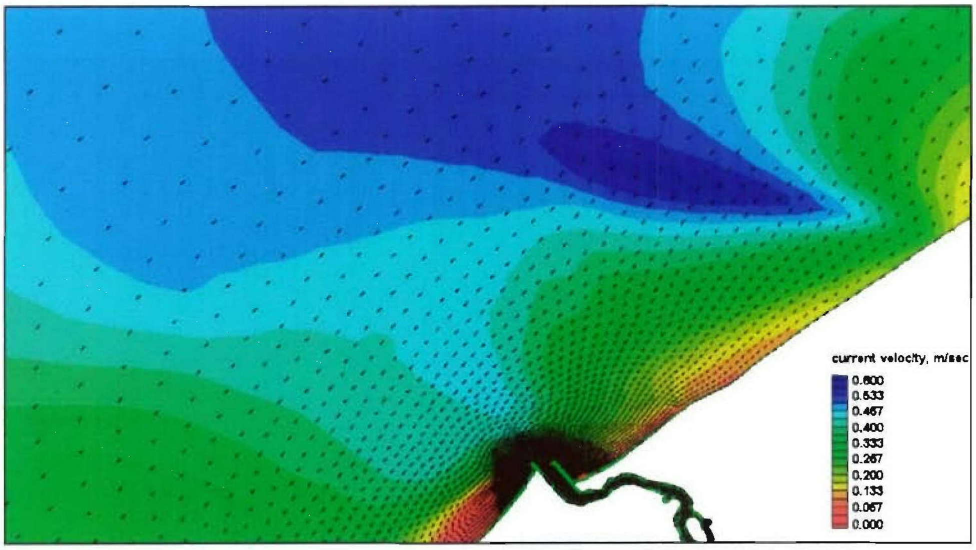

Figure 5-8a. Near-maximum flood-tide velocity, Mattituck Inlet offshore area, 1200 GMT, 7 October 2002

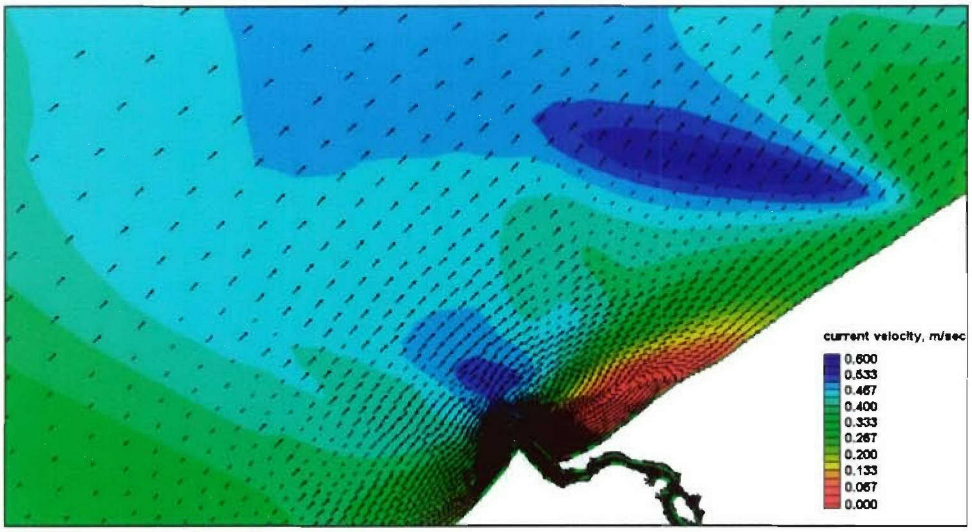

Figure 5-8b. Near-maximum ebb-tide velocity, Mattituck Inlet offshore area, 1830 GMT, 7 October 2002

Near-maximum flood and ebb current velocities in the vicinity of the inlet entrance and the offshore shoal are illustrated in Figures 5-8c and 5-8e. Figures 5-8d and 5-8f display the same current velocity vectors overlying the bathymetry for this area. The influence of the jetties at Mattituck Inlet on the direction of the depth-averaged current can be seen in Figures 5-8g and 5-8h, where eddies form and current reversals occur.

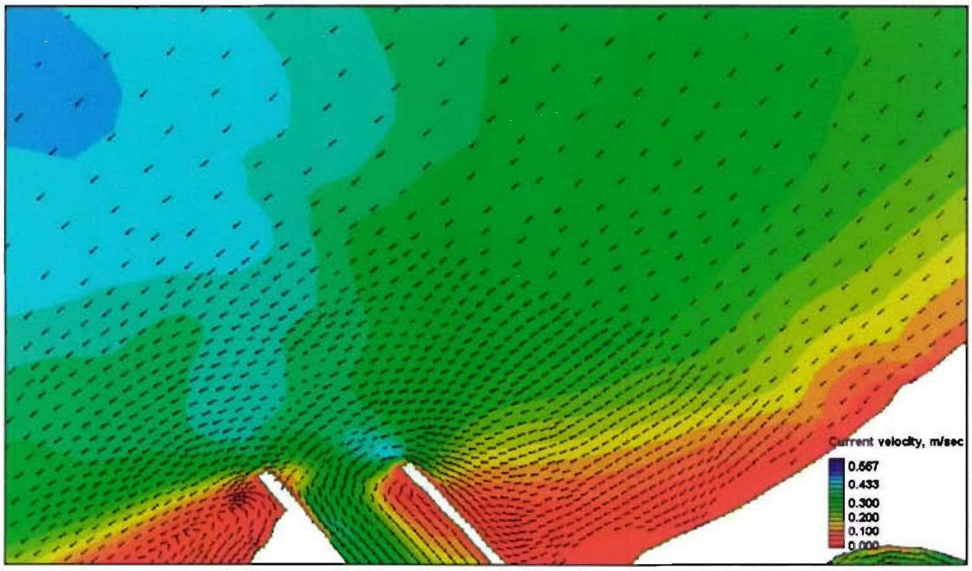

Figure 5-8c. Near-maximum flood-tide velocity, Mattituck Inlet offshore shoal area, 1200 GMT, 7 October 2002

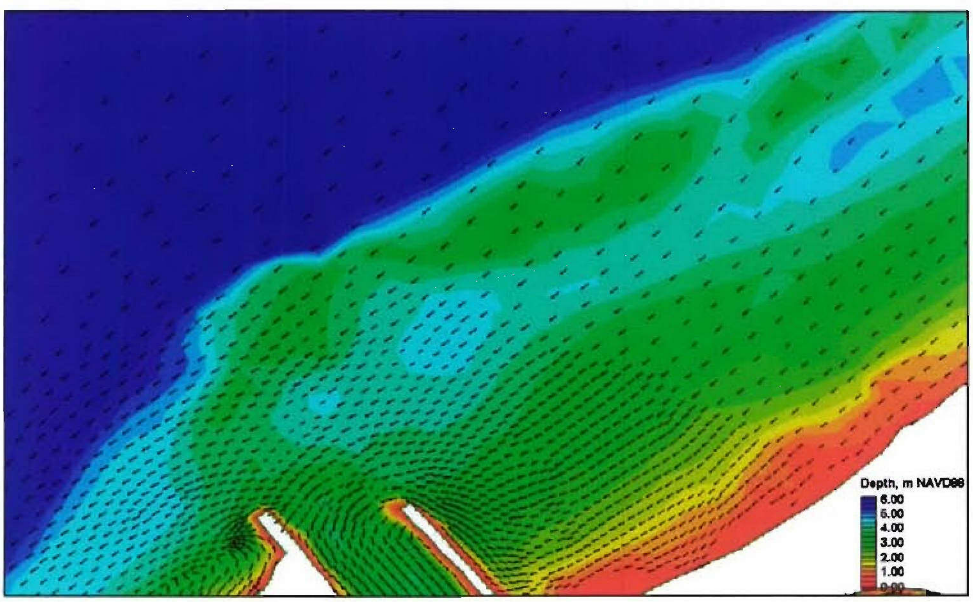

Figure 5-8d. Near-maximum flood-tide velocity and depth, Mattituck Inlet offshore shoal area, 1200 GMT, 7 October 2002

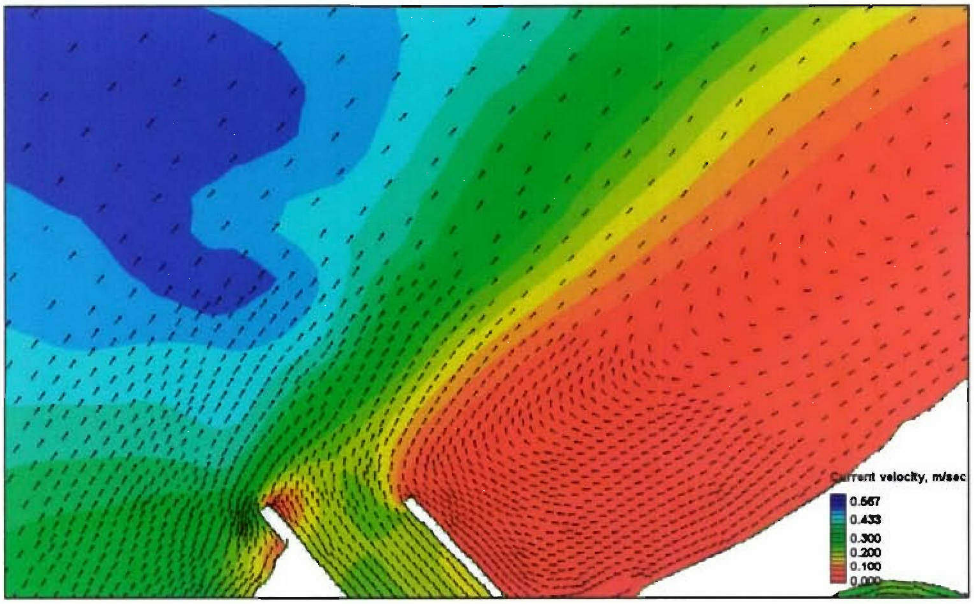

Figure 5-8e. Near-maximum ebb-tide velocity, Mattituck Inlet offshore shoal area, 1830 GMT, 7 October 2002

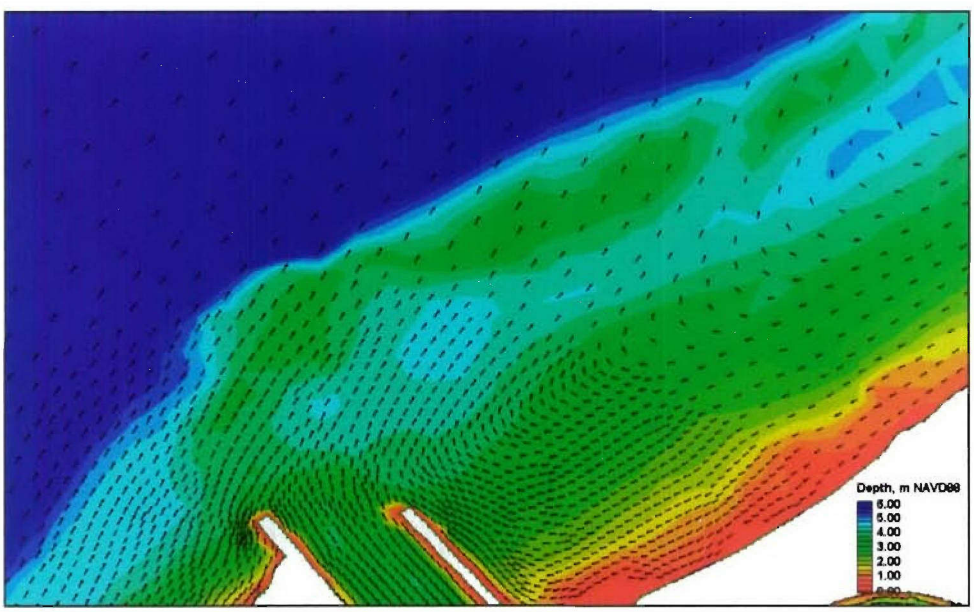

Figure 5-8f. Near-maximum ebb-tide velocity and depth, Mattituck Inlet offshore shoal area, 1830 GMT, 7 October 2002

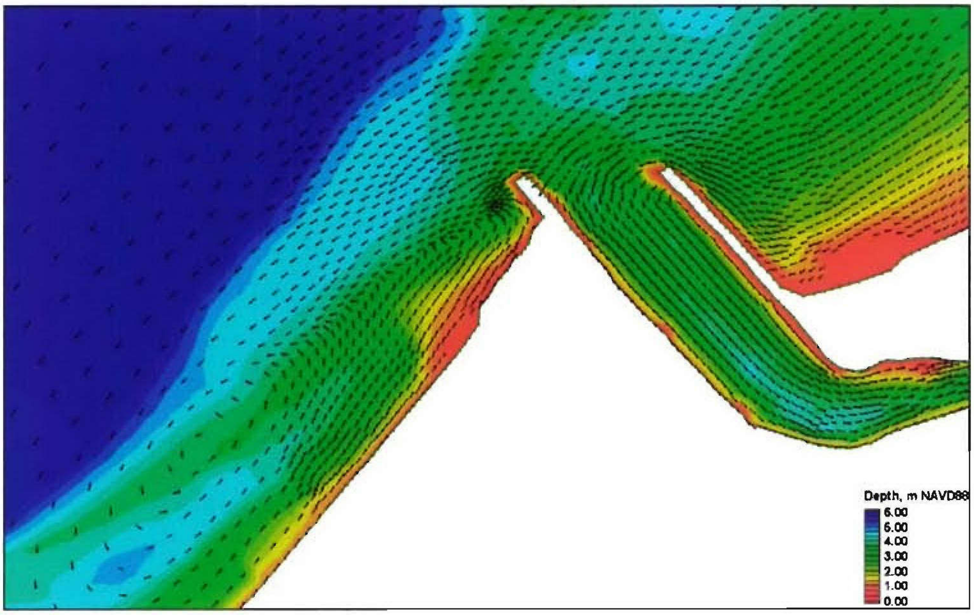

Figure 5-8g. Flood-current eddies and depth, directly west of Mattituck Inlet, 1200 GMT, 7 October 2002

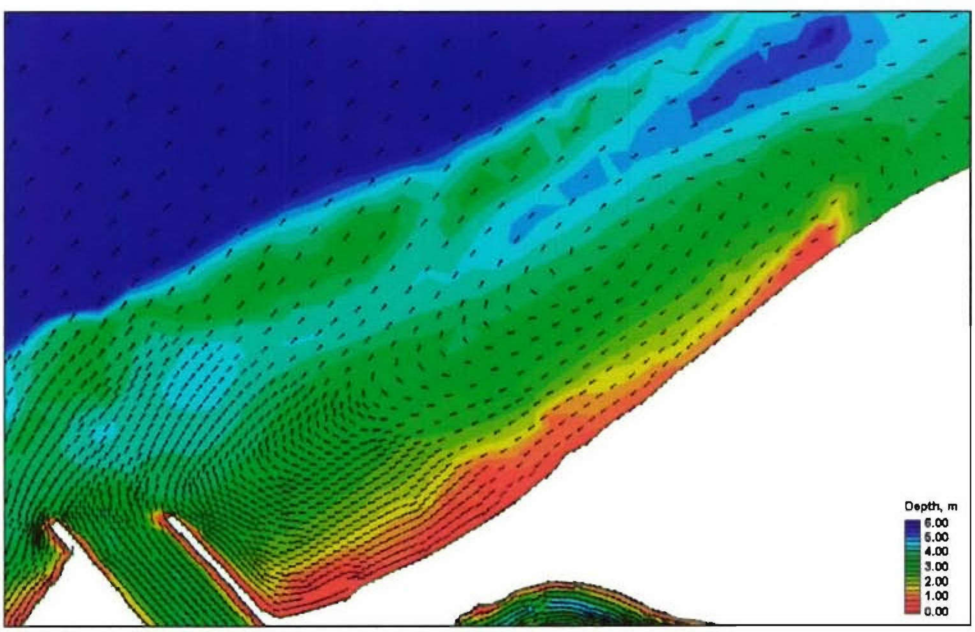

Figure 5-8h. Ebb-current eddies and depth, directly east of Mattituck Inlet, 1830 GMT, 7 October 2002

A notable result for consideration of sediment transport is that the calculated current velocity at the inlet entrance has a maximum of only about 0.5 m/sec for the spring tidal conditions simulated. The maximum current through the entrance would be less for typical tide and neap tide. It is empirically known that the annual mean-maximum velocity to maintain a minimum stable inlet channel cross section is about 1 m/sec for inlets on sandy coasts. Because the coarser sands and gravel predominant at Mattituck Inlet would require even stronger current velocity than 1 m/sec to sweep the channel clear, it can be concluded that the channel cross-sectional area is greater than the minimum (for sandy coasts).

Figures 5-9a and 5-9c display near-maximum flood- and ebb-tide current velocities within the channel. Figures 5-9b and 5-9d show these current velocity vectors overlaying the inlet and Federal navigation channel bathymetry. The greatest velocities occur adjacent to the area of the flood shoal along the east bank, opposite the area of shoaling, where Mattituck Inlet takes a sharp turn to the east and the channel becomes constricted. Magnitude of velocity reaches 0.5 m/sec.

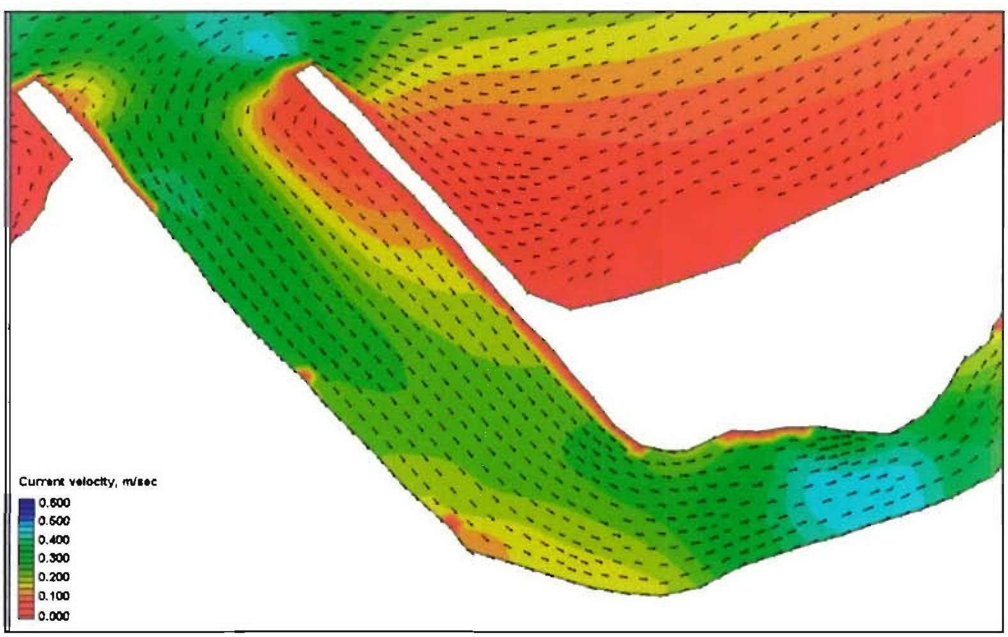

Figure 5-9a. Near-maximum flood-tide velocity, Mattituck Inlet, 1200 GMT, 7 October 2002

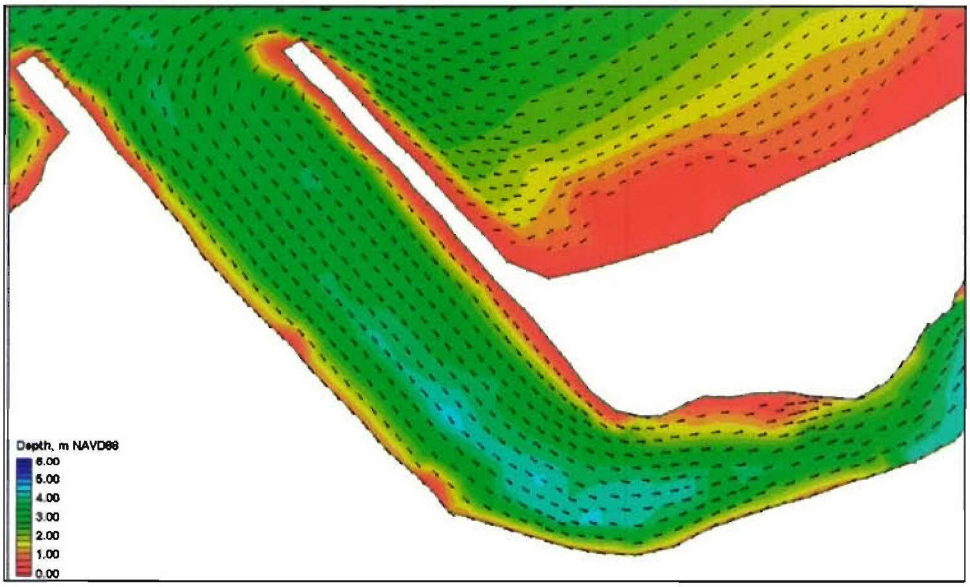

Figure 5-9b. Near-maximum flood-tide velocity and depth, Mattituck Inlet, 1200 GMT, 7 October 2002

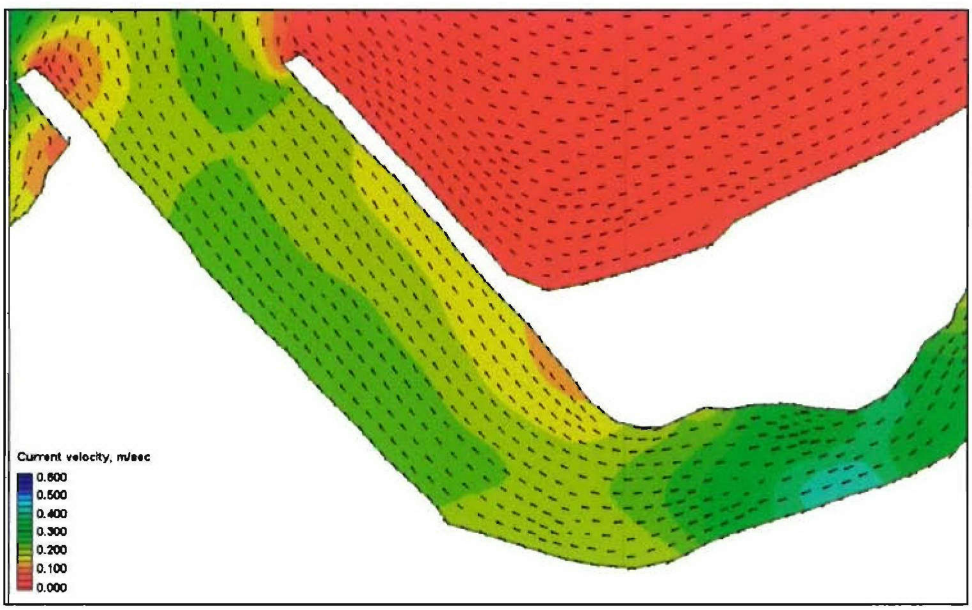

Figure 5-9c. Near-maximum ebb-tide velocity, Mattituck Inlet, 1830 GMT, 7 October 2002

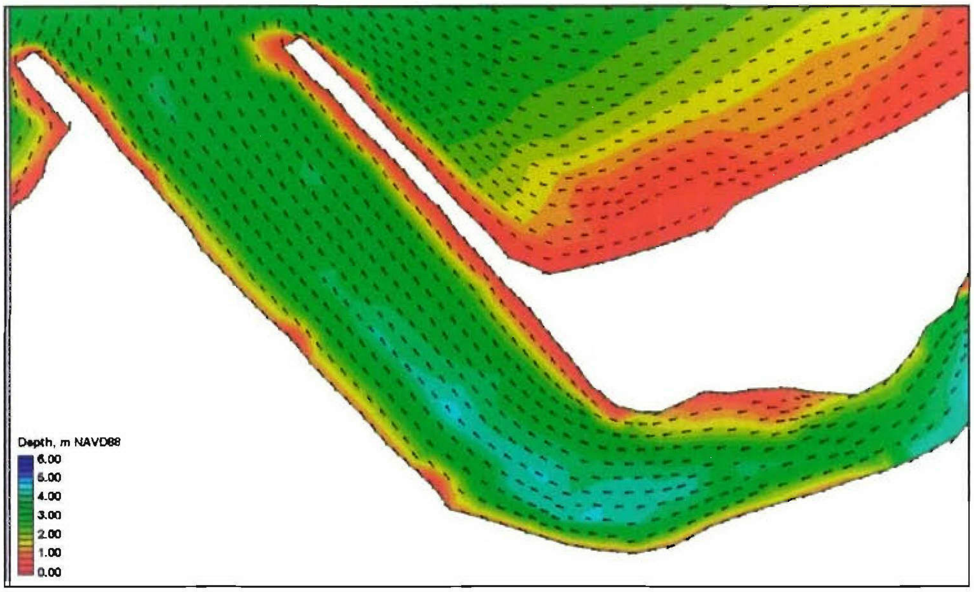

Figure 5-9d. Near-maximum ebb-tide velocity and depth, Mattituck Inlet, 1830 GMT, 7 October 2002

Figures 5-10a and 5-10c display near-maximum flood- and ebb-tide current velocities within Mattituck Inlet and the northern portion of Mattituck Creek. Figures 5-10b and 5-10d display these velocity vectors overlying the bathymetry of these areas. Current magnitude exceeds 0.5 m/sec in the creek in narrow areas.

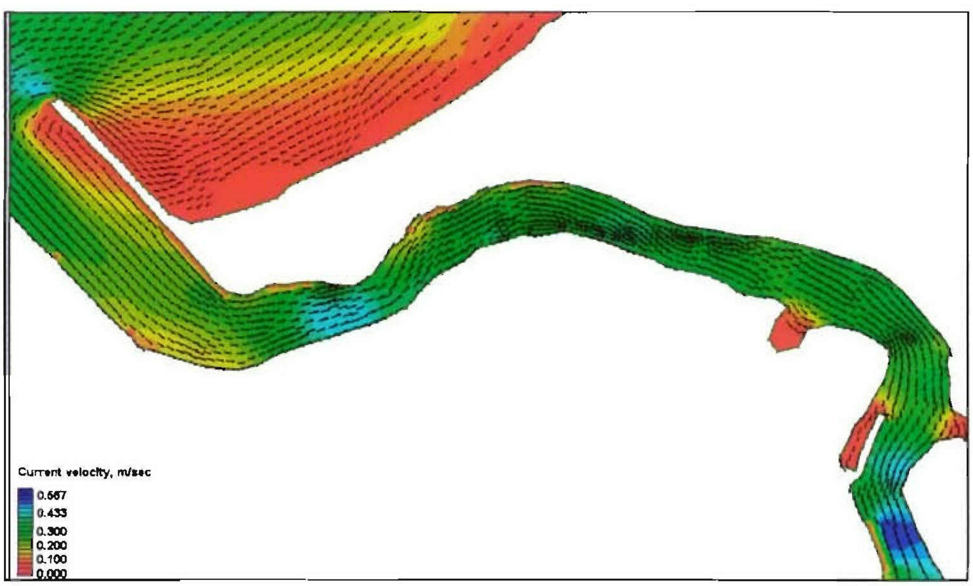

Figure 5-10a. Near-maximum flood-tide velocity, Mattituck Inlet flood shoal area, 1200 GMT, 7 October 2002

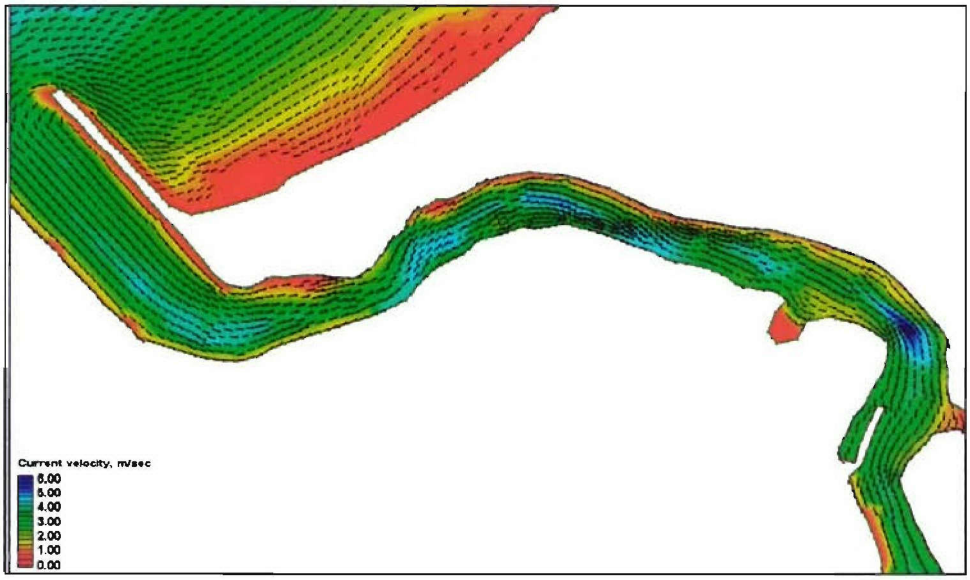

Figure 5-10b. Near-maximum flood-tide velocity and depth, Mattituck Inlet flood shoal area, 1200 GMT, 7 October 2002

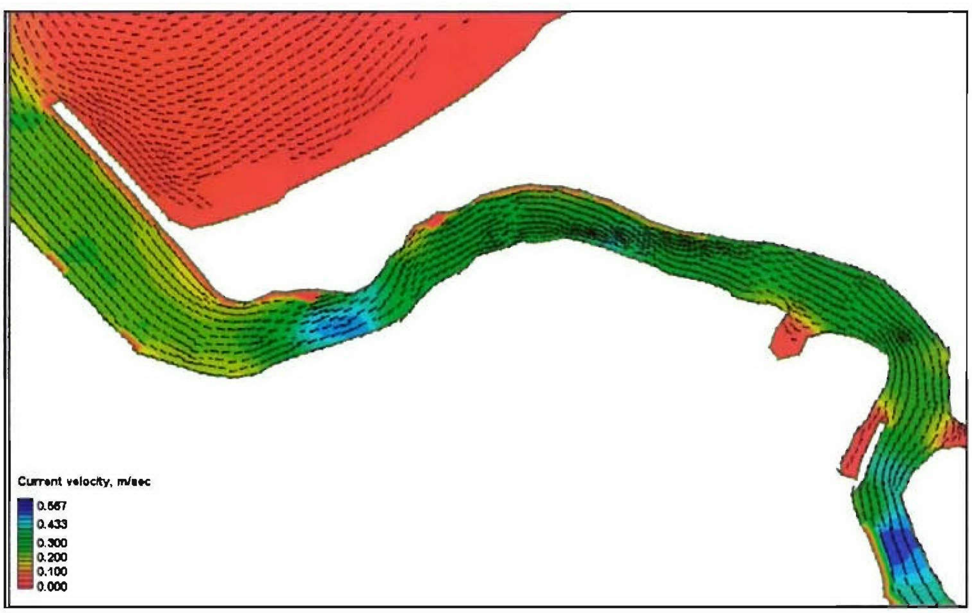

Figure 5-10c. Near-maximum ebb-tide velocity, Mattituck Inlet flood shoal area, 1830 GMT, 7 October 2002

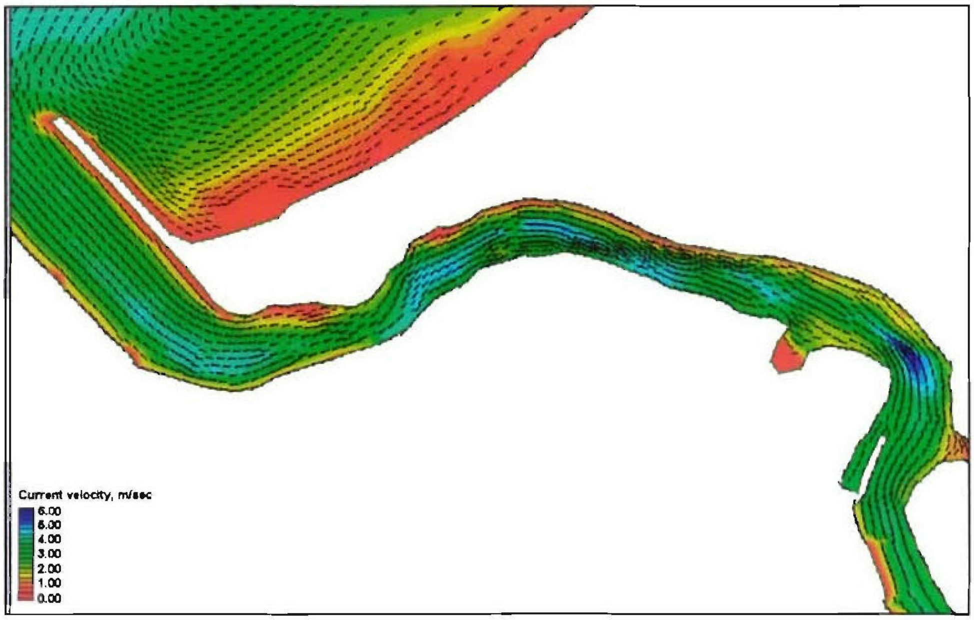

Figure 5-10d. Near-maximum ebb-tide velocity and depth, Mattituck Inlet flood shoal area, 1830 GMT, 7 October 2002

Alternative 1: Post-dredging morphology

To examine the control of the main area of shoaling on the current velocity within and around Mattituck Inlet, an alternative (synthetic) grid with this area of shoaling removed was developed. The results of this alternative are analyzed here and compared to the pre-dredging configuration of 2002. The dredged shoal configuration can be considered as an approximation of the morphology of Mattituck Inlet after the dredging of 17–24 March 2004[1]. Some differences exist, however, between the synthetic and actual dredging. The dredging of 17-24 March 2004 removed a significant portion of the shoal located on the west bank of the inlet, which is not represented in the synthetic grid. Also, the extent of the flood shoal removed from this grid is probably greater than the actual amount removed during the dredging of 2004, because sediment is expected to be removed only within the limits of the Federal navigation channel in actual dredging.

Figure 5-11a illustrates near-maximum flood current velocity near the flood shoal for the 2002 ADCIRC grid and Figure 5-11b illustrates maximum flood current velocity for this area for the dredged (flood) shoal alternative. Near-maximum ebb current velocity for this area is illustrated in Figure 5-11c (pre-dredging) and Figure 5-11d (post-dredging). The bathymetry of 6-8 October 2002 and the introduced changes in morphology for this alternative are illustrated in Figures 5-11e and 5-11f. Dredging of the flood shoal reduces velocity magnitude in the vicinity of dredging, with changes in velocity elsewhere being minor.

[1] The synthetic post-dredging grid was created and calculations performed before the March 2004 dredging took place.

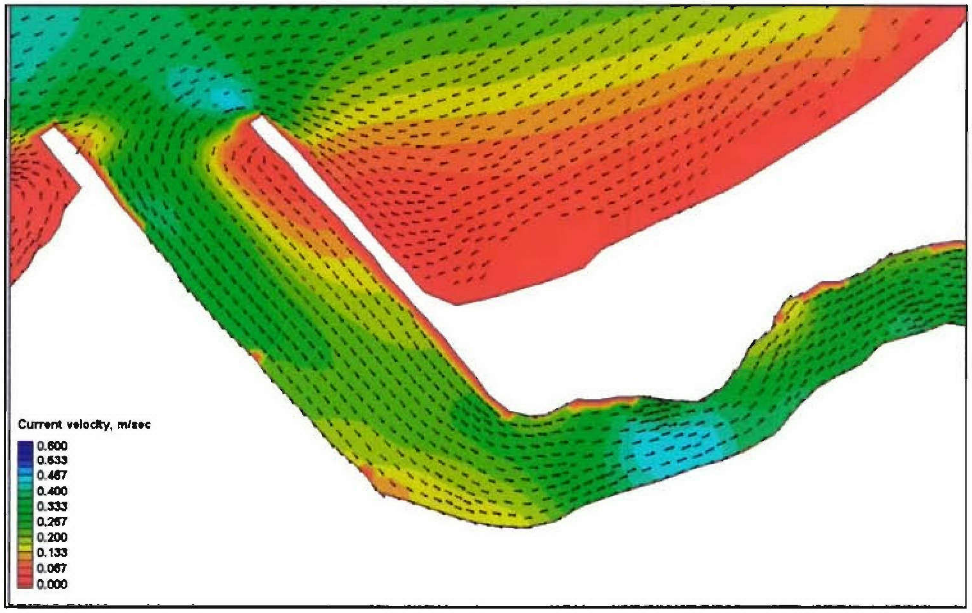

Figure 5-11a. Near-maximum flood-tide velocity, Mattituck Inlet, pre-dredging grid

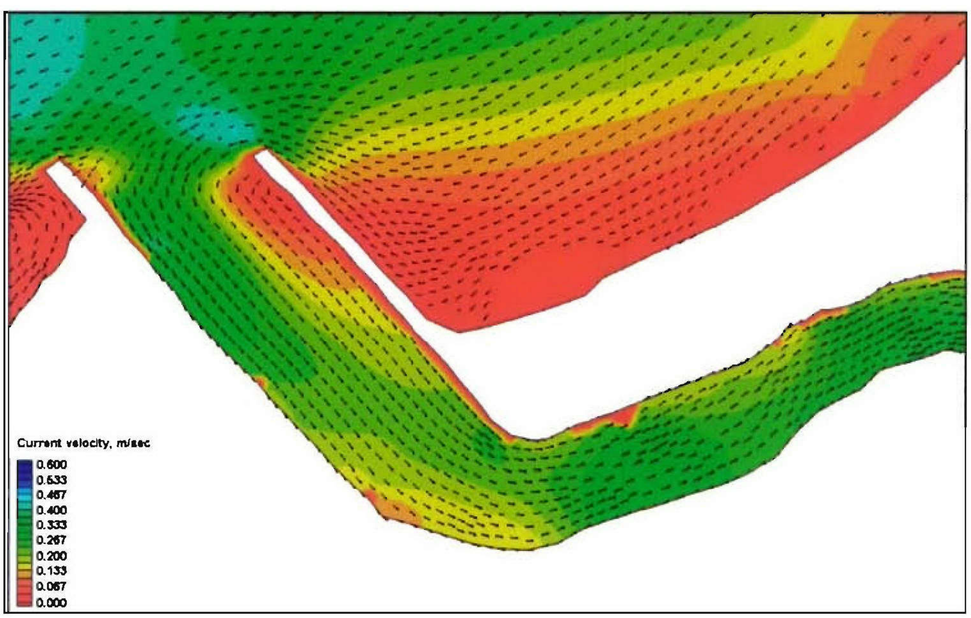

Figure 5-11b. Near-maximum flood-tide velocity, Mattituck Inlet, post-dredging grid

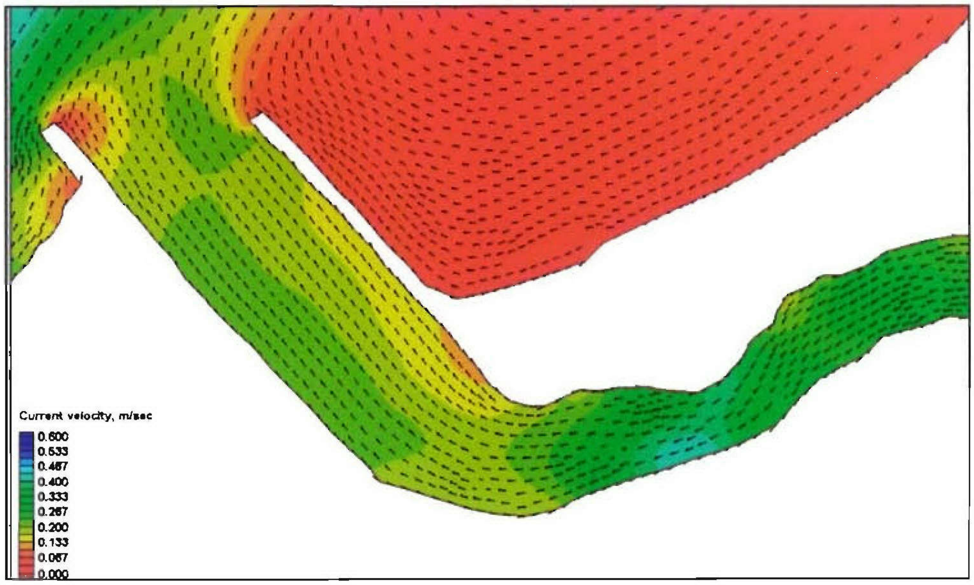

Figure 5-11c. Near-maximum ebb-tide velocity, Mattituck Inlet, pre-dredging grid

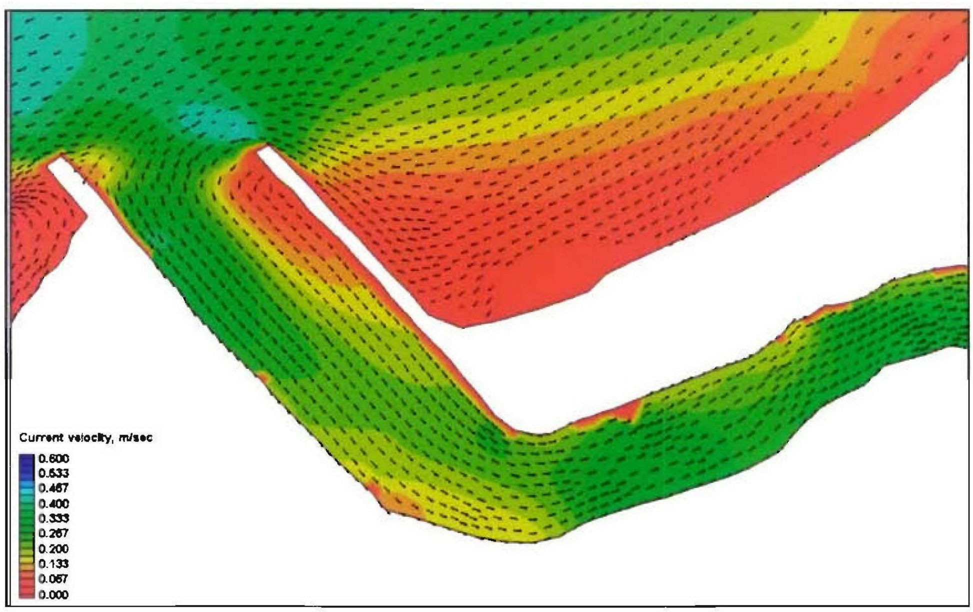

Figure 5-11d. Near-maximum ebb-tide velocity, Mattituck Inlet, post-dredging grid

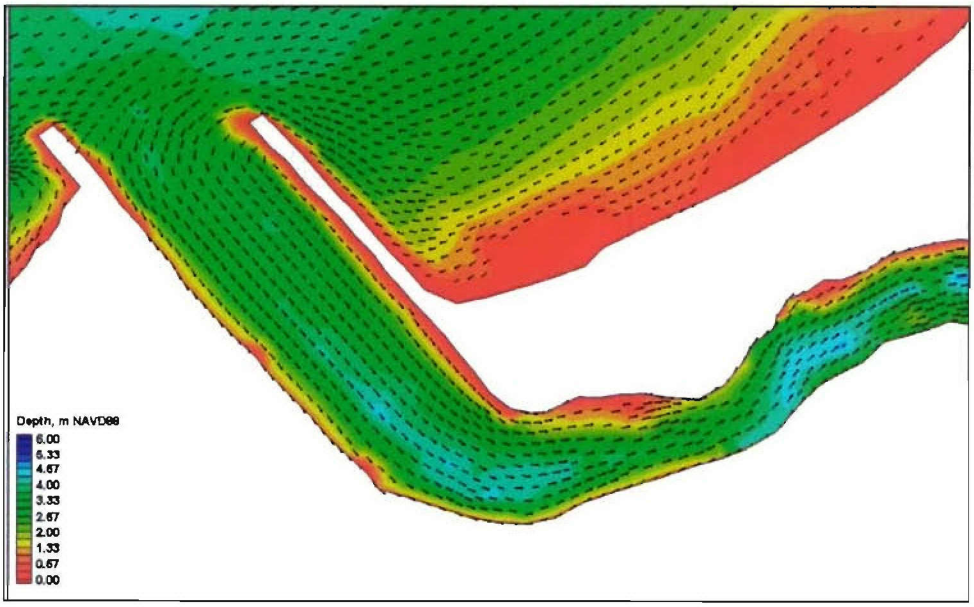

Figure 5-11e. Near-maximum flood-tide velocity and depth, Mattituck Inlet pre-dredging grid

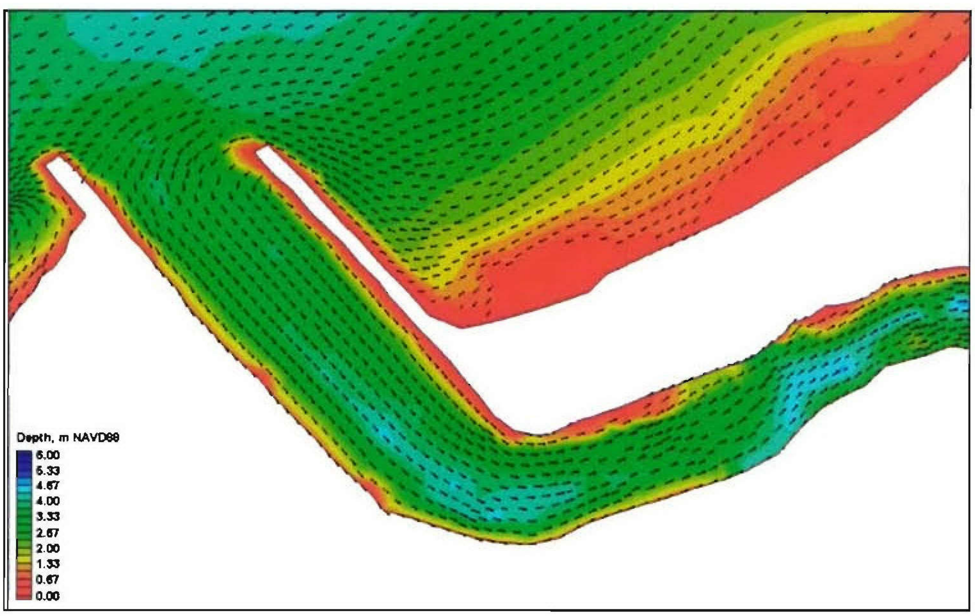

Figure 5-11f. Near-maximum flood-tide velocity and depth, Mattituck Inlet post-dredging grid

Figure 5-12 focuses on the location of synthetic dredging of the flood shoal, and current velocity at selected points is plotted in Figures 5-13a through 5-13c. The dredging of the flood shoal is calculated to reduce current velocity at the area of strongest flow by approximately 30 percent. The peaks of both ebb and flood current are reduced.

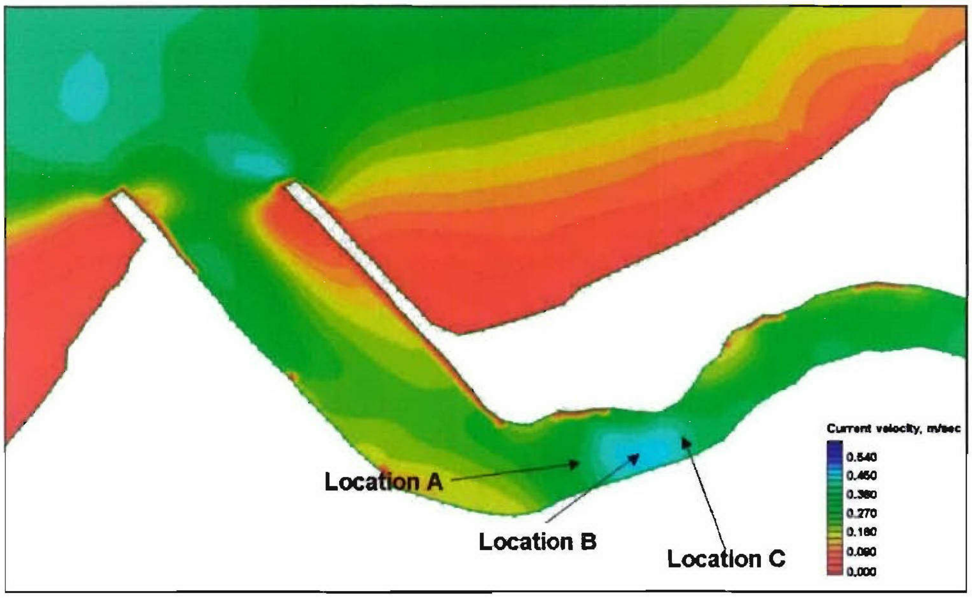

Figure 5-12. Comparative current velocity plot locations

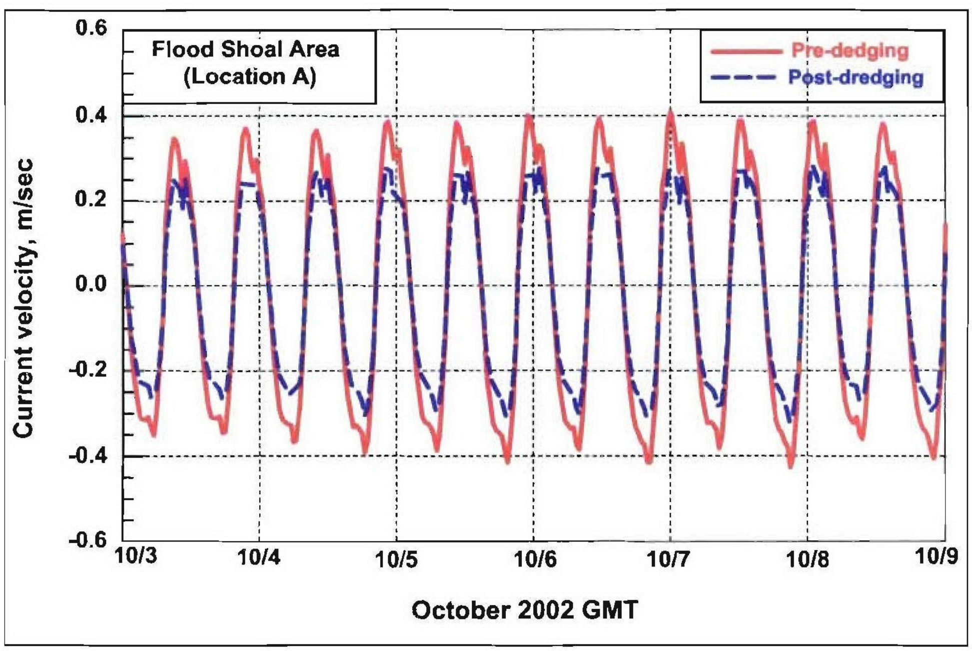

Figure 5-13a. Current velocity directly north of Mattituck Inlet east bank flood shoal, pre-dredging, and synthetic post-dredging condition (Location A)

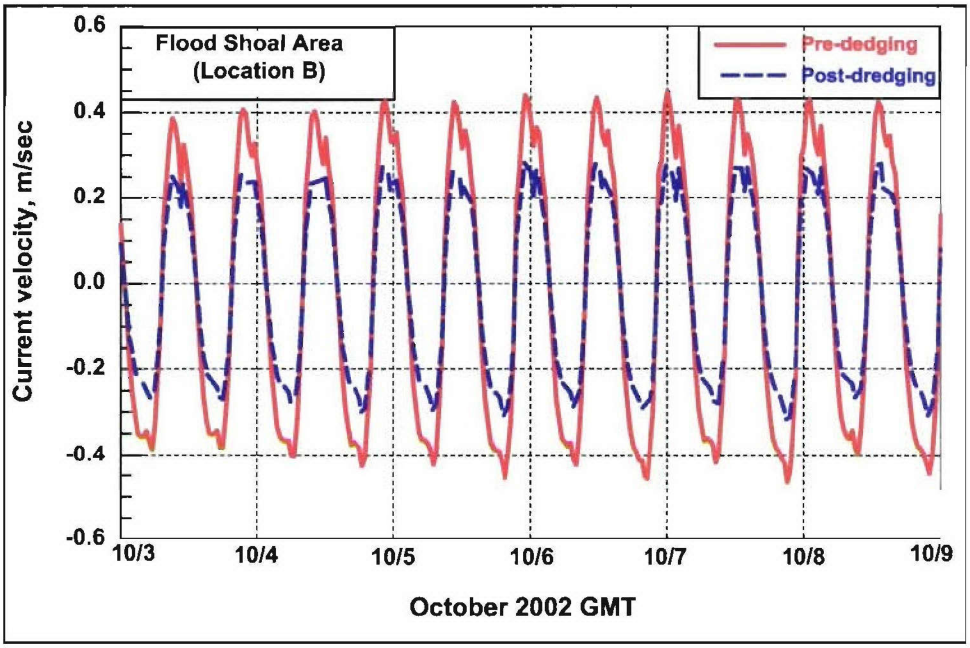

Figure 5-13b. Current velocity directly north of Mattituck Inlet east bank flood shoal, pre-dredging, and synthetic post-dredging condition (Location B)

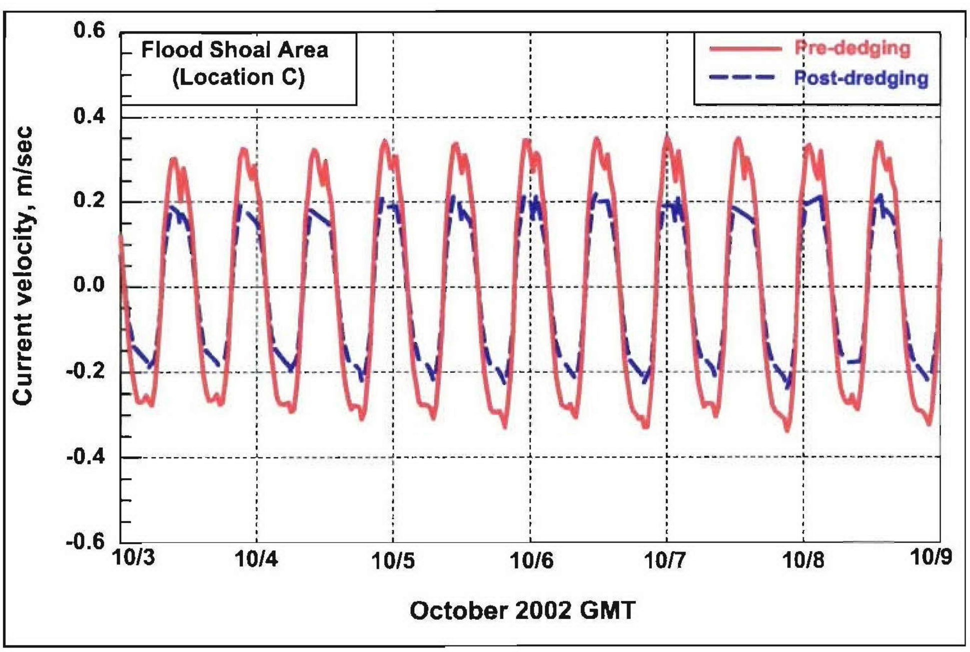

Figure 5-13c. Current velocity directly north of Mattituck Inlet east bank flood shoal, pre-dredging, and synthetic post-dredging condition (Location C)

Alternative 2: Natural morphology with offshore shoal

To examine a possible hydrodynamic, hence sediment-transport, relation between Mattituck Inlet and the offshore shoal located to the east, an alternative grid of Mattituck Inlet representative of its natural state was developed. The results of this alternative are analyzed here and compared to the pre-dredging configuration of 2002. The morphology representing the natural (pre-jetty) state is based on that of the inlet in 1891 (Figure 4-10). The east-directed spit shown in Figure 4-10 was truncated in this grid, because the apparent great spit length was not considered to be representative of Mattituck Inlet in typical natural equilibrium. The depth at the center of Mattituck Inlet and Mattituck Creek was taken to be approximately 1.3-1.5 m NAVD88. This depth was selected because the spring tide range at Mattituck Inlet is about 2 m, and there is no indication in the historic record that the inlet and Mattituck Creek became dry.

The tidal prism at Mattituck Inlet is 4.32×10^7 cu ft. Applying the Jarrett (1976) relation for Atlantic Coast inlets with no jetties (discussed in Chapter 6), $A_C = 5.37 \times 10^{-6} P^{0.107}$, the channel cross-sectional area of Mattituck Inlet in its natural state is estimated to be 794 sq ft. If the width of Mattituck Inlet in a natural state is taken to be 175 ft, the resulting average depth is 4.5 ft NAVD88, or 1.38 m. Finally, the historic presence of a tidal mill at Mattituck Inlet suggests presence of water of at least this depth.

The hydrodynamic behavior of Mattituck Inlet in its assumed (synthetic) natural state differs considerably from that of Mattituck Inlet in its present modified state. The current at the natural Mattituck Inlet displays similar properties to the present Goldsmith Inlet. The natural Mattituck Inlet is found to be strongly flood-dominant, and the phase lag between the offshore and creek water-level peaks and troughs is pronounced.

Figures 5-14a through 5-14i display calculated tidal velocities offshore of and through Mattituck Inlet for various times during a full spring tidal cycle. Figures 5-14a and 5-14b illustrate Mattituck Inlet at 1200 GMT 7 October 2002, the time of near-maximum offshore current velocity. This time is equivalent to that of the near-maximum offshore current velocity illustrated in Figure 5-8a. For comparison to Figure 5-8a, Figure 5-14a is displayed with the same contour interval range (0-0.6 m). Figure 5-14b illustrates calculation results for this time with a contour interval range of 0–3 m, for comparison to subsequent figures. During this time of near-maximum offshore flood current, the inlet is nearing the end of ebb tide.

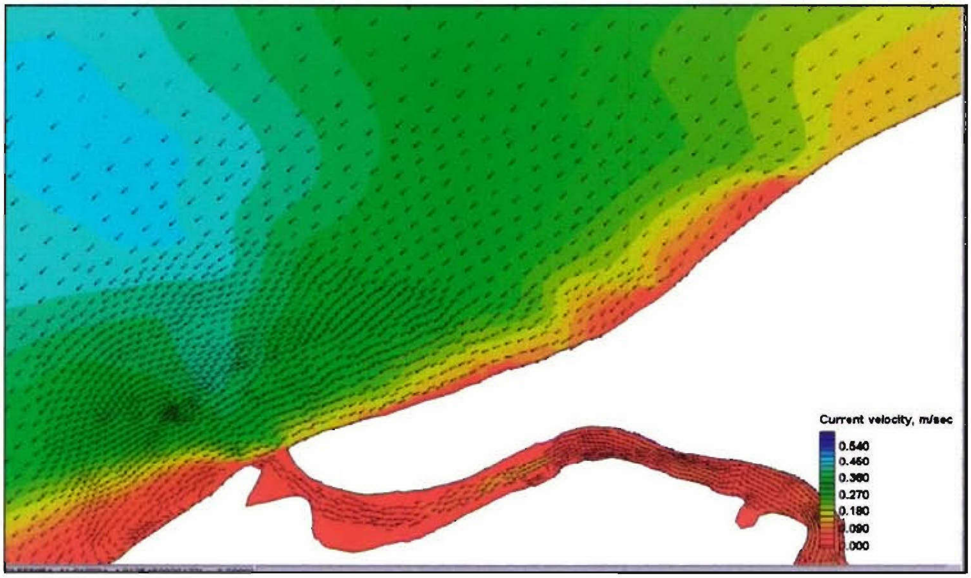

Figure 5-14a. Mattituck Inlet natural state, near-maximum offshore spring flood-tide velocity, 1200 on 7 October 2002

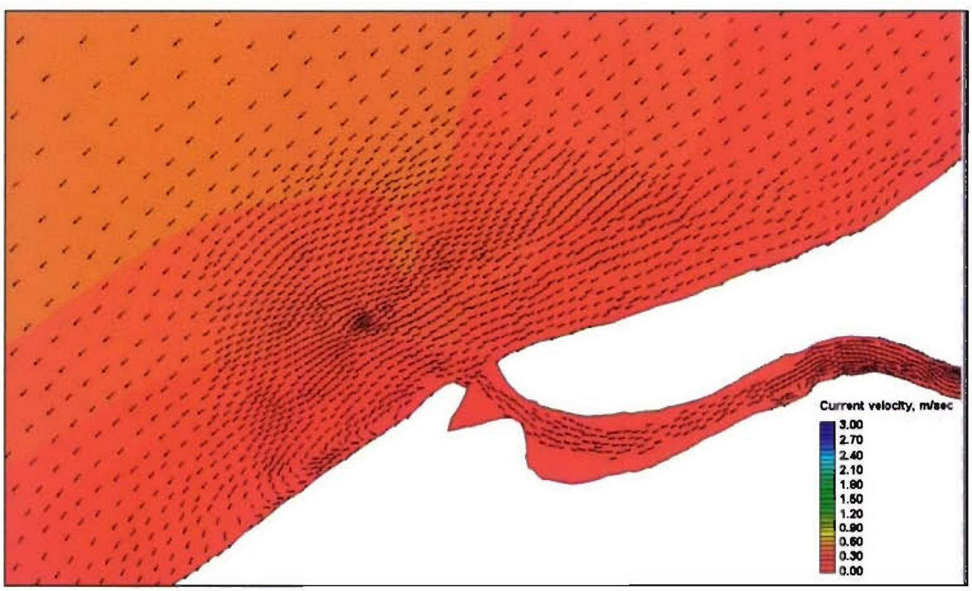

Figure 5-14b. Mattituck Inlet natural state, near-maximum offshore spring flood-tide velocity, 1200 on 7 October 2002

Figure 5-14c illustrates calculated current velocities at 1230 GMT on 7 October 2002. The offshore flood current velocities remain near peak, and the inlet has begun to flood. Current velocities at 1430 GMT on 7 October 2002 are illustrated in Figure 4-14d. This is the point of maximum flood current velocity at the mouth of the inlet, while the offshore remains in a flood portion of the tidal cycle.

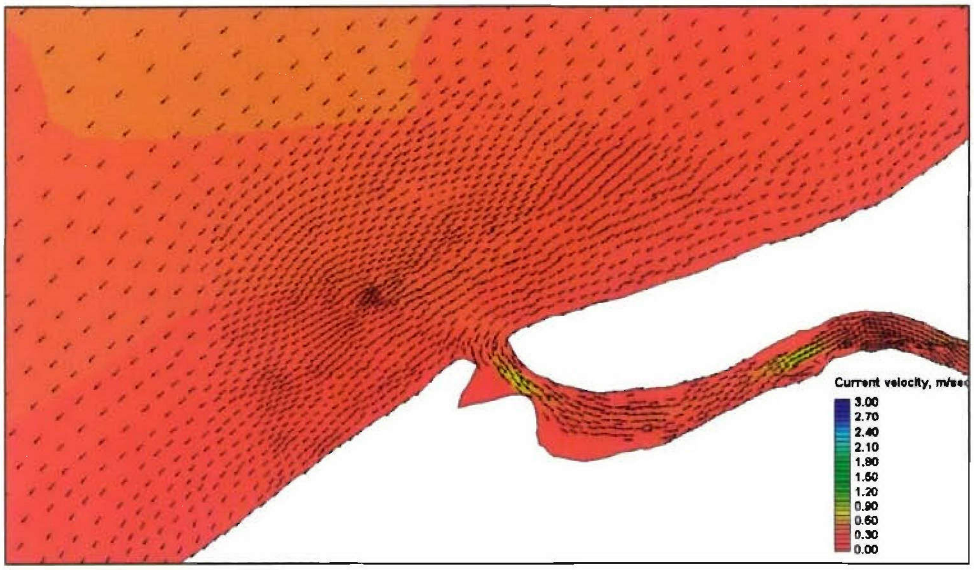

Figure 5-14c. Mattituck Inlet natural state, offshore and inlet spring flood-tide velocity, 1230 on 7 October 2002

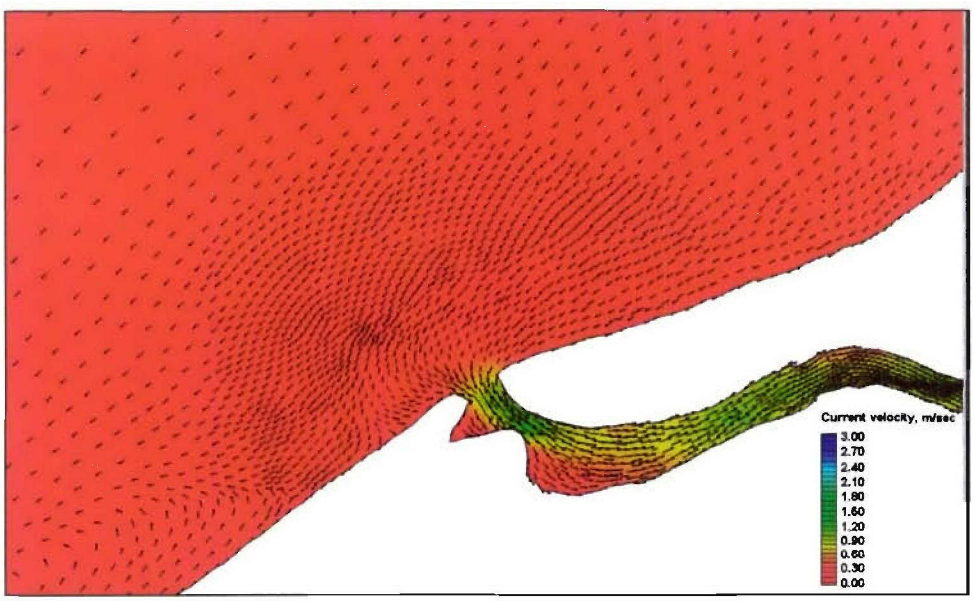

Figure 5-14d. Mattituck Inlet natural state, offshore spring flood-tide and near-maximum inlet spring flood-tide velocity, 1430 on 7 October 2002

Figure 5-14e illustrates calculated current velocity at 1530 GMT on 7 October 2002. An ebb tide has begun offshore, but the inlet continues to flood at strong velocity relative to the maximum inlet flood current velocities. The offshore flood current velocity remains near peak, and the inlet has begun to flood. Current velocities at 1830 GMT on 7 October 2002 are illustrated in Figure 5-14f. The point of near-maximum ebb current velocity has been reached offshore, and the inlet is in an ebb stage of the tidal cycle. This figure can be compared to Figures 5-17 and 5-20, which illustrates results for the same time for a representative 2002 pre-dredging morphology at Mattituck Inlet.

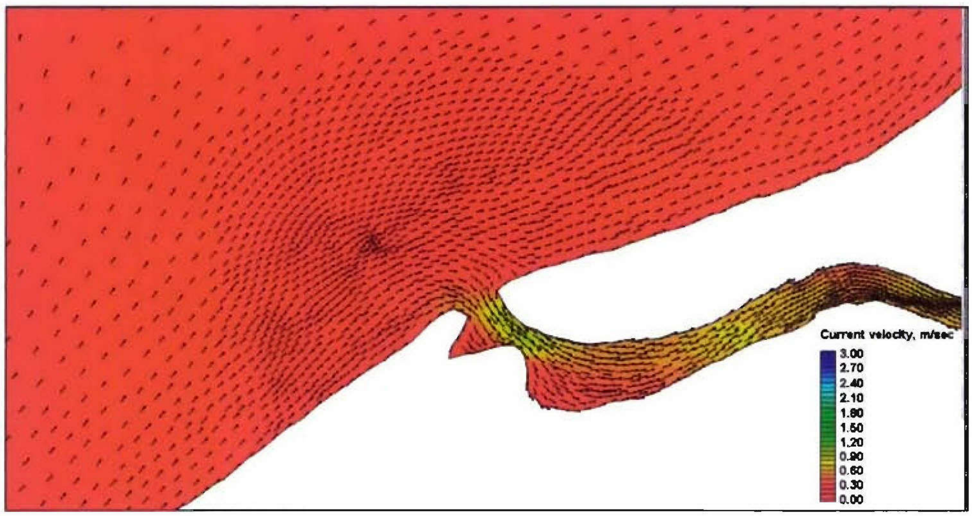

Figure 5-14e. Mattituck Inlet natural state, offshore spring ebb-tide and inlet spring flood-tide velocity, 1530 on 7 October 2002

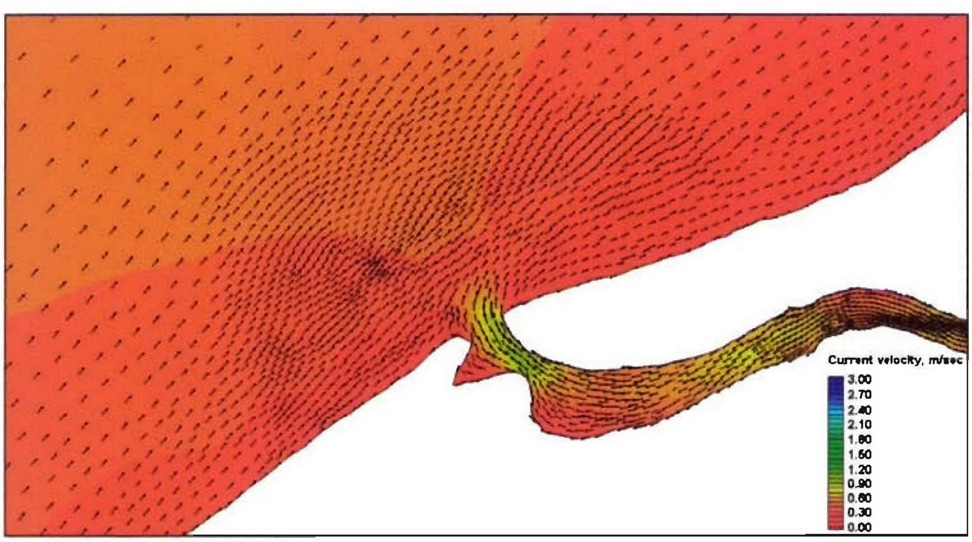

Figure 5-14f. Mattituck Inlet natural state, near maximum offshore spring ebb-tide and inlet spring ebb-tide velocity, 1830 on 7 October 2002

Figure 5-14g illustrates calculated current velocity at 2100 GMT 7 October 2002. Ebb tide current velocity at the mouth of the inlet approaches 2 m/sec, a velocity much greater than the typical calculated spring tide maximum of 0.5 m/sec found at the existing inlet. Figure 5-14h illustrates current velocity at 2200, a period when flood tide has begun offshore and the inlet remains in a stage of ebb tide. Figure 5-14i illustrates current velocity at 0030 on 8 October 2002. The area in is in a tidal stage the same as that of Figure 5-14a, the first figure in this series.

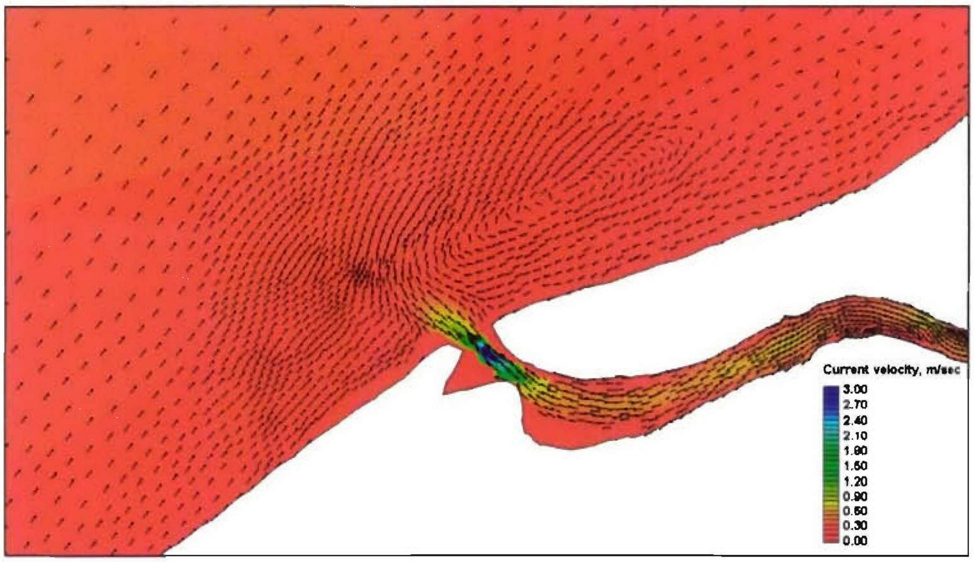

Figure 5-14g. Mattituck Inlet natural state, offshore spring ebb-tide and inlet near maximum spring ebb-tide velocity, 2100 on 7 October 2002

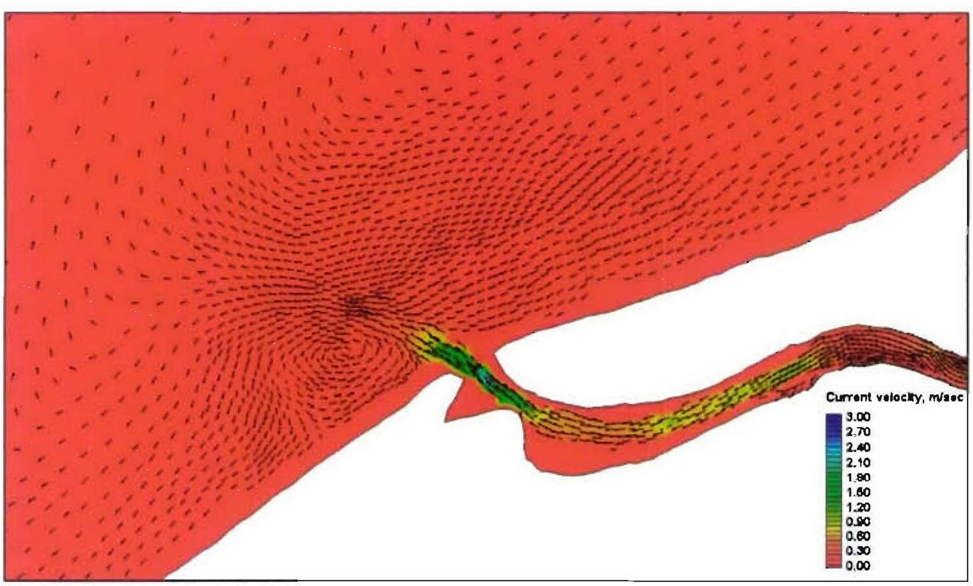

Figure 5-14h. Mattituck Inlet natural state, offshore spring flood-tide and inlet spring ebb-tide velocity, 2200 on 7 October 2002

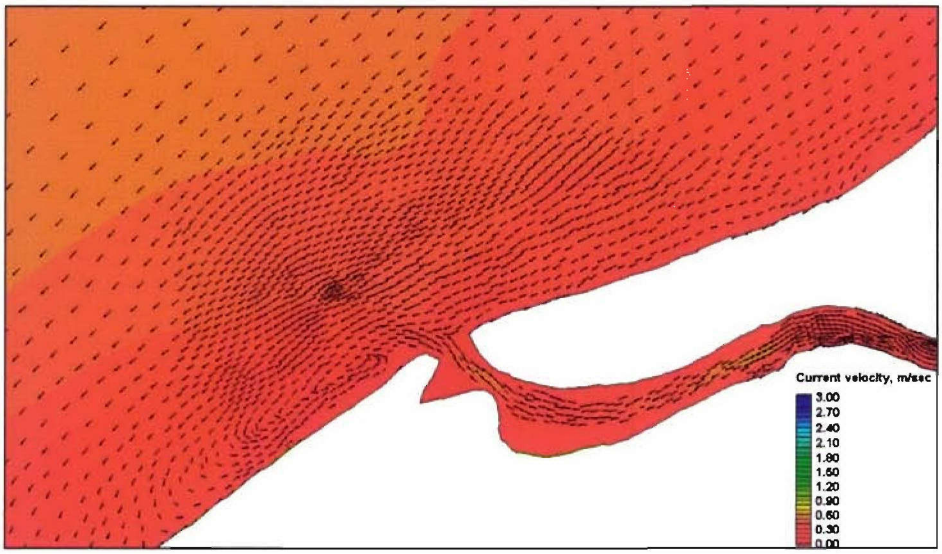

Figure 5-14i. Mattituck Inlet natural state, near maximum offshore spring flood-tide and inlet spring ebb-tide velocity, 0030 on 8 October 2002

Figure 5-15 displays locations offshore and within the inlet where water level and current velocity calculation results were extracted to examine the differences in hydrodynamic behavior between the offshore area and Mattituck Inlet in its natural state. Location C is near the present-day flood shoal, and Location D is near the site of the 19 September - 8 October 2002 water level and current meter data collection. Figures 5-16a through 5-16c illustrate differences in water-surface elevations at these locations, and Figures 5-17a through 5-17c compare current velocities.

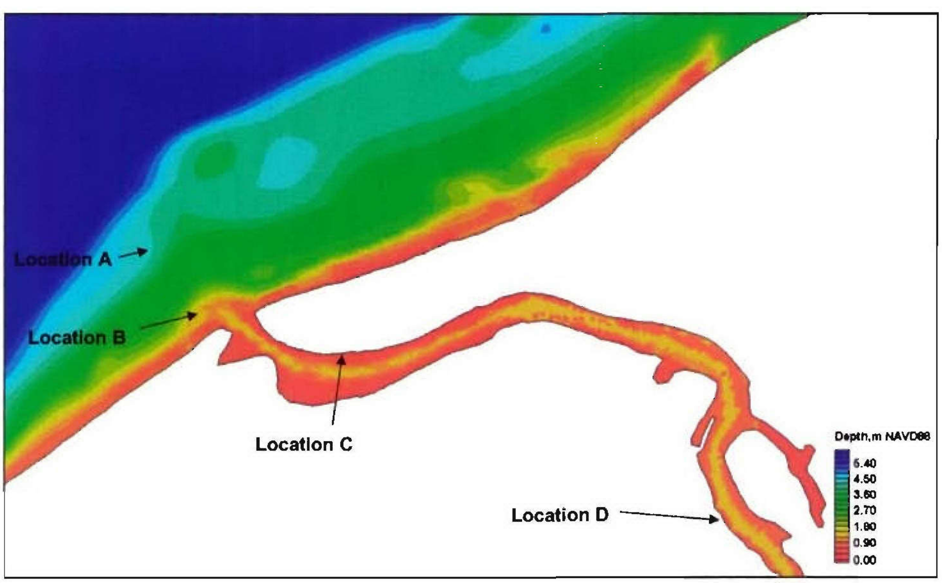

Figure 5-15. Mattituck Inlet assumed (synthetic) natural state and offshore water level and current velocity comparison locations

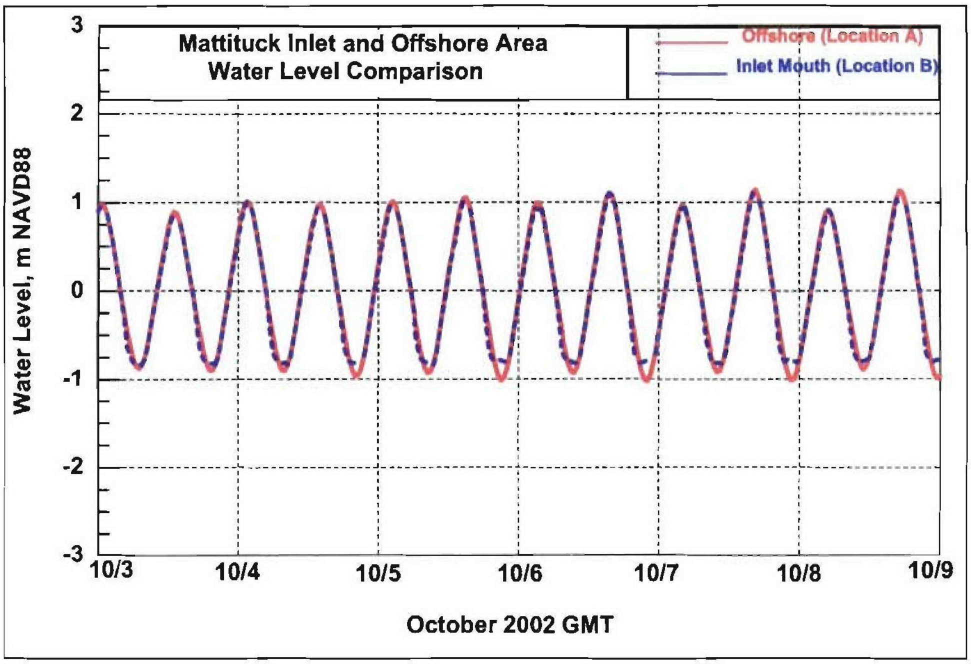

Figure 5-16a. Mattituck Inlet natural state and offshore water level comparison (Locations A and B)

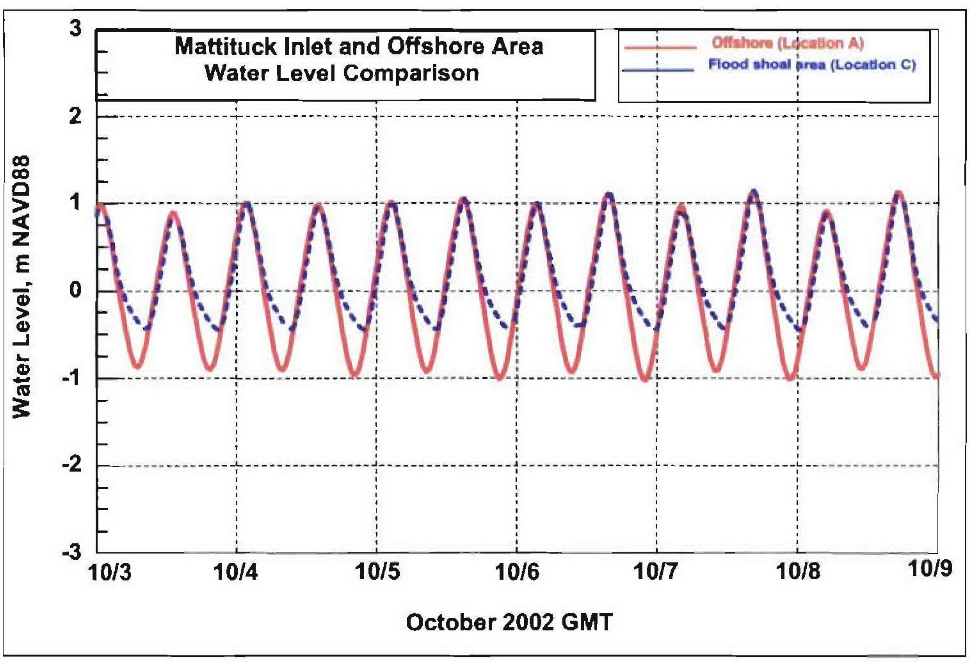

Figure 5-16b. Mattituck Inlet natural state and offshore water level comparison (Locations A and C)

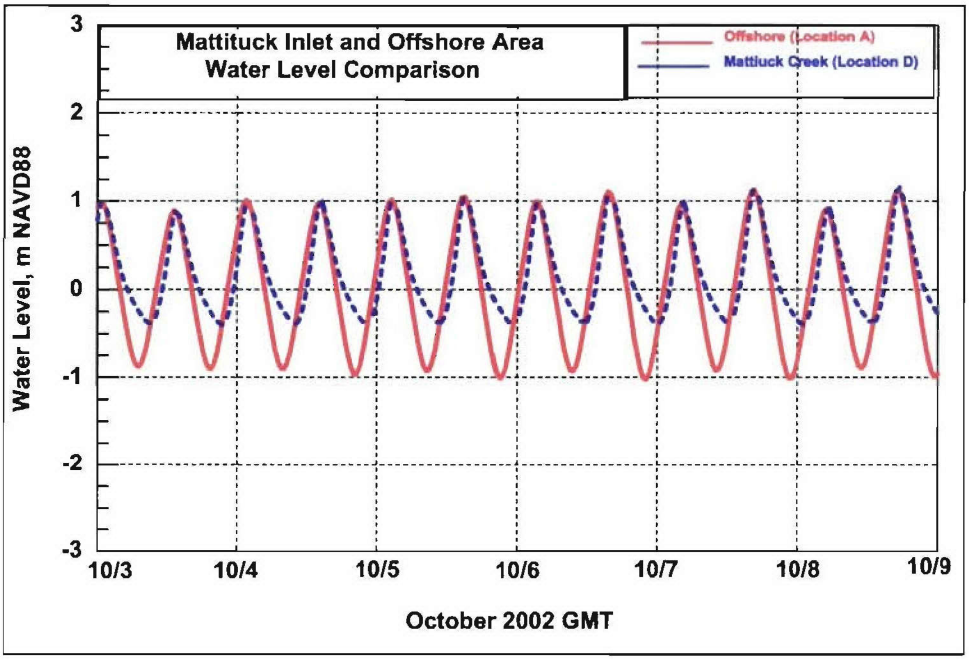

Figure 5-16c. Mattituck Inlet natural state and offshore water level comparison (Locations A and D)

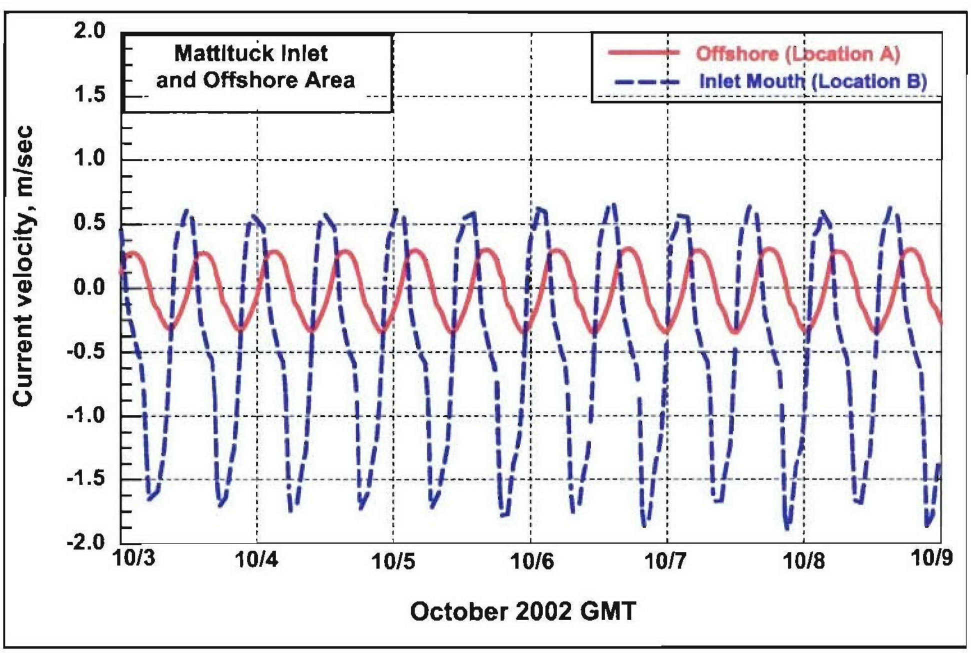

Figure 5-17a. Mattituck Inlet natural state and offshore current velocity comparison (Locations A and B)

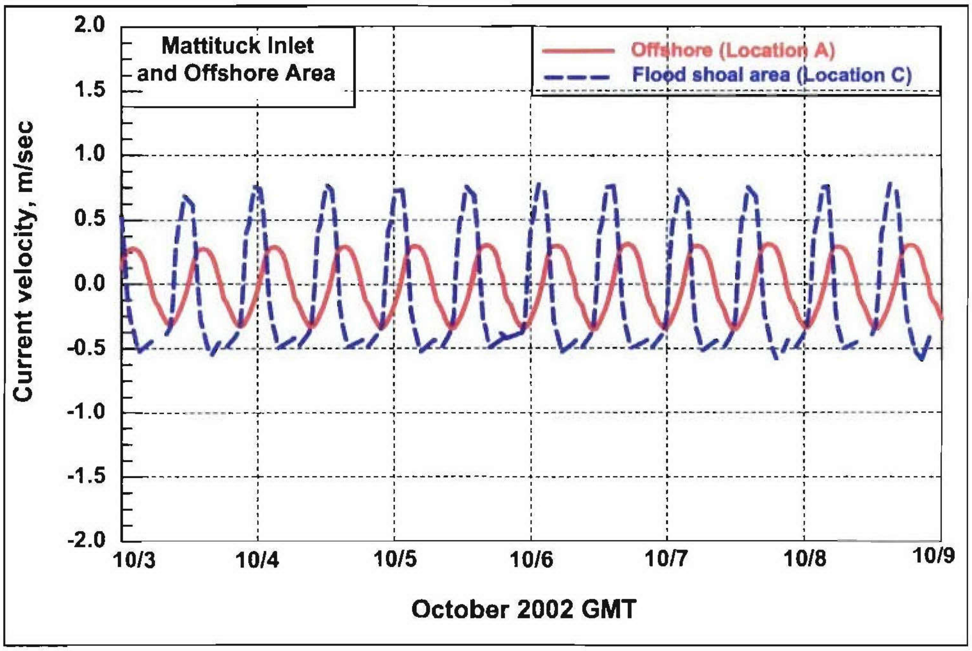

Figure 5-17b. Mattituck Inlet natural state and offshore current velocity comparison (Locations A and C)

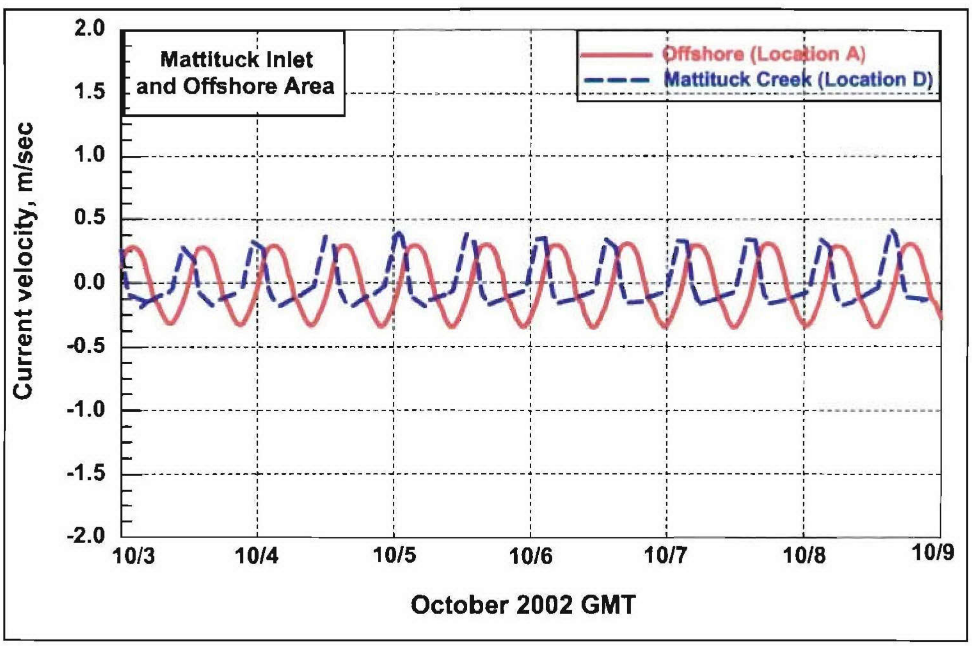

Figure 5-17c. Mattituck Inlet natural state and offshore current velocity comparison (Locations A and D)

Offshore shoal. The calculated hydrodynamics at Mattituck Inlet in a natural state and the offshore shoal located to the east are displayed in Figures 5-18a through 5-18h. This series of figures illustrates current velocity and current velocity vectors overlying bathymetry for the spring tide periods of near-maximum offshore flood current velocity, near-maximum inlet flood current velocity, near-maximum offshore ebb current velocity, and near-maximum inlet ebb current velocity, respectively. Figure 5-18a illustrates current velocity at 1200 on 7 October 2002, the time of near-maximum offshore flood current. Figures 5-18b displays the same current velocity vectors overlying the inlet and offshore shoal bathymetry.

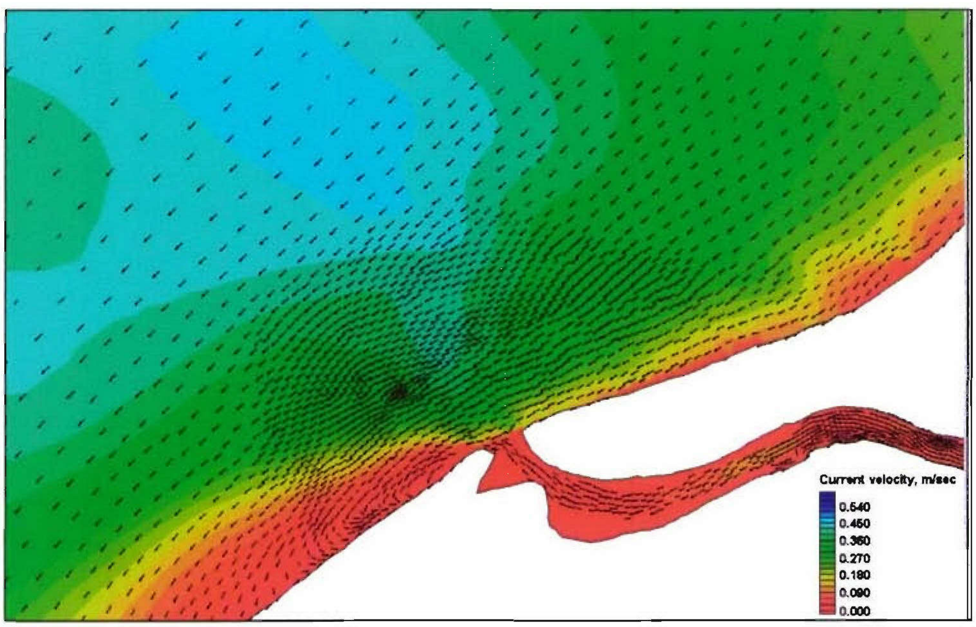

Figure 5-18a. Near-maximum offshore flood-tide velocity, Mattituck Inlet offshore shoal area, 1200 GMT on 7 October 2002

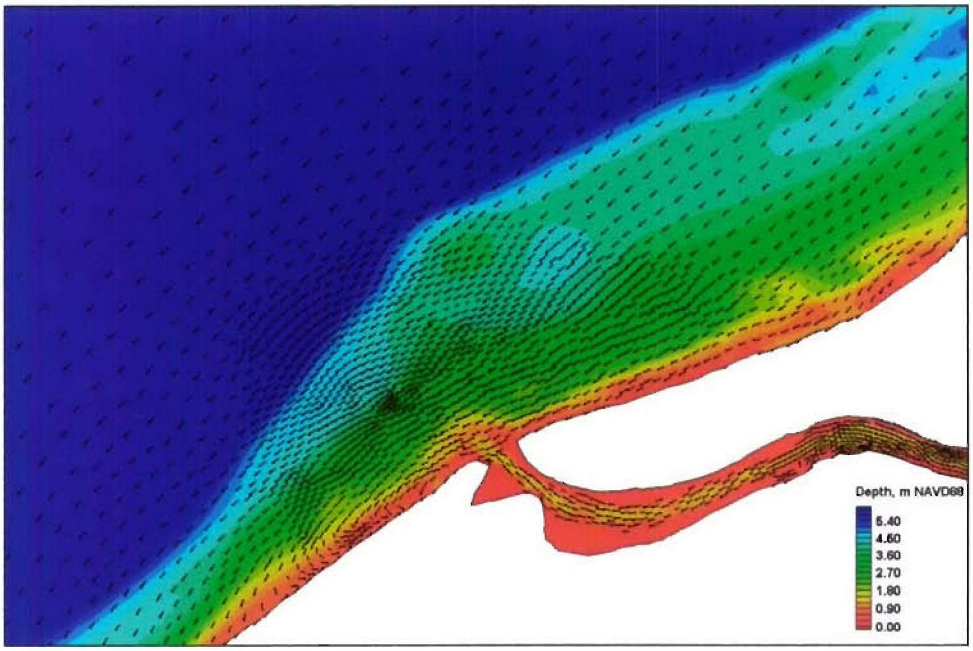

Figure 5-18b. Near-maximum offshore flood-tide velocity and depth, Mattituck Inlet offshore shoal area, 1200 GMT on 7 October 2002

Figure 5-18c illustrates current velocity at 1430 on 7 October 2002, the time of near-maximum inlet flood current. Figures 5-18d displays the same current velocity vectors overlying the inlet and offshore shoal bathymetry.

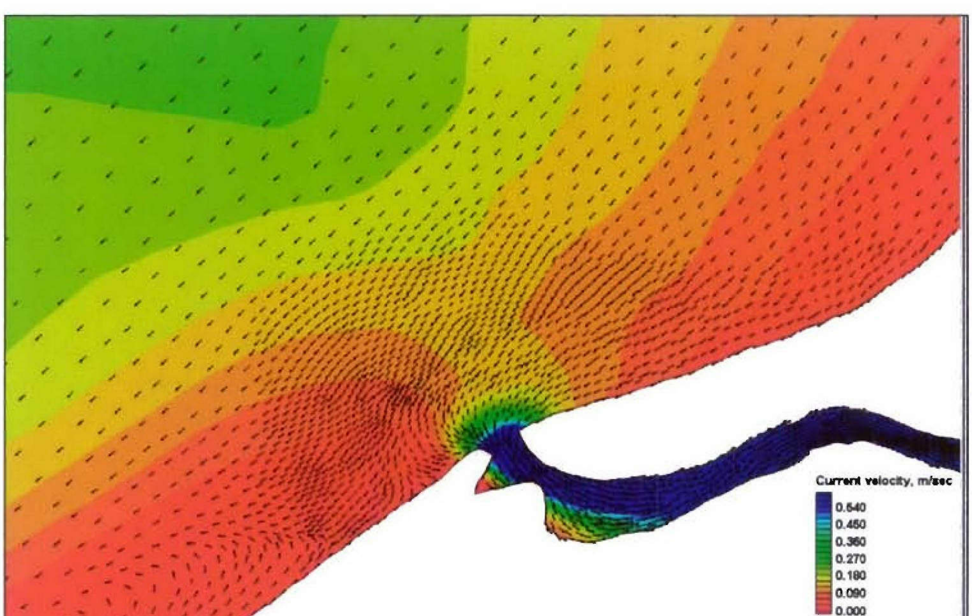

Figure 5-18c. Near-maximum inlet flood-tide velocity, Mattituck Inlet offshore shoal area, 1430 GMT on 7 October 2002

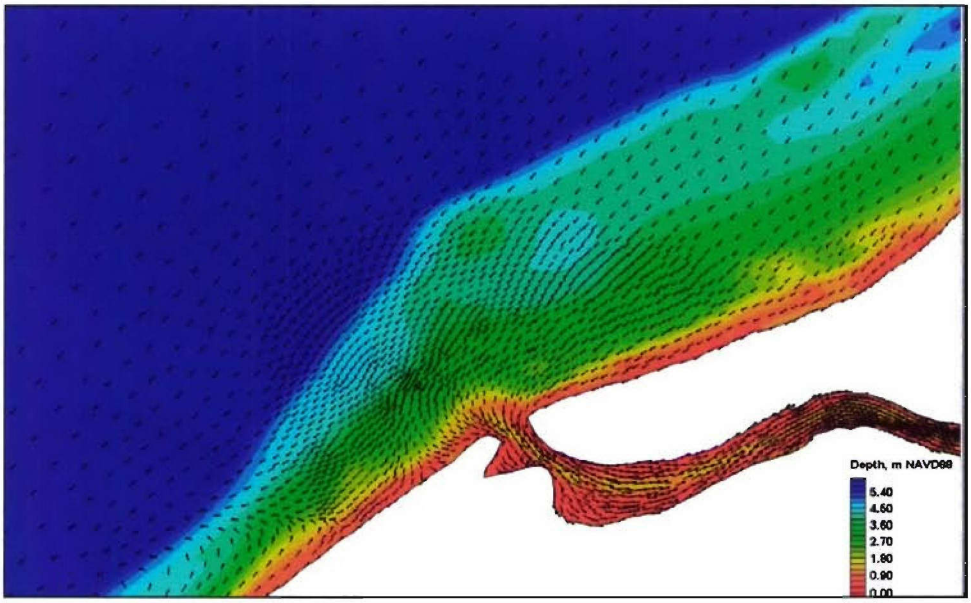

Figure 5-18d. Near-maximum inlet flood-tide velocity and depth, Mattituck Inlet offshore shoal area, 1430 GMT on 7 October

Figure 5-18e illustrates current velocity at the model at 1830 7 October 2002, the time of near-maximum offshore ebb current. Figure 5-18f displays the same current velocity vectors overlying the inlet and offshore shoal bathymetry.

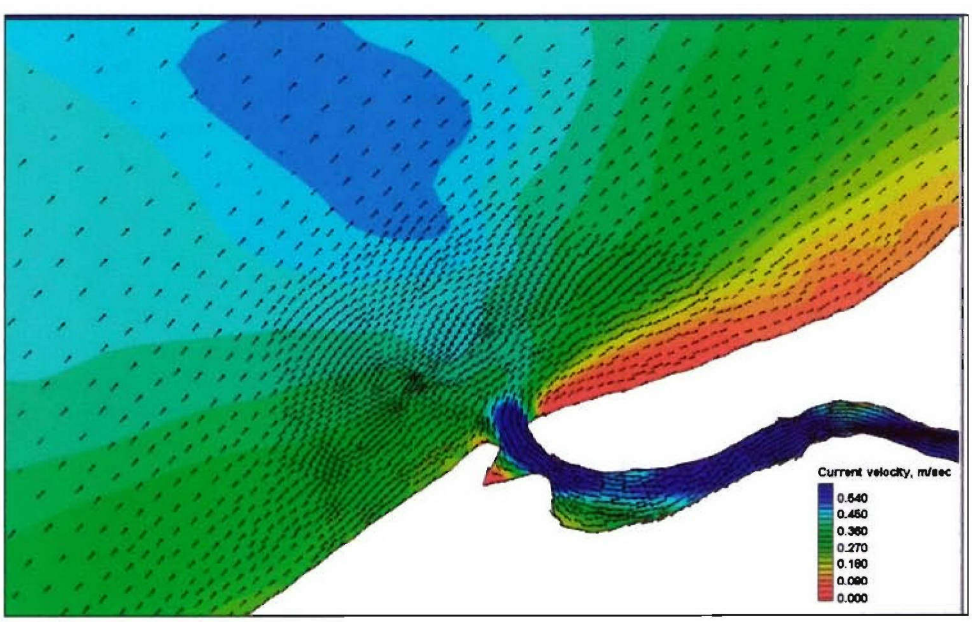

Figure 5-18e. Near-maximum offshore ebb-tide velocity, Mattituck Inlet offshore shoal area, 1830 GMT on 7 October 2002

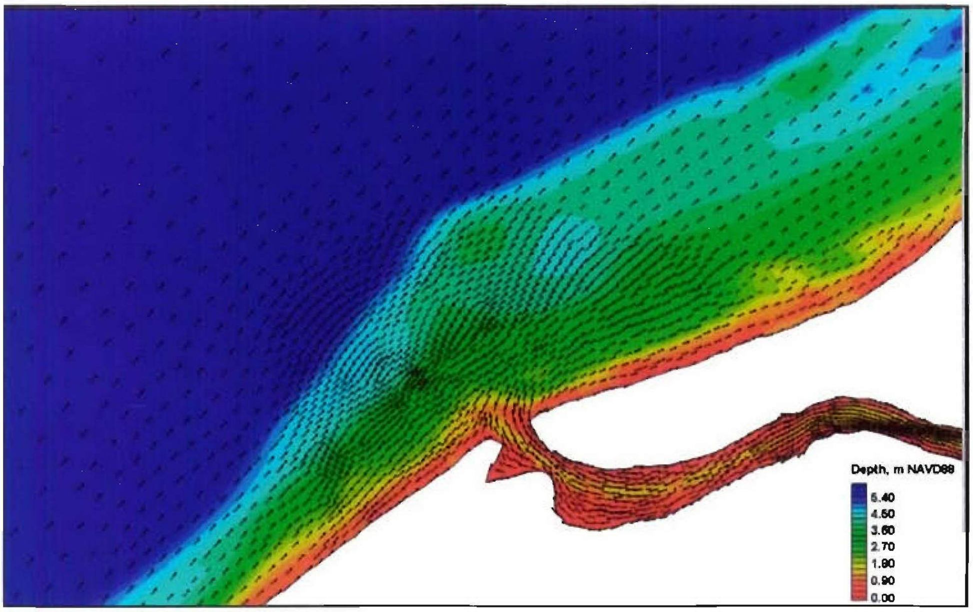

Figure 5-18f. Near-maximum offshore ebb-tide velocity and depth, Mattituck Inlet offshore shoal area, 1830 GMT on 7 October

Figure 5-18g illustrates current velocity at 2030 on 7 October 2002, the time of near-maximum inlet ebb current. Figure 5-18h displays these same current velocity vectors overlying the inlet and offshore shoal bathymetry. When the current is at its peak of near 1.87 m/sec, current velocity magnitudes diminish greatly with distance from the inlet entrance. The maximum tidal current velocity at the western extreme of the offshore shoal is calculated to be 0.36 m/sec. Figure 5-19 illustrates the locations of the current velocities plotted in Figures 5-20a and 5-20b, which include the offshore bathymetry. Current velocities shown in Figure 5-20b are nearly equivalent and are, therefore, difficult to discern.

For a configuration representing Mattituck Inlet in its natural state, prior to stabilization by jetties, the depth-averaged ebb-tidal current velocity at the offshore shoal is relatively weak, reaching about 0.35 m/sec for short durations. Such a current velocity exceeds the threshold of motion for medium sand grains, and the presence of wave orbital velocities near the bottom would further mobilize sand and make it available for transport. The direction of the calculated ebb current at maximum velocity is compatible with formation of an ebb shoal at the general location of the offshore shoal. However, the highly linear shape of the offshore shoal does not conform with the horizontal pattern of the ebb current, which tends to expand in areas beyond the location of the offshore shoal. Also, the relatively short duration when sand could be transported further indicates that the offshore shoal is not a relict ebb shoal of the historic Matttituck Inlet.

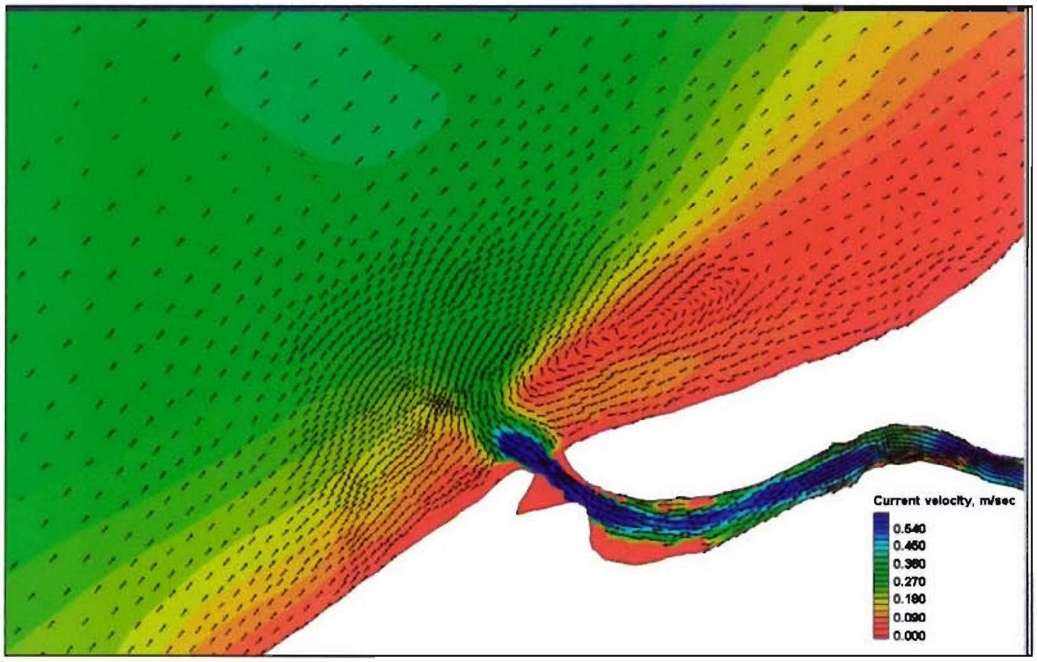

Figure 5-18g. Near-maximum inlet ebb-tide velocity, Mattituck Inlet offshore shoal area, 2030 GMT on 7 October 2002

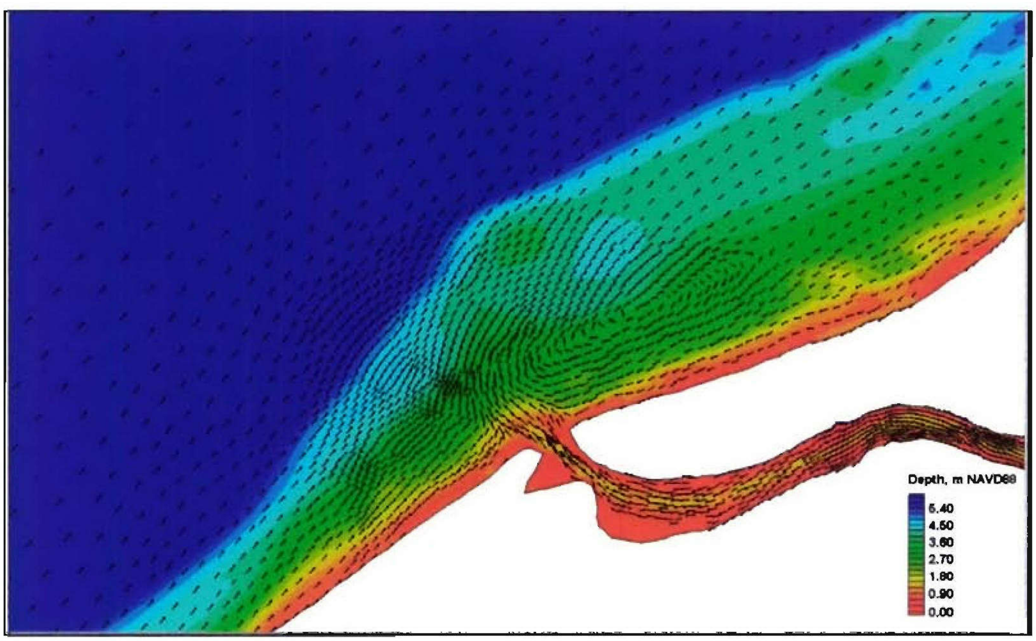

Figure 5-18h. Near-maximum inlet ebb-tide velocity and depth, Mattituck Inlet offshore shoal area, 2030 GMT on 7 October 2002

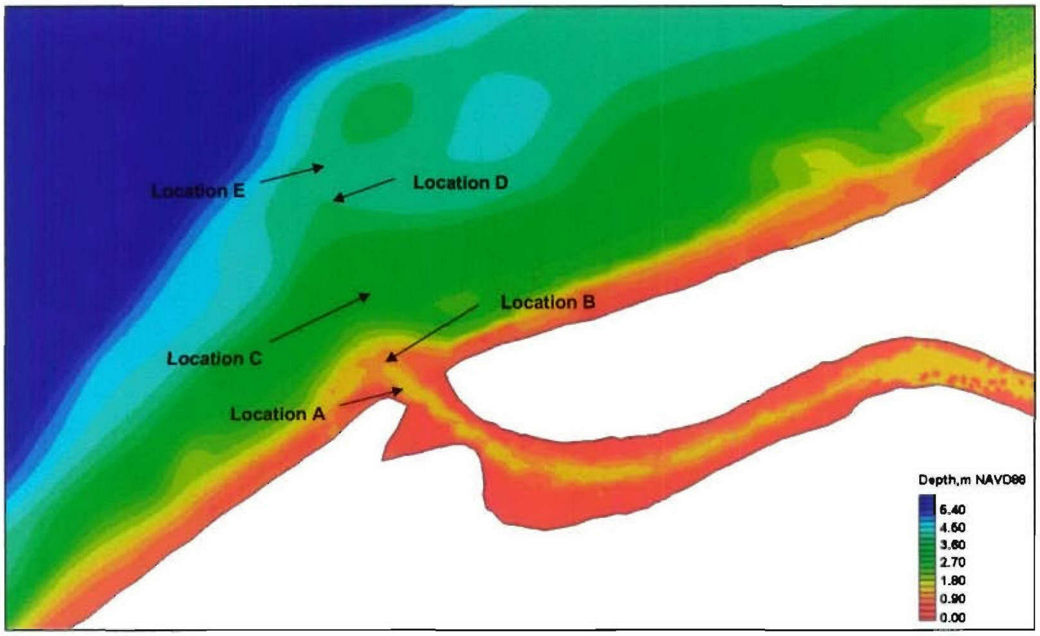

Figure 5-19. Current velocity comparison plot locations

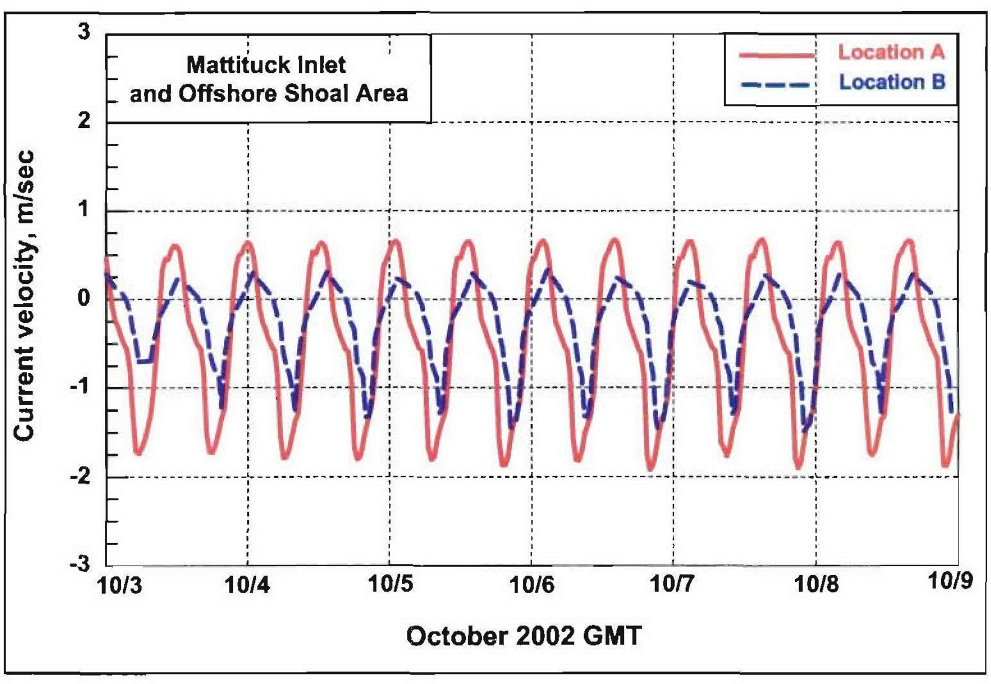

Figure 5-20a. Current velocity at Mattituck Inlet entrance (Locations A and B)

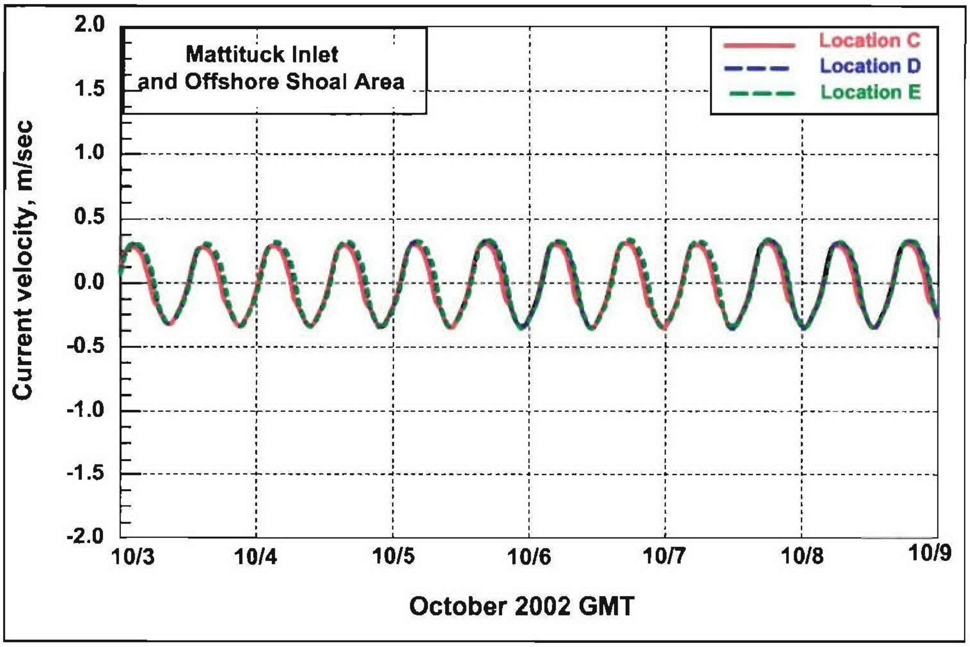

Figure 5-20b. Current velocity between Mattituck Inlet entrance and offshore shoal (Locations C through E)

Goldsmith Inlet

Water-surface elevation and current velocity at Goldsmith Inlet and Goldsmith Pond were calculated with the DYNLET model. DYNLET is well suited for applications to inlet and bay systems not expected to have complex horizontal circulation patterns. Goldsmith Inlet is such a system in which flow is directed primarily along the channel. The implicit solution method of DYNLET can efficiently calculate for shallow water and strong flows, for which an explicit solution method would require a small time-step. DYNLET can be considered as a "1-D plus" model in that it solves for current velocity at specified stations along each cross section as determined by the depth and bottom friction at each station. Water level at the nodes and velocity at the stations are calculated, with the velocity apportioned at the stations according to the bottom friction or conveyance of the channel (Amein and Kraus 1991).

Model validation

A DYNLET bathymetry grid for Goldsmith Inlet was established as a series of connected nodes that constitute a channel network originating directly offshore of Goldsmith Inlet and terminating in the back (southern end) of Goldsmith Pond (Figure 5-21). The model was forced at Node 1with water-level measurements adapted from the Mattituck Inlet jetty gauge, and a no-discharge boundary condition (current velocity of zero) was specified at Node 31 located at the back of the pond. The distance between nodes was determined so as to represent significant changes in morphology through consideration of channel or pond width, depth, and roughness of the bottom. The DYNLET grid of Goldsmith

Inlet originates approximately 200 m offshore. The distance between nodes within the channel and pond is approximately 20 m.

A uniform rectilinear bathymetry grid for Goldsmith Inlet and Goldsmith Pond was created by importing the October 2002 bathymetry survey data into DYNLET. Thirty-one nodes with cross sections of varying length were then generated (Figure 5-21). The October 2002 bathymetry survey is referenced to NAVD88 datum.

Initial DYNLET validation runs of the Goldsmith Inlet DYNLET model were not satisfactory because the channel dried occasionally in the simulations. As discussed in Chapter 4, some locations of the channel have elevations near msl. The source of the inaccuracy was concluded to be a discrepancy between the employed NAVD88 datum and msl elevation at Goldsmith Inlet. The relation between msl and NAVD88 at Goldsmith Inlet and Pond is not known. The October 2002 bathymetry survey found msl and NAVD88 to be within survey error offshore of Mattituck Inlet.

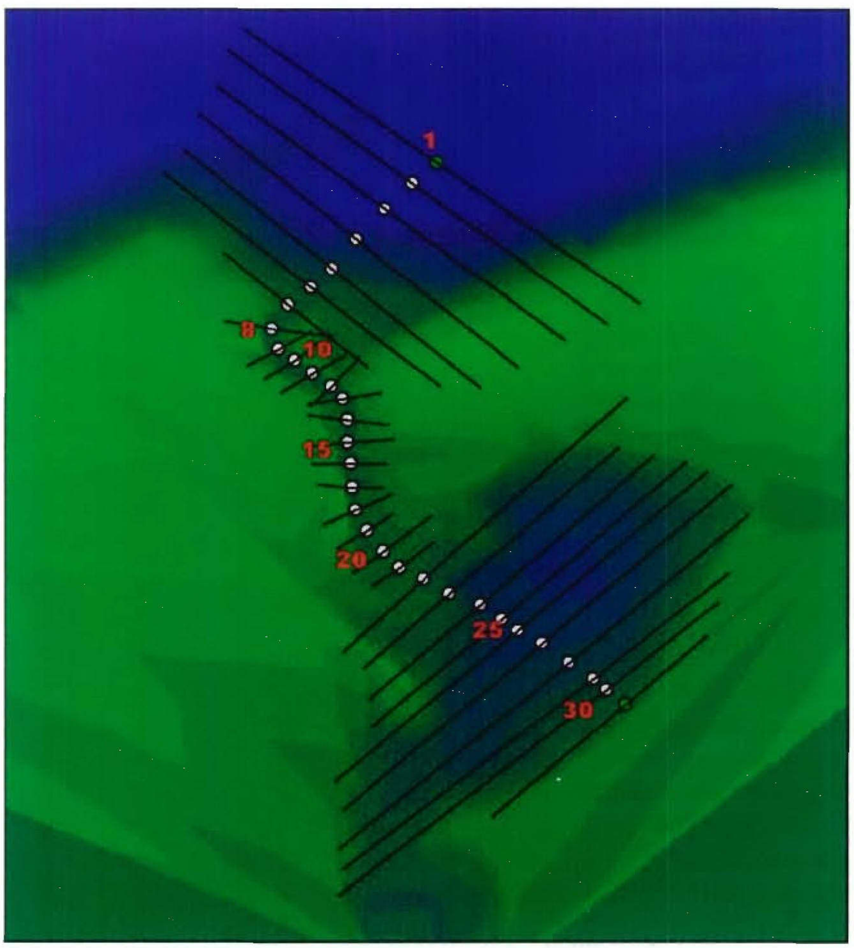

Figure 5-21. DYNLET grid of Goldsmith Inlet, with nodes and extents of nodal cross sections

Water-level measurements obtained offshore of Mattituck Inlet from 19 September to 8 October 2002 drove the model. It was found by numerical experimentation that raising the water-surface elevation in this data set by 0.25 m produced a successful model simulation that accurately represented the tidal signature recorded at Goldsmith Pond, while not drying the channel. The authors have never observed the inlet channel to dry, even during low tide. DYNLET model water-level calculations are referenced to NAVD88. The results were adjusted by subtracting 0.25 m to account for the datum shift of the input water-surface elevation. A shift upward in the driving water level is functionally equivalent to shifting the entire bathymetry grid down by the same amount.

DYNLET was calibrated by specifying larger values of the bottom friction coefficient in the Goldsmith Inlet channel, where small rocks are present and can protrude above the water surface, some of which may be remnants from jetty construction. The default value of Manning's n of 0.025 m/sec$^{1/3}$ was maintained at most nodes, but in the channel where rocks and roiling water are seen, the value was increased to 0.03 to 0.04. The time-step in the model was set to 30 sec.

In initial model runs, calculated water level at the pond gauge lagged the measurements by 36 min. A lag between calculations and measurements is expected, because Goldsmith Inlet lies 5 km east of Mattituck Inlet, and the tidal wave travels from east to west. The tidal record offshore of Mattituck Inlet was therefore adjusted forward 36 min to account for the time of tidal wave travel between the location of the tidal record and the location of the input driving the model. This adjustment implies that the tidal wave moves westward at about 0.23 m/sec along the shallow water of this portion of the north shore of Long Island.

The input boundary condition (Node 1) and the first DYNLET water-level calculation (Node 2) for the period of data collection (20 September – 8 October 2002) are plotted in Figure 5-22a. Figure 5-22b shows these water levels for the 5-8 October 2002, spring tide. A comparison of water-level measurements at Goldsmith Inlet for 20 September – 8 October 2002 and the corresponding DYNLET calculations (at Node 30) are shown in Figure 5-22c, and Figure 5-22d gives this comparison for a period of spring tide.

Current velocity measurements taken within Goldsmith Inlet for a short interval on 8 October are compared to corresponding DYNLET current velocity calculations (at Nodes 13 and 14) in Figures 5-23a and 5-32b. The calculations well reproduce the limited length of the measurements. The current velocity is seen to be strong, exceeding 1 m/sec, and the calculated current is flood dominant, meaning that the flood current has a higher peak velocity than ebb, but shorter duration. This dominance has implications for sediment transport in the inlet, discussed in the following paragraphs.

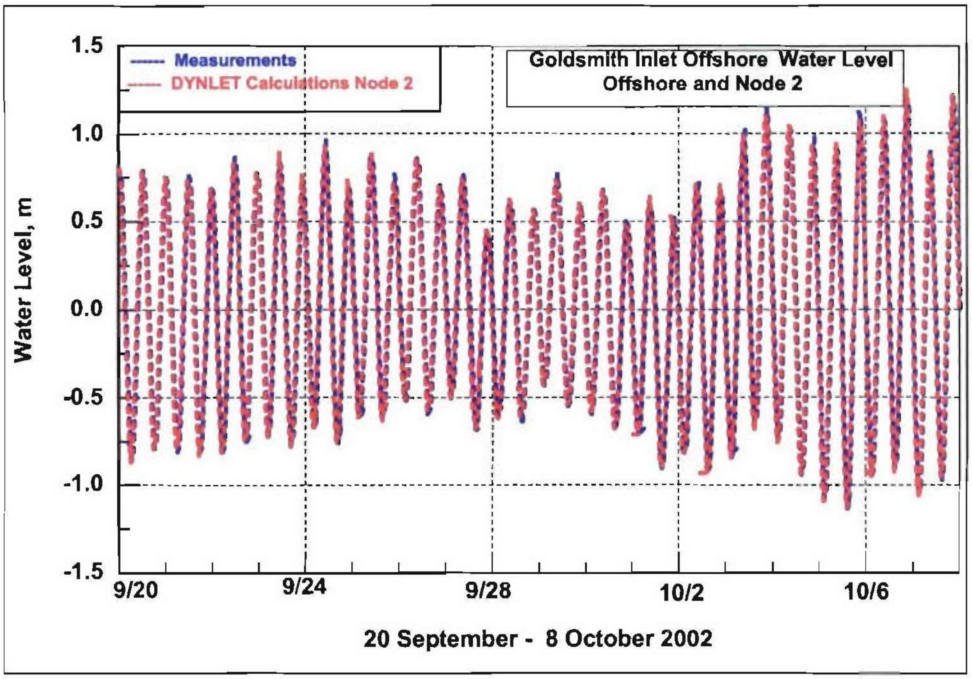

Figure 5-22a. Water-level measurements offshore of Goldsmith Inlet and Node 2 calculations, 20 September - 8 October 2002

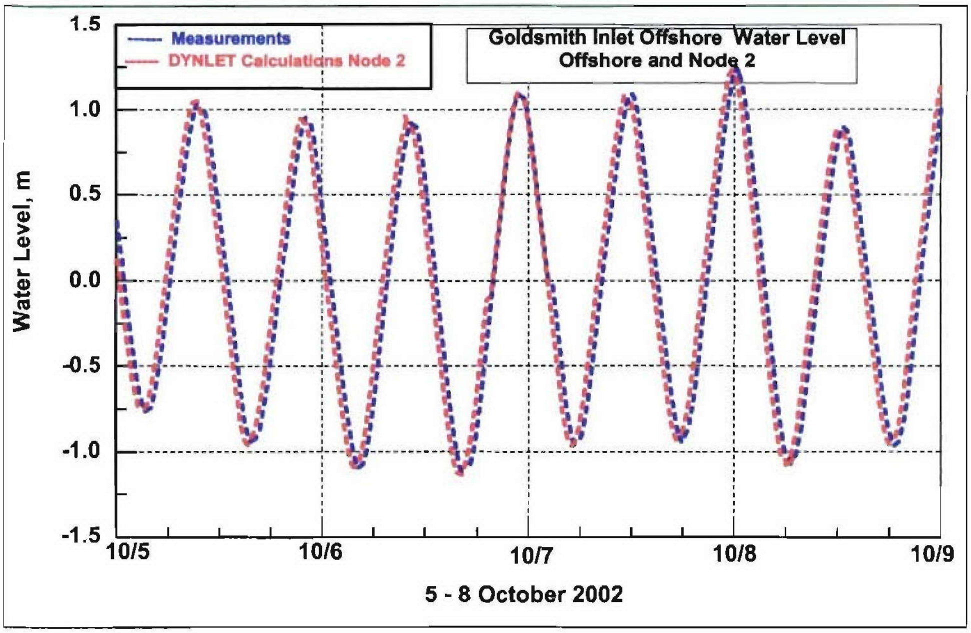

Figure 5-22b. Water-level measurements offshore of Goldsmith Inlet and Node 2 calculations, 5-8 October 2002

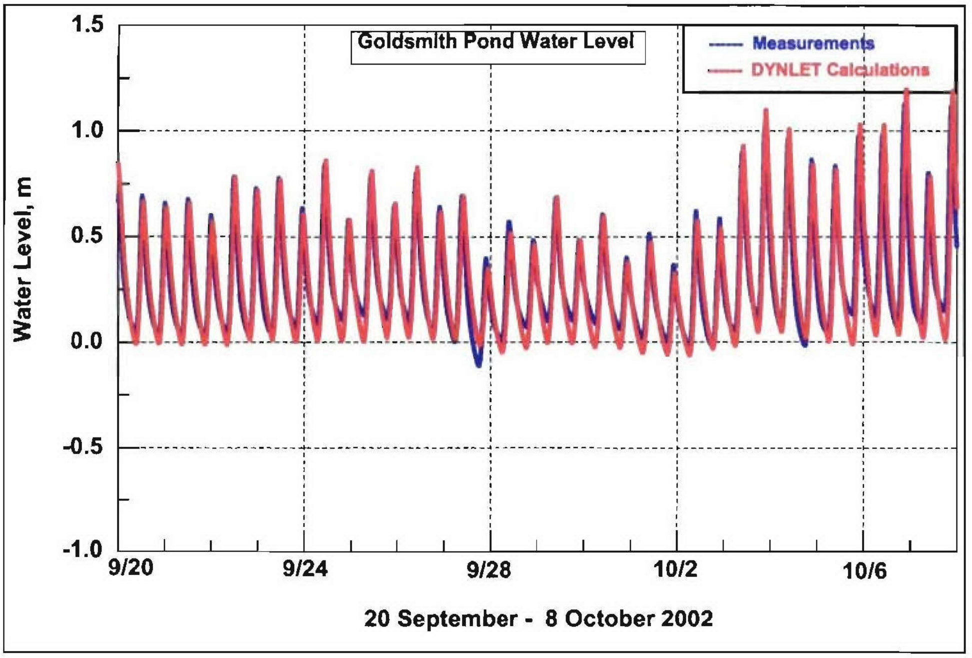

Figure 5-22c. Water-level measurements at Goldsmith Pond and DYNLET Node 30 calculations, 20 September - 8 October 2002

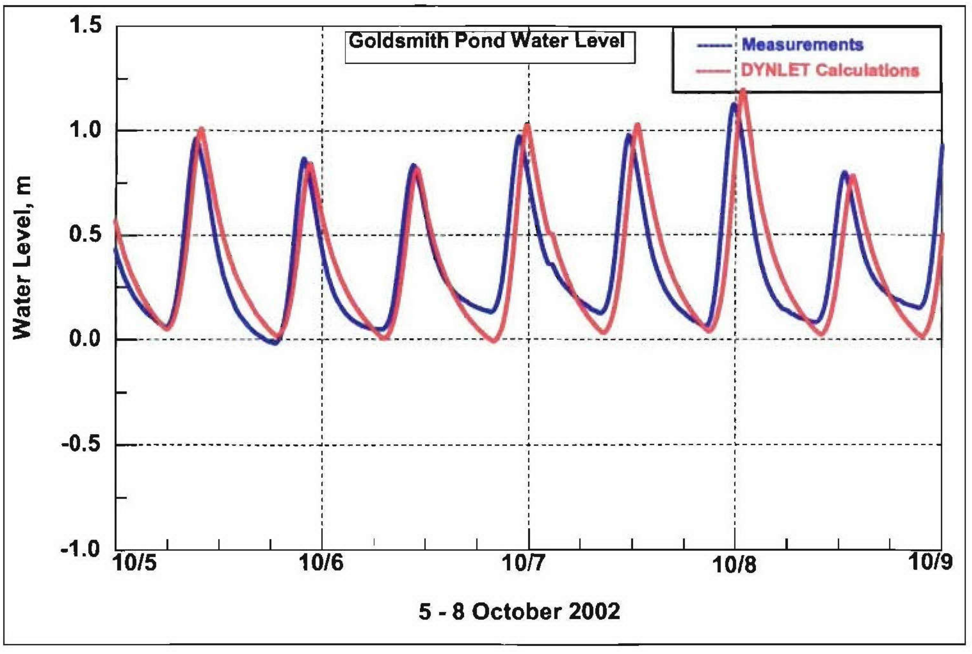

Figure 5-22d. Water-level measurement offshore of Goldsmith Pond and DYNLET Node 30 calculations, 5-8 October 2002

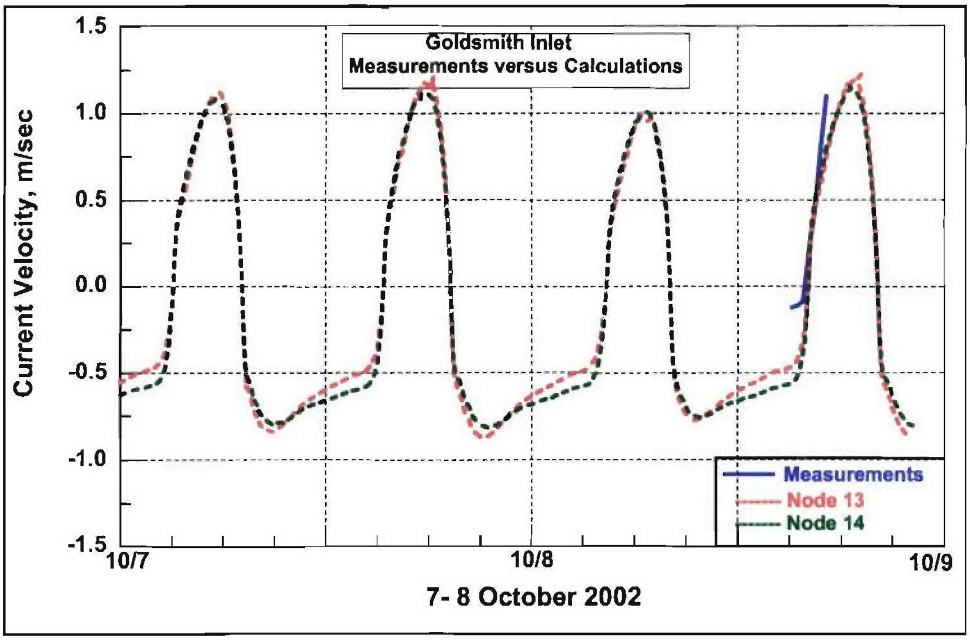

Figure 5-23a. Current velocity measurement and calculated velocities at Nodes 13 and 14, 7-8 October 2002

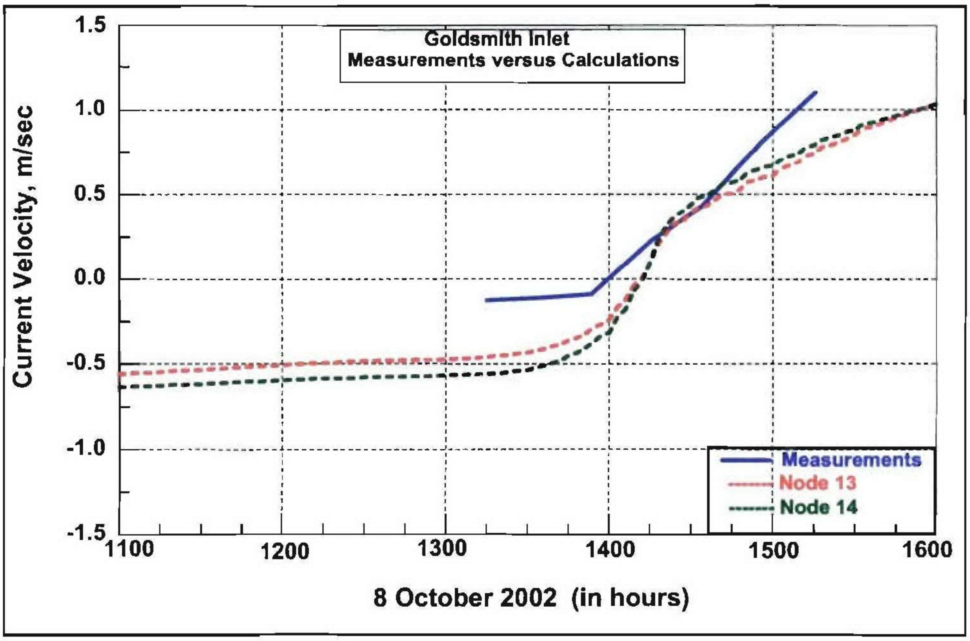

Figure 5-23b. Current velocity measurement and Nodes 13 and 14 calculations, 8 October 2002

Discussion of tidal asymmetry

Table 5-1 lists the mean and maximum depths for the DYNLET nodes. Depths are referenced to NAVD88 and were extracted from the bathymetry data of 6-8 October 2002 with a DYNLET interface utility.

Table 5-1
Goldsmith Inlet DYNLET Node Depths

Node	Mean Depth (m, NAVD88)	Maximum Depth (m, NAVD88)
1	3.57	5.74
2	3.25	5.50
3	2.81	4.23
4	2.36	3.63
5	1.66	2.59
6	0.87	1.98
7	0.71	1.8
8	0.53	1.2
9	0.34	0.50
10	0.31	0.44
11	0.31	0.42
12	0.43	0.61
13	0.46	0.61
14	0.31	0.46
15	0.45	0.63
16	0.3	0.57
17	0.19	0.30
18	0.12	0.15
19	0.14	0.22
20	0.13	0.15
21	0.1	0.14
22	0.52	1.16
23	0.92	1.6
24	1.23	1.84
25	1.29	1.85
26	1.10	1.85
27	1.09	1.83
28	0.91	1.42
29	0.69	1.01
30	0.44	0.90

Calculated tidal water levels exhibit strong asymmetric behavior at Goldsmith Inlet. Figures 5-24a through 5-24f plot water level at selected nodes along the inlet channel and the total discharge at each of these nodes. Each figure plots nodes against the input boundary condition (Node 1) and calculated elevation at a selected preceding node. The figures contain comparisons for a spring tide, 5-8 October 2002.

At nodes located near the forcing in Long Island Sound, the water-level signal is sinusoidal. With distance into the inlet, the water-level signal becomes more asymmetric, achieving a greater maximum on flood than on ebb, and with a shorter time of flood than ebb. Such water-level behavior is called flood dominance. There are three possible contributions the asymmetry. The first and likely dominant contribution is the presence of sills in the inlet. The higher water of flood can enter the inlet rapidly, because the tide wave celerity is given by the square root of the product of gravitational acceleration and depth. On the lower water of ebb, the depth is less, and the water flow must be slower. Connected with this hypsometric change in wave speed is the fact that bottom friction will retard flow more strongly for shallower water.

A second contribution to the asymmetry in water-level signal in the inlet and pond is the preferential drainage in the wetland surrounding Goldsmith Pond. It is expected that flooding water will enter the wetland more rapidly than the draining water on ebb. A third contribution for the asymmetry is the nonlinear interactions of flow components introduced by the bottom friction terms and advective terms in the equations of motion.

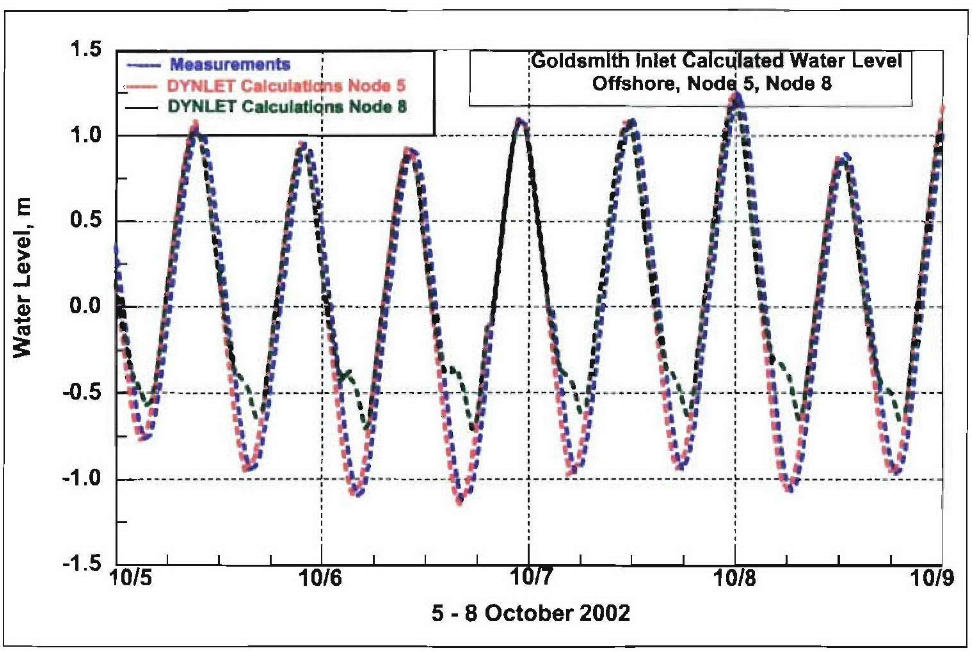

Figure 5-24a. Water-level measurements offshore of Goldsmith Inlet and DYNLET Nodes 5 and 8 calculations, 5-8 October 2002

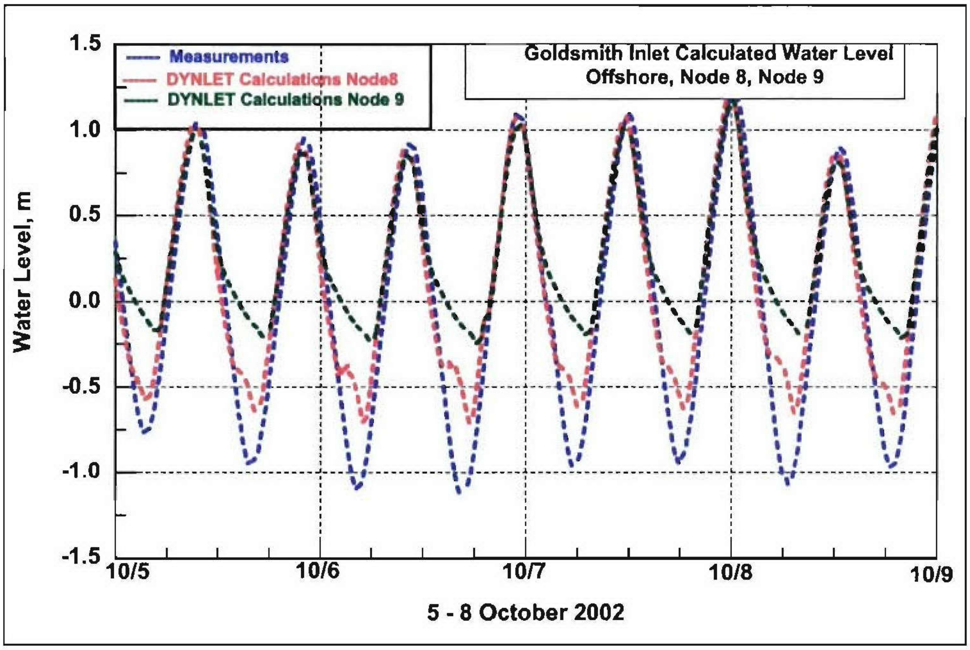

Figure 5-24b. Water-level measurements offshore of Goldsmith Inlet and DYNLET Nodes 8 and 9 calculations, 5-8 October 2002

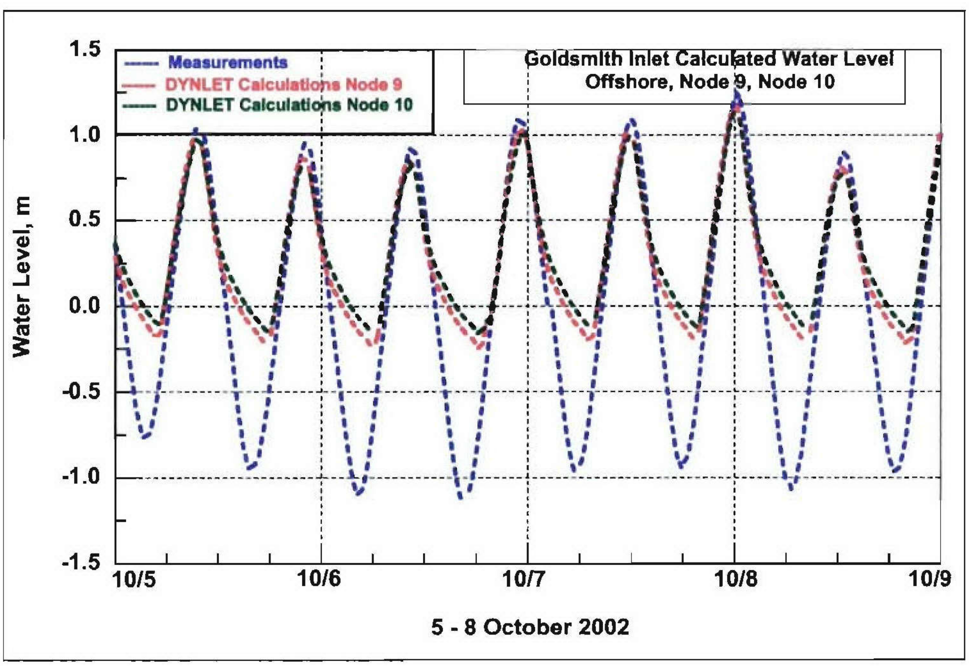

Figure 5-24c. Water-level measurements offshore of Goldsmith Inlet and DYNLET Nodes 9 and 10 calculations, 5-8 October 2002

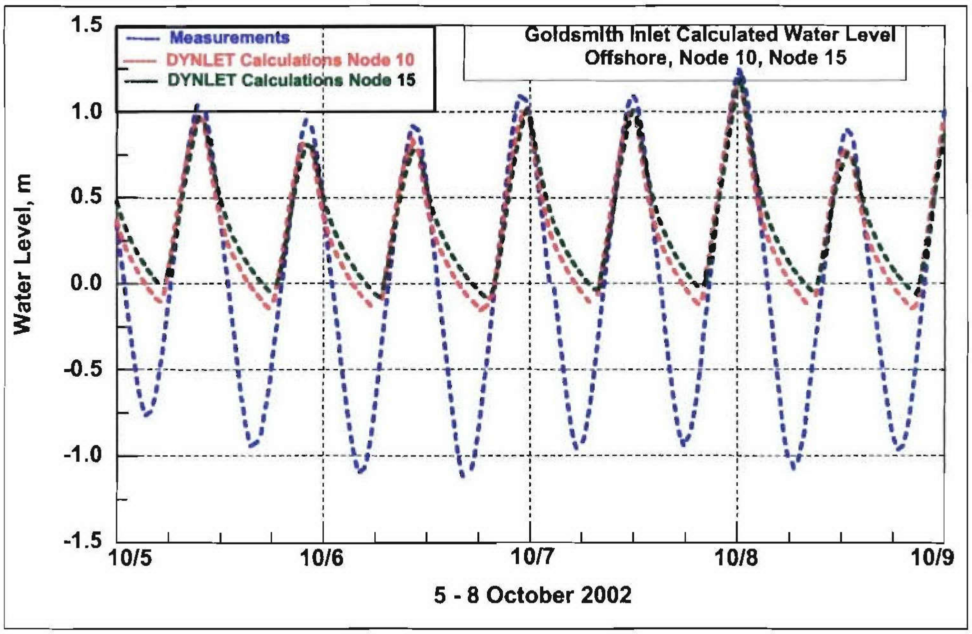

Figure 5-24d. Water-level measurements offshore of Goldsmith Inlet and DYNLET Nodes 10 and 15 calculations, 5-8 October 2002

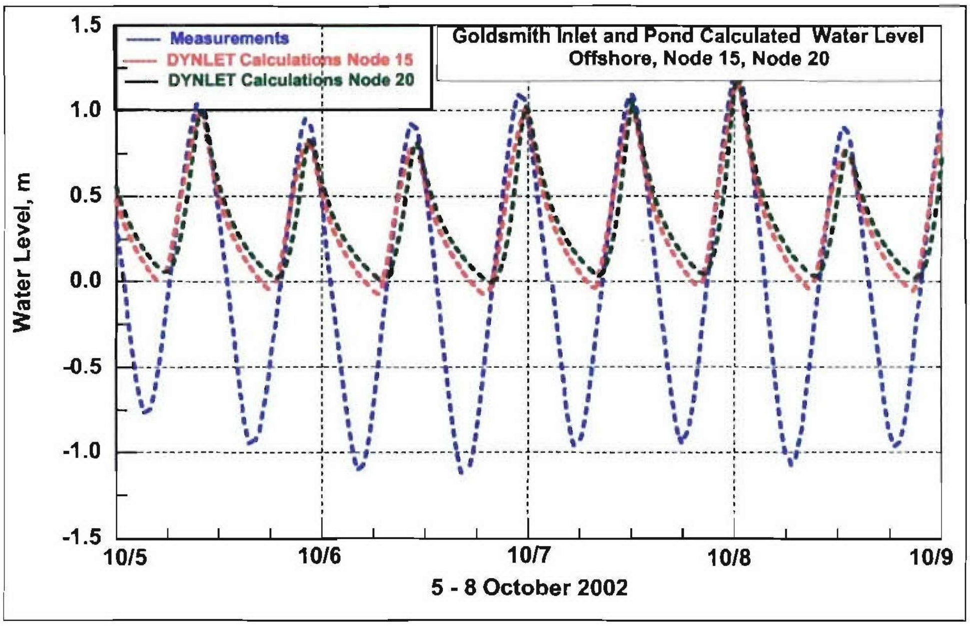

Figure 5-24e. Water-level measurements offshore of Goldsmith Inlet and DYNLET Nodes 15 and 20 calculations, 5-8 October 2002

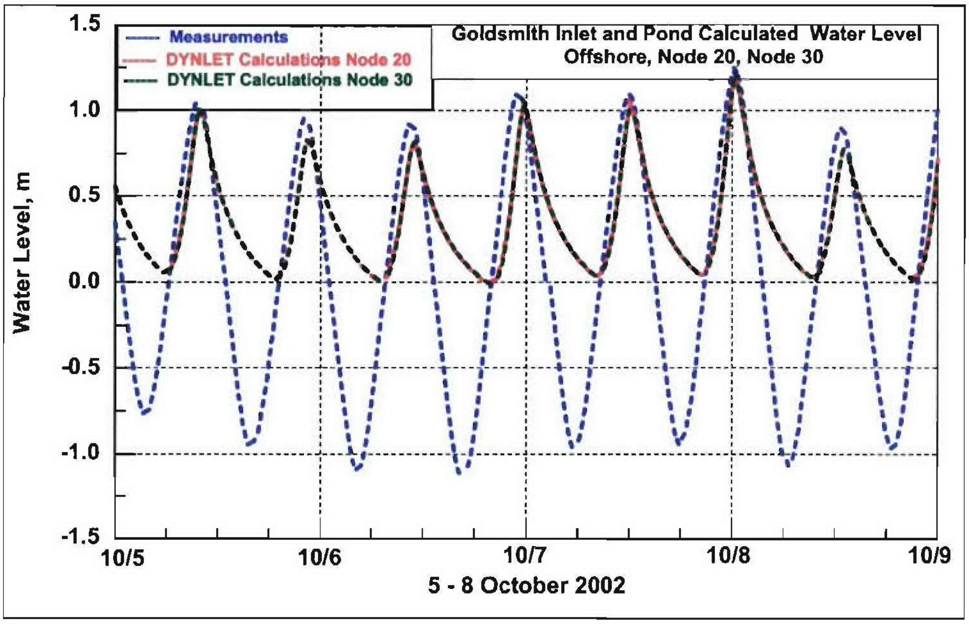

Figure 5-24f. Water-level measurements offshore of Goldsmith Inlet and DYNLET Nodes 20 and 30 calculations, 5-8 October 2002

Figures 5-25a to 5-25c plot the total discharge for the nodes referenced in Figures 5-24a through 5-24e. Flood currents are denoted as positive and ebb current as negative. The calculated discharge rates in the channel again exhibit a trend of flood dominance (stronger flood flow for shorter duration than that of the ebb flow).

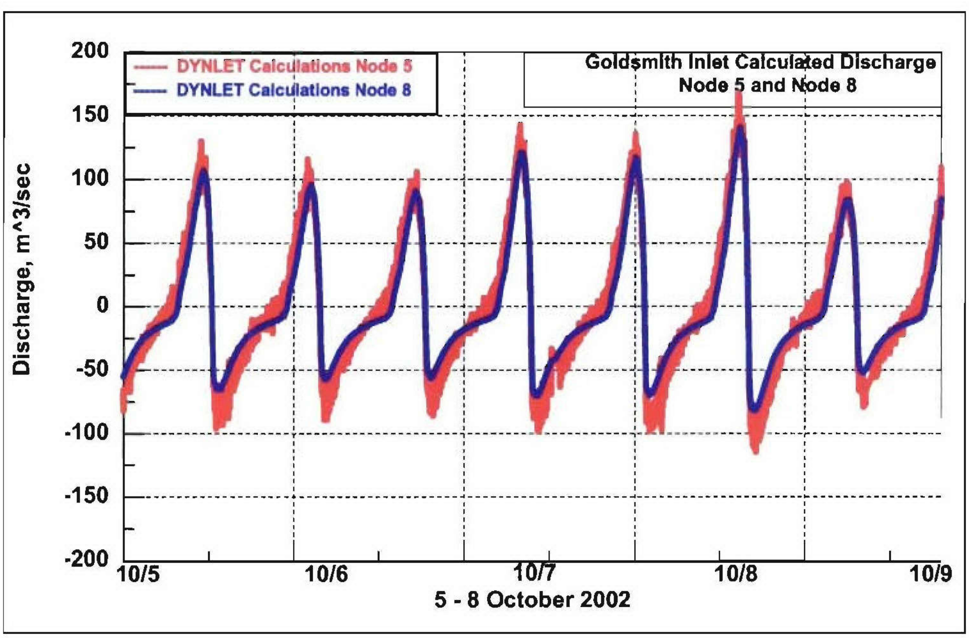

Figure 5-25a. Discharge at Goldsmith Inlet, DYNLET Nodes 5 and 8 calculations, 5-8 October 2002

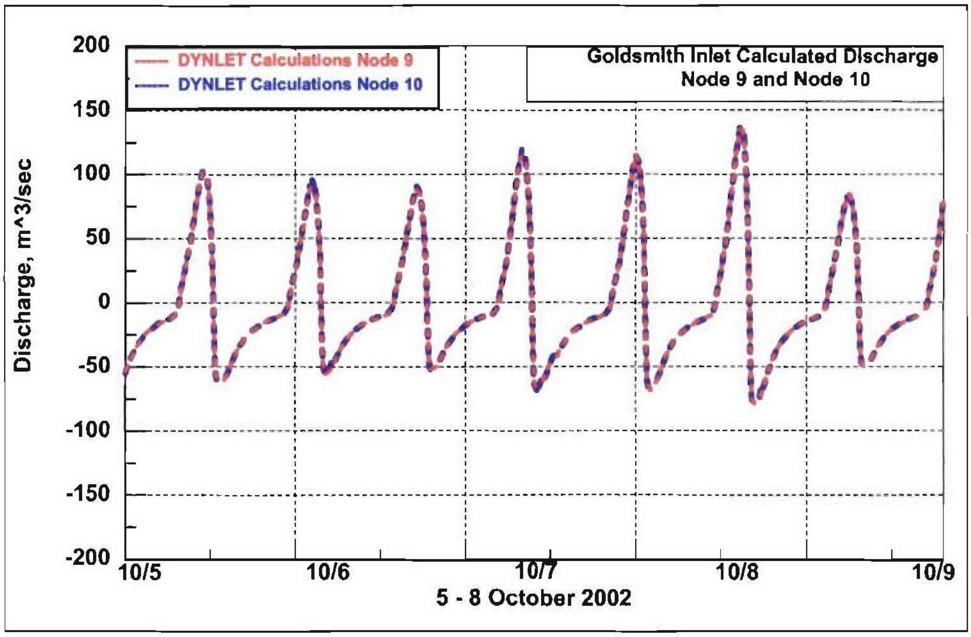

Figure 5-25b. Discharge at Goldsmith Inlet, DYNLET Nodes 9 and 10 calculations, 5-8 October 2002

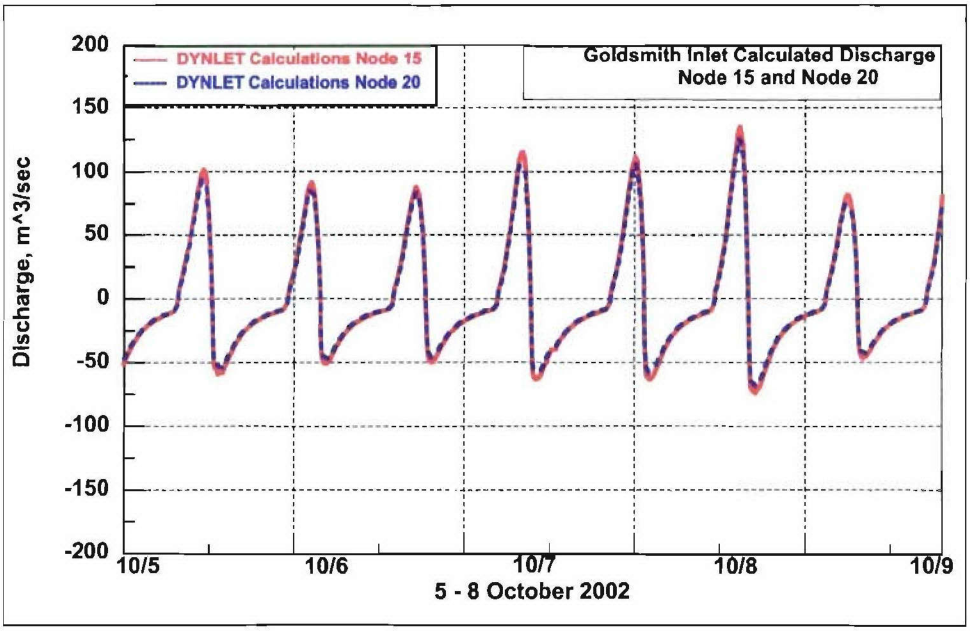

Figure 5-25c. Discharge at Goldsmith Inlet, DYNLET Nodes 15 and 20 calculations, 5-8 October 2002

Discussion of current velocity

Figures 5-26a through 5-26k plot current velocity at selected nodes across the DYNLET channel. Each figure displays calculated velocity at selected nodes and the calculated offshore velocity (Node 1), as well as a calculated velocity at a selected preceding node exhibiting a significant change in velocity. The plots contain comparisons for spring tide, 5-8 October 2002. The areas under velocity curves above and below may not be equal because these curves represent velocity at one station (one point) at a particular node. The current velocity at other stations may have different and compensating behavior. In contrast, total discharge at cross sections (all stations summed) as given in Figures 5-25a to 5-25c must show the same amount of water entering on flood as exiting on ebb for any tidal cycle (assuming no freshwater inputs to the pond).

The model calculations clearly demonstrate a relationship between limiting depths at Goldsmith Inlet and maximum velocity through it. Control by limiting depth is evident at Node 8 during times of flood current and at Nodes 8 and 21 during times of ebb current. Maximum calculated current velocity within the channel at Goldsmith Inlet increases by an order of magnitude between nodes as the flow enters the inlet mouth between Nodes 6 and 7, owing to the constriction and decrease in depth. At Node 7, the inlet mouth, the flow is still predominantly sinusoidal, but with a shift toward flood dominance. With distance into the inlet, similar to findings for calculated water level, the signal for the current velocity becomes more flood dominant.

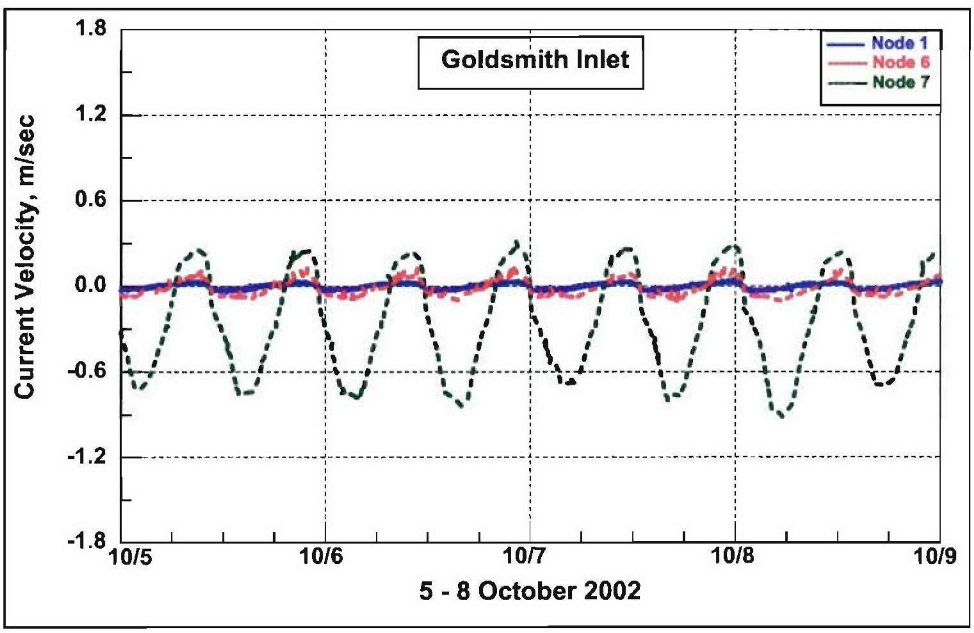

Figure 5-26a. Current velocity calculations offshore of Goldsmith Pond and DYNLET Nodes 6 and 7 calculations, 5-8 October 2002

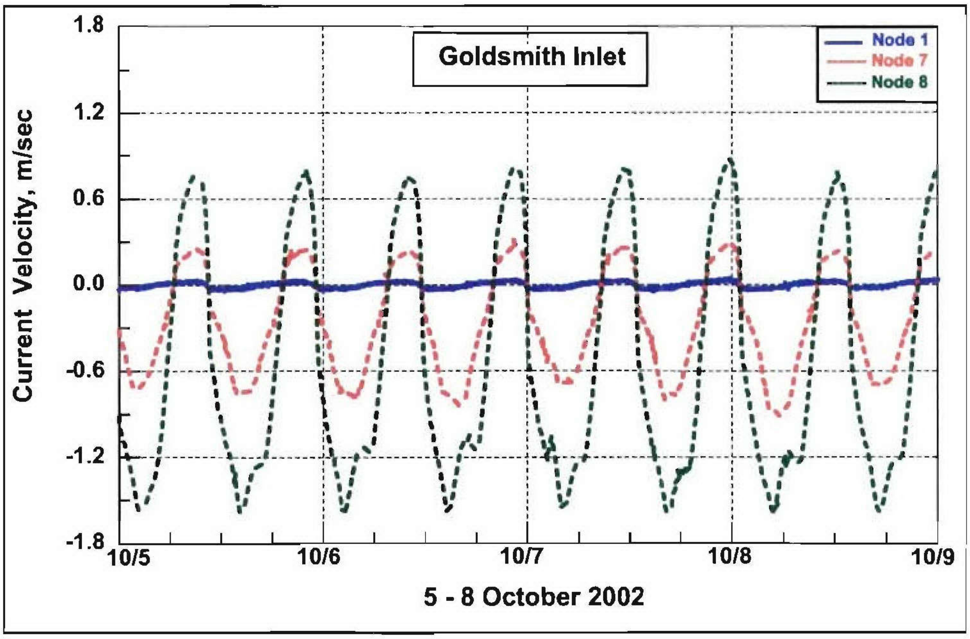

Figure 5-26b. Current velocity calculations offshore of Goldsmith Inlet and DYNLET Nodes 7 and 8 calculations, 5-8 October 2002

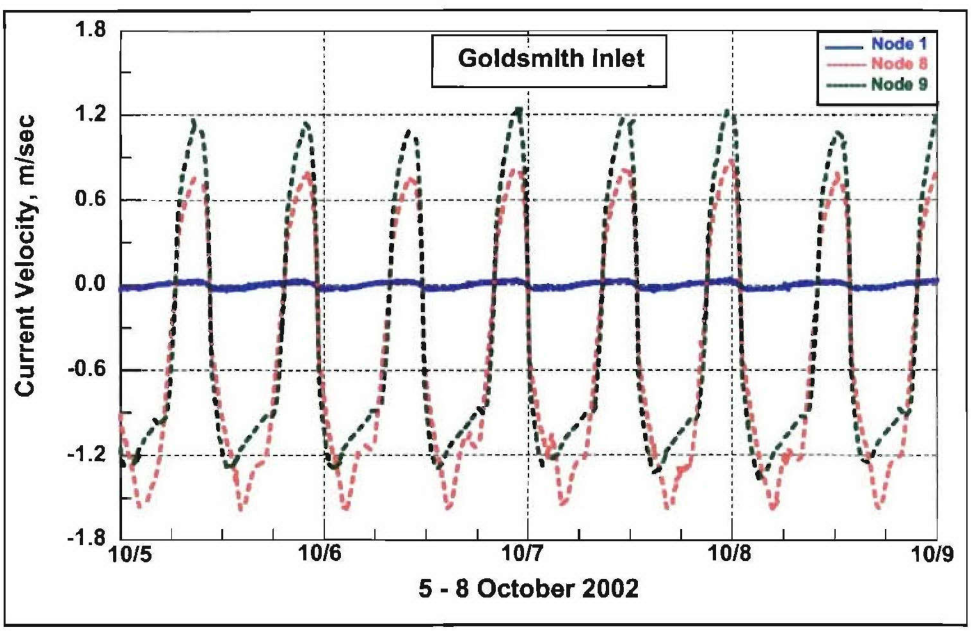

Figure 5-26c. Current velocity calculations offshore of Goldsmith Pond and DYNLET Nodes 8 and 9 calculations, 5-8 October 2002

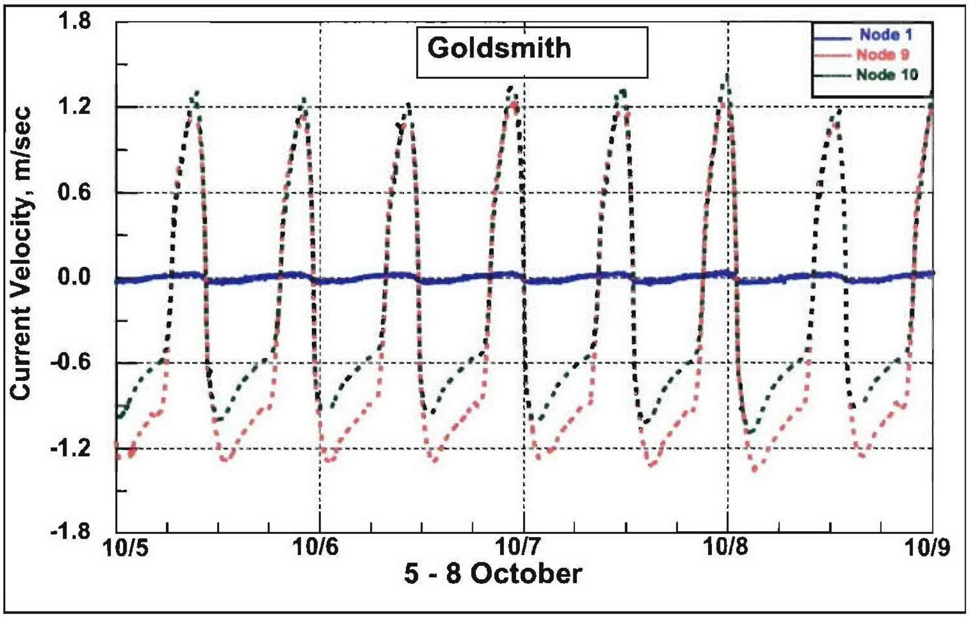

Figure 5-26d. Current velocity calculations offshore of Goldsmith Pond and DYNLET Nodes 9 and 10 calculations, 5-8 October 2002

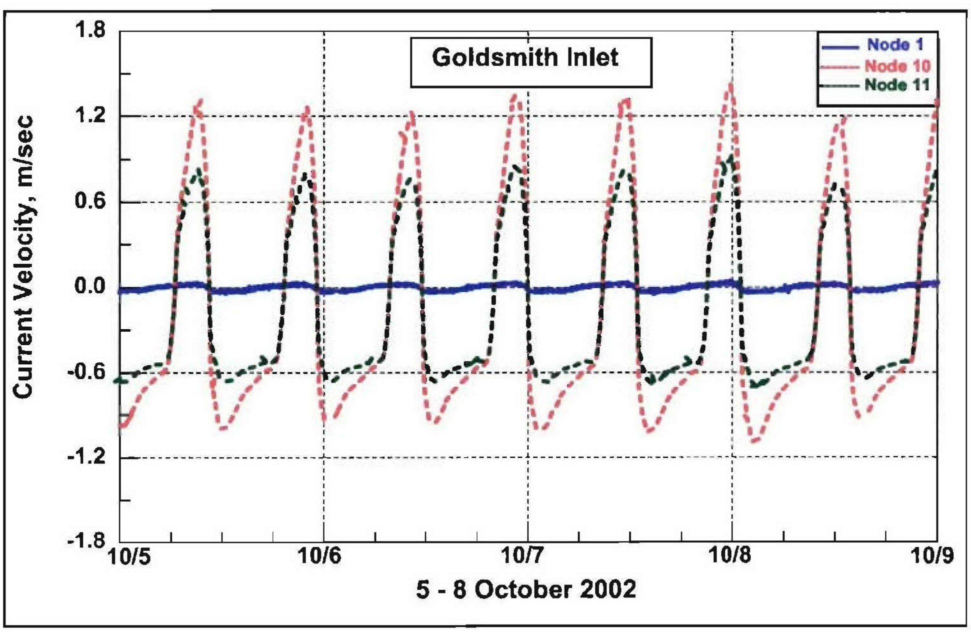

Figure 5-26e. Current velocity calculations offshore of Goldsmith Pond and DYNLET Nodes 10 and 11 calculations, 5-8 October 2002

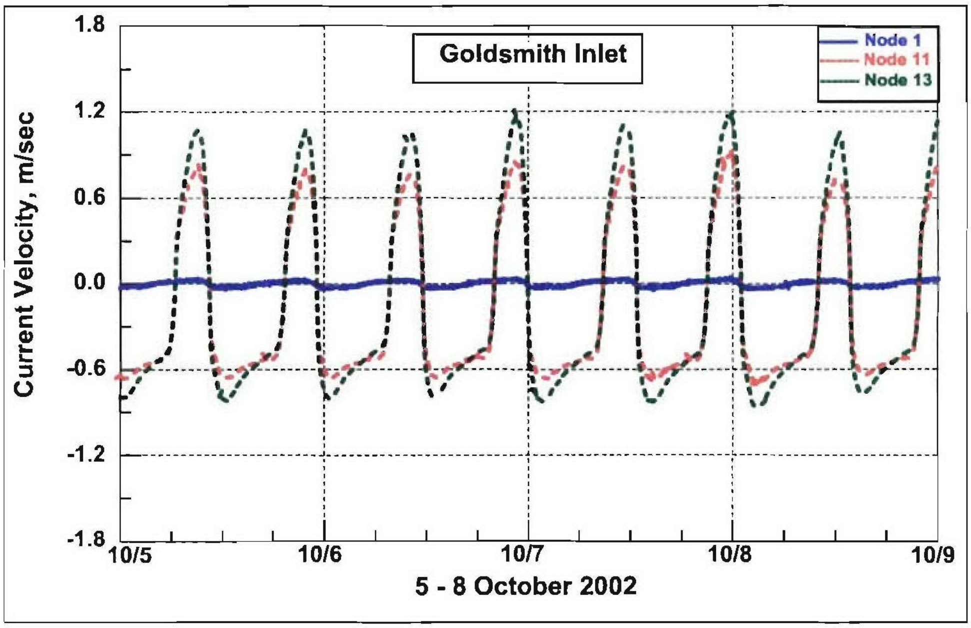

Figure 5-26f. Current velocity calculations offshore of Goldsmith Pond and DYNLET Nodes 11 and 13 calculations, 5-8 October 2002

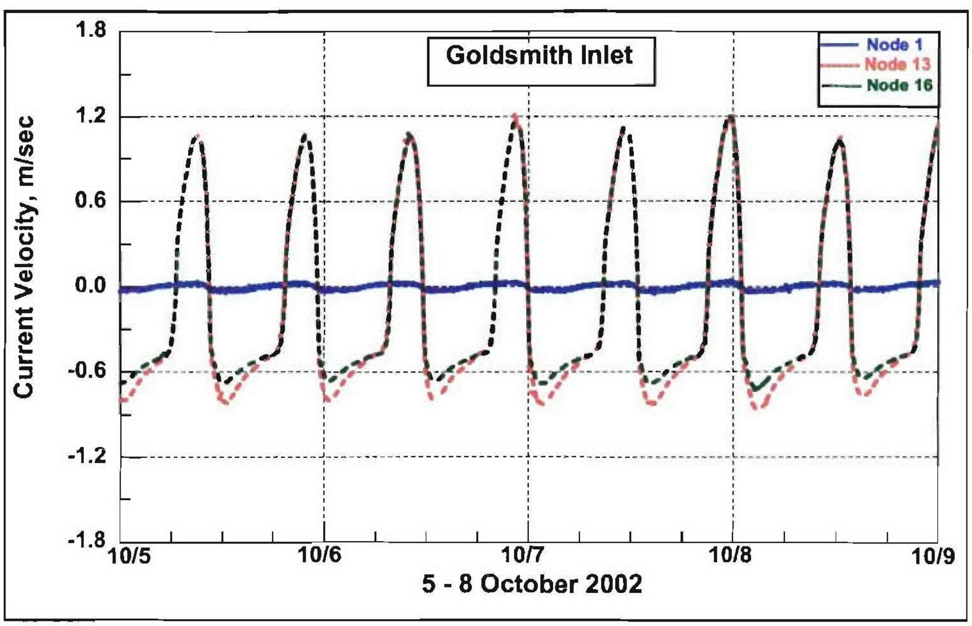

Figure 5-26g. Current velocity calculations offshore of Goldsmith Pond and DYNLET Nodes 13 and 16 calculations, 5-8 October 2002

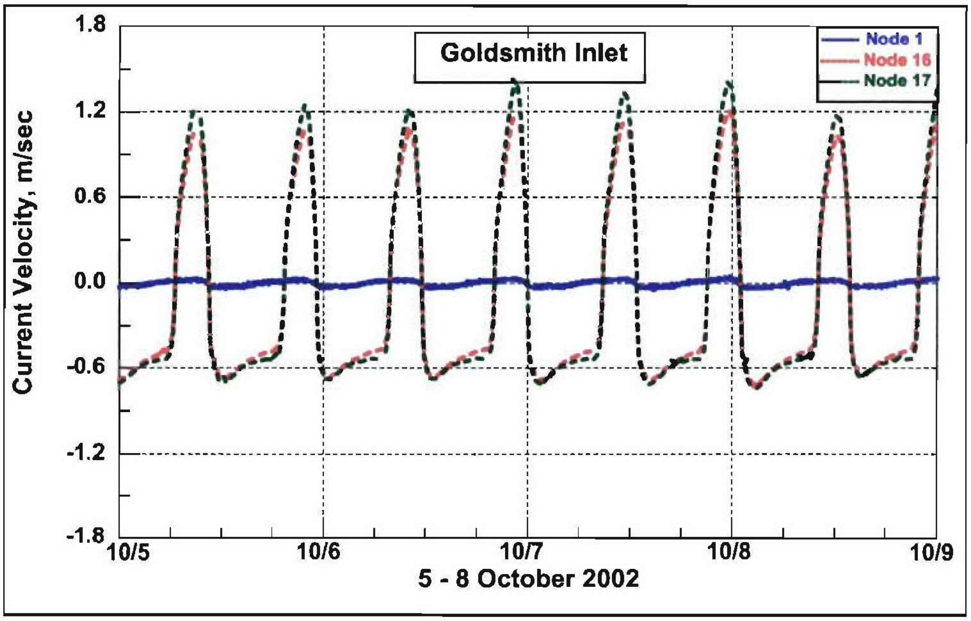

Figure 5-26h. Current velocity calculations offshore of Goldsmith Pond and DYNLET Nodes 16 and 17 calculations, 5-8 October 2002

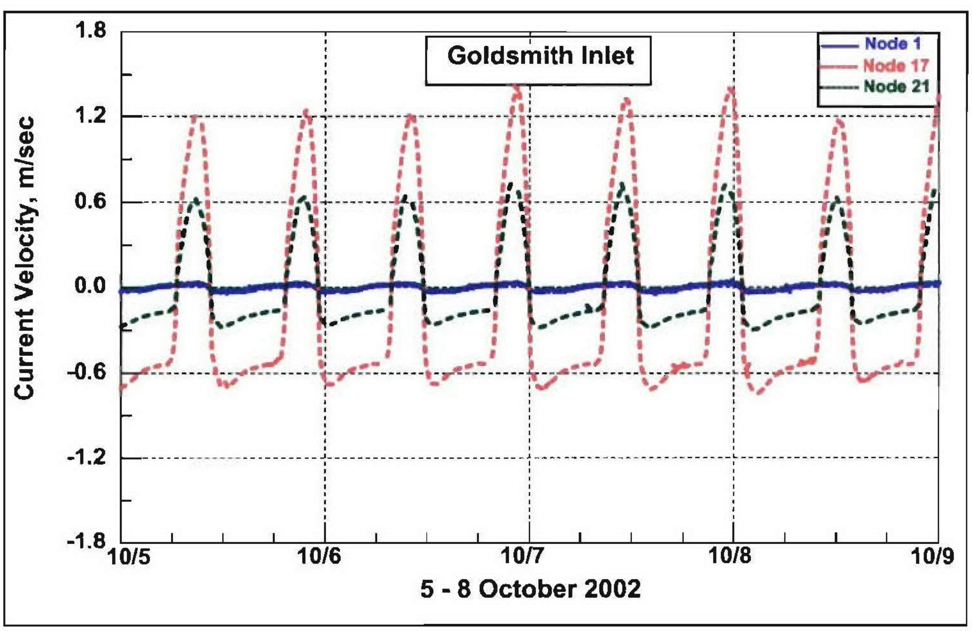

Figure 5-26i. Current velocity calculations offshore of Goldsmith Pond and DYNLET Nodes 17 and 21 calculations, 5-8 October 2002

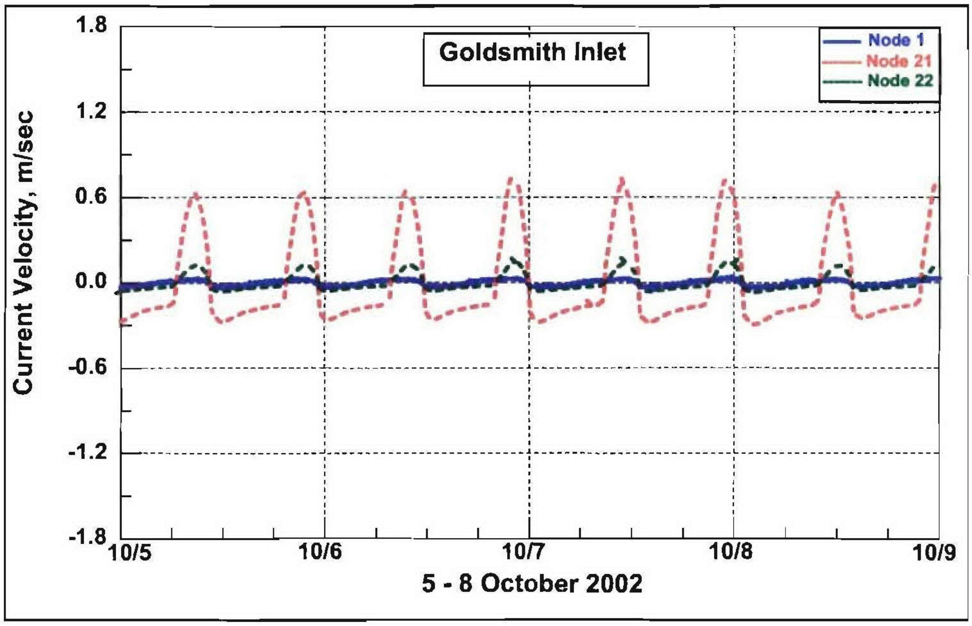

Figure 5-26j. Current velocity calculations offshore of Goldsmith Pond and DYNLET Nodes 21 and 22 calculations, 5-8 October 2002

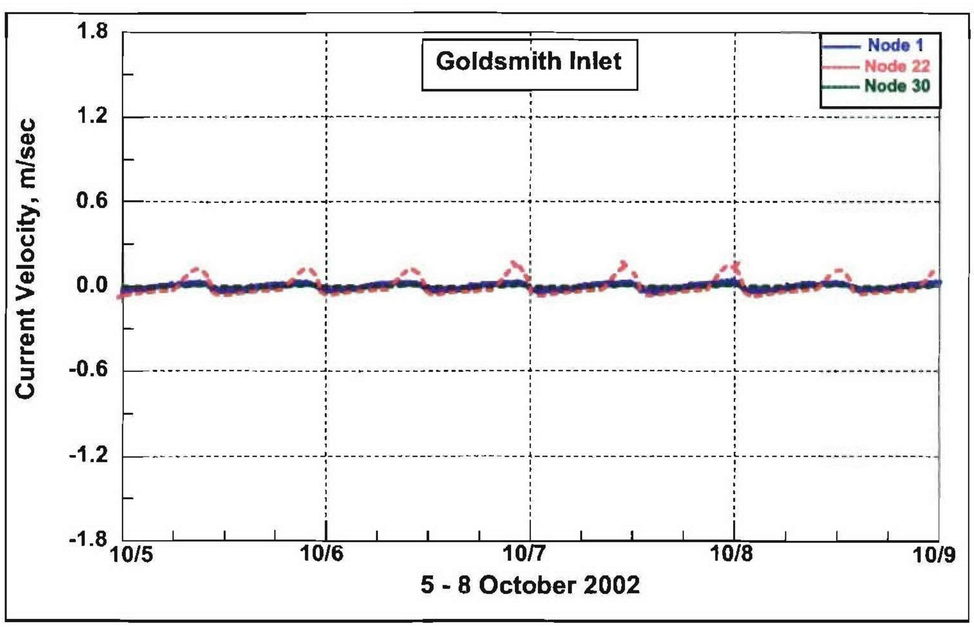

Figure 5-26k. Current velocity calculations offshore of Goldsmith Pond and DYNLET Nodes 22 and 30 calculations, 5-8 October 2002

Figure 5-27 plots the maximum calculated velocity at each node for a spring flood tide and the subsequent ebb tide on 7 October 2002, together with the elevation. The flood current had maximum velocity of 1.43 m/sec for this time interval. Strong flood-tidal currents persist to the exit of the channel into Goldsmith Pond. The ebb current at the mouth exceeds 1 m/sec.

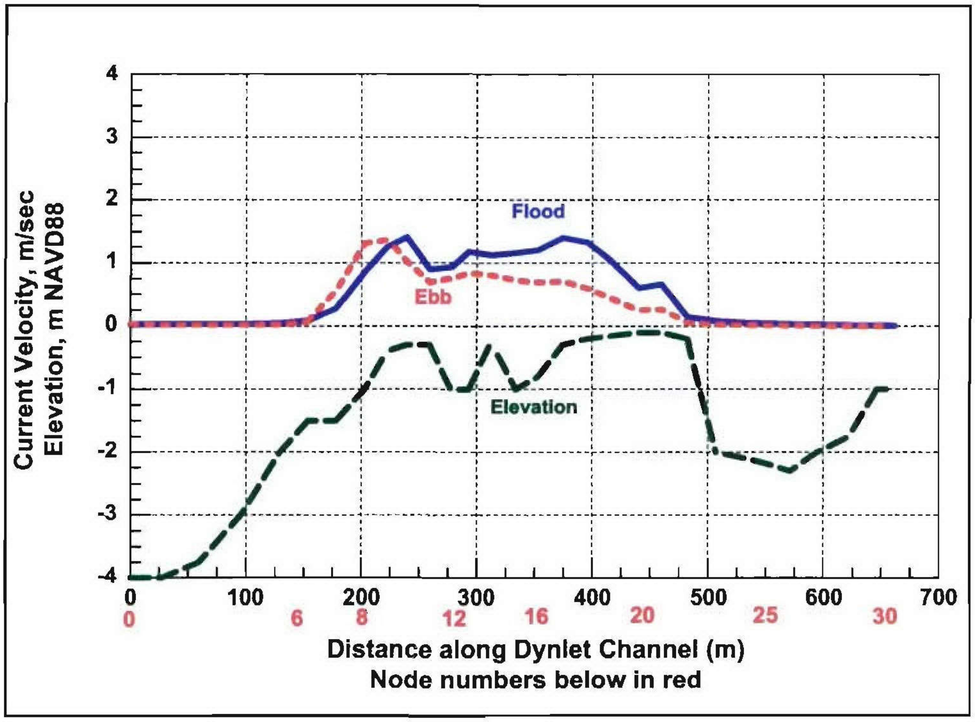

Figure 5-27. Maximum calculated flood- and ebb-spring-tide current speed and water elevation at Goldsmith Inlet, 7 October 2002

Figure 5-28a and 5-28b display composite surfaces of maximum calculated flood and ebb velocity, respectively, at all node stations for hours 400 to 450 of the model run. Larger-scale views of these velocities within the channel are shown in Figures 5-28c and 5-28d. The time interval corresponds to 7-8 October 2002, a spring tide, giving maximum velocities experienced at these locations. Figure 5-28e shows a difference map between these surfaces that illustrates the magnitude of current velocity asymmetry throughout the surface.

A strong flood current persists over the entire channel and into the pond, whereas the ebb current is weak over much of the channel and pond, except at the mouth of the inlet. Such behavior would tend to transport sediment, particular sand, toward Goldsmith Pond, promoting flood shoal development and growth. The strong ebb current at the entrance would tend to maintain the inlet by sweeping finer sediments away from the mouth. However, sediment brought into the inlet on flood will not be flushed on ebb, promoting closure by constriction inside the inlet and not necessarily at the mouth.

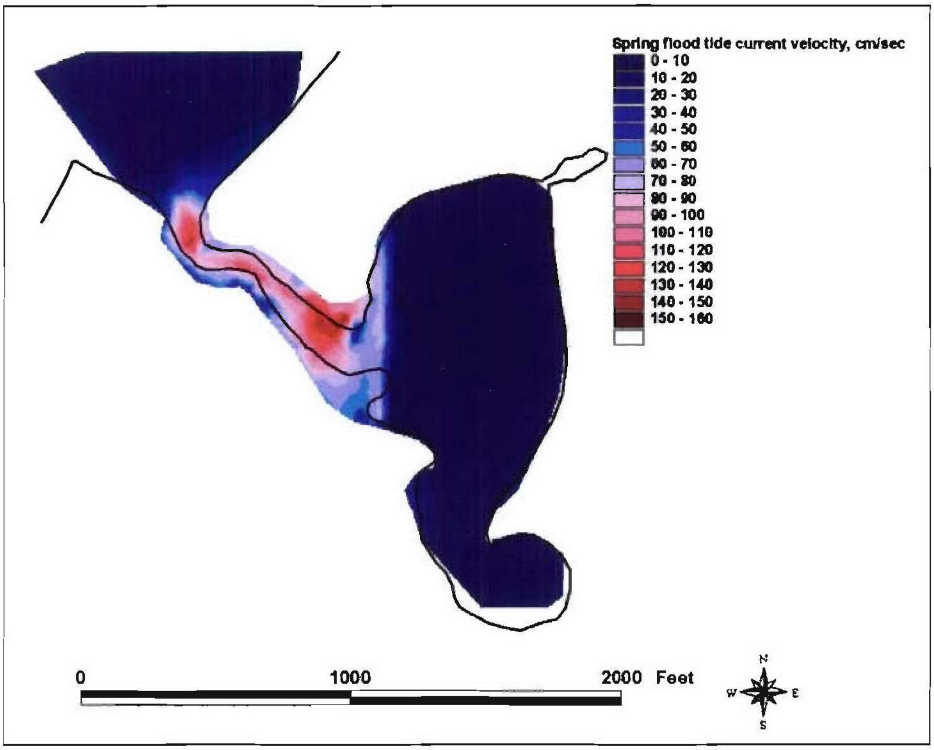

Figure 5-28a. Goldsmith Inlet spring flood-tide maximum current velocity, total calculation domain

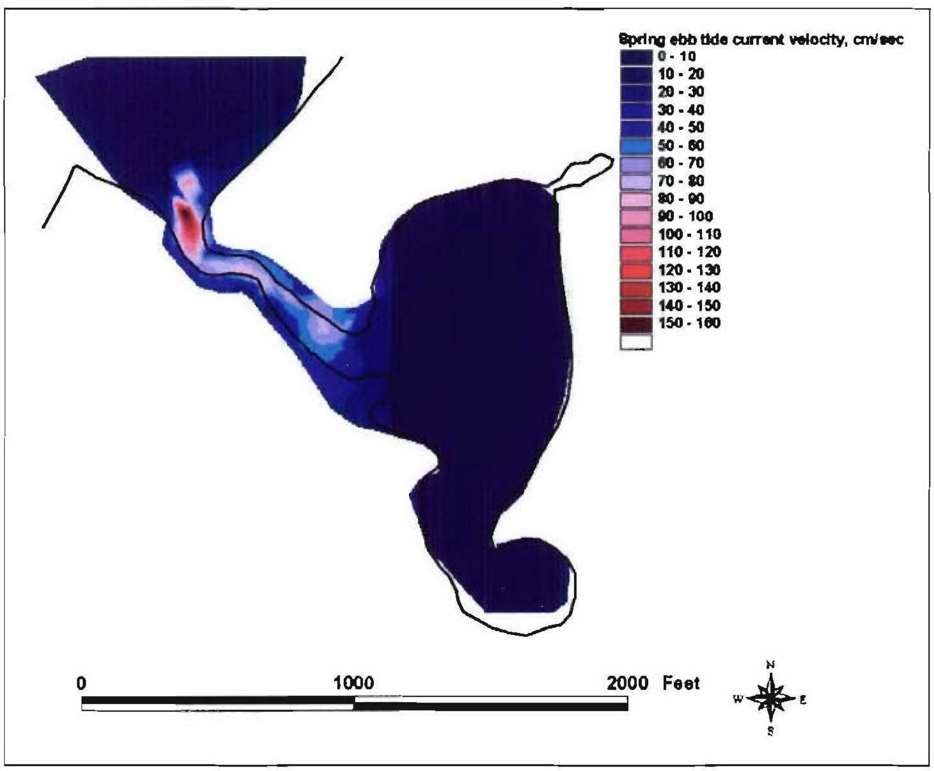

Figure 5-28b. Goldsmith Inlet spring ebb-tide maximum current velocity, total calculation domain

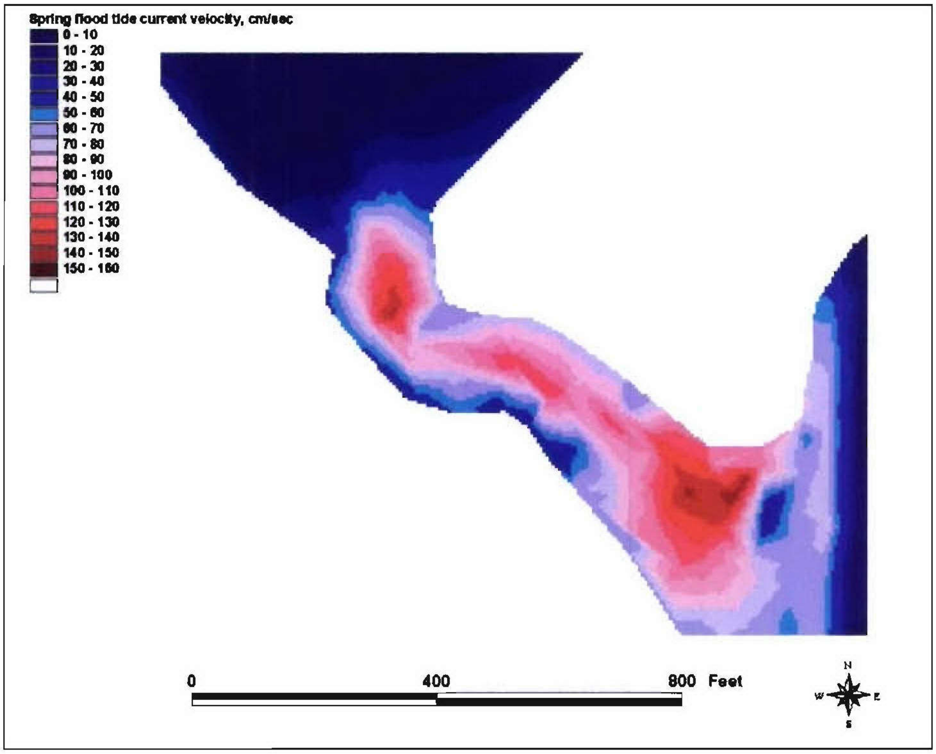

Figure 5-28c. Goldsmith Inlet spring flood-tide maximum current velocity, inlet channel

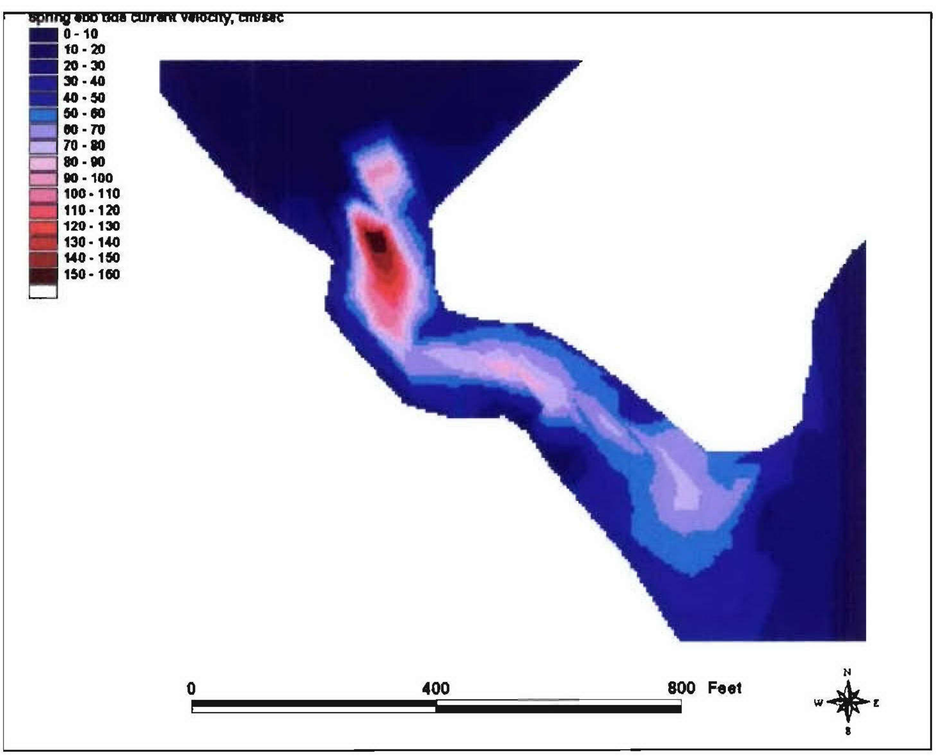

Figure 5-28d. Goldsmith Inlet spring ebb-tide maximum current velocity, inlet channel

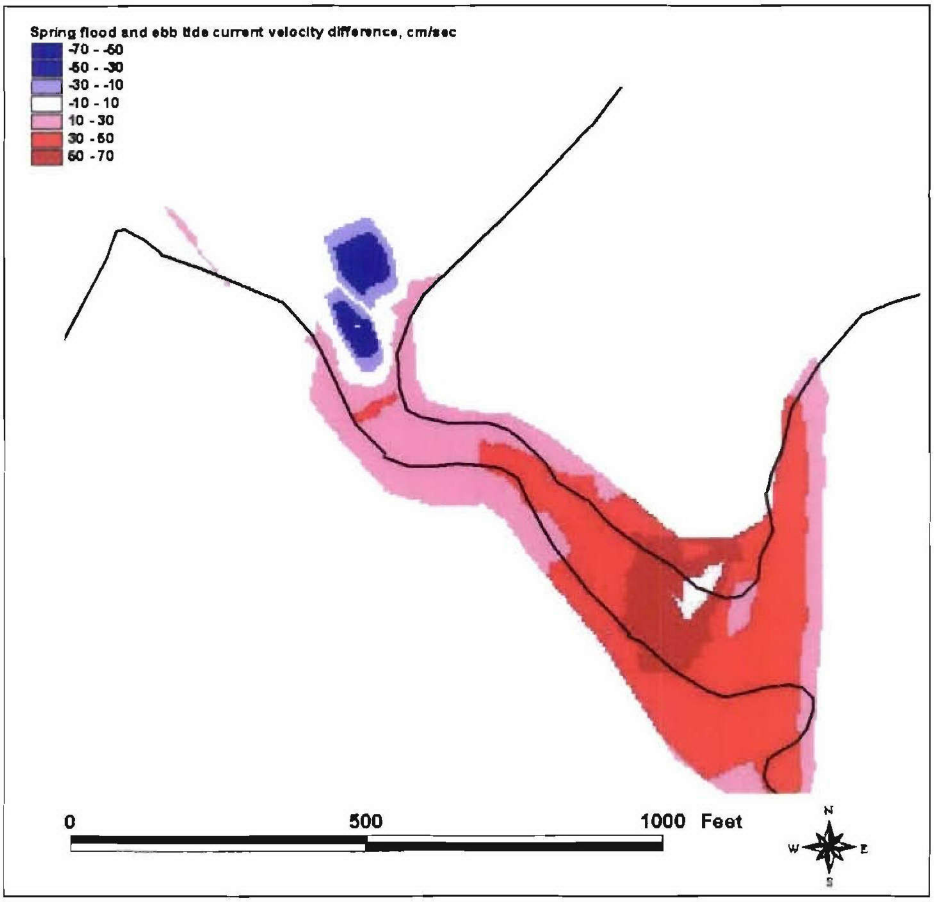

Figure 5-28e. Goldsmith Inlet spring flood-tide and ebb-tide maximum current velocity difference

6 Inlet Morphology and Stability

The morphology of an inlet is a consequence of a dynamic balance among the factors of hydrodynamic forcing, geologic setting, supply and transport of sediment in and near the inlet, and any artificial manipulations such as jetty construction and dredging. Classification methods describing the large-scale features of inlets (ebb shoal, flood shoal and inlet channel) are available (e.g., Bruun and Gerritsen 1959, 1960; Hayes 1980). Empirical relations have been derived that relate the tidal prism of an inlet to its channel cross-sectional area (e.g., LeConte 1905; O'Brien 1931, 1966; Jarrett 1976; Byrne et al. 1980), and a method for estimating inlet channel cross-sectional area stability is also available (Escoffier 1940). Jarrett (1976) and Byrne et al. (1980) examined the width-to-depth ratio *W/D* of inlet channels to characterize the hydraulic efficiency. Relations have been also been derived to predict the volume of inlet ebb shoals (Walton and Adams 1976) and flood shoals Carr de Betts (1999) based on tidal prism.

In this chapter, the channel and shoal morphologies of Mattituck Inlet and Goldsmith Inlet are examined through available qualitative and quantitative approaches, incorporating data and calculation results presented in preceding chapters.

General Inlet Properties

Studies that explore the quantitative properties of morphologic features of inlets are reviewed in this section as preparation for application to Mattituck Inlet and Goldsmith Inlet.

Inlet classification and sedimentation patterns

Hayes (1977) and Davis and Hayes (1984) introduced a classification procedure that places inlet morphology within a continuum ranging from tide dominated to wave dominated (Figure 6-1). At tide-dominated inlets, ebb shoals tend to be large (relative to the flood shoal) and intertidal at their crests. Sediment (sand) bypassing occurs through the mechanism of "tidal bypassing," (Bruun and Gerritsen 1959, 1960) by which sediment is initially brought into the inlet from the updrift side by the flood tide and then transported to the downdrift side by the ebb current. Mattituck Inlet and Goldsmith Inlet fall into the category of tide-dominate inlets according to Figure 6-1. However, there is a large gravel

and coarse-grained sediment component at these inlets that will minimize tidal bypassing, and these inlets do not possess an ebb shoal because of the large grain size of the sediment, weak wave action, and weak ebb discharges.

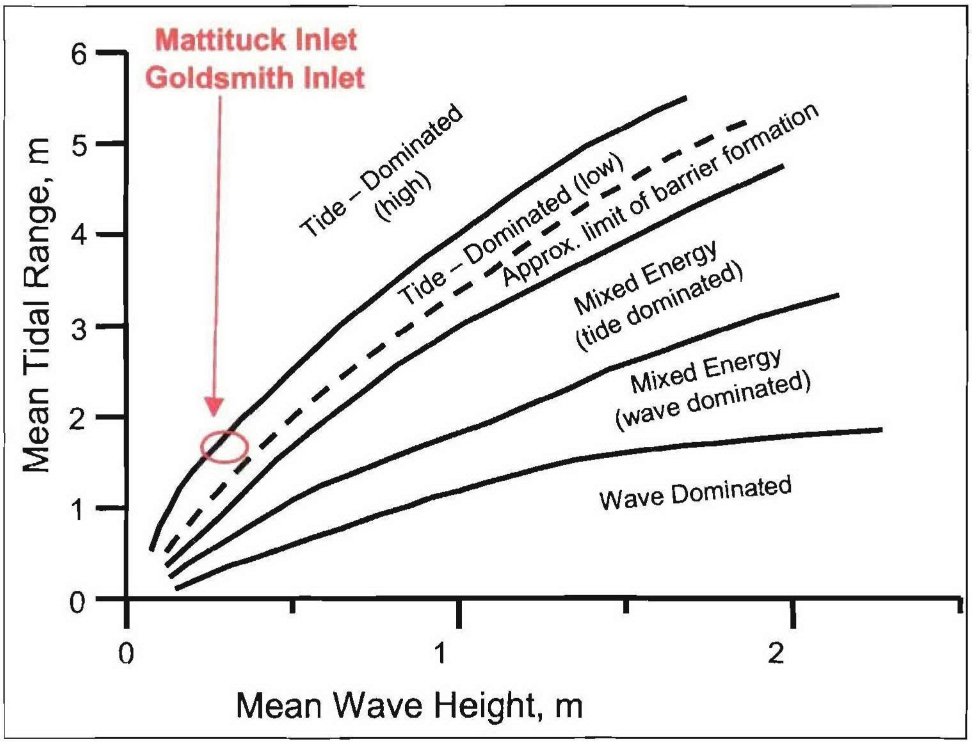

Figure 6-1. Classification of tidal inlet morphology (after Davis and Hayes 1984)

Sand bypassing at tide-dominated inlets can also occur by breaching and reconfiguring of the ebb shoal as the outer inlet channel meanders. This process pertains to inlets without stabilization structures. Breaching and reconfiguration combined with wave-driven onshore migration of sand bodies in the form of swash bars can result in large volumes of sand bypassed from the ebb shoal to the adjacent beaches (FitzGerald et al. 2000). In this process, the channel elongates while typically migrating downdrift. Hydraulic friction of the long channel reduces the inlet current that acts to maintain the inlet entrance; eventually, sediment brought to the entrance by waves closes it. The blocked flow will then break through at a narrow point in the spit located closer to the main channel prior to migration, thereby starting a possible repeat of the cycle of migration, closure, and reopening. This cyclic process may have acted at both Mattituck Inlet and Goldsmith Inlet prior to their stabilization. It probably could not occur at the present Goldsmith Inlet because of the wide beach segment located to the west, adjacent to the jetty.

In contrast, wave-dominated inlets have small ebb shoals that are submerged, and well-developed flood shoals that can be emergent at low tide. Natural sand bypassing occurs through "bar bypassing," the mechanism of wave-driven transport across the outer bar of the ebb shoal to downdrift bypass and attachment bars. The typical morphology of the ebb shoal of an inlet has been identified as an ebb shoal proper, which lies directly in front of the inlet, close to

the channel or within ebb tidal jet flow, together with bypassing bars on each side with volumes dependant on the balance of left-directed and right-directed longshore transport (Kraus 2000). At wave-dominated inlets, the longshore transport of sediment occurs by exchange of sediment among these morphologic components of the ebb shoal system. Inspection of the morphology at Goldsmith Inlet indicates that sediment bypasses the mouth under wave action, but without apparent ebb shoal or bypass bar to the east.

A third type of bypassing, episodic bypassing, occurs when large portions of sediment detach from the ebb shoal complex and migrate to shore (FitzGerald 1988; Gaudiano and Kana 2000). Episodic bypassing is not applicable to Mattituck Inlet and Goldsmith Inlet, because these inlets do not have ebb-tidal shoals or significant bypassing bars.

Bruun and Gerritsen (1959, 1960) first identified the mechanisms of bypassing by littoral transport across the outer bar (ebb shoal complex) and tidal bypassing. They defined a ratio r as:

$$r = \frac{P}{Q_g} \tag{6-1}$$

where P.= tidal prism, and Q_g = gross or total longshore sediment transport rate in 1 year (giving a volume). The tidal prism in this relation corresponds to spring tide, when the strongest current scours the inlet channel. The parameter r expresses the relative strength of the tidal flow that acts to sweep the inlet clear of sediment brought into its entrance by wave-generated longshore sediment transport. Based on the observations of Bruun and Gerritsen (1959, 1960), the r ratio allows for classification of inlet channel stability and mode of sand bypassing. Inlet characteristics associated with different r ratio ranges are summarized in Table 6-1. Inlets with low r-values have channels that are unstable experience bar bypassing (wave-dominated inlets), whereas inlets with large r-values tend to have stable channels and experience tidal bypassing (tide-dominated inlets).

Table 6-1
Inlet Bypassing and Channel Cross-Sectional Stability Classification of Inlets (Modified from Bruun and Gerritsen (1959, 1960) and Including Additional Information)

r-value	Channel Stability	Dominant Bypassing Mode
$r < 20$	Unstable. Inlet may be closed by deposition of sediment during a storm. Typically no navigable channel.	Bar bypassing
r = 20-50	Highly variable in location and area, with multiple channels possible. Dredging and jetties typically required to maintain navigable depths.	Bar bypassing; may have several bars
r = 50-150	Clear main channel and well-developed ebb shoal.	Bar bypassing and tidal bypassing
$r > 150$	Reasonably stable channel.	Episodic bypassing, tidal bypassing

Inlet Stability

Quantitative empirical relations between the equilibrium, or minimal stable cross-sectional channel area of an inlet and its tidal prism have been established for almost a century (e.g., LeConte 1905; O'Brien 1931, 1969; Jarrett 1976). This relation is expressed as:

$$A_C = CP^n \tag{6-2}$$

where A_C = minimum inlet cross-sectional channel area below msl, and C and n = empirical coefficients determined from field measurements.

The original expression has undergone refinement as measurements have become available. Research has been performed to better estimate the empirical coefficients, taking into account processes such as wave activity, degree of sheltering of the inlet from waves, presence or absence of jetties, inlet channel cross-section size, and sediment size. Jarrett (1976) analyzed 108 tidal inlets along the three oceanic coasts of the United States and quantified variations in this relation based on location and the number of jetties as none, one, or two. Table 6-2 lists the empirical coefficient values derived by Jarrett (1976). The 108 inlets examined were located on sandy (fine to medium sand) coasts.

Table 6-2
Tidal Prism (cu ft) and Minimum Channel Cross-Sectional Area (sq ft) Relationships (Jarrett 1976)

Location	All Inlets	Unjettied, Single jettied	Dual Jettied
All Inlets	$A_c = 5.74 \times 10^{-5} P^{0.95}$	$A_c = 1.04 \times 10^{-5} P^{1.03}$	$A_c = 3.76 \times 10^{-4} P^{0.86}$
Atlantic Coast	$A_c = 7.75 \times 10^{-6} P^{1.05}$	$A_c = 5.37 \times 10^{-6} P^{1.07}$	$A_c = 5.77 \times 10^{-5} P^{0.95}$
Gulf Coast	$A_c = 5.02 \times 10^{-4} P^{0.85}$	$A_c = 3.51 \times 10^{-4} P^{0.86}$	Insufficient data
Pacific Coast	$A_c = 1.19 \times 10^{-4} P^{0.91}$	$A_c = 1.91 \times 10^{-6} P^{1.10}$	$A_c = 5.28 \times 10^{-4} P^{0.85}$

Simpson (1976) investigated the hydraulics of two small gravelly inlets located within Puget Sound, WA, and found that the cross-sectional area of both inlets was smaller than the equilibrium area predicted by previously derived expressions. Byrne et al. (1980) investigated 14 small inlets they defined by the criterion $A_c < 100$ sq m (1,076 sq ft). These inlets were located within lower Chesapeake Bay, VA, on sandy shores and were not stabilized by structures. They quantified a departure from previously derived coefficients based on inlet size. This relation, expressed in American Customary Units, was found to be:

$$A_C = 1.212 \times 10^{-2} P^{0.61} \tag{6-3}$$

Byrne et al. (1980) compared their data set to that compiled by Jarrett (1976) and concluded that for small inlets, the departure from the tidal prism – minimum channel cross-sectional area relation derived for larger oceanic inlets occurs between A_c = 100 and 500 sq m (1,076 and 5,082 sq ft).

Escoffier (1940) analyzed closure conditions for a tidal inlet channel by comparing possible cross-sectional areas of the inlet with those predicted by a stability criterion such as given in Equation 6-2. As noted by Seabergh (2003), equilibrium cross-sectional area predicted through an Escoffier analysis implies that the amplitude of the water-surface elevation in the bay is close or equal to the amplitude in the tidal body connected to the inlet.

Kraus (1998) derived the form of Equation 6-2 through a process-based model that accounts for the dynamic balance between ebb-tidal sediment transport and the longshore sediment transport produced by waves. The power of n in Equation 6-2 was found to be 0.9, in agreement with values listed in Table 6-2, and the coefficient C was determined to be of the form:

$$C = \left(\frac{\alpha \pi^3 n_M^2 W_E^{4/3}}{Q_g T^3} \right)^{0.3} \qquad (6\text{-}4)$$

where

α = nondimensional coefficient with value of order unity entering the inlet sediment transport formula employed

n_M^2 = Manning's roughness coefficient squared, $\sec^2/\mathrm{m}^{2/3}$

W_E = width of inlet at equilibrium, m

Q_g = annually gross longshore transport rate, cu m/year (converted to cu m/sec)

T = dominant tidal period, which is 44,712 sec for a semidiurnal tide

Equation 6-4 does not explicitly account for a threshold of motion for transport by the ebb-tidal current or by the longshore sediment transport rate. A threshold could be significant for gravel and cobble beaches, both for transport by the tidal current in the inlet and by waves at and adjacent to the inlet. Equation 6-4 indicates that the value of C will increase if the gross longshore transport rate decreases, all other factors being equal, giving a larger value of the cross-sectional area A_C in Equation 6-2 for the same tidal prism P.

Hydraulic efficiency

Jarrett (1976) compiled information on the ratios of inlet width, W to depth, D for the 108 inlets he studied. He found that inlets with smaller W/D ratios (<100) tend to be hydraulically more efficient. This result is reasonable, because small W/D values indicate relatively greater depth, hence weaker bottom friction. A more hydraulically efficient channel implies a larger channel cross section for the same tidal prism. The average W/D ratio for all the inlets studied by Jarrett (1976) was 337, and the average W/D ratio for the 16 Atlantic coast dual-jettied inlets was 67.

Byrne et al. (1980) compiled information on W/D for their 14 studied inlets located in Chesapeake Bay and obtained an average $W/D = 23$. They conclude that the cross section of smaller channels must, therefore, become more efficient than that of larger channels to maintain stability. The observed departure in W/D characteristics between large and small inlets occurs between approximately A_C = 100 sq m to 500 sq m (1,076 sq ft to 5,082 sq ft).

Ebb shoal volume

Walton and Adams (1976) derived empirical equations based on analysis of 42 inlets that relate the volume of the ebb shoal of a mature or equilibrium inlet to its tidal prism. This relation can be expressed as

$$V_E = C_E P^{1.23} \tag{6-5}$$

where V_E= volume of the ebb shoal in cu yd, and P = tidal prism in cu ft. The value of the empirical coefficient C_E depends on wave exposure as $C_E = 8.7 \times 10^{-5}$ for highly exposed coasts (typically, Pacific Ocean coast), 10.5×10^{-5} for moderately exposed coasts (typically, northern Atlantic Ocean coast), 13.8×10^{-5} for mildly exposed coasts (typically, Gulf of Mexico and southern Atlantic coast), and 10.7×10^{-5} for all coasts.

Flood shoal volume

Carr de Betts (1999) derived empirical predictive relations that relate the volume and area of the flood shoal of an inlet to its spring tidal prism. She studied 61 inlets in Florida, 19 of them located along the Atlantic coast and 42 along the Gulf of Mexico coast. It is noted here that inlets of Florida lie on coasts containing abundant quantities of fine sand (and small shell fragments in the case of the gulf coast of Florida). Flood shoals would be expected to more easily form in coastal environments with plentiful fine material, in contrast to the coarser sediments found along the north shore of Long Island, NY.

Predictive expressions were developed for the near field (that part of the flood shoal readily visible), far field (that part spread in a thin layer further in the bay), and total flood shoal combining the near and far fields (Carr de Betts 1999). The predictive relation between inlet tidal prism and total volume of the flood shoal is:

$$V_{FT} = 2.0389 \times 10^4 P^{0.296} \tag{6-6}$$

where V_{FT} = total volume of the total flood shoal in cu m, and P = the tidal prism in cubic meters. The predictive relation between inlet tidal prism and total area of the associated flood shoal is:

$$A_{FT} = 4.7585 \times 10^4 P^{0.249} \tag{6-7}$$

where A_{FT} = total area of the flood shoal in square meters.

The predictive relationships between the tidal prism and the near field flood shoal volume and area is used to estimate flood shoal area and volume at Mattituck Inlet and Goldsmith Inlet later in this chapter. The predictive relationships between the tidal prism and the far field flood shoal volume and area is not used and is not shown here. The predictive relation between inlet tidal prism and near field volume of the flood shoal is:

$$V_{FN} = 4.056 \times 10^3 P^{0.314} \tag{6-8}$$

where V_{FN} = near field volume of the flood shoal in cu m, and P = the tidal prism in cubic meters. The predictive relation between inlet tidal prism and near field area of the associated flood shoal is:

$$A_{FN} = 1.4532 \times 10^4 P^{0.254} \tag{6-9}$$

where A_{FN} = near field area of the flood shoal in square meters.

The regression correlations for these relations were weak. In contrast to an ebb shoal, there is no significant wave force acting against the flood-tidal jet, allowing sediment to travel far into an inlet and spread in a thin layer that is difficult to measure. Older portions of flood shoals are difficult to distinguish from peripheral wetlands and marshes. Flood shoals are also manipulated through dredging. These empirical relations, however, can be useful in obtaining order-of-magnitude estimates.

Mattituck Inlet

Material introduced in the preceding sections of this chapter is applied to Mattituck Inlet in this section and to Goldsmith Inlet in the following section.

According to the classification by Davis and Hayes (1984), shown in Figure 6-1, Mattituck Inlet is a tide-dominated inlet because it experiences forcing by a diurnal mean tidal range of approximately 1.6 m and is subject to a relatively small mean wave height. Given the limited fetch of Long Island Sound, the mean annual wave height for non-calm events (when waves are present) for Mattituck Inlet is estimated to be 0.3 m and consists mainly of steep wind waves that would tend to move finer sand offshore (Batten and Kraus 2005).

Hubbard et al. (1979) classified tidal inlet morphology based on the hydrodynamic setting. Tide-dominated inlets have well-developed ebb shoals, and sand bypassing is accomplished through tidal bypassing. It has been concluded in this study that the linear shoal located offshore of Mattituck Inlet is not an ebb shoal. Evidence of tidal bypassing, however, can be seen in the depth contours between this feature and the entrance channel (Figure 3-16).

Table 6-3 lists values to calculate the *r* ratio for Mattituck Inlet. The tidal prism was calculated by multiplying the bay area of the inlet by its spring tidal range. The surface area of Mattituck Inlet and Mattituck Creek was 7.2×10^6 sq ft as interpreted from GIS analysis of an aerial photograph dated 16 April 2003. The spring tide range within the creek was 6.0 ft based on water-level data collected 19 September to 8 October 2002, consistent with the value given by NOS for the area.

Because the gross longshore sediment transport rate at Mattituck Inlet is not well known, two values (15,000 and 25,000 cu yd/year) were used to calculate the *r* ratio of Mattituck Inlet. These values are considered to represent the minimum and maximum gross longshore sediment transport rates at the inlet. Mattituck Inlet has an *r* ratio of in the range of 64 to 107 (Table 6-3). According to the classification of Bruun and Gerritsen (1959, 1960) summarized in Table 6-1, inlets with an *r* ratio of 50 to 150 have a well-developed ebb shoal (sandy beaches), and sand bypassing occurs through a combination of bar bypassing and tidal bypassing. Mattituck Inlet lacks an ebb shoal. However, sediment bypassing from the west beach may occur along the offshore shoal, and it is inferred to occur along a bypassing bar located near the tip of the west jetty. It is feasible that fine to medium sand can bypass in this way, but not coarser sand and gravel because of the small waves and weak tidal current (Chapter 5). The sand bypassing complex offshore of Mattituck Inlet is displayed in Figure 3-

14. Sand bypassing at Mattituck Inlet appears to occur through a combination of tidal bypassing and bar bypassing.

Table 6-3
Mattituck Inlet *r* Ratio and Associated Physical Quantities

Quantity	Mattituck Inlet
Tidal range (ft)	6.0
Surface area (sq ft)	7.2×10^6
Tidal Prism (cu ft)	4.32×10^7
Longshore transport rate (cu yd)[1]	15,000 -25,000
r ratio	64-107

[1] Range in longshore sediment transport rate accounts for estimated range in east-directed transport, material directed to the offshore by the west jetty, and efficiency of the present east jetty to block sediment directed at the inlet from the east.

The relatively short distance between the jetties, promotes scouring flow in the channel (small *W/D* ratio). For Mattituck Inlet, *W/D* = 43, calculated by dividing the width of the inlet between the two jetties (400 ft) by the measured hydraulic radius (9.3 ft). Jarrett (1976) notes that inlets with small *W/D* ratios (*W/D* <100) are hydraulically efficient.

Mattituck Inlet channel cross-sectional area stability

The Channel Equilibrium Area (CEA) model (Seabergh and Kraus 1997) creates an Escoffier stability curve for a given inlet and was applied to examine stability of Mattituck Inlet. The Jarrett (1976) relation for dual-jettied inlets on the Atlantic coast was selected for the analysis, of which Mattituck Inlet fits well to the trend (Figure 6-2). The one-dimensional CEA model is calibrated by inputting the dimensions of the inlet and bay from which the hydrodynamics of the inlet are calculated. The CEA model requires the tidal amplitude at an inlet, which is half the tidal range.

CEA-calculated water level and velocity are then compared to measurements at the inlet. Figure 6-3 plots measured and calculated water levels offshore of Mattituck Inlet, and Figure 6-4 plots measured and calculated water levels for within the inlet. The comparison period 5-7 October 2002 was selected because the measurement range was nearly equal to the spring tide range as reported by the NOS (6.0 ft) (Chapter 3).

Table 6-4 summarizes the physical quantities that served as input to calculate the equilibrium channel area of Mattituck Inlet. The minimum cross-sectional area of 1,600 sq ft was derived from the cross sections produced from the bathymetry survey of 6-8 October 2002. The cross section used, cross-section 9, is shown in Figure 3-20c. Cross-section 8 appears to have a smaller area, but was not selected because of inadequate survey coverage. The location of this transect, at the main area of shoaling, is shown in Figure 3-19.

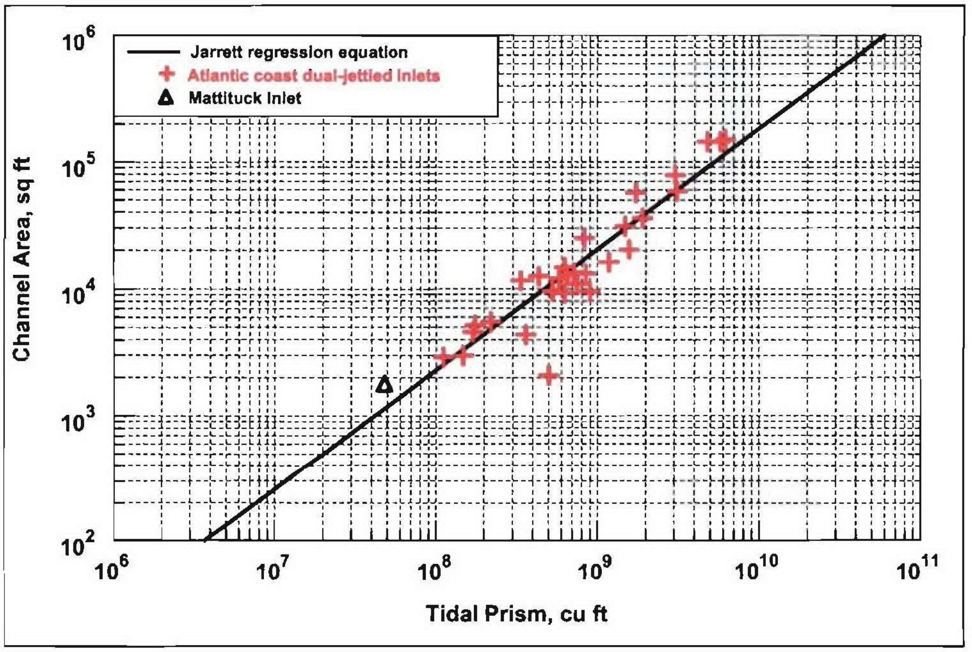

Figure 6-2. Tidal prism-channel area relation, Mattiuck Inlet and Atlantic coast dual jettied inlets

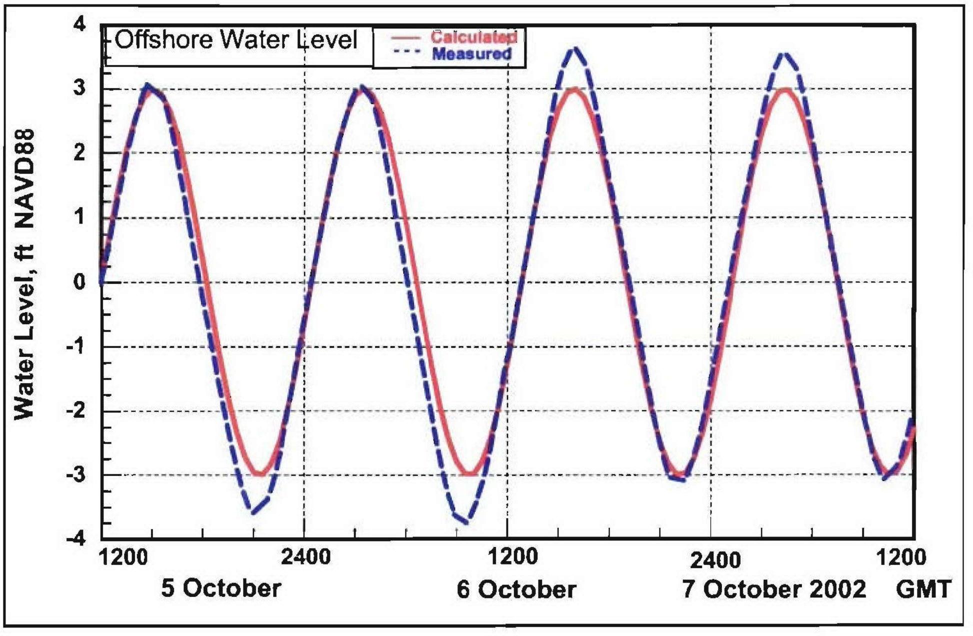

Figure 6-3. Mattituck Inlet offshore water-level measurements and calculations by CEA model

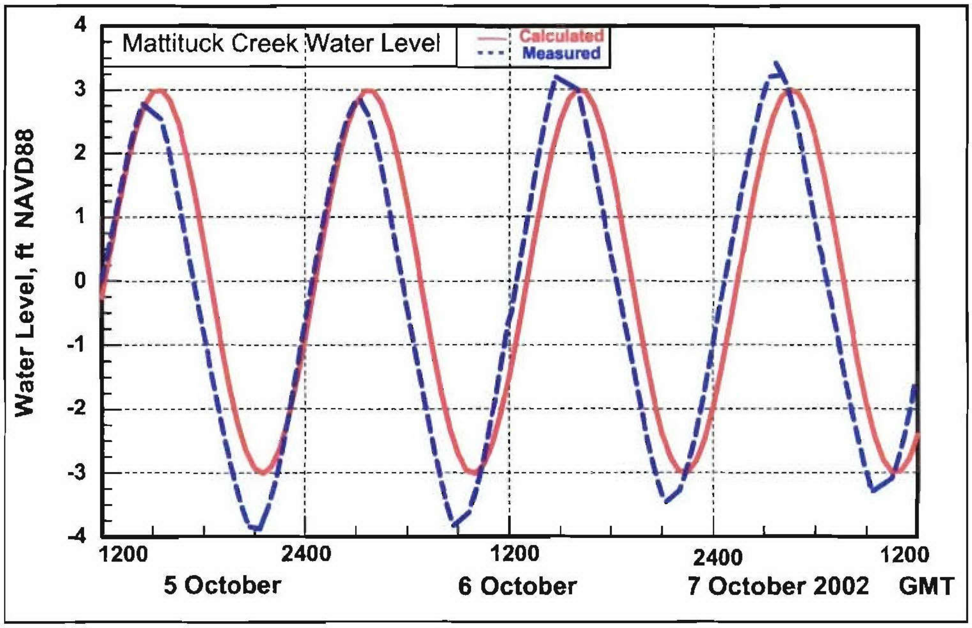

Figure 6-4. Mattituck Creek water-level measurements and calculations by CEA model

Table 6-4
Channel Equilibrium Area Model Quantities for Mattituck Inlet

Ocean tide amplitude (ft)	3.0	Channel length (ft)	3,000
Bay surface area (sq ft)	7.2×10^6	Channel width (ft)	200
Hydraulic radius (ft)	9.3	Channel area (sq ft)	1,600

The calibrated CEA model produced the stability curve shown in Figure 6-5, giving a predicted stable equilibrium area of 1,020 ft for Mattituck Inlet. In an Escoffier inlet stability analysis, if the calculated velocity for the inlet falls below the equilibrium velocity (or is tangent to it at a single point), the inlet is unstable and will close. If the two curves intersect at two points (as for Mattituck Inlet), the point on the right is identified as the stable equilibrium cross-sectional area. If the channel area is larger than this, the tidal current velocity in the inlet will decrease, promoting channel infilling and a return to the stable condition. If the channel area decreases, the tidal current velocity in the inlet will increase, scouring the channel until it returns to stable cross-sectional area. The intersection on the left side of the Escoffier curve denotes an unstable condition. If the channel area decreases beyond this point, velocity will decrease and the inlet will tend toward closure because friction will reduce the velocity further.

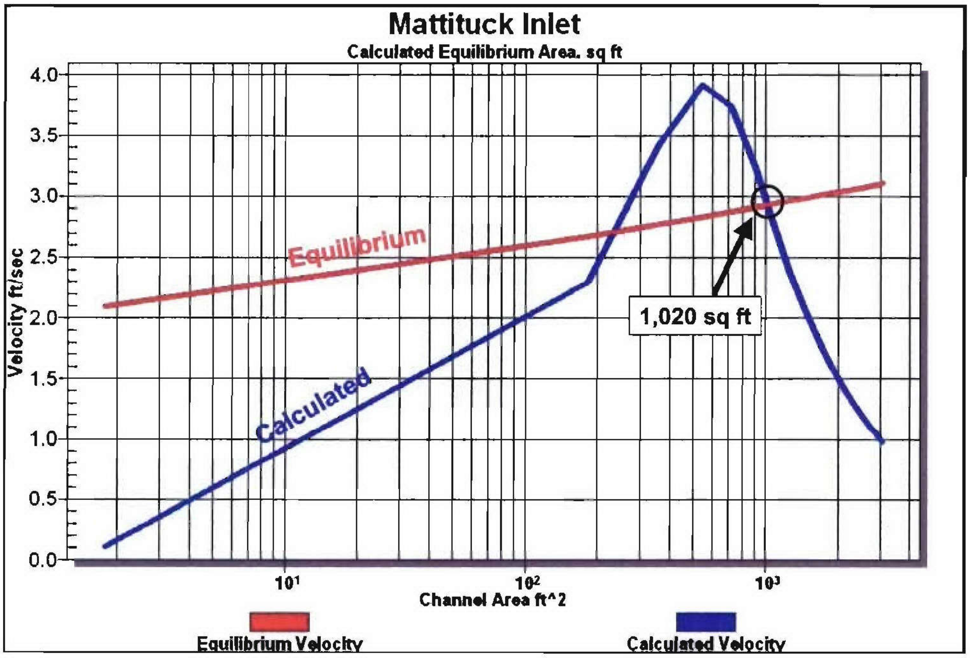

Figure 6-5. Escoffier curve calculated for Mattituck Inlet, CEA model

The Jarrett (1976) relation predicts an msl minimum stable channel cross-sectional area of 1,035 sq ft for Mattituck Inlet. The Escoffier analysis of Mattituck Inlet predicts a stable channel cross-sectional area of 1,020 sq ft, which is 36 percent smaller than the observed October 2002 measurement of 1,600 sq ft.

The measured inlet channel cross-sectional area is significantly larger than predicted. The Escoffier stability analysis is based on the implicit assumption that the bay tide range will approach or equal the ocean or forcing tide range (Seabergh 2003). This is not the case for Mattituck Inlet, yet the channel cross-sectional area is greater. Such a morphological property, a much larger-than-predicted inlet channel cross-sectional area, is anomalous.

Several factors might contribute to the unusually large channel cross-sectional area. In the judgment of the authors, in possible order of significance, these are:

a. Historic mining of the inlet channel and the adjacent west beach may have removed at least 500,000 cu yd of sand and gravel over an approximate 50-year period (1920s to 1970s), artificially increasing the area and hydraulic efficiency of the entrance channel.

b. The relatively low longshore sediment transport rate found on the north shore of Long Island and at this site, due to its shoreline orientation and protection by the west jetty, is not adequate to fill a maintained channel.

c. The relatively small *W/D* ratio of 43, indicating hydraulically efficient inlet (for fine-and medium-sized sand).

Mattituck Inlet offshore shoal

To further explore the origin of the linear offshore shoal located east of Mattituck Inlet, that is, whether or not it is an ebb-tidal shoal, the empirical

prediction of Walton and Adams (1976) was examined. The coefficient value $C_E = 8.7 \times 10^{-5}$ (Equation 6-5) for mildly exposed coasts was employed in the calculation. For the tidal prism of 4.32×10^7 cu ft, the volume of the shoal is predicted to be 340,000 cu yd. The actual volume of this feature was calculated to be 460,000 cu yd (Chapter 4).

The difference between the actual and predicted volume of this feature supports a conclusion that the feature is not a relic or active ebb-tidal shoal. Implicit in the estimation procedure of Walton and Adams (1976) is the requirement that the sediment at a site be predominantly fine to medium sand. Because the offshore shoal considered contains a significant percentage of coarse sand and gravel, it is expected that the Walton and Adams (1976) empirical relation would overestimate the volume if the feature were an ebb shoal. The underestimation of the shoal volume by the Walton and Adams (1976) relation supports the conclusion that this feature is not an ebb shoal.

Other aspects of this study further support this conclusion. The shoal is located too far east (outside the ebb-tidal jet) and possesses large gravel content, making transport of these sediment grains from the inlet to the feature doubtful. Tidal circulation modeling of Mattituck Inlet (Chapter 5) indicates that the feature is not hydraulically connected to the inlet in its present condition or in its natural condition. Finally, the feature experienced minimal growth between 1927 and 2002 (Chapter 4).

Mattituck Inlet flood shoal

The volume of the flood shoal at Mattituck Inlet can be estimated directly through bathymetry difference calculations in a GIS and compared to the empirical relation derived by Carr de Betts (1999).

The major area of shoaling at Mattituck Inlet is found on the east bank adjacent to the end of the east jetty, and there is also considerable shoaling on the opposite (west) bank. The shoaling refers to locations above the navigation channel and does not include deposition along the walls of the channel (bank encroachment). Shoaling inferred to be caused by the transport of sediment into Mattituck Inlet continues along both banks to a distance of about 2,000 ft beyond the landward end of the inlet.

A polygon that encompasses this area was created in a GIS, and a TIN was generated (Figure 6-6). The extent of the flood shoal considered here is greater than the preceding analysis of flood shoal morphology change. Morphology change analysis was based on the area of the flood shoal included in typical New York District condition surveys. Because the bathymetry survey of 6-8 October 2002 covered all of Mattituck Creek, the area of analysis is extended here. An estimate of the volume of this portion of the flood shoal was obtained by calculating the volume of sediment found above a reference datum. Two volumes with respect to two reference datums (-6 ft NAVD88 and –4 NAVD88, which correspond approximately to –3 ft mlw and –1 ft mlw) were calculated to provide an estimated range of the volume of this portion of the flood shoal.

The area considered to be part of the flood shoal included dry land to an elevation of up to +1.5 ft NAVD88. This identification was made because analysis of historical aerial photographs indicated that these areas are new features created by shoaling and landward bypassing accumulation (Figures 4-24

through 4-26b and Figures 4-37a through 4-37b). In some areas, however, portions of dry land that may be within the intertidal zone, and part of the flood shoal, were not covered by the survey. The surface area range of the 6-8 October 2002 flood shoal was calculated as 1.99×10^5 to 2.68×10^5 sq ft. The volume range was calculated to be 1.58×10^4 to 3.26×10^4 cu yd.

Bank encroachment is a significant form or mode of shoaling at Mattituck Inlet and occurs along the east channel wall. Analysis of pre-dredging surveys indicates that the length of the east channel wall subject to bank encroachment is approximately 1,000 ft. The project slope for the Mattituck Inlet navigation channel is 1:3. The resulting surface area of the east channel wall subject to encroachment is approximately 1.0×10^4 sq ft. Based on the analysis of temporal changes in channel width (Figures 4-39a through 4-39c), the 1,000-ft-long section of the east channel wall is estimated to be subject to an overall depth-averaged rate of sediment accumulation of 2 ft/year. This rate of encroachment converts to 740 cu yd/year of sediment accumulation on the east channel wall.

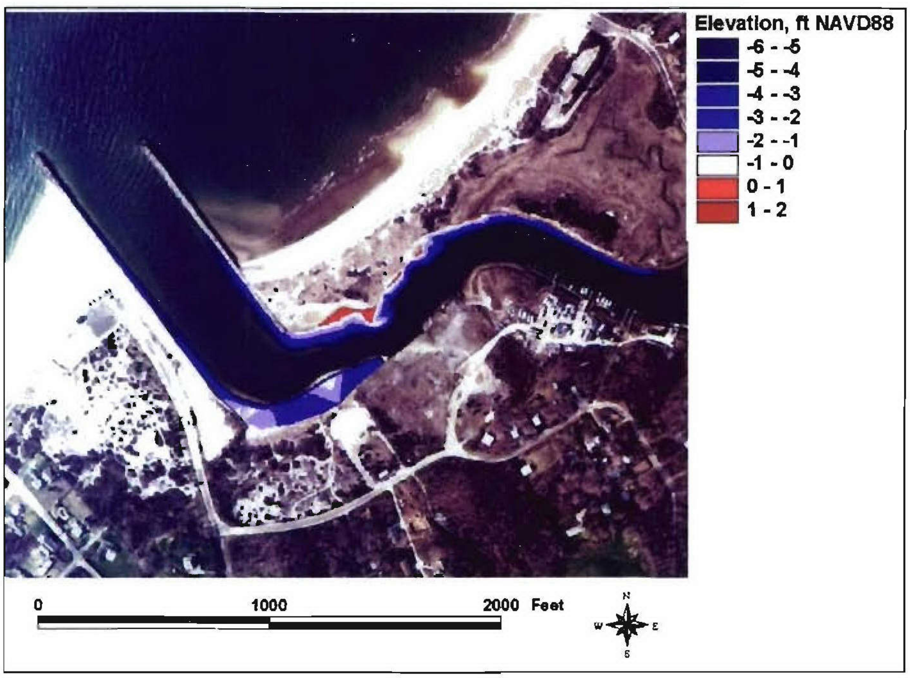

Figure 6-6. Shoaling at Mattituck Inlet and Mattituck Creek, 6-8 October 2002

Analysis of pre-dredging surveys indicates that the length of the west channel wall subject to bank encroachment is approximately 800 ft, with a resulting surface area of 8×10^3 sq ft. Based on analysis of temporal changes in width, the depth-averaged rate of sediment accumulation along the west channel wall is estimated to be 1.5 ft/year. This intrusion mode converts to an accumulation rate of 440 cu yd/year on the west channel wall.

Although the annual rate of channel infilling is difficult to quantify (because the rate produces depth change approaching survey error), a rate of 0.125 ft/year (1.5 in./year) is considered a reasonable estimate based on the measured channel elevation changes between May 1980 and October 1989. The surface area of the Federal navigation channel with the area analyzed is 2.16×10^5 sq ft. The rate of

sediment accumulation due to channel infilling is thereby estimated to be 100 cu yd/year. This estimate corresponds well to volumes dredged in recent times. The total rate of shoaling within the study area is estimated to be 1,280 cu yd/year, with the greatest amount of shoaling (1,180 cu yd/year) occurring along the channel walls.

The total flood shoal volume was estimated with the empirical relation of Carr de Betts (1999). Because the channel at Mattituck Inlet is constricted compared to a relatively open bay, and there are no other recognizable areas of shoaling, the near-field flood shoal volume predicted was considered appropriate. Applying a tidal prism of 4.32×10^7 cu ft, the total volume of the flood shoal was calculated to be 4.33×10^5 cu yd, and the total flood shoal area was calculated to be 5.50×10^6 sq ft.

The empirical relation predicts a value that is larger than the directly estimated volume by a factor of 10. Four reasons can be given for this large difference:

a. The tidal current at Mattituck Inlet is weak compared to typical Florida inlets where Carr de Betts (1999) performed her studies, and weak in general compared to other permanent inlets. A weaker flood current implies weaker transport and a smaller flood shoal.

b. The sediment on the beaches adjacent to Mattituck Inlet contains a large coarse fraction as opposed to the homogeneous fine sand on Florida beaches. Therefore, a smaller amount of fine material of the total sediment load is available to be transported to the interior channel at Mattituck Inlet.

c. Longshore sediment transport rates along the Atlantic coast and Gulf coast of Florida exceed the estimated transport rates along the north shore of Long Island by a factor of as much as 10, and 2 to 5 (including hurricanes), respectively, again indicating less material is brought to the inlet entrance and available for transport into the inlet.

d. Portions of the flood shoal in and around the navigation channel are dredged.

Goldsmith Inlet

Similar to the situation of Mattituck Inlet, Goldsmith Inlet is in the low-tide-dominated inlet classification range according to Davis and Hayes (1984) (Figure 6-1). In contrast to Mattituck Inlet, Goldsmith Inlet does not fit the description of a tide-dominated inlet identified by Hubbard et al. (1979). The morphology of Goldsmith Inlet is more similar to that of a wave-dominated inlet, having no apparent ebb-tidal shoal and a well-developed flood shoal. Because of the strong direction of net longshore transport to the east and the coarse sand and gravel predominant at the site, it is inferred that sediment bypasses the inlet relatively close to shore, typically within the swash zone.

Table 6-5 lists r-values for Goldsmith Inlet and the quantities entering the calculation. The surface area of Goldsmith Inlet and Pond was found to be 9.5×10^5 sq ft interpreted from GIS analysis of an aerial photograph dated 16 April 2003. The spring tidal range within the pond was calculated to be 3.2 ft based on the water-level data collected 19 September to 8 October 2002. As with

Mattituck Inlet a range of 15,000 to 25,000 cu/yd year was employed as the gross transport rate.

Inlets with an *r* ratio of less than 20 tend to be unstable and non-navigable, and sand bypassing is accomplished by wave-driven transport across the bypassing bars. Goldsmith Inlet is non-navigable and does not have an ebb shoal or bypassing bar, in conformance with the prediction.

Table 6-5
Goldsmith Inlet *r* Ratio and Associated Physical Quantities

Quantity	Goldsmith Inlet
Tidal range (ft)	3.2
Surface area (sq ft)	9.5×10^5
Tidal Prism (cu ft)	3.04×10^6
Transport rate (cu yd)	15,000 - 25,000
r ratio	4.5 – 7.5

Goldsmith Inlet channel cross-sectional area stability

The stability of Goldsmith Inlet was analyzed with the CEA model. Because Goldsmith Inlet is a small inlet located on a sheltered coast, the predictive equation derived by Byrne et al. (1980) for small inlets was selected and entered as a user-specified relation in the model. The minimum cross-sectional area of the inlets studied by Byrne et al. (1980) ranged from 5.4 to 270 sq ft, bracketing the minimum cross-sectional area at Goldsmith Inlet of 80 sq ft. The channel area was obtained from the bathymetry survey of 6-8 October 2002.

Table 6-6 summarizes the physical quantities that served as input to calculate the equilibrium channel area of Goldsmith Inlet. Cross-section 2 in Figure 3-44a was selected to represent the minimum cross-sectional area (80 sq ft) for Goldsmith Inlet. This cross section has a width of 55 ft at this location. Cross sections were generated based upon a limited number of data points, for which the perimeter of the inlet was not explicitly recorded. Because the indicated channel width (55 ft) was considered to be too large based on field observations, the effective wetted width was taken to be 45 ft.

Table 6-6
Channel Equilibrium Area Information for Goldsmith Inlet

Ocean tide amplitude (ft)	2.0	**Channel length (ft)**	1,300
Surface area (sq ft)	9.5×10^5	**Channel width (ft)**	45
Hydraulic radius (ft)	1.4	**Channel area (ft)**	80

A tidal range of 4 ft was employed in the stability analysis of Goldsmith Inlet to compensate for the action of the sill (higher bottom) located at the entrance and toward the opening into the pond, which limit the tide range in the pond to 3.2 ft. The range of 4 ft is considered an effective range that would exist if the entrance were not depth limited by the sills.

Figure 6-7 plots the measured water level and water level as calculated with the CEA model for Goldsmith Inlet. The CEA model cannot reproduce the asymmetry of the observed signal (as discussed in Chapter 4). The model can still give an estimate of stable channel cross-sectional area if the amplitudes correspond in the calibration.

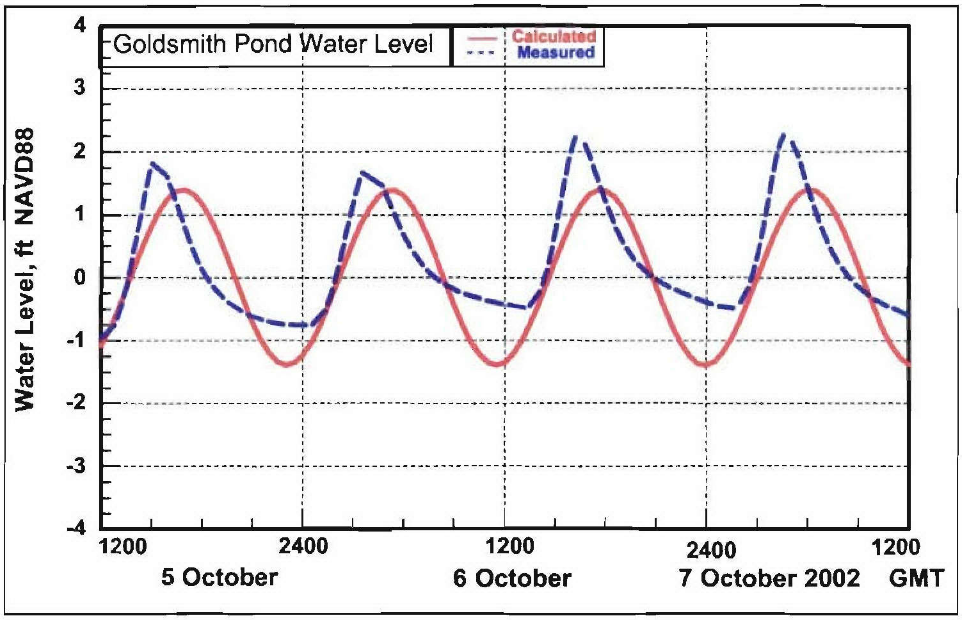

Figure 6-7. Goldsmith Pond water-level measurements and calculations by CEA model

Figure 6-8 shows the calculated maximum velocity curve and the calculated equilibrium velocity curve for Goldsmith Inlet. The empirical relation for small inlets developed by Byrne et al. (1980) predicts an equilibrium cross-sectional area of 109 sq ft for Goldsmith Inlet, and their empirical equation with the CEA Escoffier analysis gives a stable channel cross section of 114 sq ft. These calculations are close to value of the minimum channel cross-sectional area of 80 sq ft obtained from the October 2002 survey.

Figure 6-9 plots the tidal prism and channel area relation for Goldsmith Inlet with data of the inlets studied by Byrne et al. (1980) and Simpson (1976). The Goldsmith Inlet data points conforms well with the trend of the small Chesapeake Bay inlets. The two Puget Sound inlets studied by Simpson (1976), Lagoon Point Inlet and Hancock Lake Inlet, are included because they are similar to Goldsmith Inlet in being small, gravelly inlets. The inlets studied by Simpson (1976) were not protected by jetties.

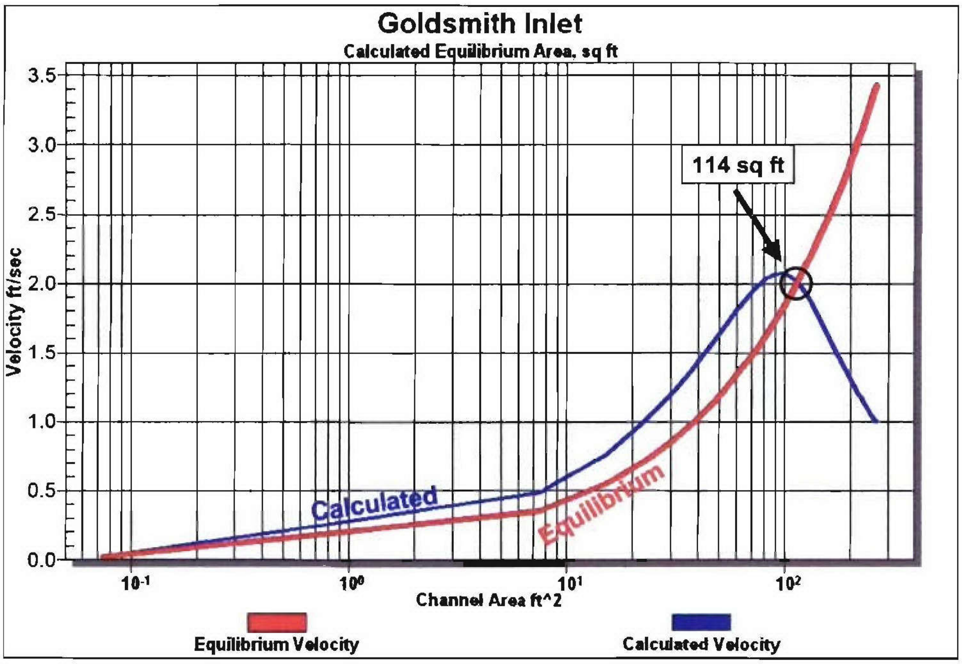

Figure 6-8. Escoffier curve calculated for Goldsmith Inlet, CEA model

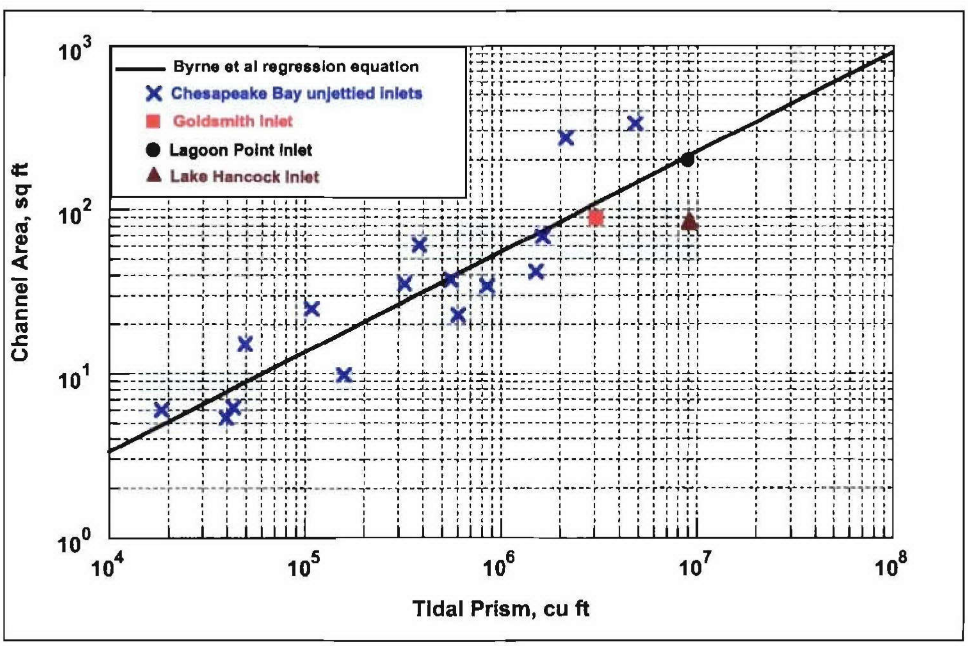

Figure 6-9. Tidal prism-channel area relation, Goldsmith Inlet, Chesapeake Bay small inlets, and Puget Sound inlets

Similar to the Chesapeake Bay inlets studied by Byrne et al. (1980), Goldsmith Inlet is small and located on a coast receiving limited longshore sediment transport. Unlike the Chesapeake Bay inlets, however, Goldsmith Inlet is protected by one jetty and comprises medium to coarse grain sediment. Blockage of longshore sediment transport by the Goldsmith Inlet jetty and the streaming of this material past the inlet mouth as discussed in Chapter 4 would reduce sediment arrival to the inlet and, therefore, promote a larger channel cross-sectional area.

For Goldsmith Inlet, the width-to-depth ratio, $W/D = 32$, based on measurements listed in Table 6-6. The inlet channel is, therefore, less efficient than the small Chesapeake Bay inlets studied by Byrne et al. (1980) where the average $W/D = 23$. However, as compared to the larger inlets studied by Jarrett (1976), it is highly hydraulically efficient.

Goldsmith Inlet ebb shoal

Goldsmith Inlet does not posses an ebb shoal, as discussed in Chapter 4. Instead, a subaqueous spit is present eastward from the jetty, in the direction of predominant eastward longshore transport. Longevity of the inlet is inferred to owe in part to eastward migration and orientation of the inlet mouth, enabling sediment that would otherwise be deposited in the entrance to bypass the inlet. The bar crossing the mouth of Goldsmith Inlet is morphologically similar to a spit growing from the large fillet that forms on the east side of the jetty. This fillet receives sediment that is transported close to shore and around the jetty from west to east.

A conventional ebb shoal is considered to form and be maintained as a balance of the ebb current that transports sediment seaward and wave-induced currents that transport sediment shoreward. For Goldsmith Inlet, the ebb current is weak as compared to the flood current, and it is doubtful that it can sustain an appreciable ebb shoal and sweep the channel clear of course sediment if the inlet were stabilized to enter normal to the shoreline, parallel to the jetty. In addition, the ebb discharge from Goldsmith Inlet is relatively small compared to the volume of water moved by obliquely incident waves. Therefore, the ebb flow is not adequate to maintain an ebb shoal. In migration of the inlet mouth to the east, the ebb current issuing from the mouth of the inlet will tend to reinforce the wave-induced longshore current directed to the east. Based on this interpretation, the most stable configuration of Goldsmith Inlet is one with the channel directed toward the east, not northward or parallel to the jetty.

Goldsmith Inlet flood shoal

The flood shoal at Goldsmith Inlet consists of three lobes that are located on the east bank, west bank, and in the channel where the inlet channel enters Goldsmith Pond (Figure 6-10). The volume of the flood shoal at Goldsmith Inlet is estimated directly through bathymetry difference calculations in a GIS, after Dean and Walton (1973) and using the empirical relation derived by Carr de Betts (1999).

Because the ambient depth in the eastern portion of Goldsmith Pond is greater than in the western portion and within the channel, two polygons were created to estimate the total volume of the flood shoal. One polygon encompassed the west and channel lobe, and the other encompassed the east lobe. No area was found that contained a clearly identifiable ambient depth, so the ambient depth was approximated from depths surveyed adjacent to each polygon. This depth was multiplied by the surface area of each lobe, yielding the volume of water located above each idealized "no-shoal" bathymetry.

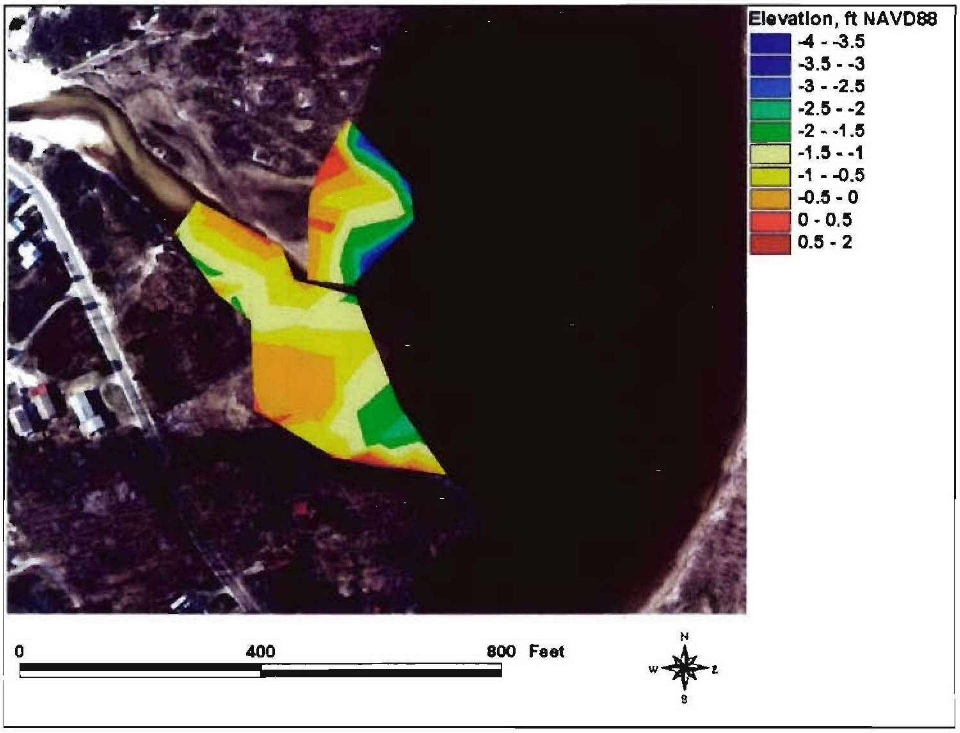

Figure 6-10. Shoaling at Goldsmith Inlet and Goldsmith Pond, 8 October 2002

A TIN was generated for each polygon and the volume of water located between each TIN and the NAVD88 datum was calculated. Subtracting the volume of the water found above each TIN from the value that represented an ambient water volume yielded an estimate of the volume of each lobe. The estimated ambient depths for the west lobe and channel lobe are 2.0 ft, and the estimated ambient depth for the east lobe is 4.5 ft. The volume of the west lobe was calculated to be 2,915 cu yd and the volume of the west lobe was calculated to be 3,715 cu yd. Quantities used to determine this estimate are summarized in Table 6-7.

Table 6-7
Goldsmith Inlet Flood Shoal and Physical Quantities

Location	West and Channel Lobe	East Lobe
Ambient depth (ft)	2	4.5
Surface Area (sq ft)	7.86×10^4	3.0×10^4
Estimated volume above ambient depth (cu yd)	5,825	5,000
Estimated volume above shoal (cu yd)	2,910	1,285
Estimated volume of flood shoal (cu yd)	2,915	3,715

The total flood shoal volume was also estimated with the empirical relation of Carr de Betts (1999). Because of the small size of Goldsmith Inlet and pond, the relation that predicts the near field ebb shoal volume was employed, as it is believed that much of the flood shoal accumulation can be observed. Applying a tidal prism of 3.04×10^6 cu ft, the total volume of the flood shoal was calculated to be 1.88×10^5 cu yd and the total flood shoal area was calculated to be 2.80×10^6 sq ft. The directly calculated volume of both lobes is 6,630 cu yd.

The empirical relation overestimates the volume derived from measurements by a factor of 30. Reasons for this are the same as presented in the analysis for Mattituck Inlet.

Discussion of Channel Cross-Sectional Area Relations

Channel cross-sectional areas of Mattituck Inlet and Goldsmith Inlet are compared here. To examine the response of cross-sectional areas of small inlets such as these to tidal forcing, the Jarrett (1976), equation for Atlantic coast dual-jettied inlets is drawn together with the Byrne et al. (1980) equation for small, inlets without jetties (Figure 6-11). Data from which the regression equations were obtained are included in the plots. Measurements for the two Puget Sound gravelly inlets from Simpson (1976) and for Mattituck Inlet and Goldsmith are also plotted.

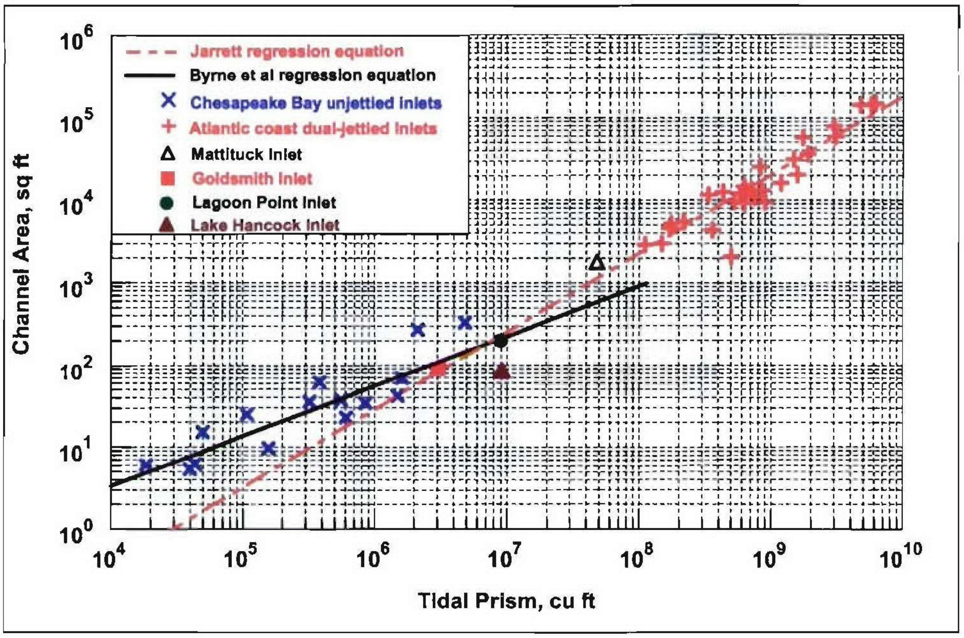

Figure 6-11. Comparison of channel cross section and tidal prism relations

The trend lines were extended beyond their empirical ranges of validity for visual comparison. The trends for the Atlantic coast dual-jetty inlets and the small natural inlets are different. On Figure 6-11, Mattituck Inlet lies at the lower end of the Atlantic Coast dual-jetty inlets and close to the regression line. In contrast, Goldsmith Inlet lies at the upper end of the small Chesapeake Bay inlets, and it almost falls on top of their regression line. The two small Puget Sound inlets are also compatible with the small-inlet trend developed from the Chesapeake Bay inlets.

It appears that the conclusion of Byrne et al. (1980) about the greater efficiency of small inlets is valid, although it can be argued that the Goldsmith Inlet and two Puget Sound Inlet data points are compatible with an extension of the Atlantic coast dual-jetty trend line. However, it is considered that the location of the Goldsmith Inlet point is accidental in plotting near the Atlantic coast dual-jetty trend line, as do a few of the Chesapeake Bay data points.

7 Comparative Analysis and Conclusions

This study of Mattituck Inlet and Goldsmith Inlet, Long Island, NY, covered the historic and geomorphic background, literature, field measurements, numerical modeling of tidal circulation, and analysis of inlet morphology. Information contained in the preceding chapters of this report is comprehensive and varied. This chapter integrates and synopsizes study results and findings of the morphologic characteristics of the two inlets for engineering applications. Recommendations are given to improve the quality of future investigations and to support coastal and navigation projects located on the north shore of Long Island.

Tidal inlets on the north shore of Long Island opening to Long Island Sound have received little study compared to those on the south shore that open to the Atlantic Ocean. It appears that most inlets on the north shore have been more stable and in existence longer than the inlets on the south shore. For example, on the south shore, Fire Island Inlet migrated several miles westward between 1824 and 1940 (Gofseyeff 1952), Moriches Inlet closed for decades in the twentieth century (Czerniak 1977), and the Great Storm of 1938 reopened Shinnecock Inlet in the twentieth century. Such extremes have not been reported for inlets located on the north shore. Inlets on the north shore, therefore, hold value for furthering understanding of basic inlet processes, in particular, of inlet stability. Knowledge and insight gained on the mechanisms contributing to the stability of Long Island north shore inlets will provide information and guidance for maintaining inlets in general.

Another motivation for the study of inlets along the north shore of Long Island is the large range in grain size of the sediments on this coast, where both coarse sand and gravel are present. In contrast, most studies and findings for inlets concern coasts consisting primarily of uniform fine-to-medium sands.

Mattituck Inlet, with a federally maintained navigable channel, is located 5.2 miles to the west and is larger than Goldsmith Inlet, although small relative to the six permanent inlets on the south shore of Long Island. Goldsmith Inlet is a small inlet and the easternmost on the north shore. Goldsmith Inlet has undergone moderate anthropogenic manipulation as compared to Mattituck Inlet. Therefore, the two neighboring inlets provide a reasonable range in physical characteristics to make comparisons and search for controlling variables on inlet stability and hydrodynamics.

Summary of Inlet Characteristics

Findings of this study on the morphology, sediment, hydrodynamics, and engineering activities at Mattituck Inlet and Goldsmith Inlet are summarized in Tables 7-1 to 7-4, respectively. These compilations are discussed in subsequent sections of this chapter.

Table 7-1
Mattituck Inlet and Goldsmith Inlet – Morphologic Characteristics

Characteristic	Mattituck Inlet	Goldsmith Inlet
r ratio	64-107	4.5-7.5
Hydrodynamic dominance	Tide dominated (low)	Tide dominated (low)
Offshore characteristics	Longshore bars west of inlet	Offshore depression on both sides of inlet
Gross longshore sediment transport rate estimate (cu yd/year)	15,000 - 25,000	16,000 - 21,000
Presence of ebb shoal	No	No
Presence of flood shoal	Yes	Yes
Bypassing mechanism	Probably small to negligible	Within swash zone
Channel shoaling mode	Bank encroachment	Channel infilling
Minimum cross-sectional area (observed) (sq ft)	1,600	80
Minimum cross- sectional area (theoretical prediction) (sq ft)	1,020	114
Average depth (ft, mlw)	9	1-2
Channel width-to-depth ratio	43	32

Table 7-2
Mattituck Inlet and Goldsmith Inlet, Nearshore Slopes and Sediment Grain Size

Characteristic	Mattituck Inlet	Goldsmith Inlet
Nearshore slope - west of Inlet	1:15	1:10
Nearshore slope - east of Inlet	1:25	1:10
Median grain size - west of Inlet (mm)	3.15	3.0
Median grain size - east of Inlet (mm)	0.49	0.49
Median grain size - channel entrance (class)	Coarse sand	Coarse gravel
Median grain size - mid-channel (class)	Medium to fine sand	Medium to fine gravel
Median grain size - channel egress (class)	Very coarse sand	Very coarse to coarse sand
Median grain size - flood shoal	(not sampled)	Very coarse to coarse sand

Table 7-3 **Mattituck Inlet and Goldsmith Inlet - Hydrodynamic Characteristics**		
Characteristic	**Mattituck Inlet**	**Goldsmith Inlet**
Tidal prism (cu ft)	4.32×10^7	3.04×10^6
Mean tide range (in creek and pond) (ft)	5.26	2.15
Spring tide range (in creek and pond) (ft)	6	2.9
Average ebb tide duration (min)	373	536
Average flood tide duration (min)	370	208
Maximum observed tidal current (m/sec)	0.4 - 0.5	1.3 and rising
Maximum calculated tidal current in inlet entrance (m/sec)	0.47	1.43

Table 7-4 **Mattituck Inlet and Goldsmith Inlet, Summary of Key Engineering Activities**		
Activity	**Mattituck Inlet**	**Goldsmith Inlet**
Jetty construction dates	1906 - 1914 (intermittent) 1937 - 1938 (west jetty seaward extension) 1946 (east jetty landward extension)	1963 - 1964
Jetty length (ft)	1,020 - east jetty 1,320 - west jetty	350-400
Width between jetties (ft)	400	NA
Average volumes dredged (cu yd)	38,000 (1921 - 1965) 17,000 (1980 - 2004)	4,700
Typical interval between dredging (years)	4.9 (1921 - 1965) 13 (1980 - 2004	1 - 1.5
Dredging depth (ft) mlw	7 plus 2	3

Comparative Analysis

This section gives an integrated comparative analysis of Mattituck Inlet and Goldsmith Inlet. Tables 7-1 to 7-4 can be consulted for additional or related information.

Forcing

Mattituck Inlet and Goldsmith Inlet experience almost the same tidal forcing, incident waves, wind, storms, and longshore sediment transport potential by waves. The average and spring tidal ranges in eastern Long Island Sound near

these inlets are 5.2 and 6.0 ft, respectively. Predominant waves are out of the west, both in height and duration of incidence. Data are lacking on the wave climatology of Long Island Sound with which to make quantitative predictions with standard engineering formulas. The long-term net longshore sediment transport is estimated to be 15,000 cu yd/year to the east at Goldsmith Inlet and somewhat less at Mattituck Inlet, based upon impoundment rates at the jetties, the orientation of the inlets relative to the predominant direction of wave incidence, and consistency with dredging records. Batten and Kraus (2005) obtained a net rate of 16,000 cu yd/year to the east at Mattituck Inlet and a gross rate of 21,000 cu yd/year based on a sediment budget analysis.

Both inlets supported tidal mills in the 1700s and 1800s, owing to the significant tidal range and relatively narrow channels. Therefore, in their natural states, the inlets must have experienced substantial tidal flow much of the year, although it is believed that the inlets would close temporarily due to presence of ice in winter and by occasional blockage from longshore sediment transport.

General features of geomorphology

Mattituck Inlet and Goldsmith Inlet share similar geologic settings characterized by coarse sediment and steep slopes, a result of the glacial origins of Long Island and a terminal moraine (Harbor Hill Moraine) located near the north shore. Each inlet lies at the center of a pocket beach bounded by headlands, and the adjacent beaches, cliffs, and the neighboring coastal cliffs of glacial origin are composed of a wide variety of grain sizes. Both inlets and their back bays are likely low-lying watersheds created by glaciers, and these areas are prone to sediment deposition.

The predominant grain size on the beaches and in the inlet entrances ranges between medium sand to gravel. In their natural states, prior to construction of jetties, the entrances to both inlets probably migrated moderately eastward (order of tens of feet for Goldsmith Inlet and hundreds of feet for Mattituck Inlet), returning to their root or original channel locations by breaking through the spit formed as part of the migration process. Mattituck Creek bends to the west before interrupting the dune line and exiting to Long Island Sound, suggesting underlying geologic control (hard bottom) that prevents direct access to the sound. A large number of glacial erratics can be observed in the nearshore on the eastern side of Mattituck Inlet. Cross-sectional channel stability of Goldsmith Inlet may also have been promoted by either a geologic control or structures to the west of the present location of the inlet.

The area offshore (12-30 ft mlw) of each inlet is composed predominantly of fine to medium grained sand. The offshore east of each inlet contains higher percentages of medium grained sand than areas west. No offshore area contains gravel, with the notable exception of the offshore shoal formation east of Mattituck Inlet, which has a gravel content estimted at 31 percent. The distribution of sediment grain sizes for the nearshore area west of both inlets is bimodal, with large percentages of medium grained sand and gravel. The nearshore area east of each inlet is composed predominantly of fine and medium sand. The sediment in the Federal navigation channel at Mattituck Inlet is a mixture of fine, medium, and coarse sand, and trends toward coarser material proceeding into the inlet. At Goldsmith Inlet, the inlet entrance is composed

predominantly of gravel and trends towards fine gravel to coarse sand proceeding south into the inlet. The difference in grain size distribution patterns observed is attributed to the difference in inlet width. At Mattituck Inlet, wave action has potential to transport coarse-grained sediment into the inlet. In contrast, the narrow width at Goldsmith Inlet prevents large waves from entering the inlet. Coarse-grained sediment is, therefore, not redistributed and remains at the inlet entrance.

The absence of ebb shoals at Mattituck Inlet and Goldsmith Inlet distinguishes them from the inlets on the south shore of Long Island (as well as from other tidal inlets on alluvial coasts), which possess ebb shoals with volumes in the range of about 8 to 40 million cu yd. Absence of an ebb shoal is a shared feature with harbors and entrances in the Great Lakes of the United States.

Anthropogenic influences

Although Mattituck Inlet and Goldsmith Inlet have similar forcing and geologic setting, there are substantial distinguishing physical characteristics. Two jetties built approximately 100 years ago have been maintained and improved to support shallow-draft navigation protecting Mattituck Inlet. Mattituck Inlet has been dredged extensively, possible to as deep as 20 ft mlw in certain locations of the Federal navigation project by commercial mining interests. Commercial mining took place on the beach directly west of the west jetty between 1960 and 1975 (and probably earlier) as well. Combined, it is estimated that these activities removed an estimated 500,000 to 900,000 cu yd of sediment from the inlet and littoral system between the 1920s and 1970s. Material dredged as part of the Federal navigation project prior to the 1946 was probably placed offshore (and could feasibly have contributed to the volume of the offshore shoal located east of the inlet), whereas material dredged between the 1960s and present has been placed on the downdrift beach.

The jetties at Mattituck Inlet are 400 ft apart, and the navigation channel is 100 ft wide at the bottom, maintained to a minimum depth of 7 ft mlw plus 2 ft allowable overdredging. The width of Goldsmith Inlet varies and is typically on the order of 25 to 75 ft, depending on the stage of tide. Two jetties fix the location of Mattituck Inlet, whereas the entrance to Goldsmith Inlet can migrate to the east, in the direction of net longshore sediment transport induced by breaking waves. There is geomorphic evidence that the mouth of Mattituck Inlet migrated west prior to construction of the jetties, but would return to its root channel, Mattituck Creek. Typical greater depths at Mattituck inlet range between 7 and 18 ft, mlw, whereas typical greater depths at Goldsmith Inlet range between 2 and 4 ft mlw.

The jetty at Goldsmith Inlet was constructed 40 years ago (1964) and is not maintained. The jetty functions as a sediment-retention structure or groin, serving no navigation purpose. The structure can be termed as a jetty only in historic context as part of a marina-development plan that was not implemented. Goldsmith Inlet has been dredged or excavated intermittently and shallowly (to maximum depth of about 3 ft mlw) in the past half century. Material dredged from Goldsmith Inlet since the 1970s has been placed on the downdrift beach. Because the jetty at Goldsmith Inlet has reached impoundment capacity, the inlet

has increasingly returned to a natural condition, where the inlet entrance is oriented at an acute angle in relation to the shoreline.

Multiple (typically, two or three) longshore bars are prominent to the west of Mattituck Inlet, but bars are absent west of Goldsmith Inlet, perhaps owing to a depression in the nearshore located just west of the jetty. Significant longshore bars are not found along the beaches directly to the east of the inlets. The shorelines to the west of both inlets have advanced considerably through impoundment at the west jetties, as compared to the position of the respective shorelines to the east, which receded after construction of the jetties at both locations. The shorelines to the west of the inlets are considerably smoother than the shorelines directly to the east. Material dredged as part of Federal navigation project channel maintenance prior to the dredging of 1946 was probably placed offshore. Condition surveys and dredging records indicate that material dredged in 1946 and later, with the exception of the dredging of 1961, was placed on the downdrift beach or in the nearshore of the downdrift beach.

Hydrodynamics and tidal shoals

The tidal prism at Mattituck Inlet is about 14 times greater than that at Goldsmith Inlet. However, the maximum current velocity through the mouth of Goldsmith Inlet can exceed 1 m/sec, whereas at Mattituck Inlet the current between the jetties rarely exceeds 0.5 m/sec. Numerical modeling of Mattituck Inlet in a representative natural condition (nineteenth century) indicated a maximum current exceeding 1 m/sec, similar to that at Goldsmith Inlet. Despite the great differences in tidal current, both inlets share geomorphic commonality in possessing flood shoals composed of fine-to-medium sand, and each lacks an ebb shoal.

Although the maximum ebb-current velocity at Goldsmith Inlet exceeds 1 m/sec and is comparable to that at other inlets that have formed ebb-tidal shoals, the volume of water flow or discharge is evidently too small to construct an ebb shoal. Sediment transported by the ebb current to the mouth of Goldsmith Inlet is moved away from the entrance by waves and the wave-induced longshore current.

Strong flood dominance exists at Goldsmith Inlet, which promotes movement of sediment, particularly fine sand, toward Goldsmith Pond, creating broad flood shoals. Numerical simulation of tidal hydrodynamics at Mattituck Inlet with a configuration representative of conditions prior to jetty construction indicates that this inlet was also flood dominant. Mattituck Inlet and Goldsmith Inlet cannot support ebb shoals because the ebb current velocity at Mattituck Inlet is too weak (maximum of 0.5 m/sec), and the discharge at Goldsmith Inlet is too small.

Channel cross-sectional area stability

The minimum channel cross-sectional area for Goldsmith Inlet agrees with the empirical prediction for small inlets in Chesapeake Bay (Byrne et al. 1980). In contrast, the minimum channel cross-sectional area of Mattituck Inlet is about one-third larger than the empirical prediction for Atlantic coast dual-jetty inlets

on sandy coasts (Jarrett 1976). The unusually large minimum cross-sectional area of the channel at Mattituck Inlet experiences a weak tidal current. The large area is attributed to a combination of overdredging of the inlet by commercial mining, low longshore sediment transport rate, and sediment blockage by the jetties.

Given their significant differences, it is remarkable that these two inlets have remained open, with the possible exception of intermittent short closings, for more than two centuries and likely much longer. The stability of inlets on the north shore derives in part from a relatively steep inner shore face, presence of geologic controls such as glacial erratics or hard points on shore, origins of ponds as low-lying areas created after glaciation, and relatively weak longshore sediment transport that is about an order of magnitude less than that on the south shore. However, other factors have entered in controlling stability, in particular, commercial mining of sediment, such as at Mattituck Inlet.

Mattituck Inlet, Conclusions

Prior to the 1938 extension of the west jetty, Mattituck Inlet experienced substantial sediment intrusion through shoal development on the west side. The extension was effective in eliminating this shoaling. Prior to the 280-ft landward extension of the east jetty in 1946, a breach and spit formation occurred on the east side of the east jetty. The 1938 seaward extension of the west jetty and the 1946 landward extension of the east jetty have effectively protected Mattituck Inlet from sediment intrusion, indicating successful modification or tuning of these coastal structures. The improvements decreased the long-term average-shoaling rate at Mattituck Inlet from approximately 8,000 cu yd/year to 1,500 to 2,000 cu yd/year.

While the breach was open, sediment was transported into the inlet entrance to the west and into the navigation channel where the channel turns eastward. At present, large dunes and a berm abut the east jetty, reducing breach potential. The presence of accretionary features on the Long Island Sound side of the east barrier indicates that shoreline position adjacent to the east jetty has become stable under typical wave conditions. Some cutting into the backside of the east barrier, adjacent to the east jetty, by the tidal current and, possibly, reflected waves is observed. This cutting should be monitored so that the integrity of the barrier near the east jetty is not compromised.

Considerable commercial mining of sand and gravel took place at Mattituck Inlet from the 1920s to the mid-1970s. The exact volumes of mining are undocumented, and some records are missing. It is estimated that mining resulted in the removal of 250,000 to 500,000 cu yd of sediment from between the jetties and that mining on the beach directly west of the west jetty removed 260,000 to 400,000 cu yd of sediment. Commercial mining permanently removed mined material from the littoral zone and beaches. Such mining contributed to maintenance of the navigation channel, and it is hypothesized in this study that the amount of commercial mining of the inlet channel increased the channel cross-sectional area beyond that supported by tidal flow. The channel will not readily return to an equilibrium cross section because of the low rate of longshore sediment transport at the site and protection of the channel by the jetties.

Commercial mining by local permit on the beach directly west of Mattituck Inlet served to prevent the west jetty from reaching impoundment capacity. The volume of the attachment fillet located there has grown considerably in recent years (Batten and Kraus 2005). Because mining of the fillet west of the jetty no longer takes place, the west jetty will eventually reach impoundment capacity. This occurrence can in turn be expected to substantially increase bypassing and sediment accumulation within the inlet.

Most dredging conducted today is performed to remove the flood shoal that forms at the base of the east jetty and along the west bank opposite this flood shoal. Sediment accumulating on the flood shoal encroaches into the channel as a steep shoal growing southward. Wave action is inferred to be a significant contributing mechanism in mobilizing finer sediments for transport by the flood tidal current. Waves have been observed to enter directly into the inlet to break on the opposing gravel beach located at the eastward turn in the channel. Sediment in this area encroaches into the channel as a steep shoal growing northward. The sediment arriving to this beach is sorted, with gravel and pebbles left behind and finer sand transported into the channel by tidal currents and wave-induced currents.

For the past approximately 50 years, Mattituck Inlet has provided a reliable channel for the shallow-draft navigation it supports, requiring maintenance dredging approximately every 10 years. Shoaling patterns occurring today are largely the same as those observed prior to the improvements of 1938 and 1946, although removed volumes have diminished.

The existence of the modern-day flood shoal can be traced to the behavior of the spit that formed in 1891 from the east bank, directed to the west. This spit migrated and reached an equilibrium position around 1980. Because the spit was subject to littoral forces over this time and is now mostly below water, it can be considered a flood shoal. The main area of shoaling occurs along the east bank where Mattituck Inlet empties into Mattituck Creek and the west bank opposite this location experiences significant shoaling. Shoaling is caused primarily by sediment brought into the inlet by storms from the northwest quadrant, to which the inlet is directly exposed. The major form of shoaling at Mattituck Inlet is in the form of bank encroachment, particularly at the location of the flood shoal. Wave action, and the production of waves by boats passing through the inlet are judged to be significant mechanisms for the redistribution of sediment onto the banks of the Federal navigation channel.

It is concluded that the morphologic feature at Mattituck Inlet that has the appearance of a relict ebb-tidal shoal is not an ebb shoal. Reasons for this conclusion are:

a. The shoal experienced minimal growth from 1927 to 2002.

b. The feature is not hydraulically connected to Mattituck Inlet. Numerical simulations of the tidal circulation for the present condition and representative natural inlet condition demonstrate that the ebb-tidal current is too weak to transport sediment to the shoal.

c. The shoal has a large gravel content, making transport to it by a weak tidal current infeasible.

d. The feature is located too far to the east to be associated with the inlet as an ebb-tidal shoal.

The origin of the offshore shoal is unknown. It may be a pre-existing geologic feature, and a portion of it may be the result of dredged material placement during the new work dredging of Mattituck Inlet.

Goldsmith Inlet, Conclusions

The presence of a tidal mill at Goldsmith Inlet in the eighteenth and nineteenth centuries indicates stability of the channel and strong tidal flow prior to the partial modifications of 1963-1964 as part of proposed and later abandoned marina development. The construction of a jetty on the west side of the entrance and the new-work dredging (1964) promoted stability of the inlet by interrupting longshore transport of sediment to the east for approximately 14 years. In 1978, the jetty at Goldsmith Inlet appears to have reached impoundment capacity.

After impoundment capacity was reached, rates of sediment intrusion into Goldsmith Inlet increased. An increased sediment supply resulted in dynamic morphological evolution within Goldsmith Inlet, partially mitigated by dredging, initially by Suffolk County and later by the Town of Southold. The increased rates of sediment intrusion resulted in the creation of an attachment fillet or spit directly east of the inlet, the eventual maturation of the flood shoal, and a subsequent increase in the rate of channel infilling.

The reestablishment of an effective natural longshore sediment bypassing system appears to have taken place sometime in the early 1980s, when the attached fillet east of the jetty reached an areal extent that promotes bypassing. Partial dredging from 1980 to 2000 apparently mitigated the continued growth and maturation of this attached fillet, and the eastward migration of the inlet entrance. The lack of dredging in recent years (in addition to the continued degradation of the jetty) has allowed for rapid growth of this feature, and resulting eastward migration of the inlet entrance (2001-2002). Reestablishment of a natural system of sediment bypassing has occurred, where sediment is transferred from this attached fillet via a bypassing bar located near the swash zone and eventually to the beach east of Goldsmith Inlet.

The current through Goldsmith Inlet is strongly flood dominant, controlled in main part by the shallow sills in the channel. Because sediment transport is proportional to a power of water velocity, such as the third power, net sediment transport is directed into Goldsmith Pond. The greater velocity magnitude at the inlet mouth entrains and transports larger grain sizes. Because the current velocity magnitude decreases with distance into the inlet, gradational deposition occurs, with the larger grain size fractions deposited and finer sediments transported further into the inlet.

Tidal asymmetry of coastal inlets has been well studied (e.g., Boon 1975; Boon and Byrne 1981; Aubrey and Speer 1985; Speer and Aubrey 1985; Speer et al. 1991), as recently summarized by Walton (2002). For example, shoaling channels truncate the lowest portion of the tide, resulting in a longer falling tide and a weaker ebb current as compared to the flood current. Such a truncation is a hypsometric effect, the control of water-surface elevation by the bathymetry or depths. In the case of Goldsmith Inlet, the elevation of the entire inlet entrance is

located near msl. At the lower water levels of ebb tide, the sills at the flood shoal and shoreline become more effective in retarding flow. In addition, water enters the fringing marsh of Goldsmith Pond on flood tide more rapidly than when it exits on ebb. The effective friction of the marsh, creating storage capacity, will release water slowly as compared to its entrance at flood tide.

The mouth of Goldsmith Inlet appears to be at or near locational equilibrium if it is oriented to the east. Past dredging practice has realigned the channel parallel to the jetty. It is hypothesized here that an orientation with the mouth directed to the east is the optimum for sediment bypassing and maintenance of inlet stability. The attached fillet to the east, between the jetty and the inlet mouth, now functions to bypass sediment via transport in the swash zone.

If the accretion fillet to the west were mined substantially, impoundment at the jetty would reduce the sediment bypassing volume, turning back the processes in time.

Recommendations for Future Studies

Wave measurements are lacking for the Long Island Sound and are essential for improving the reliability of coastal studies both for Long Island and Connecticut. Long-term measurements will allow development of a wave hindcast needed in engineering design. The USACE, New England District, and the New York District could share costs and benefits of wave gauging. At present, the University of Connecticut operates a nondirectional wave gauge in the middle of Long Island Sound. This gauge could be upgraded to directional capability for modest cost.

The amount of sediment that may be directed offshore by jetties along the north shore of Long Island is unknown. Because of the steep nearshore slope and coarse material, material directed offshore will not return to the beach. Offshore movement of sediment is an unanswered question, and it may be related to the observed reduction in required dredging volume at Mattituck Inlet. It was beyond the scope of this primarily morphologic study to apply a combined wave, current, and sediment transport model to estimate offshore sediment transport. Also, wave data are lacking to drive such a model.

It is recommended that sediment sampling be conducted in the offshore area of jetties to determine sediment texture and, as necessary, high-resolution bathymetric surveys be made to detect sediment buildup offshore. These might be done in conjunction with channel condition surveys.

The rate of channel infilling at Mattituck Inlet is low as compared to early in the twentieth century, indicating efficient protection by the jetties in their present configuration. Maintenance dredging removes the portion of the flood shoal that encroaches upon the Federal navigation channel. This formation has never been dredged in its entirety. Full removal of the portion of this shoal lying outside the navigation channel would greatly reduce shoaling at Mattituck Inlet and increase the required time interval between maintenance dredging, while supplying material to the downdrift beach. The volume of material that could be provided is estimated to be on the order of 15,000 cu yd, comparable to that removed from the channel during the typical 10-year dredging cycle. This feature appears to function as a groin in accumulating sediment, promoting channel bank

encroachment. Removal of this feature would increase the transport capacity of the flood current and promote tidal circulation in the neighboring marshes.

Numerical modeling of tidal circulation at Mattituck Inlet in a representative natural condition revealed marked hydrodynamic similarity to Goldsmith Inlet, which has a cross-sectional area relation with tidal prism similar to that of small inlets in Chesapeake Bay. A hypothesis is suggested – that the inlets along the north shore of Long Island display a unique relation between cross-sectional area and tidal prism. A regional characteristic relation is plausible given the low rates of longshore sediment transport, large sediment size, and relatively large tidal prism found in this region. The tide range within Long Island Sound increases from east to west. An increase in tidal ranges suggests that inlets along Long Island Sound will be increasingly stable proceeding east to west. It is further expected that other north shore inlets in Long Island Sound will lack an ebb shoal or have a much smaller ebb shoal as compared to the standard predictive formula. Flood shoals would be large for the shallower inlets.

References

Allee King Rosen and Fleming, Inc., Moffat and Nichols, Engineers, and The Saratoga Associates. (1995, revised 1996). "Town of Southold erosion management plan," prepared for the Town of Southold, revised by the New York Department of State, Division of Coastal Resources, and the Town of Southold.

Alpine Ocean Seismic Survey, Inc. (1998). "Final report on the geophysical investigation, Duck Pond Point to Horton Point, Southold project," prepared for the Town of Southold.

Amein, M., and Kraus, N. C. (1991). "DYNLET1: Dynamic implicit numerical model of one-dimensional tidal flow through inlets," Technical Report CERC 91-10, U.S. Army Engineer Waterways Experiment Station, Vicksburg, MS.

Aubrey, D. G., and Speer, P. E. (1985). "A study of non-linear tidal propagation in shallow inlet/estuarine systems, Part I: Observations," *Estuarine, Coastal and Shelf Science* 21, 185-205.

Batten, B. K., and Kraus, N. C. (2005). "Evaluation of shore erosion downdrift of Mattituck Inlet, New York: Section 111 study," Technical Report ERDC/CHL TR-04-xx, U.S. Army Engineer Research and Development Center, Vicksburg, MS.

Bokuniewicz, H., and Tanski, J. J. (1983). "Sediment partitioning at an eroding coastal bluff, " *Northeastern Geology* 5(2), 73-81.

Boon, J. D., III. (1975). "Tidal discharge asymmetry in a salt marsh drainage system," *Limnology and Oceanography* 20(1), 71-80.

Boon, J. D., III, and Byrne, R. J. (1981). "On basin hypsometry and the morphodynamic response of coastal inlet systems," *Marine Geology* 40, 27-48.

Bruun, P., and Gerritsen, F. (1959). "Natural by-passing of sand at coastal inlets," *Journal of the Waterways and Harbors Division* 85(WW4), American Society of Civil Engineers (ASCE), 75-107.

Bruun, P., and Gerritsen, F. (1960). "*Stability of tidal inlets*." North Holland Publishing Co., Amsterdam, 123 p.

Byrne R. J., Gammisch, R. A., and Thomas, G. R. (1980). "Tidal prism-inlet area relations for small tidal inlets," *Proceedings 17th Coastal Engineering Conference* III, ASCE, 2,517-2,531.

Carr de Betts, E. E. (1999). "An examination of flood tidal deltas at Florida's tidal inlets," M.S. thesis, Coastal and Oceanographic Engineering Department, University of Florida, Gainesville, FL.

Comes, C. R. (1954). "Peconic's Old Gristmill," *Long Island Forum* 107.

Cooke, T. W. (1985). "Sediment budget of Stony Brook Harbor, Long Island, New York," M.S. thesis, State University of New York at Stony Brook, Stony Brook, NY, 120 p.

Craven, C .E. (1906). *A history of Mattituck, LI, NY.* (Reprinted 1988), Jedediah Clauss and Sons, Amereon Ltd., Mattituck, New York, 11952-9500.

Czerniak, M. T. (1977). "Inlet interaction and stability theory verification," *Proceedings Coastal Sediments '77,* ASCE, 754-773.

Davies, D. S. (1972). "Stability of the North Shore of Long Island," Marine Environmental Studies, State University of New York at Stony Brook.

Davies, D. S., Axelrod, E. W., and O'Connor, J. S. (1971). "Erosion of the north shore of Long Island," Technical Report No. 18, State University of New York, Marine Science Research Center, 101.

Davis, Jr., R. A., and Hayes, M. O. (1984). "What is a wave dominated coast?," *Marine Geology* 60, 313-329.

Dean, R. G., and Walton, T. L. (1973). "Sediment transport processes in the vicinity of inlets with special reference to sand trapping," *Estuarine Research* II, L. E. Cronin, ed., Academic Press, 129-149.

Escoffier, F. F. (1940). "The stability of tidal inlets," *Shore and Beach* 8(4), 114-115.

Fields, L., Bosma, K. F., and Byrnes, M. R. (1999). "Historical shoreline change analysis: Western town line to Horton Point, Southold, NY, final report," Aubrey Consulting, Inc., East Falmouth, MA.

FitzGerald, D. M. (1988). "Shoreline erosional-depositional processes associated with tidal inlets," *Hydrodynamics and Sediment Dynamics of Tidal Inlets,* D. G. Aubrey, and L. Weishar, eds., Springer, Berlin, 186-225.

FitzGerald, D. M., Kraus, N. C., and Hands, E. B. (2000). "Natural mechanisms of sediment bypassing at tidal inlets," ERDC/CHETN-IV-30, U.S. Army Engineer Research and Development Center, Vicksburg, MS.

Fuller, M. L. (1914). "The geology of Long Island, New York," U.S. Geological Survey Professional Paper 82, 231 p.

Gaudiano, D. J., and Kana, T. W. (2000). "Shoal bypassing in South Carolina tidal inlets: Geomorphic variables and nine empirical predictions for nine mesoscale inlets," *Journal of Coastal Research* 17(2), 280-291.

Gofseyeff, S. (1952). "Case history of Fire Island Inlet, NY." *Proceedings of Third Conference on Coastal Engineering*, Council on Wave Research, 272-305.

Goodwin, P. (1996). "Predicting the stability of tidal inlets for wetland and estuary management," *Journal of Coastal Research* 81(23), 83-101.

Greenman-Pedersen Associates, P.C. (1981). "Report on the shoreline impacts of the Goldsmith Inlet jetty," in Town of Southold (2003), "local waterfront revitalization program," prepared by V. Scopaz, AICP Town Planner with assistance from S. Ridler, Coastal Resources Specialist, New York State Department of State Division of Coastal Resources.

Hayes. M. O. (1977). "Barrier island morphology as a function of tide and wave regime," *Proceedings Coastal Symposium on Barrier Islands*, S. Leatherman, ed., Academic Press, New York, 1-27.

Hayes, M. O. (1980). "General morphology and sediment patterns in tidal inlets," *Sedimentary Geology* 26, 139-156.

Hubbard, D. K., Oertel, G., and Nummedal, D. (1979). "The role of waves and tidal currents in the development of tidal-inlet sediment structures and sand body geometry; examples from North Carolina, South Carolina, and Georgia," *Journal of Sedimentary Petrology* 49(4), 1,072-1,092.

Hughes, S. A. (2002). "Equilibrium cross sectional area at tidal inlets," *Journal of Coastal Research* 19(1), 160-174.

Hume, T. M., and Herdendorf, C. E. (1990). "Morphologic and hydrologic characteristics of tidal inlets on a headland dominated, low littoral drift coast, northeastern New Zealand," *Proceedings Skagen Symposium, Journal of Coastal Research* SI 9, 527-563.

Jarrett, J. T. (1976). "Tidal prism-inlet area relationships," GITI Report 3, U.S. Army Engineer Waterways Experiment Station, Vicksburg, MS.

Johnson, D. W. (1919). *Shore processes and shoreline development.* John Wiley and Sons, Inc., London.

Kana, T. W. (1995). "A mesoscale sediment budget for Long Island, New York," *Marine Geology* 126, 87-110.

Koppelman, L. E., Weyl, P. K., Gross, M. G., and Davies, D. S. (1976). *The urban sea - Long Island Sound.* Praeger Publishers, New York, 223.

Kraus, N. C. (1998). "Inlet cross-sectional area calculated by process-based model," *Proceedings 26th Coastal Engineering Conference*, ASCE, 3,265-3,278.

Kraus, N. C. (2000). "Reservoir model of ebb-tidal shoal evolution and sand-bypassing," *Journal of Waterway, Port, Coastal, and Ocean Engineering* 126(6), 305-313.

Kraus, N. C., and Rosati, J. D. (1997). "Interpretation of shoreline-position data for coastal engineering analysis," Coastal Engineering Technical Note CETN-II-39, U.S. Army Engineer Waterways Experiment Station, Vicksburg, MS.

Kraus, N. C., and Rosati, J. D. (1998). "Estimation of uncertainty in coastal-sediment budgets at inlets," Coastal Engineering Technical Note CETN-IV-16, U.S. Army Engineer Waterways Experiment Station, Vicksburg, MS.

Kraus, N. C., Zarillo, G. A., and Tavolaro, J. F. (2003). "Hypothetical relocation of Fire Island Inlet, New York," *Proceedings Coastal Sediments '03*, CD-ROM published by World Scientific Press and East Meets West Productions, Corpus Christi, TX, ISBN-981-238-422-7, 14 p.

Kumar, N., and Sanders, J. E. (1974). "Geomorphic and stratigraphic analysis of Fire Island, New York, *Marine Geology* 21, 491-532.

Leatherman, S. P. (1989). "Role of inlets in geomorphic evolution of the south shore of Long Island, N.Y., USA," *Environmental Management* 13, 109-115.

Leatherman, S. P., and Allen, J. R., eds. (1985). "Geomorphologic analysis of south shore of Long Island barriers, New York," Report to U.S. Army Engineer District, New York.

Leatherman, S. P., Dean, R. G., Kana, T., and Anders, F. J. (1997). "Goldsmith Inlet and adjacent areas, north shore of Long Island, New York: Erosion problems and suggested modifications," *Shore and Beach* 65(3), 13-16.

LeConte, L. J. (1905). "Discussion on river and harbor outlets, notes on the improvement of river and harbor outlets in the United States," Paper No. 1009, by D. A. Watts, *Transactions American Society of Civil Engineers,* 306-308.

Luettich, R. A., Jr., Westerink, J. J., and Scheffner, N. W. (1992). "ADCIRC: An advanced three-dimensional circulation model for shelves coasts and estuaries, Report 1: Theory and methodology of ADCIRC-2DDI and ADCIRC-3DL," Dredging Research Program Technical Report DRP-92-6, U.S. Army Engineer Waterways Experiment Station, Vicksburg, MS, 137 p.

Lyles, S. D., Hickman, L. E., and Debaugh, H. A. (1988). "Sea level variations for the United States 1855 – 1986," National Oceanic and Atmospheric Administration, National Ocean Service, Rockville, MD, 182 p.

Militello, A., and Kraus, N.C. (2001). "Shinnecock Inlet, New York, site investigation, Report 4: Evaluation of flood and ebb shoal sediment source alternatives for the west of Shinnecock Interim Project, New York," Technical Report CHL TR-98-32, Coastal Inlets Research Program, U.S. Army Research and Development Center, Vicksburg, MS.

Militello, A., Kraus, N. C., and Brown, M. E. (2000). "Regional coastal and inlet circulation modeling with application to Long Island, New York," *Proceedings of the 13th Annual National Conference on Beach Preservation Technology*, FSBPA, Tallahassee, FL, 191-201.

Moody, J. A. (1988). "Small-scale inlets as tidal filters," *Lecture notes on coastal and estuarine studies,* D. G. Aubrey and L. Weisher, eds., Springer-Verlag New York, Inc., 137-154.

Morang, A., Rahoy, D. S., and Grosskopf, W. G. (1999). "Regional geologic characteristics along the south shore of Long Island, New York," *Proceedings Coastal Sediments '99*, ASCE, 1,568-1,583.

O'Brien, M. P. (1931). "Estuary tidal prisms related to entrance areas," *Civil Engineering* 1(8), 738-739.

O'Brien, M. P. (1966). "Equilibrium flow areas of tidal inlets on sandy coasts," *Proceedings 10th Coastal Engineering Conference* 1, 676-686.

O'Brien, M. P. (1969). "Equilibrium flow areas of inlets on sandy coasts," *Journal of Waterways, Ports, and Harbors Division* 95(WW1), 43-52.

Offshore and Coastal Technologies, Inc. (1998). "Shoreline monitoring; Southold town line to Horton Point," 500 Spencer Road Avondale, PA.

Omholt, F. L. (1974). "Effects of small groins on shoreline changes on the north shore of Suffolk County, New York," New York Ocean Science Laboratory Technical Report No. 0028, Montauk, NY.

Panuzio, T. (1968). "The Atlantic coast of Long Island," *Proceedings 11th Coastal Engineering Conference*, ASCE Press, 1,222-1,241.

Park, M. J. (1985). "Prediction of tidal hydraulics and sediment transport patterns in Stony Brook Harbor," M.S. thesis, State University of New York at Stony Brook, Stony Brook, NY, 146 p.

Ralston, R. R., U.S. Engineer Office, First District. (1928). "Report on survey of Mattituck Harbor, NY," in House of Representatives (1935) report from the Chief of Engineers on preliminary examination and survey of Mattituck Harbor, NY, House Document No. 8, 71st Congress, 1st Session, U.S. Government Printing Office, Washington, DC.

Schubel, E. J. (1976). "An assessment of the effects of the periodic removal of sand from the western jetty at Mattituck Inlet on shore erosion of contiguous shoreline segments," Marine Sciences Research Center, State University of New York, Stony Brook, NY.

Schmeltz, E. J., Sorensen, R. M., McCarthy, J. J., and Nersesian, G. (1982). Breach/inlet interaction at Moriches Inlet, *Proceedings 18th Coastal Engineering Conference*, ASCE, 1,062-1,077.

Schwaab, W. C., Thieler, E. R., Allen, J. S., Foster, D. S., Swift, B. A., Denny, J. F., and Danforth, W. W. (1999). "Geologic mapping of the nearshore area offshore Fire Island, New York," *Proceedings Coastal Sediments '99*, ASCE, 1,552-1,567.

Seabergh, W. C. (2003). "Long-term coastal inlet channel area stability," *Proceedings Coastal Sediments '03*, CD-ROM published by World Scientific Publishing Corporation, and East Meets West Productions, ISBN 981-238-422.7.

Seabergh, W. C., and Kraus, N. C. (1997). "PC program for coastal inlet stability analysis using Escoffier method," Coastal Engineering Technical Note CETN-IV-11, Coastal Engineering Rearch Center, U.S. Army Engineer Waterways Experiment Station, Vicksburg, MS.

Shepard, F.P. (1963). *Submarine geology*. Harper and Rowe Publishers, New York, 557 p.

Signell, R. S., List, J. H., and Farris, A. S. (2000). "Bottom currents and sediment transport in Long Island Sound: A modeling study," *Journal of Coastal Research* 16(3), 551-566.

Simpson, D. P. (1976). "Hydraulics of two small gravelly tidal inlets," M.S. thesis, University of Washington, Seattle, WA, 137 p.

Smith, E. R. (1988). "Case histories of Corps breakwaters and jetty structures, Report 5, North Atlantic Division," Technical Report REMR-CO-3, U.S. Army Engineer Waterways Experiment Station, Vicksburg, MS.

Speer, P. E., and Aubrey, D. G. (1985). "A study of non-linear tidal propagation in shallow inlet/estuarine systems, Part II: Theory," *Estuarine, Coastal and Shelf Science* 21, 207-224.

Speer, P. E., Aubrey, D. G., and Friedrichs, C. T. (1991). "Nonlinear hydrodynamics of shallow tidal inlet/bay systems," in *Tidal Hydrodynamics*, B. B. Parker, ed., Wiley, NY, 321-340.

Taney, N. E. (1961). "Geomorphology of the south shore of Long Island, New York," TM No. 128, U.S. Army Corps of Engineers, Beach Erosion Board, Washington, DC.

Tanski, J., Bokuniewicz, H. J., and Schubert, C. E. (1990). "An overview and assessment of the coastal processes data base for the south shore of Long Island, *Proceedings of Workshop Held April 10-21, 1989*, New York Sea Grant Program Special Report No. 104, New York State Sea Grant, Stony Brook, NY.

Tetra Tech, Inc. (1979). "Jamesport nuclear project shoreline study," Tetra Tech, Inc. Jacksonville, FL.

Town of Southold. (2003). "Local waterfront revitalization program," prepared by Valerie Scopaz, AICP Town Planner, with assistance from Steve Ridler, Coastal Resources Specialist, New York State Department of State Division of Coastal Resources.

U.S. Army Engineer District, New York. (1963) "NYSPW beach protection project 192," permit granted to the Department of Public Works, State of New York, NY.

U.S. Army Engineer District, New York. (undated). "Mattituck Harbor dredging history, 1921 - Present," New York, NY.

U.S. Army Engineer District, New York. (1969). "North Shore of Long Island Suffolk County, New York, beach erosion control and interim hurricane study (survey)," New York, NY.

U.S. Army Engineer District, New York. (2003). "Fact sheet - Mattituck Harbor, NY," New York, NY.

U.S. Engineers Office, First District. (1928). "Report on survey of Mattituck Harbor, NY," in House of Representatives (1935) "Report from the Chief of Engineers on preliminary examination and survey of Mattituck Harbor, NY," House Document No.8, 71st Congress, 1st Session, U.S. Government Printing Office, Washington, DC.

U.S. Environmental Protection Agency, and U.S. Army Corp of Engineers. (2001). "Physical oceanographic evaluation of Long Island Sound and Block Island Sound."

Walton, T. L., Jr. (2002). "Tidal velocity asymmetry at inlets," Coastal Engineering Technical Note ERDC/CHL CHETN IV-47, U.S. Army Engineer Research and Development Center, Vicksburg, MS.

Walton, T. L., and Adams, W. D. (1976). "Capacity of inlet outer bars to store sand," *Proceedings 15th Coastal Engineering Conference*, ASCE, 1,919-1,937.

Williams, S. J. (1981). "Sand resources and geological character of Long Island Sound," Technical Paper No. 81-3, Department of the Army, Coastal Engineering Research Center, Fort Belvoir, VA, 65 p.

Zarillo, G., and Park, M. (1987). "Sediment transport prediction in a tidal inlet using a numerical model - application to Stony Brook Harbor, Long Island, New York, USA," *Journal of Coastal Research* 3(4), 429-444.

REPORT DOCUMENTATION PAGE

Form Approved OMB No. 0704-0188

1. REPORT DATE *(DD-MM-YYYY)*
July 2005

2. REPORT TYPE
Final report

3. DATES COVERED *(From - To)*

4. TITLE AND SUBTITLE

Geomorphic Analysis of Mattituck Inlet and Goldsmith Inlet, Long Island, New York

5a. CONTRACT NUMBER

5b. GRANT NUMBER

5c. PROGRAM ELEMENT NUMBER

6. AUTHOR(S)

Michael J. Morgan, Nicholas C. Kraus, Jodi M. McDonald

5d. PROJECT NUMBER

5e. TASK NUMBER

5f. WORK UNIT NUMBER

7. PERFORMING ORGANIZATION NAME(S) AND ADDRESS(ES)

City University of New York, Hunter College, Department of Geography, 695 Park Avenue, New York, NY 10021;
U.S. Army Engineer Research and Development Center. Coastal and Hydraulics Laboratory, 3909 Halls Ferry Road, Vicksburg, MS 39180-6199;
U.S. Army Engineer District, New York, 26 Federal Plaza, New York, NY 10278-0090

8. PERFORMING ORGANIZATION REPORT NUMBER

ERDC/CHL TR-05-2

9. SPONSORING / MONITORING AGENCY NAME(S) AND ADDRESS(ES)

U.S. Army Corps of Engineers
Washington, DC 20314-1000

10. SPONSOR/MONITOR'S ACRONYM(S)

11. SPONSOR/MONITOR'S REPORT NUMBER(S)

12. DISTRIBUTION / AVAILABILITY STATEMENT

Approved for public release; distribution is unlimited.

13. SUPPLEMENTARY NOTES

14. ABSTRACT

This study of Mattituck Inlet and Goldsmith Inlet, Long Island, NY, covers the historic and geomorphic background, literature, field measurements, numerical modeling of tidal circulation, and analysis of inlet morphologic properties. The inlets are located 8.2 km apart on the eastern end of the north shore of Long Island, NY, facing Long Island Sound. Mattituck Inlet has a federally maintained channel and dual jetties, and it connects the sound to Mattituck Creek. Mattituck Inlet is the only major harbor on the north fork of Long Island and is a commercial and recreational boating center. The navigation channel is maintained to a depth of 7 ft mean low water with a 2-ft allowable overdraft. Goldsmith Inlet connects the sound to Goldsmith Pond. The inlet has a nonfunctional jetty on its west side and is non-navigable, with typical depths ranging from 0.5 to 3 ft.

Tidal inlets on the north shore of Long Island have received little study compared to those on the south shore that open to the Atlantic Ocean. It appears that most inlets on the north shore have been more stable and in existence longer than the inlets on the south shore. Inlets on the north shore, therefore, hold value for further understanding of basic inlet processes, in particular, of channel cross section and locational stability. Another motivation for the study of inlets along the north shore of Long Island is the large range in grain size of the sediments on this coast.

(Continued)

15. SUBJECT TERMS

ADCIRC Model	Geomorphology	Inlet stability
Coastal inlets	Hydrodynamic modeling	

16. SECURITY CLASSIFICATION OF:			17. LIMITATION OF ABSTRACT	18. NUMBER OF PAGES	19a. NAME OF RESPONSIBLE PERSON
a. REPORT	b. ABSTRACT	c. THIS PAGE			19b. TELEPHONE NUMBER *(include area code)*
UNCLASSIFIED	UNCLASSIFIED	UNCLASSIFIED		332	

14. ABSTRACT (Concluded)

Given their significant differences, it is remarkable that Mattituck Inlet and Goldsmith Inlet have remained open for more than two centuries and likely much longer. The stability of inlets on the north shore derives in part from a relatively steep inner shore face, presence of geologic controls such as glacial erratics or hard points on shore, origins of ponds as low-lying areas created after glaciation, and relatively weak longshore sediment transport that is about an order of magnitude less than that on the south shore of Long Island. However, other factors enter in controlling stability, in particular, commercial mining of sediment, such as at Mattituck Inlet.